Development of a Combat Aircraft Operational and Cost-Effectiveness Design Methodology

A Thesis
Presented
by

Flt. Lt. Otsin Nilubol

Supervisor : Prof. J. P. Fielding

In Partial Fulfillment
of the Requirements for the Degree
Doctor of Philosophy

Cranfield College of Aeronautics
School of Engineering
Cranfield University
February 2005

ABSTRACT

This study set out to develop an aircraft design methodology, which gives combat aircraft more operational and cost-effectiveness by considering these factors early in the design process. In this methodology, an aircraft will be considered as a sub-system of an overall system, representing an entire operation scenario. Measures of operational and operational cost-effectiveness indicate the quality of, and relationships between, the major design aspects; i.e. susceptibility, vulnerability, reliability, maintainability, and operational cost. These measures are functions of aircraft measures of performance and measures of effectiveness. A mission operation simulation was developed as the transformation tool, to performance and effectiveness measures.

The measures of aircraft performance developed in this methodology have been evaluated by simple, yet sufficient, models because of the paucity of available data, information and the appropriateness of such assessment methods during the early design stages. An aircraft performance in susceptibility terms is measured both in the forms of probability of detection, which is predicted through its radar cross section (RCS), and probability of hit. The RCS prediction model in this study generally uses an aircraft's external shape, and the probability of hit is also evaluated from the aircraft presented areas.

The probability of kill is a measure of aircraft performance used the vulnerability design methods. This value relates directly to number and sizes of the critical components installed in the aircraft, and their layout. The modification of the critical component layout can directly affect the aircraft probability of kill. In this study, only two major threat types are considered; i.e. contact and proximity warheads.

Manoeuvrability probability has been introduced, and been used together with the susceptibility and vulnerability probabilities to predict the overall operational survivability probability in this study.

Aircraft reliability and some maintainability probabilities are predicted by using available unclassified data and fundamental aircraft design parameters and variables by dint of statistical analysis and the Pareto principle.

Operational cost in this methodology is calculated throughout the aircraft Life Cycle Cost (LCC) by averaging the total operation cost over the total number of operational aircraft in one base and total number of flying hours for an aircraft fleet's entire life. The average operation cost in conjunction with the number of aircraft lost and of weapons released during the mission simulation gives the total operational cost for the overall scenario.

An alternative method used to integrate all probabilities into the operation mission simulation is by using the reliability block diagram technique in conjunction with an event tree diagram. The Monte Carlo simulation technique has been used to generate more accurate results by means of random value usage.

Most results from the operation mission simulation are in the form of integer numbers; therefore, the genetic algorithm optimisation method was mainly used in this study. However, the gradient-based optimisation method can also be used to give approximate predictions. The results from the optimisation can finally be used as examples of how to design a combat aircraft for operational and cost-effectiveness.

ACKNOWLEDGEMENTS

This thesis would not have been successful finished without the help of many people. The author would like to sincerely thank to all of them, including:

My supervisor, **Professor John P. Fielding** for his great supervision and valuable guidance.

The Royal Thai Air Force for sponsoring my research.

Dr. Craig Lawson for his patient and fast correction with English writing and great advice on thesis writing.

Mr. Philip Pugh for his assistance, and advice on the estimation of Life Cycle Cost.

Professor Robert Ball for his advice on probability of detection prediction.

Mr. Paul Alonze for his advise on vulnerability assessment.

Mr. Georgios Dimitriadis and **Mr. Rui Miguel Martins Pires** for their assistance on information assessment from CATIA models.

Dr. Oswald for his assistance with access to a high performance computer.

Diane Boyles, Elizabeth James, Ramesh Wadher, and all staff at Cranfield University for their supports in this research.

Finally, thanks to **my Family and Friends** for their unwavering support and love.

TABLE OF CONTENTS

ABSTRACT ii

ACKNOWLEDGEMENTS iii

LIST OF TABLES ix

LIST OF FIGURES xii

NOMENCLATURE xix

1 INTRODUCTION 1

2 DESIGN METHODOLOGY FOR AIRCRAFT OPERATIONAL AND COST-EFFECTIVENESS 4

2.1 Conventional Aircraft Design Methodology 4

2.1.1 Conceptual Design 4

2.1.2 Preliminary Design 5

2.1.3 Detail Design 5

2.2 System of Systems Design Methodology 6

2.2.1 Vehicle Level of Design 7

2.2.2 Mission Level of Design 7

2.2.3 Theatre Level of Design 8

2.3 Design Methodology for Operational and Cost-Effectiveness 8

2.3.1 Aims & Development of Methodology 8

2.3.2 Campaign Definition 11

2.3.3 Aircraft Measures of Performance and Effectiveness 11

2.3.4 Measures of Operational Effectiveness 14

2.3.5 Measures of Cost-Effectiveness 15

2.4 Chapter Summary 16

3 SURVIVABILITY ASSESSMENT 17

3.1 Susceptibility Assessment 17

3.1.1 Radar Cross Section 19

3.1.2 Probability of Detection by Radar 23

3.1.3 Conditional Probability of Hit 24

3.2 Vulnerability Assessment 30
3.2.1 Kill Tree Diagram 30
3.2.2 Shotline Technique 30
3.2.3 Vulnerable Area given by a Single Hit 31
3.2.4 Aircraft Kill Probability by a Single Hit of a Nonexplosive Penetrator 36
3.2.5 Aircraft Kill Probability by Multiple Hits of Penetrators 36
3.2.6 Aircraft Kill Probability by Proximity Warhead 38
3.2.7 Lethal Radius 39
3.3 Probability of Survivability 39
3.3.1 Probability of Manoeuvrability (Weighting Factors) 40
3.3.2 Probability of Encounter 40
3.4 Chapter Summary 43
4 RELIABILITY & MAINTAINABILITY 44
4.1 Reliability Assessment 44
4.1.1 Direct Linear Regression 44
4.1.2 Pareto Distribution 45
4.1.3 Empty Weight Functionality 46
4.1.4 Combination between Linear Regression and Pareto Distribution . 47
4.2 Maintainability Assessment 49
4.2.1 Mean Time To Repair 49
4.2.2 Scheduled Maintenance 50
4.2.3 Unscheduled Maintenance 51
4.3 Chapter Summary 53
5 LIFE CYCLE COST ESTIMATION 54
5.1 Research, Development, Test & Evaluation Cost 55
5.1.1 Airframe Development Cost 56
5.1.2 Engine Development Cost 56
5.1.3 Avionics Development Cost 57
5.2 Production Cost 57
5.3 Ground Support Equipment and Initial Spares 57

5.4 Operation and Support 58
5.4.1 Personnel Cost 58
5.4.2 Unit Level Consumption 58
5.4.3 Contracts 59
5.4.4 Sustaining Support Cost and Installation Support Funds 59
5.5 Disposal 59
5.6 Mission Operational Cost 60
5.6.1 Operational Cost during Peacetime Operations 60
5.6.2 Operation Cost during Wartime Operations 60
5.6.3 Measure of Operational Cost 61
5.7 Chapter Summary 65
6 OPERATION MISSION SIMULATION 66
6.1 Threat Analysis 66
6.1.1 Nonexplosive Penetrator or Contacted Warhead 66
6.1.2 Proximity Warhead 67
6.2 Mission Analysis 68
6.3 Operation Simulation Concept 69
6.4 Success Probability Assessment 72
6.5 Monte Carlo Simulation Technique 74
6.6 Chapter Summary 77
7 OPTIMISATION METHODS 78
7.1 Gradient-based Method 78
7.2 Genetic Algorithms 79
7.2.1 GAlib Optimisation Tools 82
7.3 Chapter Summary 85
8 RESULTS 86
8.1 Results from Susceptibility Assessment 86
8.1.1 Radar Cross Section 86
8.1.2 Signal-To-Noise Ratio 88
8.1.3 Probability of Detection 89

8.1.4 Probability of Hit 89
8.2 Results from Vulnerability Assessment 90
8.2.1 Probability of Kill 90
8.3 Results from Reliability & Maintainability Assessment 91
8.4 Results from Life Cycle Cost Estimation 94
8.5 Operation Simulation Results 97
8.5.1 Results and Effects of an Individual Aircraft Measure of Performance on Operational and Operational Cost Measures of Effectiveness 97
8.5.2 Results and Effects of Multiple Aircraft Measures of Performance on the Operational and Operational Cost Measures of Effectiveness 108
8.6 Results from Optimisation 115
8.6.1 Results from the Optimisation using the Gradient-Based Method . 116
8.6.2 Results from the Optimisation using Genetic Algorithms 116
9 DISCUSSION 119
9.1 Design Methodology for Aircraft Operational and Cost-Effectiveness . . . 119
9.2 Validation and Discussion of Susceptibility Assessment 121
9.2.1 RCS Validation 121
9.2.2 Susceptibility Assessment 122
9.3 Discussion of Vulnerability Assessment 123
9.4 Validation and Discussion of Reliability & Maintainability Assessment . . 124
9.5 Validation and Discussion of Life Cycle Cost Estimation 126
9.6 Discussion of Operation Simulation 126
9.7 Discussion of Aircraft Measures of Performance on the Operational and Operational Cost Measures of Effectiveness 127
9.8 Discussion of Optimisation Results Relative to the Operational and Cost-Effectiveness 128
9.9 Future Work 129
10 CONCLUSIONS 131
11 RECOMMENDATIONS 134
REFERENCES 135

APPENDIX A — RELIABILITY BLOCK DIAGRAM AND EVENT TREE CALCULATION METHODS 139

APPENDIX B — SURVIVABILITY ASSESSMENT MODULE 143

APPENDIX C — RELIABILITY & MAINTAINABILITY ASSESSMENT MODULE 160

APPENDIX D — LIFE CYCLE COST ESTIMATION MODULE . . . 172

APPENDIX E — OPERATION MISSION SIMULATION MODULE 190

APPENDIX F — MISSION EFFECTIVENESS ANALYSIS APPLICATION 225

LIST OF TABLES

2.1 Example of transformation from aircraft design parameter into aircraft MOPs for specific design aspect 10

2.2 Example List of Measures of Performance and Effectiveness 15

2.3 Measure of Effectiveness at the theatre level of design 15

3.1 Assumed default probability of kill of a component, given a hit on the component $P_{k/h}$ 32

3.2 Aircraft component presented areas with overlapped critical components . 34

3.3 Calculation of the kill probability of the Overlapped No. 2 35

3.4 State transition matrix $[T]$ 38

3.5 Aircraft manoeuvrability probabilities 41

6.1 Predicted value per sortie from mission simulation module 71

8.1 Comparison between selected aircraft front view RCS from published source [18] and calculated aircraft front view RCS from the susceptibility assessment sub-module 87

8.2 Calculated U-99 RCS in six main views 87

8.3 Calculated S/N of six main U-99 views for each flight phase [dBm^2] 88

8.4 Calculated average RCS and S/N for each flight phase by using manoeuvrability probability option 2 89

8.5 Average calculated S/N and P_D in each flight phase predicted by using manoeuvrability probability option 2 89

8.6 $P_{H/D}$ of three main U-99 views in each flight phase evaluated from 20 random hits 90

8.7 Calculated $P_{K/H}$ of U-99 with redundant fuel systems 91

8.8 Calculated $P_{K/H}$ of U-99 with non-redundant fuel systems 91

8.9 Comparison between real aircraft failure rate and results of the combination method and functionality method [per 1000 flying hours] 93

8.10 Comparison between real aircraft defect man-hour rate and results of the combination method and functionality method [per 1000 flying hours] . . . 94

8.11 Results of U-99 from reliability & maintainability assessment module . . . 94

8.12 Results from life cycle cost estimation sub-module 95

8.13 Comparison between U-99 LCC calculated from the LCC estimation module and from FACET [25] 95

8.14 Comparison between LCC per one U-99 [M$] during wartime and peacetime scenarios for 4 years and 20 years life time 97

8.15 Effect of increasing an individual U-99 MOP on operational and operational cost MOEs 108

8.16 Generic effects of increasing individual aircraft MOPs for survivability on operational and operational cost MOEs 111

8.17 Generic effects of increasing aircraft MOP within selected specific remaining aircraft MOPs on operational and operational cost MOEs 115

8.18 Results from the gradient-base method optimisation 116

8.19 Results from the genetic algorithm optimisation 117

B.1 Results of F-117 front view radar cross section calculation from susceptibility assessment module 145

B.2 Results of B-2 front view radar cross section calculation from susceptibility assessment module 146

B.3 Results of U-99 front view radar cross section calculation from susceptibility assessment module 146

B.4 Results of U-99 probability of detection in attack flight phase of manoeuvrability option 2 with $P_n = 3.72665 \times 10^{-6}$ 147

B.5 U-99 critical components list 149

B.6 U-99 overlapped critical components list 150

B.7 Lethal radius[m] of U-99 with and without non-redundant fuel systems . . 153

B.8 Lethal radius[Grid] of U-99 with and without non-redundant fuel systems . 153

B.9 U-99 drawing grid factor in six main aircraft views 153

C.1 Linear equations to predict aircraft failure rate in each data set 161

C.2 Aircraft design variable from Serghides [38] 163

C.3 Aircraft design variable from unpublished data [4] 163

C.4 Failure rate Pareto distribution coefficients 166

C.5 Compare results of failure rate prediction per 1000 flying hour 167

C.6 Defect man-hour rate Pareto distribution coefficients 171

C.7 Compare results of defect man-hour rate prediction per 1000 flying hour . . 171

E.1 Results from susceptibility and vulnerability assessment sub-modules with different manoeuvrability probability options 198

E.2 Results from mission simulation module with different manoeuvrability probability options 200

E.3 Total results from the gradient-based method optimisation 221
E.4 Total results from the genetic algorithms optimisation 223

LIST OF FIGURES

1.1 Aircraft design aspects 1

2.1 Conventional Design Methodology 6

2.2 System of systems design methodology [43] 7

2.3 Flowchart of the operational and cost-effectiveness design methodology . . 9

2.4 Aircraft Measures of Performance and Effectiveness for Survivability 12

3.1 Plane wave scattering by a rectangular plate [27] 20

3.2 The finish-cone geometry [13] 22

3.3 Conditional detection by threshold setting [6] 23

3.4 Probability of detection vs signal-to-noise ratio and probability of false alarm [24] 25

3.5 Aircraft presented areas represented by Shoe Box and bivariate normal miss distance distribution 27

3.6 Presented area represented by Shoe Box and Carlton methods 27

3.7 Circular symmetric miss distance [6] 28

3.8 Warhead detonation and fragment spray 29

3.9 Kill tree diagram for UAV 31

3.10 Identification of Overlapped area by shotline technique 32

3.11 Presented and vulnerable areas of critical components and aircraft [6] . . . 32

3.12 Overlapped areas from tank no.1, tank no.2 and FCS 33

3.13 Aircraft manoeuvrability in attack flight phase 40

3.14 Block diagram for independent encounters survivability probability 41

4.1 Pareto distribution 46

4.2 Failure rate as a function of empty weight 47

4.3 Failure rate distribution of aircraft P 48

4.4 Defect man-hour rate as a function of aircraft empty weight 52

5.1 Consumer Price Index, 1983 = 1.00 55

5.2 Results of U-99 LCC estimation in peacetime scenario 63

5.3 Results of U-99 LCC estimation in wartime scenario 64

6.1 Time clock for each aircraft [1] 69

6.2 Flowchart for Operation Mission Simulation Module 70

6.3 Reliability Block Diagram for Inbound phase success probability calculation 74
6.4 Example of using Monte Carlo with Reliability Block Diagram 75
6.5 Normal curve of successful sorties after 20000 trials 75
7.1 Flowchart of genetic algorithm 80
7.2 Example of mutation and crossover methods [50] 81
8.1 Results of U-99 radar cross section in dBm^2 unit 88
8.2 Comparison between the highest failure rate from the linear and exponential regression analysis 92
8.3 Comparison between the highest defect man-hour rate from linear and exponential regression analysis 92
8.4 Results from U-99 LCC estimation in peacetime scenario for 4 years life time 96
8.5 Results from U-99 LCC estimation in peacetime scenario for 20 years life time 96
8.6 Effect of the probability of detection on the operational and operational cost 98
8.7 Effect of the probability of hit on the operational and operational cost . . . 100
8.8 Effect of the probability of kill on encounter with penetrators on the operational and operational cost 102
8.9 Effect of the probability of kill on encounter with proximity warhead on the operational and operational cost 103
8.10 Effect of the reliability probability on the operational and operational cost 104
8.11 Effect of the mean time to repair defect on the operational and operational cost 105
8.12 Effect of the mean time to repair damage on the operational and operational cost 105
8.13 Effect of the defect man-hour rate on the operational and operational cost MOEs 107
8.14 Effect of P_D and $P_{K_{Non}}$ with increasing $P_{K_{Ext}}$ and constant P_H on the number of the total sorties flown 109
8.15 Effect of P_D and $P_{K_{Non}}$ with increasing $P_{K_{Ext}}$ and constant P_H on the total operational cost 110
8.16 Effect of aircraft defect arising rate with increasing $MTTR_{Defect}$ on numbers of the total sorties flown and the total targets killed 111
8.17 Effect of aircraft defect arising rate, P_D, $P_{K_{Non}}$, $P_{K_{Ext}}$ and $MTTR_{Defect}$ with a constant DMHR on the total number of sorties flown 113
8.18 Effect of aircraft defect arising rate, P_D, $P_{K_{Non}}$, $P_{K_{Ext}}$ and $MTTR_{Defect}$ with a constant DMHR on cost[$]/target 114

A.1 Two components series system 140
A.2 Two components parallel system 140
A.3 Reduced Event Tree Sample 141
B.1 Flowchart of survivability assessment module 143
B.2 Flowchart of probability of detection prediction 144
B.3 Susceptibility assessment dialog 145
B.4 Graph for evaluation detection probability dialog 147
B.5 Flowchart of probability of hit determination 148
B.6 Application dialog for probability of hit determination 149
B.7 Flowchart of vulnerability assessment module 150
B.8 Vulnerability assessment module application dialog 151
B.9 Critical component overlapped area presented area tab dialog 151
B.10 Semi-automatic Grid counting 152
B.11 Transition matric for U-99 top/bottom view without critical components overlapping consideration 154
B.12 Transition matric for U-99 right/left view without critical components overlapping consideration 155
B.13 Transition matric for U-99 front/rear view without critical components overlapping consideration 155
B.14 Transition matric for U-99 right/left view without shielding effect of critical components overlapping consideration 156
B.15 Transition matric for U-99 right/left view with shielding effect of critical components overlapping consideration 156
B.16 Transition matric for U-99 front/rear view without shielding effect of critical components overlapping consideration 157
B.17 Transition matric for U-99 front view with shielding effect of critical components overlapping consideration 158
B.18 Transition matric for U-99 rear view with shielding effect of critical components overlapping consideration 158
B.19 Lethal radius estimation application dialog 159
C.1 Flowchart of reliability & maintainability assessment module 161
C.2 Reliability & Maintainability assessment application dialog 162
C.3 Pareto distribution of real data in 1985, 1993, and 1996 165

C.4 Comparison between the highest failure rate from the real data and from the Pareto distribution representative 165
C.5 Failure rate Pareto distribution coefficient calculation tab dialog 166
C.6 Defect man-hour rate Pareto distribution coefficient calculation tab dialog 167
C.7 Defect man-hour rate as a function of aircraft empty weight 168
C.8 Pareto distribution of real data in 1985 and 1993 170
C.9 Comparison between the highest defect man-hour rate from the real data and from the Pareto distribution representative 170
D.1 Life Cycle Cost estimation application dialog 172
D.2 Flowchart of LCC estimation module 173
D.3 Result of F-16 LCC estimation in peacetime scenario 186
D.4 Result of F-16 LCC estimation in wartime scenario 187
D.5 Result of Eurofighter LCC estimation in peacetime scenario 188
D.6 Result of Eurofighter LCC estimation in wartime scenario 189
E.1 Flowchart of entire application 190
E.2 Flowchart of air superiority mission 191
E.3 Flowchart of patrol mission 192
E.4 Flowchart of long penetration mission (Hi-Lo-Lo-Hi) 193
E.5 Flowchart of escort mission 194
E.6 Flowchart of reconnaissance mission 195
E.7 Flowchart of reconnaissance mission (continue) 196
E.8 Flowchart of bombing mission 197
E.9 Fives alternatives of manoeuvrability probability 199
E.10 Effect of probability of detection 200
E.11 Effect of probability of hit 201
E.12 Effect of probability of kill on encounter with penetrators 201
E.13 Effect of probability of kill on encounter with proximity warhead 202
E.14 Effect of defect arising rate 202
E.15 Effect of mean time to repair defect 203
E.16 Effect of probability of mean time to repair damage 203
E.17 Effect of probability of defect man-hour rate 204

E.18 Effect of P_D and $P_{K_{Non}}$ with increasing $P_{K_{Ext}}$ and $P_H = 0.5$ on the total number of sorties flown 204

E.19 Effect of P_D and $P_{K_{Non}}$ with increasing $P_{K_{Ext}}$ and $P_H = 0.75$ on the total number of sorties flown 205

E.20 Effect of P_D and $P_{K_{Non}}$ with increasing $P_{K_{Ext}}$ and $P_H = 0.25$ on the total number of targets killed 205

E.21 Effect of P_D and $P_{K_{Non}}$ with increasing $P_{K_{Ext}}$ and $P_H = 0.5$ on the total number of targets killed 206

E.22 Effect of P_D and $P_{K_{Non}}$ with increasing $P_{K_{Ext}}$ and $P_H = 0.75$ on the total number of targets killed 206

E.23 Effect of P_D and $P_{K_{Non}}$ with increasing $P_{K_{Ext}}$ and $P_H = 0.5$ on the total operational cost 207

E.24 Effect of P_D and $P_{K_{Non}}$ with increasing $P_{K_{Ext}}$ and $P_H = 0.75$ on the total operational cost 207

E.25 Effect of P_D and $P_{K_{Non}}$ with increasing $P_{K_{Ext}}$ and $P_H = 0.25$ on the cost[$]/sortie 208

E.26 Effect of P_D and $P_{K_{Non}}$ with increasing $P_{K_{Ext}}$ and $P_H = 0.5$ on the cost[$]/sortie208

E.27 Effect of P_D and $P_{K_{Non}}$ with increasing $P_{K_{Ext}}$ and $P_H = 0.75$ on the cost[$]/sortie 209

E.28 Effect of P_D and $P_{K_{Non}}$ with increasing $P_{K_{Ext}}$ and $P_H = 0.25$ on the cost[$]/target 209

E.29 Effect of P_D and $P_{K_{Non}}$ with increasing $P_{K_{Ext}}$ and $P_H = 0.5$ on the cost[$]/target210

E.30 Effect of P_D and $P_{K_{Non}}$ with increasing $P_{K_{Ext}}$ and $P_H = 0.75$ on the cost[$]/target 210

E.31 Effect of aircraft defect arising rate, P_D and $MTTR_{Defect}$ on the total number of sorties flown with $P_{K_{Non}} = P_{K_{Ext}} = 0.00$ 211

E.32 Effect of aircraft defect arising rate, P_D and $MTTR_{Defect}$ on the total number of sorties flown with $P_{K_{Non}} = P_{K_{Ext}} = 0.25$ 211

E.33 Effect of aircraft defect arising rate, P_D and $MTTR_{Defect}$ on the total number of sorties flown with $P_{K_{Non}} = P_{K_{Ext}} = 0.50$ 212

E.34 Effect of aircraft defect arising rate, P_D and $MTTR_{Defect}$ on the total number of sorties flown with $P_{K_{Non}} = P_{K_{Ext}} = 0.75$ 212

E.35 Effect of aircraft defect arising rate, P_D and $MTTR_{Defect}$ on cost[$]/sortie with $P_{K_{Non}} = P_{K_{Ext}} = 0.25$ 213

E.36 Effect of aircraft defect arising rate, P_D and $MTTR_{Defect}$ on cost[$]/sortie with $P_{K_{Non}} = P_{K_{Ext}} = 0.50$ 213

E.37 Effect of aircraft defect arising rate, P_D and $MTTR_{Defect}$ on cost[$]/sortie with $P_{K_{Non}} = P_{K_{Ext}} = 0.75$ 214

E.38 Effect of aircraft defect arising rate, P_D and $MTTR_{Defect}$ on the total number of targets killed with $P_{K_{Non}} = P_{K_{Ext}} = 0.00$ 214

E.39 Effect of aircraft defect arising rate, P_D and $MTTR_{Defect}$ on the total number of targets killed with $P_{K_{Non}} = P_{K_{Ext}} = 0.25$ 215

E.40 Effect of aircraft defect arising rate, P_D and $MTTR_{Defect}$ on the total number of targets killed with $P_{K_{Non}} = P_{K_{Ext}} = 0.50$ 215

E.41 Effect of aircraft defect arising rate, P_D and $MTTR_{Defect}$ on the total number of targets killed with $P_{K_{Non}} = P_{K_{Ext}} = 0.75$ 216

E.42 Effect of aircraft defect arising rate, P_D and $MTTR_{Defect}$ on cost[$]/target with $P_{K_{Non}} = P_{K_{Ext}} = 0.00$ 216

E.43 Effect of aircraft defect arising rate, P_D and $MTTR_{Defect}$ on cost[$]/target with $P_{K_{Non}} = P_{K_{Ext}} = 0.25$ 217

E.44 Effect of aircraft defect arising rate, P_D and $MTTR_{Defect}$ on cost[$]/target with $P_{K_{Non}} = P_{K_{Ext}} = 0.50$ 217

E.45 Effect of aircraft defect arising rate, P_D and $MTTR_{Defect}$ on cost[$]/target with $P_{K_{Non}} = P_{K_{Ext}} = 0.75$ 218

E.46 Effect of aircraft defect arising rate, P_D and $MTTR_{Defect}$ on the total operational cost [$] with $P_{K_{Non}} = P_{K_{Ext}} = 0.00$ 219

E.47 Effect of aircraft defect arising rate, P_D and $MTTR_{Defect}$ on the total operational cost [$] with $P_{K_{Non}} = P_{K_{Ext}} = 0.25$ 219

E.48 Effect of aircraft defect arising rate, P_D and $MTTR_{Defect}$ on the total operational cost [$] with $P_{K_{Non}} = P_{K_{Ext}} = 0.50$ 220

E.49 Effect of aircraft defect arising rate, P_D and $MTTR_{Defect}$ on the total operational cost[$] with $P_{K_{Non}} = P_{K_{Ext}} = 0.75$ 220

E.50 Development of the possible minimum cost[$]/target solution by using the gradient-based method 221

E.51 Development of the possible minimum cost[$]/sortie solution by using the gradient-based method 222

E.52 Development of the possible maximum targets killed solution by using the gradient-based method 222

E.53 Development of the possible maximum sorties flown solution by using the gradient-based method 222

E.54 Improvement of minimum cost[$]/target solution populations optimised by the genetic algorithms 222

E.55 Improvement of minimum cost[$]/sortie solution populations optimised by the genetic algorithms 223

E.56 Improvement of maximum targets killed solution populations optimised by the genetic algorithms 223

E.57 Improvement of maximum sorties flown solution populations optimised by the genetic algorithms 224

F.1 Complete flow chart of mission effectiveness analysis application 226

F.2 Operation mission simulation application dialog 227

F.3 Monte Carlo Simulation Dialog 228

F.4 Simple numerical graphical result display 229

F.5 Simple line graph result display 230

F.6 Simple semi-animate graphical result display 230

F.7 Results from an operation simulation with manoeuvrability probability option 2 232

F.8 Data Management Dialog 233

F.9 Vulnerability Assessment Dialog 233

F.10 Lethal Radius Assessment Dialog 234

F.11 Semi-Automatic Grid Counter Dialog 235

F.12 Zooming and Moving Image Possibility 235

F.13 Susceptibility Assessment Dialog 236

F.14 Pre-Calculated Graph Display Dialog 237

F.15 Probability of Hit Assessment Tab Dialog 238

F.16 Reliability & Maintainability Assessment Dialog 239

F.17 Life Cycle Cost Estimation Dialog 240

Nomenclature

α_1, α_2	Leading and trailing fragment spray angles from the axis of the static warhead detonation [Degree]
δ_1, δ_2	Angle of leading and traling fragment spray [Degree]
γ	Constant value = 1.781072
λ	Radar wavelength [m]
μ_x, μ_y	Mean value of x and y
ϕ	Angle between incident wave and x axis of the target [Degree]
π	Constant value = 3.14159
Ψ	Elevation angle of the missile [Degree]
$\rho(x, y)$	Probability density function of miss distance
σ	Radar cross section [m^2]
σ_x, σ_y	Standard deviation of x and y
θ	Angle between incident wave and z axis of the target [Degree]
a, b, l	Dimension of geometrical object in cartesian coordinated system [m]
A_p	Presented area [m^2]
A_{v_i}	Vulnerable area [m^2]
Alt	Maximum altitude [m]
B_n	Noise bandwidth [Hz]
$C_{\overline{Operation}}$	Average operation & support cost per aircraft per flying hour [$]
$C_{Contract}$	Total contract cost [$]
$C_{Disposal}$	Disposal cost [$]
C_{FH}	Flying hour cost [$]
$C_{Flyaway}$	Flyaway cost [$]
C_{Fuel}	Total fuel cost [$]
$C_{GSE\&IS}$	Ground support equipment and initial spares cost
$C_{Install}$	Installation support funds [$]
$C_{Maintenance}$	Average operational maintenance cost per aircraft per flying hour [$]

$C_{Mission}$	Total operation & support cost for entire fleet during mission simulation [$]
$C_{Operation}$	Operation and Support Cost [$]
$C_{Personnel}$	Total personnel cost [$]
$C_{Production}$	Production Cost [$]
$C_{RDT\&E}$	Research, Development, Test, and Evaluation Cost [$]
C_{Sortie}	Sortie cost [$]
$C_{SuccessfulSortie}$	Successful sortie cost [$]
$C_{Sustain}$	Total sustaining support cost [$]
C_{Target}	Target cost ('Bang per Buck') [$]
$C_{Training}$	Service allowance, personnel support and training cost [$]
C_{Unit}	Unit level consumption cost [$]
C_{Weapon}	Weapon cost [$]
C_{Fuel}	Cost of fuel per litre [$]
$CD_{Airframe}$	Total cost of airframe development [$]
$CD_{Avionics}$	Total cost of avionics development
$CP_{Avionics}$	Total avionics production cost [$]
CP_{Engine}	Total cost of engine production [$]
DEF	Deflated rate factor
$DMHR(100)$	Highest aircraft's component defect man-hour rate [Hour/ 1000 flying hours]
$DMHR(70)$	Lowest aircraft's component defect man-hour rate [Hour/ 1000 flying hours]
DR	Defect rate [per 1000 flying hours]
E_i	Expected number of encounters by ith threat type
E_t	Threshold setting
FH	Aircraft flying hours [Hour]
FHY	The average annual flight time [Hour]
$FR(100)$	Highest aircraft component's failure rate per 1000 FH
$FR(70)$	Lowest aircraft component's failure rate per 1000 FH

FT	Effective temperature [K]
G	Gain of transmitting antenna
H	Aircraft height [m]
k	The Boltzmann's constant = $1.3806503 \times 10^{-23}$ $[J/degree]$
k_1	Constant = $2\pi/\lambda$
L	Loss factor
M	Mach number
$M_{A/C}$	Aircraft mission mass [kg]
$M_{Airframe}$	Airframe-only mass [kg]
M_{Fuel}	Aircraft fuel load [kg]
$MAT_{Composite}$	Percentage of composite materials in airframe
$MTBF$	Mean time between failure [Hour]
$MTTR$	Mean time to repair [Hour]
$MTTR(100)$	Highest aircraft's component mean time to repair [Hour]
N	Number of fragments in the warhead
n	Number of fragment hits on aircraft
N_E	Number of engines per aircraft
N_{FH}	Number of flying hour
N_{Kill}	Number of target kill
N_{LARGE}	Number of largest single buy from the program
N_{Lost}	Number of aircraft kill
$N_{Operation}$	Number of aircraft in operation
N_{PROD}	Number of production aircraft
$N_{RDT\&E}$	Number of test aircraft
N_{STAT}	Number of stationary test aircraft
$N_{Take-off}$	Number of take-off during the mission simulation
$N_{SuccessfulSorties}$	Number of successful sorties during the mission simulation
P	Power of the transmitter radar [Watt]
P_n	The false alarm probability

P_A, P_a	The probability of threat being active
$P_D, P_{D/A}$	The Probability of aircraft being detected
$P_{F/I}, P_{F/D}$	The probability that the proximity warhead fuses the aircraft
$P_{H/I}, P_{H/D}$	The probability that threat propagator hits the aircraft
$P_{I/L}, P_i$	The probability that the threat weapon intercepts the aircraft
$P_{L/D}, P_l$	The probability of threat weapon being launched
P_{View_i}	The Manoeuvrability Probability or Weighting Factor of i aircraft view in a specific flight phase, i = Front, Rear, Left, Right, Top, Bottom
P_H	The probability of being hit
$P_{K/H}$	The probability kill, given a hit
P_K	The kill probability
P_S	The survivability probability
$P_{K/F}$	The probability that aircraft is killed given fusing
R	Distance between antenna and aircraft [m]
RED	Economic discount rate [%]
$ROAC$	Packing density of the fuselage $[kg/m^3]$
s	Distance between detonation to the fragment spray [m]
S/N	The signal to noise ratio
SM	Total aircraft schedule maintenance [Man-hout per flying hour]
$SM_{2-Propulsion}$	Schedule maintenance for 2^{nd} line schedule engine inspection and maintenance [Man-hour per flying hour]
$SM_{Avionics}$	Schedule maintenance for 2^{nd} line avionics maintenance [Man-hour per flying hour]
$SM_{Post-Flight}$	Schedule maintenance for post-flight [Man-hour per flying hour]
$SM_{Pre-Flight}$	Schedule maintenance for pre-flight [Man-hour per flying hour]
$SM_{Propulsion}$	Schedule maintenance for 1^{st} line propulsion inspection and maintenance [Man-hour per flying hour]
$t_{Maintenance}$	Time in maintenance occurrence [Hour]
$T_{SL_{Max}}$	Uninstalled engine maximum thrust at sea level [N]
T_{Sortie}	Sortie time [Hour]
$Thrust$	Total thrust $[kN]$

TIF	Technology improvement factor
$TLIFE$	Operated aircraft life [Year]
$TT4$	Maximum turbine inlet temperature [^{o}R]
V_f	Average fragment speed respecting to a stationary warhead [m/s]
V_m	Missile speed [m/s]
V_t	Target (aircraft) horizontal speed when encountered by proximity warhead [m/s]
V_{Max}	Maximum true airspeed [m/s]
W_a	Aircraft wing area [m^2]
W_e	Aircraft empty weight [kg]
WV	Uninstalled avionics mass [lb]
x, y	Cartesian coordinate
$YR52$	Years from first flight year relative to 1952 [Years]
CDAE	Engineering cost for development airframe [$]
CDDS	Development support cost [$]
CDE	Engine development cost [$]
CDEF	Cost of engine fit for the development aircraft
CDFT	Flight test cost [$]
CDMME	Manufacturing material and equipment cost [$]
CDQL	Quality control cost [$]
CDV	Avionics development cost [$]
CDVF	Cost of the avionics fit for the development aircraft [$]
CEP	Circular Error Probable
CJA	Disposal advanced material cost [$]
CJM	Disposal labour effort cost [$]
CJMAT	Disposal composite material cost [$]
CJT	Disposal cost ['then-year' dollar]
CLE	Engineering rate [$/hour]
CLM	Manufacturing labour rate [$/hour]

CLT	Quality/tooling labour rate [$/hour]
COAC	Mechanical contract cost [$]
COCS	Supply contract cost [$]
CODLR	Depot level reparable cost [$]
COEC	Engine contract cost [$]
COF	Cost of Fuel, other petroleum, oil, and lubricants [$]
COM	Total operation personnel cost [$]
COMMAT	Maintenance material cost [$]
COMSS	Miscellaneous support supply cost [$]
COTAD	Temporary additional duty cost [$]
COUTRN	Transport cost [$]
COVC	Avionics contract cost [$]
CPAE	Production engineering cost for development airframe [$]
CPE	Engine production cost [$]
CPI	Consumer Price Index
CPMME	Manufacturing material and equipment cost [$]
CPQL	Quality control cost [$]
CPR	Average annual civilian payment [$]
CSASTT	Total service allowance, personnel support and training cost [$]
CSEK	Replacement support equipment and modification kit procurement cost [$]
CSEPCS	Enlisted permanent change station cost [$]
CSET	Enlisted training cost [$]
CSISF	Installation support funds [$]
CSM	Total support personnel cost [$]
CSOPCS	Officer permanent change station cost [$]
CSOT	Officer training cost [$]
CSSE	Sustaining engineering support cost [$]
CSST	Total sustaining support cost and installation support funds [$]

CSTF	Training fund [$]
DAR	Depot arrival rate [Hour]
EDML	Development manufacturing cost [$]
EDTP	Tooling cost [$]
EPML	Development manufacturing cost [$]
EPR	Average annual enlisted payment [$]
EPTP	Tooling cost [$]
ERM	Unit cost for an engine repair [$]
ERO	Unit cost for an engine overhaul [$]
FADT	Advanced design tool factor
FAMA	Advanced materials cost factor [$]
FATF	Advanced technology factor
FATT	Advanced technology testing factor
FCS	Flight control system
FLO	Low-observable features factor
FMOF	Crew-ratio
FPROR	Overhaul/repair ratio
FS	Security factor
GALib	Genetic Algorithm Library in C++ langauge
GSE&IS	Ground Support Equipment and Initial Spares
LCC	Life Cycle Cost [M$]
MOE	Measure of Effectiveness
MOEs	Measures of Effectiveness
MOP	Measure of Performance
MOPs	Measures of Performance
NOM	Total number of operation personnel
NOMC	Number of operation civilian
NOME	Number of operation enlisted
NOMO	Number of operation officer

NOMOF	Number of active flight-crew member
NPART	Number of partners
NSMC	Number of support civilian
NSME	Number of support enlisted personnel
NSMO	Number of support office
O&S	Operation and Support
OPR	Average annual officer payment [$]
RAF	Royal Air Force
RATE	Production rate during manufacture [/month]
RBD	Reliability Block Diagram
UAV	Unmanned Air Vehicle
YRACC	Accounting year

CHAPTER 1

INTRODUCTION

Since end of the cold war, military budgets have been dramatically reduced; however, new aircraft are still required to replace the old ones. To fulfil all possible military requirements with few aircraft types, a new generation of combat aircraft is being developed. These aircraft will be multi-role and also be more operationally and cost-effective. Thus, more efficient design in the early stage which considers most possible design aspects has to be done (see Fig.1.1).

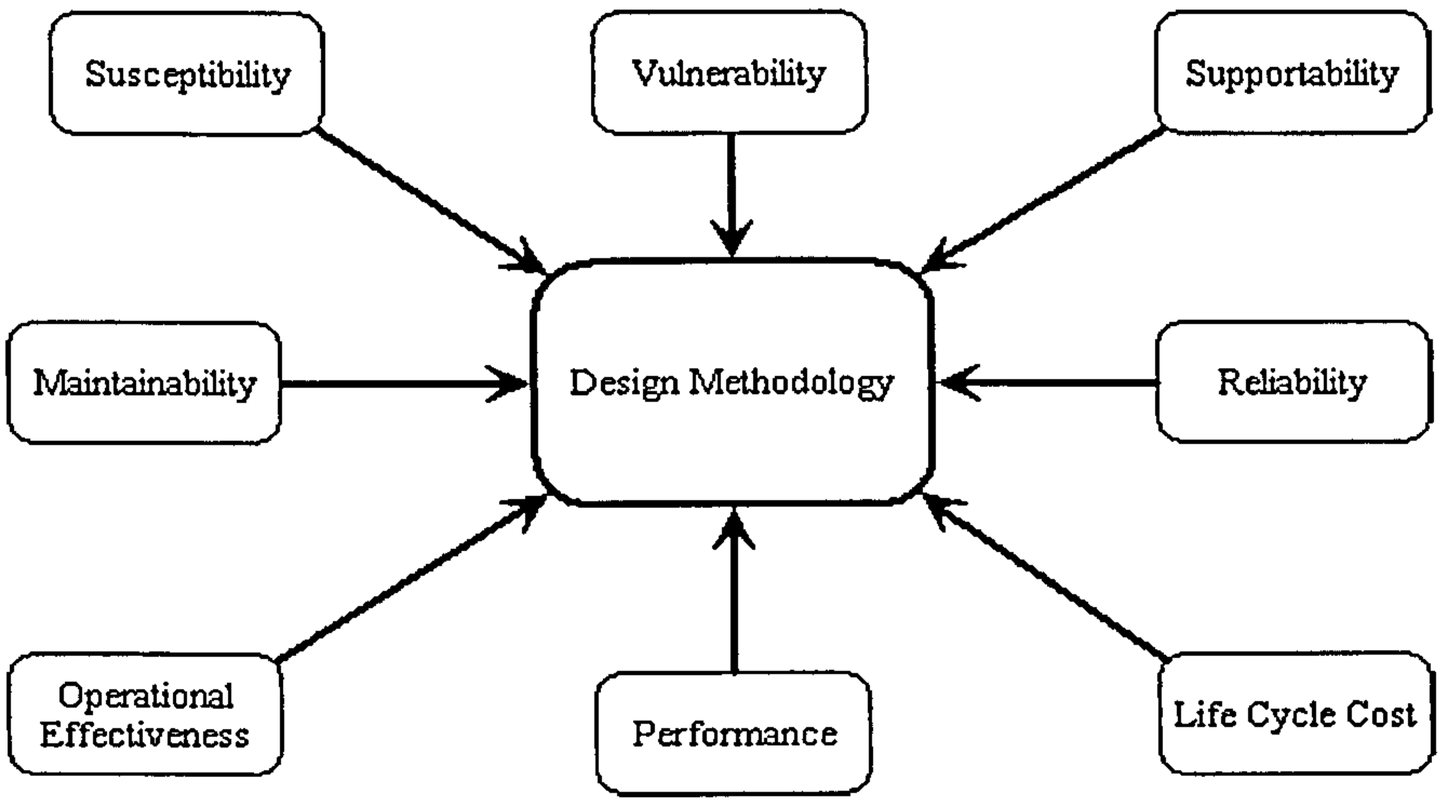

Figure 1.1: Aircraft design aspects

Some of these aspects have been developed and integrated into either the conceptual or preliminary design processes [1,38]; such as Reliability & Maintainability (R&M); Supportability; Survivability and Life Cycle Cost (LCC). Some previous works have been also developed methodologies, designed to integrate models of aircraft component effectiveness and life cycle costs into either the conceptual or preliminary design processes [2,28,44,54]. Due to restricted subject such the survivability, some developed methodology or assessment model cannot be published in details [23]. Nevertheless, all published previous works took only one design aspect into account. One such methodology integrates operation simulation and cost estimation into the early design process at the same time as the other design disciplines will be described in this thesis.

This research aimed to develop a combat aircraft design methodology for operational and cost-effectiveness mainly by considering the survivability, reliability & maintainability, and life cycle cost. An approach to achieve this research objective is to develop a software application using as a tool to measure the aircraft measures of performance and also to measure the aircraft operational and operational cost measures of effectiveness.

To measure an aircraft performance for specific design aspect and integration all together with the mission simulation to measure aircraft operational and operational cost effectiveness, the assessment methodologies for the specific design aspects have to be developed. An application with several pop-up dialog is programmed by using Microsoft Develop Studio C++ as a compiler. This compiler offers graphic display, drag & drop features, and also object oriented capacity. The main application name is 'Mission Effectiveness Analysis'.

To measure an aircraft operational effectiveness in the forms of the total number of specific sorties, targets, and aircraft, the mission simulation has to be integrated within the methodology. By using the reliability bock diagram in conjunction with the event tree diagram, these operational measures of effectiveness in the required format can be determined.

The aircraft life cycle cost estimation model used for this research is based on previous work. With some validations, in some variables and sub-models, an aircraft life cycle cost during both peacetime and wartime scenarios can be predicted. Through this cost, the operational cost for an entire fleet in one base can be predicted. Together with the weapons released expense and aircraft lost cost, which are calculated directly from the mission simulation, the total operational cost for an entire mission operation can be thus evaluated.

By combination of all sub-modules with the mission simulation, the operational and operational cost measures of effectiveness can be predicted. Used in conjunction with the Monte Carlo simulation technique, this gives more accurate predicted values.

Two different optimisation methods have also been integrated within this methodology to search for the optimum solution for combat aircraft operational and cost-effectiveness.

The Cranfield Unmanned Air Vehicle (U-99), which has been designed by MSc Students at Cranfield University, has been chosen as a case study because of the design performance requirements and data availability.

The results from the optimisation can firstly be used as an indication to design the U-99 for operational and/or operational cost effectiveness.

Additionally, by using the developed tool, trade-offs between aircraft measures of performance can be perform to achieve or improve the objective values.

CHAPTER 2

DESIGN METHODOLOGY FOR AIRCRAFT OPERATIONAL AND COST-EFFECTIVENESS

In this chapter, three different design methodologies are described. The first two methods, developed and demonstrated by Raymer [36], Roskam [37] and Soban [42–44], use different concepts of aircraft definition. The third methodology is a combination of the first two methodologies, which also gives an opportunity to integrate several design aspects and an operation simulation early into the design process [16,17,32]. This makes the third design methodology, therefore, wider-ranging in that it assesses operationally and cost-effectiveness.

2.1 Conventional Aircraft Design Methodology

This design methodology is commonly used as the fundamental process of aircraft design in aeronautical engineering. An aircraft is defined as an object throughout the design methodology. Three stages of aircraft design have been identified with different levels of detail, i.e. conceptual design, preliminary design, and detail design [36,37].

Figure 2.1 shows that before the first design process can begin, the aircraft fundamental requirements and performance have to be defined. These requirements come mostly from the customer; for example the government in the case of combat aircraft, and the airline company in the case of commercial aircraft. Sometimes these requirements may be modified during the design processes due to new customer specifications, updates of technologies or decreases in budget. Thus, the design process has to be repeated. It leads to increased expense and time consumption.

2.1.1 Conceptual Design

A combat aircraft conceptual design usually begins with a specific set of design requirements, established by the prospective customer, rather than a company-generated guess as to what future customers may need. These design requirements include parameters such as aircraft range and payload, take off and landing distance, manoeuvrability and

speed requirements, and so on. With these specifications, the first conceptual sketch of the entire aircraft, and some major components and systems can be characterised. Therefore, all fundamental design parameters and variables can be estimated. The first look at cost and manufacturing is also made at this time.

An initial layout is analysed to determine if it really will perform the required mission. Predicted aerodynamics, weights, and installed propulsion characteristics are also analysed, and subsequently used to do detailed sizing calculations. Furthermore, the performance capabities of the design are calculated and compared to the requirements. The details of the configuration are therefore, subject to change. All of this work will be done on paper, or on a computer.

2.1.2 Preliminary Design

Before this design stage can start, most of the major aspects of the conceptual design have to be finalished, and also the configuration has to be frozen. Thus, the specialist in particular areas will design and analyse their own portion of the aircraft. Testing is initiated in areas such as aerodynamics, propulsion, structures, and stability and control.

Lofting, which is the mathematical modelling of the outside skin of the aircraft with sufficient accuracy to insure proper fit between its different parts, is performed in this design process. The objective of this design stage is to ready the company for the detail design stage, also called full-scale development, and also to establish confidence that the aircraft can be built on time and at the estimated cost.

2.1.3 Detail Design

This detail design begins with the actual pieces to be fabricated being designed. For example, during conceptual and preliminary design the wing box will be designed and analysed as a whole. During the detail design, that whole will be broken down into individual ribs, spars, and skins, each of which must be separately designed and analysed. This design stage also includes production design. Specialists determine how the aircraft will be fabricated, starting with the smallest and simplest subassemblies and building up to the final assembly process.

During the detail design, the testing effort intensifies. The actual structure of the aircraft is fabricated and tested. Control laws for the flight control system are tested, and a detailed working model of the actuators and flight control surfaces is produced. This

design stage ends with the fabrication of the aircraft.

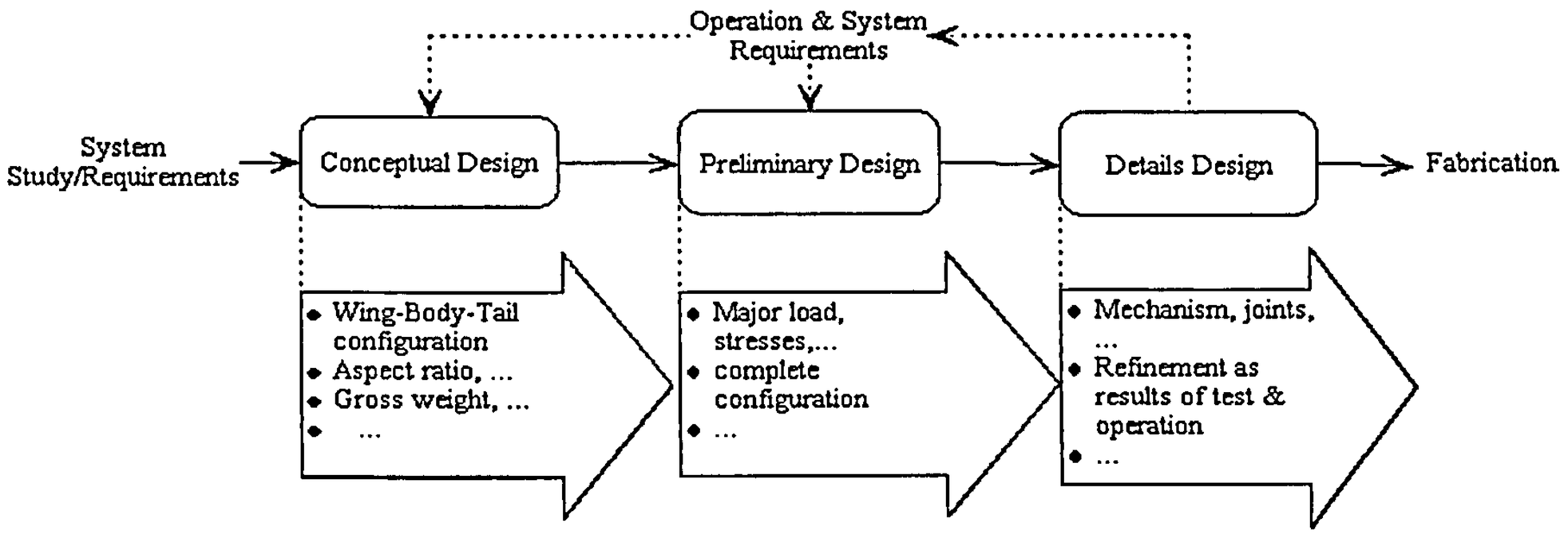

Figure 2.1: Conventional Design Methodology

2.2 System of Systems Design Methodology

Soban [43] presented an alterative design methodology, "system of systems", which integrates survivability assessment into an aircraft design process. This method can show the effect of this design aspect during the preliminary design process, earlier than in the conventional design methodology. This allows for sufficient trade-offs and resource allocations to be made by measuring the effectiveness of the aircraft at a high level of design, i.e. theatre or campaign level. The theatre level is the highest of three levels in this design methodology (see Fig. 2.2). In using this method, an aircraft is treated as a sub-system of the overall system, which represents an operation or campaign. Various aspects of each system are measured to indicate their qualities, which are dependent on the system's level. The measures of each level are in the forms of Measure of Performance (MOP) or Measure of Effectiveness (MOE), which have been described more detail in section 2.3.3. Similar models have also been studied and presented by Simkins [39] and by Kitowski [28].

The following are some examples for classifications of system level:

- Vehicle level: An aircraft A is more likely to be detected.
- Mission level: Number of aircraft available at the end of a sortie
- Theatre level: Total number of targets destroyed

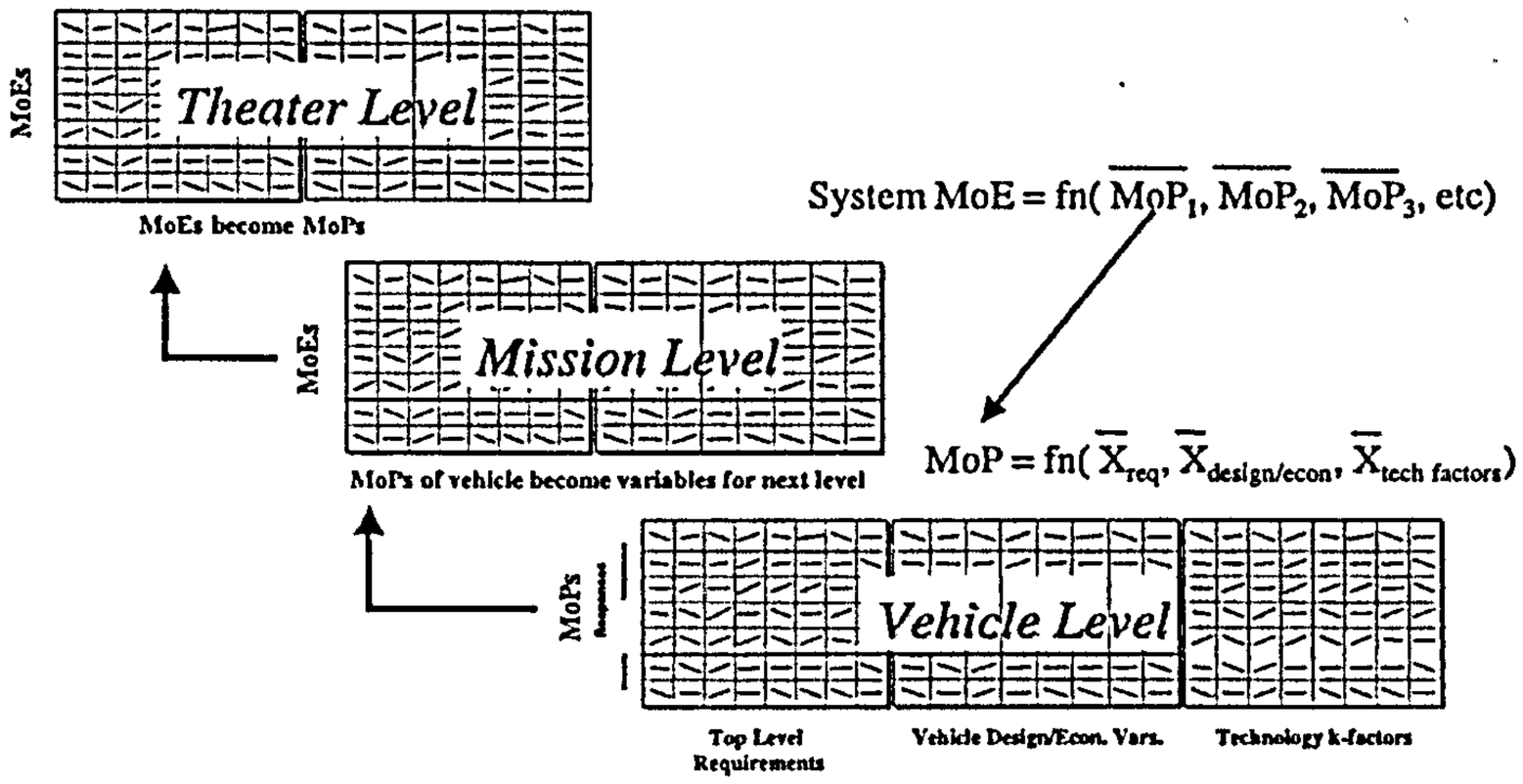

Figure 2.2: System of systems design methodology [43]

2.2.1 Vehicle Level of Design

In this level of design, only an aircraft is defined as a system. With its Measures of Performance (MOPs) in major design aspects, the "goodness" of the aircraft in these design points of view can be indicated in the form of probability values. These values are only functions of the aircraft design variables and parameters. For example, an aircraft geometric dimension is used to calculate its probability of detection, which indicates how easily the aircraft can be detected.

As an output of vehicle level of design, aircraft MOPs can be passed to the mission level of design to measure the aircraft mission effectiveness.

2.2.2 Mission Level of Design

The objective function of this level of design is to link the vehicle level to the theatre level of design. Mission level of design is required because the outputs from the vehicle level of design are in the form of aircraft MOPs, and they do not usually map directly to be used as the inputs to theatre level of design. The inputs to theatre level of design are in the form of aircraft Measures of Effectiveness (MOEs). Therefore, the MOPs of vehicle level are transformed to be variables in mission level of design.

A short time-scale of operation model; such as sortie or operational day, is defined as a system, in which an aircraft is referred to as a sub-system. The MOPs of the aircraft are used to measure the aircraft effectiveness at the mission level of design. For instance, an attack flight phase in a sortie during the entire operation is defined as a system. One

of the aircraft MOEs in the mission level of design is the aircraft probability of success in this flight phase, which is a function of the aircraft MOPs in several different design aspects, such as probability of detection, probability of kill, and probability of encounter by a different threat.

Therefore, the output of the mission level of design is in the form of aircraft MOEs, and will be treated as mission MOPs for the theatre level of design.

2.2.3 Theatre Level of Design

Finally, the theatre becomes the system, and the aircraft and short time-scale operation (sortie or operational day) are relegated to be components of this new system. The theatre thus becomes a system of systems and is a function of the vehicle and mission levels of design. Therefore, the theatre level of design is a function of the components of the vehicle and mission levels of design, including aircraft and sorties. In other words, mission MOEs from the mission level of design become mission MOPs and are input variables for the theatre level of design.

The campaign MOEs at the theatre level of design are used as a measure of the aircraft "goodness" for the entire campaign. Tradeoffs can thus be made between vehicle design and mission requirements in the lower levels of design. These requirements, when optimised to fulfill theatre level goals and objectives, become the requirements to which the vehicle is then designed.

2.3 Design Methodology for Operational and Cost-Effectiveness

2.3.1 Aims & Development of Methodology

The design methodology aimed to combine conventional design and "system of systems" design methods. This was to be achieved by integrating operation simulation, survivability assessment, reliability & maintainability assessment and life cycle cost estimation into a methodology for use in the conceptual and preliminary design stages (see Fig. 2.3). The aim was to measure aircraft operational and operational cost effectiveness as a function of aircraft MOPs in several design aspects, such as survivability, reliability, and operational cost. The final aim was to facilitate tradeoffs between aircraft MOPs using an optimiser to fulfill the main theatre objective functions, such as maximum number of sorties flown,

maximum number of targets destroyed, sortie cost, target cost, and so on.

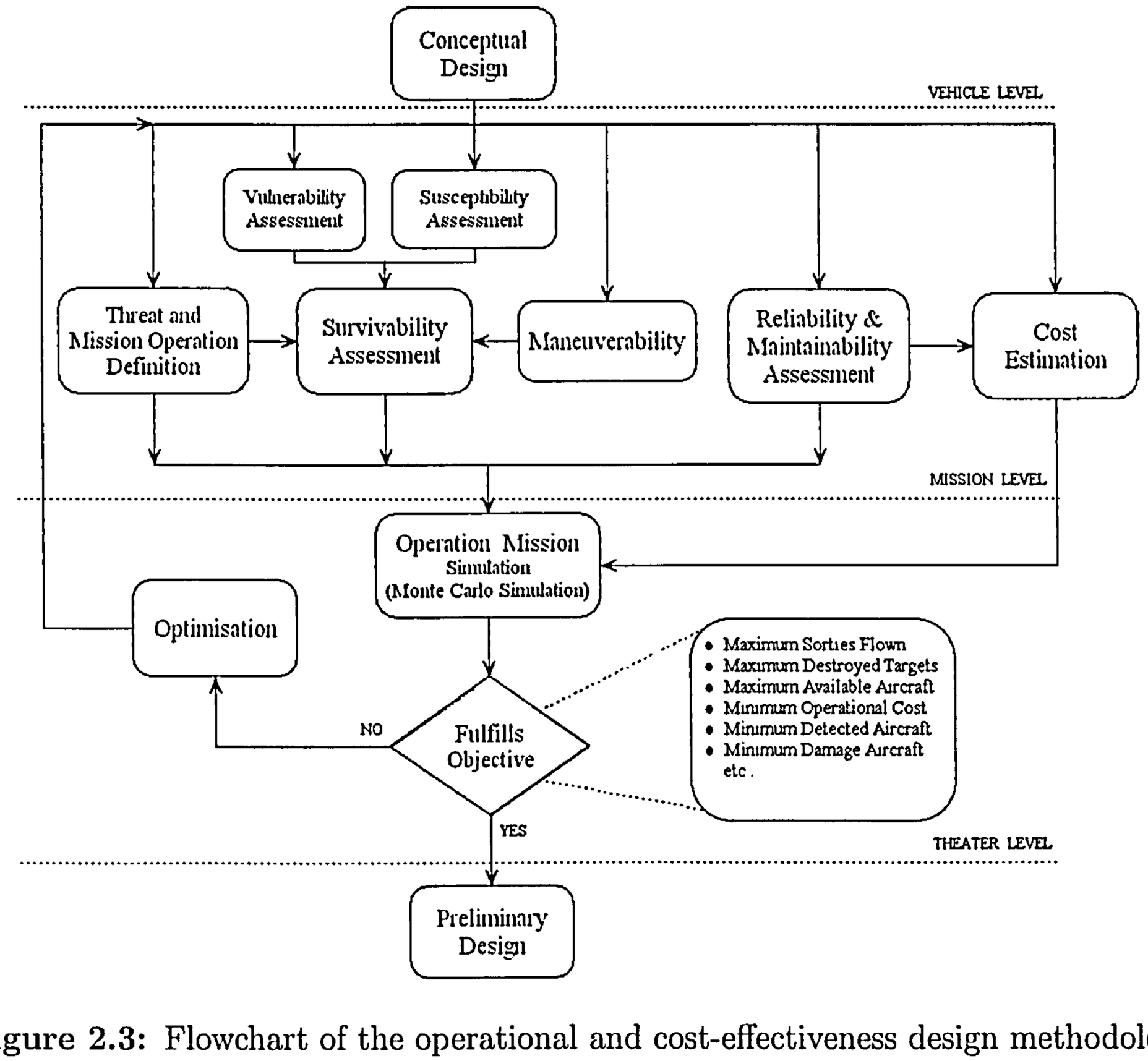

Figure 2.3: Flowchart of the operational and cost-effectiveness design methodology

The aircraft performance aspects of this methodology was to be firstly measured in three main design aspects, i.e. survivability, reliability & maintainability, and operation cost. Integration of an operation simulation, tradeoffs between aircraft MOPs in these design aspects should be be executed directly after the conceptual design. With results of optimised aircraft MOPs in these three design aspects, the operational and cost-effectiveness aircraft design parameters and variables should then be calculated. These include most of the aircraft design parameters, aircraft performance, sketchy aircraft geometry, and major internal critical components or systems layout. Examples of these are wing area, aircraft empty weight, aircraft height, maximum altitude, and so on. The results of these evaluations will be subsequently fed into more detailed design processes; i.e. preliminary and detail design.

Within the operational and cost-effectiveness design methodology, the aircraft MOPs in all the design aspects below are predicted directly from aircraft conceptual design

parameters and variables at the vehicle level of design, considering only aircraft hardware. These MOPs are indicative of the quality in each design aspect the aircraft has.

The application namely 'Mission Effectiveness Analysis' has been implemented based on the flow chart, as illustrated in Fig. 2.3. This application comprises several pop-up dialogs, which represent each design aspect studied in this research . The purpose of this application is to transform the aircraft design variable into aircraft MOPs, aircraft operational and operational cost MOEs (details and rough user manual, see Appendix F). Table 2.1 shows an example of the transformation from aircraft design parameter into aircraft MOPs for specific design aspect.

Table 2.1: Example of transformation from aircraft design parameter into aircraft MOPs for specific design aspect

Design Aspect	Design parameters (Inputs)	Measures of performance (Outputs)
Susceptibility	external geometry, and presented areas	$P_D, P_{F/I} or P_{H/I}$
Vulnerability	critical internal components and systems, external presented areas	$P_{K/H}$
Reliability	Height, Empty weight, Altitude, Thrust, Wing areas, Number of engine	Defect arising rate per 1000 flying hours
Maintainability	Empty weight, Altitude, Height, Thrust, Wing areas, Number of engine	DMHR, Scheduled maintenance
Manoeuvrability	-	Weighting factor

One of the greatest difficulties in developing this methodology was the security and commercial restrictions placed upon the data required. Another difficulty was the complexity of the assessment required for the design aspects involved, such as probability of kill/hit of aircraft critical components, mean time to repair, and avionics development costs. The result of this complexity was that either the assessment could not be performed, or the timescales involved would be too long. Some constraints and assumptions, therefore, had to be made in this methodology, as shown in later chapters and appendices.

The transformation methods from conceptual design parameters to Measures of Performance (MOPs) value in survivability design are described in chapter 3. These include susceptibility and vulnerability. The MOPs in reliability & maintainability are described in chapter 4. The functionality of the survivability, reliability & maintainability, and life cycle cost modules are explained in chapter 6. These are used to measure aircraft

operational and cost-effectiveness.

One approach to measure mission effectiveness was to use a Reliability Block Diagram (RBD) in conjunction with an event tree diagram to combine many aircraft probability values together (aircraft MOPs). This could give probability values in each flight phase during a sortie (mission MOPs). The calculation and methods used are described in chapter 6.

2.3.2 Campaign Definition

This methodology was designed to show how operationally effective a new design of combat aircraft will be, by measuring its operational effectiveness at the theatre level. In other words, the designed aircraft will be examined for its operational requirements in computational simulation early during the design process. For example, the number of aircraft lost in ten days of operation, exposed to high levels of opponent's defenses, can be directly estimated after the first conceptual design. Therefore, an operational simulation of the aircraft mission requirements has to be established early and then merged into the design process. Additionally, some design aspect assessments refer directly to campaign definition. For example, an opponent's defensive systems affect the aircraft MOPs and MOEs in terms of vulnerability.

An entire campaign includes both friendly and foe armaments, defenses, capabilities, campaign duration, and so on. Therefore, it is not very easy to obtain this information at the early design stage. Additionally, it is too complex to simulate and also it is not necessary to consider all details. So, some constraints and assumptions have thus been made (for details, see Chapter 6).

2.3.3 Aircraft Measures of Performance and Effectiveness

Through this methodology, the aircraft design variables and parameters become aircraft MOPs for several design aspects through survivability assessment, reliability & maintainability assessment, and life cycle cost estimation sub-modules. This section introduces principles by which these variables and parameters are transformed into aircraft MOPs for major design aspects.

2.3.3.1 Measurement of Survivability

The aircraft MOP in the case of survivability design is a probability value of aircraft survival, which is a function of two other aircraft MOPs, i.e. probability of aircraft being hit (susceptibility) and probability of aircraft being killed by a given hit (vulnerability). Both aircraft MOPs, which are outputs of the vehicle level of design, are functions of fundamental aircraft design parameters and variables. With an integration of threat analysis and aircraft manoeuvrability at the mission level of design, the aircraft Measure of Effectiveness (MOE) for survivability design can be evaluated.

$$MOE_{Survivability} = f(MOP_{Susceptibility}, MOP_{Vulnerability}, MOP_{Manoeuvrability}, \ldots)$$

In other words, the aircraft MOE for survivability design integrates an ordinary aircraft MOP for survivability (P_s), and the aircraft MOP for manoeuvrability (Weighting Factors). Aircraft manoeuvrability is simply represented in this study as a weighting factor (for details, see chapter 3 and Fig. 3.13).

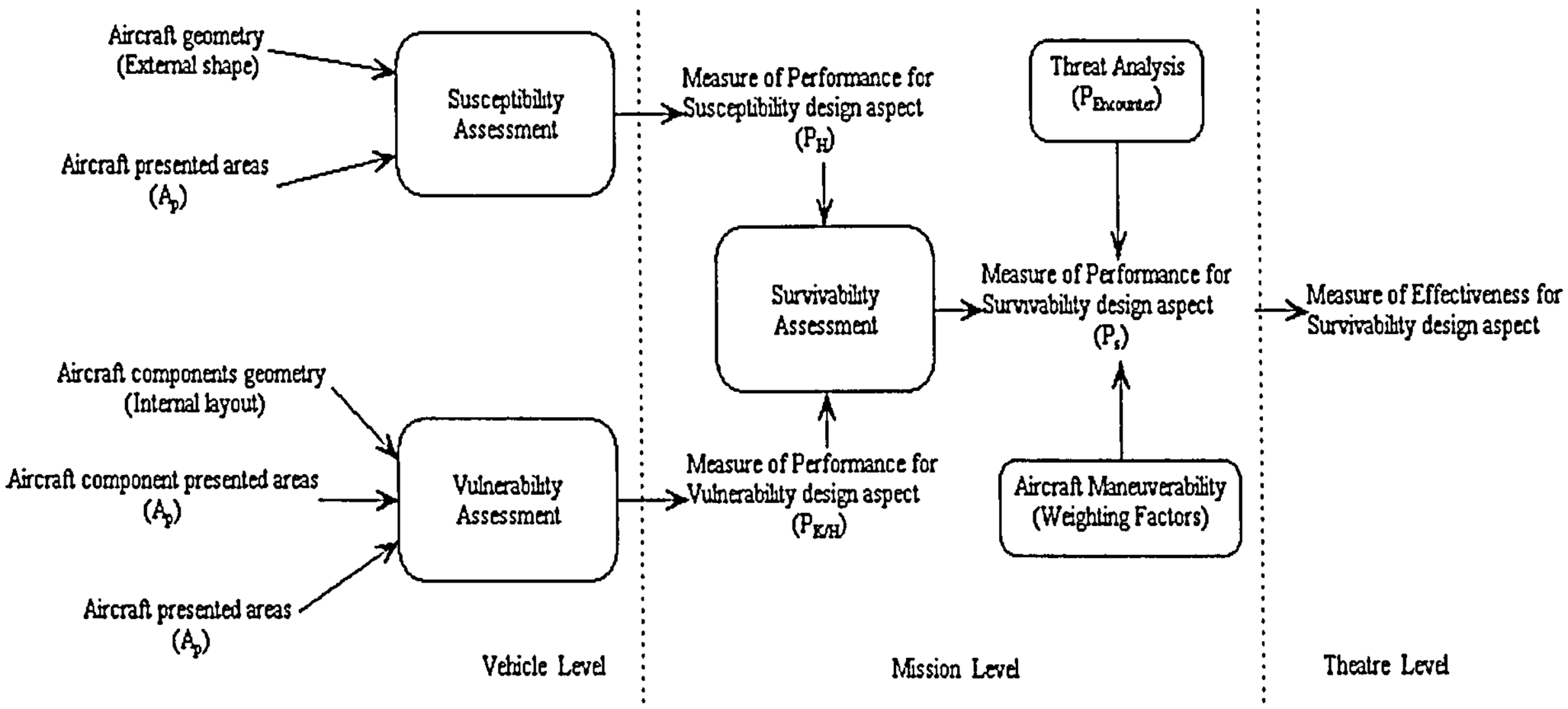

Figure 2.4: Aircraft Measures of Performance and Effectiveness for Survivability

2.3.3.1.1 Measurement of Susceptibility

The aircraft MOP for susceptibility can be represented as the probability of being hit (P_H), which is mainly a function of another two aircraft MOPs, i.e. the probability of detection (P_D) and conditional probability of hit ($P_{H/I}$ or $P_{F/I}$).

The first aircraft MOP is the probability of detection (P_D), which measures how easily an aircraft is detected by the opponent searching systems during the campaign. This

measure is mainly a function of aircraft signatures. Ball [6] introduced three major aircraft signatures with different characteristics and assessment methods; i.e. radar, infrared, and visual signatures. Due to major threat types dominated in this study, the radar signature in the form of radar cross section (σ) had been chosen to evaluate an aircraft probability of detection (for details, see Section 3.1.2).

On the other hand, the second aircraft MOP, the conditional probability of hit ($P_{H/I}$ or $P_{F/I}$), measures how likely the possibility is that the aircraft will be hit by threats. This measure mainly depends on threat type (penetrator or external explosive) and specific aircraft presented areas (for details, see Section 3.1.3).

2.3.3.1.2 Measurement of Vulnerability

The aircraft MOP for vulnerability can be expressed as the probability of a kill by a given hit ($P_{K/H}$). This value is a function of three aspects related to aircraft critical components, namely; system presented areas, layout, and probability of a kill by a given hit (for details, see Section 3.2).

The aircraft MOP for survivability from vehicle level of design refers directly to the aircraft itself, but the mission MOP (or aircraft MOE) for survivability, from the mission level of design refers to the nature of the environment in which the aircraft operates, and aircraft behaviour during short-timescale operations (See Fig. 2.4).

2.3.3.2 Measurement of Reliability

For this design aspect, an aircraft failure rate can represent one of aircraft MOPs, by characterising how reliable aircraft are per 1000 flying hours. This value is a function of several conceptual design parameters and variables, such as maximum empty weight, aircraft height, maximum altitude and so on. Details of MOE in reliability and reliability assessment methodology are described in Chapter 4.

In mission level of design, aircraft MOP for reliability is one of the main direct effects on aircraft MOE. For example, the aircraft operational defect arising rate, which is defined as 10% of failure rate per flying hour, results in a direct impact on the probability of successful flight phase, probability of aircraft availability for next sortie, and so on.

2.3.3.3 Measurement of Maintainability

There are numerous alternatives which represent aircraft MOPs for maintainability at the vehicle level of design. Two of these are Defect Man-Hour Rate per 1000 flying hour (DMHR) and Scheduled Maintenance (SM). The first value, DMHR, indicates how many man-hours of maintenance the aircraft requires during 1000 flying hours. The second aircraft MOP for maintainability shows how regularly the aircraft has to be inspected, components replaced, and also repaired.

At the vehicle level of design, for this methodology, these two values have their own measurement methods (see Section 4.2). However, both values are used at the mission level of design to measure aircraft effectiveness in terms of operational cost per flying hour (for details, see Chapter 5).

2.3.3.4 Measurement of Manoeuvrability

Several forms of aircraft MOP can represent aircraft ability to manoeuvre during a mission. One of these aircraft manoeuvrability-performance measures is predicted using a weighting factor to indicate an average percentage of aircraft visible to the threat in each mission flight phase. This MOP shows how quickly an aircraft changes its flight characteristics in each flight phase, and thus its manoeuvrability.

2.3.4 Measures of Operational Effectiveness

Before aircraft operational effectiveness at the campaign level can be measured, the aircraft effectiveness in a short operation timescale, or at a mission level of design, first has to be evaluated. These aircraft MOEs are functions of aircraft MOPs and campaign definition.

In other words, at the theatre level of design, aircraft MOEs become mission MOPs, and are used as variables to measure operational effectiveness, through utilising a RBD. In this way, aircraft MOPs become indirect variables for operational MOEs; therefore, an aircraft can be measured for operational effectiveness.

It is very hard to give a general definition of operational effectiveness, because it depends on overall mission, campaign, and organisation of operations. Table 2.2 shows examples of MOPs and MOEs at all three levels.

Table 2.2: Example List of Measures of Performance and Effectiveness

Measure of Performance (Vehicle level)	Measure of Effectiveness (Mission level)	Measure of Effectiveness (Theatre level)
Probability of detection	Probability of successful flight phase	Number of sorties flown
Probability of kill/hit	Probability of survival of aircraft	Number of killed aircraft
Weighting factors	Probability of target destruction	Number of destroyed targets
Defect man-hour rate	Probability of aircraft being in maintenance	Number of aircraft in maintenance
Defect arising rate	Probability of availability of aircraft for next sortie	Number of available aircraft

2.3.5 Measures of Cost-Effectiveness

This methodology also aims to measure operational cost-effectiveness, which can help to integrate the best design alternatives [48] into an early design stage. However, the exact spend during real missions cannot easily be estimated. One possibility is to evaluate the operational cost through the Life Cycle Cost (LCC) at the vehicle level of design. Operational cost-effectiveness together with operational MOEs can be measured at the theatre level of design; for instance, sortie cost, weapon cost, aircraft loss cost. This method has been used here, and is presented in chapter 5.

Finally, measures of both operational and cost-effectiveness can be evaluated together at the theatre level of design. This activity completed the development of the overall methodology.

Table 2.3 shows the aircraft measures of both operational and cost-effectiveness at the theatre level of design.

Table 2.3: Measure of Effectiveness at the theatre level of design

Operational Effectiveness	Cost-Effectiveness	Operational and cost-effectiveness
Total number of sorties flown	Total operation cost	Operation cost per sortie
Total number of destroyed targets	Total weapon cost	Cost per destroyed target
Total number of available aircraft	Total aircraft lost cost	

2.4 Chapter Summary

This chapter has:

- introduced a "system of systems" design methodology, which has defined an aircraft as a subsystem of the overall system, namely the campaign [44].

- shown a newly developed design methodology for operational and cost effectiveness, by merging the conventional design methodology and the "system of systems" design methodology. together with cost-effectiveness measures.

- clarified aircraft MOPs, and MOEs in terms of susceptibility, vulnerability, survivability, reliability, maintainability, manoeuvrability, and cost.

- shown how missions and campaigns can be measured for operational and cost-effectiveness.

- explained relationships between aircraft MOPs, aircraft MOEs, mission MOEs, and campaign MOEs, in selected design aspects.

CHAPTER 3

SURVIVABILITY ASSESSMENT

This design aspect is one of the most important for combat aircraft design. An important issue is that most of the data and also the assessment methods are often military classified. Therefore, simple models for predicting a survivability probability value have been developed and introduced. This gives an opportunity to adequately evaluate aircraft MOP in survivability during conceptual design.

Aircraft combat survivability is defined as capability to avoid and/or withstand a man-made hostile environment. Firstly, the capacity to avoid guns, missiles, radars and all of the other elements of opponent's defense that make up the man-made hostile mission environment is referred to as the susceptibility. On the the other hand, the aircraft inability to withstand the man-made hostile environment is referred to as the vulnerability [6].

Aircraft survivability can be measured by the parameter, called the probability of survival (P_S), which in turn is related to the probability of kill (P_K). The probability of kill is the product of two survivability concepts: susceptibility (P_H) and vulnerability ($P_{K/H}$). Hence the survivability probability can be determined as:

$$P_S = 1 - P_K = 1 - P_H P_{K/H} \tag{3.1}$$

In this chapter, the main concepts and models to evaluate aircraft survivability will be explaining; the rest of the theory and models, including results are described and illustrated in Appendix B.

3.1 Susceptibility Assessment

Susceptibility is the probability that the aircraft will be detected and be hit. This value is a function of those things that would make the aircraft more difficult to be seen and tracked, such as stealth, manoeuvrability, tactics, and avionics. The probability of hit (P_H) can be divided into five categories with conditional probabilities as follows:

- The probability of the threat being active when the aircraft arrives (P_A)

- The probability of the aircraft being detected, given the threat is active ($P_{D/A}$)
- The probability of the threat weapon being launched, given the threat is active and detects the aircraft ($P_{L/D}$)
- The probability that the threat weapon intercepts the aircraft, given that the threat propagator was launched ($P_{I/L}$)
- The probability that the threat propagator hits the aircraft or the proximity warhead fuses, given the propagator intercepts the aircraft. This is called the conditional probability of hit ($P_{H/I}$ or $P_{F/I}$).

In the operational and cost-effectiveness design methodology, the susceptibility assessment has the function of transforming aircraft design parameters and/or variables into aircraft MOP for susceptibility at the vehicle level of design; which means only $P_{D/A}$, $P_{F/I}$, and $P_{H/I}$ are measured directly from the susceptibility assessment. The rest of the conditional probabilities can be defined as the opponent weapons, which are input into the campaign definition for this methodology. Therefore, subscripts of these probabilities have been redefied to indicate their source. This is done by using lowercase letters for probabilities valued by the campaign definition (P_a, P_l, P_i), and using uppercase letters for probabilities valued by susceptibility assessment ($P_D, P_{H/D}, P_{F/D}$). The probability of hit can be thus split into two groups and be calculated as follows:

$$\begin{aligned} P_H &= P_A P_{D/A} P_{L/D} P_{I/L} (P_{H/I} \text{ or } P_{F/I}) \\ &= \{(P_{H/D} \text{ or } P_{F/D}) P_D\}_{Susceptibility} \{P_a P_l P_i\}_{Campaign} \end{aligned} \tag{3.2}$$

In this chapter, only the probability values evaluated by the susceptibility module will be described. Aircraft signature is one of the susceptibility assessment results, which leads to the calculation of the probability of detection, P_D. An aircraft has many different kinds of signature, such as the radar signature, the infrared signature, visual and the aural signatures. All of the signatures, except for the aural signature, are electromagnetic in origin. Due to the wide-ranging disciplines to be integrated into this design methodology, only the radar signature has been chosen to evaluate the probability of detection. This is because this kind of aircraft signature can be detected from a great distance, and although radar is only one of several sensors that is considered in design of a low-observable platform [27]. It is the dominant one.

3.1.1 Radar Cross Section

Hovanessian [24] has defined the Radar Cross Section (RCS) of a target as an equivalent area producing the same amount of energy returned to the radar as would be produced by target scatterer. The RCS of a target can represent the size of the target as well as the geometric shape and discontinuities, such as corners.

Radar Cross Section is then defined as a measurement value used to estimate the size of the aircraft signature (σ) by using the combination of transmitting and receiving radar signals. The RCS depends strongly upon the direction from which the signal arrives, the direction of the receiving antenna, and the size and shape of the object. The total cross section of a complex object can be computed by an assembly of simpler shapes and by a number of techniques of differing levels of complexity [9].

The scattering characteristics of a target are strongly dependent upon the frequency of the incident wave. At high-frequency regions, called the optical region, all dimensions of the target are large compared to the wavelength, and thus the cross section can be approximated by the theory of geometrical or ray optics and of physical or wave optics [5]. Additionally, most long-range ballistic missile defense radars operate with frequencies greater than 1 GHz (L band and above); therefore, simple shapes cross section approximation models are used in this region.

This methodology aims to integrate susceptibility assessment into an early design stage to measure the aircraft performance in this design aspect. To calculate the exact RCS, requires more details of aircraft design, complex calculation, and consideration of the Radar Absorbing Material (RAM), which has been used in most of new generation of combat aircraft; such design details are not available at the early design stage. They have modest levels of accuracy, but can not be consistently for accurate comparison of alternative configurations; therefore, some complex shape will be neglected; such as cavity and joint edges. The following approximate predictions for simple shape cross section are thus adequate for this methodology.

3.1.1.1 Sphere Cross Section

Spheres have a symmetrical shape, therefore their radar cross section is obviously independent of aspect angle. For this reason spherical shapes can be used as a standard target without concern for their exact orientation with respect to the radar. Also, if it

is in motion, its cross section will not fluctuate with change of aspect. The sphere cross section can be approximately calculated as:

$$\sigma = \pi a^2 \tag{3.3}$$

where a is a radius of the sphere.

3.1.1.2 Rectangular Flat Plate

To predict radar cross section of a flat plate is not easy due to the unsymmetrical shape. However, Blake [9] divided flat plate cross section calculation into two categories; large plane surface and general rectangular flat plate.

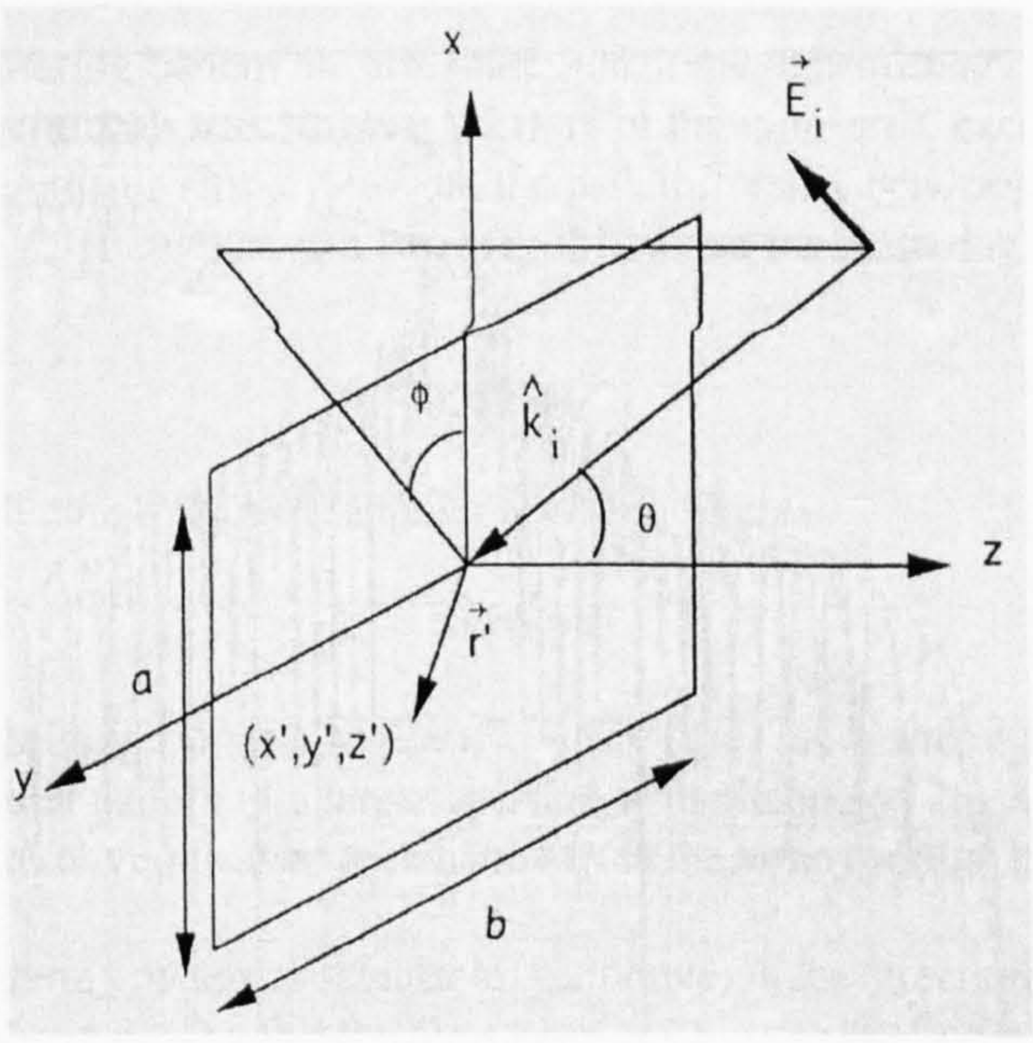

Figure 3.1: Plane wave scattering by a rectangular plate [27]

In general terms a rectangular plate has a predefined edge dimension a in the x coordinate and b in the y coordinate system, where the coordinate system is defined such that the x-y plane coincides with the plane of the plate itself. So, the angle between an incident wave and the z axis of the plate, or normal vector of the plate, is defined as θ. ϕ is defined as the angle between the incident wave and the x axis of the plate (see Fig. 3.1). If the incident wave is assumed to be lying on the y-z plane of the plate coordinated system, the radar cross section of the plate will be calculated with Eqn.(3.4). If not lying on the y-z plane, the flat plate cross section can be evaluated with the Eqn.(3.5).

$$\sigma(\theta) = \frac{4\pi A^2}{\lambda^2}\left[\frac{\sin(k_1 a \sin\theta)}{k_1 a \sin\theta}\right]\cos^2\theta \tag{3.4}$$

$$\sigma(\theta,\phi) = \frac{4\pi A^2}{\lambda^2}\left[\frac{\sin(k_1 a\sin\theta\cos\phi)}{k_1 a\sin\theta\cos\phi}\frac{\sin(k_1 b\sin\theta\sin\phi)}{k_1 b\sin\theta\sin\phi}\right]^2\cos^2\theta \tag{3.5}$$

where a, b are edge dimensions, λ is the radar wavelength, A is the flat plate area, and $k_1 = 2\pi/\lambda$.

However, if a plate is flat, with the conducting surface perpendicular to the direction of radar line of sight, and only if the overall dimensions of the plate in any direction are large compared to the wavelength, then this cross section can be shown as:

$$\sigma = \frac{4\pi A^2}{\lambda^2} \tag{3.6}$$

3.1.1.3 Circular Cylinder

The cylinder has proved to be very useful in modeling portions of aircraft such as fuselage, wing tanks, and engine nacelles. Very thin circular cylinders whose radii are very small in comparison with the radar wavelength have been extremely useful in modeling the sharp edges of some wing surfaces. Very thin cylinders are referred to here as thin wires.

Unlike the sphere, the cylinder is, in general, polarisation-sensitive. However, very large cylinders (with all dimensions much larger than a wavelength) are polarisation-insensitive. If the cylinder axis is perpendicular to the direction of propagation, the cross section for a large cylinder is simply:

$$\sigma = \frac{2\pi a l^2}{\lambda} \tag{3.7}$$

where a is the cylinder radius and l is the cylinder length.

If the angle between the radar line of sight and the cylinder (θ), is fairly large ($(4\pi a\sin\theta)/\lambda \gg 1$), then the exact expression for the radar cross section is quite complicated:

$$\sigma = \frac{a\lambda\sin\theta}{2\pi}\left\{\frac{\sin[(2\pi l/\lambda)\cos\theta]}{\cos\theta}\right\}^2 \tag{3.8}$$

Crispin [13] derived a general equation to calculate the cross-section for a cylinder whose dimensions are small in comparison to the wavelength, such as a wire, sharp leading edge (thin wire). Eqn.(3.9) where the effective cross-section for θ is not close to 90°:

$$\sigma = \frac{\lambda^2\tan^2\theta\cos^4\phi}{16\pi\left[(\frac{\pi}{2})^2 + \left(\ln\frac{\lambda}{\gamma\pi a\sin\theta}\right)^2\right]} \tag{3.9}$$

where $\gamma = 1.781072$, θ is the angle between the wire and the direction of incidence, and ϕ is the angle between the polarisation direction and the plane formed by the wire and the direction of incidence.

In the case where $\theta = 90°$, equation(3.9) can be reduced to:

$$\sigma = \frac{\pi l^2 cos^4 \phi}{\left(\frac{\pi}{2}\right)^2 + \left(ln\frac{\lambda}{\gamma\pi a}\right)^2} \tag{3.10}$$

3.1.1.4 Finite Cone

The finite cone can be used to model wing surfaces and portions of a fuselage surface. If the cone base is circular with radius a, and has a finite length of L, then the radar cross section of this simple finite cone shape for $\theta = 90°$ is given by:

$$\sigma = \frac{8\pi L^3 \sin\alpha}{9\lambda \cos^4 \alpha} \tag{3.11}$$

where λ is the radar wavelength, and α is the half cone angle (see Fig. 3.2).

And for the $\theta \neq 90°$, the cross-section can be calculated with Eqn.(3.12).

$$\sigma = \left(\frac{\lambda L \tan\alpha}{8\pi \sin\theta}\right) \tan^2(\theta - \alpha) \tag{3.12}$$

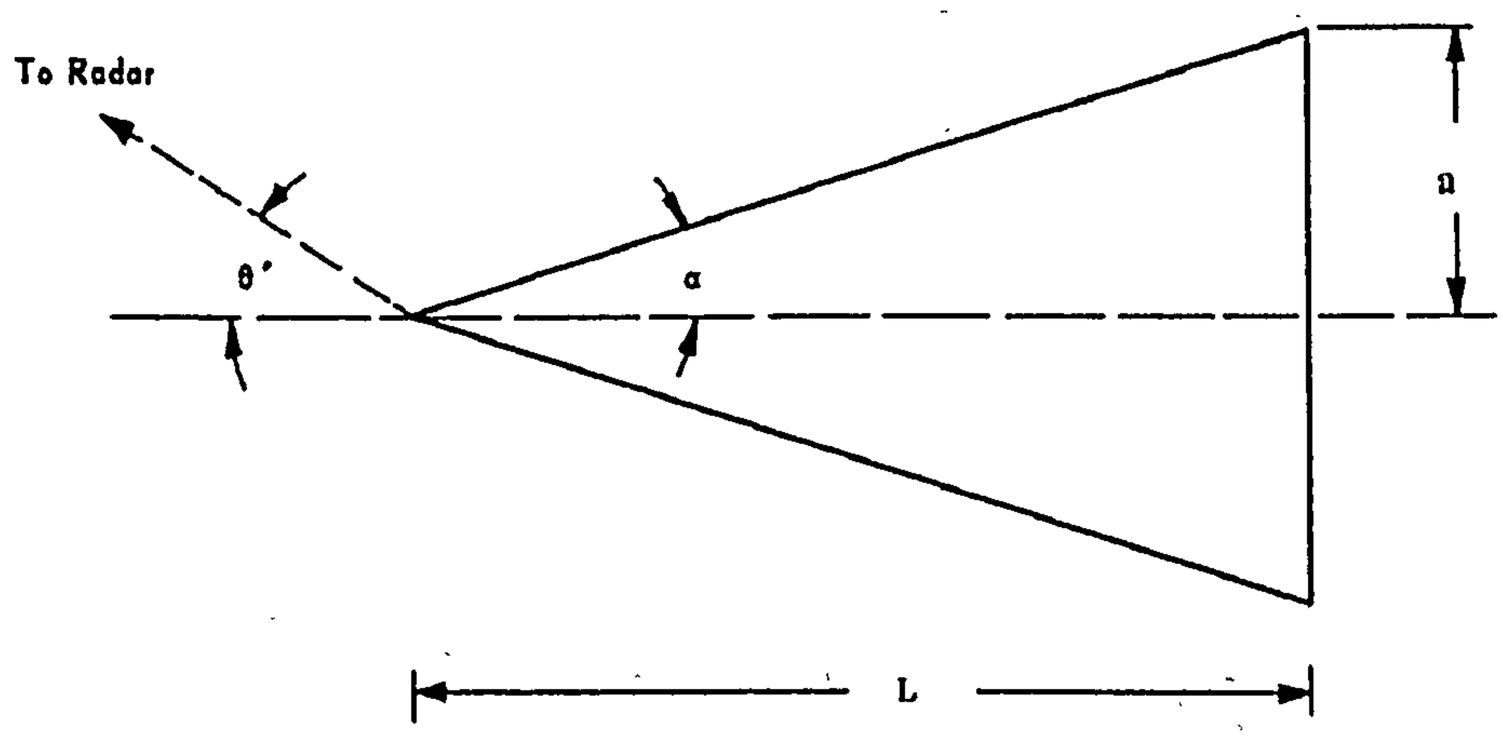

Figure 3.2: The finish-cone geometry [13]

3.1.1.5 Large, Smooth, Curved Surfaces

For a very large surface, it can be assumed that the principal radii of curvature is very large compared to the wavelength, but is finite. The simple calculation of cross-section for this kind of shape is given by Eqn.(3.13):

$$\sigma = \pi R_1 R_2 \tag{3.13}$$

where R_1 and R_2 are the principal radii of curvature of the surface at the point where the radar wave front first strikes it.

3.1.1.6 Complex Targets

The electromagnetic problem of cross section calculation can become very complicated for the above described simple geometric shapes, thus, necessitating the use of approximation techniques. It is understandable that exact calculation of the cross sections of more complicated targets is virtually impossible. However, techniques of approximate calculation have been developed, yielding results that are in reasonable agreement with experiment [9]. This approximation, called the *random phase method*, simply averages the contributions of all σ's of simple geometric shape assemblies of the target over all possible phase angles. This leads to the formula:

$$\sigma_{total} = \sum_{k=1}^{N} \sigma_k \tag{3.14}$$

3.1.2 Probability of Detection by Radar

A detection by radar occurs when the total power level processed by the radar receiver, Signal and Noise $(S + N)$, is above a selected power level called the threshold (see Fig. 3.3). The signal-to-noise ratio (S/N), when $S + N$ is equal the threshold, is defined as $(S/N)_{min}$ [6]. Therefore, the probability of detection (P_D) is then a function of the signal to noise ratio (S/N) and the false alarm probability (P_n), and can also be calculated as follows [24]:

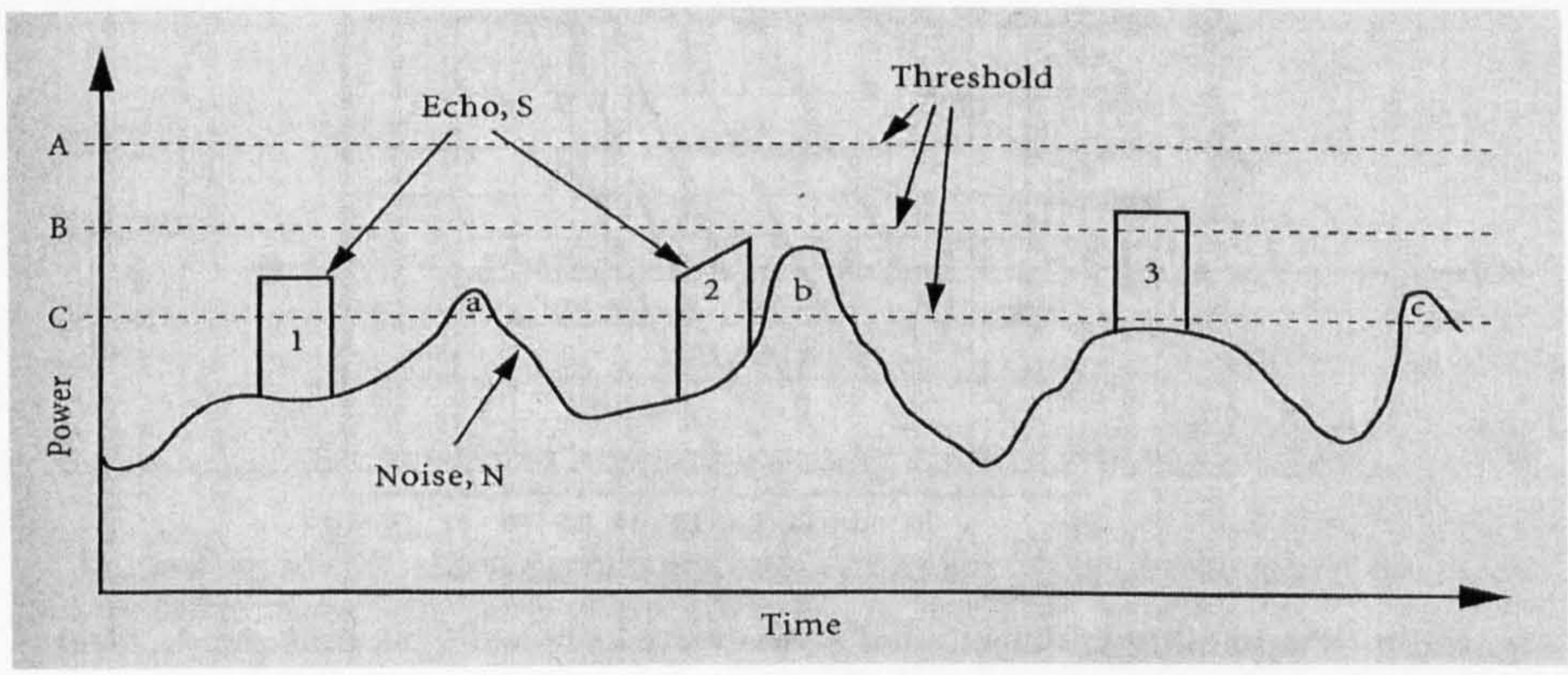

Figure 3.3: Conditional detection by threshold setting [6]

$$P_D = 1 - e^{-S/N} \int_{P_n}^{1} I_0 \left\{ \sqrt{-4(S/N)ln(u)} \right\} du \tag{3.15}$$

where

$$S/N = \frac{PG^2\lambda^2\sigma}{(4\pi)^3 R^4 FkTB_nL} \tag{3.16}$$

$$u(E_t) = P_n = \exp\{-E_t^2/2\} \tag{3.17}$$

Where S/N is signal-to-noise ratio of the radar with G gain transmission power. R is the distance between radar and aircraft. FT is the effective temperature, L is signal and echo power loss factor. k is the Boltzmann's constant, and B_n is the noise power that lies within the signal bandwidth of radar receiver.

Signal-to-noise ratio is a function of power processed by a radar receiver and is direct proportional to aircraft cross section (σ), as shown in equation (3.16). Additionally, S/N is also the reciprocal to the distance between aircraft and radar receiver to the fourth power. On the other hand, the probability of false alarm (P_n) can be determined directly from the threshold setting of radar.

Hovanessian [24] showed some typical results from equation (3.15) - (3.17) in Fig. 3.4, which can be used as a simple alternative to predict probability of detection by radar.

3.1.3 Conditional Probability of Hit

After an aircraft has been detected, the enemy then engages the aircraft with their weapon, which generally can be divided into two main categories; contact warhead (penetrator) and proximity warhead (blast and fragments). The contact warhead has to hit directly to kill or damage the aircraft. On the other hand, the proximity-fused warhead detonates outside the aircraft at a detonation distance. Its blast and fragments will then hit and kill or damage the aircraft. It is not necessary for all shot penetrators and fragments from the detonation to hit the aircraft. Some will hit and some may miss the aircraft. This matter will also affect the conditional probability of hit. Additionally, the conditional probability of hit depends on the threat weapon type which intercepts the aircraft; a contact warhead ($P_{H/D}$) or a proximity warhead ($P_{F/D}$).

3.1.3.1 Miss Distance

The measure of the threat system's ability to position a warhead within the vicinity of the aircraft is the closet point of approach of the propagator with respect to the aircraft. This miss distance is essentially an error. In general, the miss distance is a function of the

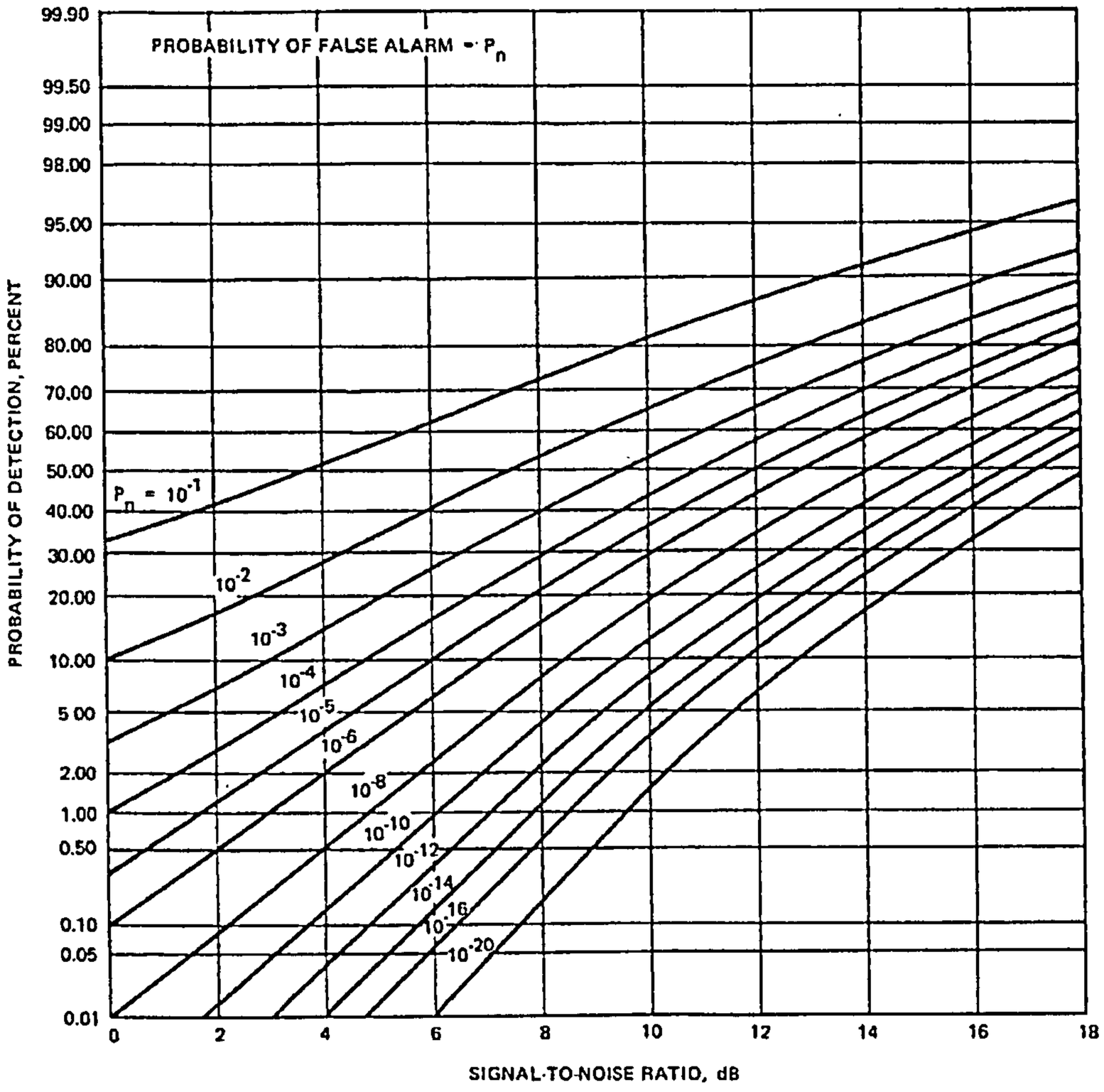

Figure 3.4: Probability of detection vs signal-to-noise ratio and probability of false alarm [24]

three spatial coordinates (x, y, z) whose origin is centred at the aim point of the target (normally the centre of gravity of the aircraft). However, in simple evaluations the two spatial coordinates (x, y) and sometimes only one dimension (r) are used (see Fig. 3.7).

3.1.3.2 Conditional Probability of Hit by a Contact Warhead

The probability that the aircraft is hit, when it is detected ($P_{H/D}$), depends upon the miss distance distribution and upon the physical size of the aircraft presented area to the propagator. Assuming that an aircraft has been shot with N propagators at N different locations of x, y pairs, the distance from the aircraft aim point to any x, y pair is the miss distance for that shot, and the distances x and y are the coordinate errors. If the N miss distances are independent from one another and there is no correlation between the x and y components of the miss distance, the assumption is made that the probability density function of the miss distance $\rho(x, y)$ can be represented by two dimensional normal

distribution as:

$$\rho(x,y) = \frac{1}{2\pi\sigma_x\sigma_y}\exp\left(-\frac{(x-\mu_x)^2}{2\sigma_x^2} - \frac{(y-\mu_y)^2}{2\sigma_y^2}\right) \tag{3.18}$$

where σ_x and σ_y are the standard deviation of miss distances x and y respectively; μ_x and μ_y are mean values of miss distance x and y.

If the two means (μ_x, μ_y) are found, or assumed, to be equal to zero, and if the two standard deviations (σ_x, σ_y) are found, or assumed, to be equal, the bivariate distribution simplifies to the circular normal distribution given by:

$$\rho(r) = \frac{1}{2\pi\sigma_r^2}\exp\left(-\frac{r^2}{2\sigma_r^2}\right) \tag{3.19}$$

The presented area of the aircraft in the miss distance plane, which is defined as a plane that contains the miss distance vector and is normal to the relative propagator path, is given by:

$$A_P = \iint_L L(x,y)dxdy \tag{3.20}$$

An aircraft is hit only when x and y define a location within the physical extent of the aircraft; location of (x, y) pairs outside the aircraft boundary are misses. Consequently, the probability of a propagator hit on the presented area of the aircraft is given by integral of $\rho(x, y)$ over the extent of the aircraft:

$$P_{H/D} = \iint_L \rho(x,y)dxdy \tag{3.21}$$

Due to the complexity of evaluating for a general aircraft external shape, two alternative approximated aircraft shape representations can be used, i.e. the "Shoe Box" and the "Carlton". The difference between the two methods is that the "Shoe Box" defines a rectangular area with side lengths x_0 and y_0 as shown in Fig 3.5. Therefore, $A_P = x_0 y_0$.

On the other hand, Carlton, or the diffused Gaussian method uses a function $H(x, y)$, which defines the probability that locations (x, y) lie on the aircraft presented area (see Fig. 3.6). Aircraft presented area can be then evaluated as:

$$A_P = \int_{-\infty}^{\infty}\int_{-\infty}^{\infty} H(x,y)dxdy \tag{3.22}$$

Then $P_{H/D}$ with N propagators becomes:

$$P_{H/D} = \int_{-\infty}^{\infty}\int_{-\infty}^{\infty} \rho(x,y)H(x,y)dxdy \tag{3.23}$$

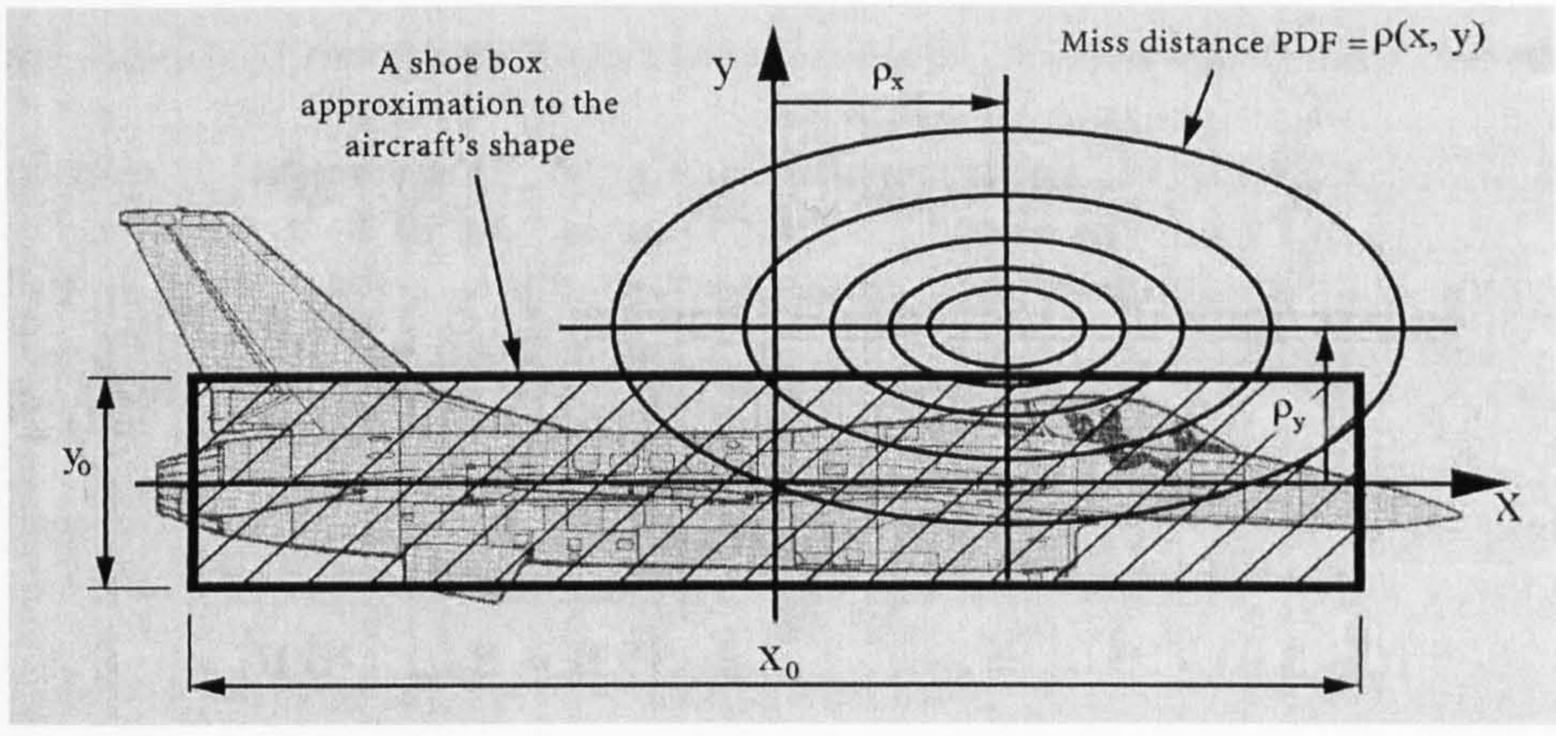

Figure 3.5: Aircraft presented areas represented by Shoe Box and bivariate normal miss distance distribution

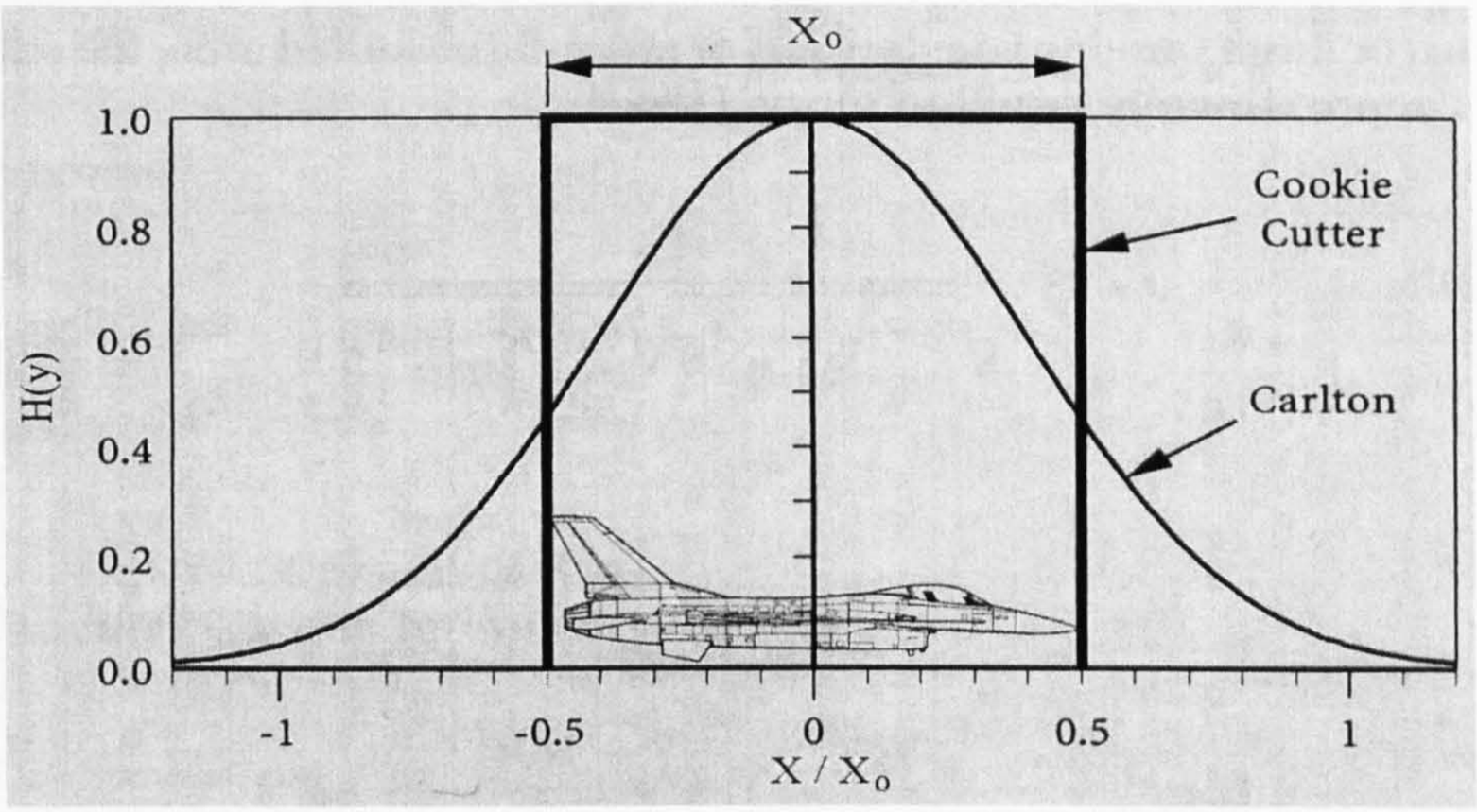

Figure 3.6: Presented area represented by Shoe Box and Carlton methods

If circular symmetry about the aim point is assumed for the miss distance distribution, and if the aircraft presented area is taken as a circle of radius r_0, and $\sigma_x = \sigma_y = \sigma_r$. Then the aircraft presented area can be determined as the circle area of this radius ($A_p = \pi r_0^2$), as illustrated in Fig. 3.7. Thus, the $P_{H/D}$ can be estimated from one of following equations [6]:

$$P_{H/D} = \begin{cases} 1 - \exp\left(\frac{-A_p}{2\pi\sigma_r^2}\right) & \text{Shoe Box} \\ \frac{A_p}{2\pi\sigma_r^2 + A_p} & \text{Carlton} \end{cases} \tag{3.24}$$

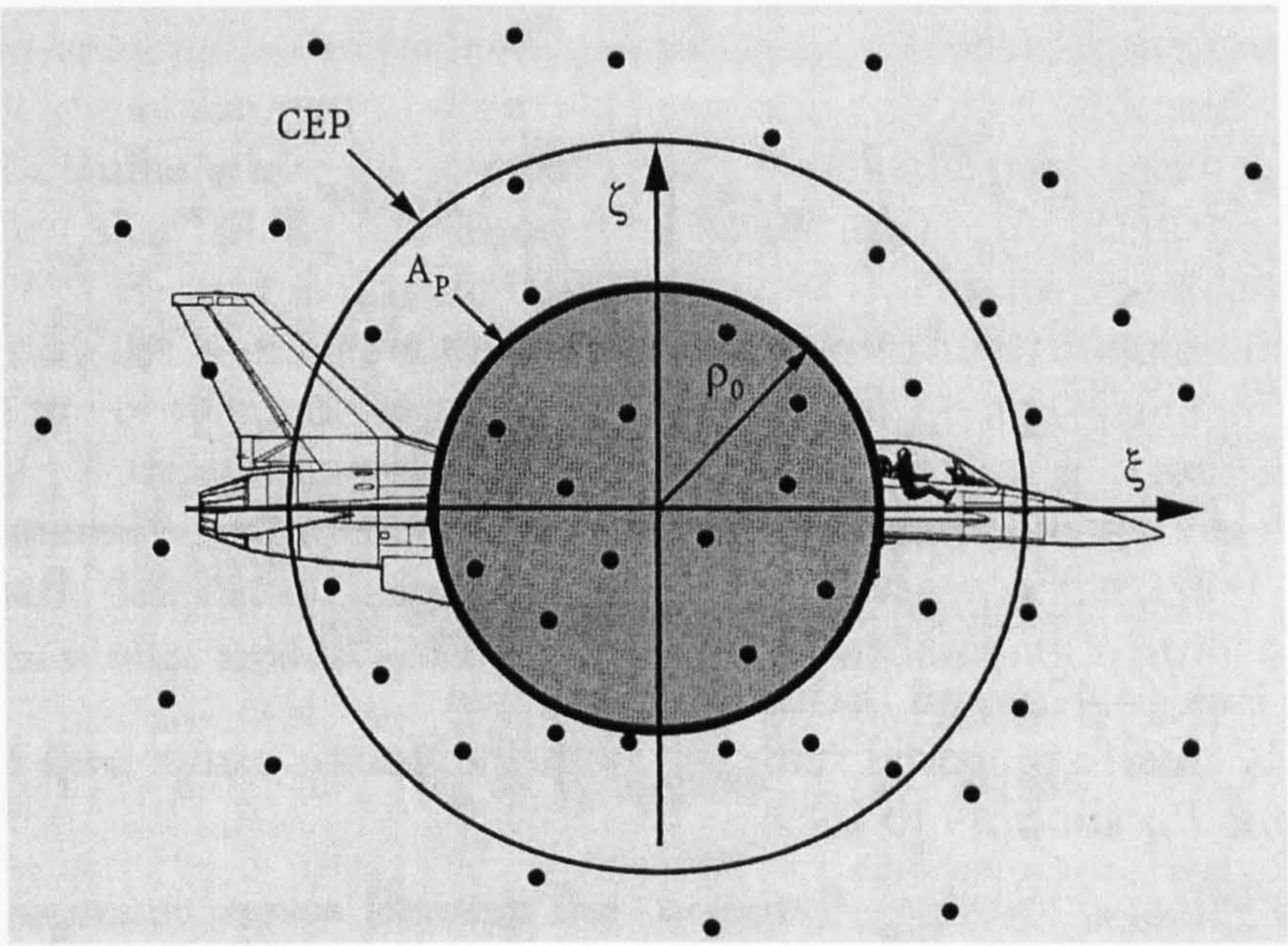

Figure 3.7: Circular symmetric miss distance [6]

3.1.3.3 Conditional Probability of Hit by Proximity Warhead

On the other hand, a propagator with a proximity warhead does not have to hit the aircraft to kill or damage it. Instead, the aircraft is killed when the proximity warhead fuses in a location that causes one or more warhead fragments, discrete rod, continuous rod, or penetrators to hit the aircraft. Additionally these hits must be sufficient to kill the aircraft. If the warhead detonates close enough, the blast effect may also damage and/or kill the aircraft. Most of the current air target warheads are designed to kill the target with fragment spray, whose kill or damage mechanism is similar to the kill or damage mechanism inflicted by multiple hits of contact warheads or penetrators. Therefore, the blast-fragment warhead is chosen to represent the proximity warhead.

From a susceptibility point of view, the miss distance of each fragment from a proximity warhead detonation and the number of fragments penetrating the target are the major factor in the evaluation of this threat type. The number of fragments penetrating the aircraft depends on the number of fragments in the proximity warhead, fragment impact locations, and the terminal effects parameters; such as the fragment mass, impact velocity, and detonation distance (see Fig. 3.8). In general, the fragments will be randomly distributed throughout the fragment spray zone. The expected number of hits on the aircraft can be estimated by assuming that a presented area of the aircraft is hit with

a uniform density spray of fragment [5]. This is expressed in Eqn.(3.25).

$$n = \frac{NA_p}{2\pi s^2(\cos\delta_1 - \cos\delta_2)} \tag{3.25}$$

where N is the number of fragments in the warhead, and s is the detonation distance between fragment spray and the warhead. δ_1 and δ_2 are the leading and the trailing fragment spray angles which are defined as:

$$\delta_i = \arctan\left[\frac{V_m \sin\Psi + V_f \sin(\Psi + \alpha_i)}{V_m \cos\Psi + V_f cos(\Psi + \alpha_i) - V_t}\right] - \Psi, \quad i = 1, 2 \tag{3.26}$$

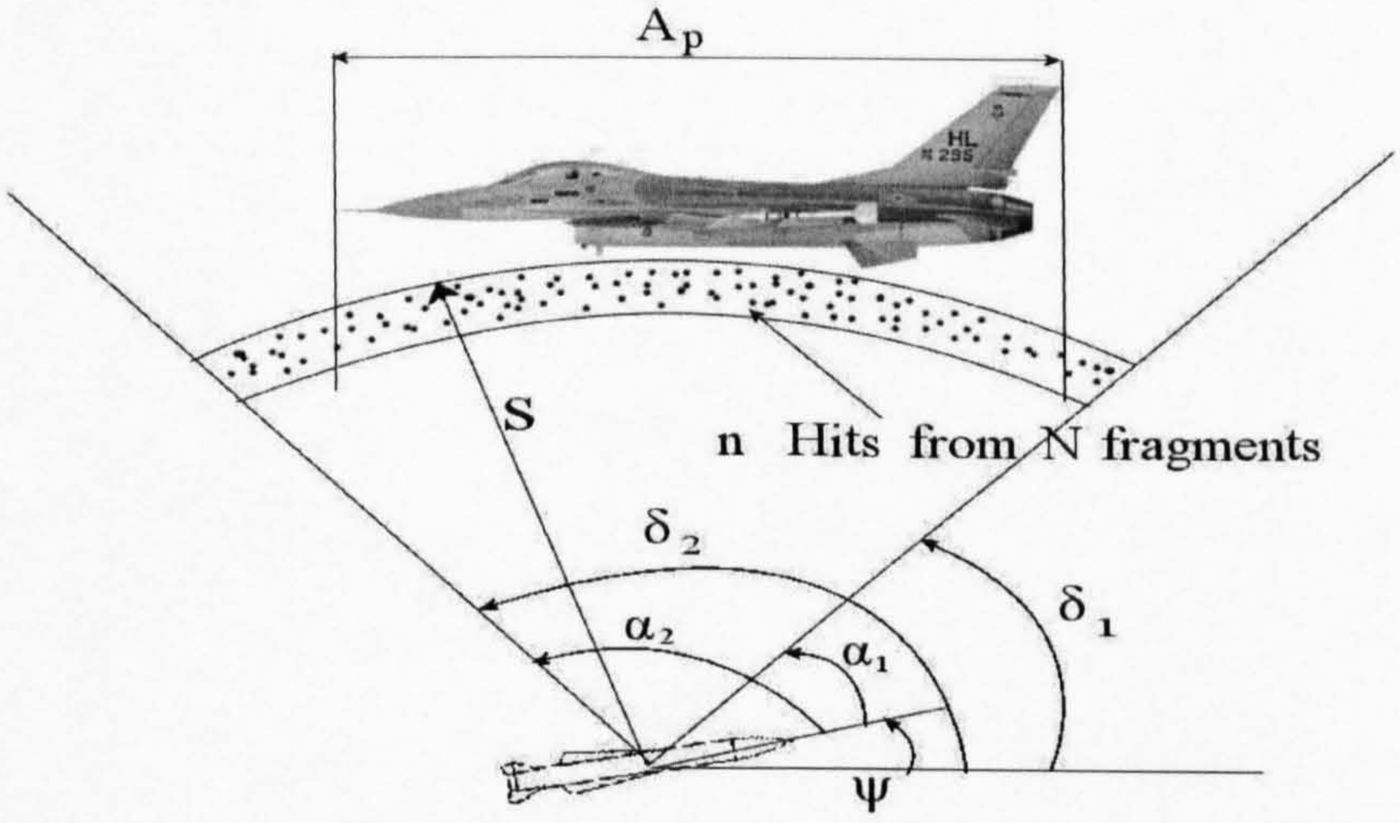

Figure 3.8: Warhead detonation and fragment spray

where V_t is the target horizontal speed, V_m is the speed of the missile, Ψ is the elevation angle of the missile, V_f is the average fragment speed with respect to a stationary warhead, and α_1 and α_2 are the leading and trailing fragment spray angles from the axis of the static warhead detonation, respectively.

The number of fragments, which supposedly directly hit the aircraft is dependent upon detonation distance and the number of fragments along the aircraft length. In this case, the probability of fuse ($P_{F/D}$) becomes 1.0 for all n direct fragment hits, and the probability of hit can be calculate as n hits by contact warhead (see Fig. 3.8). In other words, a hit by a proximity warhead becomes n multiple hits by a contact warhead with a $P_{H/D}$ of 1.00 for detonated fragments within aircraft presented area.

3.2 Vulnerability Assessment

Vulnerability is the probability that the aircraft will be killed if hit [6], and is a function of aircraft critical component configurations, including specific armament, system locations and redundancies. An aircraft consists of many components, and each individual component has a level of vulnerability; thus, each component vulnerability contributes in some measures to the overall vulnerability of the aircraft. The aircraft vulnerability is indicated by the probability of kill given a hit, $P_{K/H}$. This probability can be evaluated using the following procedures:

- Identification of the critical components considering redundancy level
- Identification of each critical component Damage-Caused Failure Mode
- Calculation of each individual critical component vulnerability
- Identification of overlapped areas of these critical components
- Calculation of each overlapped area critical component vulnerability
- Summation of each individual critical component and each overlapped area of these critical components vulnerability considering to their layout (Shielding Effect for Overlapped Area)

3.2.1 Kill Tree Diagram

A kill tree diagram is a logic symbology, which shows a top-down approach that starts with aircraft kill event and then determines what event or combination of events can cause the aircraft kill event. The kill tree diagram can be illustrated by the generic fault tree as shown in Fig. 3.9. At the bottom of each branch of the diagram, all critical components resulting is an aircraft kill event are shown. With the basic logic gates (AND, OR), critical component redundancy can be illustrated.

3.2.2 Shotline Technique

This technique has been used to identify the overlapped area of critical components by superimposing a planar grid over the aircraft model and then passing parallel shotlines or ray towards the grid nodes [1]. A list of the penetrated components is then generated.

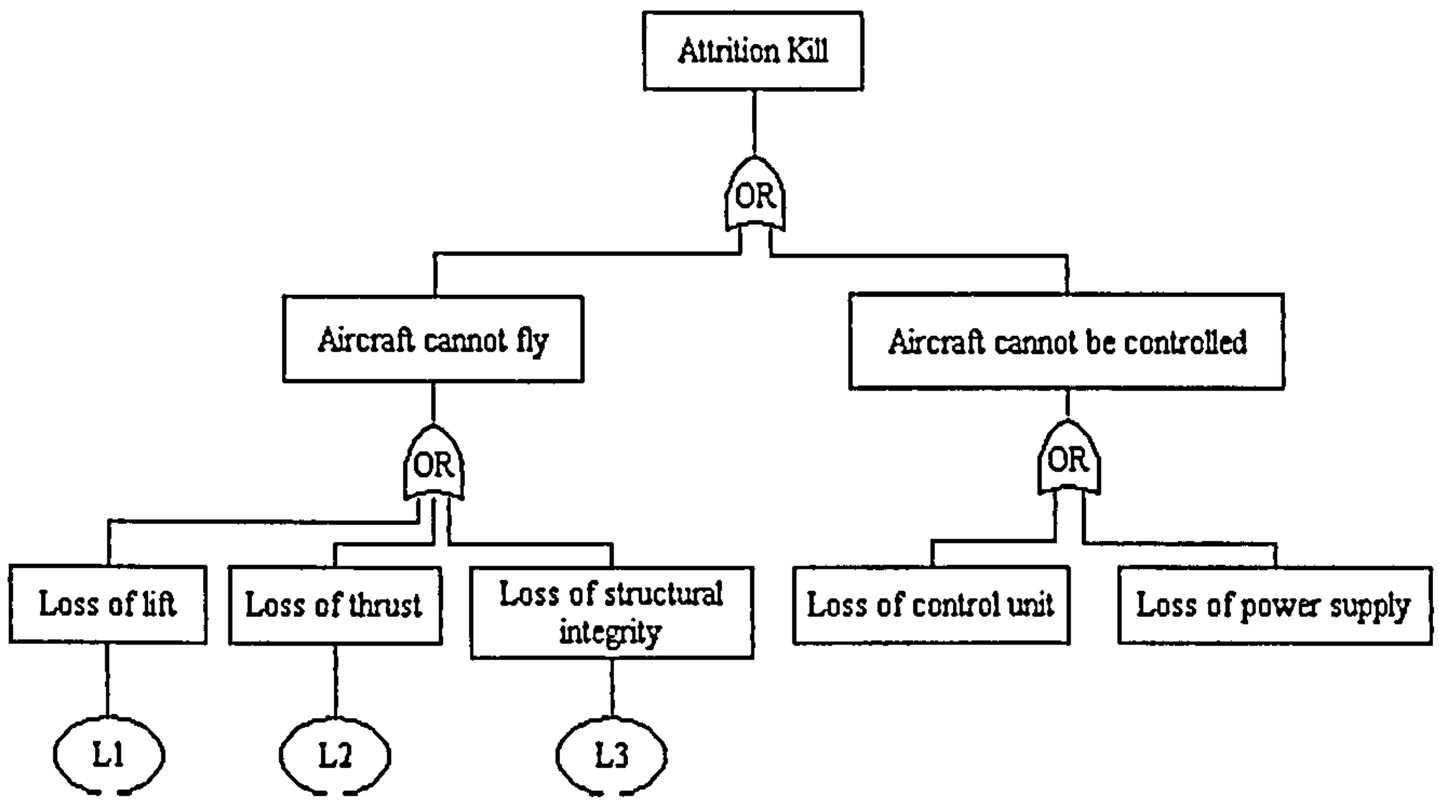

Figure 3.9: Kill tree diagram for UAV

In the vulnerability assessment module used for this methodology, the overlapped area of the critical components within the same shotline (see Fig. 3.10) can be examined in two categories; i.e. shielding effect and non-shielding effect. For shielding effect, the front critical component may be used as a shield for the critical components behind. On the other hand, for non-shielding effect the overlapped areas of the critical component will be redefined as an additional non-redundant critical component. The components behind are automatically killed when the front component of the overlapped area is killed. Therefore, the total number of critical components increases. The effect of these two definitions of overlapped area will be discussed later.

3.2.3 Vulnerable Area given by a Single Hit

The vulnerable area technique is a theoretical threat-presented area that, if hit by a damage mechanism, would result in an aircraft or components kill [6]. The vulnerable area of the ith component (A_{v_i}) depends on the presented area of the component in the plane normal to the approach direction of the threat (A_{p_i}) as illustrated in Fig. 3.11. The probability of component kill, given a hit on the component (P_{k/h_i}) is as follows:

$$A_{v_i} = A_{p_i} P_{k/h_i} \tag{3.27}$$

The determination of the $P_{k/h}$ of each component is a very difficult undertaking. It requires a combination of complete analysis of critical data and sound engineering judgment. There is no universal methodology for arriving at a numerical value for $P_{k/h}$ [6].

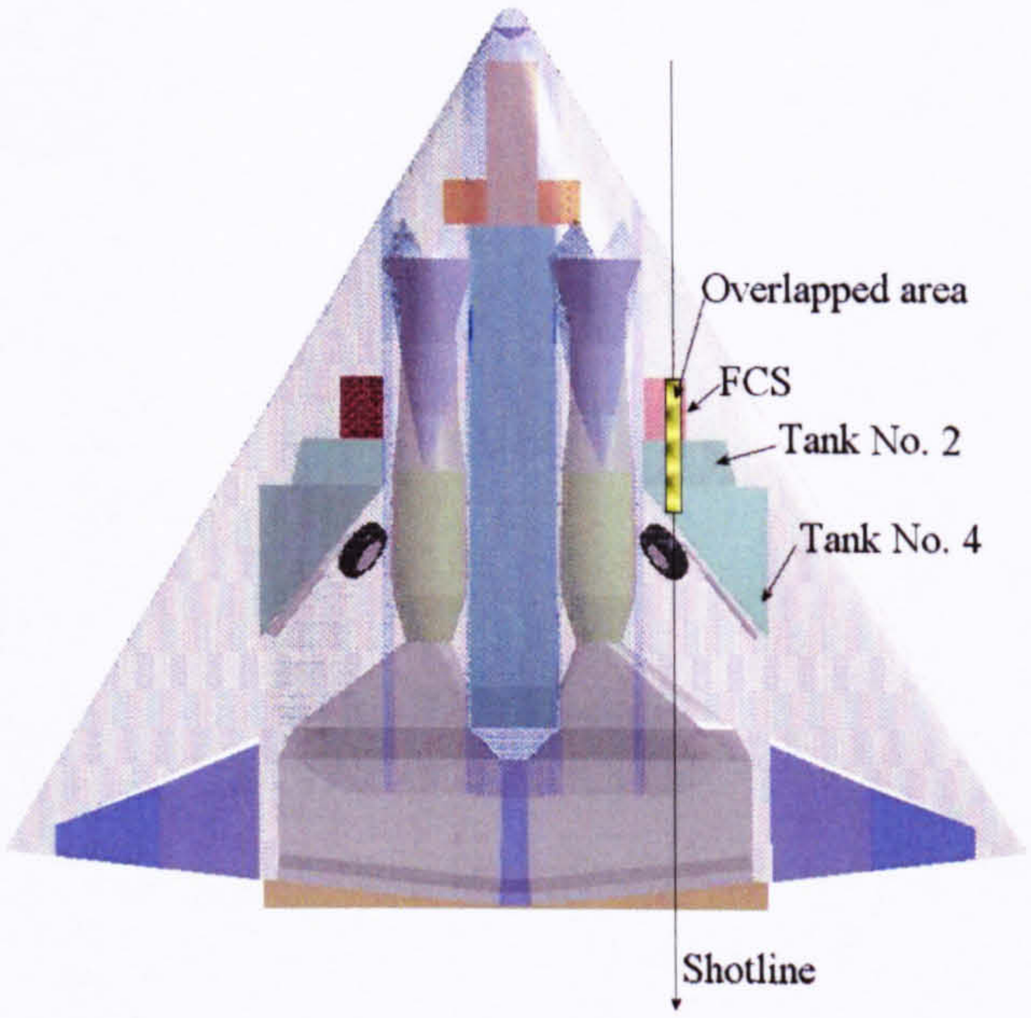

Figure 3.10: Identification of Overlapped area by shotline technique

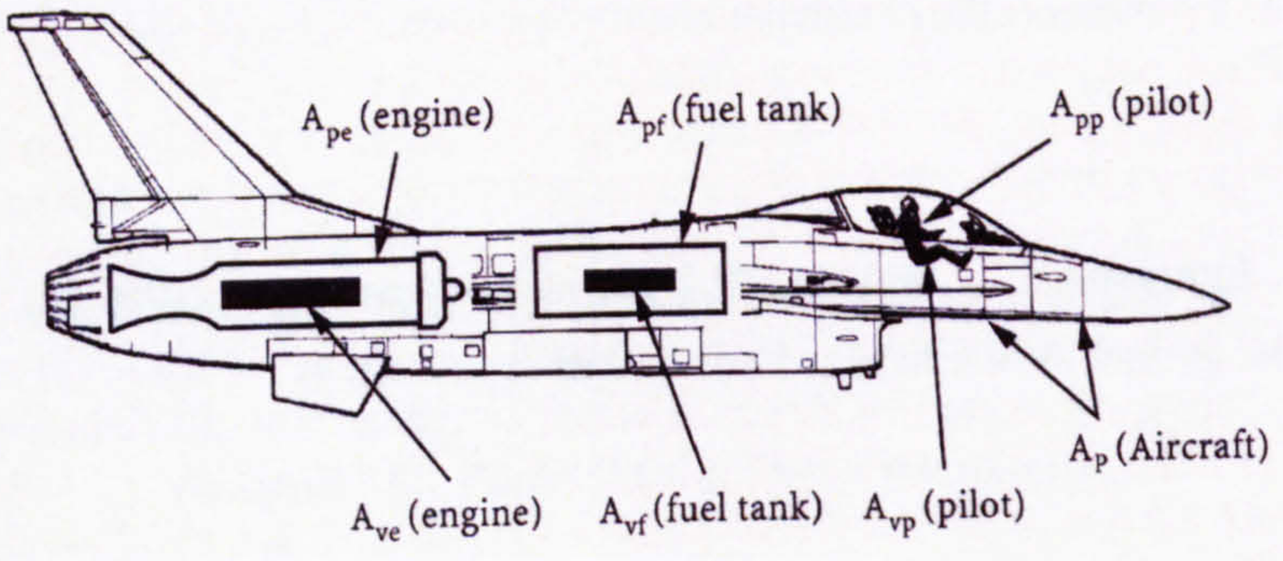

Figure 3.11: Presented and vulnerable areas of critical components and aircraft [6]

Therefore, the assumed $P_{k/h}$ in Table 3.1 are chosen as guideline and/or default value in vulnerability assessment. These values have been assumed by Ball [6].

Table 3.1: Assumed default probability of kill of a component, given a hit on the component $P_{k/h}$

Critical component	$P_{k/h}$
Pilot	1.0
Fuel system	0.3
Engine	0.6 - 0.7
Avionic	0.8 - 0.9

Before the vulnerable areas of the overlapped areas of the critical components can be determined, the probability of kill given a hit, and presented area of overlapped critical

components both have to be defined and calculated depending on their redundancy. The presented area of overlapped critical components is defined as the intersection of presented areas of all overlapped critical components, arranged by the same shotline (see Fig. 3.12). It is possible to acquire redundant overlapped areas if an aircraft has symmetrically redundant critical components; unless overlapped critical components are always defined and considered as non-redundant components.

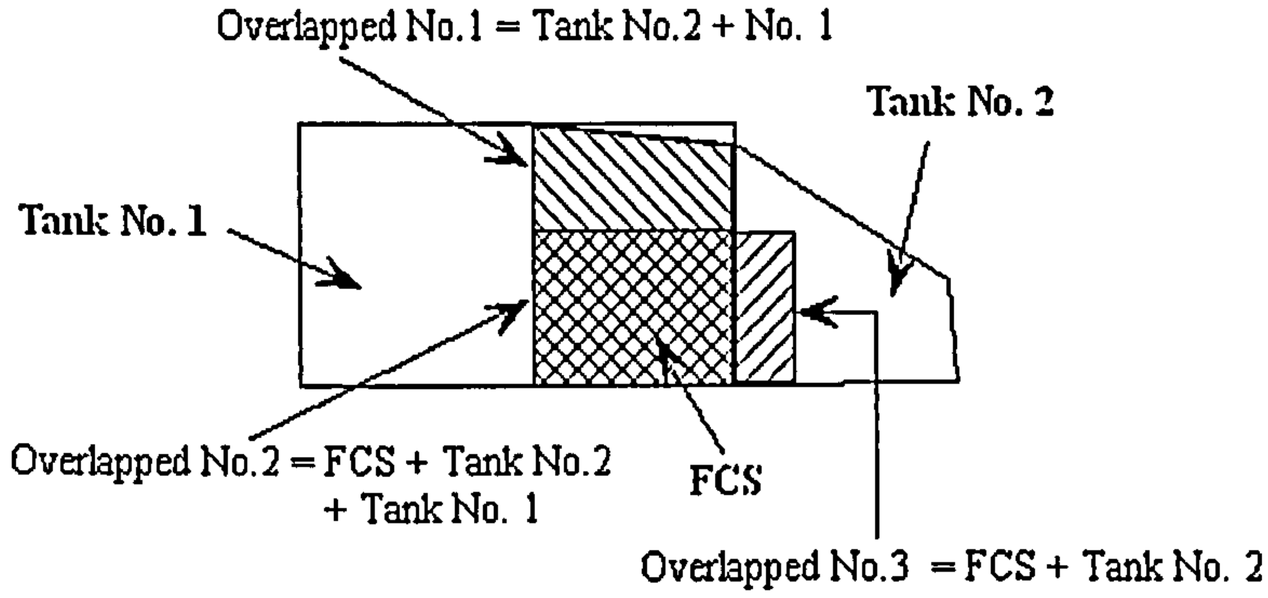

Figure 3.12: Overlapped areas from tank no.1, tank no.2 and FCS

The probability of a kill of an overlapped area, given a hit on the overlapped area, has to be determined. This determination depends mainly on the redundancy level of the overlapped critical components, which can be classified as follows.

3.2.3.1 Overlap of Non-Redundant Critical Components

A hit in this overlapped area can kill one or more of the components intersected by the shotline. Thus, the component kills along the shotline are not mutually exclusive. Assume there are C non-redundant critical components along all shotlines within the overlapped area. This overlapped area, with its C components, can be considered to be a composite non-redundant critical component. The probability that all C components survive the hit (P_{s/h_O}) is given by the joint probability that each of the C components survives the hit.

$$P_{s/h_O} = P_{s/h_1} P_{s/h_2} P_{s/h_3} ... P_{s/h_C} = \prod_{i=1}^{C} (1 - P_{k/h_i}) \tag{3.28}$$

Hence, the probability of kill of an overlapped area of non-redundant critical components given a hit is given by:

$$P_{k/h_O} = 1 - \prod_{i=1}^{C} (1 - P_{k/h_i}) \tag{3.29}$$

3.2.3.2 Overlap of Redundant Critical Components

If redundant critical components overlap each other, or another redundant component, a single hit on the overlapped region can kill all redundant critical components. Therefore, an overlapped area of redundant critical components becomes automatically non-redundant, unless there is another identical overlapped redundant component onboard the aircraft. The probability of kill of this kind of overlapped area can be evaluated as:

$$P_{k/h_O} = P_{k/h_1} P_{k/h_2} P_{k/h_3} \ldots P_{k/h_C} = \prod_{i=1}^{C} P_{k/h_i} \tag{3.30}$$

3.2.3.3 Overlap of Redundant and Non-Redundant Critical Components

In this case, an overlapped area comprises $C1$ non-redundant critical components and $C2$ redundant critical components. The overlapped region can be killed by killing one of the $C1$ non-redundant critical components or by killing all $C2$ redundant critical components. Hence, the probability of kill for such an area can be calculated as:

$$P_{k/h_O} = 1 - \left(\{ \prod_{i=1}^{C1} (1 - P_{k/h_i}) \} \{ 1 - \prod_{j=1}^{C2} P_{k/h_j} \} \right) \tag{3.31}$$

Finally, the vulnerable areas of overlapped critical components can be evaluated according to Eqn. (3.27), and their redundancy can be categorised as described above.

An effect on consider for overlapped area of critical components is the determination of the vulnerable areas of the non-overlapped regions of the critical components. The presented area of these critical components are deducted, or sometimes replaced by the intersection of the presented areas. For instance, three intersection regions from fuel tank no.1, no.2, and the flight control system, shown in Fig. 3.12, can therefore be evaluated. The results are shown in Table 3.2.

Table 3.2: Aircraft component presented areas with overlapped critical components

Component	$A_p[ft^2]$	$P_{k/h}[-]$	$A_v[ft^2]$	Redundancy
Fuel Tank No.1	20 (45 - 25)	0.3	6.0	redundant
Fuel Tank No.2	15 (45 - 25 - 5)	0.3	4.5	redundant
FCS	0 (20 - 15 - 5)	0.95	0.0	non-redundant
Overlapped No.1	25	0.09	2.25	non-redundant
Overlapped No.2	15	0.9545	14.181	non-redundant
Overlapped No.3	5	0.965	4.825	non-redundant
Total	**80**	-	**21.256**	-

3.2.3.4 Shielding Effect applied to Overlapped Critical Components

One possible to reduce the vulnerable areas of the critical component overlapped area is to use the front critical component of the overlapped area as a shield for the behind critical components. The assumed shield capability in this study is 10%. That means the probability of kill of the behind critical components will be reduced by 10%. Additionally, the reconfiguration of the critical component layout by moving the less critical component to the front of the overlapped area is another method to supplementary reduction of kill probability of the overlapped area. This effect is valid within the overlapped area only. By this approach, the kill probability of the overlapped area reduces. Table 3.3 shows an example of calculation of the kill probability of the Overlapped No. 2. In this example, the FCS has been positioned between the fuel tank No. 1 and No. 2 for the reconfiguration layout.

Table 3.3: Calculation of the kill probability of the Overlapped No. 2

Component	Probability of kill		
	Non-Shielding Effect	Shielding Effect	
		Original Layout	Reconfigurated Layout
Fuel Tank No.1	0.3	0.27	0.27
Fuel Tank No.2	0.3	0.27	0.3
FCS	0.95	0.95	0.855
Total	**0.9545**	**0.953645**	**0.866745**

The total aircraft vulnerable area calculated from a single hit is then the summation of all non-redundant critical components and non-redundant overlapped critical components, which can be more or less than the total aircraft vulnerable areas resulting from a single hit without overlapped areas. This depends on the layout of the critical components and the consideration of the shielding effect of the front component of the overlapped area. For instance, if the aircraft designer rearranges these three critical components so that no overlapped areas of critical components exists; its vulnerable areas will be 19 ft^2, instead of 21.256 ft^2. In case that the front critical component in the overlapped area can be used as a shield for the behind critical components, the aircraft vulnerable areas will be reduced to 21.147475 ft^2 for the original layout, and to 19.518 ft^2 for the reconfiguration layout.

3.2.4 Aircraft Kill Probability by a Single Hit of a Nonexplosive Penetrator

The aircraft kill probability, given a random single hit on the aircraft ($P_{K/H}$), is the summation of the kill probabilities of the non-redundant critical components, given a random hit on the aircraft (P_{k/H_i}). This can be calculated as:

$$\begin{aligned} P_{k/H_i} &= P_{h/H_i} P_{k/h_i} = (A_{p_i}/A_p)(A_{v_i}/A_{p_i}) \\ &= A_{v_i}/A_p \end{aligned} \tag{3.32}$$

In the case that an aircraft has been hit by a single nonexplosive penetrator, it is impossible to kill an aircraft by killing only one of the redundant critical components. Hence, the kill probability given a random single hit on the aircraft with C non-redundant critical components and overlapped areas is evaluated as:

$$P_{K/H} = \sum_{i=1}^{C} P_{k/H_i} = \sum_{i=1}^{C} \frac{A_{v_i}}{A_p} \tag{3.33}$$

3.2.5 Aircraft Kill Probability by Multiple Hits of Penetrators

It is assumed that the random distribution of hits by more than one penetrator or fragment over the aircraft is uniform, and all hits are assumed to travel along parallel shotlines from the same direction. Ball [6] offers five alternatives to estimate these probability values; i.e. Binomial approach for N hits, Poisson approach for E expected hits, Tree diagram, Markov chain, and Simplified approach. With the first two methods, the effects of critical component redundancy cannot be considered in kill probability by multiple hits. The third method, the tree diagram, examines kill expressions for each hit, considering redundant and non-redundant critical components, and the sum of these values up to aircraft kill probability by N hits. A disadvantage of tree diagram is that it is too detailed and time consuming. The Markov chain or state matrix method offers an opportunity to determine aircraft, kill probability by multiple hits of nonexplosive penetrators with consideration of redundancy for less detailed calculation for each hit. The results of the tree diagram and Markov chain will be identical because both methods use the same principle. The last method is the simplified approach, which considers that more than one component can be killed by one hit and that the kill of one component has no effect on the kills of the other components, given N hits (or E expected hits). The aircraft kill probability by this method is a logical summation of all redundant and non-redundant critical components

kill probabilities after N hits (or E expected hits), which can be calculated by either binomial or poisson methods.

Ball has also shown that the results from the Markov chain, the simplified approach by the binomial method, and the simplified approach by the poisson method are very similar. Hence, the Markov chain method has been chosen to determine $P_{K/H}$ by multiple hits of nonexplosive penetrators or fragments in this methodology because the matrix can be simple constructed and be less complicated used.

Markov Chain or state matrix method defines the state vector $\{S\}$, which describes all redundant critical component kill states and all possible aircraft kill states given a single hit as:

- One or more of the non-redundant critical components or overlapped critical components have been killed, resulting in an aircraft kill, denoted by $Knrc$.
- One of the redundant critical components Cm has been killed, denoted by $Krc_{n \text{ in } Cm}$.
- All of the redundant critical components Cm have been killed, resulting in an aircraft kill, denoted by Krc_{Cm}.
- None of the non-redundant critical components and none of the redundant critical components are killed, denoted by NK.

Note that a summation of all state probability values in $\{S\}$ must always be unity; or in other words, the aircraft must exist in one of the possible states.

$$\{S\} = \{Knrc \quad Krc_{1 \text{ in } C1} \quad Krc_{2 \text{ in } C1} \quad Krc_{C1} \quad \ldots \quad NK\}^T \tag{3.34}$$

The transition matrix of probability $[T]$ specifies how the aircraft will translate from one state to another as a result of a hit on the aircraft. The state vector after ith hits, where $i = 0, 1, 2, \ldots$ N, is shown in Eqn. (3.35). For instance, if an aircraft includes three non-redundant critical components and one set of two redundant critical components, the transit matrix of probability $[T]$ can be evaluated, as shown in Table 3.4.

where $A_{P_{AC}}$ is an aircraft presented area; $A_{P_{Knrc}}$ is the total presented area of all non-redundant critical components. $A_{P_{Krc_{n \text{ in } Cm}}}$ represents the area of the nth critical component of the mth redundant critical component set. $A_{P_{NK}}$ is the total presented area of all non-critical components. Therefore, the state vector $\{S\}^{(i+1)}$ can be given by:

$$\{S\}^{(i+1)} = [T]\{S\}^{(i)} \tag{3.35}$$

Table 3.4: State transition matrix $[T]$

$1/A_{P_{AC}}$	Probability of transition from this state					To this state
	$Knrc$	$Krc_{1 \text{ in } C1}$	$Krc_{2 \text{ in } C1}$	Krc_{C1}	NK	
	$A_{P_{AC}}$	$A_{P_{Knrc}}$	$A_{P_{Knrc}}$	0	$A_{P_{Knrc}}$	$Knrc$
	0	$A_{P_{NK}} + A_{P_{Krc_{1 \text{ in } C1}}}$	0	0	$A_{P_{Krc_{1 \text{ in } C1}}}$	$Krc_{1 \text{ in } C1}$
$1/A_{P_{AC}}$	0	0	$A_{P_{NK}} + A_{P_{Krc_{2 \text{ in } C1}}}$	0	$A_{P_{Krc_{2 \text{ in } C1}}}$	$Krc_{2 \text{ in } C1}$
	0	$A_{P_{Krc_{2 \text{ in } C1}}}$	$A_{P_{Krc_{1 \text{ in } C1}}}$	$A_{P_{AC}}$	0	Krc_{C1}
·	0	0	0	0	$A_{P_{NK}}$	NK

An aircraft kill is defined by those states that specify either a kill of any of non-redundant components ($Knrc$) or a kill of the members of the m sets of redundant components (Krc_{Cm}). Hence, the probability the aircraft is killed after ith hits is given by

$$P_{K/H}^{(i)} = Knrc^{(i)} + Krc_{C1}^{(i)} + Krc_{C2}^{(i)} + \ldots + Krc_{Cm}^{(i)} \tag{3.36}$$

3.2.6 Aircraft Kill Probability by Proximity Warhead

The proximity-fused high explosive warhead produces primary damage from the blast and high velocity fragments or penetrators generated by the detonation. An aircraft vulnerability given by an external blast is usually expressed as an envelope about the aircraft where the detonation of a specified charge weight high explosive will result in a specified level of damage or kill to the aircraft [6]. Detonation outside of these envelopes will result in little or no damage to the aircraft or in a lesser kill level. Envelopes are determined for a variety of encounter conditions that allow for variations in aircraft speed and altitude, as well as aspect (aircraft view). Aircraft critical components vulnerable to the external blast consist principally of portions of the structure and control surface, which are out of scope of this design methodology. Therefore, the blast damage effect is excluded from the vulnerability assessment module.

On the other hand, penetrators or fragments spray from warhead detonation can directly damage the aircraft following the same principle as multiple hits by contacted warheads or penetrators, as shown in Fig. 3.8. The measure of vulnerability on encounter with this threat is the probability that the aircraft is killed given fusing, $P_{K/F}$. To determine this value, the actual number or expected number of fragments that hit the aircraft has to be calculated first (see Section 3.1.3.3). Then, the aircraft kill probability by those fragment hits can be evaluated using the same kill probability calculation principle as the multiple hits by penetrators (see Section 3.2.5).

3.2.7 Lethal Radius

The lethal radius is an alternative measure of aircraft vulnerability. It is defined as the detonation distance between the proximity warhead and an aircraft, where the aircraft kill probability is 0.5, neglecting of the threat blast effect. The $P_{F/D}$ of proximity warheads can thus be described as a function of the number of fragments (N) depending on detonation distance (s) (details see Section 3.2.6). Assuming that the threat proximity warhead detonates within the lethal radius, the aircraft is then killed. Therefore, the lethal radius can indicate only how good an aircraft is in terms of vulnerability, and will not be considered in this design methodology.

$$P_{F/D} \simeq P_{K/D_{(N\ hits)}} = f(N(s)) = f(s) \tag{3.37}$$

3.3 Probability of Survivability

Aircraft survivability is measured as P_S, which is a function of $P_{K/H}, P_{K/F}, P_{H/D}, P_{F/D}$ and P_D depending on encounter threat types:

$$P_S = 1 - P_K = \begin{cases} 1 - P_D P_{H/D} P_{K/H} & \text{Penetrator} \\ 1 - P_D P_{F/D} P_{K/F} & \text{Proximity warhead} \end{cases} \tag{3.38}$$

Survivability depends upon the encounter threat type, aspect (or aircraft view), and scenario. The survivability assessment for this methodology includes survivability on encounter with both nonexplosive penetrator and proximity warhead (external explosive) in the six main aircraft views; i.e. front, rear, right, left, top and bottom views. In a real combat scenario, an aircraft cannot fly only in one attitude (appearance) (see Fig. 3.13) and $P_D, P_{K/H}, P_{H/D}, P_{K/F}, P_{F/D}$ also depend on the aircraft aspect facing the threat. Therefore, an alternative way to consider this effect is to define the manoeuvrability probability P_{View} (or weighting factors) and to integrate this value into survivability assessment as:

$$P_S = 1 - \sum_{i=Front}^{Top} P_{View_i} P_{D_i} (P_{H/D_i} P_{K/H_i} \text{ or } P_{F/D_i} P_{K/F_i}) \tag{3.39}$$

So, aircraft survivability of each aircraft view (appearance) facing the threat in each flight phase can be determined. The average survivability in each flight phase can finally be evaluated by the summation of the survivability values in each view.

3.3.1 Probability of Manoeuvrability (Weighting Factors)

Due to the real flying and mission specification, an aircraft has to change its aspect (view) facing the threat encounter direction. Therefore, probability of a specific aspect facing the threat (or weighting factors) has been defined and used to determine an average aircraft aspect facing threat encounter direction during a specific flight phase. In this research, this probability of a specific aspect is renamed to probability of manoeuvrability. The probability of manoeuvrability is therefore, defined as the probability of each of the six aircraft views directly facing the threat encounter direction in a specific phase during a sortie. By assuming that threat encounter directions are constant and uniform throughout the mission; multiple aircraft views during each flight phase can be seen by threat weapons, as illustrated in Fig. 3.13. Sometime in the real situation, an aircraft may use terrain to reduce these probability of manoeuvrability in some specific flight phase. If in this case, the total manoeuvrability probability may be less than unity. Unfortunately, this case is out of scope of this research. Therefore, the total manoeuvrability probability in each flight phase for this research has to always be unity.

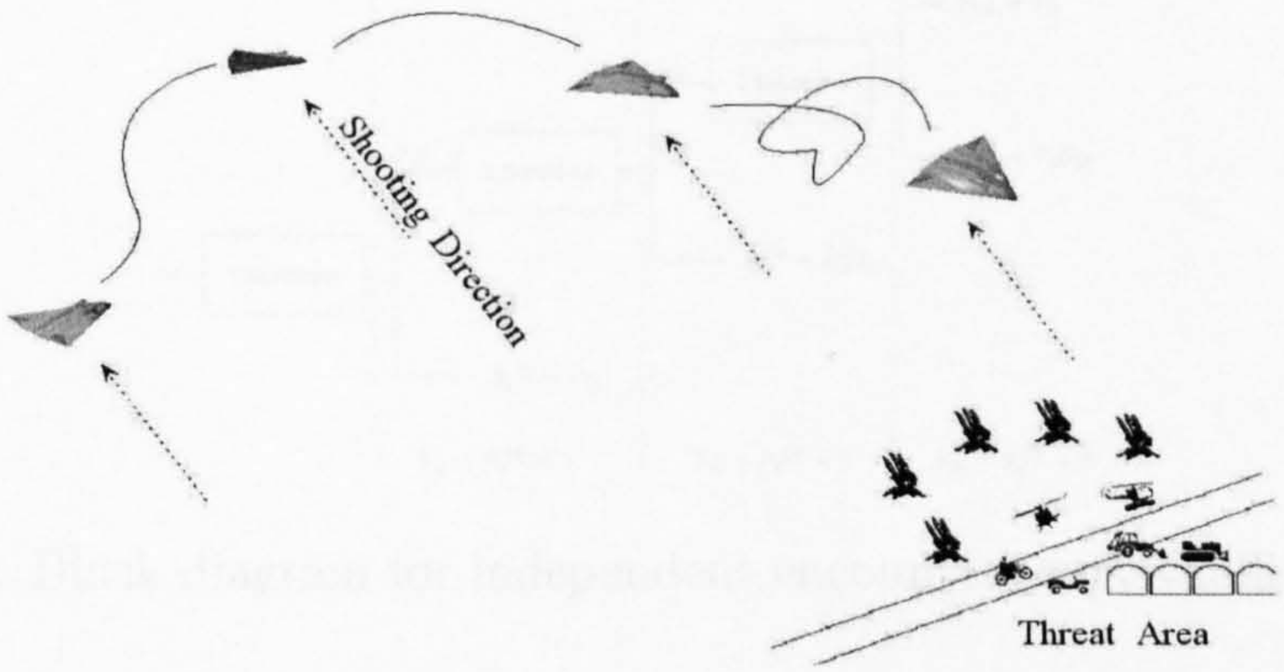

Figure 3.13: Aircraft manoeuvrability in attack flight phase

Table 3.5 shows an example of aircraft manoeuvrability probabilities during the mission simulation. These values will be set up as default values and be used as option 2 of the results shown in chapter 8.

3.3.2 Probability of Encounter

In real combat situations, not only the aircraft manoeuvrability has to be taken into account, but the probability of single or multiple encounters by one or more different threat types during the mission have to be examined. In this section, the effect of probability of

Table 3.5: Aircraft manoeuvrability probabilities

Flight phase	Aircraft views					
	Top	Right	Left	Front	Rear	Bottom
Preflight	0.25	0.00	0.00	0.75	0.00	0.00
Outbound	0.05	0.15	0.15	0.60	0.00	0.05
Attack	0.15	0.15	0.15	0.40	0.00	0.15
Inbound	0.05	0.15	0.15	0.00	0.60	0.05
Postflight	0.25	0.00	0.00	0.00	0.75	0.00

encounter by two main weapon types after each other (cannot be at the same time) on aircraft survivability is introduced.

In a flight phase during a sortie, an aircraft may be shot at several times by one or more weapon types. It is assumed that each threat can encounter only one aircraft and is independent of other threats. The aircraft mission survivability depends on the number of encounters and types of weapon. An aircraft can survive the mission only when it survives each encounter during the mission. The probability that the aircraft survives the ith encounter refers to its $(i-1)$th encounter survivability probability (see Fig. 3.14).

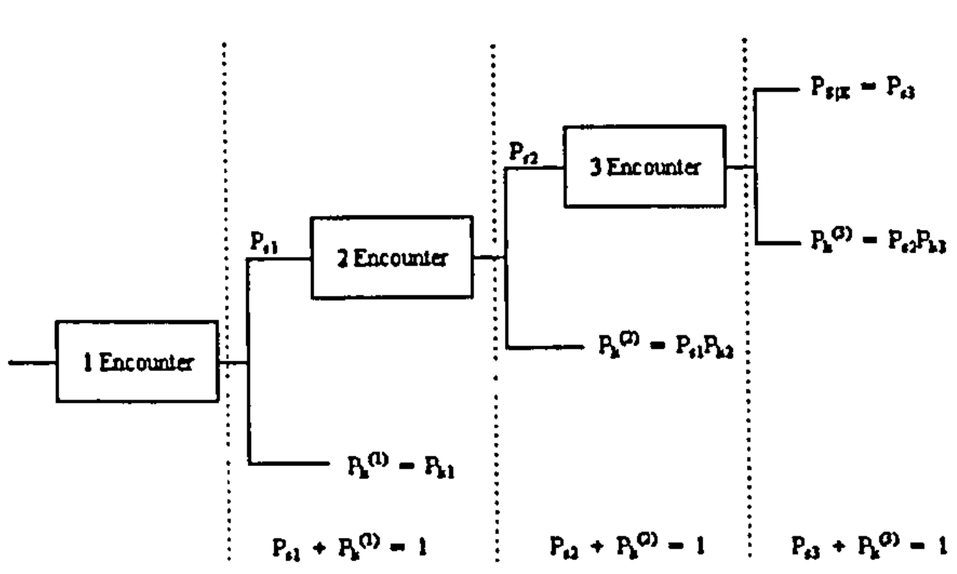

Figure 3.14: Block diagram for independent encounters survivability probability

In the other words, the aircraft can survive the encounters only when it survives all shots. Therefore, an aircraft survivability probability given N encounters from the same weapon type can be determined as follows:

$$\begin{aligned} P_S &= P_{S_1}P_{S_2}P_{S_3}\cdots P_{S_N} = \prod_{i=1}^{N} P_{S_i} \\ &= (1-P_{K_1})(1-P_{K_2})(1-P_{K_3})\cdots(1-P_{K_N}) \\ &= \prod_{i=1}^{N}(1-P_{K_i}) \end{aligned} \tag{3.40}$$

where P_{S_i} is the probability of aircraft survivability given the ith encounter; and P_{K_i} is also the aircraft kill probability given the ith encounter.

If an aircraft encounters N weapon types; each type has an expected number E_i. The aircraft mission survivability is hence calculated as follows:

$$\begin{aligned} P_{S(\text{mission})} &= P_{S(\text{weapon type 1})} P_{S(\text{weapon type 2})} \cdots P_{S(\text{weapon type N})} \\ &= (1 - P_{K_1})^{E_1} (1 - P_{K_2})^{E_2} (1 - P_{K_3})^{E_3} \cdots (1 - P_{K_N})^{E_N} \\ &= \prod_{i=1}^{N} \exp(-E_i P_{K_i}) \end{aligned} \tag{3.41}$$

3.4 Chapter Summary

This survivability assessment chapter has:

- shown an overview of the survivability model.
- presented a simple model to evaluate aircraft RCS by using simple geometric shapes to represent an aircraft.
- shown the determination method of aircraft probability of detection through its radar cross section and opponent radar performance.
- presented alternative simple methods to determine aircraft probability of being hit by contact and proximity warheads.
- explained the vulnerability probability determination methods for the two main threat weapon types.
- introduced manoeuvrability probability and integrated this into the survivability probability.
- explained how aircraft mission survivability probability can be determined through considering susceptibility, vulnerability, and manoeuvrability probabilities.

CHAPTER 4

RELIABILITY & MAINTAINABILITY

Reliability & Maintainability (R&M) is another important design aspect which has to be considered during the combat aircraft design process, because the reliability & maintainability will directly affect to aircraft available for the next sortie, which is one of the objective functions of this research.

Prediction of realistic R&M figures for a combat aircraft during the conceptual and/or preliminary design phases is a continuing problem for both designers and operators. This is primarily due to paucity of hardware details. Theses details are generally not available for analysis and evaluation during the early design stage. A statistical approach is used to estimate the aircraft reliability. On the other hand, aircraft maintainability can be indirectly evaluated by a model used in aircraft life cycle cost estimation.

The main concepts and results will be shown in this chapter, and the rest of principles, methods, models, and results are demonstrated in Appendix C.

4.1 Reliability Assessment

Reliability can be quantified as the probability of successfully completing the mission without failure. Due to the lack of system and component details during the conceptual and preliminary design stage, historical data were statistically analysed and used to develop the reliability probability prediction techniques.

In this section, four reliability assessment alternatives are examined and explained; i.e. Direct linear regression, Pareto distribution, Combination between linear regression and Pareto distribution, and Empty weight functionality.

4.1.1 Direct Linear Regression

Serghides [38] introduced a method to estimate the reliability and maintainability of each aircraft component by using the historical data with statistical analysis. The main principle of this method is to select the two best design parameters in the following criteria to create a linear equation to estimate for both military and civilian aircraft thirteen

component defect rates (DR).

1. Highest linear correlation between aircraft defect rate data with the aircraft design parameter.

2. Engineering judgement basis, for example a design parameter which can indicate size of a system, such as height or weight.

With the selected design parameters, the linear regression equation can be built in the form:

$$DR_{System} = b_0 + b_1 \cdot X_1 + b_2 \cdot X_2$$

where $b_0, b_1,$ and b_2 are constant equation coefficients, and $X_1$and X_2 are selected aircraft design parameters for each particular system.

Serghides also developed a technology improvement factor (TIF) based on the year 1952 to validate his prediction method and multiply this value with the pre-calculated system DR. Hence, the total aircraft DR can finally be calculated by summing all thirteen aircraft components DR:

$$DR_{Aircraft} = \sum_{i=1} DR_{System_i}$$

A newer model was required to ensure correct prediction for modern aircraft, the development was undertaken by Whittle [52]. This model has been used by Woodford [53] to predict total personnel and unit level consumption costs.

4.1.2 Pareto Distribution

Al-Ahmed [1] showed that finding a realistic relationship between the R&M and the conceptual and/or preliminary design variables could be difficult for each system because each aircraft consists of more than thirty different systems. Many of these system's R&M figures are not directly related to the way the aircraft is designed.

Al-Ahmed also discovered that if the aircraft reliability data are sorted in a descending order, this graph follows Pareto distribution regardless of the aircraft age. This means that the whole aircraft reliability can be predicted by a few system reliabilities of aircraft systems failure rate distribution, which contribute 80% of the total failure rate by using Pareto principle [30].

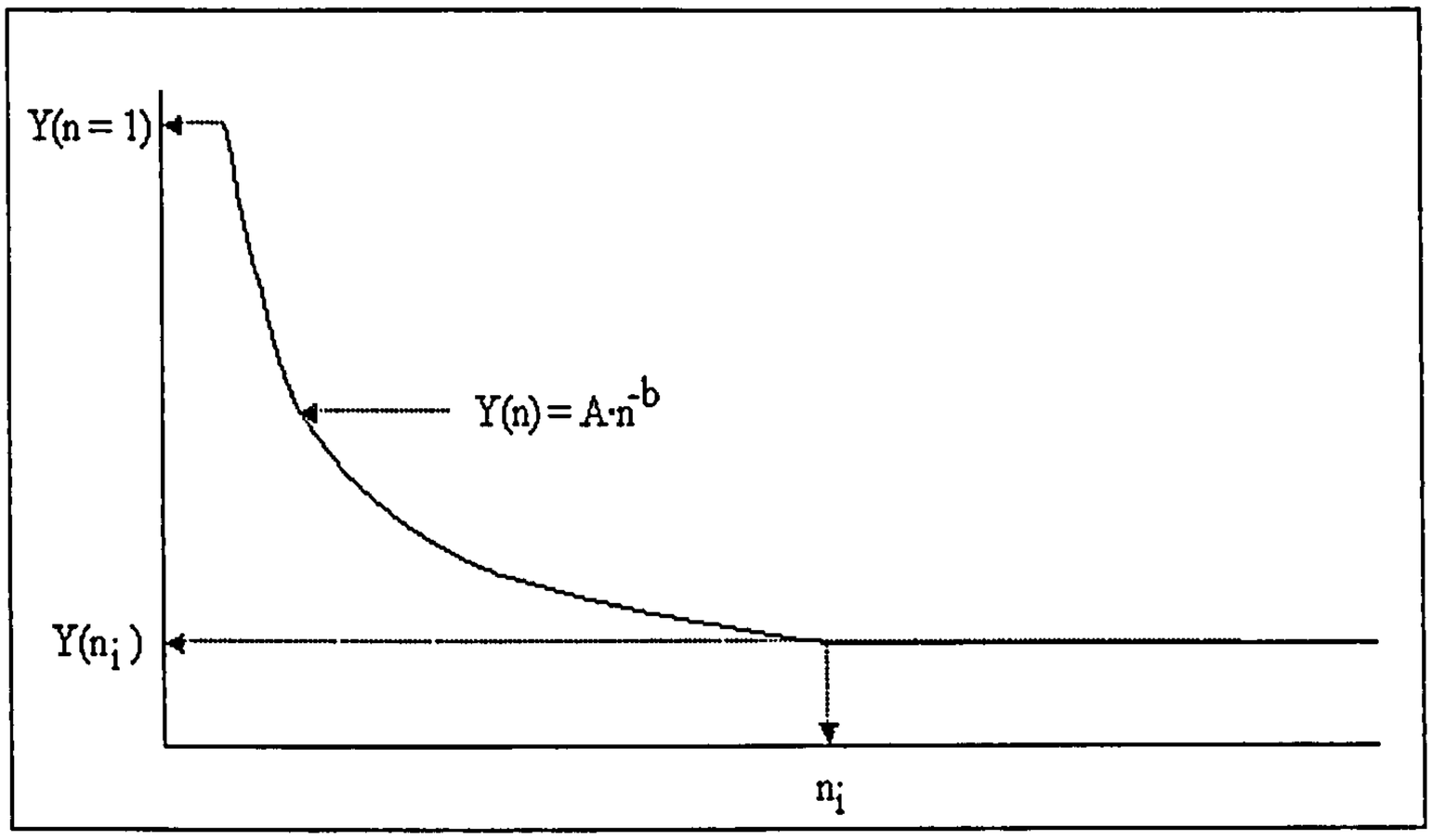

Figure 4.1: Pareto distribution

To approximate this failure rate distribution of aircraft main systems, Al-Ahmed had developed equations to estimate the following parameters, which are necessary to define the Pareto curve, as shown in Fig. 4.1.

1. The highest failure rate figure, $FR(1)$.

2. The lowest failure rate figure, $FR(8)$.

3. Number of systems per aircraft, NoS

Hence, the rest of aircraft system failure rates can also be calculated by using the Pareto distribution in the form:

$$FR(n) = FR(1) \cdot n^{-b} \tag{4.1}$$

4.1.3 Empty Weight Functionality

An alternative to predict an aircraft failure rate is to develop a function of an aircraft empty weight [3], unfortunately this method needs a large number of reliability data, which is not easy to collect due to restriction. However, four linear graphs from available reliability data (1985, 1987, 1993, 1996) are plotted; and show that aircraft failure rate may be possible a function of aircraft empty weight as shown in Fig 4.2.

By using all available aircraft reliability data, an average linear equation for aircraft failure rate evaluation has been discovered as:

$$FR = 0.0476 + 0.0666 \cdot W_e \tag{4.2}$$

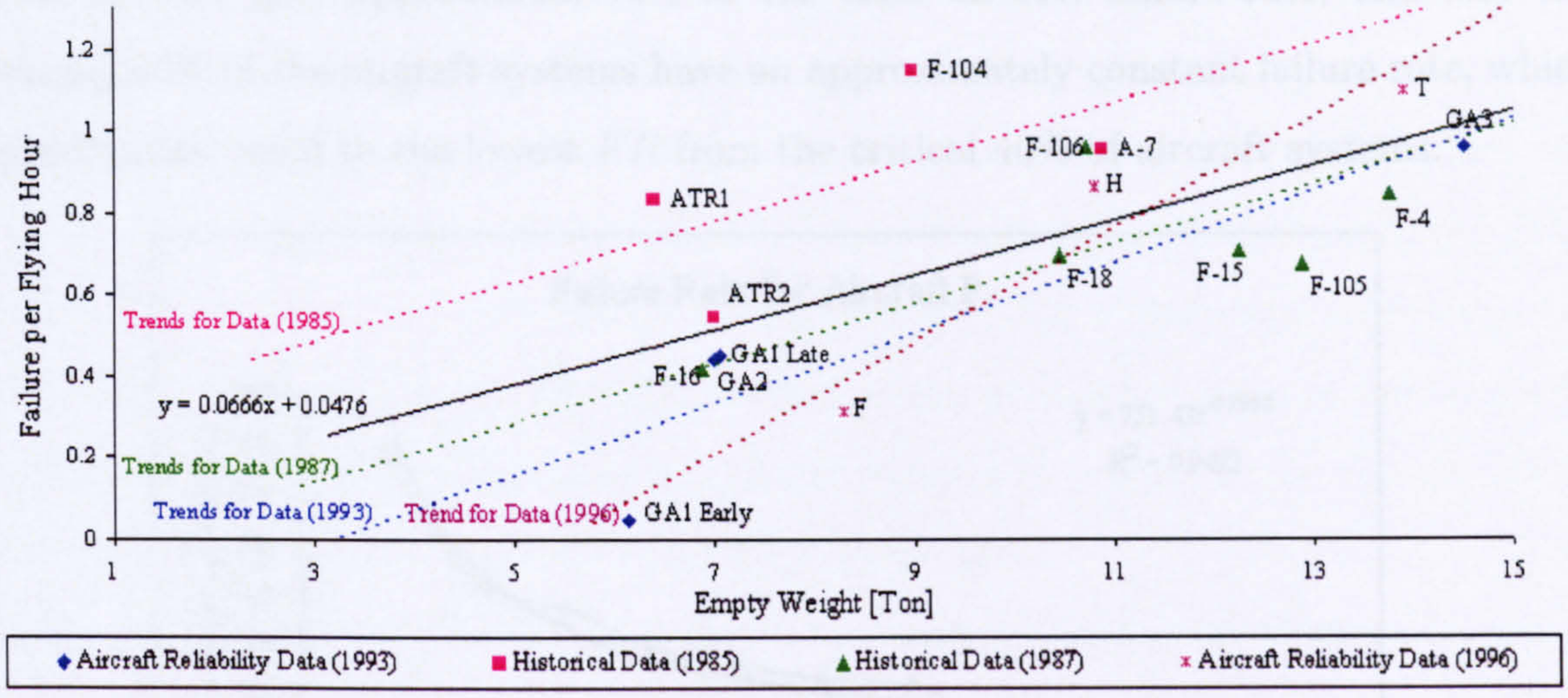

Figure 4.2: Failure rate as a function of empty weight

4.1.4 Combination between Linear Regression and Pareto Distribution

Both Serghides and Al-Ahmed had their own data to produce their models to predict the aircraft reliability, and they are not comparable with each other due to the different aircraft classifications and aircraft technologies used. Additionally, it was possible to predict aircraft reliability by using a combination of the two above aircraft reliability prediction methods with classified data [4].

Firstly, six aircraft design parameters, which relate to almost major aircraft systems, are selected to investigate their linear and exponential correlation with the entire aircraft failure rate. These parameters are

- Aircraft empty weight, W_e
- Number of engines per aircraft, N_e
- Altitude, Alt
- Gross wing area, W_a
- Aircraft height, H
- Total thrust, $Thrust$

Secondly, failure rate distributions of all available data have been plotted and analysed. The 40:70 portion has been found as shown in Fig. 4.3. In other words, 40% of major

aircraft systems give approximate 70% of the total aircraft failure rate; and also the remaining 60% of the aircraft systems have an approximately constant failure rate, which is approximate equal to the lowest FR from the critical 40% of aircraft systems.

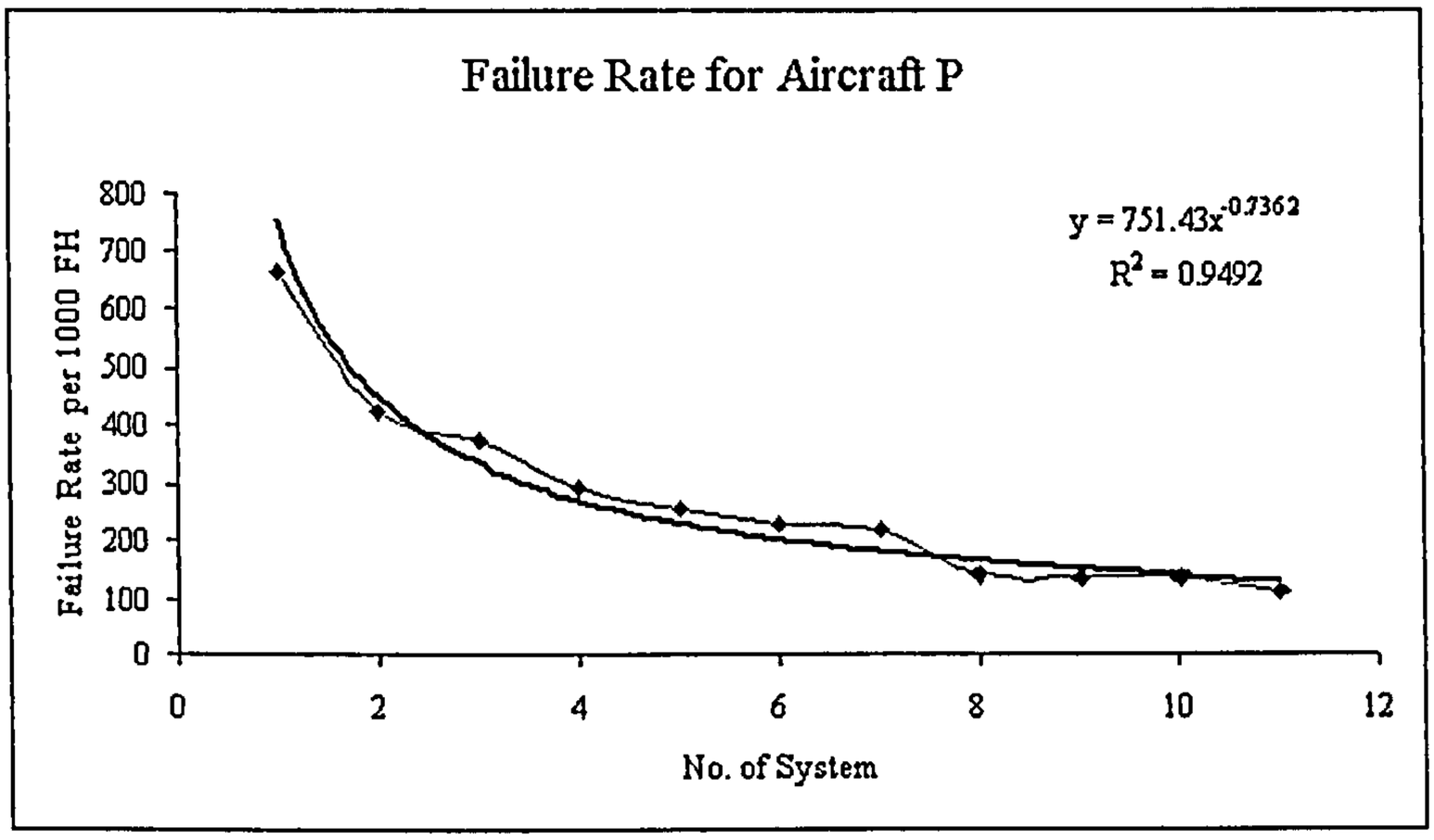

Figure 4.3: Failure rate distribution of aircraft P

The next step is to develop either exponential and/or linear regression equations to predict the highest and the lowest failure rate from two almost complete available data sets [4,38]. The results from these analyses show that linear regression equations are the best solution to predict the highest and the lowest failure rates by assuming that aircraft consist of thirteen major systems (details see Appendix C). The aircraft system failure rate distribution, which is evaluated from these two linear regression equations firmly supports the 40:70 portion of the Pareto principle. The highest and the lowest failure rate are given by:

$$\begin{aligned} FR(100) =& 122.245 - 61.126 \cdot H + 2.299 \cdot Thrust + 0.0149 \cdot W_e + 0.00166 \cdot Alt \\ & + 125.517 \cdot N_E - 1.465 \cdot W_a \end{aligned} \tag{4.3}$$

$$\begin{aligned} FR(70) =& 90.896 - 1.806 \cdot H - 4.9641 \cdot Thrust - 0.0197 \cdot W_e + 0.04018 \cdot Alt \\ & - 232.866 \cdot N_E + 15.88 \cdot W_a \end{aligned} \tag{4.4}$$

$$b = -0.8977117177 \cdot (\log\{FR(70)\} - \log\{FR(100)\}) \tag{4.5}$$

where b is power variable in the Pareto distribution form. $FR(100)$ is the predicted highest failure rate, and $FR(70)$ is the predicted lowest failure rate. Failure rate is assumed to be constant for the remaining 60% of aircraft system.

Because the data used to develop the $FR(100)$ and $FR(70)$ were collected in 90's, they are not quite appropriate with the new design technology used in present aircraft. Therefore, a technology improvement factor has to be examined and be added into the equations. Serghides [38] used the predicted system defect rate and the number of years measured from a reference date (1952) to the first flight of a prototype to develop the TIF for each aircraft system. But this method is too detailed and is not applicable to this design methodology, which expects a simple method to predict whole aircraft failure rate during the conceptual and/or preliminary design process.

With regard to the decreasing trends of the new generation of combat aircraft in terms of both empty weight and failure rate (see Fig. 4.2), an alternative to the TIF development with these relationship may be possible and found as follows:

$$\text{Unmanned Aircraft} \begin{cases} W_e \geq 5000 \text{ kg}, & TIF = 1/3 \\ W_e < 5000 \text{ kg}, & TIF = 1/4 \end{cases}$$

$$\text{Manned Aircraft} \begin{cases} W_e \geq 12000 \text{ kg}, & TIF = 1/2 \\ W_e < 12000 \text{ kg}, & TIF = 1/3 \end{cases}$$

The total aircraft failure rate collected after the year 1985 can thus be evaluated by the summation of thirteen aircraft system failure rates, which are calculated from distribution equations (see Eqn.(4.1)):

$$FR_{Aircraft} = TIF \cdot \sum_{n=1}^{13} FR(n) \tag{4.6}$$

4.2 Maintainability Assessment

Maintainability is defined as the inherent characteristic of an item related to its ability to be restored when the specified maintenance task is performed as required [29]. There are several possibilities to measure the maintainability; such as mean time to repair ($MTTR$), defect man-hour rate ($DMHR$), scheduled maintenance (SM) and so on. In this section, these major three maintainability measures, which relate directly to mission simulation, are described.

4.2.1 Mean Time To Repair

Knezevic [29] introduced methods to measure $MTTR$ by using probability theory. This method can be used when aircraft maintainability function, which is a probability density

function of aircraft $MTTR$, is known. If the number of aircraft systems (N) is known, the $MTTR$ can be given by:

$$MTTR = \int_0^\infty (t \times m(t))dt \tag{4.7}$$

where $m(t)$ is the probability density function of maintainability.

The only available maintainability data set [1] in the form of $MTTR$ were examined with the Pareto distribution approach; it was found that $MTTR$ followed approximately the 40:60 relationship. This method can provide a probability density function in a form of a power expression. The possible methods to predict $MTTR_{Aircraft}$ are:

1. Using Pareto distribution as a probability density function of maintainability:

$$MTTR_{Aircraft} = \int_1^N (n \cdot (MTTR(100) \cdot n^b))dn = \frac{MTTR(100)}{2+b}(N^{(2+b)} - 1)$$

2. Using direct integration on Pareto distribution curve:

$$MTTR_{Aircraft} = \int_1^N (MTTR(100) \cdot n^b)dn = \frac{MTTR(100)}{1+b}(N^{(1+b)} - 1)$$

3. Using Pareto principle 40:60 portion: This method is similar to the above aircraft failure rate evaluation; the difference is that the portion of the total $MTTR$ is given by a small number of aircraft systems.

4. Using assumed value: Burleigh [10] calculated $MTTR_{Defect} = 1.53$ hours from HAWK data and $MTTR_{Damage} = 2.6$ hours from A-10 data. These two values are used as default assumed values throughout this research due to lack of maintainability data in the form of $MTTR$.

4.2.2 Scheduled Maintenance

Woodford [53] presented a scheduled maintenance requirement for aircraft with the model taken from a paper by Harmon [14]. The method predicts the scheduled inspection and maintenance effort requirements based on a systematic approach, and can be split into five discrete sections; pre-flight, post-flight, periodic (avionics), special (propulsion), and periodic (shop-propulsion).

Pre-flight:

$$SM_{Pre-Flight} = \frac{(0.3763 + 3.9462E-5 \cdot M_{A/C})}{\sqrt{(1 - MAT_{Composit})}} \times 0.99^{YR52} \quad (4.8)$$

Post-Flight:

$$SM_{Post-Flight} = \frac{(1.2556 + 1.807772E-5 \cdot M_{A/C})}{\sqrt{(1 - MAT_{Composit})}} \times 0.99^{YR52} \quad (4.9)$$

Periodic (Avionics):

$$SM_{Avionics} = (0.3266 + 2.06252E-3 \cdot WV + 2.41588E-3 \cdot ROAC) \times 0.98^{YR52} \quad (4.10)$$

Special (Propulsion):

$$SM_{Propulsion} = (0.344 + 1.04991E-5 \cdot T_{SL_{Max}}) \times 0.985^{YR52} \quad (4.11)$$

Periodic (Shop-Propulsion):

$$SM_{2-Propulsion} = (0.1603 + 4.968525E-6 \cdot T_{SL_{Max}}) \times 0.985^{YR52} \quad (4.12)$$

Total aircraft scheduled maintenance (SM):

$$SM = SM_{Pre-Flight} + SM_{Post-Flight} + SM_{Avionics} + SM_{Propulsion} + SM_{2-Propulsion} \quad (4.13)$$

These models are very simple because they are based mainly on mass and thrust. Unfortunately, there are paucity data available for scheduled maintenance; therefore, it is extremely difficult to check the accuracy of this model [53].

4.2.3 Unscheduled Maintenance

With the same principles as aircraft failure rate prediction, an aircraft defect-man hour rate ($DMHR$) will be predicted. The 40:70 ratio described in section 4.1.4 was again been observed. Due to the limited data avaiable [4,38] to develop models for $DMHR(100)$, $DMHR(70)$ and TIF, only two possible alternatives are examined and shown in this methodology, as follows:

1. Combination between linear regression and Pareto distribution: This method uses the same principle, aircraft design parameters, and number of aircraft components

assumption as the model for FR calculation. By using historical data [4,38], the $DMHR$ equations can be given as:

$$DMHR(100) = 4615.4050 - 230.2682 \cdot H + 24.0820 \cdot Thrust - 0.0501 \cdot W_e - 0.2296 \cdot Alt + 696.7274 \cdot N_E - 9.7865 \cdot W_a \quad (4.14)$$

$$DMHR(70) = 518.5990 - 19.6558 \cdot H - 3.7209 \cdot Thrust - 0.00054 \cdot W_e - 0.02297 \cdot Alt + 59.4110 \cdot N_E - 1.8700 \cdot W_a \quad (4.15)$$

$$b = -0.8977117177 \cdot (\log\{DMHR(70)\} - \log\{DMHR(100)\}) \quad (4.16)$$

$$DMHR_{Aircraft} = \sum_{n=1}^{13} DMHR(n) = \sum_{n=1}^{13} DMHR(100) \cdot n^b \quad (4.17)$$

2. Functionality of aircraft empty weight: From available maintainability data, two linear $DMHR$ against aircraft empty weight traces were plotted. However, only two data sets are available, but the both trends of $DMHR$ against empty weight can be clearly identified as shown in Fig. 4.4. Therefore, an average trend can be also used to predict general aircraft DMHR as:

$$DMHR = 12.221 - 0.8009 \cdot W_e \quad (4.18)$$

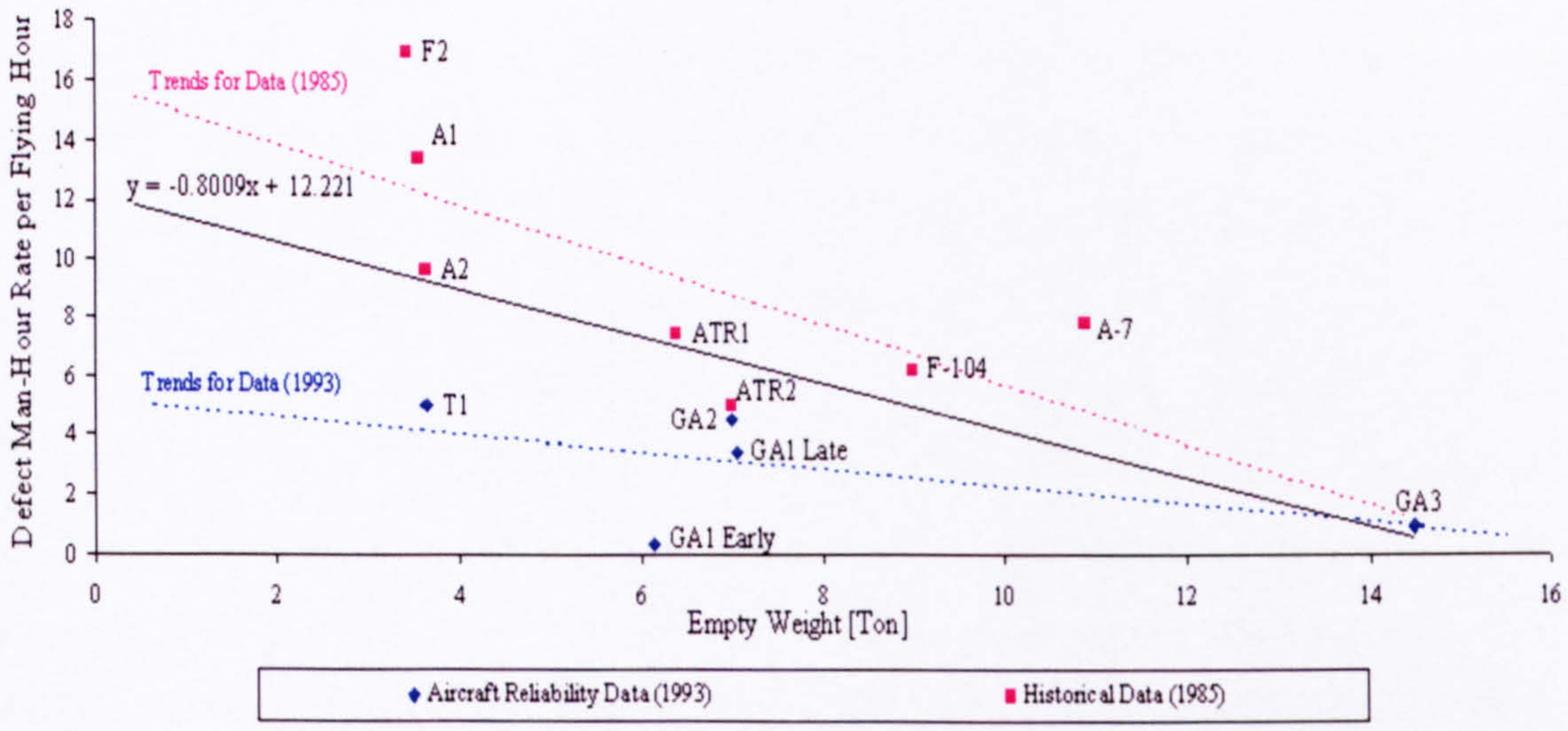

Figure 4.4: Defect man-hour rate as a function of aircraft empty weight

4.3 Chapter Summary

This chapter has

- introduced a possible method to estimate aircraft reliability by using historical data with statistical analysis in the form of linear correlation and regression [38].
- shown a possible method to estimate aircraft reliability by using Pareto distribution [1].
- presented a developed alternative model to predict aircraft failure rates by combining the above mentioned two models with consideration of technology improvement factors.
- shown a very simple model to estimate aircraft failure rate as a function of its empty weight.
- presented three alternative measures of maintainability; i.e. MTTR, Scheduled and Unscheduled maintenance.
- shown alternative models to predict these three measures.

CHAPTER 5

LIFE CYCLE COST ESTIMATION

This methodology attempts to integrate an operational cost analysis into the early design stage by dint of using mission simulation, taking aircraft mission requirement into account. However, there are some unpredictable parameters during aircraft design processes; such as threat performance, military readiness requirement, and mission strategy and so on. The accurate operation cost is therefore more difficult to predict. An alternative to evaluate this value is reversed calculation from aircraft Life Cycle Cost (LCC).

There are numerous number of studies and bodies of research to model LCC, which differ in the details that they consider [11,25,37,45,46,53] . However, LCC can generally be split into five main sections; i.e. Research, Development, Test and Evaluation; Production; Ground Support Equipment and Initial Spares; Operation and Support; and Disposal Costs.

$$LCC = C_{RDT\&E} + C_{Production} + C_{GSE\&IS} + C_{Operation} + C_{Disposal} \tag{5.1}$$

The model used in this methodology is based on the model from Woodford [53], which can predict aircraft LCC mainly during the peacetime operation. The operation cost in LCC includes all costs, which can occur during aircraft life time. Therefore, the total operational cost per flying hour, which include operation, personnel, support and maintenance cost per flying hour, can be evaluated. Additionally, an aircraft lost cost and weapon expense during a mission from a mission simulation module will be added up to estimate the total mission operational cost (details see section 5.6).

Because of variation in inflation and foreign currency values, price can fluctuate according to local economic condition. Therefore, LCC will be simply represented as a 'then-year' value, which is defined as a constant base year dollar value including the effects of inflation or escalation, and/or reflect the price levels expected to prevail during the year of issue [15,31]. To include this inflation in the life cycle cost estimation, the Consumer Price Index (CPI) is integrated into most equations. The CPI has been normalised to 1983 dollars, with regard to the definition given by the U.S. Department of Labor, Bureau of the Labor Statistics [49].

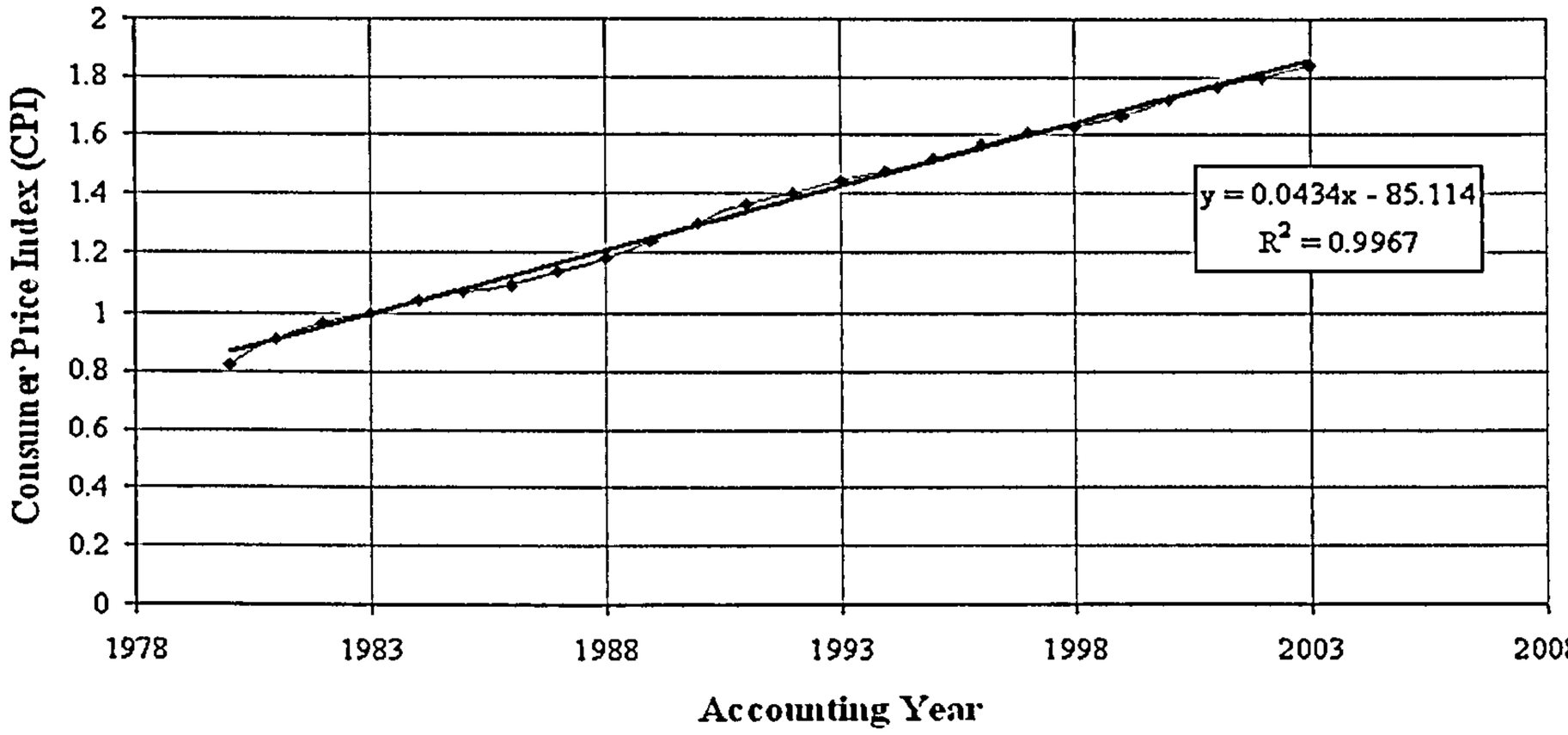

Figure 5.1: Consumer Price Index, 1983 = 1.00

Fig. 5.1 shows the average CPI from 1978 to 2003 published monthly by the United States Department of Labor, Bureau of Labour Statistics [49], which can be simply modelled as a linear equation as:

$$CPI = 0.0434(YRACC - 1983) - 85.114 \tag{5.2}$$

In this chapter, the principle method to predict an operational cost used in mission simulation will be introduced. Complete calculation methods and results are described in Appendix D.

5.1 Research, Development, Test & Evaluation Cost

The Research, Development, Test & Evaluation (RDT&E) cost covers all areas of research and development prior to full-scale production of the aircraft. This cost typically makes up about 15-20% of the LCC of modern, low-production combat aircraft, and is obviously affected by the number of aircraft over which this cost can be amortised.

The model of RDT&E cost estimation is based on Burns [11] and Birkler [8] with validation by Woodford [53]. This method breaks the RDT&E cost into airframe development cost, engine development cost, and avionics development cost. These procedures obtain many different activities, and can thus be thought of as a 'Activity-Based Costing' procedure, which are calculated as an effort quantity (hours) and will be multiplied with the labour rates to estimate these costs (for the full model see Appendix D).

5.1.1 Airframe Development Cost

There are several activities to complete an airframe development. Each activity cost depends on its effort quantity (hours) and labour rate as follows:

1. Engineering cost for the airframe development can be estimated as a function of airframe unit weight, maximum true velocity, number of developed aircraft, number of partners, percentage of advanced material usage and also engineering labour rate.

2. During the airframe development, all development support attributed to engineering cost can be evaluated as a function of airframe unit weight, maximum true velocity, number of developed aircraft, consumer price index, security factor and number of partner.

3. Flight testing cost includes all costs incurred by the aircraft manufacturer to complete flight testing, except the cost of the production of the flight test aircraft. This cost can be estimated as a function of airframe unit mass, maximum true velocity, number of developed aircraft, consumer price index, security factor and advanced technology testing factor.

4. Tooling cost mainly depends on the aircraft production rate, high production rates result in higher tooling cost. This cost also depends on airframe unit mass, maximum true velocity, number of developed aircraft, number of partners, and tooling labour rate.

5. Development manufacturing labour cost includes all costs necessary for machining, fabricating, assembly of the major structure, installation of purchased parts, government furnished equipment, and subcontractor assemblies and components.

6. Manufacturing material and equipment cost is based on the low-observable features usages, this cost excludes engines and avionics.

5.1.2 Engine Development Cost

The engine development cost estimation methodology is based on the model developed by Birkler [8] and validated by Woodford [53]. This model can estimate the engine development cost before entry into service as a function of engine sea-level static gross thrust, mach number for supersonic design, and the maximum turbine inlet temperature.

However the cost of the engines for the development aircraft can be estimated differently. Mr. P. Pugh, formerly of the Directorate Project, Time, and Cost Analysis (DPTCAn), a division of the Ministry of Defence, suggested that production engine cost is an approximately 75% of the development engine cost. With the number of engines purchased for the RDT&E, depending on the number of test aircraft and the number of engines per aircraft, the total cost of engine for development aircraft can be found.

5.1.3 Avionics Development Cost

The avionics development cost estimation is contrary to the other development cost estimation because development and production cost of individual avionics systems are more dependent on the performance of that particular system, which is not measured in aircraft design terms.

An alternative model to estimate avionics cost model is based on the uninstalled avionics mass, which is approximated 90% of the total avionics mass [11,46].

5.2 Production Cost

Production cost is typically about 45-50% of the total LCC of modern combat aircraft, and also includes production engineering design, production investment (manufacturing facilities, tooling, jigs and fixtures), manufacturing labour, quality control, material and equipment, profit, overheads, administration, and purchasing of engines and avionics systems. This cost per aircraft decreases with the number of aircraft built, as learning curve theory and economies of scale are applied [54].

Most estimation models for the production cost, except engine production cost, are similar to the model of RDT&E cost estimation, only they use both total number of developed aircraft and total number of production aircraft instead of number of just developed aircraft.

5.3 Ground Support Equipment and Initial Spares

The Ground Support Equipment and Initial Spares (GSE&IS) cost is very difficult to estimate, but with suggestions made by several members of the costing community, GSE&IS cost is simply set to 10% of the aircraft recurring flyaway cost [53], which is equivalent to

the total production cost divided by number of production aircraft. This gives approximately 5% of total LCC.

5.4 Operation and Support

The operation and support (O&S) cost is the biggest portion of the total LCC and the most relevant to this design methodology. O&S costs for modern combat aircraft can be split into several major parts as follows:

5.4.1 Personnel Cost

Personnel costs depends on the number of officers, enlisted staffs, and civilian personnel in the first and second lines operation, and in support. The number of the first line operation personnel depends mainly on the scheduled maintenance, number of operational aircraft, and annual flying hours. On the other hand, the number of the second line operation personnel, which consists of officers, enlisted and civilian personnel, depends on unscheduled maintenance, DMHR (for details see chapter 4). This cost also includes the personnel cost for the service allowances, personnel support and training

5.4.2 Unit Level Consumption

This cost attempts to include all costs for consumables used in maintaining the aircraft, maintenance materials, miscellaneous support supplies, depot level repares, and temporary additional duty. The unit level consumption estimation model can be divided into eight main categories as follows:

1. Annual used fuel cost.
2. The cost of other petroleum, oil and lubricants.
3. Maintenance material cost.
4. Miscellaneous support supply.
5. Depot level repares.
6. Temporary additional duty.
7. Transport.
8. Other.

5.4.3 Contracts

This cost has been modified to calculate an annual contract value, rather than using the work-breakdown approach like the one for first and second line maintenance [53]. This cost consists of the three main aircraft systems; i.e. airframe, propulsion, and avionics and supplies.

5.4.4 Sustaining Support Cost and Installation Support Funds

This cost includes the replacement support equipment cost; cost of modification kit procurement; sustaining engineering support; and cost incurred by the personnel pay and allowance, material, and utilities needed for the maintenance of the base.

Normally an aircraft will be operated for a life of approximately 20 - 30 years. However, the summation of all of the previously calculated costs is an approximate expense only for one year of operation and support in the form of 'then year' dollars (or 'accounting-year' dollars). Therefore, the economic discount rate (RED) at 6 % per annum has to be added for each year of operation and support. This rate is used for the majority of government projects [53].

5.5 Disposal

The disposal cost consists of disassembly labour, disposal of non-reusable material, sale of scrap material, and resale of on-board equipment. Depending on the relative values of these different components, the total disposal figure could be positive (cost), or negative (credit).

The chosen model used in this methodology, developed by Woodford [53] is to add the estimated cost of labour to dismantle the aircraft, the cost of disposing of the non-reusable items, and subtract the value of the reusable items. The resale of systems is thought to be unlikely for the moment, as technology in these areas changes so quickly; the value of these items has been neglected.

Total aircraft LCC can be calculated as the summation of the above mentioned costs as Eqn. 5.1 shows. Fig. 5.2 - 5.3 shows the results of LCC estimation of the U-99 aircraft during peacetime and wartime operations.

5.6 Mission Operational Cost

The mission operational cost depends mainly on mission scenario, i.e. wartime or peacetime. As described above, the model used to estimate aircraft LCC in this methodology is based on peacetime operations; therefore, some maintenance costs will be deducted from total O&S cost during wartime operations. The weapon expense and aircraft lost cost will be included into the operation & support cost during wartime operations instead.

5.6.1 Operational Cost during Peacetime Operations

In peacetime operations, aircraft will be well maintained subject to high mission readiness. In this case, the entire four maintenance lines in Woodford's [53] model are included to predict the total operation & support cost. But the predicted total cost is an approximate operation & support expense for the entire aircraft life; therefore, an average O&S cost per aircraft per flying hour can be given as:

$$C_{\overline{Operation}} = \frac{C_{Operation}}{N_{Operation} \cdot TLIFE \cdot FHY} \tag{5.3}$$

Hence, the total mission operational cost during peacetime operation in this methodology can be estimated as:

$$C_{Mission} = C_{\overline{Operation}} \cdot \sum_{i=1}^{N_{Operation}} FH_i \tag{5.4}$$

5.6.2 Operation Cost during Wartime Operations

On the other hand, for the calculation of O&S cost during a wartime scenario in this mission simulation, the third and the forth line maintenance (contract cost) will be omitted. Additionally, expense of weapons and aircraft lost will be taken into account instead. Hence, an aircraft operation cost in LCC calculation has to be calculated as:

$$C_{Operation} = C_{Unit} + C_{Sustain} + C_{Personnel} + C_{Install} + C_{Training} \tag{5.5}$$

Therefore, the total mission operational cost in wartime scenario in mission simulation can be given as:

$$C_{Mission} = C_{Weapon} \cdot N_{Weapon} + C_{Flyaway} \cdot N_{Lost} + C_{\overline{Operation}} \cdot \sum_{i=1}^{N_{Operation}} FH_i \tag{5.6}$$

where $C_{\overline{Operation}}$ is an average operational cost per aircraft per flying hour in wartime, which can be estimated as shown in Eqn. (5.3). N_{Weapon} is the number of released

weapons in a mission simulation and N_{Lost} is the number of aircraft lost during the same simulation.

5.6.3 Measure of Operational Cost

As described above, an operational cost includes all expenses, which occur during mission simulation. There is lots of information hidden in this cost, which can be linked and be used in conjunction with aircraft MOPs for specified design aspects. For instance, the total maintenance cost during the mission simulation can be linked with aircraft MOPs in reliability & maintainability in the form of $FR, DMHR,$ and SM. The explanation is that FR directly affects the number of maintenance aircraft in a mission simulation; and maintenance cost is also a function of aircraft $DMHR$ and SM (for the complete equation see Appendix C).

From the aircraft life cycle cost estimation, the following cost can be broken down and may be used in this methodology to measure aircraft operational cost effectiveness.

1. Operational maintenance cost: This cost covers all consumables used in maintaining the operational aircraft throughout the simulation excluding fuel, petroleum, oil, and lubricant. The operational maintenance cost per aircraft per flying hour can be estimated from following equation:

$$C_{Maintenance} = \frac{(C_{Unit} - C_{Fuel})(1 - DEF)}{RED \cdot N_{Operation} \cdot TLIFE \cdot FHY} \tag{5.7}$$

$$DEF = (1 + RED)^{-TLIFE} \tag{5.8}$$

2. Flyaway cost: This cost is used to indicate the average expense to build an aircraft, which can be estimated as:

$$C_{Flyaway} = \frac{C_{PROD}}{N_{PROD}} \tag{5.9}$$

3. Mission operational cost: This cost includes all expenses occurring in the mission simulation, which covers released weapon cost and aircraft lost cost.

4. Flying hour cost: This rate will indicate how much the flying hour cost is for each aircraft.

$$C_{FH} = \frac{C_{Mission}}{N_{FH} \cdot N_{Operation}} \tag{5.10}$$

5. Cost[$] / Target: This cost is one of the main objectives of this research, by calculating a ratio between all expenses occurring in the mission simulation and the number of targets killed ('Bang per Buck').

$$C_{Target} = \frac{C_{Mission}}{N_{Kill}} \tag{5.11}$$

6. Cost[$] / Sortie: This cost can be used to indicate how much every take-off will cost.

$$C_{Sortie} = \frac{C_{Mission}}{N_{Take-off}} \tag{5.12}$$

7. Cost[$] / Successful Sortie: This cost shows an average cost for each sortie, in which an aircraft releases a weapon and returns to base, regardless of whether the target is damaged or destroyed.

$$C_{SuccessfulSortie} = \frac{C_{Mission}}{N_{SuccessfulSorties}} \tag{5.13}$$

Aircraft Name : U-99 in PEACE TIME

Airframe Mass	941.69	Kg	Uninst. Avionic Mass	151.72	Kg	Aircraft Mass	4547.23	Kg	Fuel Mass	488.52	kg
Max. Thrust	19.82	kN	Max. Velocity	437.69	Km/h	Max. Mach	1.00		Max. Inlet-Temperature	1055.05	K
Adv. Materials	33.520	%	Disposal Labour	5.000	%	Economic Discount	6.000	%	Account Year	2004	
Year Entry Service	2006		Develop Aircraft	5		Static Aircraft	4		Test Aircraft	5	
Production Aircraft	500		Operation Aircraft	10		Aircraft Crew	1		Annual Flying	125.00	Hrs
Life Time	4.00	Years									
Development			Production			Operation & Support			Disposal		
Airframe	157.624	M$	Airframe	1268.113	M$	Personnel	11.204	M$	Advanced Materials	0.008	M$
Avionic	533.537	M$	Avionic	1228.460	M$	Service Training	1.525	M$	Composite Materials	-6.481	M$
Engine	58.950	M$	Engine	103.912	M$	Contract	2.699	M$	Labour	39.775	M$
Software	2627.400	M$	Unit & Flyaway	5.201	M$	Install Support	1.015	M$			
						Unit Level	0.824	M$			
						Sustain Support	0.471	M$			
Total	3377.511	M$	Total	2600.484	M$	Total	17.738	M$	Total	33.303	M$
			Ground Support	260.048	M$	Total 4.00 Yr	61.463	M$	Deflated Disposal	26.379	M$
Total LCC			Discount LCC/AC			Cost/AC/FH					
RDT&E	3377.511	M$		6.688	M$	Personnel	7764.326	$			
Production	2600.484	M$		5.149	M$	Contract	553.285	$			
Ground Support	260.048	M$		0.520	M$	Unit Level	571.335	$			
Operation	61.463	M$		6.146	M$	Ground	1040.194	$			
Disposal	26.379	M$		0.052	M$	Operation	12292.561	$			
Total	6325.885	M$		18.556	M$	Fly Away	5.201	M$			

Figure 5.2: Results of U-99 LCC estimation in peacetime scenario

Aircraft Name : U-99 in WAR TIME

Airframe Mass	941.69	Kg	Uninst. Avionic Mass	151.72	Kg	Aircraft Mass	4547.23	Kg	Fuel Mass	488.52	kg
Max. Thrust	19.82	kN	Max. Velocity	437.69	Km/h	Max. Mach	1.00		Max. Inlet-Temperature	1055.05	K
Adv. Materials	33.520	%	Disposal Labour	5.000	%	Economic Discount	6.000	%	Account Year	2004	
Year Entry Service	2006		Develop Aircraft	5		Static Aircraft	4		Test Aircraft	5	
Production Aircraft	500		Operation Aircraft	10		Aircraft Crew	1		Annual Flying	125.00	Hrs
Life Time	4.00	Years									
Development			Production			Operation & Support			Disposal		
Airframe	157.624	M$	Airframe	1268.113	M$	Personnel	10.205	M$	Advanced Materials	0.008	M$
Avionic	533.537	M$	Avionic	1228.460	M$	Service Training	1.454	M$	Composite Materials	-6.481	M$
Engine	58.950	M$	Engine	103.912	M$	Contract	0.000	M$	Labour	39.775	M$
Software	2627.400	M$	Unit & Flyaway	5.201	M$	Install Support	0.932	M$			
						Unit Level	0.675	M$			
						Sustain Support	0.352	M$			
Total	3377.511	M$	Total	2600.484	M$	Total	13.618	M$	Total	33.303	M$
			Ground Support	260.048	M$	Total 4.00 Yr	47.189	M$	Deflated Disposal	26.379	M$
Total LCC			Discount LCC/AC			Cost/AC/FH					
RDT&E	3377.511	M$		6.688	M$	Personnel	7072.335	$			
Production	2600.484	M$		5.149	M$	Contract	449.668	$			
Ground Support	260.048	M$		0.520	M$	Unit Level	467.718	$			
Operation	47.189	M$		4.719	M$	Ground	1040.194	$			
Disposal	26.379	M$		0.052	M$	Operation	9437.881	$			
Total	6311.612	M$		17.129	M$	Fly Away	5.201	M$			

Figure 5.3: Results of U-99 LCC estimation in wartime scenario

5.7 Chapter Summary

This chapter has

- introduced a model to integrate the aircraft life cycle cost estimation into a conceptual/preliminary design process.
- shown an alternative to convert part of LCC to mission operational cost during an early design stage.
- presented measures of aircraft operational-cost effectiveness in this design methodology.

CHAPTER 6

OPERATION MISSION SIMULATION

Due to the fact that the environment of a real mission is far too complex. Therefore, a simulation is used as a tool to examine the relationships between aircraft design aspects and to predict mission and operation measures of performance and effectiveness in the designed aircraft operational environments. Some constraints, assumptions and also definitions of the simulation are described here in this chapter.

6.1 Threat Analysis

From statistical data from the Gulf War in 1991, only 14 aircraft from over 923 USAF combat aircraft were lost. There were all lost to ground-based air defense, and none were lost in air-to-air combat [20,35]. Therefore, the two major weapon types examined and considered within the mission operation simulation in this study are anti-aircraft artillery (AAA), which are represented by nonexplosive penetrator or contacted warheads, and surface to air missile (SAM), which are represented by proximity warheads.

6.1.1 Nonexplosive Penetrator or Contacted Warhead

In this study, the nonexplosive penetrator or contacted warhead represents the threat posed by bullets or cannon sizes from 14.5 - 57.0 mm. These threat types can be anti-aircraft self-propelled, towed and machine guns; such as ZPU-series 14.5-mm towed anti-aircraft guns, ZSU-57-2 self-propelled anti-aircraft gun systems, and ZSU 23-4 self-propelled anti-aircraft guns. The maximum altitude of the shell when fired in the anti-air role for these systems can be up to 15000 m depending on their caliber size [26].

Kill methodology for this threat type is to penetrate along the shotline through the aircraft from one side to another side. Aircraft components, which are on this shotline, will not be functional regardless of their kill level. But in this simulation, the contemplation of timescale during a sortie is not a relevant issue; therefore, every kill level given to an aircraft component will be considered as an immediate kill in that flight phase.

Because of high revolution rate of automatic machine guns installed in these systems,

an aircraft will probably encounter several shots, even if the aircraft flies through this defense system in a short period. By assuming that the shots keep constant direction and parallel with each other, and attack perpendicular to aircraft view, the probability of kill by this threat type will be estimated via Markov matrix with random numbers of hits.

6.1.2 Proximity Warhead

The surface to air missile represents a proximity warhead in this mission simulation. This threat system can be deployed from fixed installations or mobile launchers, their tracking and guidance system may use radar, infrared, or laser. High explosive warheads with internally grooved fragmentation can be proximity, contact and also command fused. Target initial detection range depends on the frequency of the installed radar system.

Kill mechanism for this kind of threat can be given as:

1. Explosion inside aircraft or on contact with aircraft: In this case, detonation occurs immediately or shortly after warhead impacting target. The results are detonation on or inside the aircraft with the accompanying blast and fragment spray in many directions. To predict this kill method exceeds the scope of this study.

2. Blast: The missile explodes its warhead outside the target within explosion distance. In most externally detonating warheads the blast is a secondary damage mechanism, which will be neglected in this study.

3. Fragments: After warhead detonation, internal fragments will spread around the warhead within the fragment spray zone (see Chapter 3). Fragments can also be treated as penetrators with the assumption of uniform constant direction and velocity. The number of fragment hits depends on the detonation distance and target presented area.

As described above, in this mission simulation, blast effect will be neglected and the SAM is always assumed to be proximity fused with random detonation distance. The kill methodology of this threat type can be converted into multiple hits by fragments, and its kill probability can be also determined as the same principle using the multiple hits by penetrators.

Probability of encounter by one threat type is a ratio of the number of single types

of weapon to the number of aircraft flying throughout the mission. In this mission simulation the probability of encounter by penetrator ($E_{Penetrator}$) and by proximity warhead ($E_{Proximity}$) will be assumed as constant values of 0.05 and 0.02.

6.2 Mission Analysis

Military aircraft are designed to execute one or more roles; but each category needs specific performance to complete every particular task during the mission. Generally, military missions can be divided into two main categories: tactical and strategic combat; and combat support mission.

Tactical and strategic combat mission has been chosen for this design methodology concept with several alternative missions studied; such as combat patrol, air superiority, and escort. Finally, bombing mission has been selected to be the primary mission due to the case study aircraft (U-99) specification used. The flowcharts of studied missions are shown in Appendix E.

The bombing mission used in this mission simulation using the U-99 specification [40,41] can be described as:

- There are five main flight phases in a sortie; Pre-Flight, Outbound, Attack or Penetration, Inbound, and Post-Flight phase.
- Outbound and Inbound phases include a cruise segment of 750 nm or 1389 km with a cruise speed of Mach 0.78 at 40000 ft or 12192 m.
- U-99 releases its weapon during the attack or penetration phase at 25000 ft or 7620 m with 1.5 turn.
- Take-off and landing distance should be less than 3500 ft or 1066.8 m.
- The weapon carried is a Joint Direct Attack Munition (JDAM) which is installed in the weapons bay above the main fuel tank. Its weight is approximately 454 kg. Therefore, U-99 has to fly upside down before releasing its weapon during the attack phase and turn back over afterwards.

6.3 Operation Simulation Concept

Burleigh [10] showed a simple methodology to predict combat aircraft mission readiness by using approximated default values of aircraft reliability, maintainability and survivability in mission simulation. His method used all parameters as average constants throughout the simulation. Number of sorties flown, aircraft kills and so on, can hence be calculated by multiplying those values and the total number of aircraft, operation days, sorties per day and so on.

For instance, the number of aircraft kills at the end of the operation day is a summation of the total aircraft kills in each sortie, which is a result of the multiplication of the probability of attrition and the number of available aircraft in that sortie as:

$$N_{\text{A/C kill}} = \sum_{i=1}^{\text{sorties per day}} (P_{s1} N_{\text{Available in } i\text{th sortie}})$$

where P_{s1} is an average constant attrition probability.

From the above equation, the number of aircraft kills in ith sortie become a floating point value, but his model need only the integer number. Hence, this number has to be revalued by ignoring the floating point numbers.

An alternative to evaluate the number of available aircraft is to use separate time clock for each aircraft and its system component to identify when the component and/or aircraft obtains failure status during the simulation [1]. By this method, each aircraft will launch, be repaired, or be in maintenance separately depending on Mean Time To Repair ($MTTR$) and Mean Time Between Failure ($MTBF$).

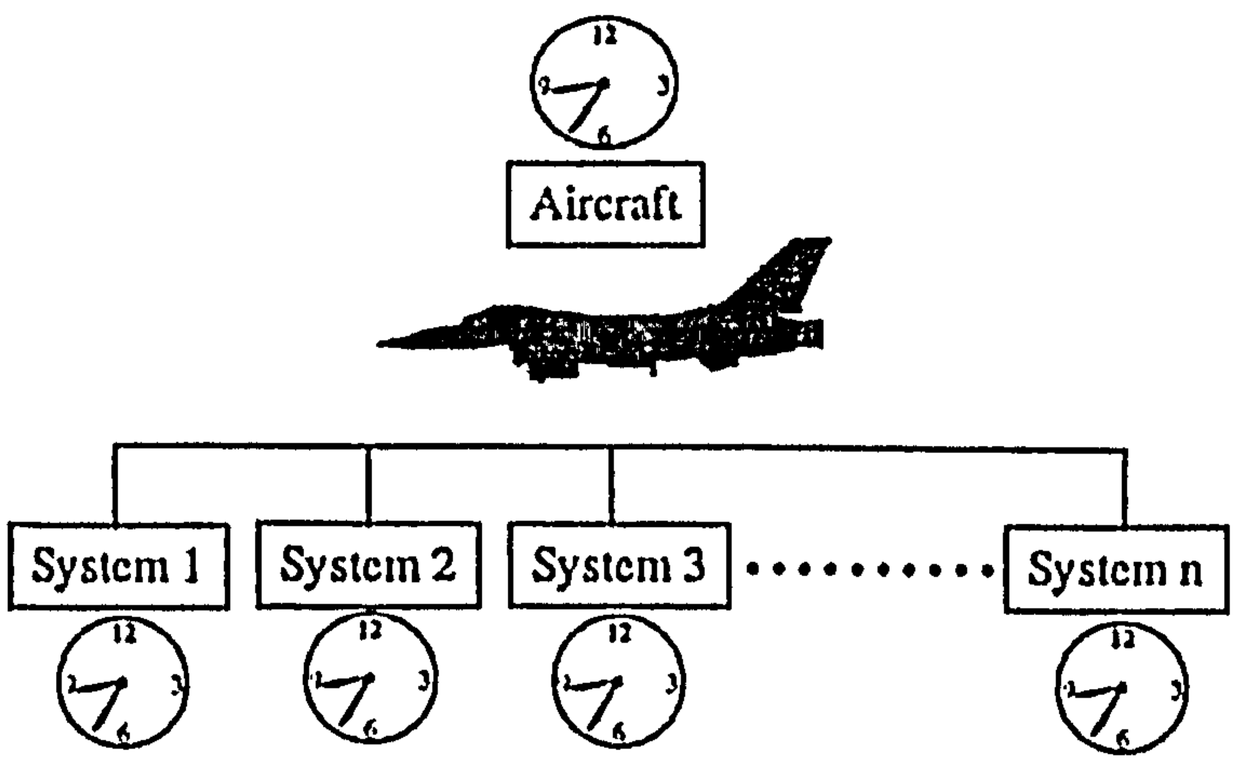

Figure 6.1: Time clock for each aircraft [1]

Another possible method used to evaluate the number of sorties flown during the mission, is reliability block diagram analysis. This method will evaluate the event success probability, such as the success probability of each flight phase, of maintenance, of aborting the mission and of failure [17]. The number of aircraft, which can get through preflight phase, is defined as the number of sorties flown by individual aircraft. At the end of operational day, the total number of sorties flown in that operational day is the summation of all the sorties flown in that operational day. The summation of the total sorties flown in every operational day throughout the mission simulation gives the total number of sorties flown in the mission simulation.

On the other hand, the number of complete sorties is defined as the number of aircraft which returns to their own base after a sortie, in an operational day, or in the mission simulation. Another measure related to sorties in this study is the successful sorties, which has a similar definition to the complete sortie. The difference between complete and successful sorties is that aircraft achieving a successful sortie have released their weapons during the penetration phase and returned to their own base. Such numbers can be used to measure an aircraft operational effectiveness.

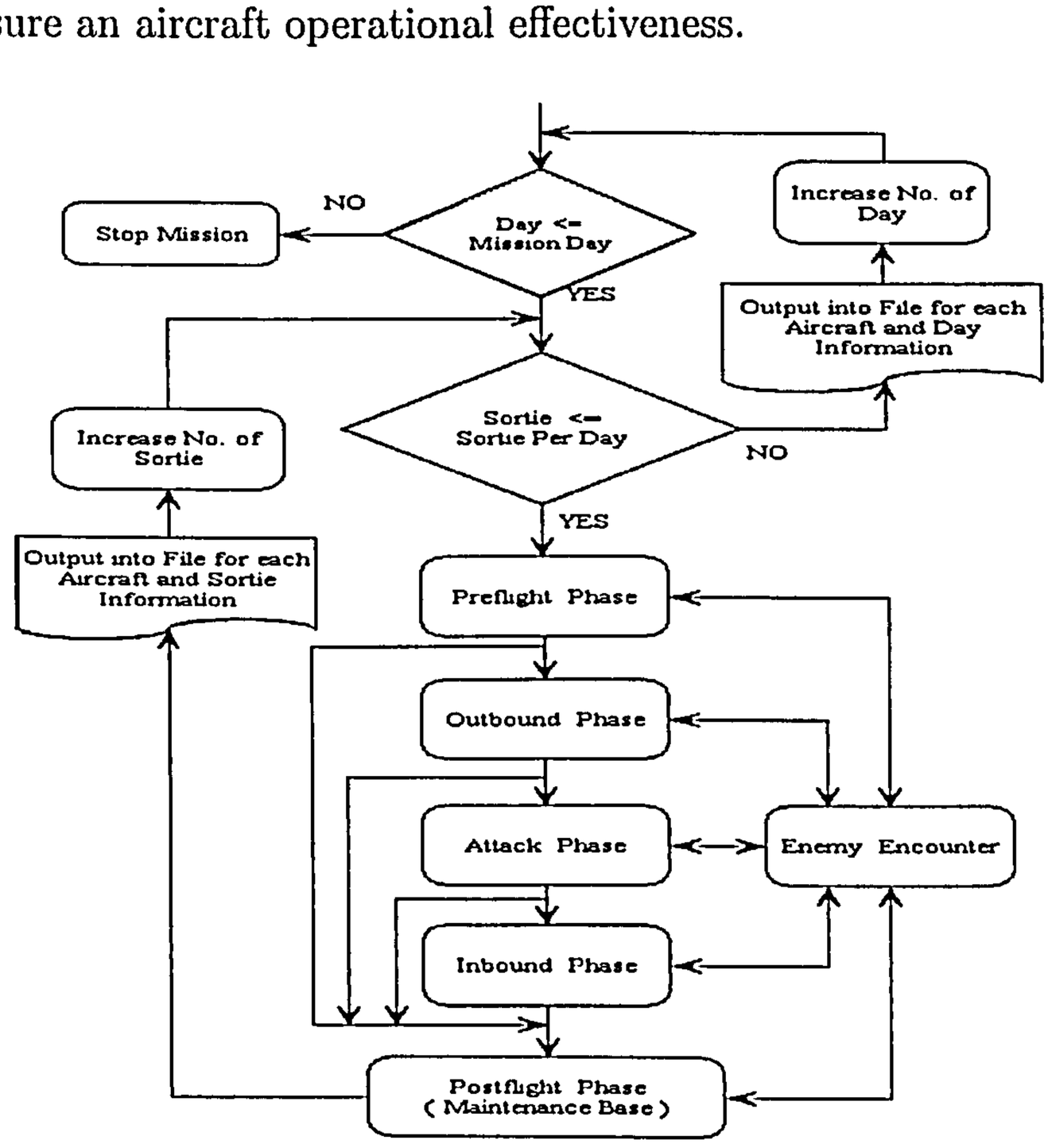

Figure 6.2: Flowchart for Operation Mission Simulation Module

Because most aircraft measures of performance and effectiveness are in the form of probability values, the Reliability Block Diagram (RBD) with the event trees is an alternative to predict such numbers of sorties flown, complete sorties, successful sorties, targets killed and so on. The fundamental of RBD and event trees calculation has been explained in Appendix A. This method decides that an event can occur if the occurrence value is greater than or equal to the probability of the specific event, which can be added and subtracted depending on its event tree diagram.

By using this method, each aircraft will obtain a different random value in each flight phase to compare with the flight phase success probability, which will be explained in a later section. Integer numbers which indicate how many aircraft have or have not achieved an event are recorded and passed to the subsequent events. This procedure will continue until the aircraft completes the sortie and the mission. A similar principle has been used to predict the following values:

Table 6.1: Predicted value per sortie from mission simulation module

Value	Calculation method
Number of sorties flown	Number of aircraft which achieve pre-flight phase successfully.
Number of complete sorties	Number of aircraft which can approach post-flight phase by following sortie route.
Number of successful sorties	Number of aircraft which achieve complete sortie and release their weapon during attack phase.
Number aircraft in maintenance	Number of aircraft which still remain in maintenance in post-flight phase.
Number of killed aircraft	Number of aircraft which obtains event probability greater than or equal to kill event in flight phase.
Number of available aircraft	Number of total aircraft deducted by Number of killed aircraft.
Number of targets detected	Number of weapons which are released during the attack phase due to assumption of using smart bomb.
Number of targets killed	Number of targets which obtain random value greater than the default target kill probability.

Table 6.1 shows the concept of how to predict an integer number of specific aircraft, sorties, and targets in each sortie, which can be added up at the end of the operational day and entire mission to obtain the total results for the operational days and the mission. For instance, total number of sorties flown for the entire mission of m operational day,

and k sorties per day can be calculated as:

$$N_{Total\ sorties\ flown} = \sum_{i=1}^{m\ operation\ day} N_{Total\ sorties\ flown\ in\ i\ day}$$
$$= \sum_{i=1}^{m\ operation\ day} \left\{ \sum_{j=1}^{k\ sortie\ per\ day} N_{Total\ sorties\ flown\ of\ j\ sortie\ in\ i\ day} \right\}$$

6.4 Success Probability Assessment

To evaluate final successful event probability, every opportunity which can possibly occur during this event has to be drawn and linked together regarding their logical consequence (RBD), an example has been shown in Fig. 6.3. Together with the logical 'AND', 'OR' and 'NOT' combination (RBD) and the event trees diagram, the final successful probability value can be evaluated. All possible occurrences, their definitions, and their logistical combinations can be described as:

1. System failure: This can happen due to either defect arising rate in every flying hour, which is assumed as 10% of total aircraft failure rate, or damage rate from being attacked in previous flight phase. By using RBD parallel connection (logical 'OR' combination), these two possible events can be combined together. The probability calculation from the new combined event can be evaluated as Eqn. (6.1). If an aircraft achieves this occurrence, mission abort status has to be called with the consequence that the aircraft will be returning to the own base.

$$P_{System\ failure} = 1 - (1 - P_{Damage\ previous\ occurrence})(1 - P_{Defect}) \tag{6.1}$$

2. System not failure: This occasion is the opposite of system failure. The probability value can be evaluate by using logical 'NOT' combination.

$$P_{System\ not\ failure} = 1 - P_{System\ failure} \tag{6.2}$$

3. Survive: This occasion can occur if an aircraft achieves the 'system not failure' occurrence. For survival probability itself, an aircraft has to survive all encounters occurring during this flight phase, which includes several SAM and AAA threats (details see chapter 3). The combination of more encounters and 'system not failure' events can be linked together as the RBD series combination (logical 'AND'

combination). The survive event probability value can be thus calculated as:

$$P_{Survive} = P_{System\ not\ failure} \times P_{Survive\ all\ encounters} \tag{6.3}$$

4. Not survive: This is the opposite from 'survive' occurrence, and the number of aircraft, which achieves this occurrence, will obtain status 'KILL' and be added to the number of killed aircraft.

$$P_{Not\ survive} = P_{System\ not\ failure} \times (1 - P_{Survive}) \tag{6.4}$$

5. Damage: This occurrence will happen if the aircraft gets through 'survive' occurrence; but it has been shot and obtains component damaged. The damage value will be randomly generated and be added into the aircraft damage rate.

$$P_{Damage} = P_{Survive} \times P_{Damage\ rate} \tag{6.5}$$

6. No damage: An aircraft achieves this either by not being hit or by being hit but not being damaged.

$$P_{None\ damage} = P_{Survive} \times (1 - P_{Damage}) \tag{6.6}$$

7. Mission abort: This will occurs if the aircraft gets damaged with a certain damage rating, which causes the aircraft to return for repair. The probability of abort mission in each event is assumed constant as 0.38% for this mission simulation.

$$P_{Mission\ abort} = P_{Damage} \times P_{Abort} \tag{6.7}$$

8. Mission not aborted or Continue: This possibility is the second alternative to continue a sortie, even if an aircraft gets damaged but it is still functional and able to complete the designed mission.

$$P_{Mission\ not\ abort} = P_{Damage} \times (1 - P_{Mission\ abort}) \tag{6.8}$$

9. Maintenance: An aircraft will still stay in the 'maintenance' event if the aircraft needs to be repaired as a result of component damage or due to a mission abort occurrence

$$P_{Maintenance\ against\ damage} = 1 - e^{(-\frac{t_{Maintenance}}{MTTR_{Damage}})} \tag{6.9}$$

$$P_{Maintenance\ against\ mission\ abort} = 1 - e^{(-\frac{t_{Maintenance}}{MTTR_{Defect}})} \tag{6.10}$$

$$P_{Maintenance} = P_{Maintenance\ against\ damage} \times P_{Maintenance\ against\ mission\ abort} \tag{6.11}$$

10. Successful flight phase: This probability value is a summation of all possibility probable value that allow the mission to continue except for post-flight phase, which concerns only the probability that an aircraft will be available for the next sortie. (see an example in Fig. 6.3)

$$P_{Successful\ flight\ phase} = P_{None\ Damage} + P_{Mission\ not\ abort} \tag{6.12}$$

11. Unsuccessful flight phase: This is the opposite to the above occurrence.

$$\begin{aligned} P_{Unsuccessful\ flight\ phase} &= P_{System\ failure} + P_{Not\ survive} + P_{Mission\ abort} \\ &= 1 - P_{Successful\ flight\ phase} \end{aligned} \tag{6.13}$$

In every flight phase in this mission simulation, a similar sequence of occurrences is obtained. Fig. 6.3 shows an example of the event tree diagram to evaluate the successful inbound phase probability value.

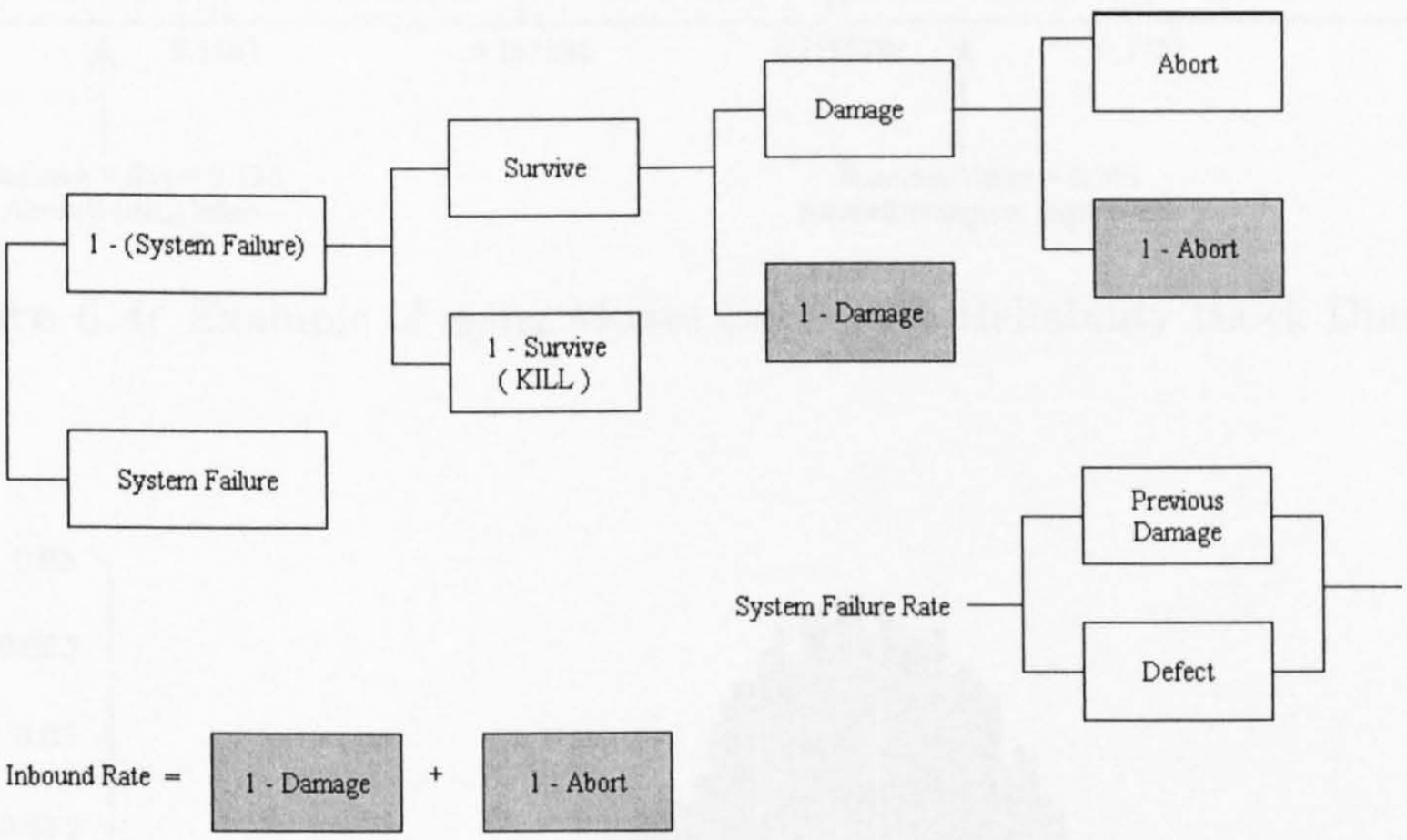

Figure 6.3: Reliability Block Diagram for Inbound phase success probability calculation

6.5 Monte Carlo Simulation Technique

Monte Carlo simulation methods are stochastic techniques, which means that they are based on the use of random numbers and probability statistics to investigate problems. This method provides approximate solutions with tolerance errors [19].

There are several methods to use Monte Carlo simulation technique to predict solutions to the problem, but one of these is to use a random value to compare with the event

probability to decide which event will occur. The number of occurring events will be recorded and statistically analysed. After a certain number of trials, the probability distribution of an event occurring can thus be plotted similar to the graph shown in Fig. 6.5.

The principle of using Monte Carlo simulation technique with Reliability Block Diagram is that every possible occurrence in each flight phase in this mission simulation has to be examined and calculated regarding its event tree diagram. These values can be used to compare with the generated random value to determine which event an aircraft will achieve. For example every occurrence probability in outbound phase can be evaluated and shown as in Fig. 6.4. If the generated random value is 0.123, an aircraft will be killed. On the other hand, if the generated random value is 0.345, the aircraft will achieve successful outbound phase and will continue to post-flight phase.

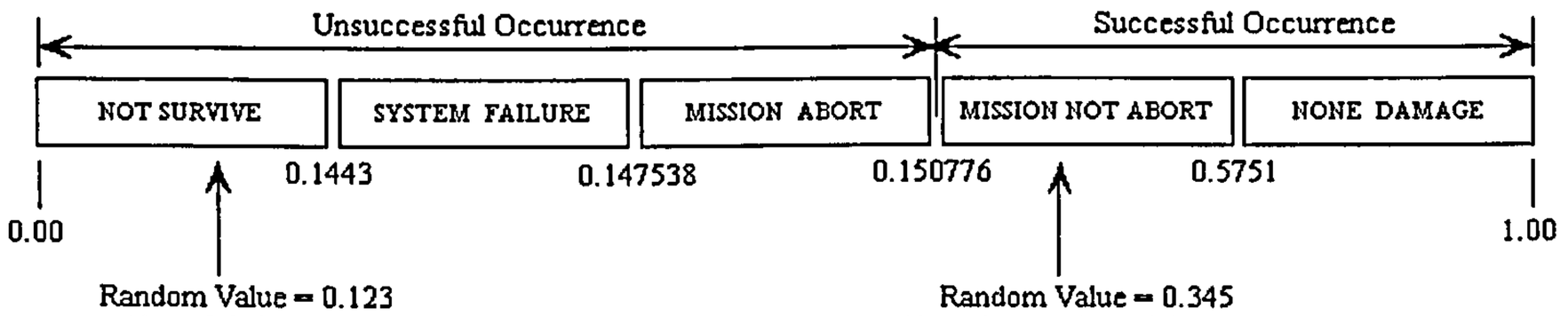

Figure 6.4: Example of using Monte Carlo with Reliability Block Diagram

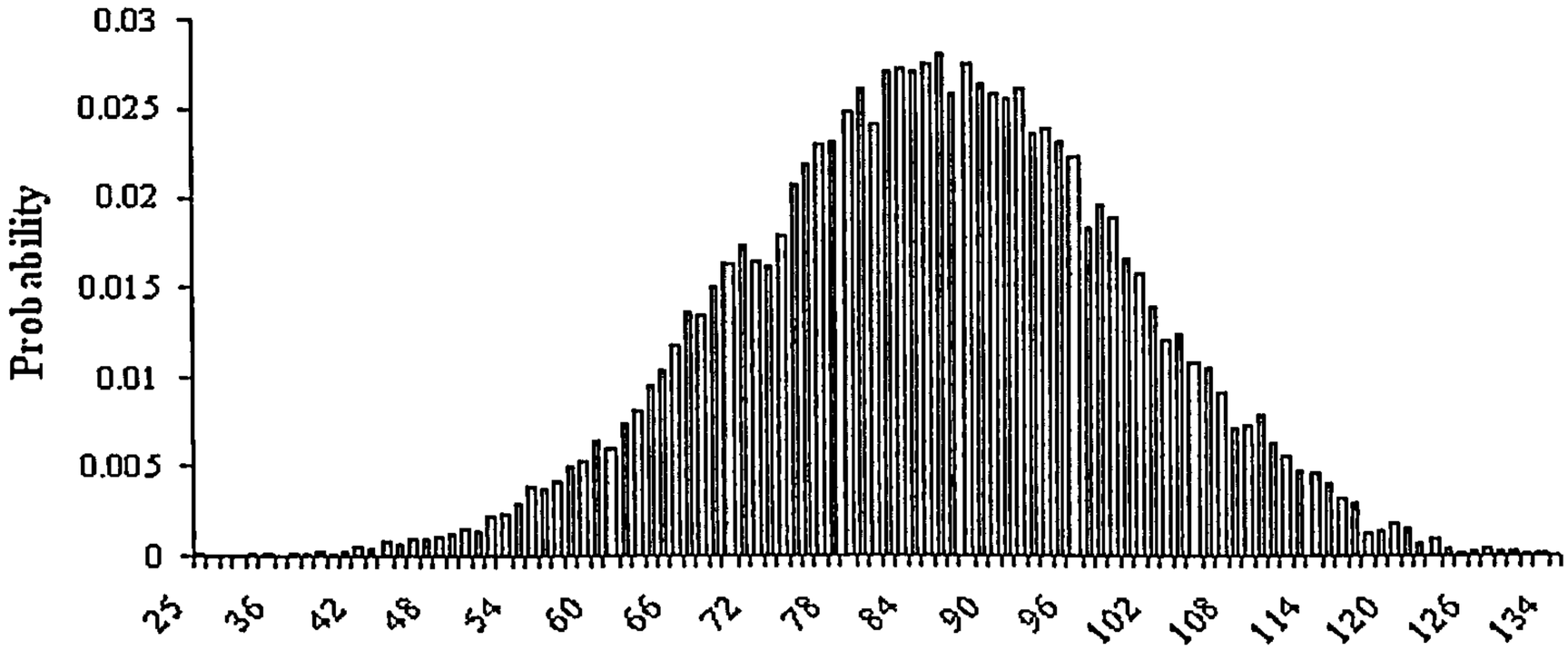

Figure 6.5: Normal curve of successful sorties after 20000 trials

The number of specific aircraft, target, and sorties can be thus evaluated by summation of the number of aircraft and targets in specific categories. For instance, the number of

aircraft which achieve successful pre-flight occurrence can be used as the number flown in that sortie, and will give the total sorties flown in the operation day and the entire mission.

With this principle, every flight phase will generate a random value to predict which occurrence of event tree diagram will occur. The specific number of sorties, aircraft, and targets can be calculated at the end of each simulation run. After a certain number of simulation runs or trials, statistical analysis of specific integer objective values can be processed as shown in Fig. 6.5. The mean and mode values from the analysis can be thus represented as the result of mission simulation [32].

6.6 Chapter Summary

This chapter has

- analysed specific threats used in this mission simulation.
- examined and classified a bombing mission to simulate mission model for this study.
- introduced a simple method to predict the total number of specific sorties, aircraft and targets by using directly probability and separate clock time.
- described another alternative to predict the total number of specific sorties, aircraft, and targets by using RBD with event trees.
- shown all possible occurrences in each flight phase in a sortie.
- examined the successful and unsuccessful flight phase probability values, which are used to predict the numbers of specific sorties, aircraft, and targets.
- introduced Monte Carlo simulation technique to predict integer number results for this mission simulation.

CHAPTER 7

OPTIMISATION METHODS

This chapter introduces two major optimisation methods used in this research; Gradient-based method and Genetic algorithms. The first method is commonly used to solve engineering problems; but it is not perfectly appropriate with the problem in this research due to the use of objective values in the form of integers. However, the gradient-based method can be used to guide variable trends and approximate objective values. On the other hand, the genetic algorithms do not use any gradient or partial differentials to search for the local/global minimum/maximum, but instead uses the objective value of a particular variable set to measure how good this variable is, compared to the other variable set.

The first optimisation tool is an evaluation version of a commercial product, which can be of limited use. However, this version is still sufficient for the problem in this research. On the other hand, the second optimisation tool is freeware, and provides source code for future development. Nevertheless, no development was performed on the optimisation during this research, as the basic codes are sufficient.

7.1 Gradient-based Method

This method is commonly used to minimise or maximise the objective function in engineering and science. The fundamental principle of the gradient-based approach is used to predict the direction in which the search for the minimum/maximum objective function should proceed by using the first derivatives of the objective function and constraints with respect to the vector of the aircraft design variables.

Because some objective values in this study are integer numbers, the gradient-based method can therefore cause particular problems or difficulties to find local and global minimum/maximum as the differential of a function with respect to the relevant variable will obtain a value constant of zero.

The Solver DLL from Frontline Systems Ltd. [21] has been chosen because of the following reasons:

1. The company also provides an evaluation version, which can be downloaded free from the internet.

2. A limit of the evaluation version is the maximum of ten variables that can be used; however, this number is sufficient to solve the problem in this study.

3. This program can handle almost all possible problems, such as linear, quadratic, nonlinear, and nonsmooth.

7.2 Genetic Algorithms

Goldberg [22] introduced simple genetic algorithms as a search for best fit algorithms based on the mechanics of natural selection and natural genetics. They combine survival of the fittest among string structures with a structured yet randomised information exchange, to form a search algorithm with some of the innovative flair of a human search. In every generation, a new set of artificial creatures is created using bits and pieces of the fittest of the old; an occasional new part is tried for good measure. While randomised, genetic algorithms are no simple random walk. They efficiently exploit historical information to speculate on new search points with expected improved performance. The principles of this method are follows:

1. Defining a representation: A single solution of the problem has to be represented as a single data structure (Genome). The population of solutions based on this data structure will be created depending on representation type.

2. Defining genetic operator: The genetic algorithm will define how the population evolution takes place.

3. Fitness scaling: An objective function will be used to determine how fit each genome is for survival.

4. Selection/replacement: The genome operator uses selection/replacement strategies to generate new individuals.

A typical genetic algorithm stop criteria is a number of generations, for which an optimiser should run. However, there are alternative stop criteria, such as measure of goodness of best solution, and convergence of population [50].

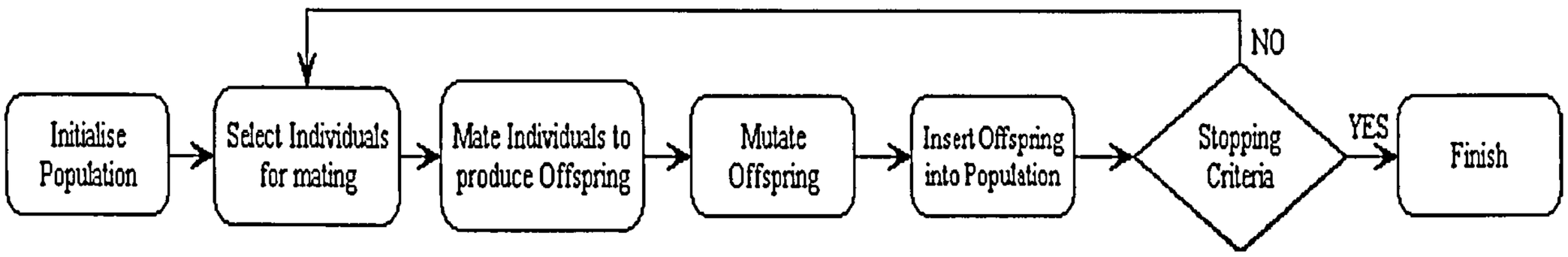

Figure 7.1: Flowchart of genetic algorithm

Defining a Representation

It is necessary to use a data structure which is appropriate for the problem because the representation has to be able to represent any solution to the problem. The number of possible representations is endless. These may be in purely numerical representation such as an array of real numbers or in Goldberg style, of a string of bits that map to a real number.

Genome Operators

Each genome has three primary operators: Initialisation, mutation, and crossover. With these operators, the populations will be created and evolved throughout the optimisation process as follows:

1. The initialisation operator determines how the genome is initialised by stuffing the genomes with the primordial genetic material from which all solutions will evolve.

2. The Mutation operators define the procedure for mutating each genome mutation, which means here different things for different data types. These should be able to introduce new genetic material as well as modify existing material. For example, a typical mutation for a binary string genome is flipping the bits in the string with a given probability.

3. The crossover operator defines the procedure for generating a child from two parent genomes. Similar to mutation, crossover is specific to the data type, but it involves multiple genomes. The traditional crossover generates two children from two parents.

4. The objective function has to be defined, and is used to evaluate genomes. Therefore, the genetic algorithm can determine which individuals are better than others.

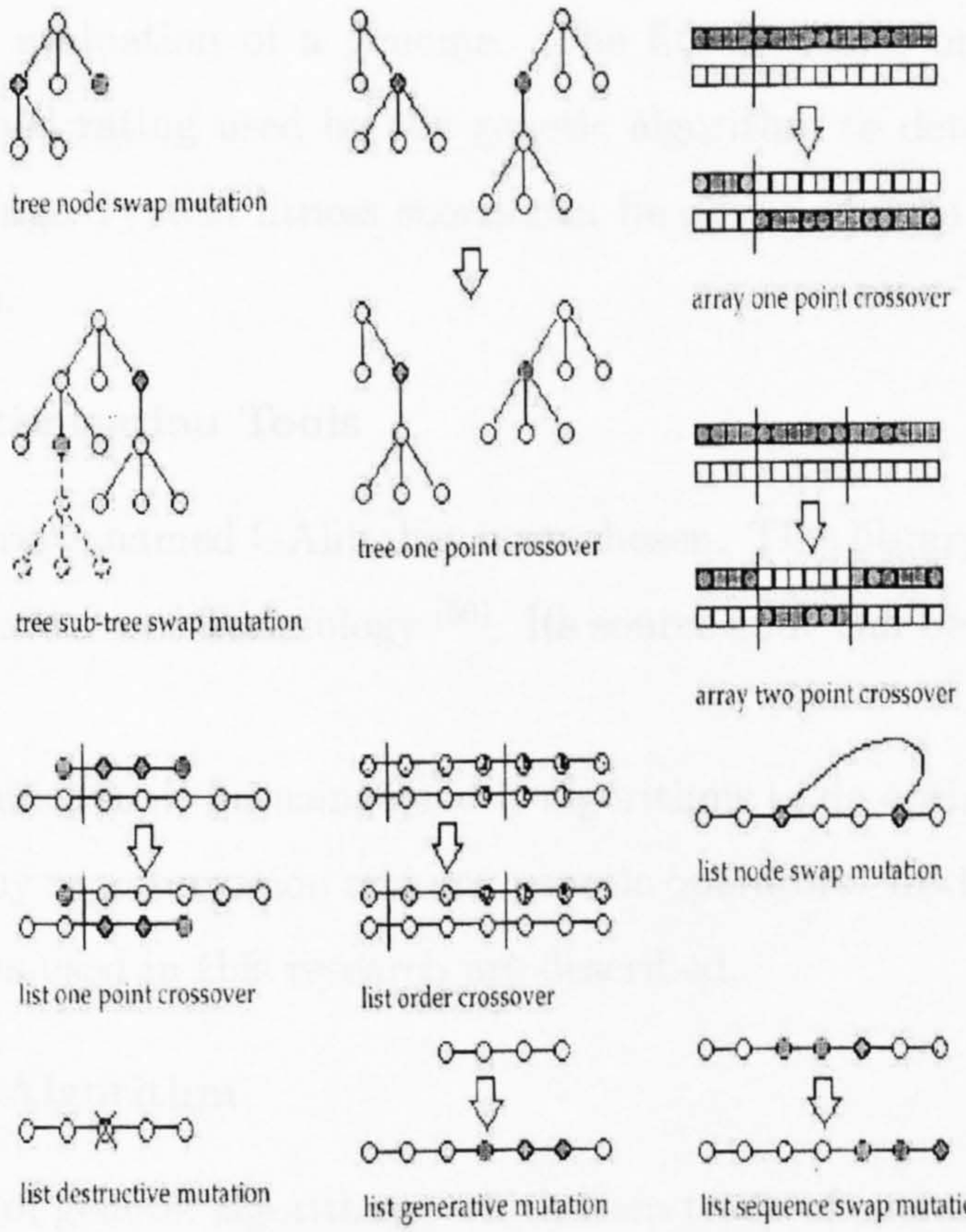

Figure 7.2: Example of mutation and crossover methods [50]

The Population Object

The population object is a container of genomes, and each genome object has its own initialiser and evaluator for each individual in the population. It also keeps track of the best, average, derivation, and so on for the population. In this object, mating method and algorithm have to be defined.

Each population object has a scaling scheme objective associate with it. The scaling scheme object converts the objective score of each genome to a fitness score that the genetic algorithm uses for selection.

Objective Functions and Fitness Scaling

This is the major difference between genetic algorithms and gradient-based methods. Genetic algorithms require only a single measure of how good a single individual is, compared to the other individuals, which is provided by objective function. Gradient-based methods use complicated differential equations or a smooth search score.

The objective score is the value calculated directly from the objective function; it

is raw performance evaluation of a genome. The fitness score, on the other hand, is a possibly-transformed rating used by the genetic algorithm to determine the fitness of individuals for mating. Typical fitness scores can be obtained by a linear scaling of the raw objective scores.

7.2.1 GAlib Optimisation Tools

A freeware C++ library, named GAlib, has been chosen. This library has been developed at Massachusetts Institute of Technology [50]. Its source code can be downloaded directly from the internet.

This library includes tools for using genetic algorithms to do optimisation in any C++ program by using any representation and any genetic operators. In this section, the major classes and functions used in this research are described.

Class GAGeneticAlgorithm

This is a base class of genetic algorithms, which keep track of evolution statistics such as number of mutations, number of crossovers, number of evaluations, best/mean/worst in each generation, and initial/current population statistics. It also defines the terminator, a number function that specifies the stopping criterion for the algorithm.

The 'evolve' member function first calls 'initialize', then calls the 'step' member function until the 'done' member function returns 'gaTrue'.

Class GASimpleGA

This class is based on GAGeneticAlgorithm, and uses non-overlapping populations method to clone the individuals for its own population. This simple genetic algorithm creates an initial population by cloning the individual or population, which has been passed when this is created. Each generation the algorithm creates an entirely new population of individuals by selecting from the previous population then mating to produce the new offspring for the new population. This process continues until the stopping criteria are met.

Elitism is chosen by passing 'gaTrue' value into 'elitism' member function, so the best individual from each generation is carried over to the next generation.

Function Terminators

The 'done' member function simply calls the 'completion' function to determine whether or not the genetic algorithm should continue. The 'completion' function returns 'gaTrue' when the genetic algorithm should finish, and 'gaFalse' when the genetic algorithm should continue.

The number of generation stopping criteria is set by default, in which the function compares the current generation to the specified number of generations. If the current generation is less than the requested number of generation, it returns 'gaFalse'. Alternative of stopping criteria is convergence of best individual scores, in which the function compares the population average to the score of the best individual in the population. If the population average is within 'pConvergence' of the best individual's score, it return 'gaTrue'.

Class GAGenome

The genome is a virtual base class. It defines a number of constants and function prototypes specific to the genome and its derived classes.

The 'score' member function returns the objective score of the genome using the objective function assigned to the genome.

Class GABin2DecGenome

This genome class converts binary strings to decimal values. Before using this genome, a mapping of bits to a decimal value has to be created by specifying how many bits will be used to represent the designed bounded numbers.

The 'phenotype' member function can get or set the mapping from binary to decimal numbers.

Class GABin2DecPhenotype

This class defines the mapping from binary to decimal values by using 'add' member function to create a mapping that tells the 'phenotype' that **n** bits should be used to represent a floating point number from given minimum and maximum values.

GAStatistics

The statistics object contains information about the current state of the genetic algorithm objects. 'BestIndividual' member function returns the best individual encountered by the genetic algorithm, which can be used for future analysis.

7.3 Chapter Summary

This chapter has:

- briefly introduced the gradient-base optimisation method.
- nominated an alternative tool to gradient-base method for integrating in the main program.
- presented an alternative method to optimise integer objective value, the genetic algorithm.
- introduced an optimisation tool for the genetic algorithm optimisation.

CHAPTER 8

RESULTS

Some assumptions had to be made due to military restrictions and limited data and information availability. This also applied to assessment methods in some parts of the simulation (details see chapter 6). This chapter will show only general results generated from the application 'Mission Effectiveness Analysis' by using the case study aircraft, U-99. The general results of individual sub-modules and their combination with the main application will be described. The remaining results of individual sub-module in details are shown separately in the relevant Appendices.

8.1 Results from Susceptibility Assessment

The susceptibility assessment sub-module is one part of the survivability assessment sub-module; its objective is to measure aircraft susceptibility performance; i.e. probability of being detected (P_D), probability of being hit or fused when being detected ($P_{H/D}$ or $P_{F/D}$).

As described in section 3.1, the aircraft probability of detection (P_D) depends on the signal-to-noise ratio, which is a function of its RCS, threat's radar performance, and the distance between an aircraft and the signal-receiving radar system. In this section, the results of U-99's probability of detection are shown.

8.1.1 Radar Cross Section

RCS is commonly measured in the terms of dBm^2 or m^2 in many different angles. It is so difficult to access data to validate this sub-module, due to the fact that only limited details of aircraft front view RCS can be found in text books [18]. The B-2 and F-117 aircraft have thus been chosen to calculate their RCS, aiming to validate this sub-module. Another reason for choosing these aircraft is that their external shapes can be straightforwardly represented by simple geometrical shapes (details see Appendix B).

Table 8.1 compares the calculated RCS generated from the susceptibility assessment sub-module with the RCS data from an open source [18]. The discrepancy between the

B-2 RCS predicted by this sub-module and the RCS value from the open source (approximately 26 %) is significantly higher than an discrepancy in the case of the F-117 RCS (approximate 0.28%). There are two reasons for this discrepancy in the case of the B-2 compared to the case of the F-117. Firstly, the complexity of the shape of the B-2 compared to the F-117 leads to a much higher discrepancy in calculation for the B-2. Secondly, the B-2 has significantly better usage of RAM than the F-117, and the sub-module ignores the effects of RAM. However, the discrepancy between the predicted aircraft RCS by the susceptibility assessment module and the aircraft RCS quoted from published source may be less or more than the values shown in Table 8.1. It depends on radar frequency used to calculate an aircraft RCS in the susceptibility assessment module. This assumed radar frequency used here may be not the same as used to predict in the published source, because there is no such information about the radar frequency used to predict aircraft RCS quoted from the published source.

Table 8.1: Comparison between selected aircraft front view RCS from published source [18] and calculated aircraft front view RCS from the susceptibility assessment sub-module

Aircraft	RCS $[m^2]$	Calculated RCS $[m^2]$	Discrepancy [%]
B-2	0.1	0.12613468	26
F-117	0.025	0.02492856	0.28576
U-99	-	0.0061	-

The aircraft RCS depends primarily on the aircraft external geometrical shapes in each aircraft view; therefore, each aircraft view RCS has to be separately calculated. The results of U-99 RCS in the six main aircraft views can be shown in Table 8.2.

Table 8.2: Calculated U-99 RCS in six main views

View	RCS $[m^2]$	RCS [dBm^2]
Top	2807183.5	64.4827
Left	0.01133908	-19.4542
Right	0.01133908	-19.4542
Front	0.00610207	-22.1452
Rear	1.17095530	0.6854
Bottom	2807183.5	64.4827

An alternative way to present aircraft RCS is to plot these values in a concentric manner, as shown in Fig. 8.1. This method can show the aircraft RCS in the four main views compared, with each other.

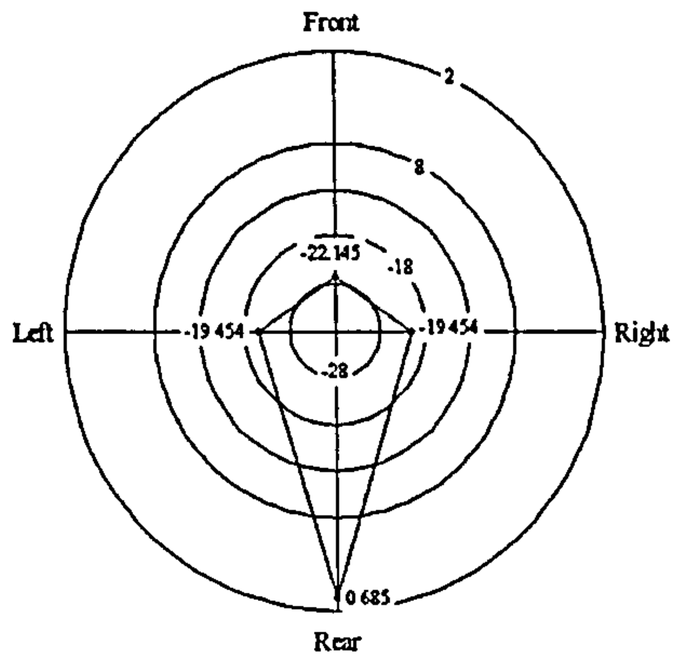

Figure 8.1: Results of U-99 radar cross section in dBm^2 unit

8.1.2 Signal-To-Noise Ratio

As described in Chapter 3, the probability of detection cannot be predicted directly from the aircraft RCS, but can be predicted from the aircraft S/N. The aircraft S/N depends on several parameters, but most of them are assumed as constant throughout the mission simulation; such as temperature (no weather change), radar receiving system. The aircraft S/N in this research will thus vary only depending on aircraft RCS and distance between aircraft and radar receiving system in each flight phase. Therefore, the S/N for each aircraft view in each flight phase has to be independently evaluated. Table 8.3 shows the S/N of all six main aircraft views in every flight phase in a sortie.

Table 8.3: Calculated S/N of six main U-99 views for each flight phase [dBm^2]

Flight Phase	Top	Left	Right	Front	Rear	Bottom
Pre-Flight	44.7216	-39.2153	-39.2153	-41.9063	-19.0757	44.7216
Outbound	52.5295	-31.4075	-31.4075	-34.0985	-11.2679	52.5295
Attack	79.1151	-4.8218	-4.8218	-7.5128	15.3178	79.1151
Inbound	52.5295	-31.4075	-31.4075	-34.0985	-11.2679	52.5295
Post-Flight	44.7216	-39.2153	-39.2153	-41.9063	-19.0757	44.7216

An average S/N in each flight phase can be calculated through Eqn. (3.16) by using an average RCS, which is the result of the multiplication of each aircraft view RCS and the manoeuvrability probability (weighting factors) for the particular aircraft view in the particular flight phase. The manoeuvrability probability table option 2 (see Fig. E.9) has been chosen to generate the results in this study. Table 8.4 shows the average U-99 RCS and S/N in each flight phase with manoeuvrability probability option 2.

Table 8.4: Calculated average RCS and S/N for each flight phase by using manoeuvrability probability option 2

Flight Phase	RCS [dBm^2]	S/N [dBm^2]
Pre-Flight	58.4621	38.9264
Outbound	54.4827	42.7058
Attack	59.2539	73.8863
Inbound	54.4827	42.7058
Post-Flight	58.4621	38.9264

8.1.3 Probability of Detection

With the assumed threshold setting default value of the receiveing radar system, the probability of false alarm, P_n, can be thus evaluated as 3.72665×10^{-6}. Together with this P_n value and the average S/N, the average probability of detection by the radar of the U-99 in each flight phase can be simply discovered by dint of the pre-calculated graph (see Fig. 3.4). Table 8.5 shows P_D predicted by using average S/N in each flight phase and a threshold setting default value.

Table 8.5: Average calculated S/N and P_D in each flight phase predicted by using manoeuvrability probability option 2

View	Pre- and Post-Flight		Out- and Inbound		Attack	
	S/N	P_D	S/N	P_D	S/N	P_D
Top & Bottom	44.7216	≈ 0.95	52.5295	≈ 0.95	79.1151	≈ 0.98
Left & Right	-39.2153	≈ 0.001	-31.4075	≈ 0.001	-4.8218	≈ 0.006
Front	-41.9063	≈ 0.001	-34.0985	≈ 0.001	-7.5128	≈ 0.003
Rear	-19.0757	≈ 0.001	-11.2679	≈ 0.001	15.3178	≈ 0.65
Average	38.701	≈ 0.95	42.5294	≈ 0.95	73.8863	≈ 0.98

8.1.4 Probability of Hit

Table 8.6 shows the results of the probability of hit predicted from both 'Carlton' and 'Shoe-Box' models used to represent the aircraft presented area (see Fig. 3.6). The miss distance distribution, σ_r, is calculated from an assumed 20 generated random hits, and miss distances in conjunction with the 'Carlton' and the 'Shoe-Box' model illustrating aircraft presented areas.

Table 8.6: $P_{H/D}$ of three main U-99 views in each flight phase evaluated from 20 random hits

View	Carlton			Shoe-Box		
	σ_r	A_P	$P_{H/D}$	σ_r	A_P	$P_{H/D}$
Top & Bottom	282.287	28.5571	0.578458	240.795	28.5571	0.799853
Left & Right	44.0028	11.8748	0.603518	60.6532	11.8748	0.668563
Front & Rear	33.5298	10.6451	0.61617	23.0322	10.6451	0.903382

8.2 Results from Vulnerability Assessment

In this methodology, only two main threat types have been considered; i.e. penetrator (represented by AAA) and proximity warhead (represented by SAM). The principle kill mechanism for the penetrator threat type is to destroy and/or damage aircraft components, which are on the shotline (definition see Chapter 3). The measure of aircraft MOP in vulnerability encountered by this threat type is probability of kill, P_K.

On the other hand, the proximity warhead in this study is assumed to detonate outside the aircraft and produce fragments, which directly hit the aircraft afterwards. The number of fragments can be evaluated from the detonation distance. In this case, each fragment is considered as an individual penetrator. Therefore, the probability of kill by all fragments can be determined by using the same principle of multiple hits by penetrators. The lethal radius can be discovered, and can be used to represent the $P_{K_{Ext}}$ (details see Chapter 3).

8.2.1 Probability of Kill

The probability of kill is mainly a function of critical component vulnerable areas value (A_V). This value can be calculated from the critical component presented areas, which depend on the component layout, and kill probability by given hit on the component. Three alternative critical component layouts have been examined; i.e. non-overlapped area existence (non-overlapped), shielding effect of frontal critical component of the overlapped area (shielding overlapped), and non-shielding effect of frontal critical component of the overlapped area (non-shielding overlapped). Redundancy is another consideration effecting the kill probability calculations.

Table 8.7 shows the comparison of kill probability values of the U-99 in different critical component layouts, with consideration of fuel system redundancy. On the other hand, Table 8.8 shows the results of kill probability calculation without consideration of fuel system redundancy. Due to the semi-automatic grid counter method used to predict the

presented areas of both critical components and aircraft (see Appendix B), the vulnerable areas will be thus calculated in Grid unit, which can be convert into the SI unit, metre, by using factors shown in Table B.9.

Table 8.7: Calculated $P_{K/H}$ of U-99 with redundant fuel systems

	Top/Bottom		Left/Right		Front		Rear	
	A_V [Grid]	$P_{K/H}$	A_V [Grid]	$P_{K/H}$	A_V [Grid]	$P_{K/H}$	A_V [Grid]	$P_{K/H}$
Non-Overlapped	25.60	0.00999	22.40	0.05056	28.80	0.08090	22.80	0.08090
Non-Shielding Overlapped	25.60	0.00999	26.46	0.05972	30.48	0.08562	30.48	0.08562
Shielding Overlapped	25.60	0.00999	24.48	0.05526	30.31	0.08515	29.55	0.08301

In this methodology, the incendiary threat type has not been taken into account; therefore, the redundancy of fuel system can reduce the aircraft P_K.

Table 8.8: Calculated $P_{K/H}$ of U-99 with non-redundant fuel systems

	Top/Bottom		Left/Right		Front		Rear	
	A_V [Grid]	$P_{K/H}$	A_V [Grid]	$P_{K/H}$	A_V [Grid]	$P_{K/H}$	A_V [Grid]	$P_{K/H}$
Non-Overlapped	149.80	0.05847	93.80	0.21174	93.00	0.26124	93.00	0.26124
Non-Shielding Overlapped	149.80	0.05847	93.86	0.21188	91.64	0.25743	91.64	0.25743
Shielding Overlapped	149.80	0.05847	87.93	0.19848	90.61	0.25451	88.92	0.24992

8.3 Results from Reliability & Maintainability Assessment

The reliability & maintainability models used in this methodology are based on the combination method, or the functionality of empty weight method, both described in Chapter 4. By using statistical analysis of historical data, both models can be thus developed and produced the results shown in this section.

In the first method, the highest and the lowest values of reliability and maintainability for use in the prediction model were firstly developed. Fig. 8.2 shows the comparison between the actual highest failure rate and predicted highest failure rates from two developed models; i.e. linear and logarithm regressions. An average error for the highest FR calculated by the linear regression model is approximately 8.5%, whereas 12% was found for the highest FR determined by the logarithmic regression model.

Fig. 8.3 shows the calculated highest $DMHR$ from linear and logarithm regressions, together with the actual data. An average error for the highest DMHR calculated from the logarithm regression model is approximately 13%, and approximately 12% for the value calculated from the linear regression model.

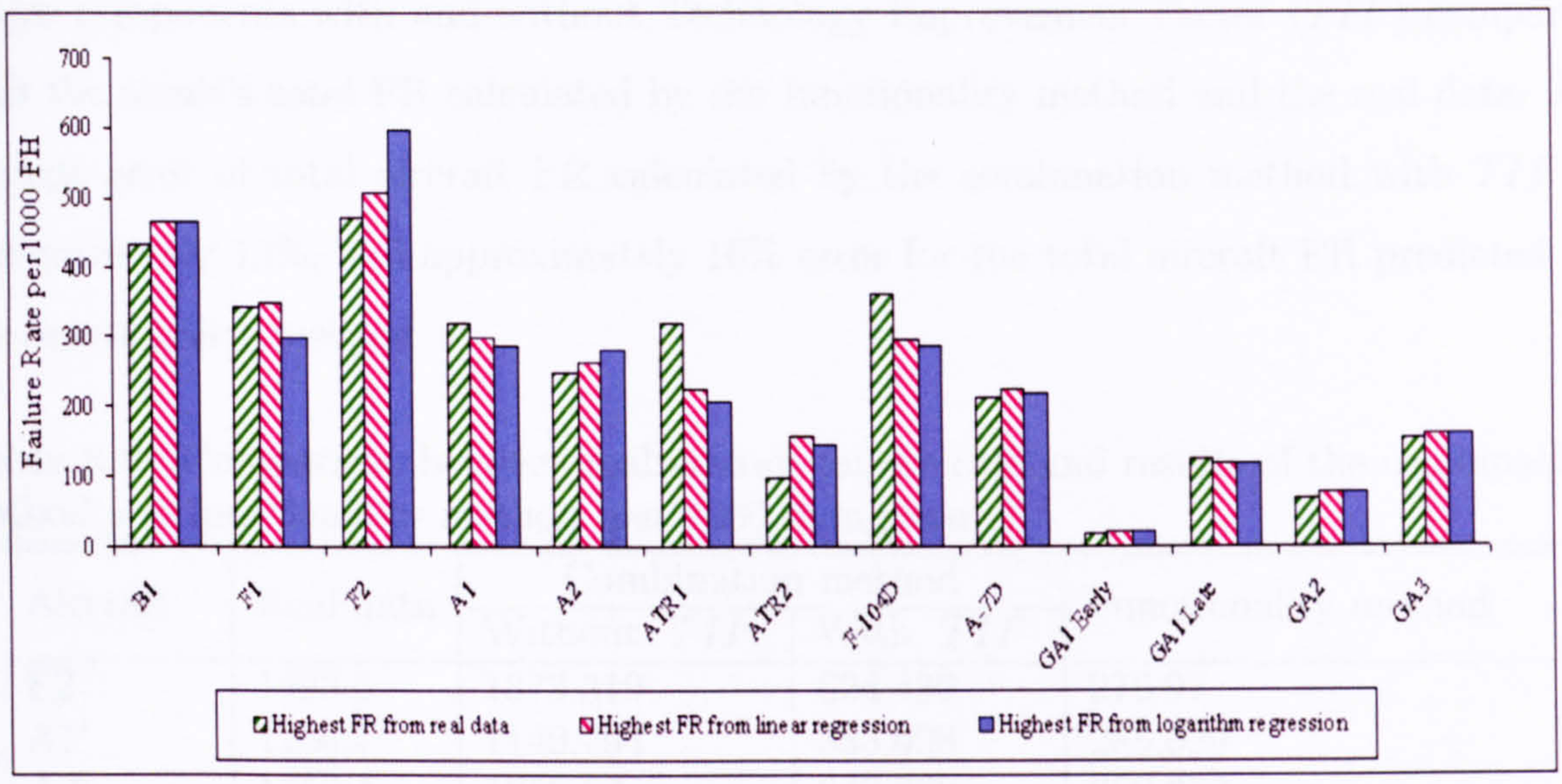

Figure 8.2: Comparison between the highest failure rate from the linear and exponential regression analysis

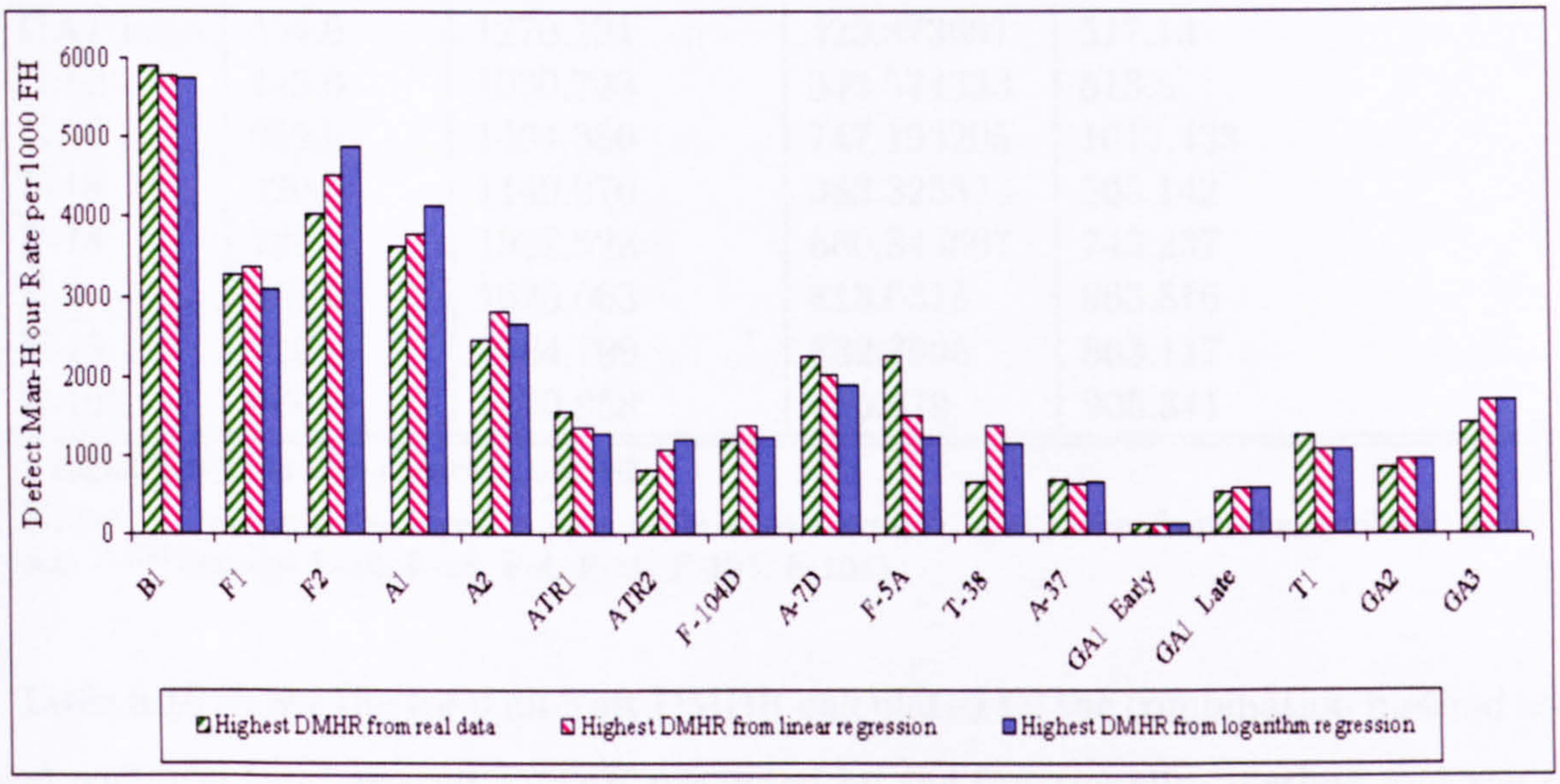

Figure 8.3: Comparison between the highest defect man-hour rate from linear and exponential regression analysis

The linear regression model has, therefore, been chosen to predict the highest and the lowest FR and DMHR in this methodology. The Pareto distribution b coefficient could then be evaluated. At the final stage, aircraft FR and DMHR distribution over all 13 major systems were evaluated by dint of Pareto distribution coefficients. The total aircraft FR and DMHR are simply a summation of all 13 major system FR and DMHR. Table 8.9 shows the total FR calculated by the combination method, with the assumption of thirteen

major components with and without Technology Improvement Factor (TIF) compared with the result's total FR calculated by the functionality method and the real data. An average error of total aircraft FR calculated by the combination method with TIF is approximately 13%, and approximately 16% error for the total aircraft FR predicted by the functionality method.

Table 8.9: Comparison between real aircraft failure rate and results of the combination method and functionality method [per 1000 flying hours]

Aircraft	Real data	Combination method		Functionality method
		Without TIF	With TIF	
F2*	1493.5	1873.319	624.439	276.97
A1*	1250.7	1149.294	383.098	285.029
A2*	1052.4	1043.67	347.890	289.278
ATR1*	832.8	803.302	267.767	472.974
ATR2*	547.4	661.507	220.502	513.8
F-104*	1147.2	1119.292	373.097	645.535
A-7*	958.5	882.449	294.149	772.634
GA1 Late	454.0	1270.121	423.373667	517.13
GA2	445.0	1030.723	343.574333	513.8
GA3	959.0	1494.386	747.193205	1013.433
F-16	420.0	1149.976	383.325333	505.142
F-18	700.0	1982.528	660.842667	743.237
F-4	850.0	1626.063	813.0315	963.816
F-15	710.0	1664.799	832.3995	863.117
F-105	680.0	1170.958	585.479	905.341

* Reliability data was collected in 1985

Note: All aircraft displayed in this table were renamed, and taken from the available data sets [4,38] (except F-16, F-18, F-4, F-15, F-105, F-104)

Table 8.10 shows the total aircraft DMHR calculated by the combination method compared with the total aircraft DMHR predicted by the functionality method and the real data. An average error for the combination method is approximately 57% and approximately 41% for the functionality method.

Table 8.11 shows the result of the U-99 FR and DMHR predicted by the combination method and the functionality method. The Pareto 40:70 portion has been chosen to predict the FR and DMHR in conjunction with TIF. The difference between these predicted values from two prediction methods is approximately 11% for the FR, and approximately 22% for the DMHR.

Table 8.10: Comparison between real aircraft defect man-hour rate and results of the combination method and functionality method [per 1000 flying hours]

Aircraft	Real data	Combination method	Functionality method
F2	17029.7	17580.38	9462.7
A1	13405.5	14248.79	9365.792
A2	9584.4	10698.21	9314.694
ATR1	7459.6	5118.266	7105.652
ATR2	4990.7	4282.271	6614.7
F-104	6216.3	5711.828	5030.52
A-7	7810.6	7867.151	3502.082
GA1 Late	3430.0	10744.59	6574.655
GA2	4500	8384.919	6614.7
GA3	959.0	3283.273	606.348
T1	5040.0	4383.341	9309.729

Note: All aircraft displayed in this table were renamed, and taken from the available data sets [4,38] (except F-104)

Table 8.11: Results of U-99 from reliability & maintainability assessment module

Method	Variable	Failure rate	Defect man-hour rate
Combination method	Highest (100)	401.7737	3368.80371
	Lowest (70)	20.48245	406.2553
	b coefficient	-1.160382	-0.824707
	Aircraft with TIF	298.681	-
	Aircraft without TIF	1194.726	12285.26
Functionality method	Aircraft	265.315	9602.858

8.4 Results from Life Cycle Cost Estimation

The Life Cycle Cost (LCC) estimation model is based on Woodford's [53] model. This predicts the total aircraft LCC for the entire aircraft life in peacetime, by using mostly aircraft conceptual design parameters. The model has been partly validated and modified to be able to predict the total aircraft LCC during wartime (see Chapter 5). However, only operation cost and flyaway cost are used to evaluate the total operational cost during either peacetime or wartime in this study. The operation cost will be averaged out over the total number of flying hours and over the total number of operational aircraft in one base throughout the aircraft lifetime, as shown in Table 8.12. The Operation cost per flying hour for U-99 is the highest due to only 500 flying hours for its entire life time.

The difference between the F-16 LCC during peacetime, calculated from Woodford's model and from the LCC estimation model in this methodology is approximately 4%, and approximately 3% for Eurofighter. Regarding the flyaway cost in FY92$M values quoted

Table 8.12: Results from life cycle cost estimation sub-module

Aircraft	LCC [M$/AC]		Flyaway Cost [M$]		Operation Cost [$/FH/AC]	
	Peacetime	Wartime	Peacetime	Wartime	Peacetime	Wartime
U-99	18.556	17.129	5.201	5.201	12292.561	9437.881
F-16	57.701	43.621	20.095	20.095	5212.074	3011.974
Eurofighter	123.646	101.355	51.818	51.818	5932.708	2960.647

by Woodford [53], the flyaway cost for F-16 calcuated from the LCC estimation model was apporximately 12% less than from the quoted price. Similar to the flyaway cost for Eurofighter, the difference is approximately 4.5%.

An alternative method used to predict the aircraft LCC is to use the FACET [25] commercial program. Mr. Pugh, formerly of the Directorate Project, Time, and Cost Analysis (DPTCAn), a division of the Ministry of Defence, used this program to estimate the U-99 LCC, as shown in Table 8.13. The difference between the U-99 flyway cost calculated from the FACET program and from the LCC estimation model in this methodology is approximately 4.4%. Regarding U-99 LCC predicted by FACET program, receiving directly from Mr. Pugh, the development cost does not take the avionics software development cost into account; therefore, the development cost discrepancy from both methods is significant high (approximately 86%).

Table 8.13: Comparison between U-99 LCC calculated from the LCC estimation module and from FACET [25]

Cost	LCC estimation module [M$]	FACET [M$]
Development	3377.511	1817.874
Production	2600.484	2717.604
Flyaway	5.201	5.4351

Fig. 8.4 shows the percentage of the operation cost over 4 years of peacetime scenario. An average operation cost is approximately $49,000 /aircraft/flying hour.

In the case of the U-99 life being increased to 20 years, nearly a half of LCC has to be spent on the operation cost, as illustrated in Fig. 8.5. The average operation cost per aircraft per flying hour also increases to $461,000 by assuming that the U-99 can be used for a total of 500 flying hours, as in its design specification.

Table 8.14 shows an overall U-99 LCC per aircraft during peacetime and wartime scenario comparing between 4 years and 20 years life time. The operation cost during the wartime scenario calculated from the LCC estimation model still excludes the weapons

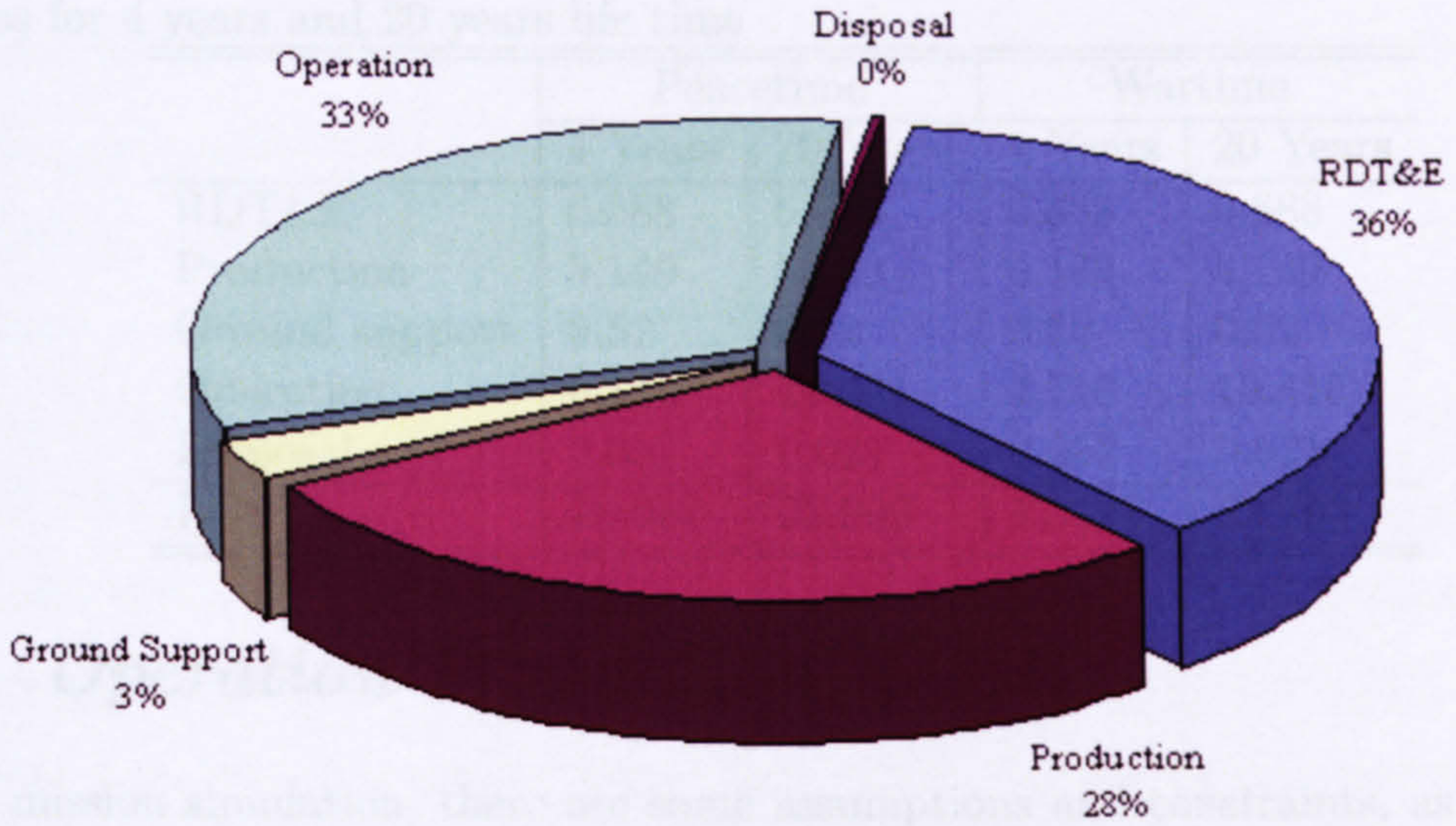

Figure 8.4: Results from U-99 LCC estimation in peacetime scenario for 4 years life time

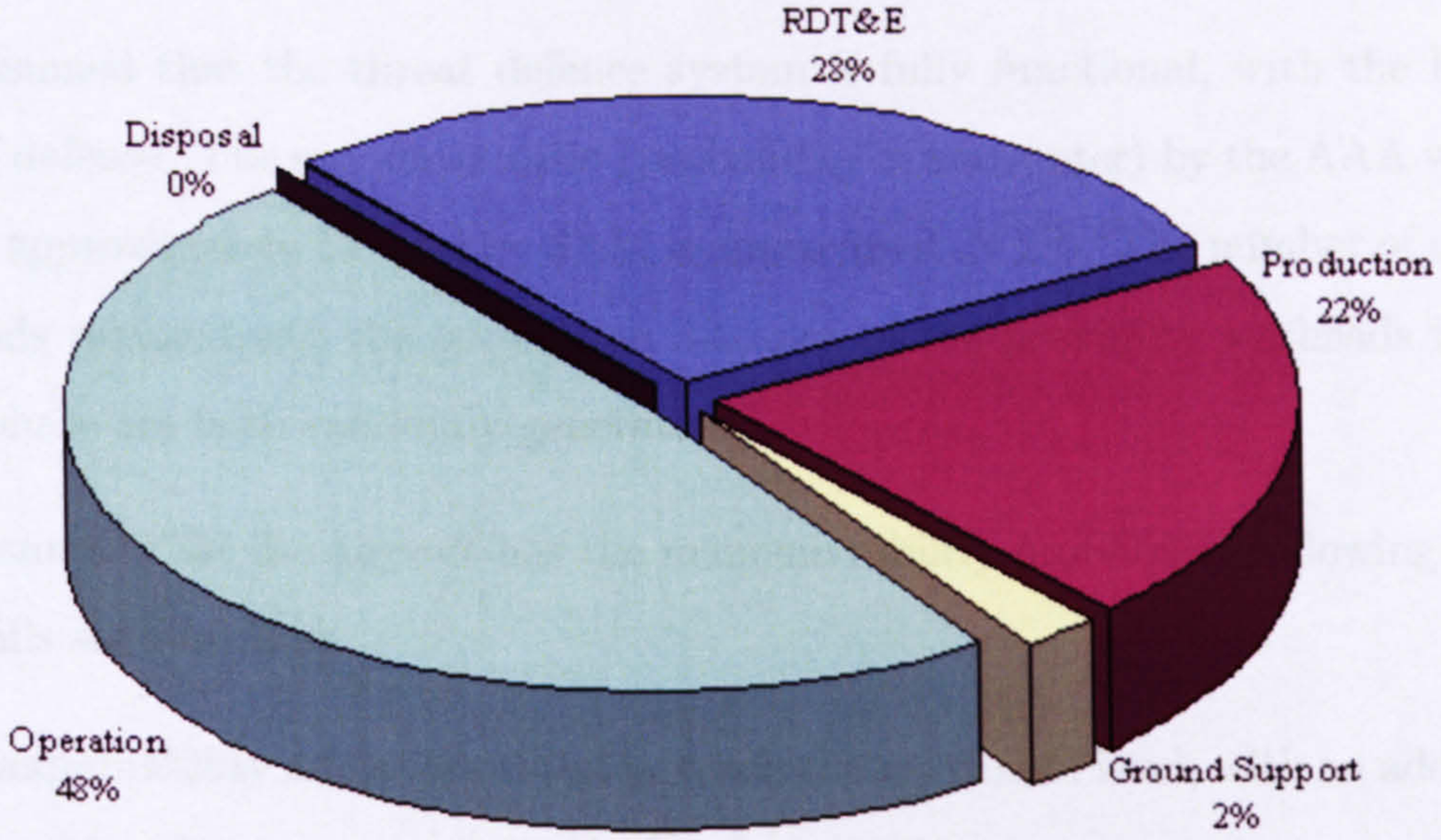

Figure 8.5: Results from U-99 LCC estimation in peacetime scenario for 20 years life time

released cost and the aircraft lost cost, which will be added later in the operation simulation module. The sum over these three major costs will be defined as the total operational cost.

Table 8.14: Comparison between LCC per one U-99 [M$] during wartime and peacetime scenarios for 4 years and 20 years life time

	Peacetime		Wartime	
	4 Years	20 Years	4 Years	20 Years
RDT&E	6.688	6.688	6.688	6.688
Production	5.149	5.149	5.149	5.149
Ground support	0.52	0.52	0.52	0.52
Operation	6.146	11.531	4.719	10.415
Disposal	0.052	0.021	0.052	0.021
LCC	18.087	23.909	17.128	22.793

8.5 Operation Simulation Results

In this mission simulation, there are some assumptions and constraints, as described in Chapter 6, which can be concluded as follows:

1. The mission scenario takes 10 operation days with a maximum of 2 operation sorties per day. The fleet size comprises 10 U-99 aircraft flying in the bomber role.

2. It is assumed that the threat defence system is fully functional, with the highest level of defense. The encounter ratio (probability of encounter) by the AAA weapon type is approximately 5% and by SAM is approximately 2%. The number of contact warheads released and the detonation distance of the proximity warheads in each flight phase are both randomly generated.

3. It is assumed that the aircraft has the manoeuvrability probability following option 2 (details see Fig. E.9).

4. The maintainability and supportability reach the maximum level, with an additional 12 hours of maintenance at the end of each operation day.

8.5.1 Results and Effects of an Individual Aircraft Measure of Performance on Operational and Operational Cost Measures of Effectiveness

The results from the operation simulation process, where only one specific aircraft MOP becomes a constant value throughout the simulation, will be presented in this section. With these results, the direct effect of an individual aircraft MOP on the operational and cost MOEs can be identified. The major aircraft MOPs investigated in this study are probability of detection (P_D), probability of hit (P_H), probability of aircraft kill on encounter with penetrators ($P_{K_{Non}}$), probability of aircraft kill on encounter with proximity

warhead, considering detonation distance ($P_{K_{Ext}}$), defect arising rate or failure rate (FR), mean time to repair defect ($MTTR_{Defect}$), mean time to repair damage ($MTTR_{Damage}$), and defect man-hour rate ($DMHR$).

To only evaluate the effect of aircraft probability of detection on the operational and operational cost MOEs, without any interference of of the other aircraft MOPs, the probability of detection for every aircraft view in every flight phase will be held at the same constant values. Fig. 8.6 shows the effect of the probability of detection on the entire operation and operational cost. Best fit linear modelling of the number of sorties flown, of complete sorties, of successful sorties, and of targets killed have been chosen to represent the actual data from the mission simulation. High order polynomial curves are not used to represent the data because, although the data is non-linear, it is every nearly linear and therefore, a linear approximation is sufficient in most cases. The remaining linear and polynomial curves representing the number of sorties flown, of complete sorties, and of successful sorties have been shown in Appendix E.

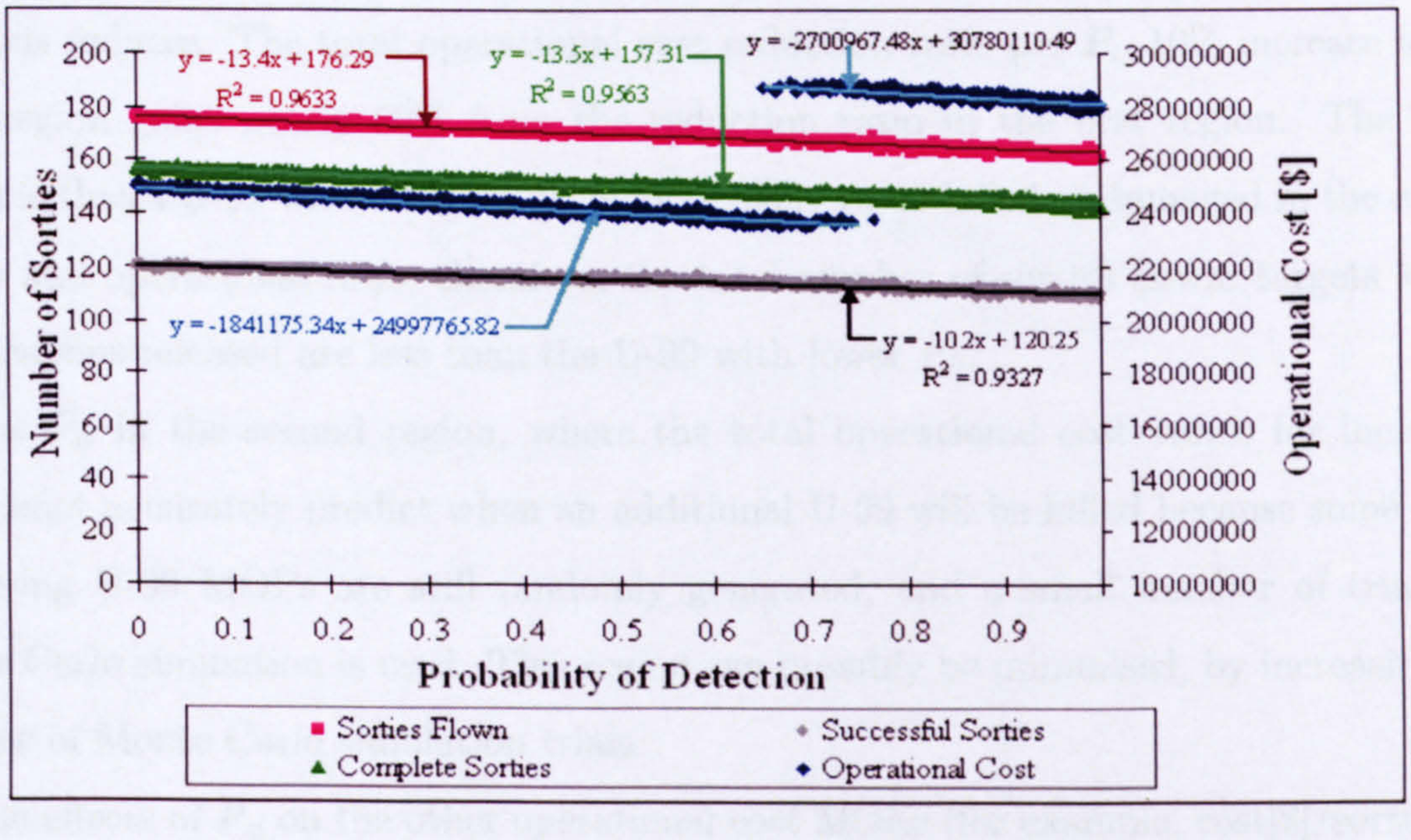

Figure 8.6: Effect of the probability of detection on the operational and operational cost

The number of sorties flown, complete sorties, successful sorties and also targets killed show decreases, of approximately 1.0 - 1.35 sortie reduction for every 10% increase in P_D. The target killed reduction is slightly less. The reduction of these operational MOEs appear to be more likely to be linear, with constant inclination because of very low percentage reduction (less than 1%). On the other hand, the reduction of the operational

cost MOEs consist of bounds over certain P_D regions. For example, the effects of P_D variation on the total operational cost can be divided into three P_D regions.

1. P_D between 0.0 - 0.65: In this region, the total operational cost reduces approximately \$184,000 for every 0.1 P_D increase.

2. P_D between 0.65 - 0.75: The total operational cost fluctuates with a range of approximately 5 M\$ over this P_D region due to Monte Carlo simulation effect.

3. P_D between 0.75 - 1.0: The reduction ratio in this region is approximately \$270,000 per 0.1 P_D increase.

An explanation for the first and the third regions, where the total operational cost reduces continuously, is that the number of U-99 flying hours decreases due to the higher possibility of detection in an early sortie and/or in an early operational day. Consequently, the U-99 is more likely to be hit, damaged, or defective in the early mission simulation period. Hence, the number of U-99 take-offs decrease and the number of weapons released also thus reduces. The total operational cost reduction ratio per P_D 10% increase in the third region gains nearly 50% from the reduction ratio in the first region. The main reason is that a U-99 with a higher P_D is more likely to be killed or damaged in the earlier sorties and operational days; therefore, the total number of sorties flown, targets killed, and weapons released are less than the U-99 with lower P_D.

The P_D in the second region, where the total operational cost varies for increased P_D, cannot accurately predict when an additional U-99 will be killed because some other remaining U-99 MOPs are still randomly generated, and a small number of trials for Monte Carlo simulation is used. This region can possibly be minimised, by increasing the number of Monte Carlo simulation trials.

The effects of P_D on the other operational cost MOEs (for example, cost[\$]/sortie and cost[\$]/target) are quite similar to the effect on the total operational cost. These operational cost MOEs can be considered as constant throughout the first and the third regions. For instance, cost[\$]/target decreases by approximately \$20 over a 0.1 P_D increase in the first region (see Fig. E.10). Comparing this \$20 decrease to the original cost[\$]/target of approximately \$200,000, this reduction is only approximately 0.01%, which can be neglected. The reason for the very small cost[\$]/target reduction percentages is that the reduced percentage over 10% increase in P_D compared to the original value of number of

targets killed (approximately 0.831%), and of the total operational cost (approximately 0.7365%) are both extremely small and close to each other.

Using a similar approach to present the effect of the probability of detection, the impact of the aircraft probability of hit on the operational and operational cost has been illustrated in Fig. 8.7. The discontinuities of operational cost appear in the specific regions, where an additional aircraft is killed. Additionally, the slope of each discontinuity increases, but are nearly constant, due to the substantial reductions in the amount of service time and weapons released. This decrease operational cost, due to both service time and weapons released reductions, is small. This leads to increases only in the reduction inclination, and does not cause any step changes. The remaining effects of the probability of hit (P_H) are similar to the effects of the P_D. The number of sorties flown, complete sorties, successful sorties and targets killed are defined as the number of specific sorties and targets. The number of specific sorties and targets, however, reduces more, and also the total operational cost fluctuates in several P_H regions.

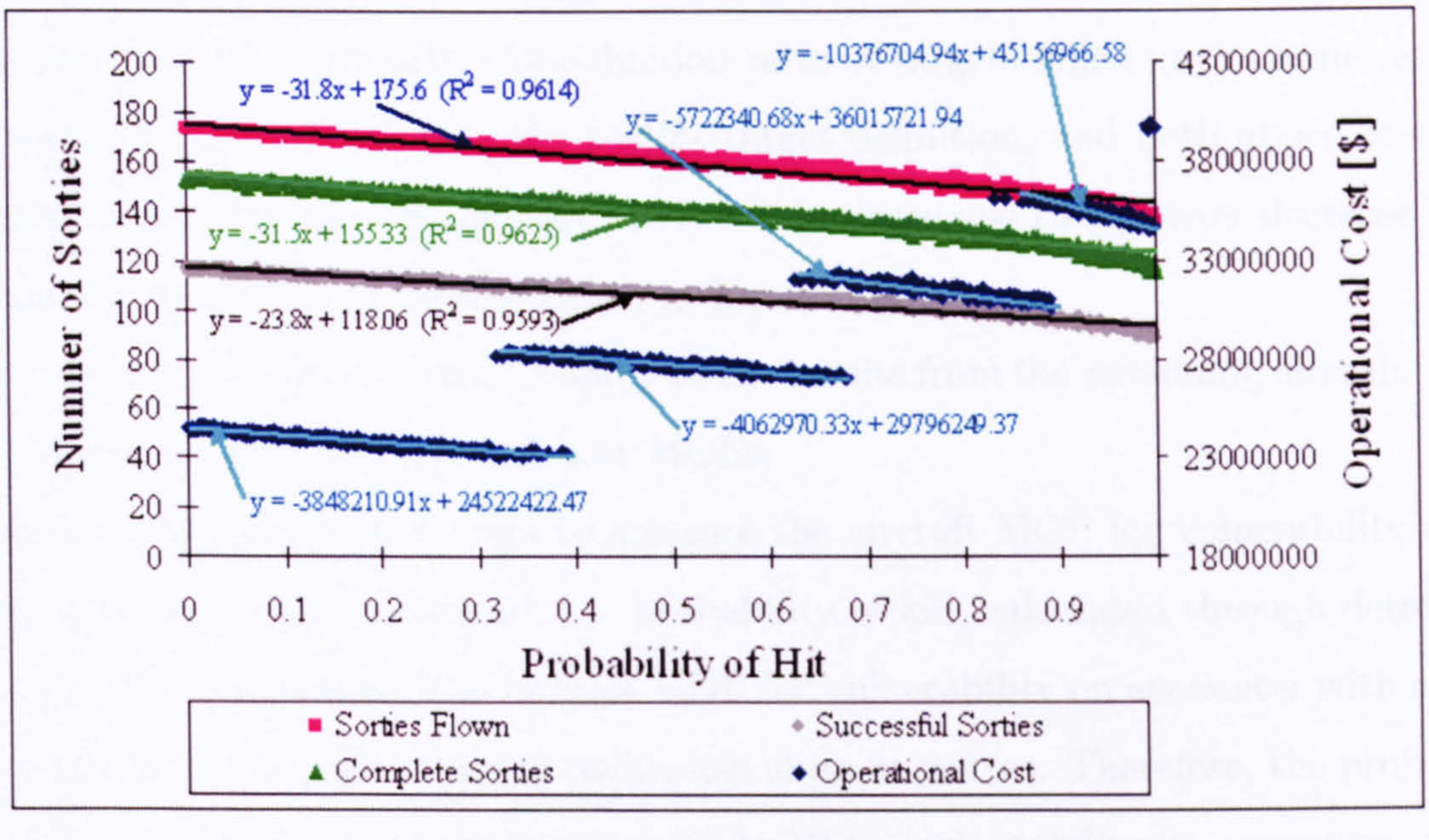

Figure 8.7: Effect of the probability of hit on the operational and operational cost

The trends of the specific sorties and targets reduction appear to increase over the P_H, and may be plotted as exponential curves. The regions where the number of the specific sortie inclination increases, are the same regions, where the total operational cost has a step change. This shows that the increasing of the specific sorties inclinations relates to the increasing number of aircraft lost. The same relationship for the change in gradient

for number of targets killed against P_H, as shown in Appendix E.

In the high P_H region, the number of specific sorties, targets killed, and the total operational cost reduce much more than in the lower P_H, due to aircraft being killed in an earlier stage of the mission simulation (see Fig. 8.7). The reason for this is the high P_D value of the U-99 case study aircraft. The trend of the reduction of specific sorties and targets killed in this region can be represented by an exponential curve. However, the reduction for an overall P_H range is still sufficiently represented by traces (see Fig. E.11).

The effects of P_H are different to these of P_D for the remaining operational cost MOEs; such as cost[$]/sortie, cost[$]/target and cost[$]/successful sortie. These operational cost MOEs increase with higher ratio within higher P_H regions, due to smaller numbers of specific sorties and/or targets killed. Higher increasing cost ratios result from the operational cost MOEs definition (see Chapter 5), in conjuction with the higher precentage reduction of the specific sorties and/or targets killed, compared to the reduced percentage of total operational costs within the high P_H region (see Fig. E.11). For instance; in the forth discontinuity area of the total operational cost, the reduction ratio in this region is approximately 2.3%. Similarly, the reduction ratio of targets killed in the same region is approximately 3.5%. Regarding the cost[$]/target definition, and both above described reduction ratios, this operational cost MOE will increase due to a greater decrease in the denominator, reduction of targets killed, in Eqn.(5.11).

The above explanations can also apply to the results from the remaining aircraft MOPs on the operational and operational cost MOEs.

There are two alternative ways to measure the aircraft MOP for vulnerability on encounter with a proximity warhead, i.e. probability of kill, calculated through detonation distance, and lethal radius. The aircraft MOP for vulnerability on encounter with a proximity warhead in the form of lethal radius has units in metres. Therefore, the probability of aircraft kill, which represents the aircraft MOP for vulnerability on encounter, with a proximity warhead calculated through detonation distance, has been chosen so that both two values (probability of aircraft kill on encounter with a proximity warhead and with penetrator) can be directly compared. The effect of the aircraft vulnerability on encounter with a non-explosive (penetrator) has been shown in Fig. 8.8, by keeping the aircraft kill probability on encounter with penetrators value constant in every flight phase, throughout the simulation, regardless the number of hits. The kill probability on encounter with a

proximity warhead is also calculated through generated random detonation distances in every flight phase.

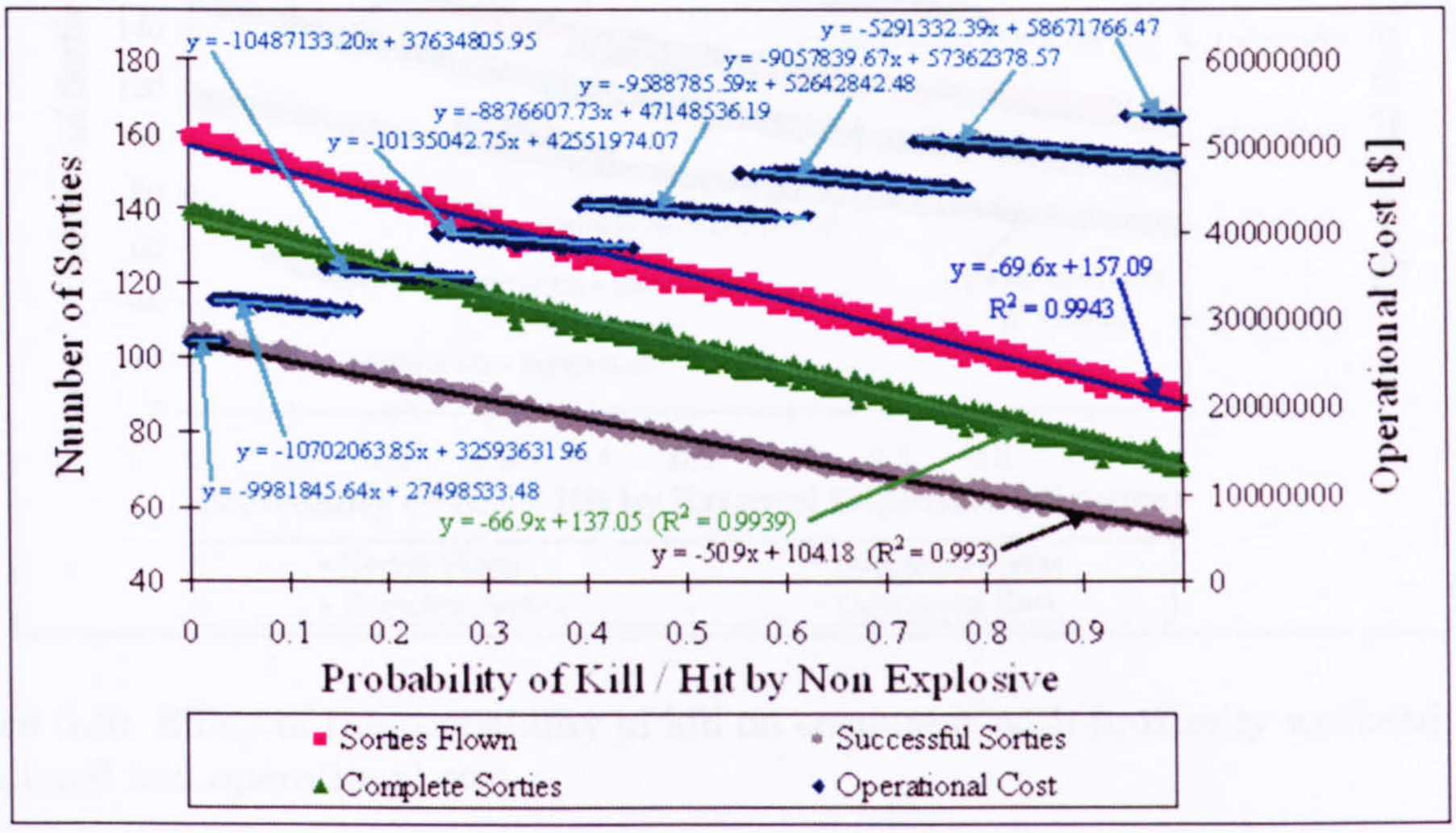

Figure 8.8: Effect of the probability of kill on encounter with penetrators on the operational and operational cost

Fig. 8.9 shows the effect of the aircraft kill probability on encounter with proximity warheads on operational and operational cost-effectiveness. In this approach, the probability of kill on encounter with proximity warhead is set as a constant value instead.

The impact of both P_K on encounter with penetrators and P_K on encounter with proximity warheads, calculated through a random detonation distance, are quite similar to the impact of the P_H. The specific sorties and targets killed reduction ratios over increasing P_K on encounter with penetrators tend to be constant and higher than the reduction ratios over P_K on encounter with proximity warheads. However, the reduction ratios of specific sorties and targets for increasing P_K on encounter with proximity warheads seem to reduce (divergence). The causes of these phenomena are:

I.) The probability of encounter by penetrators has been set higher than by proximity warheads. Therefore, the reduction ratios of specific sorties and targets for increasing P_K on encounter with penetrators are higher than the reduction ratios for increasing P_K on encounter with proximity warheads.

II.) The reduction ratio of specific sorties and targets for increasing P_K on encounter

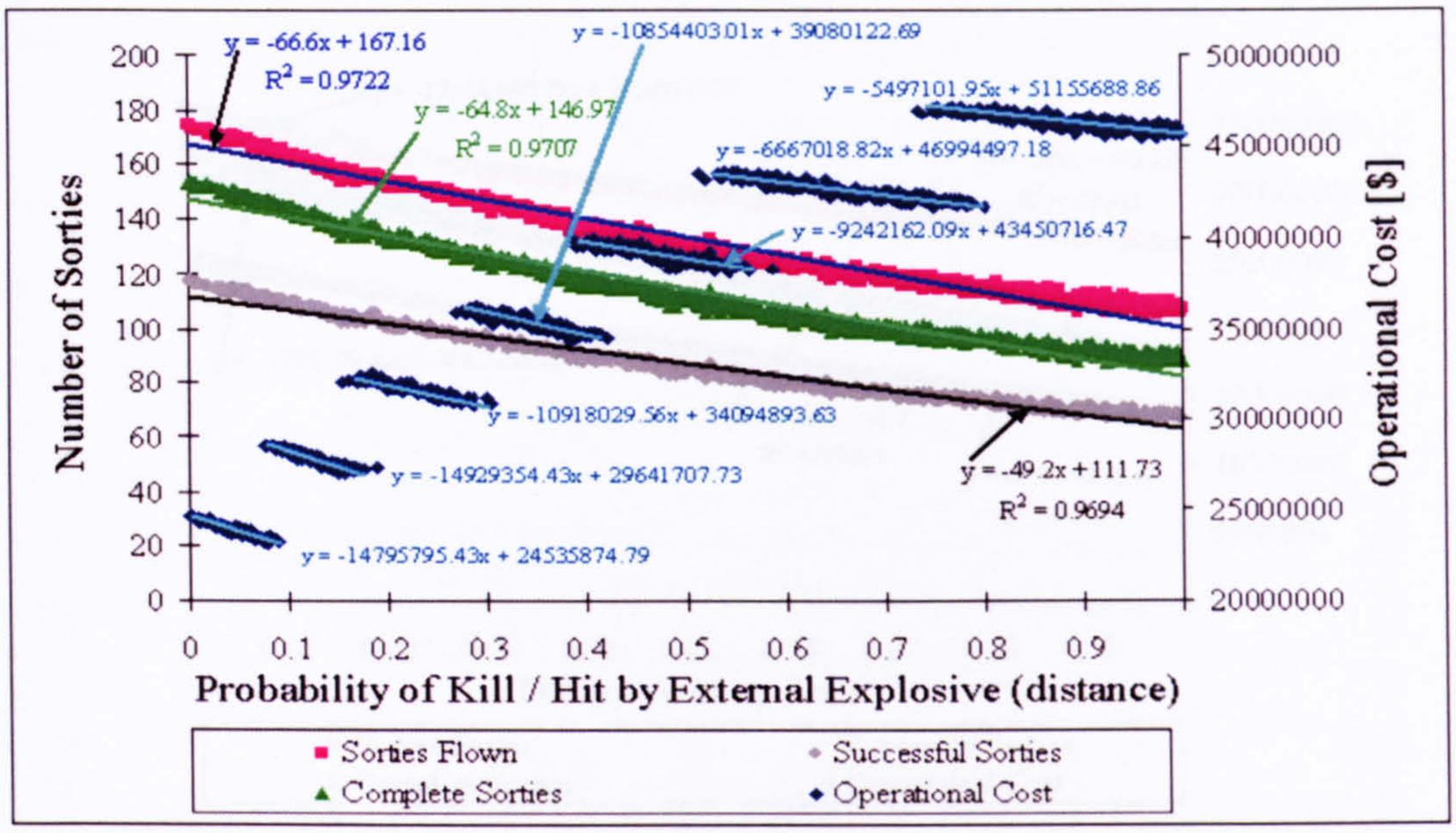

Figure 8.9: Effect of the probability of kill on encounter with proximity warhead on the operational and operational cost

with proximity warheads is reduced due to the lower probability of encounter by proximity warheads. In this case the aircraft would be more likely to be killed in a later sortie, and in a later operational day. Therefore, the total number of specific sorties and targets would not reduce much, even if the number of aircraft killed increased.

The trends of the total operational cost reduction ratio follow the trends of the total number of sorties flown reduction ratio, for the same reason as described above. The remaining operational cost MOEs are similar to that of P_H, in that there is an increasing ratio rise, yet in a different order, depending on the specific sorties, targets killed, and the total operational cost reduction ratios over increasing P_K on encounter with penetrators and proximity warheads.

The reliability probability effect on the operational and operational cost has been shown in Fig. 8.10. The maximum reliability probability value studied in this methodology has been set as 0.1 due to the assumption that the operational reliability is approximately 10% of the aircraft reliability.

The effects of the aircraft MOP for reliability on the operational MOEs are quite similar to the effects of the other aircraft MOPs, in which the specific sorties or targets killed approximately decreases steadily with different inclinations. The effect of reliability

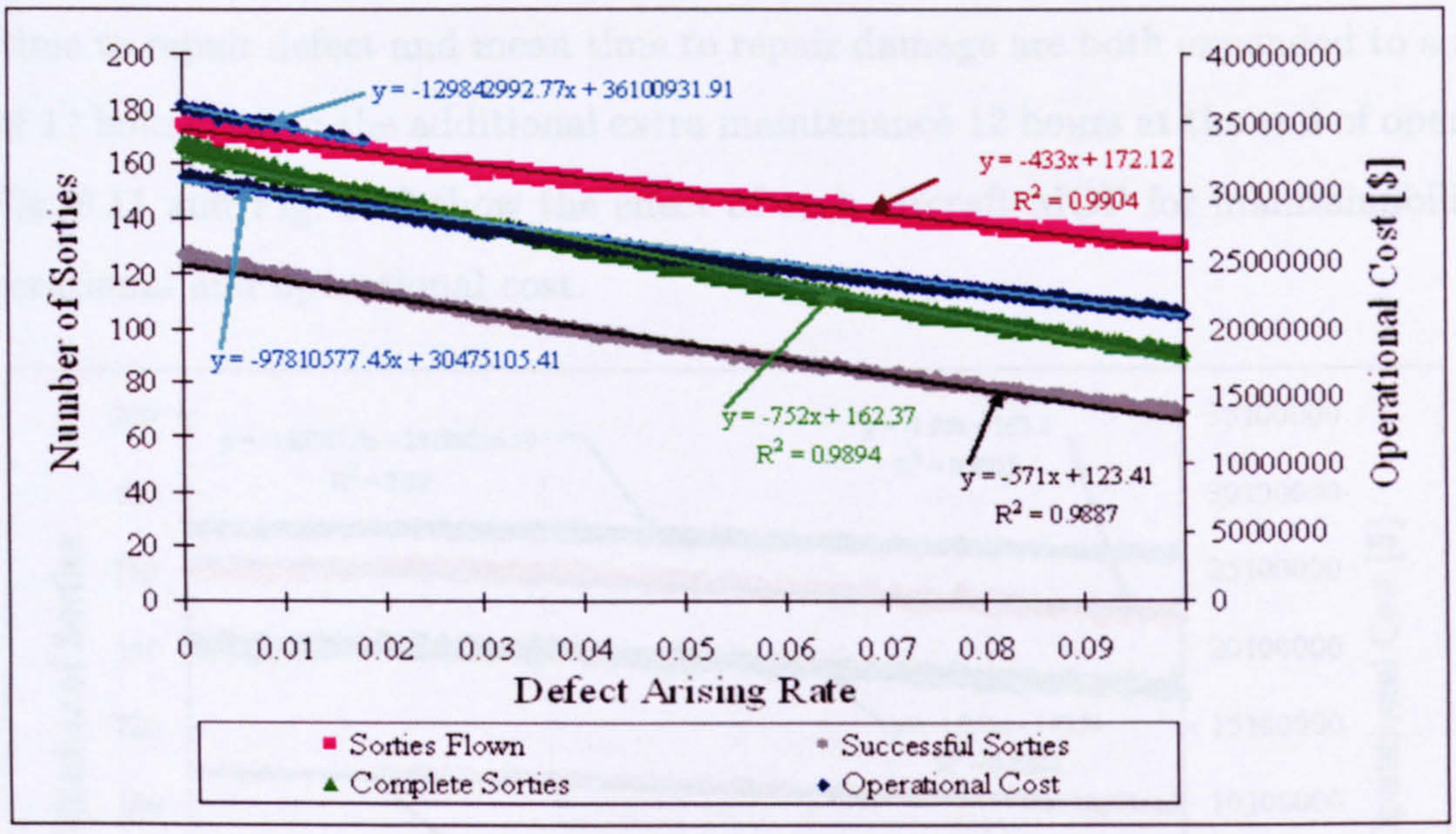

Figure 8.10: Effect of the reliability probability on the operational and operational cost

on the total operational cost fluctuated at the very low defect arising rate region. The costs decrease continuously instead. This shows that the effect of this design aspect directly affects the number of aircraft being killed, in the opposite way from the effects of the other aircraft MOPs. In the case that an aircraft had a high defect arising rate, this aircraft would be less likely to be killed. The main reason is that aircraft with high defect arising rate would operate in the mission simulation for a shorter time due to more maintenance being required. In the other words, for an aircraft frequently aborting a sortie, there was less risk of being attacked. The total number of aircraft killed, the total service time, and the total number of weapons released consequently reduced.

Due to the research time-scale and because of LCC estimation modelling, the maintenance cost was included within the total O&S cost, which was averaged over the total number of operational aircraft in one base and the total flying hours for the entire aircraft life.

The effects of the reliability on the remaining operational cost MOEs are quite similar to the effects of the other aircraft MOPs. Trends of these operational cost MOEs depend on the specific sorties or targets killed reduction proportion, compared to the total operational cost reduction ratio, as discussed above.

On the other hand, the maximum maintainability probability values represented by

mean time to repair defect and mean time to repair damage are both expanded to a maximum of 12 hours due to the additional extra maintenance 12 hours at the end of operation day. Fig. 8.11 and Fig. 8.12 show the effect of each aircraft MOP for maintainability on the operational and operational cost.

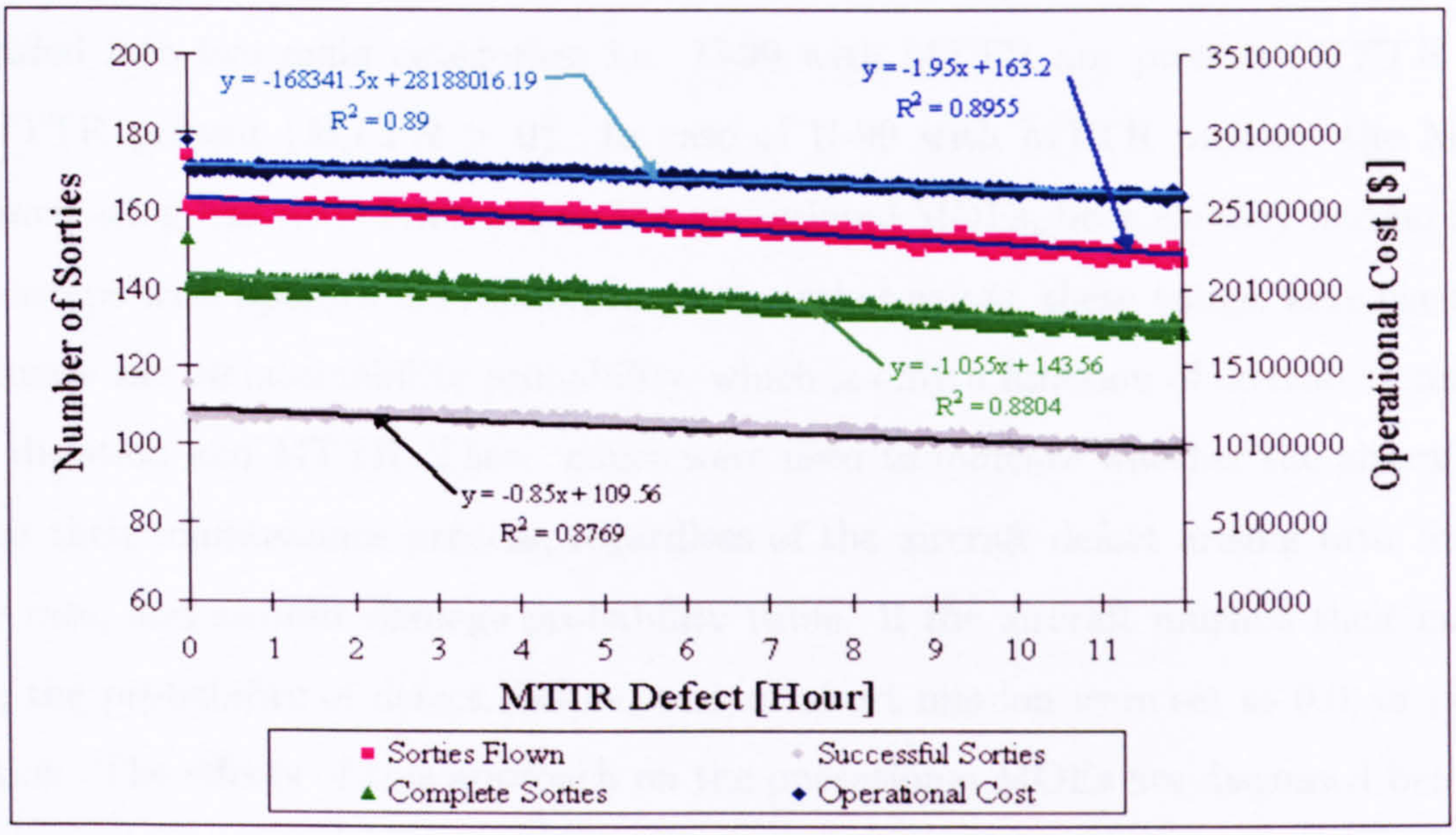

Figure 8.11: Effect of the mean time to repair defect on the operational and operational cost

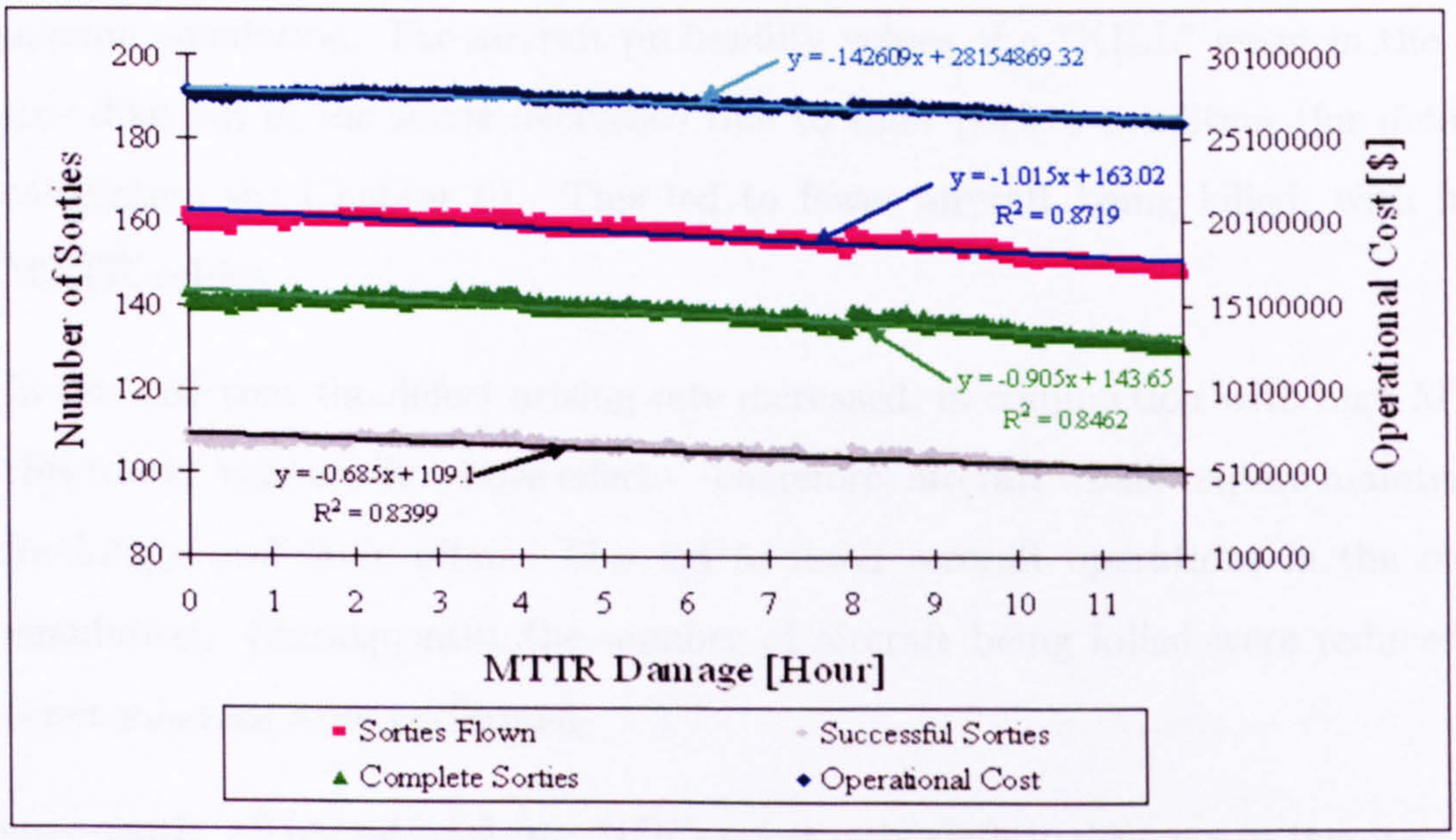

Figure 8.12: Effect of the mean time to repair damage on the operational and operational cost

The effects of the $MTTR_{Defect}$ and of the $MTTR_{Damage}$ on the operational and operational cost are very similar, shown by the traces and linear regression equations illustrated in Fig. 8.11 - 8.12. Therefore, the effect of $MTTR_{Defect}$ represents the aircraft MOP for maintainability in this study.

In this study, the effects of U-99 MOP for maintainability in the form of MTTR could be divided into two main categories; i.e. U-99 with MTTR not present ($MTTR = 0$) and MTTR present ($MTTR > 0$). In case of U-99 with MTTR present, the MTTR value increasing had little influence on the operational MOEs, because they had no direct relationships with operational reliability. In the other words, these values were used only to estimate the maintainability probability, which is only a function of aircraft in maintenance duration and MTTR. These values were used to indicate whether the aircraft had finished their maintenance process, regardless of the aircraft defect arising rate, aircraft failure rate, and aircraft damage probability value. If the aircraft finished their maintenance, the probability of defect, failure, and/or abort mission were set as 0.0, or perfect condition. The effects of this approach on the operational MOEs are discussed below:

I.) The total service time and total number of weapons released decrease due to the longer maintenance requirement and fewer sorties flown.

II.) Due to the longer maintenance required, there were fewer aircraft operating in the mission simulation. The aircraft probability values of a "KILL" event in the event tree diagram in the sortie decreased due to their perfect condition (for details of calculation see Chapter 6). This led to fewer aircraft being killed, with higher MTTR values.

III.) In the case that the defect arising rate increased, in conjunction with high MTTR, this would increase the above effects. Therefore, aircraft would require maintenance for longer and more often. This led to fewer aircraft operations in the mission simulation. Consequently, the number of aircraft being killed were reduced, but fewer missions were performed.

Consequently, all operational cost MOEs constantly slightly decrease or increase, without any bounds (step changes). Their inclinations depend on the specific sorties or targets killed reduction ratio compared to the total operational cost reduction ratio.

In the case of U-99 with MTTR not present, U-99 did not require any maintenance after operational sorties. They were consequently in perfect condition and immediately ready for the next operational sortie. Unlike the case of MTTR present, here the U-99 could be ready, at the earliest for the operational sortie after the next immediately operational sortie. Therefore, there were no significant effects of increasing MTTR values.

In this study, scheduled maintenance and DMHR were not taken into account during the operation mission simulation. Hence, they only affect the operational cost, and do not affect the number of sorties during the mission operation simulation, as illustrated in Fig. 8.13. Therefore, the effect of scheduled maintenance will not be presented in this study.

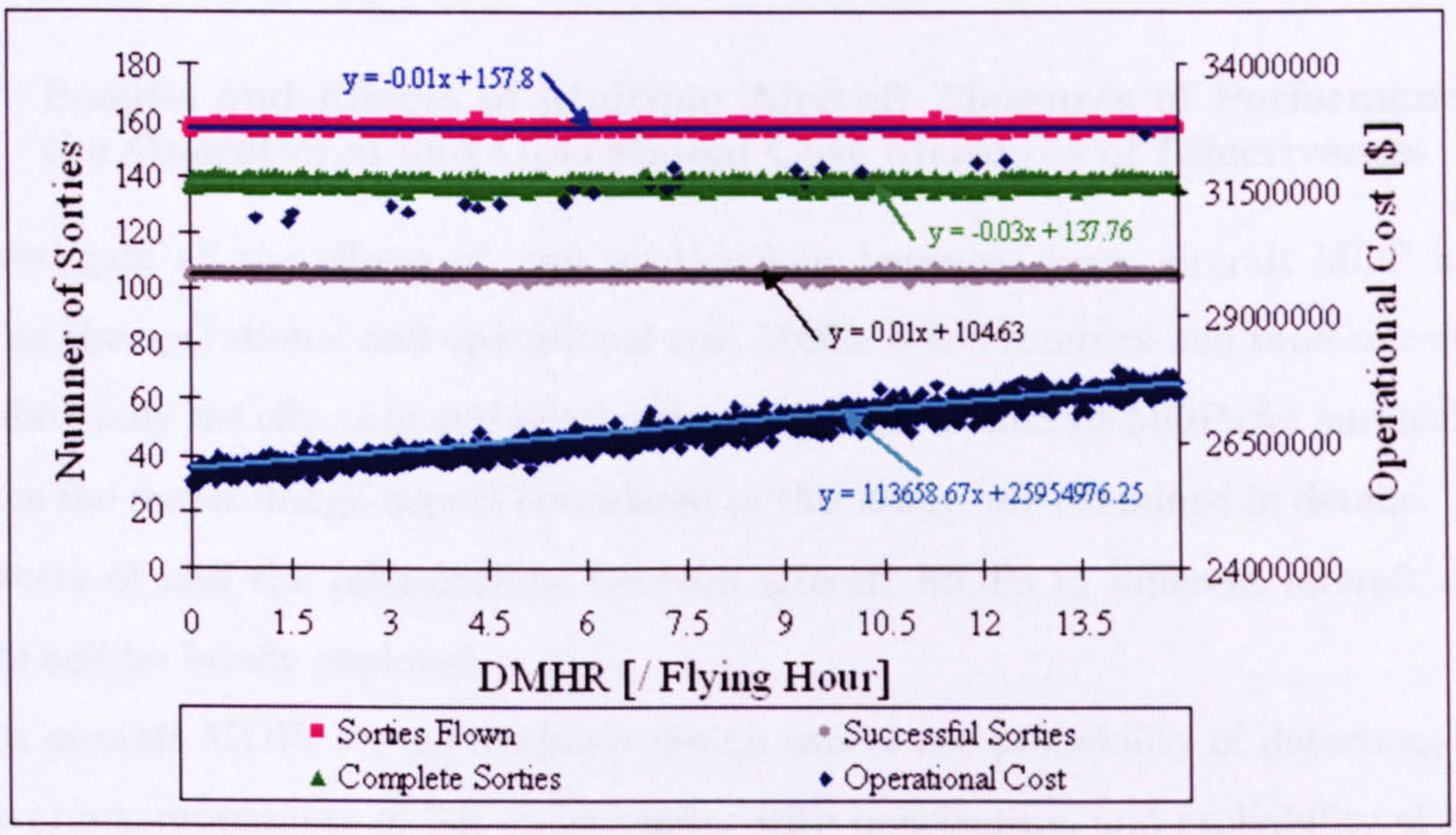

Figure 8.13: Effect of the defect man-hour rate on the operational and operational cost MOEs

The DMHR had a direct impact on the total operational cost via an average operational cost per aircraft per flying hour (for details see Chapter 5). By increasing this value, the operational cost MOPs would also rise.

The effects of increasing an individual U-99 MOP on the operational and operational cost MOEs are summaried and shown in Table 8.15. This can be used to indicate the approximate effects of this U-99 MOP on the number of specific sorties and targets, total operational cost, cost[$]/specific sortie, and cost[$]/target.

Table 8.15: Effect of increasing an individual U-99 MOP on operational and operational cost MOEs

	P_D	P_H	P_K	$P_{Encounter}$	Defect Arising	MTTR	DMHR
Effect on number of specific sorties and targets	- +	-	- -	-	- -	- +	X
Effect on the total operational cost	+ -	+	+	+	- -	- +	+ -
Effect on the remaining operational cost MOEs	+ -	+ -	++	+	+/-	+ -	+ -

X = No Effect	+/- = May increase or decrease
- + = Slight decrease	+ - = Slight increase
- = Decrease	+ = Increase
- - = Significant decrease	++ = Significant increase

8.5.2 Results and Effects of Multiple Aircraft Measures of Performance on the Operational and Operational Cost Measures of Effectiveness

To investigate all the effects of, and relationships between, every aircraft MOP in this study on the operational and operational cost MOEs is too complex and time-consuming. Therefore, only the effects of and relationships between all aircraft MOPs for survivability, which is the major design aspect considered in this study, are examined in details. Then, the effects of and the relationships between aircraft MOPs in different aircraft design aspects will be briefly explored.

The aircraft MOPs for survivability design aspect are probability of detection, probability of hit, probability of kill on encounter with penetrators, and probability of kill on encounter with proximity warheads, calculated through the detonation distance. Fig. 8.14 shows the effects of aircraft probability of detection and aircraft probability of kill on encounter with penetrators, by increasing aircraft probability of kill on encounter with a proximity warhead, and constant aircraft probability of hit. Complete results and charts of these effects and relationships have been shown in Appendix E.

Survivability is a combination of susceptibility (P_D and P_H) and vulnerability ($P_{K_{Non}}$ and $P_{K_{Ext}}$). Therefore, the effects of, and relationships between, both design aspects can be shown, and will be discussed here as follows:

I.) In the case that an aircraft has a low probability of detection, the reduction ratio of the total number of specific sorties and targets slightly decreased for increases in P_K

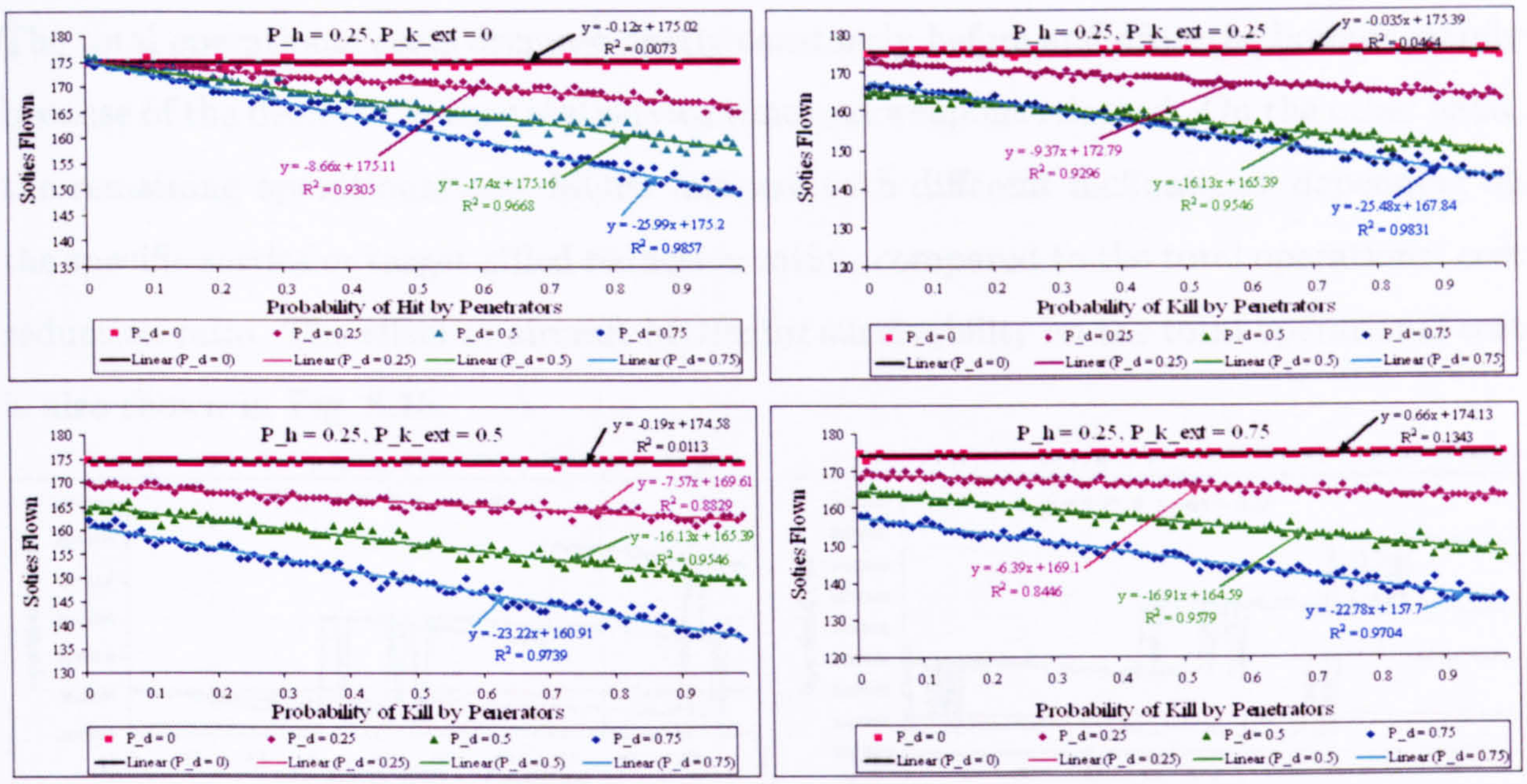

Figure 8.14: Effect of P_D and $P_{K_{Non}}$ with increasing $P_{K_{Ext}}$ and constant P_H on the number of the total sorties flown

and P_H. Additionally, reduction ratios seemed to decrease slightly with increasing P_K. The explanation of this matter is that additional aircraft were killed, but were not killed earlier in the sortie and the operational day.

II.) In the case that an aircraft has a high probability of detection, the reduction ratio of the total number of specific sorties and targets dramatically increases, and significantly increases for high regions of P_H and P_K. The main reason is that additional aircraft were killed, and earlier in the sortie and in the operational day.

III.) In the case that the aircraft probability of hit increases, but the remaining probabilities are unchanged, then the relationships between the aircraft MOPs for survivability are also unchanged. The only effect of increasing probability of hit on the operational MOEs is that the total number of specific sorties and targets reduces.

IV.) In the case that the probability of threat encounter in the mission simulation increases, the reduction of the total number of specific sorties and targets will slightly increase due to the supplemental effect of increasing the probability of encounter.

The total operational cost, cost[$]/target, cost[$]/sortie and the other operational cost MOEs generally vary over increasing aircraft MOPs for survivability in the form of discontinuity curves, mainly due to increases in the numbers of aircraft being killed.

The total operational costs decrease nearly constantly before and after the bounds mainly because of the decrease in the total service time and weapons released. On the other hand, the remaining operational cost MOEs increase with different inclinations, depending on the specific sorties or target killed reduction ratios, compared to the total operational cost reduction ratio. The effect of aircraft MOPs for survivability on the total operational cost is also shown in Fig. 8.15.

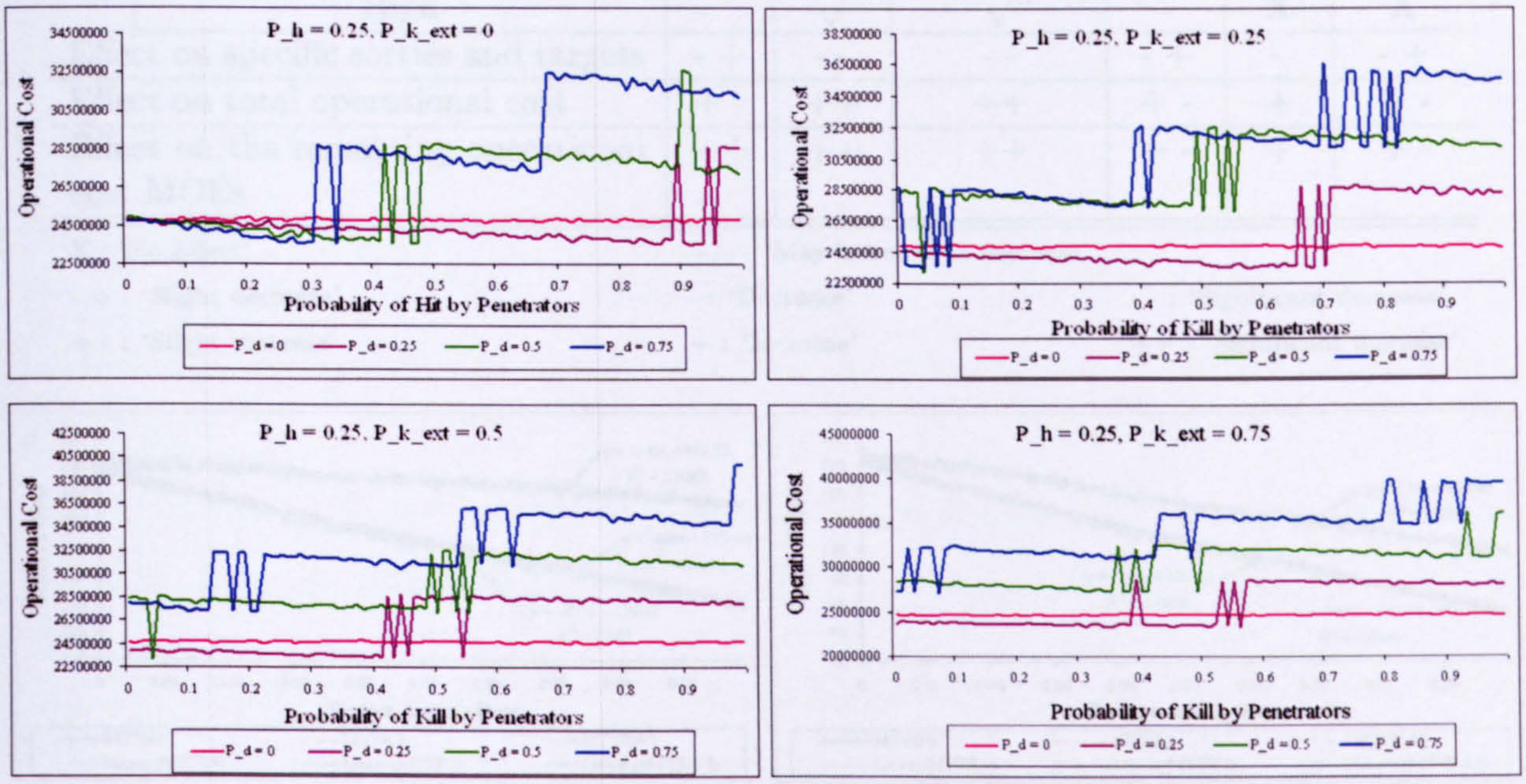

Figure 8.15: Effect of P_D and $P_{K_{Non}}$ with increasing $P_{K_{Ext}}$ and constant P_H on the total operational cost

Survivability consists of susceptibility and vulnerability; therefore, the aircraft MOP for survivability can be affected by increasing susceptibility or vulnerability, or by increasing both values. This can be summerised and shown in Table 8.16.

Only the effects of reliability & maintainability will be examined in this study due to research time scale and the paucity of information in this design aspect. Therefore, each aircraft MOP for reliability & maintainability is considered separately, unlike aircraft MOPs for survivability. However, simple relationships between aircraft defect arising rate and the aircraft mean time to repair defect related to the operational and the operational cost MOEs can be discovered. Fig. 8.16 shows the effect of, and the relationship between, the aircraft MOP for reliability (defect arising rate) and aircraft MOP for maintainability ($MTTR_{Defect}$) on the operational MOE.

In the case that the $MTTR_{Defect}$ value is not equal to zero (aircraft with $MTTR_{Defect}$

Table 8.16: Generic effects of increasing individual aircraft MOPs for survivability on operational and operational cost MOEs

		P_D		P_H		P_K	
		Low	High	Low	High	Low	High
P_D	Low	X	X		√		√
	High	X	X	√		√	
P_H	Low	√		X	X		√
	High		√	X	X	√	
P_K	Low	√			√	X	X
	High		√	√		X	X
Effect on specific sorties and targets		- +	- -	- -	- +	-	- +
Effect on total operational cost		+ -	++	++	+ -	+	+ -
Effect on the remaining operational cost MOEs		++	++	++	+ -	+	+ -

X : 'No Effect' +/- : 'May increase or decrease'

- + : 'Slight decrease' - : 'Decrease' - - : 'Significant decrease'

+ - : 'Slight increase' + : 'Increase' ++ : 'Significant increase'

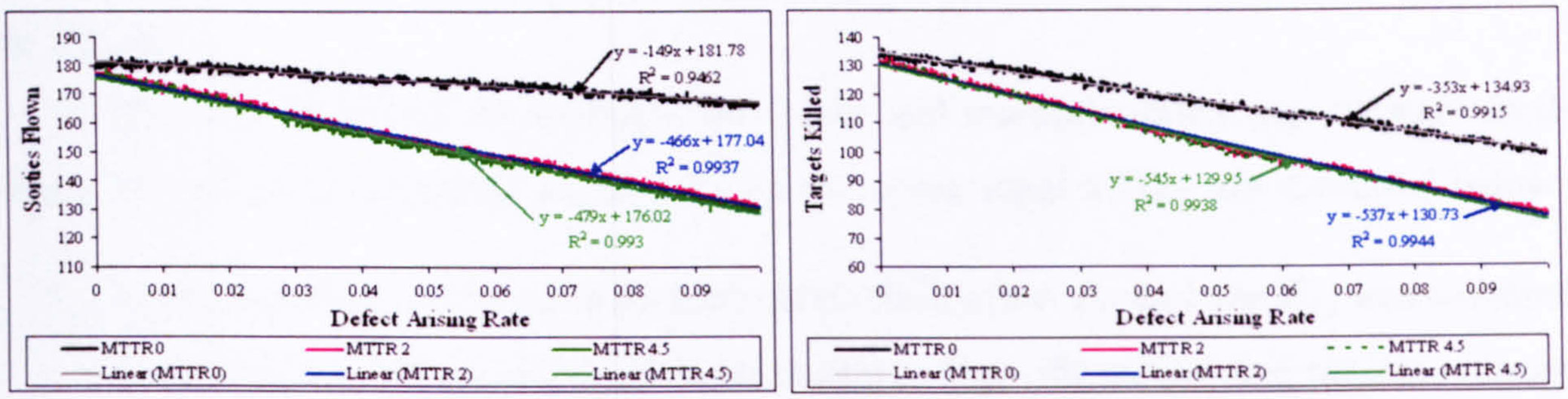

Figure 8.16: Effect of aircraft defect arising rate with increasing $MTTR_{Defect}$ on numbers of the total sorties flown and the total targets killed

present), the effects of this value on the total number of sorties flown and of targets killed are more significant than the effect in case that $MTTR_{Defect}$ value is equal to zero (aircraft with $MTTR_{Defect}$ not present). On the other hand, the effect of increasing the $MTTR_{Defect}$ of the aircraft with $MTTR_{Defect}$ present are quite small. Therefore, only 2 assumed $MTTR_{Defect}$ values (2 and 4.5) have been integrated to investigate the effect of aircraft MOP for maintainability, in conjunction with the other aircraft MOPs.

In the case that an aircraft was predicted to have 100% survival ($P_D = 0$ and/or $P_K = 0$), the total number of specific sorties and targets continuously decreased, with increasing inclinations resulting from the increase of the reliability and maintainability probability values. The explanation is that aircraft stayed longer in maintenance, had earlier and more frequently-aborted missions. Therefore, the total operational cost decreased. The remaining operational cost MOEs, however, increased or decreased with approximately

constant inclinations, depending on the total operational cost reduction ratio, compared to specific sorties or targets killed reduction ratios. Some operational cost MOE inclinations were nearly the same regardless of the variation in maintainability. This could be caused by the fact that the reduction ratio of the total operational cost, compared to the reduction ratio of the specific sorties or targets killed for each MTTR value, were very close to each other. The physical explanation was that the survivability was not taken into account; therefore, none of the operational aircraft were killed. The reduction of targets killed was caused only by the aircraft abort frequency, and required longer maintenance duration, as described above.

By combining all major aircraft MOPs in this study together, such as defect arising rate, $P_D, P_{K_{Non}}, P_{K_{Ext}}, MTTR_{Defect}$ and $DMHR$, the effects of all design aspects in this study on the operational and operational cost effectiveness can be shown, as illustrated in Fig. 8.17.

In the cases where all survivability, reliability and maintainability aspects were modelled, the effects of increasing P_D and P_K on the operational MOEs are discussed below:

I.) In the case that an aircraft with high survivability (low P_H and low P_K) was assumed not to require maintenance, the total number of specific sorties and targets reduced slightly due only to the effect of aircraft defect arising rate.

II.) In the case that an aircraft with low survivability (high P_H and high P_K) was assumed not to require maintenance, the total number of specific sorties and target increased slightly over increasing defect arising rate. The reason is that aircraft aborted their mission more often and in earlier sortie phase, and in earlier operational days, rather than being killed. This led to the fact that there were more operational aircraft in later sorties and later operational days, which could increase the number of take-offs (sorties flown). However, this did not guarantee that the other specific sorties and targets would also increase.

III.) In the case that an aircraft with high survivability was assumed to require maintenance, the effects of aircraft with low MTTR present and aircraft with high MTTR present on the total number of specific sorties and targets were quite small due to there being no direct relationship between MTTR and defect arising rate, as described above. The total number of specific sorties and targets decrease resulted

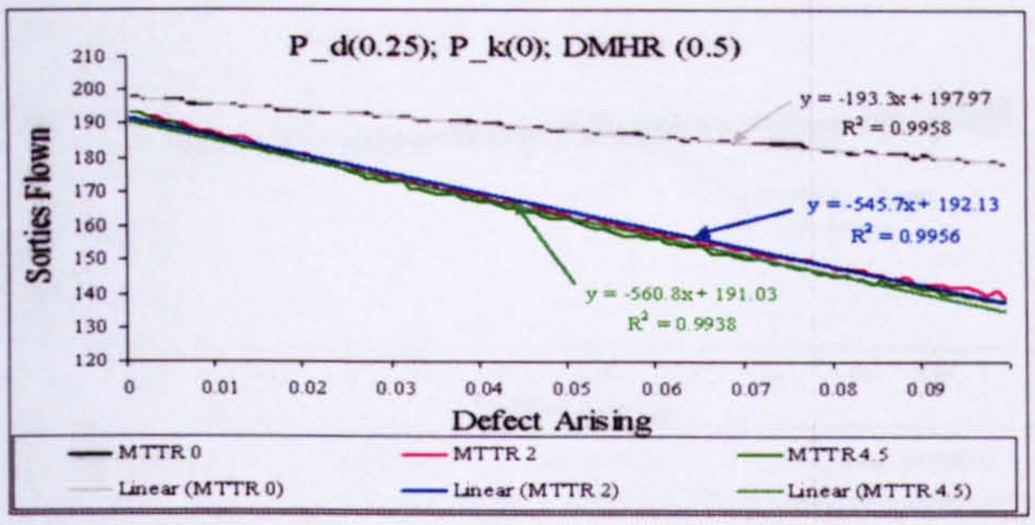

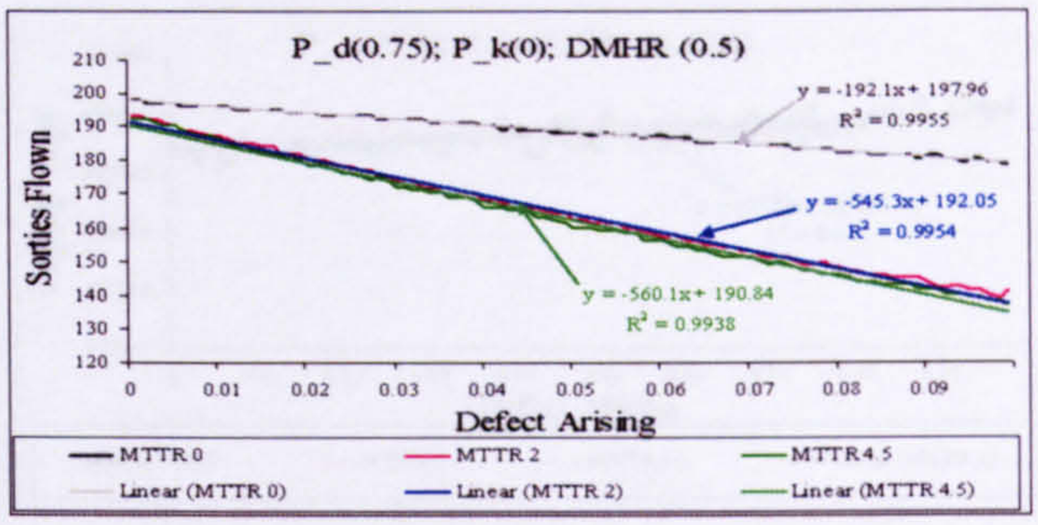

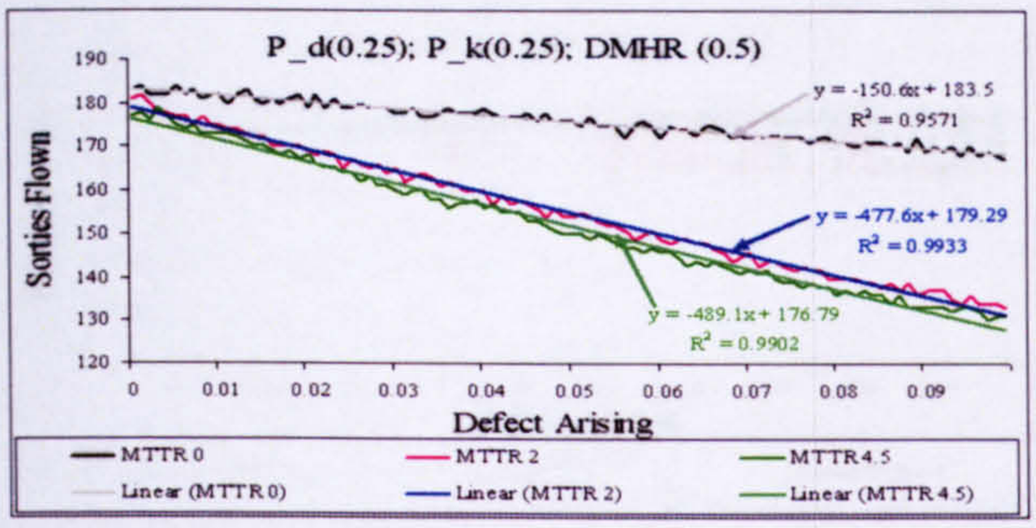

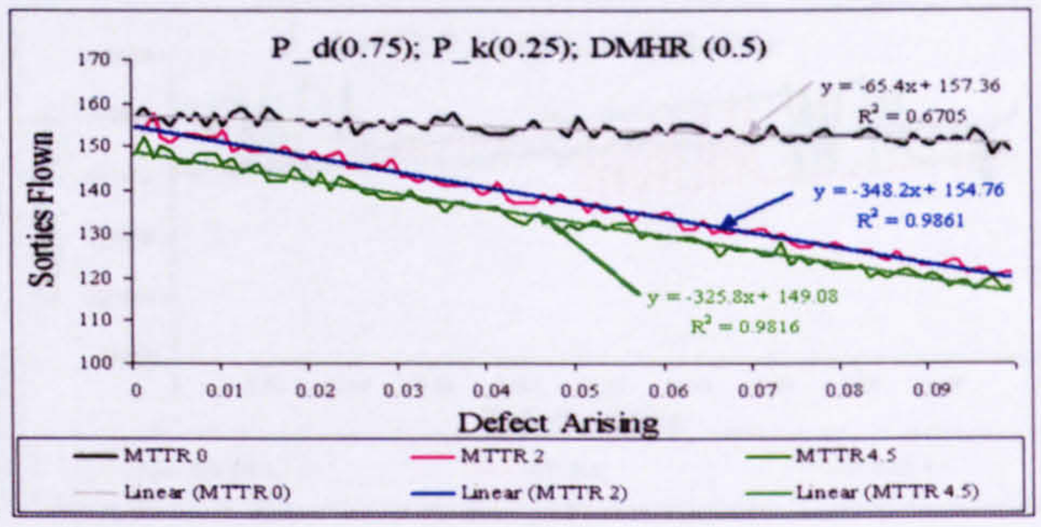

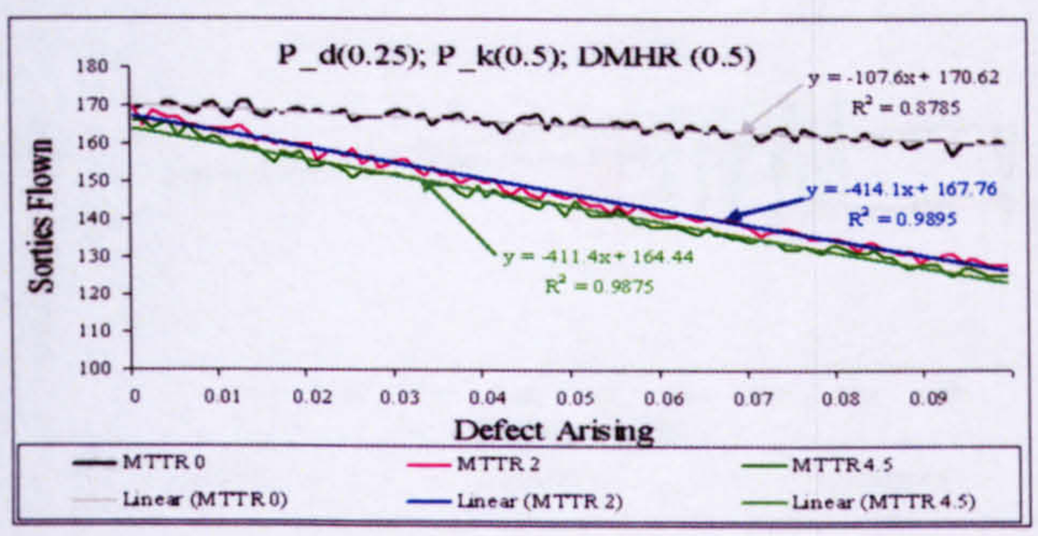

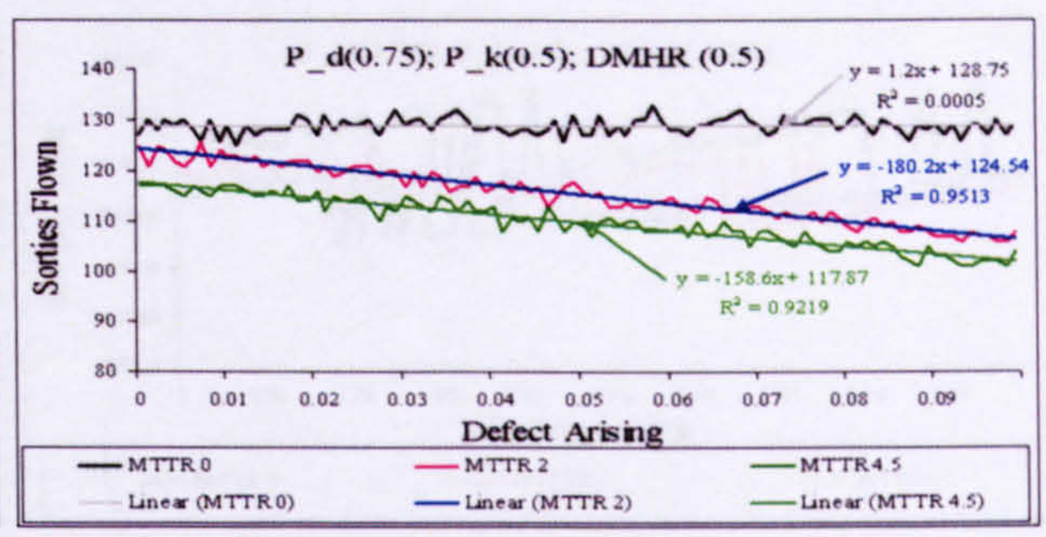

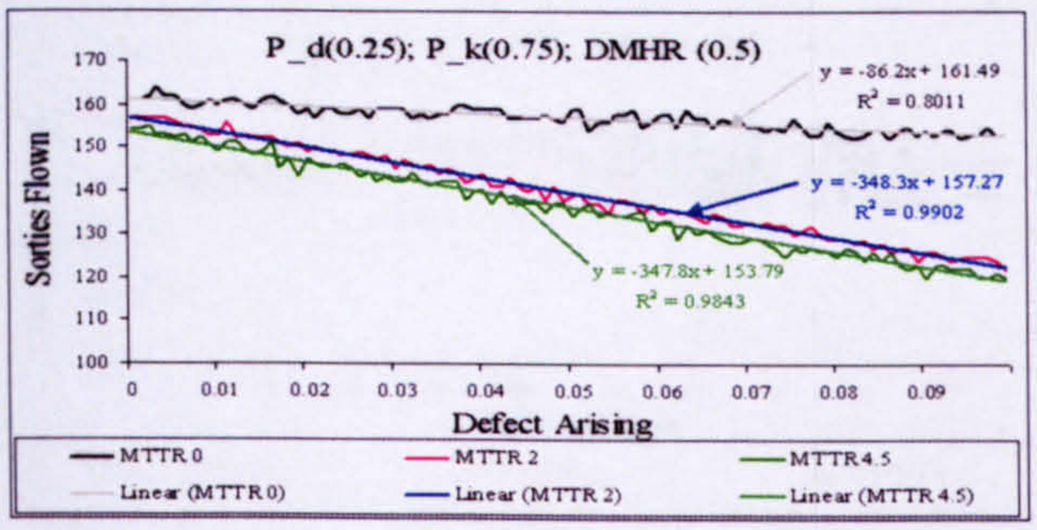

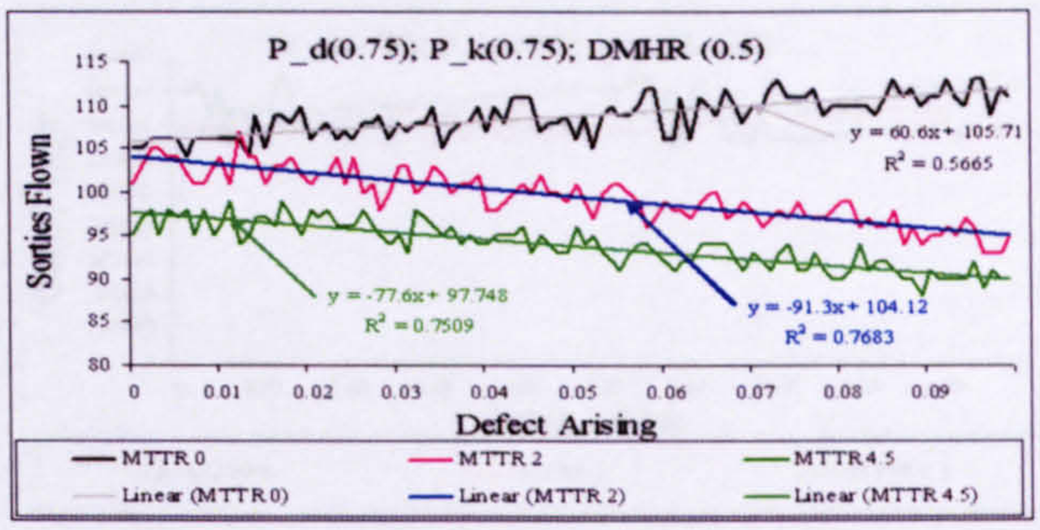

Figure 8.17: Effect of aircraft defect arising rate, P_D, $P_{K_{Non}}$, $P_{K_{Ext}}$ and $MTTR_{Defect}$ with a constant DMHR on the total number of sorties flown

mainly from the effect of defect arising rate.

The effects of these aircraft MOPs on the other remaining operational MOEs are quite similar to the effect on the total number of sorties flown, as shown in Appendix E.

On the other hand, the effects of aircraft MOPs on the cost[$]/sortie and cost[$]/target are slightly different from the effect on the operational cost. However, there is a similar trend of increasing and/or decreasing of all three operational cost MOEs. For instance, all cost decreasing or increasing traces have a constant gradient for every P_D and P_K.

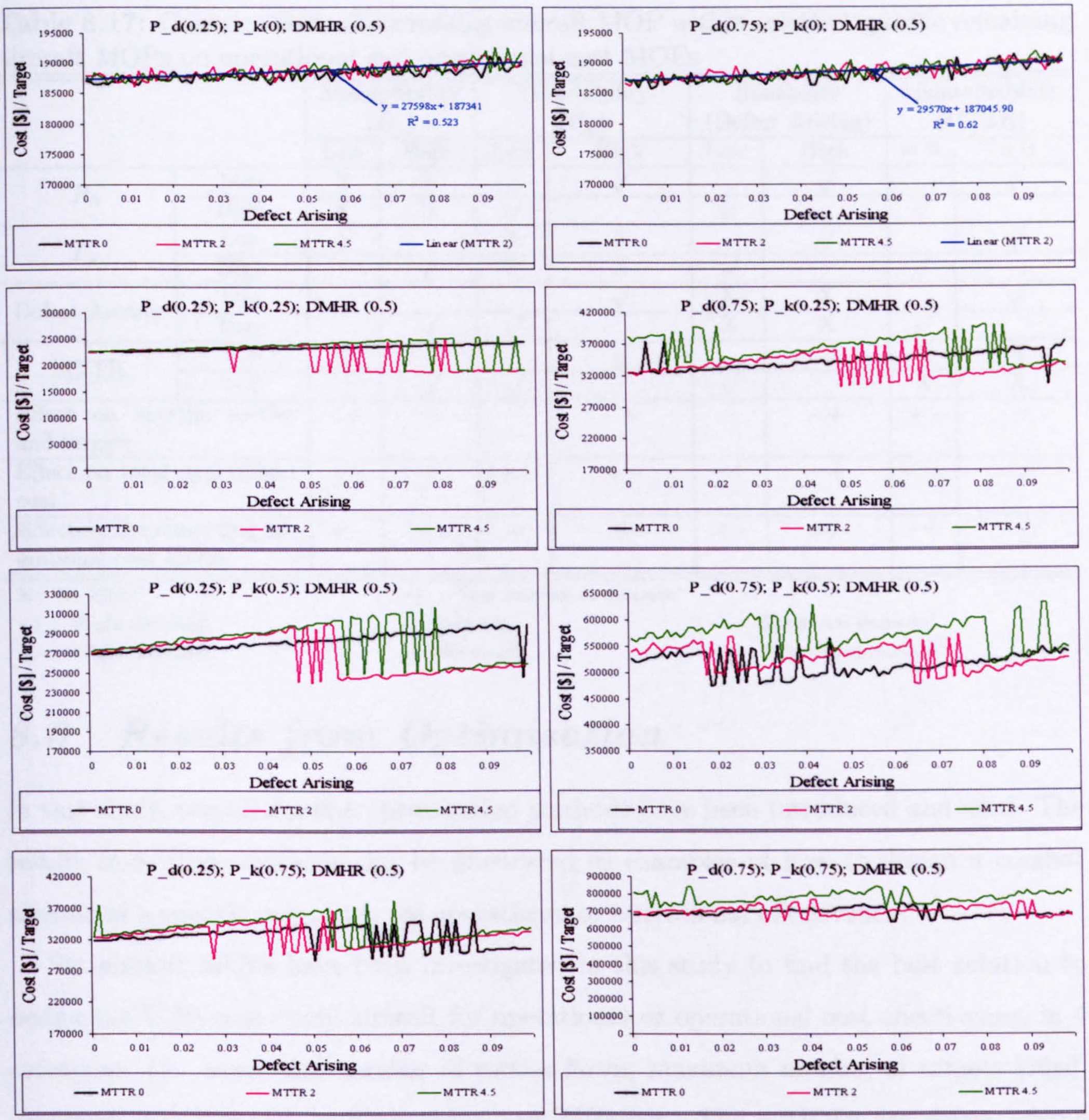

Figure 8.18: Effect of aircraft defect arising rate, P_D, $P_{K_{Non}}$, $P_{K_{Ext}}$ and $MTTR_{Defect}$ with a constant DMHR on cost[$]/target

Fig. 8.18 shows the effect of aircraft defect arising rate, P_D, $P_{K_{Non}}$, $P_{K_{Ext}}$ and $MTTR_{Defect}$ with a constant DMHR on cost[$]/target.

Table 8.17 shows a summary of the effects of increasing multiple aircraft MOPs on the operational and operational cost MOEs. The '+' and '-' signs illustrated in the table are used to indicate the effect of increasing aircraft MOP within selected specific remaining aircraft MOP regions on operational and operational cost MOEs.

Table 8.17: Generic effects of increasing aircraft MOP within selected specific remaining aircraft MOPs on operational and operational cost MOEs

		Susceptibility (P_D)		Vulnerability (P_K)		Reliability (Defect Arising)		Maintainability (MTTR)	
		Low	High	Low	High	Low	High	= 0	> 0
P_D	Low	X	X		√		√		√
	High	X	X	√		√		√	
P_K	Low	√		X	X		√		√
	High		√	X	X	√		√	
Defect Arising	Low	√			√	X	X		√
	High		√	√		X	X	√	
MTTR	= 0	√			√		√	X	X
	> 0		√	√		√		X	X
Effect on specific sorties and targets		- +	- -	-	- +	-	- +	+ -	- +
Effect on total operational cost		+ -	+	++	+ -	- +	- +	- +	- +
Effect on the remaining operational cost MOEs		+ -	++	+	+-	+ -	+/-	- +	+/-

X : 'No Effect'
+/- : 'May increase or decrease'
- + : 'Slight decrease'
- : 'Decrease'
- - : 'Significant decrease'
+ - : 'Slight increase'
+ : 'Increase'
++ : 'Significant increase'

8.6 Results from Optimisation

In this study, two alternative optimisation methods have been introduced and used. The results from these methods can be illustrated as examples of how to design a combat aircraft in a specific operation, for operational or operational effectiveness.

Six aircraft MOPs have been investigated in this study to find the best solution to design the U-99 case study aircraft for operational or operational cost effectiveness in 4 categories; i.e. maximum number of sorties flown, maximum number of targets killed, minimum cost[$]/sortie, and minimum cost[$]/target. The 6 MOPs are defect arising rate, probability of detection, probability of aircraft kill on encounter with penetrators, probability of aircraft kill on encounter with proximity warheads, mean time to repair defect, and defect man-hour rate. The following are the fundamental constraints of these variables:

1. Maximum and minimum values of aircraft defect arising rate are 0.0 and 0.1.

2. All aircraft probability ranges ($P_D, P_{K_{Non}}, P_{K_{Ext}}$) are 0.0 - 1.0.

3. $MTTR_{Defect}$ has the upper limit of 5 hours.

4. $DMHR$ maximum value is 15.00 man-hours/flying hour.

5. The number of Monte Carlo simulation trials is 200 runs in each iteration.

Due to non usage of multiobjective optimisation, and a wide range of variable constraints applied to the optimisation problems, the results from the optimisation are, therefore, part of several alternative solutions with the same constraints.

8.6.1 Results from the Optimisation using the Gradient-Based Method

As described in Chapter 7, the gradient-based method has been used to predict the approximate optimum solution due to some objective functions being in the forms of integer numbers.

Table 8.18 shows the major results from the gradient-base "Solver" optimisation [21]. The remaining results are shown in Appendix E.

Table 8.18: Results from the gradient-base method optimisation

	Minimise		Maximise	
	Cost[$]/Target	Cost[$]/Sortie	Targets Killed	Sorties Flown
Defect Arising	0.029519	0.099899	0.00494	0.00
P_D	0.062758	0.117555	0.29574	0.00
$P_{K_{Non}}$	0.371593	0.485130	0.007653	0.618059
$P_{K_{Ext}}$	0.515784	0.216124	0.148098	0.330151
$MTTR_{Defect}$	4.180827	6.534311	0.6544909	0.00
DMHR	0.00	5.374156	5.092504	4.074727
Objective Value	187454.6562	117821.8125	136	198
Ideal Value			200	200
Iterations	232	244	205	868

8.6.2 Results from the Optimisation using Genetic Algorithms

There are two main alternatives to stop the "GAlib" genetic algorithms optimisation [50], i.e. convergence of populations and number of generations. To show the difference between the results from the optimisation using the gradient-based method and this optimisation method, the number of generations termination mechanism has been chosen to produce the results.

Table 8.19 shows the major results from the "GAlib" optimisation with a maximum of 100 generations of 100 populations. Another two parameters required for this optimisation method are percentage of mutation and percentage of crossover, which are set up by default as 10% for mutation and 60% for crossover (for details see Chapter 7). The rest of the results from this method are shown in Appendix E

Table 8.19: Results from the genetic algorithm optimisation

	Minimise		Maximise	
	Cost[$]/Target	Cost[$]/Sortie	Targets Killed	Sorties Flown
Defect Arising	0.011719	0.098817	0.000194	0.000938
P_D	0.0857886	0.169359	0.030381	0.002472
$P_{K_{Non}}$	0.927993	0.279011	0.048066	0.57612
$P_{K_{Ext}}$	0.138689	0.456199	0.000565	0.03917
$MTTR_{Defect}$	1.505455	7.514457	0.408179	0.730907
DMHR	0.075532	4.2682538	2.873198	0.236438
Objective Value	185332.7812	113487.3984	146	193
Ideal Value	200		200	

The results from the genetic algorithms were slightly better than from the gradient-based method in the case of the integer objective function. The reason is that the gradient-based method uses the derivatives of the objective function and constraints to directly search for solutions and also to stop the optimisation. On the other hand, the results in the form of floating points from the gradient-based method are much closer to the results from the genetic algorithm. This shows how accurate the optimised solutions were from both methods. The gradient-based optimisation method usually required fewer iterations than was required by the genetic algorithms.

The genetic algorithms use the objective function to determine the quality of the solution (population), which contains a set of all 6 variables (Genome). The stop criteria for the optimisation used in this study was the maximum number of solution developments (generation). In each development, a specific number of the best fit populations will survive for the next generation, the rest will be taken away. All genomes in these populations will be mutated and/or exchange their parts relative to given values. This method, however, requires enormous amounts of time to achieve the best optimum.

For this study, either optimised operational or operational cost MOEs can be achieved by several solutions; therefore, the results from the optimisation can be used as a guideline for the best solution. For instance, an alternative solution for maximum sorties flown is gained from attempting to obtain the lowest values of defect arising rate and P_D as the primary condition, then followed by the $P_{K_{Non}}$, $P_{K_{Ext}}$, MTTR, and DMHR in that order.

Only one objective function can be considered for each optimisation run in this study, due to the research time scale. Therefore, the results have to be investigated further to see if they are reasonable. For example, the minimum cost[$]/sortie is approximately

CHAPTER 9

DISCUSSION

One of the objectives of this study was to develop tools to simply, yet sufficiently, assess aircraft measures of performance for three major design aspects; i.e. survivability including susceptibility and vulnerability, reliability & maintainability, and life cycle cost. The reasons for this were that the developed methodology could be published, and used by a wide range of people. It was aimed to help aircraft designer and operational personnel to make decisions quickly, without the need for access to restricted data, at a stage of aircraft design that had been hitherto impossible. The results from using these tools were to be used to contribute to aircraft design knowledge, as discussed in this chapter.

The results from the individual sub-modules and from the main module will be further clarified and discussed. The effects of, and the relationships between, the individual aircraft design aspects will be described and be discussed, relative to the results obtained from the use of the operation simulation module, together with optimisation.

9.1 Design Methodology for Aircraft Operational and Cost-Effectiveness

The design methodology developed in this research aimed to integrate all fundamental aircraft design aspects into the early design process, with consideration of operational and cost-effectiveness. This methodology was based mainly on two fundamental aircraft design methodologies; i.e. the conventional and the "system of systems" design methodologies.

The fundamental approach of the new design methodology was an integration of the "system of systems" design methodology within the design processes of the conventional design methodology. The best, and most appropriate, position in the design cycle was between the conceptual and the preliminary design processes, because of the definition of input at the vehicle level of design used in the "system of systems" design methodology. The "system of systems" design methodology aimed to measure the performance and effectiveness of the system by using the performance of sub-systems to indicate system

effectiveness. An aircraft was defined as a sub-system of the system representing the entire operation scenario; therefore, its performance, basic design parameters and variables resulting from the conceptual design process could be used to measure performance of an aircraft in the terms of susceptibility, vulnerability, reliability, maintainability, manoeuvrability, and life cycle cost.

An entire mission, representing the overall system, in conjunction with the aircraft measures of performance, therefore, could be used to measure aircraft operational and cost-effectiveness. By this approach, the aircraft design parameters and variables could directly show trends and be used to improve the aircraft effectiveness for operational and operational-cost during the early design stage.

The aircraft measures of performance could be represented in the form of the probability values, which indicate the quality of an aircraft in a specific design aspect. On the other hand, the aircraft operational measures of effectiveness could be expressed in the form of numbers of specific sorties, targets, and aircraft. The aircraft life cycle cost together with aircraft operational measures of effectiveness could then indicate the operational cost measures of effectiveness in terms of cost per specific sortie, target, and aircraft. Procedures to assess these measures of performance and effectiveness were then developed, as follows:

I.) Measures of aircraft performance assessment: The susceptibility, vulnerability, and survivability design aspects could be individually predicted in the forms of probability values. On the other hand, the reliability and maintainability were predicted in the forms of failure rate and defect man-hour rate per flying hour. However, the aircraft measures of performance for reliability and maintainability could be evaluated in the form of probability values during the evaluation of the aircraft operational measures of effectiveness. The assessment methodologies in this study were simplified due to restriction of data, information, assessment methods, and research time-scale limits. However, the assessment methodologies were sufficient to meet the project objectives.

II.) Integration of the aircraft measures of performance: One method to combining probability values was to use the reliability block diagram, together with the event tree diagram. This process combines and evaluates the success probability of a specific event in the mission simulation. However, the results from these methods

were still in the form of probability values.

III.) The aircraft operational and operational cost measures of effectiveness evaluation: Mission simulation was used to measure the aircraft operational and operational cost-effectiveness in the forms of the numbers of specific sorties, targets, and aircraft. The simulation transforms the probability values into the required formats. Additionally, with the results from both the modified life cycle cost and the mission simulation, the aircraft operational cost-effectiveness could also be expressed in the appropriate forms. To accurately achieve the numbers of specific sorties, targets, and aircraft, the Monte Carlo simulation technique was applied. This method can evaluate a number of aircraft in the specific events of the mission. This leads to the evaluation of the remaining required numbers of sorties, targets, and aircraft.

Due to the research time-scale limits, only the aircraft measures of performance were optimised, instead of the aircraft design parameters and variables. The results could however, be used as guidelines for design of combat aircraft for operational and cost-effectiveness. Further developments are also required and will be clarified later in this chapter.

9.2 Validation and Discussion of Susceptibility Assessment

9.2.1 RCS Validation

One of the objectives in this study was to develop a simple susceptibility assessment tool to help in the prediction of an aircraft probability of detection (P_D) through the aircraft RCS. The difference between the RCS predicted by this assessment sub-module and the published RCS for the F-117 aircraft was extremely small, unlike that for the B-2 aircraft (approximately 26% error). The reasons are:

1. The external shape of B-2 is more complicated to divide into simple geometrical shapes than the external shape of F-117. This is due to the rounded edges and the curvature of the top view of the B-2. These estimation and assumption for the B-2 were therefore, less accurate than for the F-117.

2. The effect of radar absorbing material (RAM) is also neglected in this study. Therefore, the B-2 RCS predicted by the assessment sub-module is approximately 25%

higher than the published value.

3. There is no information about the radar system, or the specific radar wave frequency, used to evaluate the published RCS values. The default radar wave frequency used in this assessment sub-module was 5.6 GHz based on an average SAM acquisition radar system, but this might be different from that used in the published B-2 and F-117 RCS evaluation.

9.2.2 Susceptibility Assessment

Considering only the external geometrical shape, the U-99 RCS in the front view has the lowest value, compared to the remaining 5 views, because the radar wave incident angles coming from the front view are smaller than from the other aircraft views with the same geometrical size and shape. Therefore, the radar signal reflecting from the front view is less than the other aircraft views. On the other hand, the U-99 RCS in the top and bottom views are the largest because of their geometrical shapes (assumed as flat plates) and large incident angle (approximately 90°).

The manoeuvrability probability option 2 has been set as default because the percentages of each aircraft view in every flight phase are more sensible and appropriate to the U-99 case study aircraft specification (more details see Chapter 6), compared to options 1 and 5. Additionally, the differences of susceptibility results between using option 2, 3, and 4 are, on average, negligible in comparison to the results using option 1 or 5 (see Table E.1). The susceptibility assessment results corresponding to option 5 achieve the optimum average RCS in this study because of the high percentage of front view and no view appearance of the top and bottom views during the attack phase, so the attitudes limit detection probability. This option may be applied in the case where the aircraft exhibits high manoeuvrability, to reduce the probability of exposing vulnerable views.

The aircraft probability of detection (P_D) for this study was predicted by using pre-calculated signal-to-noise ratios (S/N), in conjunction with the default assumed probability of false alarm (P_n) to derive P_D from one of the two available pre-calculated charts [24]. The probability of detection considering the scintillation effect against signal-to-noise ratio with variations of P_n (see Fig. 3.4) has been chosen to predict the U-99 P_D for this study. The scintillation, or multiple continuous illuminations as seen by radar, is produced by RCS variation with a period in the order of one second.

The results predicted by using this method are inexact, yet adequate, because the graph trends in the chart used for this study (with scintillation effect) appear to be constant over the maximum and the minimum scales in the chart. Additionally, the P_D varies very little over the maximum and the minimum S/N regions. A further consideration is that the methodology is to be used for consistent comparisons of different aircraft configurations, where absolute accuracy is less important than relative accuracy.

9.3 Discussion of Vulnerability Assessment

Regarding threat analysis in this study, two major threat types have been used to encounter the U-99 in the mission simulation; i.e. penetrator or contact warhead, and proximity warhead. An aircraft MOP for vulnerability on encounter with penetrators is the probability of kill ($P_{K_{Non}}$).

The probability of aircraft kill on encounter with a single random penetrator varies with the total aircraft vulnerable area, which is the sum of the vulnerable areas of Non-Redundant critical components. Therefore, an aircraft P_K will be decreased by making critical components redundant. For example, the U-99 P_K in the top/bottom view reduces by nearly 83% if all fuel tanks can be considered as redundant critical components.

A second possible P_K reduction method has been discovered by using reconfiguration of critical component layout. However, this method does not necessarily always reduce an aircraft P_K, depending upon how, and which critical components are reconfigured. In the case that an overlapped area of more than one critical component exists, an aircraft P_K variations can occur as follows:

I.) Overlapped area of redundant critical components: This overlapped area will increase the number of non-redundant critical components regardless of shielding and non-shielding effects of the front redundant critical component of the overlapped area. Consequently, the total vulnerable areas increase and also P_K respectively. However, an aircraft P_K using the front redundant critical component of the overlapped area as a shield (shielding effect) is still, yet slightly, less than the one without the shielding effect. The shielding effect can decrease P_K more if the front critical component of the overlapped area increases its shielding capacity.

II.) Overlapped area of non-redundant critical components with non-shielding effect: An aircraft P_K usually decreases because the total vulnerable areas also decreases,

even if the number of non-redundant components increase. The main reason is that the presented areas of the overlapped critical components reduce by the presented areas of the intersection. This leads to a reduction of the vulnerable areas of one of the intersected non-redundant critical components.

III.) Overlapped area of non-redundant critical components with shielding-effect: The shielding effect of the front critical component in the overlapped area reduced the overlapped area P_K by decreasing P_K of the shielded critical components. This can be made more efficient by reconfiguration of the critical component layout in the overlapped area, in which the lower P_K critical component is positioned in front of the higher P_K critical component. This is an explanation of the fact that the U-99 P_K in the rear view is lower than in the front view because of shielding effects.

IV.) Overlapped area of redundant and non-redundant critical components: This kind of overlapped area, either with or without the shielding effect, cannot be used to directly judge whether the total vulnerable areas increase or decrease. It depends on how many non-redundant critical components are involved, how large are the intersections, and how the critical components are positioned. More details and full investigation are required in this case.

The principle of the reduction of an aircraft lethal radius is to reduce the detonation distance of the proximity warhead, where is delivers as P_K value of 0.5 to the aircraft. An aircraft lethal radius can be thus reduced by the same way as described above (reconfiguration of the critical component layout). More details about lethal radius have been shown in Appendix E.

9.4 Validation and Discussion of Reliability & Maintainability Assessment

The aircraft MOP for reliability used in this study is the total aircraft failure rate (FR), which was predicted by the 2 different methods developed for this design methodology; i.e. the combination and functionality methods.

During the development of the combination method, the best fitting mathematical model was investigated to predict the highest and the lowest aircraft system failure rate. The results in the previous chapter show that the highest and the lowest aircraft system FR

could be predicted from available reliability data sets by using statistical linear regression based on the 6 most major R&M related design parameters, and engineering judgement; i.e. W_e, N_e, Alt, W_a, H, and $Thrust$.

The most complete reliability data sets available consisted of 13 - 15 major critical-failure systems. Most aircraft of the available data sets have 13 systems. Considering the failure rate distribution of each aircraft from the available reliability data sets, most aircraft failure rates follow the Pareto distribution, with a portion of 40:70 - 40:80. Therefore, the constant number of 13 major critical failure components and 40:70 Pareto distribution portion were set as the default values used to predict the aircraft MOP for reliability (total aircraft failure rate).

In conjunction with the available reliability data sets, based on aircraft empty weight, a Technology Improvement Factor (TIF) was discovered. Most aircraft reliability predicted by the combination method with this developed TIF are closer to the actual aircraft FR, especially data collected after the year 1985. Unfortunately, there was very limited reliability data for unmanned air vehicles (UAV); therefore, the TIF developed for this type of aircraft was based only on the results of U-99 and U-3 [47] FR predictions from both the combination and functionality methods.

Another simple FR prediction model was also developed, based on the last 2 available reliability data sets, in conjunction with the other 2 almost complete reliability data sets. The failure rates predicted from this model were more approximate, yet less complicated to use than the failure rates predicted from the combination method.

Using a similar approach, to an aircraft FR prediction, one of the aircraft MOPs for maintainability, namely defect man-hour rate (DMHR), could also be predicted by using the same principle as the highest and the lowest FR predictions. 6 major design parameters, in conjunction with assumed 13 major critical maintained systems, and also the 40:70 Pareto distribution portion were applied for the DMHR prediction. Unfortunately, there were not sufficient maintainability data to develop the TIF, and a more accurate functionality model. This meant that the average difference of DMHR predicted from the combination and the functionality methods was larger than the average difference of the FR predictions.

9.5 Validation and Discussion of Life Cycle Cost Estimation

The aircraft LCC predicted by the LCC estimation sub-module in this study is quite good because it has very small differences between the LCC predicted by this sub-module and LCC quoted from both published sources and a commercial program, as shown in Chapter 8. The LCC estimation model for this study was based on previous work with validation in some parameters, and sub-modules based on restricted literature.

The aircraft LCC comprises several costs over the entire aircraft life time. One of these costs is the total operational cost, which includes all necessary expense to operate and support an aircraft fleet on one base for the entire aircraft life. This cost can therefore, be averaged over both the total number of operational aircraft and total flying hours. By this approach, the total operational cost per aircraft over a specific mission duration can be thus calculated by multiplying the average operational cost per aircraft per flying hour and the total aircraft flying hours. The summation of all operational aircraft operation costs gives the total operational costs for the entire fleet on one base.

The operation cost predicted from the LCC estimation sub-module for the wartime scenario is less than for peacetime scenario due to excluding additional costs during wartime. These are aircraft lost cost, weapons released expense, and auxiliary maintenance and support. In this methodology, only the aircraft lost cost and weapons released expense, which are evaluated directly in the mission simulation, are taken into account, and added into the total operation cost. This makes the total operational cost in this study more sensible.

9.6 Discussion of Operation Simulation

Most of the aircraft MOPs are in the form of probability values; therefore, a reliability block diagram was developed in conjunction with an event tree diagram to predict the success probability for each flight phase in a sortie. They considered all possible occurring events in each flight phase. Some unpredictable or more complexly evaluated values in this study were, however, randomly generated. The success probability for each flight phase was used to indicate to which event an aircraft would proceed; such as aircraft being killed, the target being killed, and aircraft completing the flight phase. The number of specific sorties, targets, and aircraft could therefore be precisely determined in the form of realistic integer numbers. By this approach, the flying hours of every operational aircraft,

or in service time, could be recorded and be used to predict the operational cost for the entire mission simulation.

The Monte Carlo simulation technique was applied, with the aim of producing more accurate prediction results. This technique was based on statistical analysis, and the predicted result accuracy depends upon both the number of trials and the range of the predicted results. This process was very time consuming and demanded high computational power and performance. A number of trials were thus investigated to discover the optimum trial number to achieve sufficiently reliable predicted results. The number of 200 trials was found to be suitable and was used as the default in this study. This is the main reason for the fluctuations, discontinuity curves, and overlapped intervals in some of results shown in the previous chapter.

9.7 Discussion of Aircraft Measures of Performance on the Operational and Operational Cost Measures of Effectiveness

As shown in Table 8.15 - 8.17 in previous chapter, increase aircraft individual and/or several MOPs mostly leads to decrease total number of specific sorties and targets. The main reason is that the total service time (flying hours) and total number of weapons released for entire fleet during mission simulation reduce The reduction ratio of total specific sorties and targets depends on the combination of aircraft MOPs, which leads to earlier abort, additional aircraft lost, and/or aircraft lost in earlier sortie and operational day. The followings show the major combinations of aircraft MOPs and their effects on the total number of specific sorties and targets:

I.) Aircraft with low vulnerability and susceptibility probabilities: The total number of specific sorites and target slightly reduces.

II.) Aircraft with high vulnerability probability and low susceptibility probability: The total number of specific sorties and targets also sightly reduces due to that additional aircraft being killed takes places in later sortie and/or operational day.

III.) Aircraft with low vulnerability probability but high susceptibility probability: The total number of specific sorties and target reduces due to that additional aircraft being killed takes places in earlier sortie and/or operational day.

IV.) Aircraft with high vulnerability and susceptibility probabilities: The total number of specific sorties and targets significant reduces due to that additional aircraft being killed happens more and takes places in earlier sortie and/or operational day.

V.) Aircraft with high defect arising rate, which represent reliability: The total number of specific sorties and target mostly reduce due to that aircraft abort their mission often and spend their most of the time in maintenance.

VI.) Aircraft with high vulnerability and survivability probabilities associate with high defect arising rate and mean time to repair: The total number of specific sorties and targets significant reduces due to that aircraft abort their mission often and additional aircraft lost also take place in earlier sortie and operational day.

The effect of the combinations of aircraft MOPs on the total operational cost, on the other hand, increase or give in the opposite direction as the effects on the total number of specific sorties and target due to mainly that additional lost significant increase the total operational cost. Unfortunately, an average operation & support cost per flying hour per aircraft calculated directly from the aircraft life cycle cost in this research includes also the maintenance cost; therefore, reduction in total service time (flying hours) of entire fleet due to longer maintenance requirement leads to reduction of operation & support cost during the mission simulation. This reduction makes not much sense; therefore, further study to separate the maintenance cost from average operation & support cost per flying hour has to be performed in the future work.

9.8 Discussion of Optimisation Results Relative to the Operational and Cost-Effectiveness

The optimisation results are used as examples of this design methodology, specifically applied to the U-99 case study. Two alternative optimisation methods were shown in the previous chapter.

The results from both optimisation methods show that the U-99 could achieve maximum sorties flown or targets killed if the U-99 obtains very low P_D and defect arising rate, as shown in Table 8.18 - 8.19. The total number of sorties flown and targets killed could also increase if the U-99 vulnerability probability decreased.

A similar approach to optimise the total number of specific sorties and targets, the operational cost MOEs can also be minimised by using the same principle. Additionally, these costs could supplementally reduce by decreasing MTTR and DMHR.

Regarding LCC results shown in Table 8.12, the operation cost from aircraft LCC was averaged over the total operational aircraft in one base in conjunction with the number of annual flying hours and the total number of aircraft life time. Therefore, the operation cost of U-99, F-16 and Eurofighter could not be directly compared due to their difference in number of operational aircraft in one base, annual flying hours, and total number of entire aircraft life time.

9.9 Future Work

Due to the limited research time scale, restriction of data, information, and assessment methodology, several assumptions had to be made. This leads to the development of simple assessments. The results from these assessments are therefore approximate, but sufficient, to show trends as discussed above. However, to increase the accuracy of this design methodology, further developments are still required, and will be discussed below.

In this study, only the radar signature has been taken into account for the evaluation of aircraft probability of detection. This can only be used for specific threat types. Other aircraft signatures, namely the infrared signature and optics signature, should also be taken into account to cover most threat types currently used.

The radar cross section prediction method in this study was based only on the aircraft external shape. This method may not be sufficient to predict RCS of the new generation of combat aircraft which use more radar absorbing material. Therefore, the effects of the radar absorbing material has to be considered within the assessment methodology. Additionally, the aircraft external shape partition method used in this study is quite simple, but it may be improved with the assistance of a CAD program.

The limited research time scale, and a wide-range of design aspect assessment methodologies developed for this study, meant that the probability of detection was determined directly from pre-calculated charts. To improve prediction accuracy, the probability of detection could be calculated more quickly by using computational methods, which would require an extra sub-module due to the complexity of the equations.

The manoeuvrability probability used in this study is quite a simple model, based

on assumed and logical values. To assess these values is quite difficult during the early design stage. However, further research and investigation to assess this value should be continued.

The vulnerable area assessment model developed for this study uses simple graphical methods to predict the critical components and aircraft presented areas, by overlapping a generated grid over a graphic image. A semi-automatic grid counter has been developed. The values predicted by this method are approximate due to round edges and limited detail in the graphic image. More detailed use of CAD is another possibility to improve the accuracy of the presented areas predictions.

The maintainability assessment model used in this study uses assumed default values, due to the limited research time scale and restricted data. This assessment methodology should be further researched and developed the relationship between reliability and maintainability in the mission simulation.

To achieve more accurate prediction results using the Monte Carlo simulation technique, requires much computational time on high performance computers. An alternative method to reduce time consumption is to use computational parallelisation, which allows one application to use several processors simultaneously.

In this study, either operational or operational cost-effectiveness can be optimised. To extend the design methodology for combining optimisation of operational and cost-effectiveness, further development in optimisation has to be performed. The multiobjective optimisation technique is one of the alternatives to be studied.

Expansion of optimisation feedback could also be improved. The feedback variables used in this study are in the form of aircraft MOPs, which cannot be used directly at the vehicle level of design. Therefore, further developments of every sub-module should allow the conversion of the aircraft MOPs to fundamental aircraft design parameters. By this approach, the results from optimisation can be used in the conceptual and/or preliminary design stages.

CHAPTER 10

CONCLUSIONS

This combat aircraft design methodology for operational and cost effectiveness has been developed with the aim of integrating all fundamental aircraft design aspects and the operation simulation into the early design stage. The aircraft design aspects included in this design methodology are susceptibility, vulnerability, reliability, maintainability, manoeuvrability, and life cycle cost. An aircraft will be considered as a sub-system of an overall system representing an entire operation scenario. By this approach, aircraft measures of performance for an individual design aspect can be evaluated in the form of probability values. Therefore, aircraft operational effectiveness can be measured in the forms of number of specific sorties, targets, and aircraft remaining; such as total number of successful sorties, number of targets killed, and number of aircraft killed. Due to the aircraft life cycle cost prediction, aircraft operational cost-effectiveness can be thus measured in the forms of both total cost of and cost per specific sortie, target, or aircraft loss. The results in the form of either operational or operational cost measures of effectiveness indicate which aircraft design aspects have to be considered further and/or can be sacrificed to achieve the optimum objective function.

The method used to evaluate the aircraft operational measures of effectiveness from the aircraft measures of performance is through the use of the reliability block diagrams in conjunction with the event tree diagram, in the mission simulation. With the assistance of the Monte Carlo simulation technique, the aircraft operational measures of effectiveness can be more accurately predicted.

An aircraft measure of performance for susceptibility is represented by the aircraft probability of detection. A simple aircraft probability of detection assessment method, developed in this research, is to use the pre-calculated aircraft radar cross section indirectly to determine the probability of detection value from published charts. An aircraft radar cross section prediction method in this study is based only on the aircraft external shape.

The aircraft probability of kill represents an aircraft measure of performance for the vulnerability design aspect. The principle assessment of this value is to predict and sum

the vulnerable areas of non-redundant critical components. The influence of reconfiguration of the non-redundant and redundant critical components layout has been discovered and can be used to vary the probability of kill. An alternative measure of performance for vulnerability on encounter with a proximity warhead is that the lethal radius can also be varied by the same principle.

The measure of aircraft performance for manoeuvrability has been introduced as weighting factors, defining the percentage of aircraft view appearing to the threat encounter direction. These values directly influence the aircraft performance in survivability because each aircraft view obtains separate probabilities of kill and of detection value.

Alternative reliability and maintainability assessments developed in this research are based on statistical analysis cooperating with the Pareto principle, by using historical, published and unpublished data. This method predicts the aircraft reliability and maintainability using the fundamental aircraft design parameters, instead of details of all aircraft components. Additionally, another possible method is to assess these values is by using the relationship between both the reliability and maintainability and the aircraft empty weight.

The operational cost during a wartime scenario throughout the mission simulation can be estimated via aircraft life cycle cost. Finding the operation cost per aircraft per flying hour is the main objective of this sub-module. This cost can be evaluated by averaging the total operation cost over the number of operational aircraft in one base and total flying hours for the aircraft entire life time. By considering the number of flying hours, together with weapons released, and aircraft being killed during the mission simulation, the total operational cost can be determined.

The optimisation methods used in this research are the gradient-based method and the genetic algorithms. Both methods have been used in this study, firstly to evaluate only the optimum solutions either for operational effectiveness or operational cost-effectiveness. Due to the optimisation feedback variables in the forms of aircraft MOPs, the solutions from the optimisation can be used just to indicate the design direction to fulfill the selected objective function.

By increasing an individual aircraft MOP, the operational MOEs mostly reduce in different inclination depending on which aircraft MOP has been considered. However, by combine several aircraft MOPs, the reduction inclination may increase or decrease

depending also on which and how the aircraft MOPs have been combined. On the other hand, the effects on the operational cost MOEs are mostly opposite as the effect on the operational MOEs.

For the unmanned air vehicle, U-99, used as a case study in this research, the probability of detection and defect arising rate are the most appropriate parameters to be considered for both maximum operational MOEs and minimum operational cost MOEs. The next most appropriate parameters are probability of kill, followed by probability of hit. Additional appropriate parameters are MTTR and DMHR.

Additionally, some alternative trade-offs with the aircraft MOPs to improve the operational and operational cost MOEs can also be examined with these developed applications.

However, there are still some improvements, further development and research required to extend this design methodology, such as increased accuracy of aircraft MOPs assessment, and application of multiobjective optimisation. It should be made possible to use target values of aircraft MOPs to drive aircraft design parameters, such as span, mass etc, to optimised aircraft configurations.

CHAPTER 11

RECOMMENDATIONS

In this study, several assumptions, constraints, and simple models have been applied, due to the research time scale, restricted data, and assessment methodology. The following are some recommendations, which should be performed to improve this design methodology.

1. Improvement of RCS prediction models to consider the effect of the radar absorbing material.

2. Development of the methodology to include the assessment of an aircraft's infrared signature in order to improve the aircraft's probability of detection assessment methodology.

3. Development or improvement of the manoeuvrability probability assessment methodology.

4. Improvement of the optimisation to consider more than one objective function.

5. Improvement on all sub-modules to convert the aircraft MOPs back to the fundamental aircraft design parameters.

REFERENCES

[1] AL–AHMED, S. M., *Integration Combat Effectiveness Disciplines into the Aircraft Conceptual/Preliminary Design.* PhD thesis, Cranfield University, College of Aeronatics, 1996.

[2] AL-AHMED, S. and FIELDING, J. P., "Vulnerability Prediction Method for Use in Aircraft Conceptual Design," *The Aeronautical Journal, The Roayl Aeronautical Society*, pp. 309–315, June 1999.

[3] ANONYMOUS, "Reliability Data." [Unpublished], 1987.

[4] ANONYMOUS, "Aircraft Data." [Unpublished], 1993.

[5] BALL, R. E., *The Fundamental of Aircraft Combat Survivability Analysis and Design.* AIAA Education Series, New York: AIAA, 1985.

[6] BALL, R. E., *The Fundamentals of Aircraft Combat Survivability Analysis and Design.* AIAA Education Series, Reston: AIAA, second edition ed., 2003.

[7] BILLINTON, R. and ALLAN, R. N., *Reliability Evaluation of Engineering Systems.* New York: Plenum, second ed., 1992.

[8] BIRKLER, J. L., GARFINKLE, J. B., and MARKS, K. E., "Development and Production Cost Estimating Relationships for Aircraft Turbine Engine," Technical Paper N-1882-AF, RAND, October 1982.

[9] BLAKE, L. V., *Radar Range-Performance Analysis.* Toronto: LexingtonBooks, 1980.

[10] BURLEIGH, C. D., "Mission Readiness of Combat Aircraft," Master's thesis, Cranfield University, College of Aeronatics, 1981.

[11] BURNS, J. W., "Aircraft Cost Estimation Methodology and Value of a Pound Derivation for Preliminary Design Development Applications," in *53th Annual Conference of Society Allied Weight Engineers, Inc.*, vol. SAWE 2228, (Long Beach, CA), May 1994.

[12] COST ANALYSIS AND IMPROVEMENT GROUP, "Operating and Support Cost-Estimating Guide," May 1992.

[13] CRISPIN, J. W. and SIEGEL, K. M., *Methods of Radar Cross-Section Analysis.* Electrical Science Series, New York and London: Academic Press, 1968.

[14] DONNA F. HARMON, PATRICIA A. PATES, D. G., "Maintainability Estimating Relationships," in *Proceedings 1975 Annual Reliability and Maintainability Symposium*, (Washington D.C.), January 1975.

[15] FEDERATIONS OF AMERICAN SCIENTISTS, "Space Based Laser [SBL] Glossary of Term." http://www.fas.org/spp/starwars/program/sbl/10-10-July_GOT.htm. [accessed 10 November 2004].

[16] FIELDING, J. P. and NILUBOL, O., "A Design Assessment Methodology for Combat Aircraft Operational Effectiveness," in *2nd AIAA "Unmanned Unlimited" Systems, Technologies, and Operations - Aerospace, Land, and Sea Conference and Workshop & Exhibit*, vol. AIAA 2003-6551, (San Diego, CA, USA), September 2003.

[17] FIELDING, J. P. and NILUBOL, O., "Integration of Survivability Assessment into Combat Aircraft Initial Design," in *International Congress of the Aeronautical Sciences 2004*, vol. ICAS 2004-1.5.1, (Yokohama, Japan), August 2004.

[18] FIELDING, J. P., *Introduction to Aircraft Design.* Cambridge: Cambridge University Press, 1999.

[19] FISHMAN, G. S., *Monte Carlo: concepts, algorithms, and applications.* New York: Springer-Verlag, 1995.

[20] FRONTLINE, "The Gulf War." http://www.pbs.org/wgbh/pages/frontline/gulf. [accessed 22 November 2004].

[21] FRONTLINE SYSTEM INC., "Solver DLL V3.5 Evaluation Kit." http://www.solver.com/dwndllv35kit.php. [accessed 12 January 2002].

[22] GOLDBERG, D. E., *Genetic Algorithms in Search, Optimization and Machine Learning.* Addison-Wesley Publishing Company, INC., 1989.

[23] HALL, D., "Integrated Survivability Assessment (ISA," *Aircraft Survivability*, vol. Fall 2004, pp. 20–23, 2004.

[24] HOVANESSIAN, S. A., *Radar Detection and Tracking System.* Dedham, Massachusetts: ARTECH HOUSE, INC., 1973.

[25] HVR CONSULTING SERVICE LIMITED, "Why should one trust FACET," September 2000. Ref: PV/11/039.

[26] IRONSIDES, "Anti-Aircraft Weapons." http://ironsides.8m.com/afv/sam.html. [accessed 24 June 2003].

[27] JENN, D. C., *Radar and Laser Cross Section Engineering.* AIAA Education Series, Washington: AIAA, 1995.

[28] KITOWSKI, J. V., "Combat Effectiveness Methodology as a Tool for Conceptual Fighter Design," in *1992 Aerospace Design Conference*, vol. AIAA 92-1197, (Irvine, USA), February 1992.

[29] KNEZEVIC, J., *Reliability, Maintainability and Supportability.* Maidenhead, England: McGraw Hill, 1993.

[30] KOCH, R., *The 80/20 Principle.* London: Nicholas Brealey Publishing, 2001.

[31] NASA PRIVACY, "Present Value, Inflation, and Discounting." http://ceh.nasa.gov/webhelpfiles/Present_Value,_Inflation,_and_Discounting.htm. [accessed 10 November 2004].

[32] NILUBOL, O. and FIELDING, J. P., "An Integration of Survivability into Combat Aircraft Design Methodology for Operational Effectiveness," in *German Aerospace Congress 2004*, vol. DGLR-2004-129, (Dresden, Germany), September 2004.

[33] OFFICE OF PERSONNEL MANAGEMENT, "Special Salary Rate." http://apps.opm.gov/SSR/tables/index.cfm. [accessed 12 November 2004].

[34] OFFICE OF THE SECRETARY OF DEFENSE, "Military Compensation." http://www.defenselink.mil/militarypay/index.html. [accessed 12 November 2004].

[35] PELTZ, E., SHULMAN, H. L., TRIPP, R. S., RAMEY, T., and DREW, J. G., "Supporting Expeditionary Aerospace Force: An Analysis of F-15 Avionics Option," Tech. Rep. MR-1174-AF, RAND, 2000.

[36] RAYMER, D. P., *Aircraft Design: A Concepture Approach.* AIAA Education Series, New York: AIAA, third ed., 1999.

[37] ROSKAM, J., *Airplane Design*, vol. I - VIII. Lawewncs, Kansas: University of Kansas, 1985.

[38] SERGHIDES, V. C., "Development of a Reliability and Maintainability Prediction Methodology for the Aircraft Conceptual Design Process," Master's thesis, Cranfield University, College of Aeronatics, 1985.

[39] SIMKINS, D. and BREYER, D., "Mission Modelling of Helicopter Combat Effectiveness," in *AIAA AHS/ASEE Aircraft Design, Ssytems and Operatios Conference*, vol. AIAA 89-2146, (Seattle, USA), August 1989.

[40] SMITH, H., "U-99 unihabited tactical aircraft preliminary structural design," *Aircraft Engineering and Aerospace Technology*, vol. 73, no. 1, pp. 31–55, 2001.

[41] SMITH, H., "U-99 unihabited tactical aircraft preliminary systems design," *Aircraft Engineering and Aerospace Technology*, vol. 73, no. 3, pp. 244–265, 2001.

[42] SOBAN, D. S. and MAVRIS, D. N., "Formulation of a Methodology for the Probabilistics Assessment of System Effectiveness," in *AIAA Missile Science Conference*, (Montoney, CA, USA), November 2000. unclassified.

[43] SOBAN, D. S. and MAVRIS, D. N., "Methodology for Assessing Survivability Tradeoffs in the Preliminary Design Process," in *2000 World Aviation Conference*, vol. 2000-01-5589, (San Diego, CA, USA), SAE, October 2000.

[44] SOBAN, D. S., *A Methodology for the Probability Assessment of System Effectiveness as Applied to Aircraft Survivability and Susceptibility.* PhD thesis, Georgia Institute of Technology, November 2001.

[45] STAHL, J. W., ARENA, J. A., and KNAPP, M. I., "Cost-Estimating Relationships for Tactical Combat Aircraft," IDA Memorandum Report M-14, AD-A151 575, Institute for Defense Analyses, November 1984.

[46] STERNBERGER, N. L., "The Modular Life Cycle Cost Model for Advanced Aircraft Systems an Overview," in *39th Annaul Conference of the Society of Allied Weight Engineers, Inc.*, vol. SAWE 1351, (St. Louis Missouri), May 1980.

[47] STOCKING, P., "U-3 "Spectre" Project Executive Summary," tech. rep., Department of Power, Propoulsion & Aerospace Engineering, School of Engineering, Cranfield University, May 2004. restricted.

[48] STRETCHBERRY, D. M. and HEIN, G. F., "General Methodology: Costing, Budgeting, and Techniques for Benefit-Cost and Cost-Eeffectiveness Analysis," Technical Paper TM X-2614, NASA, Ohio, 1972.

[49] U.S. DEPARTMENT OF LABOR BUREAU OF LABOR STATISTICS, "Customer Price Index." http://www.bls.gov/cpi/home.htm. [accessed 12 November 2004].

[50] WALL, M., "GALib: A C++ Library of Genetic Algorithm Components." http://lancet.mit.edu/ga. [accessed 12 January 2002].

[51] WHITFORD, R., *Fundamental Of Fighter Design.* Shrewsbury, ENGLAND: Airlife Publishing LTD, 2000.

[52] WHITTLE, R., *Development of the Low Support Vehicle.* PhD thesis, Imperial College, 1998.

[53] WOODFORD, S., *The Minimization of Combat Aircraft Life Cycle Cost through Concepture Design Optimisation.* PhD thesis, Cranfield University, College of Aeronatics, 1999.

[54] WOODFORD, S. and SMITH, H., "The Minimization of Combat Aircraft Life Cycle Cost Through Concepture Design Optimization," in *AIAA and SAE World Aviation Conference*, vol. AIAA 98-5567, SAE 985567, (Anaheim, CA, USA), Septmeber 1998.

APPENDIX A

RELIABILITY BLOCK DIAGRAM AND EVENT TREE CALCULATION METHODS

Due to several sub-events can be occur after each other or conditional in an event; therefore, the reliability block diagram (RBD) will be used to group those sub-events and the event tree diagram will be applied to evaluate each sub-event and event probability values.

In this appendix, the probability concept will be firstly introduced, then the fundamental of the reliability block diagram and of the event trees will be briefly described.

A.1 Probability Concept

The probability has a strict technical meaning and is a scientific 'measure of chance', i.e., the probability indicates quantitatively the likelihood of an event or events. It can be indicated as a numerical value between zero, which defines an absolute impossibility, to unity, which defines an absolute certainly [7].

Each event or events will have at least two possible outcomes, one of which can be considered as the favourable outcome or success and the other as the unfavourable outcome or failure. For an event that has more than two outcomes, it is possible to group together those outcomes which can be called favourable or successes and those which can be called unfavourable or failures.

A.2 Reliability Block Diagram calculation

RBD is a diagrammatic representation of system in which each item is represented by a box. The relationship between items is determined by the effect that the failure or success of each one has on the functionality of the system as a whole. The total probability of each system or each box is unity, which can be represented in numerical form as follows:

$$P_{\text{success}} + P_{\text{Failure}} = 1 \tag{A.1}$$

There are two main principle to combine system with each others; i.e., series and

parallel. Additionally, some systems may contain a combination of more than one types.

A.2.1 Series system

This type of combination has been shown in Fig. A.1, which all sub-systems have to be connected after each other. The consequence is that the system requirement for success is so 'all sub-systems' must be working. If one of sub-system in this type of combination is failure, the entire system will be failure. The probability of system success can be thus given as

$$P_{\text{System success}} = P_{\text{A success}} P_{\text{B success}} \tag{A.2}$$

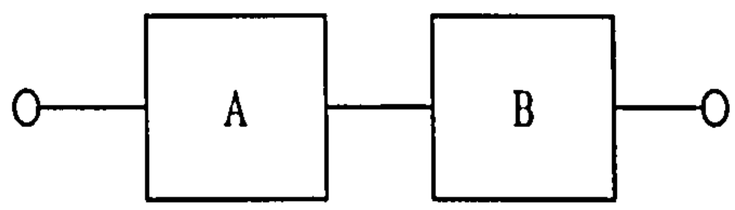

Figure A.1: Two components series system

A.2.2 Parallel system

Fig. A.2 shows an example of this parallel combination system, in which all sub-systems are connected parallel. In this case, the system requirement is that only one sub-system needs to be working for system success. Or in other words, the entire system will be failure, only if all sub-system are failure. The probability of system success can be thus obtained as the complement of the system failure or by using the expression of 'either A or B or both' constitutes success to give

$$\begin{aligned} P_{\text{System success}} &= 1 - P_{\text{System failure}} = 1 - P_{\text{A failure}} P_{\text{B failure}} \\ &= 1 - (1 - P_{\text{A success}})(1 - P_{\text{B success}}) \end{aligned} \tag{A.3}$$

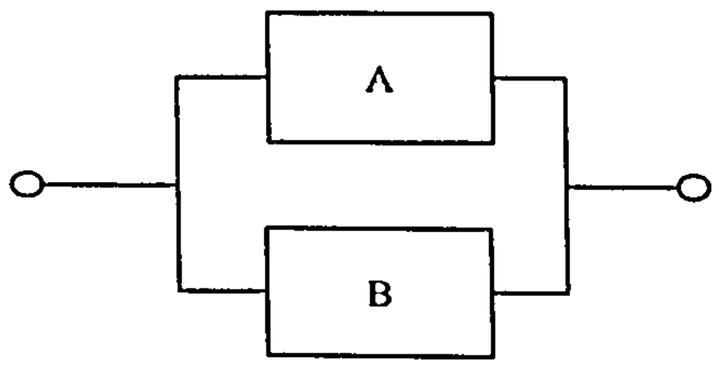

Figure A.2: Two components parallel system

A.2.3 Series-parallel System

The general principle used is to reduce sequentially the complicated configuration by combining appropriate series and parallel branches of the system until a single equivalent sub-system remains. This equivalent sub-system then represents the entire system of the original configuration.

A.3 Event Trees

An event tree is a pictorial representation of all the events which can occur in a system. It is defined as a tree because the pictorial representation gradually fans out like the branches of a tree as an increasing number of events are considered [7].

With any system, in which the operation of a particular sub-system is dependent on the success or failure of another sub-system, the sequence of events must be considered in the chronological order, in which they occur.

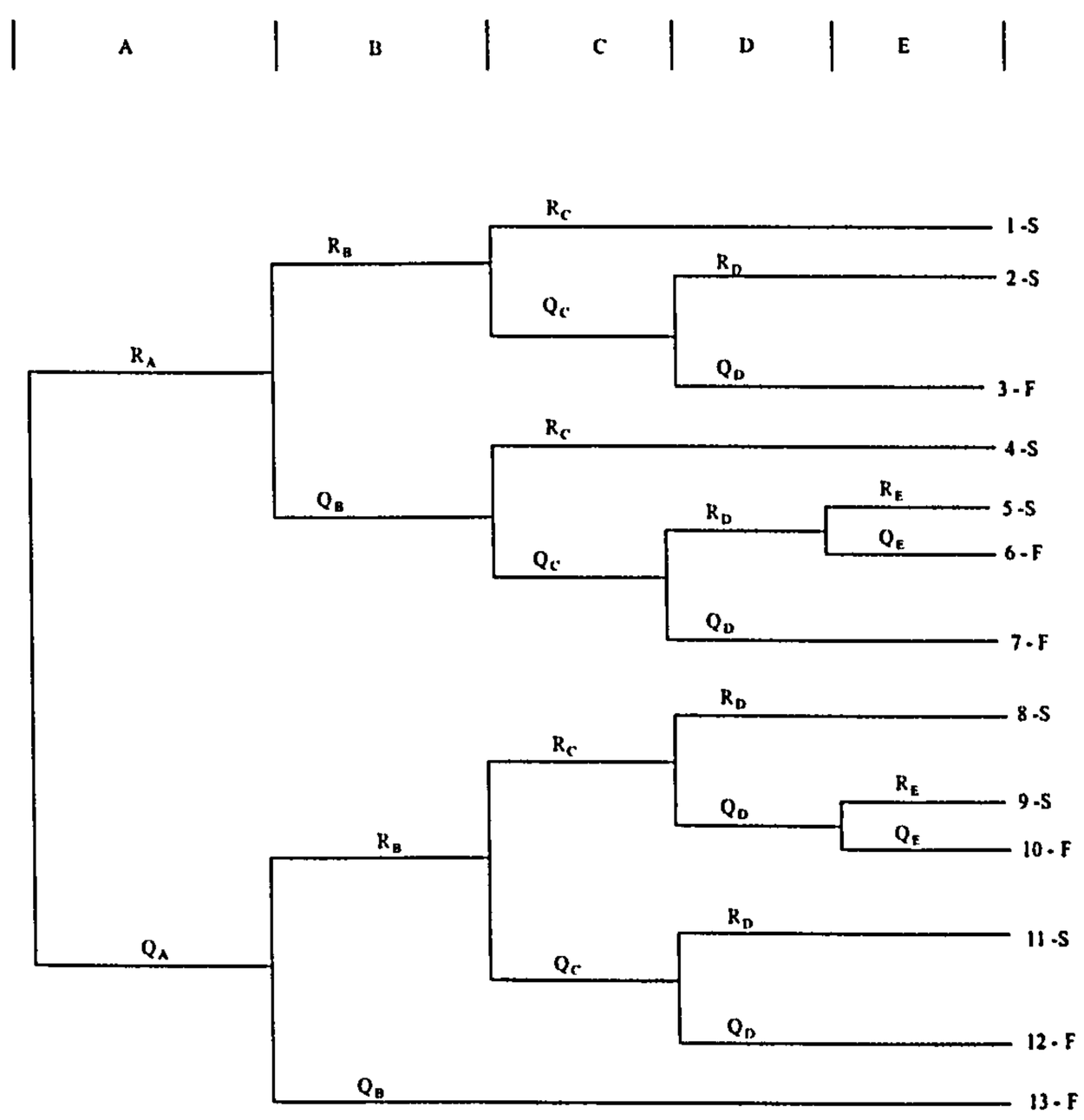

Figure A.3: Reduced Event Tree Sample

Fig A.3 shows a reduced event tree of a system of five components. This is deduced by considering each sub-system or event with considering of outcome deduction, that can be made before each new sub-system or event is considered. If, at each of these

deductions, it is known that a particular outcome is reached by a path irrespective whether subsequent sub-systems or events are successful or not, there is no need to consider further development of this event path. The success probability of this deduced system can be evaluated as

$$
\begin{aligned}
P_{\text{System success}} &= P_{\text{Path 1}} + P_{\text{Path 2}} + P_{\text{Path 4}} + P_{\text{Path 5}} + P_{\text{Path 8}} + P_{\text{Path 9}} + P_{\text{Path 11}} \\
&= P_{\text{A success}} P_{\text{B success}} P_{\text{C success}} + P_{\text{A success}} P_{\text{B success}} P_{\text{C failure}} P_{\text{D success}} + \\
&\quad P_{\text{A success}} P_{\text{B failure}} P_{\text{C success}} + P_{\text{A success}} P_{\text{B failure}} P_{\text{C failure}} P_{\text{D success}} P_{\text{E success}} + \\
&\quad P_{\text{A failure}} P_{\text{B success}} P_{\text{C success}} P_{\text{D success}} + P_{\text{A failure}} P_{\text{B success}} P_{\text{C success}} P_{\text{D failure}} P_{\text{E success}} + \\
&\quad P_{\text{A failure}} P_{\text{B success}} P_{\text{C failure}} P_{\text{D success}}
\end{aligned}
$$

APPENDIX B

SURVIVABILITY ASSESSMENT MODULE

This appendix will explain and show flowchart, algorithms, program dialogs and results of survivability assessment module, which can be split into two main sub-modules; susceptibility assessment and vulnerability assessment modules.

In the real program procedure, the vulnerability assessment module has to be first separately executed to determine presented areas of aircraft; therefore, the probability of hit or of fuse, when aircraft is detected, can be consequently evaluated from the susceptibility assessment module. With manoeuvrability probability, which is represented by weighting factors for each flight phase in a sortie, and uniform random of hits or explosion distance, an average survivability probability in each flight phase can be thus assessed as shown in Fig. B.1.

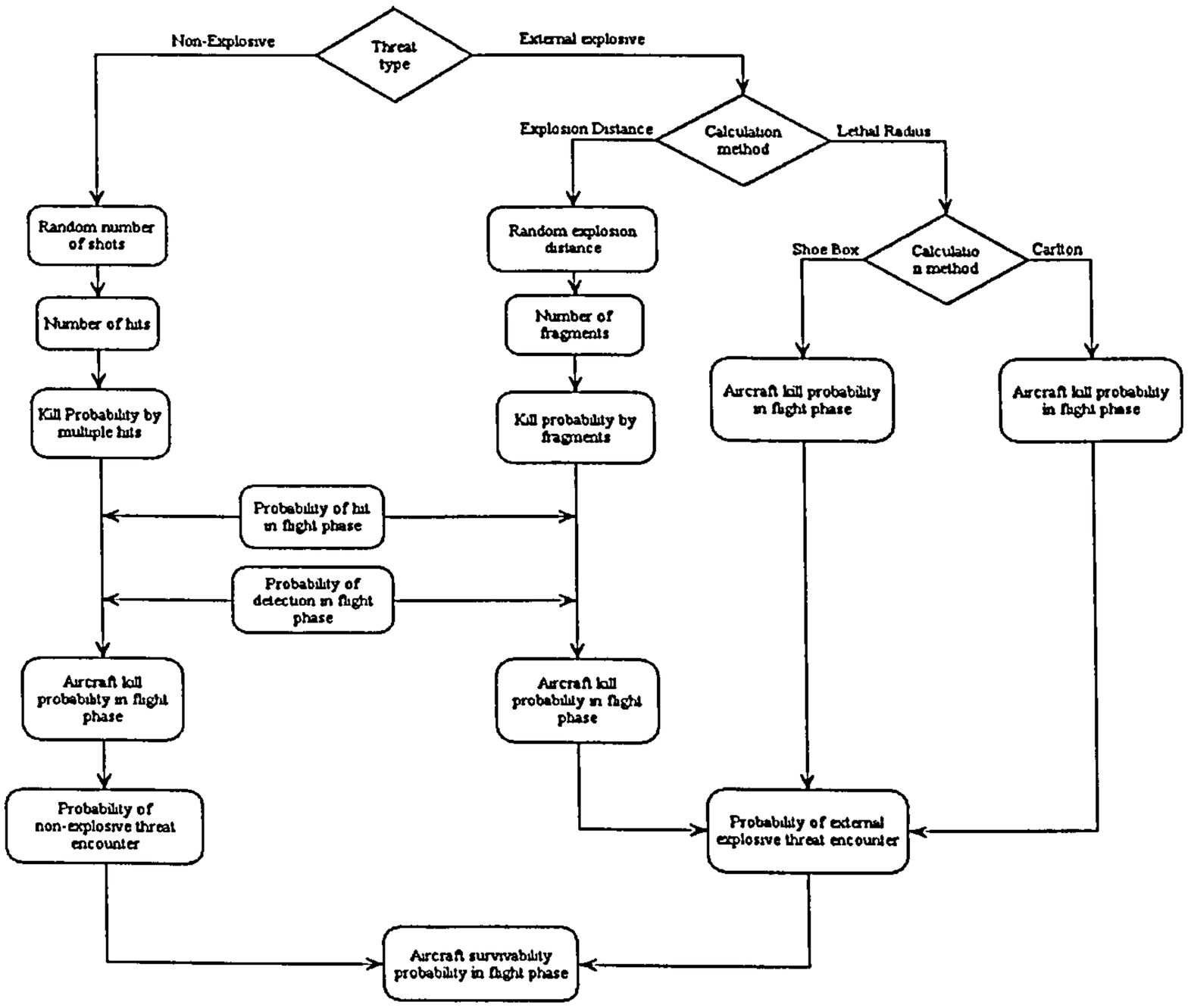

Figure B.1: Flowchart of survivability assessment module

B.1 Susceptibility Assessment Module

In this module, the probability of detection and probability of hit or of fuse, when aircraft get detected, are the main results. The probability of detection for each aircraft view can immediately determined, but for the probability of hit or of fuse evaluation needs to obtain aircraft presented areas from vulnerability assessment module before the actual determination can start. The flowchart of this module can be shown in Fig. B.2.

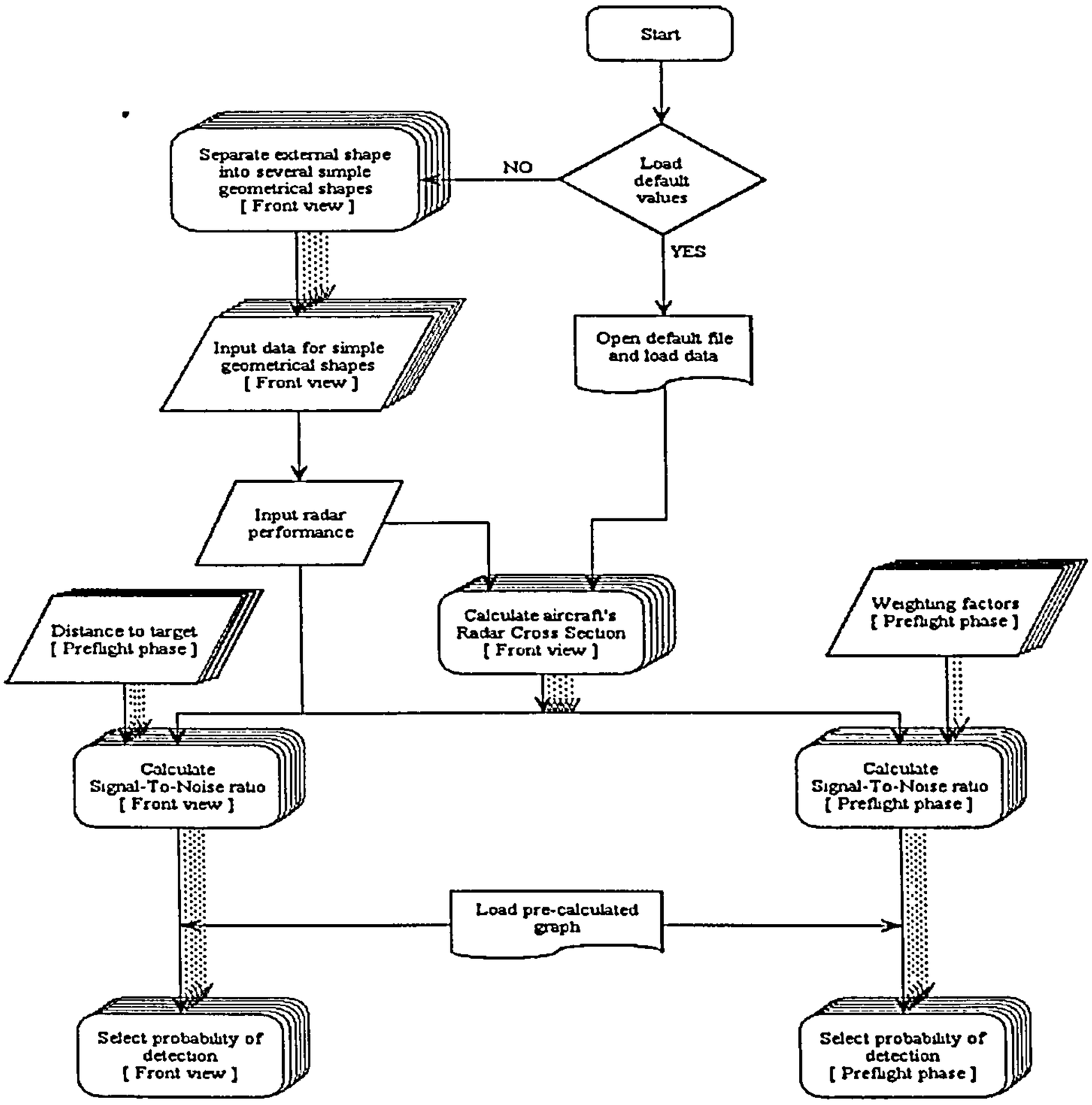

Figure B.2: Flowchart of probability of detection prediction

Input variables for each aircraft view for this module can be loaded directly from default files or be given direct in the program dialog.

B.1.1 Radar Cross Section Prediction

This module mainly calculates the aircraft RCS and the false alarm probability and shows these values in the dialog (Fig. B.4). All simple shape data of the aircraft external geometry in all six aircraft views and radar performance can be either loaded from a data

file or filled directly in this application dialog page. Consequently, the aircraft RCS in each view can be thus determined.

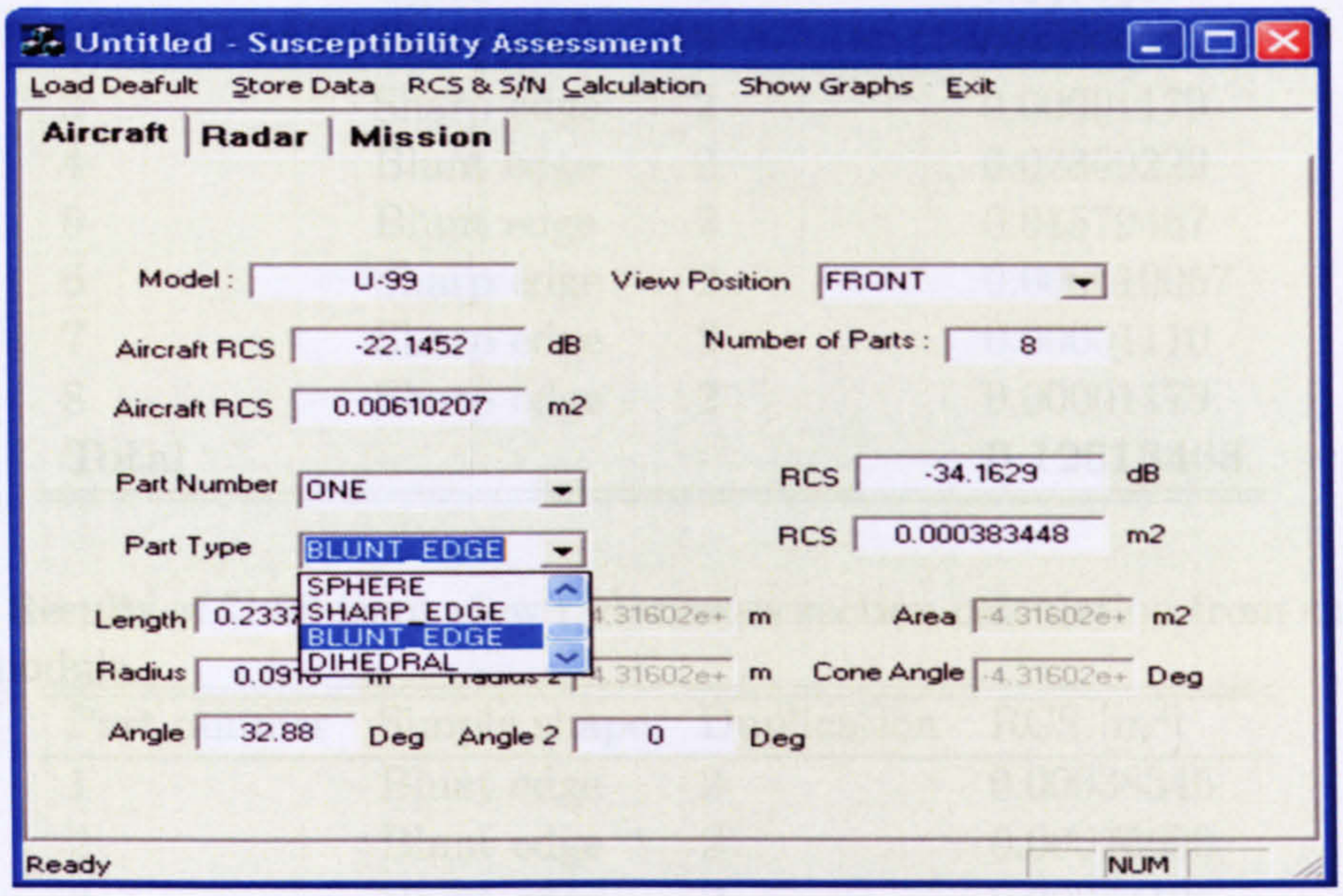

Figure B.3: Susceptibility assessment dialog

Table B.1 - B.3 show the results of front view radar cross section calculation from three different aircraft by using AN/FPS-16 radar system, which has approximate frequency of 5 GHz, to represent the general frequency of Hight Finder, Aircraft, SAM transportable, and SAM mobile radar systems [51]

Table B.1: Results of F-117 front view radar cross section calculation from susceptibility assessment module

Part number	Simple shape	Duplication	RCS $[m^2]$
1	Flat plate	2	0.00007246
2	Flat plate	2	0.00004680
3	Flat plate	2	0.00000400
4	Flat plate	2	0.00003193
5	Flat plate	2	0.00000131
6	Flat plate	2	0.00006247
7	Flat plate	2	0.00000063
8	Flat plate	2	0.01224193
9	Flat plate	2	≈0.00000000
10	Sharp edge	2	0.00000204
11	Sharp edge	2	0.00000072
Total	-	-	**0.02492856**

Table B.2: Results of B-2 front view radar cross section calculation from susceptibility assessment module

Part number	Simple shape	Duplication	RCS $[m^2]$
1	Ogive	1	0.04706017
2	Flat plate	2	0.00000557
3	Sharp edge	2	0.00001179
4	Blunt edge	2	0.02369229
5	Blunt edge	2	0.01579467
6	Sharp edge	2	0.000010057
7	Sharp edge	2	0.00001110
8	Sharp edge	2	0.00001179
Total	-	-	**0.12613468**

Table B.3: Results of U-99 front view radar cross section calculation from susceptibility assessment module

Part number	Simple shape	Duplication	RCS $[m^2]$
1	Blunt edge	2	0.00038345
2	Blunt edge	2	0.00076690
3	Blunt edge	2	0.00051126
4	Blunt edge	2	0.00060282
5	Blunt edge	2	0.00076690
6	Sharp edge	2	0.00000967
7	Sharp edge	2	0.00000796
8	Sharp edge	2	0.00000208
Total	-	-	**0.00610207**

B.1.2 Probability of Detection Estimation

As described in chapter 3, the P_D is a function of S/N and P_n; therefore, the both necessary parameters have to be firstly evaluated. The P_n is a direct function of radar threshold from Eqn.(3.17). The threshold can be loaded from default file or be directly filled in the dialog application. On the other hand, the S/N depends upon several parameters; one of them is distance between aircraft and radar system, which is subject to flight phase. Another influential parameter is aircraft RCS, which depends on the aircraft view. With the aircraft being seen view probability (manoeuvrability probability) and distance between aircraft and opponent radar system in each flight phase, an average S/N can be thus evaluated.

Once, the necessary parameters for the average aircraft detection probability in each flight phase in a mission sortie determination have been calculated, the user has to interpolate value from the pre-calculated graph to receive the probability of detection (see

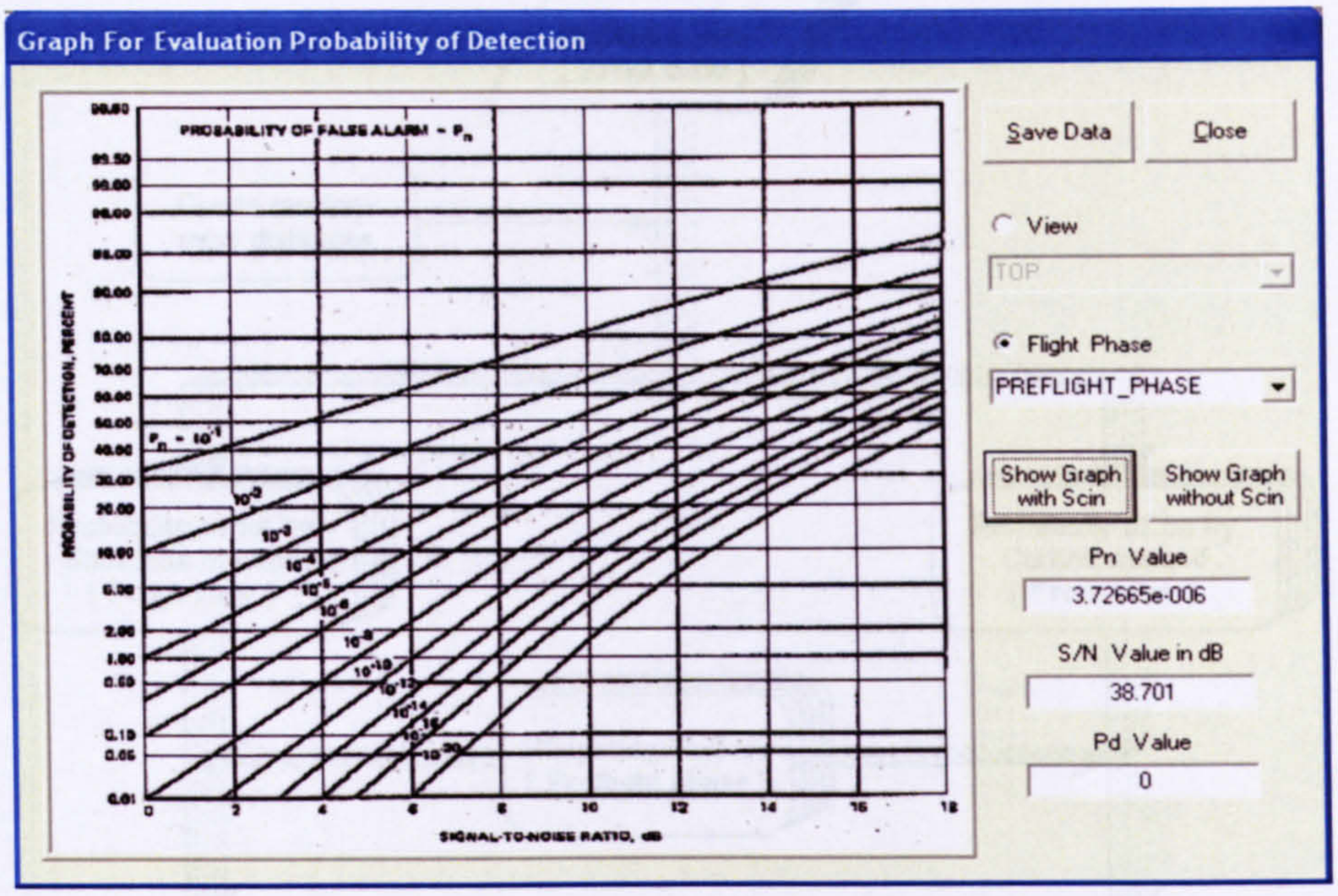

Figure B.4: Graph for evaluation detection probability dialog

Fig. B.4). By using the same principle, the detection probability of each aircraft view in each flight phase can therefore determined.

Table B.4: Results of U-99 probability of detection in attack flight phase of manoeuvrability option 2 with $P_n = 3.72665 \times 10^{-6}$

View	RCS $[dBm^2]$	$S/N[dBm^2]$	P_{View}	P_D
Top	64.4827	79.1151	0.15	≈0.99
Right	-19.4542	-4.8218	0.15	≈0.006
Left	-19.4542	-4.8218	0.15	≈0.006
Front	-22.1452	-7.5128	0.40	≈0.001
Rear	0.6854	15.3178	0.00	≈0.65
Bottom	64.4827	79.1151	0.15	≈0.99
Total	**59.2539**	**73.8863**	-	**≈0.98**

B.1.3 Probability of hit or of fuse Evaluation

This application dialog offers two models to evaluate the probability of hit or of fuse, when aircraft is detected; i.e. Shoe-Box and Carlton (details see Chapter 3). Fig. B.5 shows the program procedure to evaluate this value by using uniform random miss distance and statistical analysis.

The probability of hit or fuse, when aircraft is detected, depends on aircraft presented area; therefore, $P_{H/D}$ for each aircraft view has to be separately evaluate (see Fig.B.6).

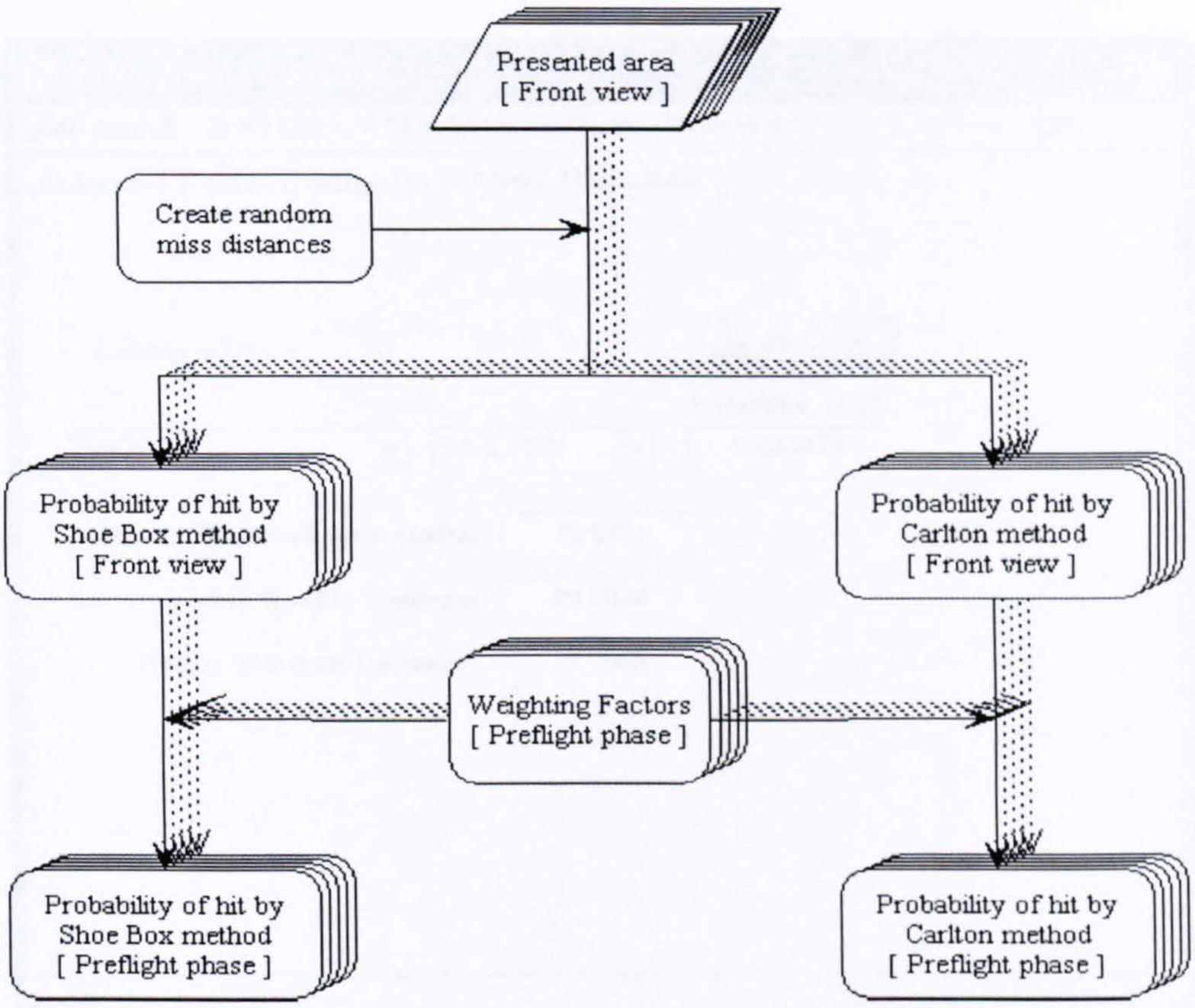

Figure B.5: Flowchart of probability of hit determination

On the other hand, $P_{F/D}$ will obtain value 1.0 because after the proximity warhead detonates, the fragments encounter directly aircraft, which can be treated as multiple hits by penetrators (more details see Section 3.1.3).

B.2 Vulnerability Assessment Module

This module calculates mainly the probability of aircraft kill given a single random hit and random multiple hits by contact warheads or penetrators. The flowchart for the vulnerability assessment module can be shown in Fig B.7:

Input parameters have to be loaded from stored files or directly given through the dialog application; and also some condition for vulnerability estimation have to be selected (see Fig. B.8)

B.2.1 Critical and Overlapped Critical Components Definition

From the kill tree diagram, the critical components are identified; this identification can be given by loading from default file or by completing in the application dialog. The component redundancy can also obtain as the same way.

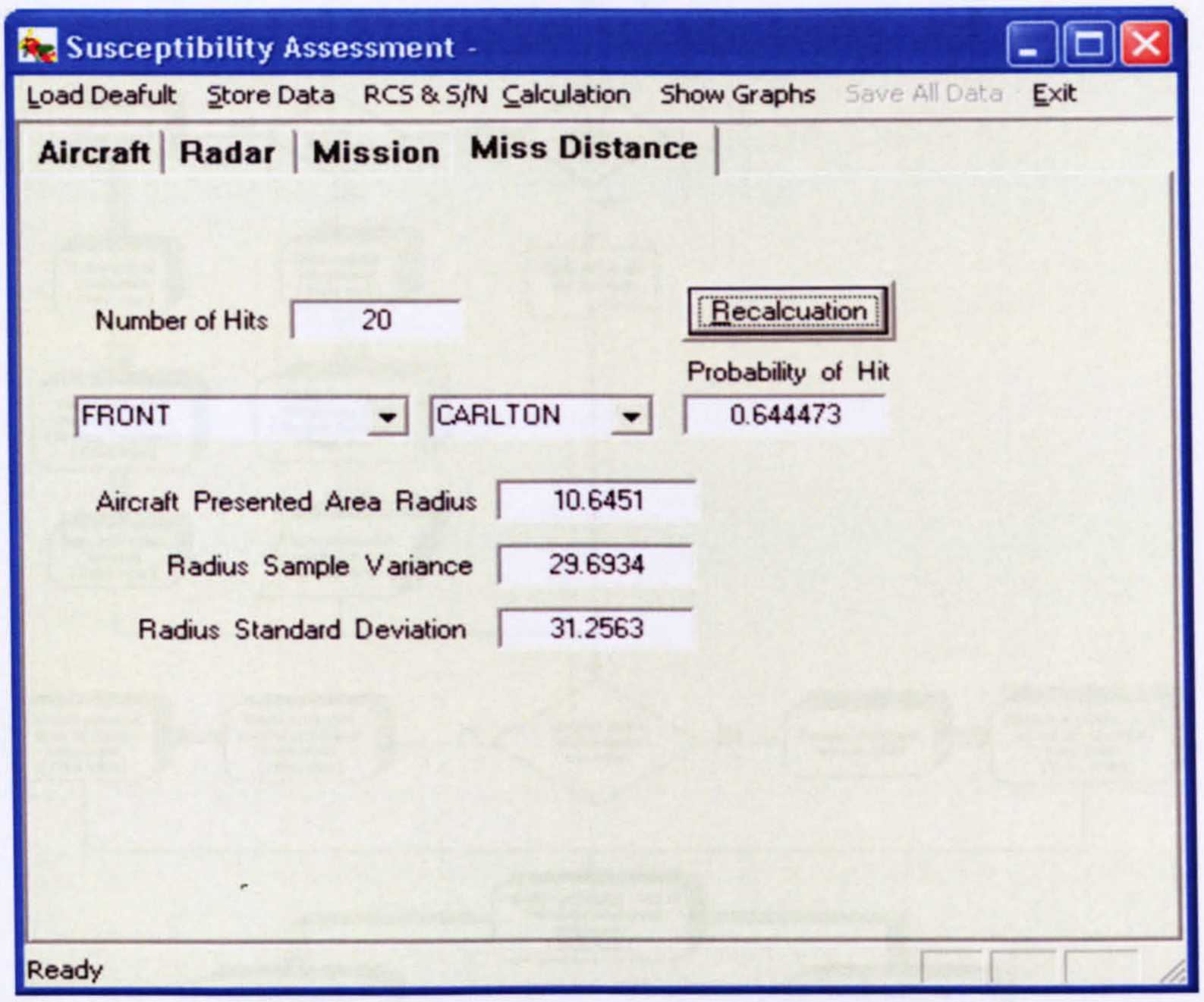

Figure B.6: Application dialog for probability of hit determination

Table B.5: U-99 critical components list

Component	Redundancy
Fuel system	5
Engine	2
Flight Control system (FCS)	2
Air Data (AD)	1
Control Unit (CU)	1
Global Positioning System (GPS)	1

With the shotline technique, overlapped critical components in each view can be identified as shown in Table B.6.

With the definition as shown in Table B.6, the presented areas, probability of kill of these critical component overlapped area for each aircraft view can be evaluated as shown in Fig. B.9.

B.2.2 Presented Area Prediction

In this module, there are three options to obtain aircraft, critical component, and overlapped presented areas; i.e. directly load from default file, directly input in the application dialog, and semi-automatic grid counting.

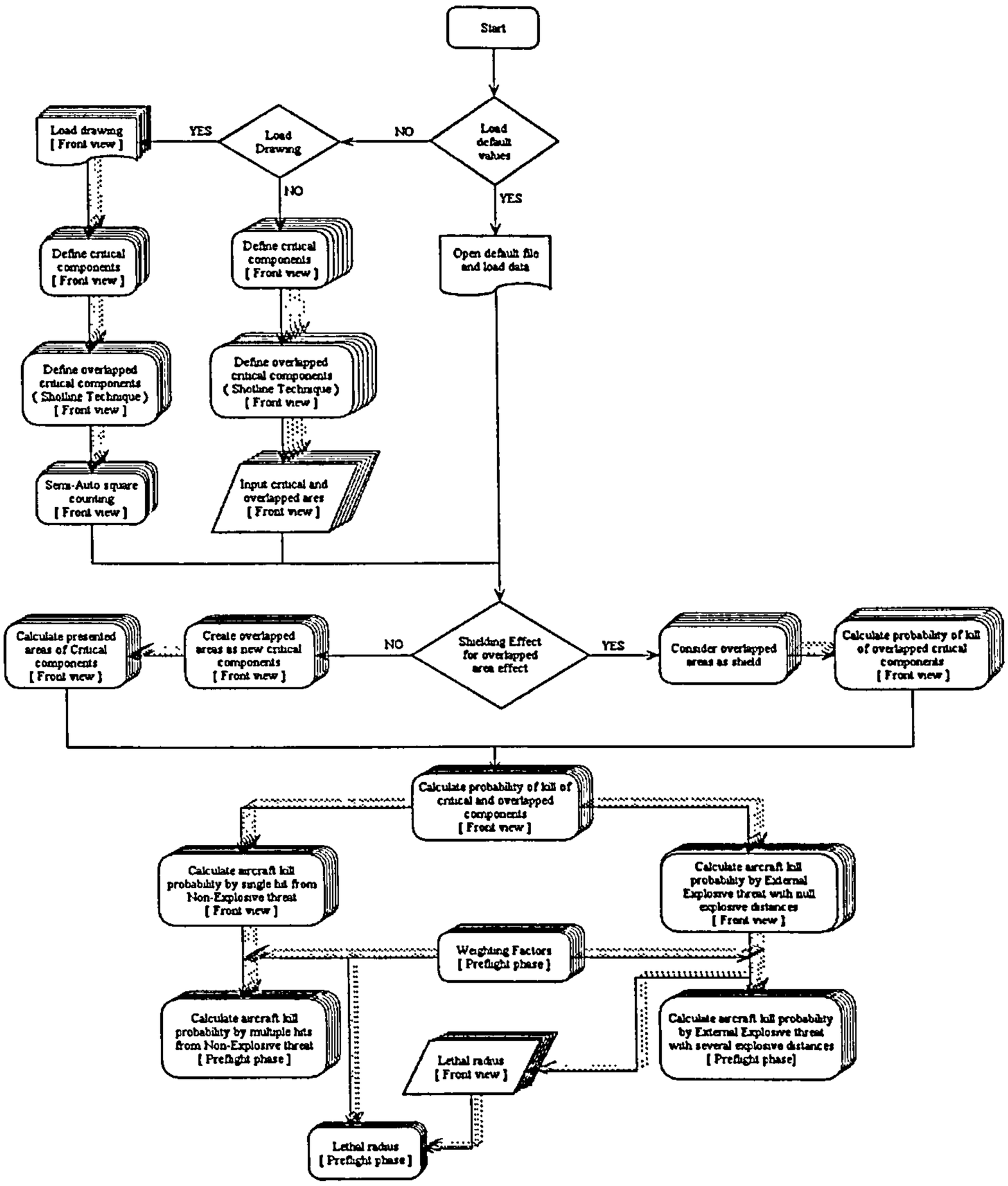

Figure B.7: Flowchart of vulnerability assessment module

Table B.6: U-99 overlapped critical components list

No.	Right/Left	Front/Rear
1	FCSs + Tank No.1	AD + Tank No.1
2	Tank No.1 + No.4 + No.5	CU + Engine No.1
3	Tank No.4 + No.5	GPS + Engine No.2
4	Tank No.4 + No.5 + Engines	FCS + Tank No.3 + No.5
5	Tank No.1 + No.4 + No.5 + Engines	Tank No.3 + No.5
6	Tank No.2 + No.3 + Engines	FCS + Tank No.2 + No.4
7	Tank No.1 + No.2 + No.3	Tank No.2 + No.4
8	GPS + CU	
9	Engine No.1 + No.2	

In the third option, information about aircraft and/or critical component presented areas are not available either from default file or from drawing, a semi-automatic grid counter option offers a simple alternative to count presented area of aircraft and/or critical

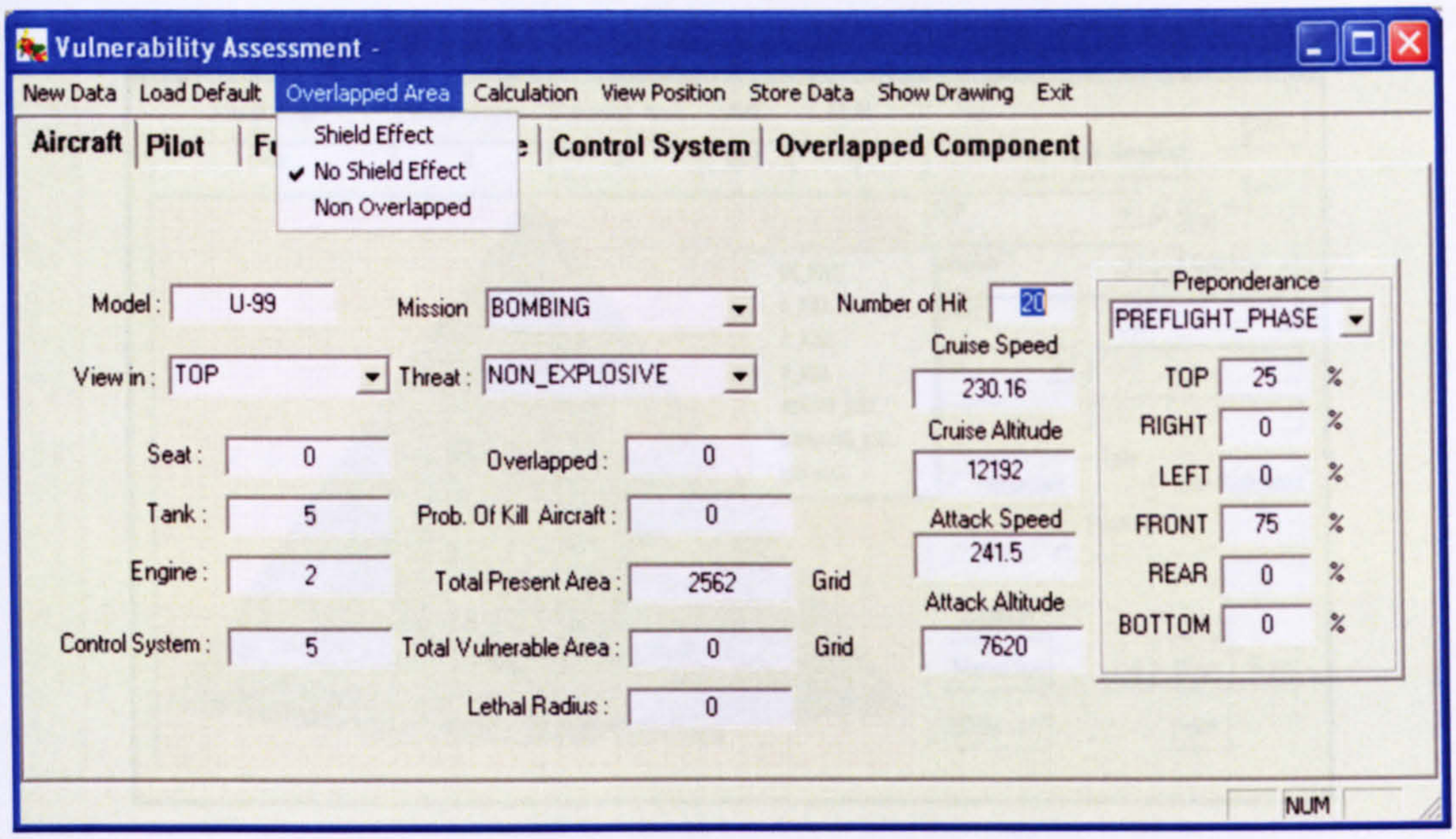

Figure B.8: Vulnerability assessment module application dialog

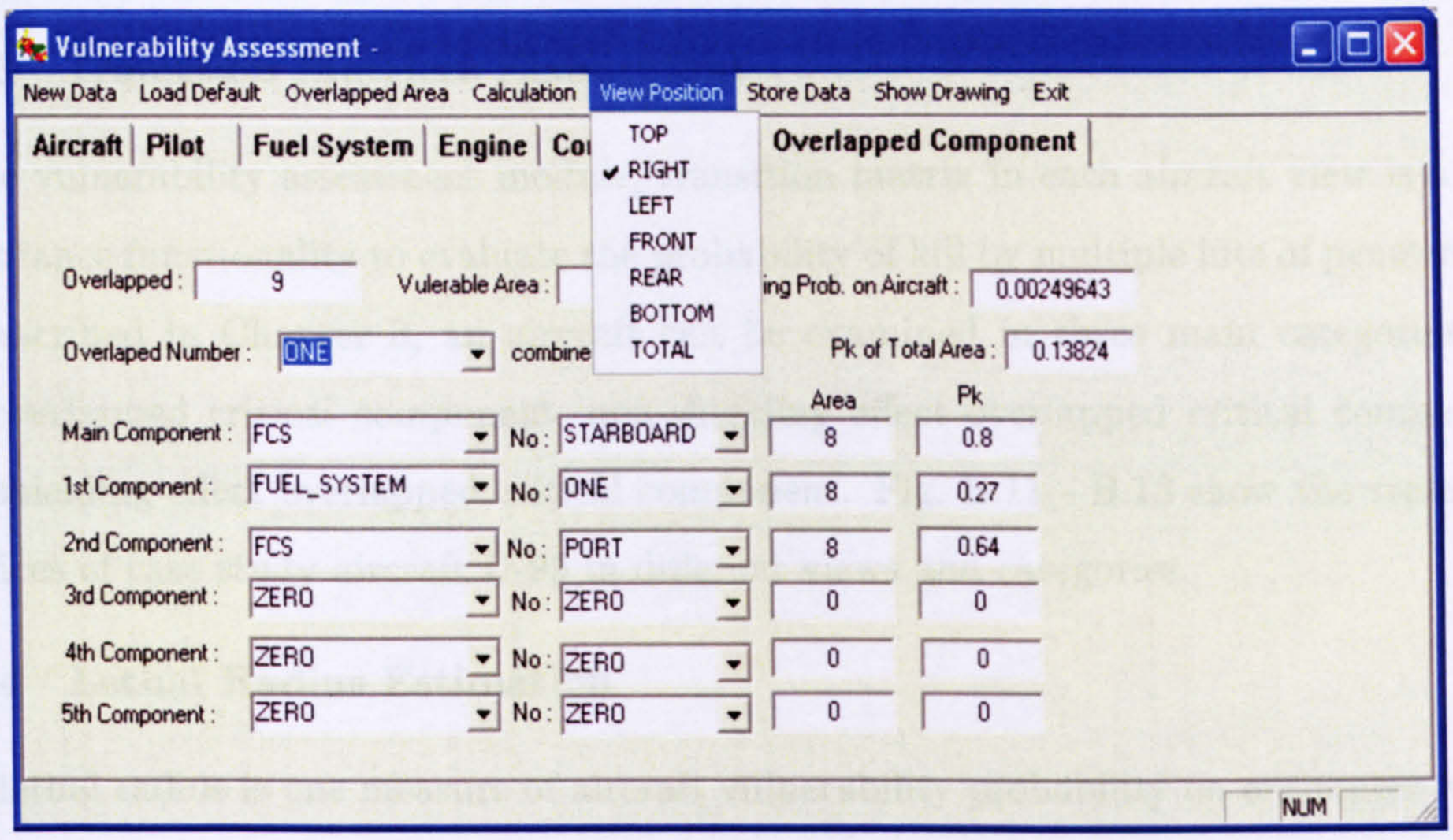

Figure B.9: Critical component overlapped area presented area tab dialog

components including overlapped areas in each aircraft view in Grid unit as shown in Fig. B.10. The generated grid can be resized; and the drawing can be moved and zoomed to mark component and/or aircraft presented areas more precisely.

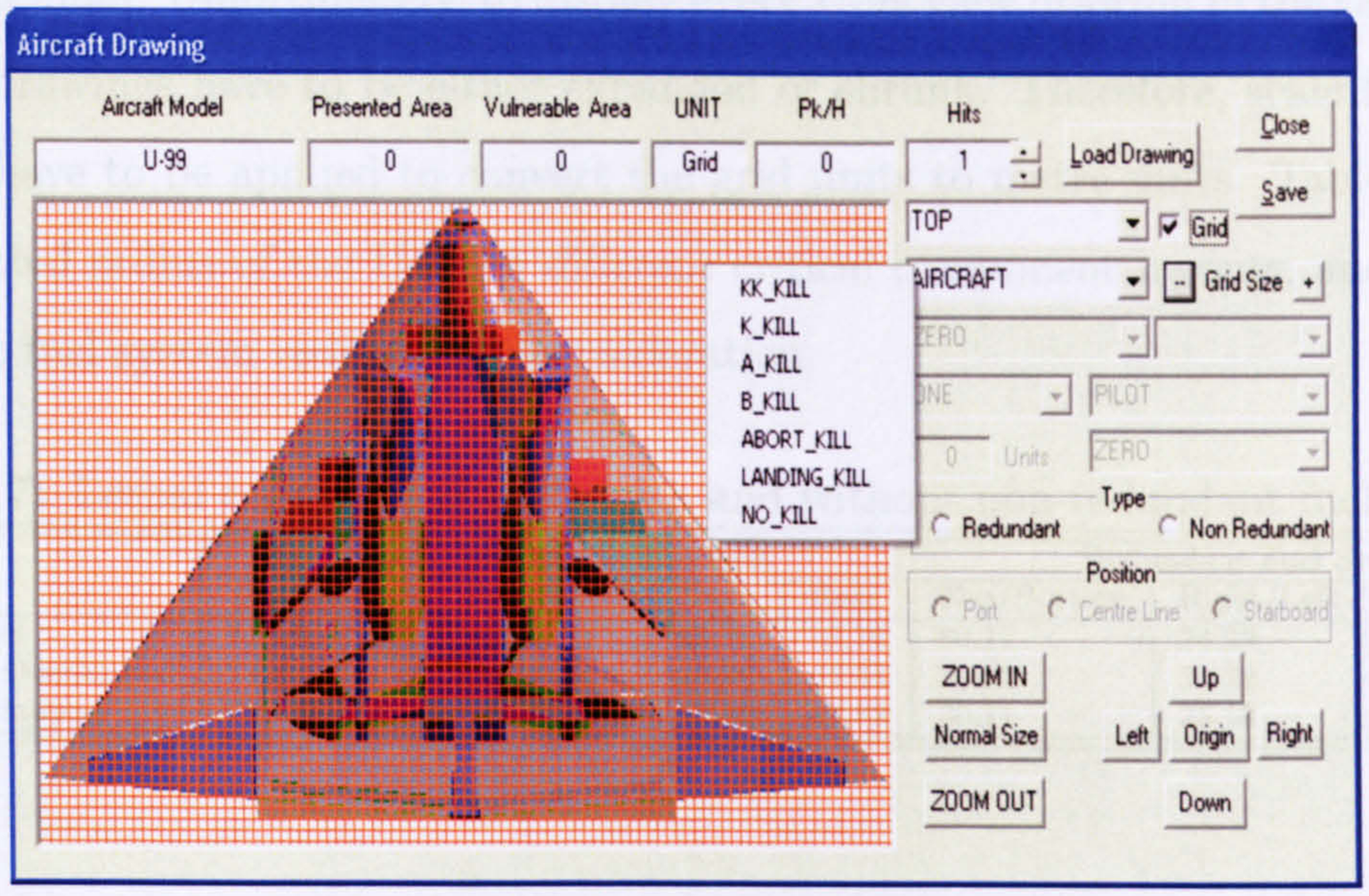

Figure B.10: Semi-automatic Grid counting

B.2.3 Transition Matrices Elaboration

In the vulnerability assessment module, transition matrix in each aircraft view is a very importance functionality to evaluate the probability of kill by multiple hits of penetrators. As described in Chapter 3, an aircraft can be examined in three main categories; i.e. non-overlapped critical component, non-shielding effect overlapped critical component, and shielding effect overlapped critical component. Fig. B.11 - B.18 show the transition matrices of case study aircraft U-99 in different views and categories.

B.2.4 Lethal Radius Estimation

The lethal radius is one measure of aircraft vulnerability probability on encounter with a proximity warhead. The expected number of fragments impacting on the aircraft depends mainly on the detonation distance. It is assumed that all fragments (n) from the spray zone, whose shotline are within the aircraft presented area (see Fig. 3.8), hit the aircraft. The probability of kill given an encounter with this warhead is thus a function of the detonation distance. If the detonation distance resulting enough fragments impacting on the aircraft, such that the probability of kill is equal to 0.5. This distance will be defined as lethal radius [6].

By using the same U-99 drawings as usual in the determination of the U-99 presented areas for all 6 main aircraft views, the lethal radius of each U-99 view can be thus evaluated

firstly in grid units. Unfortunately, to display every U-99 view drawing in the same display dialog, the drawings have to be either expanded or shrunk. Therefore, scale factors (see Table B.9) have to be applied to convert the grid units to metre units. Table B.7 - B.8 show the lethal radius of the U-99 in different critical component layouts, and also with and without fuel system redundancy consideration.

Table B.7: Lethal radius[m] of U-99 with and without non-redundant fuel systems

	Non-Redundant Fuel System				Redundant Fuel Systems			
	Top/Bottom	Right/Left	Front	Rear	Top/Bottom	Right/Left	Front	Rear
Non-Overlapped	71.48	48.26	43.76	43.76	30.11	24.29	24.64	24.64
Non-Shielding Overlapped	71.48	48.27	43.34	43.34	30.11	26.12	25.21	25.21
Shielding Overlapped	71.48	46.75	43.16	42.82	30.11	25.18	25.16	24.90

Table B.8: Lethal radius[Grid] of U-99 with and without non-redundant fuel systems

	Non-Redundant Fuel System				Redundant Fuel Systems			
	Top/Bottom	Right/Left	Front	Rear	Top/Bottom	Right/Left	Front	Rear
Non-Overlapped	642.94	507.36	504.87	504.87	270.84	255.37	284.34	284.34
Non-Shielding Overlapped	642.94	507.55	500.00	500.00	270.84	274.61	290.89	290.89
Shielding Overlapped	642.94	491.51	497.96	494.07	270.84	264.69	290.25	287.31

The lethal radius can be read from graph between P_K and s as shown in Fig. B.19.

Due to different scale of U-99 drawing in each view, the ratios of drawing grid in each aircraft view to the actual size of U-99 have been investigate and shown, as in Table B.9

Table B.9: U-99 drawing grid factor in six main aircraft views

	Span			Length		
	Grid	Metre	Factor	Grid	Metre	Factor
Top/Bottom	57	7.8	0.136842	76	6.5	0.08552
Left/Right	82	7.8	0.095122	-	-	-
Front/Rear	-	-	-	75	6.5	0.08667

Knrc	*Tank* 1	*Tank* 2	*Tank* 3	*Tank* 4	*Tank* 5	*Tank*	*Engine* 1	*Engine* 2	*Engine*	*FCS* 1	*FCS* 2	*FCS*	*NK*
1.00000000	0.00999219	0.00999219	0.00999219	0.00999219	0.00999219	0.00000000	0.00999219	0.00999219	0.00000000	0.00999219	0.00999219	0.00000000	0.00999219
0.00000000	0.92193604	0.02903981	0.02903981	0.02903981	0.02903981	0.00000000	0.02903981	0.02903981	0.00000000	0.02903981	0.02903981	0.00000000	0.02903981
0.00000000	0.00737705	0.90027326	0.00737705	0.00737705	0.00737705	0.00000000	0.00737705	0.00737705	0.00000000	0.00737705	0.00737705	0.00000000	0.00737705
0.00000000	0.00737705	0.00737705	0.90027326	0.00737705	0.00737705	0.00000000	0.00737705	0.00737705	0.00000000	0.00737705	0.00737705	0.00000000	0.00737705
0.00000000	0.00234192	0.00234192	0.00234192	0.89523816	0.00000000	0.00000000	0.00234192	0.00234192	0.00000000	0.00234192	0.00234192	0.00000000	0.00234192
0.00000000	0.00000000	0.00000000	0.00000000	0.00000000	0.89523816	0.00000000	0.00234192	0.00234192	0.00000000	0.00234192	0.00234192	0.00000000	0.00234192
0.00000000	0.00234192	0.00234192	0.00234192	0.00234192	0.00234192	1.00000000	0.00000000	0.00000000	0.00000000	0.00000000	0.00000000	0.00000000	0.00000000
0.00000000	0.02014052	0.02014052	0.02014052	0.02014052	0.02014052	0.00000000	0.91303670	0.00000000	0.00000000	0.02014052	0.02014052	0.00000000	0.02014052
0.00000000	0.02349727	0.02349727	0.02349727	0.02349727	0.02349727	0.00000000	0.00000000	0.91639346	0.00000000	0.02349727	0.02349727	0.00000000	0.02349727
0.00000000	0.00000000	0.00000000	0.00000000	0.00000000	0.00000000	0.00000000	0.02349727	0.02014052	1.00000000	0.00000000	0.00000000	0.00000000	0.00000000
0.00000000	0.00249805	0.00249805	0.00249805	0.00249805	0.00249805	0.00000000	0.00249805	0.00249805	0.00000000	0.89539427	0.00000000	0.00000000	0.00249805
0.00000000	0.00249805	0.00249805	0.00249805	0.00249805	0.00249805	0.00000000	0.00249805	0.00249805	0.00000000	0.00000000	0.89539427	0.00000000	0.00249805
0.00000000	0.00000000	0.00000000	0.00000000	0.00000000	0.00000000	0.00000000	0.00000000	0.00000000	0.00000000	0.00249805	0.00249805	1.00000000	0.00000000
0.00000000	0.00000000	0.00000000	0.00000000	0.00000000	0.00000000	0.00000000	0.00000000	0.00000000	0.00000000	0.00000000	0.00000000	0.00000000	0.89289623

Figure B.11: Transition matric for U-99 top/bottom view without critical components overlapping consideration

Knrc	*Tank* 1	*Tank* 2	*Tank* 3	*Tank* 4	*Tank* 5	*Tank*	*Engine* 1	*Engine* 2	*Engine*	*FCS* 1	*FCS* 2	*FCS*	*NK*
1.00000000	0.05056434	0.05056434	0.05056434	0.05056434	0.05056434	0.00000000	0.05056434	0.05056434	0.00000000	0.05056434	0.05056434	0.00000000	0.05056434
0.00000000	0.69841993	0.08261851	0.08261851	0.08261851	0.08261851	0.00000000	0.08261851	0.08261851	0.00000000	0.08261851	0.08261851	0.00000000	0.08261851
0.00000000	0.03250565	0.64830703	0.03250565	0.03250565	0.03250565	0.00000000	0.03250565	0.03250565	0.00000000	0.03250565	0.03250565	0.00000000	0.03250565
0.00000000	0.03250565	0.03250565	0.64830703	0.03250565	0.03250565	0.00000000	0.03250565	0.03250565	0.00000000	0.03250565	0.03250565	0.00000000	0.03250565
0.00000000	0.00677201	0.00677201	0.00677201	0.62257338	0.00000000	0.00000000	0.00677201	0.00677201	0.00000000	0.00677201	0.00677201	0.00000000	0.00677201
0.00000000	0.00000000	0.00000000	0.00000000	0.00000000	0.62257338	0.00000000	0.00677201	0.00677201	0.00000000	0.00677201	0.00677201	0.00000000	0.00677201
0.00000000	0.00677201	0.00677201	0.00677201	0.00677201	0.00677201	1.00000000	0.00000000	0.00000000	0.00000000	0.00000000	0.00000000	0.00000000	0.00000000
0.00000000	0.07178330	0.07178330	0.07178330	0.07178330	0.07178330	0.00000000	0.68758470	0.00000000	0.00000000	0.07178330	0.07178330	0.00000000	0.07178330
0.00000000	0.07178330	0.07178330	0.07178330	0.07178330	0.07178330	0.00000000	0.00000000	0.68758470	0.00000000	0.07178330	0.07178330	0.00000000	0.07178330
0.00000000	0.00000000	0.00000000	0.00000000	0.00000000	0.00000000	0.00000000	0.07178330	0.07178330	1.00000000	0.00000000	0.00000000	0.00000000	0.00000000
0.00000000	0.01444695	0.01444695	0.01444695	0.01444695	0.01444695	0.00000000	0.01444695	0.01444695	0.00000000	0.63024837	0.00000000	0.00000000	0.01444695
0.00000000	0.01444695	0.01444695	0.01444695	0.01444695	0.01444695	0.00000000	0.01444695	0.01444695	0.00000000	0.00000000	0.63024837	0.00000000	0.01444695
0.00000000	0.00000000	0.00000000	0.00000000	0.00000000	0.00000000	0.00000000	0.00000000	0.00000000	0.00000000	0.01444695	0.01444695	1.00000000	0.00000000
0.00000000	0.00000000	0.00000000	0.00000000	0.00000000	0.00000000	0.00000000	0.00000000	0.00000000	0.00000000	0.00000000	0.00000000	0.00000000	0.61580139

Figure B.12: Transition matric for U-99 right/left view without critical components overlapping consideration

Knrc	*Tank* 1	*Tank* 2	*Tank* 3	*Tank* 4	*Tank* 5	*Tank*	*Engine* 1	*Engine* 2	*Engine*	*FCS* 1	*FCS* 2	*FCS*	*NK*
1.00000000	0.08089888	0.08089888	0.08089888	0.08089888	0.08089888	0.00000000	0.08089888	0.08089888	0.00000000	0.08089888	0.08089888	0.00000000	0.08089888
0.00000000	0.69634825	0.05393258	0.05393258	0.05393258	0.05393258	0.00000000	0.05393258	0.05393258	0.00000000	0.05393258	0.05393258	0.00000000	0.05393258
0.00000000	0.04382022	0.68623590	0.04382022	0.04382022	0.04382022	0.00000000	0.04382022	0.04382022	0.00000000	0.04382022	0.04382022	0.00000000	0.04382022
0.00000000	0.04382022	0.04382022	0.68623590	0.04382022	0.04382022	0.00000000	0.04382022	0.04382022	0.00000000	0.04382022	0.04382022	0.00000000	0.04382022
0.00000000	0.01938202	0.01938202	0.01938202	0.66179770	0.00000000	0.00000000	0.01938202	0.01938202	0.00000000	0.01938202	0.01938202	0.00000000	0.01938202
0.00000000	0.00000000	0.00000000	0.00000000	0.00000000	0.66179770	0.00000000	0.01938202	0.01938202	0.00000000	0.01938202	0.01938202	0.00000000	0.01938202
0.00000000	0.01938202	0.01938202	0.01938202	0.01938202	0.01938202	1.00000000	0.00000000	0.00000000	0.00000000	0.00000000	0.00000000	0.00000000	0.00000000
0.00000000	0.03202247	0.03202247	0.03202247	0.03202247	0.03202247	0.00000000	0.67443818	0.00000000	0.00000000	0.03202247	0.03202247	0.00000000	0.03202247
0.00000000	0.03735955	0.03735955	0.03735955	0.03735955	0.03735955	0.00000000	0.00000000	0.67977524	0.00000000	0.03735955	0.03735955	0.00000000	0.03735955
0.00000000	0.00000000	0.00000000	0.00000000	0.00000000	0.00000000	0.00000000	0.03735955	0.03202247	1.00000000	0.00000000	0.00000000	0.00000000	0.00000000
0.00000000	0.01348315	0.01348315	0.01348315	0.01348315	0.01348315	0.00000000	0.01348315	0.01348315	0.00000000	0.65589881	0.00000000	0.00000000	0.01348315
0.00000000	0.01348315	0.01348315	0.01348315	0.01348315	0.01348315	0.00000000	0.01348315	0.01348315	0.00000000	0.00000000	0.65589881	0.00000000	0.01348315
0.00000000	0.00000000	0.00000000	0.00000000	0.00000000	0.00000000	0.00000000	0.00000000	0.00000000	0.00000000	0.01348315	0.01348315	1.00000000	0.00000000
0.00000000	0.00000000	0.00000000	0.00000000	0.00000000	0.00000000	0.00000000	0.00000000	0.00000000	0.00000000	0.00000000	0.00000000	0.00000000	0.64241570

Figure B.13: Transition matric for U-99 front/rear view without critical components overlapping consideration

Knrc	*Tank 1*	*Tank 2*	*Tank 3*	*Tank 4*	*Tank 5*	*Tank*	*Engine 1*	*Engine 2*	*Engine*	*FCS 1*	*FCS 2*	*FCS*	*Overlap 1*	*Overlap 2*	*Overlap 3*	*Overlap*	*NK*
1.00000	0.05972	0.05972	0.05972	0.05972	0.05972	0.00000	0.05972	0.05972	0.00000	0.05972	0.05972	0.00000	0.05972	0.05972	0.05972	0.00000	0.05972
0.00000	0.93810	0.05655	0.05655	0.05655	0.05655	0.00000	0.05655	0.05655	0.00000	0.05655	0.05655	0.00000	0.05655	0.05655	0.05655	0.00000	0.05655
0.00000	0.00000	0.88156	0.00000	0.00000	0.00000	0.00000	0.00000	0.00000	0.00000	0.00000	0.00000	0.00000	0.00000	0.00000	0.00000	0.00000	0.00000
0.00000	0.00000	0.00000	0.88156	0.00000	0.00000	0.00000	0.00000	0.00000	0.00000	0.00000	0.00000	0.00000	0.00000	0.00000	0.00000	0.00000	0.00000
0.00000	0.00000	0.00000	0.00000	0.88156	0.00000	0.00000	0.00000	0.00000	0.00000	0.00000	0.00000	0.00000	0.00000	0.00000	0.00000	0.00000	0.00000
0.00000	0.00000	0.00000	0.00000	0.00000	0.88156	0.00000	0.00000	0.00000	0.00000	0.00000	0.00000	0.00000	0.00000	0.00000	0.00000	0.00000	0.00000
0.00000	0.00000	0.00000	0.00000	0.00000	0.00000	1.00000	0.00000	0.00000	0.00000	0.00000	0.00000	0.00000	0.00000	0.00000	0.00000	0.00000	0.00000
0.00000	0.00000	0.00000	0.00000	0.00000	0.00000	0.00000	0.88156	0.00000	0.00000	0.00000	0.00000	0.00000	0.00000	0.00000	0.00000	0.00000	0.00000
0.00000	0.00000	0.00000	0.00000	0.00000	0.00000	0.00000	0.00000	0.88156	0.00000	0.00000	0.00000	0.00000	0.00000	0.00000	0.00000	0.00000	0.00000
0.00000	0.00000	0.00000	0.00000	0.00000	0.00000	0.00000	0.00000	0.00000	1.00000	0.00000	0.00000	0.00000	0.00000	0.00000	0.00000	0.00000	0.00000
0.00000	0.00000	0.00000	0.00000	0.00000	0.00000	0.00000	0.00000	0.00000	0.00000	0.88156	0.00000	0.00000	0.00000	0.00000	0.00000	0.00000	0.00000
0.00000	0.00000	0.00000	0.00000	0.00000	0.00000	0.00000	0.00000	0.00000	0.00000	0.00000	0.88156	0.00000	0.00000	0.00000	0.00000	0.00000	0.00000
0.00000	0.00000	0.00000	0.00000	0.00000	0.00000	0.00000	0.00000	0.00000	0.00000	0.00000	0.00000	1.00000	0.00000	0.00000	0.00000	0.00000	0.00000
0.00000	0.00030	0.00030	0.00030	0.00030	0.00030	0.00000	0.00030	0.00030	0.00000	0.00030	0.00030	0.00000	0.88186	0.00030	0.00030	0.00000	0.00030
0.00000	0.00041	0.00041	0.00041	0.00041	0.00041	0.00000	0.00041	0.00041	0.00000	0.00041	0.00041	0.00000	0.00041	0.88196	0.00041	0.00000	0.00041
0.00000	0.00146	0.00146	0.00146	0.00146	0.00146	0.00000	0.00146	0.00146	0.00000	0.00146	0.00146	0.00000	0.00146	0.00146	0.88302	0.00000	0.00146
0.00000	0.00000	0.00000	0.00000	0.00000	0.00000	0.00000	0.00000	0.00000	0.00000	0.00000	0.00000	0.00000	0.00000	0.00000	0.00000	1.00000	0.00000
0.00000	0.00000	0.00000	0.00000	0.00000	0.00000	0.00000	0.00000	0.00000	0.00000	0.00000	0.00000	0.00000	0.00000	0.00000	0.00000	0.00000	0.88156

Figure B.14: Transition matric for U-99 right/left view without shielding effect of critical components overlapping consideration

Knrc	*Tank 1*	*Tank 2*	*Tank 3*	*Tank 4*	*Tank 5*	*Tank*	*Engine 1*	*Engine 2*	*Engine*	*FCS 1*	*FCS 2*	*FCS*	*Overlap 1*	*Overlap 2*	*Overlap 3*	*Overlap*	*NK*
1.00000	0.05525	0.05526	0.05526	0.05526	0.05526	0.00000	0.05526	0.05526	0.00000	0.05526	0.05526	0.00000	0.05526	0.05526	0.05526	0.00000	0.05526
0.00000	0.94311	0.05655	0.05655	0.05655	0.05655	0.00000	0.05655	0.05655	0.00000	0.05655	0.05655	0.00000	0.05655	0.05655	0.05655	0.00000	0.05655
0.00000	0.00000	0.88656	0.00000	0.00000	0.00000	0.00000	0.00000	0.00000	0.00000	0.00000	0.00000	0.00000	0.00000	0.00000	0.00000	0.00000	0.00000
0.00000	0.00000	0.00000	0.88656	0.00000	0.00000	0.00000	0.00000	0.00000	0.00000	0.00000	0.00000	0.00000	0.00000	0.00000	0.00000	0.00000	0.00000
0.00000	0.00000	0.00000	0.00000	0.88656	0.00000	0.00000	0.00000	0.00000	0.00000	0.00000	0.00000	0.00000	0.00000	0.00000	0.00000	0.00000	0.00000
0.00000	0.00000	0.00000	0.00000	0.00000	0.88656	0.00000	0.00000	0.00000	0.00000	0.00000	0.00000	0.00000	0.00000	0.00000	0.00000	0.00000	0.00000
0.00000	0.00000	0.00000	0.00000	0.00000	0.00000	1.00000	0.00000	0.00000	0.00000	0.00000	0.00000	0.00000	0.00000	0.00000	0.00000	0.00000	0.00000
0.00000	0.00000	0.00000	0.00000	0.00000	0.00000	0.00000	0.88656	0.00000	0.00000	0.00000	0.00000	0.00000	0.00000	0.00000	0.00000	0.00000	0.00000
0.00000	0.00000	0.00000	0.00000	0.00000	0.00000	0.00000	0.00000	0.88656	0.00000	0.00000	0.00000	0.00000	0.00000	0.00000	0.00000	0.00000	0.00000
0.00000	0.00000	0.00000	0.00000	0.00000	0.00000	0.00000	0.00000	0.00000	1.00000	0.00000	0.00000	0.00000	0.00000	0.00000	0.00000	0.00000	0.00000
0.00000	0.00000	0.00000	0.00000	0.00000	0.00000	0.00000	0.00000	0.00000	0.00000	0.88656	0.00000	0.00000	0.00000	0.00000	0.00000	0.00000	0.00000
0.00000	0.00000	0.00000	0.00000	0.00000	0.00000	0.00000	0.00000	0.00000	0.00000	0.00000	0.88656	0.00000	0.00000	0.00000	0.00000	0.00000	0.00000
0.00000	0.00000	0.00000	0.00000	0.00000	0.00000	0.00000	0.00000	0.00000	0.00000	0.00000	0.00000	1.00000	0.00000	0.00000	0.00000	0.00000	0.00000
0.00000	0.00022	0.00022	0.00022	0.00022	0.00022	0.00000	0.00022	0.00022	0.00000	0.00022	0.00022	0.00000	0.88678	0.00022	0.00022	0.00000	0.00022
0.00000	0.00037	0.00037	0.00037	0.00037	0.00037	0.00000	0.00037	0.00037	0.00000	0.00037	0.00037	0.00000	0.00037	0.88692	0.00037	0.00000	0.00037
0.00000	0.00105	0.00105	0.00105	0.00105	0.00105	0.00000	0.00105	0.00105	0.00000	0.00105	0.00105	0.00000	0.00105	0.00105	0.88761	0.00000	0.00105
0.00000	0.00000	0.00000	0.00000	0.00000	0.00000	0.00000	0.00000	0.00000	0.00000	0.00000	0.00000	0.00000	0.00000	0.00000	0.00000	1.00000	0.00000
0.00000	0.00000	0.00000	0.00000	0.00000	0.00000	0.00000	0.00000	0.00000	0.00000	0.00000	0.00000	0.00000	0.00000	0.00000	0.00000	0.00000	0.88656

Figure B.15: Transition matric for U-99 right/left view with shielding effect of critical components overlapping consideration

Knrc	*Tank* 1	*Tank* 2	*Tank* 3	*Tank* 4	*Tank* 5	*Tank*	*Engine* 1	*Engine* 2	*Engine*	*FCS* 1	*FCS* 2	*FCS*	*Overlap* 1	*Overlap* 2	*Overlap* 3	*Overlap* 4	*Overlap*	*NK*
1.000	0.08562	0.08562	0.08562	0.08562	0.08562	0.000	0.08562	0.08562	0.000	0.08562	0.08562	0.000	0.08562	0.08562	0.08562	0.08562	0.000	0.08562
0.000	0.79971	0.04382	0.04382	0.04382	0.04382	0.000	0.04382	0.04382	0.000	0.04382	0.04382	0.000	0.04382	0.04382	0.04382	0.04382	0.000	0.04382
0.000	0.02444	0.78033	0.02444	0.02444	0.02444	0.000	0.02444	0.02444	0.000	0.02444	0.02444	0.000	0.02444	0.02444	0.02444	0.02444	0.000	0.02444
0.000	0.02444	0.02444	0.78033	0.02444	0.02444	0.000	0.02444	0.02444	0.000	0.02444	0.02444	0.000	0.02444	0.02444	0.02444	0.02444	0.000	0.02444
0.000	0.00000	0.00000	0.00000	0.75588	0.00000	0.000	0.00000	0.00000	0.000	0.00000	0.00000	0.000	0.00000	0.00000	0.00000	0.00000	0.000	0.00000
0.000	0.00000	0.00000	0.00000	0.00000	0.75589	0.000	0.00000	0.00000	0.000	0.00000	0.00000	0.000	0.00000	0.00000	0.00000	0.00000	0.000	0.00000
0.000	0.00000	0.00000	0.00000	0.00000	0.00000	1.000	0.00000	0.00000	0.000	0.00000	0.00000	0.000	0.00000	0.00000	0.00000	0.00000	0.000	0.00000
0.000	0.02528	0.02528	0.02528	0.02528	0.02528	0.000	0.78117	0.00000	0.000	0.02528	0.02528	0.000	0.02528	0.02528	0.02528	0.02528	0.000	0.02528
0.000	0.02949	0.02949	0.02949	0.02949	0.02949	0.000	0.00000	0.78538	0.000	0.02949	0.02949	0.000	0.02949	0.02949	0.02949	0.02949	0.000	0.02949
0.000	0.00000	0.00000	0.00000	0.00000	0.00000	0.000	0.02949	0.02528	1.000	0.00000	0.00000	0.000	0.00000	0.00000	0.00000	0.00000	0.000	0.00000
0.000	0.00000	0.00000	0.00000	0.00000	0.00000	0.000	0.00000	0.00000	0.000	0.75589	0.00000	0.000	0.00000	0.00000	0.00000	0.00000	0.000	0.00000
0.000	0.00000	0.00000	0.00000	0.00000	0.00000	0.000	0.00000	0.00000	0.000	0.00000	0.75589	0.000	0.00000	0.00000	0.00000	0.00000	0.000	0.00000
0.000	0.00000	0.00000	0.00000	0.00000	0.00000	0.000	0.00000	0.00000	0.000	0.00000	0.00000	1.000	0.00000	0.00000	0.00000	0.00000	0.000	0.00000
0.000	0.00121	0.00121	0.00121	0.00121	0.00121	0.000	0.00121	0.00121	0.000	0.00121	0.00121	0.000	0.75710	0.00121	0.00121	0.00121	0.000	0.00121
0.000	0.00430	0.00430	0.00430	0.00430	0.00430	0.000	0.00430	0.00430	0.000	0.00430	0.00430	0.000	0.00430	0.76019	0.00430	0.00430	0.000	0.00430
0.000	0.00121	0.00121	0.00121	0.00121	0.00121	0.000	0.00121	0.00121	0.000	0.00121	0.00121	0.000	0.00121	0.00121	0.75710	0.00121	0.000	0.00121
0.000	0.00430	0.00430	0.00430	0.00430	0.00430	0.000	0.00430	0.00430	0.000	0.00430	0.00430	0.000	0.00430	0.00430	0.00430	0.76019	0.000	0.00430
0.000	0.00000	0.00000	0.00000	0.00000	0.00000	0.000	0.00000	0.00000	0.000	0.00000	0.00000	0.000	0.00000	0.00000	0.00000	0.00000	1.000	0.00000
0.000	0.00000	0.00000	0.00000	0.00000	0.00000	0.000	0.00000	0.00000	0.000	0.00000	0.00000	0.000	0.00000	0.00000	0.00000	0.00000	0.000	0.75589

Figure B.16: Transition matric for U-99 front/rear view without shielding effect of critical components overlapping consideration

Knrc	*Tank* 1	*Tank* 2	*Tank* 3	*Tank* 4	*Tank* 5	*Tank*	*Engine* 1	*Engine* 2	*Engine*	*FCS* 1	*FCS* 2	*FCS*	*Overlap* 1	*Overlap* 2	*Overlap* 3	*Overlap* 4	*Overlap*	*NK*
1.000	0.08515	0.08515	0.08515	0.08515	0.08515	0.000	0.08515	0.08515	0.000	0.08515	0.08515	0.000	0.08515	0.08515	0.08515	0.0851*s*	0.000	0.08515
0.000	0.80172	0.04382	0.04382	0.04382	0.04382	0.000	0.04382	0.04382	0.000	0.04382	0.04382	0.000	0.04382	0.04382	0.04382	0.04382	0.000	0.04382
0.000	0.02444	0.78234	0.02443	0.02444	0.02444	0.000	0.02444	0.02444	0.000	0.02444	0.02444	0.000	0.02444	0.02444	0.02444	0.02444	0.000	0.02444
0.000	0.02444	0.02444	0.78234	0.02444	0.02444	0.000	0.02444	0.02444	0.000	0.02444	0.02444	0.000	0.02444	0.02444	0.02444	0.02444	0.000	0.02444
0.000	0.00000	0.00000	0.00000	0.75790	0.00000	0.000	0.00000	0.00000	0.000	0.00000	0.00000	0.000	0.00000	0.00000	0.00000	0.00000	0.000	0.00000
0.000	0.00000	0.00000	0.00000	0.00000	0.75790	0.000	0.00000	0.00000	0.000	0.00000	0.00000	0.000	0.00000	0.00000	0.00000	0.00000	0.000	0.00000
0.000	0.00000	0.00000	0.00000	0.00000	0.00000	1.000	0.00000	0.00000	0.000	0.00000	0.00000	0.000	0.00000	0.00000	0.00000	0.00000	0.000	0.00000
0.000	0.02528	0.02528	0.02528	0.02528	0.02528	0.000	0.78318	0.00000	0.000	0.02528	0.02528	0.000	0.02528	0.02528	0.02528	0.02528	0.000	0.02528
0.000	0.02949	0.02949	0.02949	0.02949	0.02949	0.000	0.00000	0.78739	0.000	0.02949	0.02949	0.000	0.02949	0.02949	0.02949	0.02949	0.000	0.02949
0.000	0.00000	0.00000	0.00000	0.00000	0.00000	0.000	0.02949	0.02528	1.000	0.00000	0.00000	0.000	0.00000	0.00000	0.00000	0.00000	0.000	0.00000
0.000	0.00000	0.00000	0.00000	0.00000	0.00000	0.000	0.00000	0.00000	0.000	0.75790	0.00000	0.000	0.00000	0.00000	0.00000	0.00000	0.000	0.00000
0.000	0.00000	0.00000	0.00000	0.00000	0.00000	0.000	0.00000	0.00000	0.000	0.00000	0.75790	0.000	0.00000	0.00000	0.00000	0.00000	0.000	0.00000
0.000	0.00000	0.00000	0.00000	0.00000	0.00000	0.000	0.00000	0.00000	0.000	0.00000	0.00000	1.000	0.00000	0.00000	0.00000	0.00000	0.000	0.00000
0.000	0.00087	0.00087	0.00087	0.00087	0.00087	0.000	0.00087	0.00087	0.000	0.00087	0.00087	0.000	0.75877	0.00087	0.00087	0.00087	0.000	0.00087
0.000	0.00387	0.00387	0.00387	0.00387	0.00387	0.000	0.00387	0.00387	0.000	0.00387	0.00387	0.000	0.00387	0.76177	0.00387	0.00387	0.000	0.00387
0.000	0.00087	0.00087	0.00087	0.00087	0.00087	0.000	0.00087	0.00087	0.000	0.00087	0.00087	0.000	0.00087	0.00087	0.75877	0.00087	0.000	0.00087
0.000	0.00387	0.00387	0.00387	0.00387	0.00387	0.000	0.00387	0.00387	0.000	0.00387	0.00387	0.000	0.00387	0.00387	0.00387	0.76177	0.000	0.00387
0.000	0.00000	0.00000	0.00000	0.00000	0.00000	0.000	0.00000	0.00000	0.000	0.00000	0.00000	0.000	0.00000	0.00000	0.00000	0.00000	1.000	0.00000
0.000	0.00000	0.00000	0.00000	0.00000	0.00000	0.000	0.00000	0.00000	0.000	0.00000	0.00000	0.000	0.00000	0.00000	0.00000	0.00000	0.000	0.75790

Figure B.17: Transition matric for U-99 front view with shielding effect of critical components overlapping consideration

Knrc	*Tank* 1	*Tank* 2	*Tank* 3	*Tank* 4	*Tank* 5	*Tank*	*Engine* 1	*Engine* 2	*Engine*	*FCS* 1	*FCS* 2	*FCS*	*Overlap* 1	*Overlap* 2	*Overlap* 3	*Overlap* 4	*Overlap*	*NK*
1.000	0.08301	0.08301	0.08301	0.08301	0.08301	0.000	0.08301	0.08301	0.000	0.08301	0.08301	0.000	0.08301	0.08301	0.08301	0.08301	0.000	0.08301
0.000	0.80385	0.04382	0.04382	0.04382	0.04382	0.000	0.04382	0.04382	0.000	0.04382	0.04382	0.000	0.04382	0.04382	0.04382	0.04382	0.000	0.04382
0.000	0.02444	0.78447	0.02444	0.02444	0.02444	0.000	0.02444	0.02444	0.000	0.02444	0.02444	0.000	0.02444	0.02444	0.02444	0.02444	0.000	0.02444
0.000	0.02444	0.02444	0.78447	0.02444	0.02444	0.000	0.02444	0.02444	0.000	0.02444	0.02444	0.000	0.02444	0.02444	0.02444	0.02444	0.000	0.02444
0.000	0.00000	0.00000	0.00000	0.76003	0.00000	0.000	0.00000	0.00000	0.000	0.00000	0.00000	0.000	0.00000	0.00000	0.00000	0.00000	0.000	0.00000
0.000	0.00000	0.00000	0.00000	0.00000	0.76003	0.000	0.00000	0.00000	0.000	0.00000	0.00000	0.000	0.00000	0.00000	0.00000	0.00000	0.000	0.00000
0.000	0.00000	0.00000	0.00000	0.00000	0.00000	1.000	0.00000	0.00000	0.000	0.00000	0.00000	0.000	0.00000	0.00000	0.00000	0.00000	0.000	0.00000
0.000	0.02528	0.02528	0.02528	0.02528	0.02528	0.000	0.78531	0.00000	0.000	0.02528	0.02528	0.000	0.02528	0.02528	0.02528	0.02528	0.000	0.02528
0.000	0.02949	0.02949	0.02949	0.02949	0.02949	0.000	0.00000	0.78953	0.000	0.02949	0.02949	0.000	0.02949	0.02949	0.02949	0.02949	0.0000	0.02949
0.000	0.00000	0.00000	0.00000	0.00000	0.00000	0.000	0.02949	0.02528	1.000	0.00000	0.00000	0.000	0.00000	0.00000	0.00000	0.00000	0.0000	0.00000
0.000	0.00000	0.00000	0.00000	0.00000	0.00000	0.000	0.00000	0.00000	0.000	0.76003	0.00000	0.000	0.00000	0.00000	0.00000	0.00000	0.000	0.00000
0.000	0.00000	0.00000	0.00000	0.00000	0.00000	0.000	0.00000	0.00000	0.000	0.00000	0.76003	0.000	0.00000	0.00000	0.00000	0.00000	0.000	0.00000
0.000	0.00000	0.00000	0.00000	0.00000	0.00000	0.000	0.00000	0.00000	0.000	0.00000	0.00000	1.000	0.00000	0.00000	0.00000	0.00000	0.000	0.00000
0.000	0.00087	0.00087	0.00087	0.00087	0.00087	0.000	0.00087	0.00087	0.000	0.00087	0.00087	0.000	0.76091	0.00087	0.00087	0.00087	0.000	0.00087
0.000	0.00387	0.00387	0.00387	0.00387	0.00387	0.000	0.00387	0.00387	0.000	0.00387	0.00387	0.000	0.00387	0.76390	0.00387	0.00387	0.000	0.00387
0.000	0.00087	0.00087	0.00087	0.00087	0.00087	0.000	0.00087	0.00087	0.000	0.00087	0.00087	0.000	0.00087	0.00087	0.76091	0.00087	0.000	0.00087
0.000	0.00387	0.00387	0.00387	0.00387	0.00387	0.000	0.00387	0.00387	0.000	0.00387	0.00387	0.000	0.00387	0.00387	0.00387	0.76390	0.000	0.00387
0.000	0.00000	0.00000	0.00000	0.00000	0.00000	0.000	0.00000	0.00000	0.000	0.00000	0.00000	0.000	0.00000	0.00000	0.00000	0.00000	1.000	0.00000
0.000	0.00000	0.00000	0.00000	0.00000	0.00000	0.000	0.00000	0.00000	0.000	0.00000	0.00000	0.000	0.00000	0.00000	0.00000	0.00000	0.000	0.76003

Figure B.18: Transition matric for U-99 rear view with shielding effect of critical components overlapping consideration

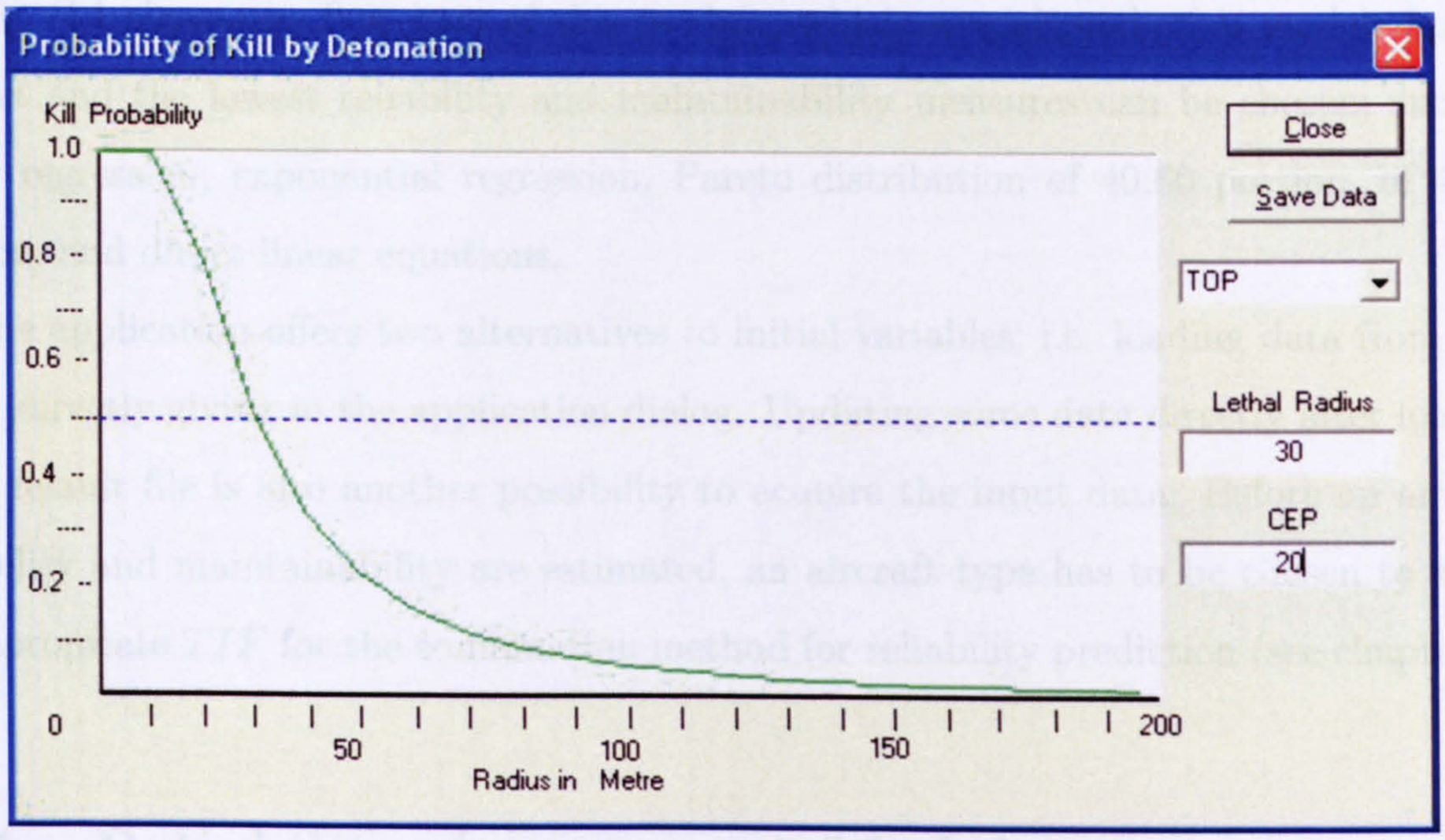

Figure B.19: Lethal radius estimation application dialog

APPENDIX C

RELIABILITY & MAINTAINABILITY ASSESSMENT MODULE

This appendix shows and explains mainly how the reliability & maintainability assessment module works. All regression equations and results from several models will be additionally shown in this appendix.

Fig. C.1 shows the flowchart of this module, which several prediction models for the highest and the lowest reliability and maintainability measures can be chosen; such as linear regression, exponential regression, Pareto distribution of 40:60 portion, of 40:70 portion, and direct linear equations.

The application offers two alternatives to initial variables; i.e. loading data from text file or directly giving in the application dialog. Updating some data directly after loading from default file is also another possibility to acquire the input data. Before an aircraft reliability and maintainability are estimated, an aircraft type has to be chosen to select an appropriate TIF for the combination method for reliability prediction (see chapter 4).

C.1 Reliability Assessment Module

In this section, equations and prediction method of the third (functionality of aircraft empty weight) and the fourth (combination method between linear regression and Pareto distribution) reliability models are described. The fourth method has been used in this design methodology, as shown in Reliability & Maintainability application dialog (see Fig. C.2).

C.1.1 Empty Weight Functionality Model

This model offers the simplest prediction method of aircraft reliability from four limit data sets (1985, 1987, 1993, and 1996). Due to limit data and timescale to develop this module, all data have been used to find an average failure rate prediction equation to

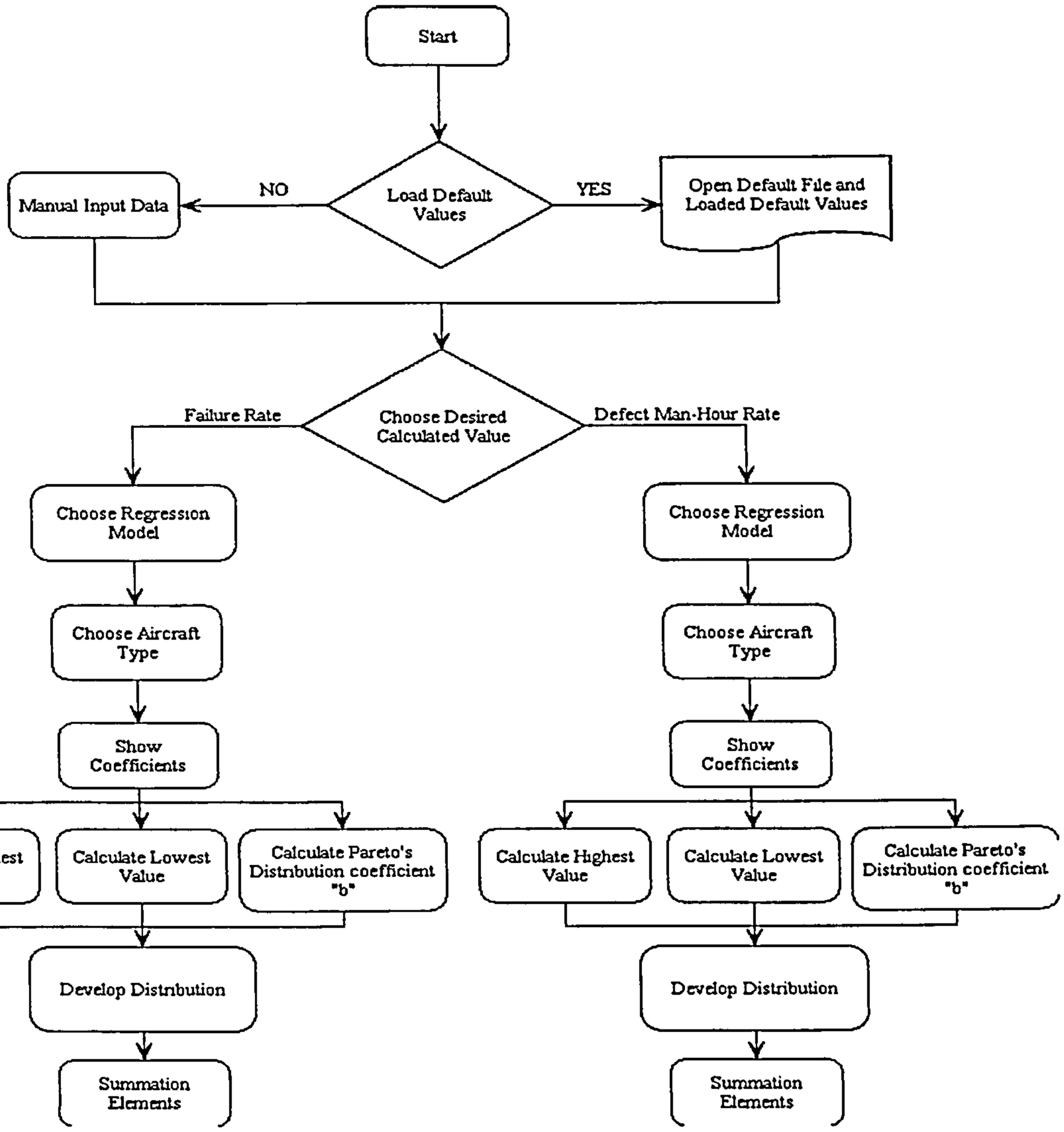

Figure C.1: Flowchart of reliability & maintainability assessment module

cover all aircraft types and generations as shown in Table C.1.

Table C.1: Linear equations to predict aircraft failure rate in each data set

Data in	Linear Equation
1985	$FR(W_e) = 0.0726 \cdot W_e + 0.268$
1987	$FR(W_e) = 0.0733 \cdot W_e - 0.0844$
1993	$FR(W_e) = 0.0870 \cdot W_e - 0.2776$
1996	$FR(W_e) = 0.1372 \cdot W_e - 0.7499$
All sets	$FR(W_e) = 0.0666 \cdot W_e + 0.0476$

C.1.2 Combination Model

As described in Chapter 4, this model contains following procedures (see Fig. C.1):

1. Determination of the highest and the lowest FR via linear regression or exponential

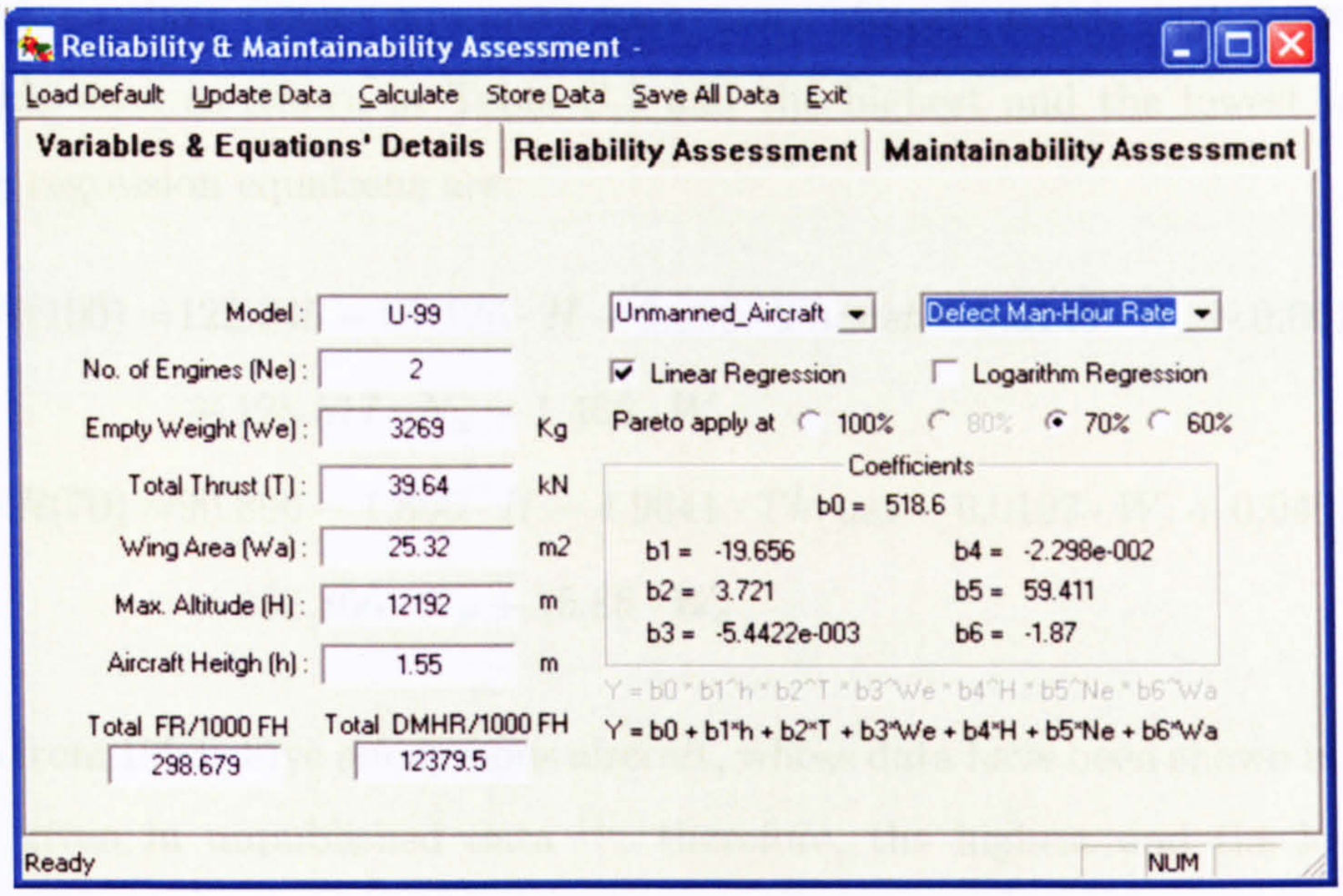

Figure C.2: Reliability & Maintainability assessment application dialog

regression.

2. Evaluation of the Pareto distribution b coefficient.

3. Determine the FR distribution values of the rest 60% aircraft systems.

4. Sum all aircraft system FR

C.1.2.1 Linear Regression Model

With this model, linear equations to evaluate the highest and the lowest failure rate from several variables by using the linear regression analysis. The six aircraft design variables are $Thrust$, W_e, H, Alt, N_E, and W_a.

Only two full details data sets with anonymous aircraft name were available (data in 1985 and 1993). The first reliability data set was collected in middle of 90's and based on the technology in that time, but the second data set was collected in early $20th$ century; therefore, both data sets could not directly used with each other without any TIF. Due to limit data and timescale, any development to integrate these two data sets could not be done in this research.

The linear equations to predict the highest and the lowest aircraft component failure rate can be here presented as follows:

1. Data from 1985: There were nine anonymous aircraft in this data set with design variable data as shown in Table C.2 and the highest and the lowest failure rate linear regression equations are:

$$FR(100) = 122.245 - 61.126 \cdot H + 2.299 \cdot Thrust + 0.0149 \cdot W_e + 0.00166 \cdot Alt + 125.517 \cdot N_E - 1.465 \cdot W_a \quad \text{(C.1)}$$

$$FR(70) = 90.896 - 1.806 \cdot H - 4.9641 \cdot Thrust - 0.0197 \cdot W_e + 0.04018 \cdot Alt - 232.866 \cdot N_E + 15.88 \cdot W_a \quad \text{(C.2)}$$

2. Data from 1993: Five anonymous aircraft, whose data have been shown in Table C.3, were given in unpublished data [4]; therefore, the highest and the lowest linear regression equations can be given:

$$FR(100) = 49.442 + 76.511 \cdot H - 30.247 \cdot Thrust - 0.082 \cdot W_e + 0.1962 \cdot Alt + 1633.004 \cdot N_E + 89.427 \cdot W_a \quad \text{(C.3)}$$

$$FR(70) = -196.905 - 16.280 \cdot H - 4.893 \cdot Thrust - 0.0245 \cdot W_e + 0.0465 \cdot Alt - 211.153 \cdot N_E + 17.958 \cdot W_a \quad \text{(C.4)}$$

Table C.2: Aircraft design variable from Serghides [38]

A/C	Thrust	Empty Weight	Height	Altitude	Engine	Wing Area	$FR(100)$	$FR(70)$
B1	355.83	2540.2	8.28	19800	4	370	464.55	74.253
F1	143.18	2650.0	5.97	18300	2	39	393.3	71.685
F2	186.82	3444.0	5.02	18300	2	49	471.48	57.394
A1	98.07	3565.0	4.95	12192	2	48	310.91	46.942
A2	64.94	3628.8	4.89	14000	2	24	248.86	38.251
ATR1	19.57	6387.0	2.69	14630	1	16	261.76	31.986
ATR2	24.03	7000.0	4.09	14630	1	17	99.048	20.455
F-104D	70.26	8978.0	4.11	17680	1	18.22	302.3	43.458
A-7D	63.40	10886.4	4.93	12192	1	34.83	236.95	37.868

Table C.3: Aircraft design variable from unpublished data [4]

A/C	Thrust	Empty Weight	Height	Altitude	Engine	Wing Area	$FR(100)$	$FR(70)$
GA1 Early	95.94	6139	3.63	15605	1	18.68	19.843	1.867
GA1 Late	95.6	7050	3.55	15240	1	21.37	117.98	13.767
T1	23.13	3635	4	15240	1	16.9	2225.7	364.705
GA2	46.8	7000	4.89	14000	2	24.18	75.65	13.581
GA3	80.96	14502	5.95	21335	2	26.6	162.02	29.415

C.1.2.2 Exponential Regression Model

This model is an alternative to predict the highest and the lowest failure rate by using exponential regression analysis. The same six design variables have been used to evaluate the $FR(100)$ and $FR(70)$, which can be given for two data sets as:

1. For data in 1985:

$$FR(100) = 52.93115866 \cdot 0.717544857^{H} \cdot 1.008068746^{Thrust} \cdot 1.000142602^{W_e} \cdot 1.000012109^{Alt} \cdot 3.132437067^{N_E} \cdot 0.991647611^{W_a} \quad \text{(C.5)}$$

$$FR(70) = 8.87061032 \cdot 0.994149478^{H} \cdot 1.004561319^{Thrust} \cdot 1.00005692^{W_e} \cdot 1.000017867^{Alt} \cdot 1.625167302^{N_E} \cdot 0.994925813^{W_a} \quad \text{(C.6)}$$

2. For data in 1993:

$$FR(100) = 9739866.727 \cdot 0.913310811^{Thrust} \cdot 1.000980832^{W_e} \cdot 7.201939508^{H} \cdot 0.999151797^{Alt} \cdot 0.0000954549^{N_E} \cdot 1.300577901^{W_a} \quad \text{(C.7)}$$

$$FR(70) = 11786500000 \cdot 26.3778653^{H} \cdot 0.90033209^{Thrust} \cdot 1.001602189^{W_e} \cdot 0.998460316^{Alt} \cdot 0.00000949137^{N_E} \cdot 1.078421347^{W_a} \quad \text{(C.8)}$$

C.1.2.3 Pareto Distribution Model

Because the fourth method of aircraft failure rate prediction is using Pareto principle to evaluate the whole aircraft failure rate; therefore, the real data of aircraft reliability has to be investigated and proved that it follows this principle as shown in Fig. C.3.

Fig. C.4 shows that the comparison between the real highest failure rate and the one from results of using Pareto distribution presentation. It shows that the Pareto distribution predicted highest failure rates are close to the original data. Hence, the highest and the lowest aircraft component failure rate from evaluated from Pareto distribution will represented the highest and the lowest failure rate of the real data to be used in development the linear regression the highest and the lowest failure rate equations. Consequently, Pareto distribution of each aircraft can be thus evaluated with the assumption that every aircraft obtains constant thirteen aircraft components as shown in Fig. C.5.

With the highest and the lowest FR, calculated by linear or exponential regression equations, the Pareto distribution b coefficient can be determined by using Eqn. (4.5). Table C.4 shows the Pareto distribution coefficients from example aircraft based on available

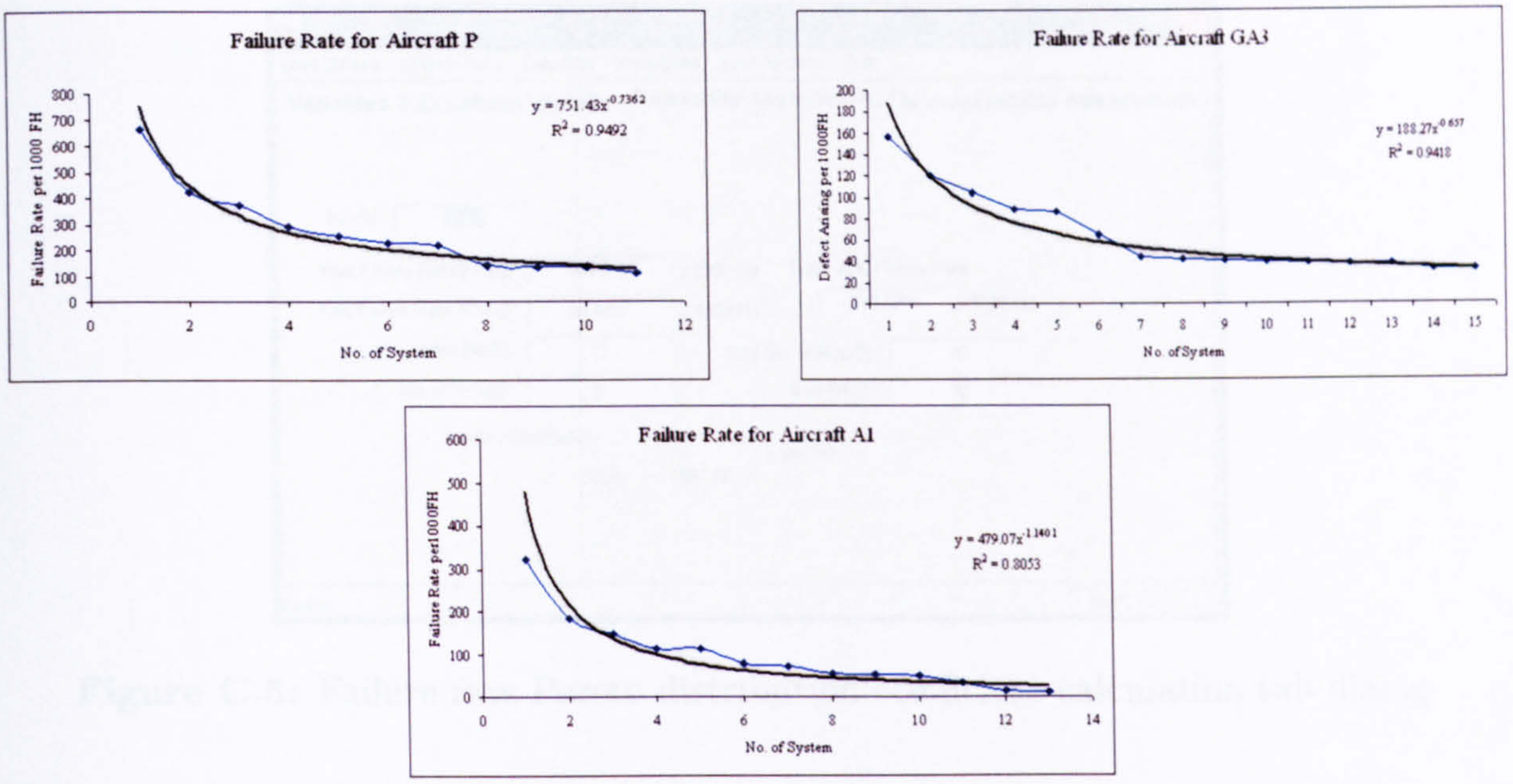

Figure C.3: Pareto distribution of real data in 1985, 1993, and 1996

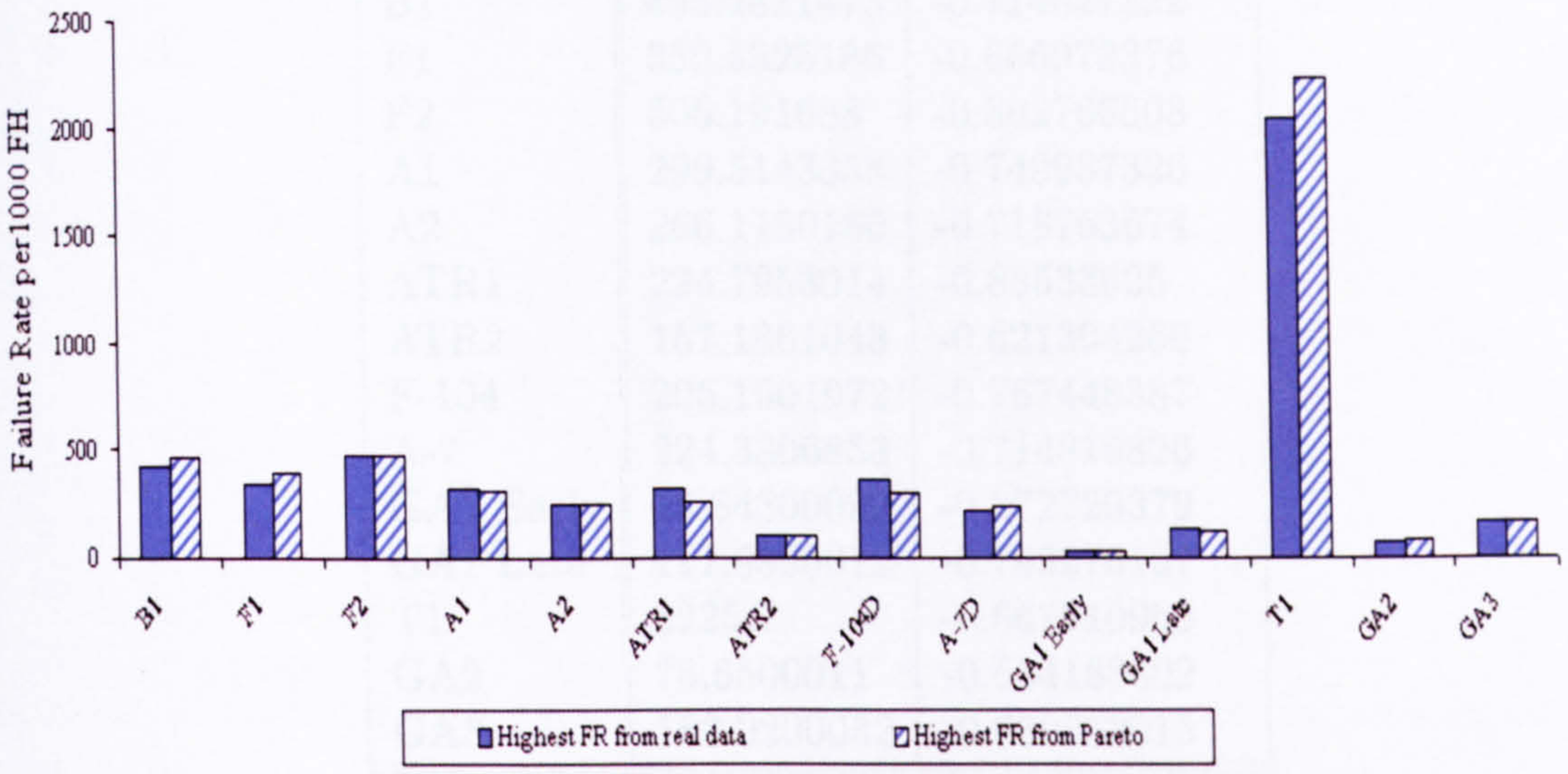

Figure C.4: Comparison between the highest failure rate from the real data and from the Pareto distribution representative

data.

Table C.5 shows the comparison between calculated results from the third and the forth failure rate prediction methods in this methodology and the real values.

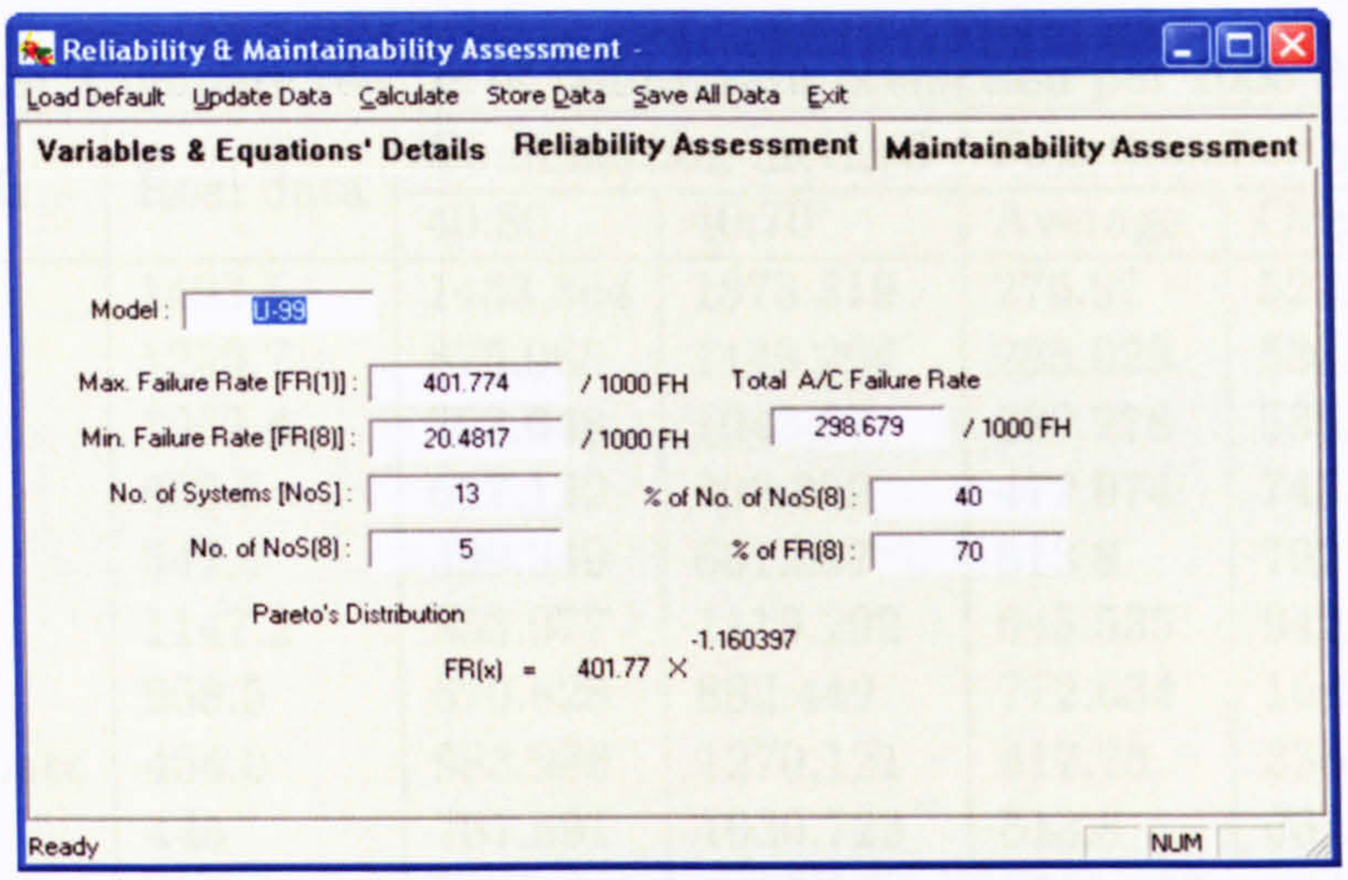

Figure C.5: Failure rate Pareto distribution coefficient calculation tab dialog

Table C.4: Failure rate Pareto distribution coefficients

Aircraft	Pareto distribution coefficient	
	$FR(100)$	b
B1	465.2821473	-0.714627222
F1	350.5325186	-0.666972376
F2	506.191688	-0.802766808
A1	299.5143338	-0.749937326
A2	266.1150186	-0.718763674
ATR1	224.7953014	-0.85533625
ATR2	157.1861043	-0.621304266
F-104	295.1601972	-0.767448387
A-7	224.3806853	-0.714819826
GA1 Early	19.84300092	-0.872729379
GA1 Late	117.9800012	-0.793275107
T1	2225.7	-0.667910969
GA2	75.6500011	-0.634183602
GA3	162.0200032	-0.630053015

C.2 Maintainability Assessment Module

Similar difficulties to an aircraft failure rate prediction, but there were much less available data to develop a certain prediction model; therefore, only a simple model as a function of aircraft empty weight is firstly examined. And the $DMHR$ equations from linear and exponential regression analysis of six design variables with assumption that an aircraft obtains thirteen component have been then developed, in which the combination method can be examined. Fig. C.6 shows the application tab dialog in this reliability & maintainability assessment module.

Table C.5: Compare results of failure rate prediction per 1000 flying hour

Aircraft	Real data	Combination method		Functionality method	
		40:80	40:70	Average	Original
F2	1493.5	1433.364	1873.319	276.97	521.744
A1	1250.7	875.968	1149.294	285.029	530.94
A2	1052.4	793.648	1043.67	289.278	535.7888
ATR1	832.8	617.122	808.302	472.974	745.4728
ATR2	547.4	499.349	661.507	513.8	792.00
F-104	1147.2	853.977	1119.292	645.535	942.328
A-7	958.5	670.828	882.449	772.634	1087.3664
GA1 Late	454.0	983.986	1270.121	517.73	335.75
GA2	445	787.591	1030.723	513.8	331.4
GA3	959	1145.412	1493.86	1013.433	984.074
F-16	420.0	873.134	1149.976	505.142	419.171
F-18	700	1532.18	1982.528	743.237	681.2185
F-4	850	1254.931	1626.063	968.716	923.9881
F-15	710	1278.09	1664.799	863.117	813.1585
F-105	680	887.399	1170.958	905.341	859.6307

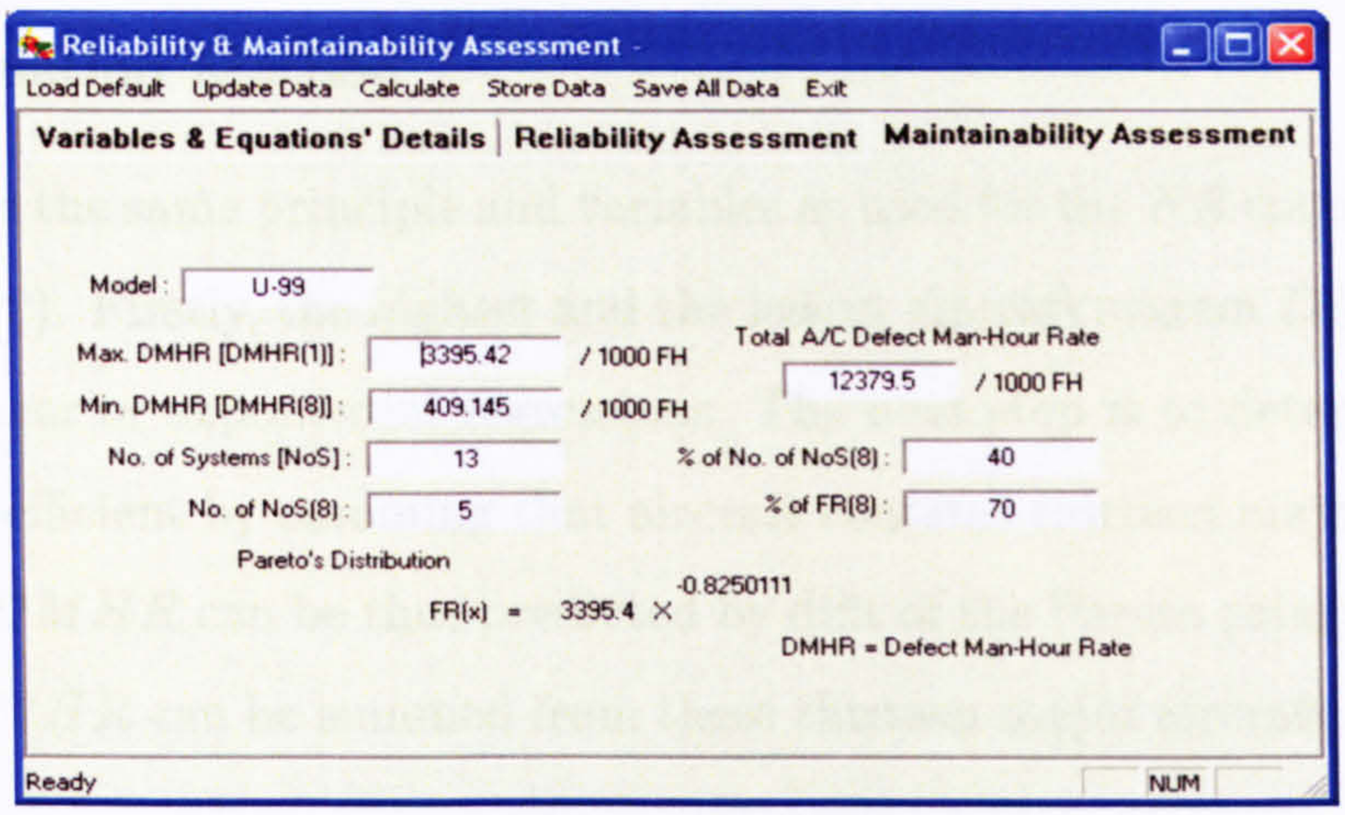

Figure C.6: Defect man-hour rate Pareto distribution coefficient calculation tab dialog

C.2.1 Functionality of Aircraft Empty Weight

There were very less maintainability data available than of reliability. Only two linear equations can be investigated, and be shown as in Fig. C.7.

Therefore, an average aircraft $DMHR$ per 1000 flying hour linear equation can be developed and shown as the following equations:

$$DMHR_{Aircraft} = 12221 - 0.8009 \cdot W_e \tag{C.9}$$

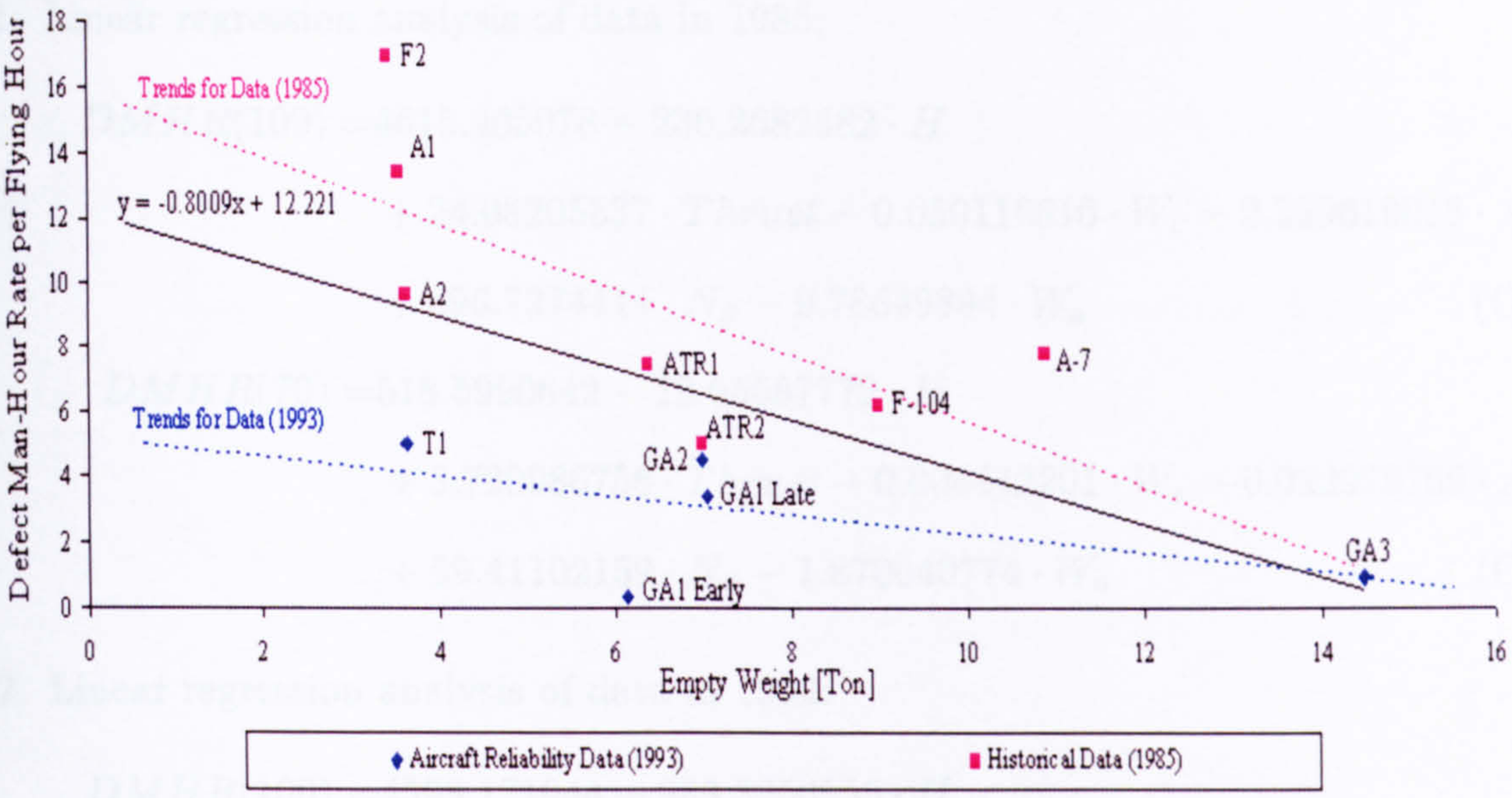

Figure C.7: Defect man-hour rate as a function of aircraft empty weight

C.2.2 Combination Method

This method uses the same principle and variables as used for the FR combination method (see Section C.1.2). Firstly, the highest and the lowest aircraft system $DMHR$ have to be evaluated via linear or exponential regressions. The next step is to determine the Pareto distribution b coefficient by assuming that aircraft contains thirteen major systems. Each aircraft system $DMHR$ can be thus predicted by dint of the Pareto principle. Finally, the total aircraft $DMHR$ can be summed from these thirteen major aircraft system $DMHR$.

C.2.2.1 Linear Regression Model

Similar as the highest and the lowest failure rate predictions, the only two data sets could not be used together due to different technology and aircraft types.

1. Linear regression analysis of data in 1985:

$$\begin{aligned} DMHR(100) =& 4615.405078 - 230.2682582 \cdot H \\ &+ 24.08205537 \cdot Thrust - 0.050116816 \cdot W_e - 0.229619018 \cdot Alt \\ &+ 696.7274414 \cdot N_E - 9.78649894 \cdot W_a \end{aligned} \tag{C.10}$$

$$\begin{aligned} DMHR(70) =& 518.5990642 - 19.65587772 \cdot H \\ &+ 3.720986756 \cdot Thrust - 0.005442201 \cdot W_e - 0.022979769 \cdot Alt \\ &+ 59.41102159 \cdot N_E - 1.870040774 \cdot W_a \end{aligned} \tag{C.11}$$

2. Linear regression analysis of data in 1993:

$$\begin{aligned} DMHR(100) =& 4598.171944 + 989.3250555 \cdot H \\ &- 20.55090072 \cdot Thrust + 0.441361581 \cdot W_e - 0.392431133 \cdot Alt \\ &- 2379.658742 \cdot N_E - 5.152069 \cdot W_a \end{aligned} \tag{C.12}$$

$$\begin{aligned} DMHR(70) =& 855.1331753 + 209.8118117 \cdot H \\ &- 3.350542173 \cdot Thrust + 0.080594332 \cdot W_e - 0.082597689 \cdot Alt \\ &- 492.851663 \cdot N_E + 0.372898482 \cdot W_a \end{aligned} \tag{C.13}$$

C.2.2.2 Exponential Regression Model

The exponential model can be also used to predicted the highest and the lowest $DMHR$ by using two available maintainability data sets as follows:

1. Exponential regression analysis of data in 1985:

$$\begin{aligned} DMHR(100) =& 8491.619193 \cdot 0.935621878^{H} \cdot 1.010783441^{Thrust} \cdot 0.999968623^{We} \\ &\cdot 0.999871213^{Alt} \cdot 1.290320816^{N_E} \cdot 0.99448234^{W_a} \end{aligned} \tag{C.14}$$

$$\begin{aligned} DMHR(70) =& 1010.2661880.944147718^{H} \cdot 1.010921795^{Thrust} \cdot 0.999976427^{We} \\ &\cdot 0.999899442^{Alt} \cdot 1.086936452^{N_E} \cdot 0.994702854^{W_a} \end{aligned} \tag{C.15}$$

2. Exponential regression analysis of data in 1993:

$$\begin{aligned} DMHR(100) =& 2147374.605 \cdot 12.00683986^{H} \cdot 0.956821917^{Thrust} \cdot 1.000883348^{We} \\ &\cdot 0.998972826^{Alt} \cdot 0.001303594^{N_E} \cdot 1.164114963^{W_a} \end{aligned} \tag{C.16}$$

$$\begin{aligned} DMHR(70) =& 293832.5362 \cdot 15.86936996^{H} \cdot 0.947961121^{Thrust} \cdot 1.000966956^{We} \\ &\cdot 0.99883298^{Alt} \cdot 0.000284034^{N_E} \cdot 1.355441031^{W_a} \end{aligned} \tag{C.17}$$

C.2.2.3 Pareto Distribution Model

Similar to reliability prediction, the real data of aircraft maintainability has to be investigated and proved that it follows this principle as shown in Fig. C.8.

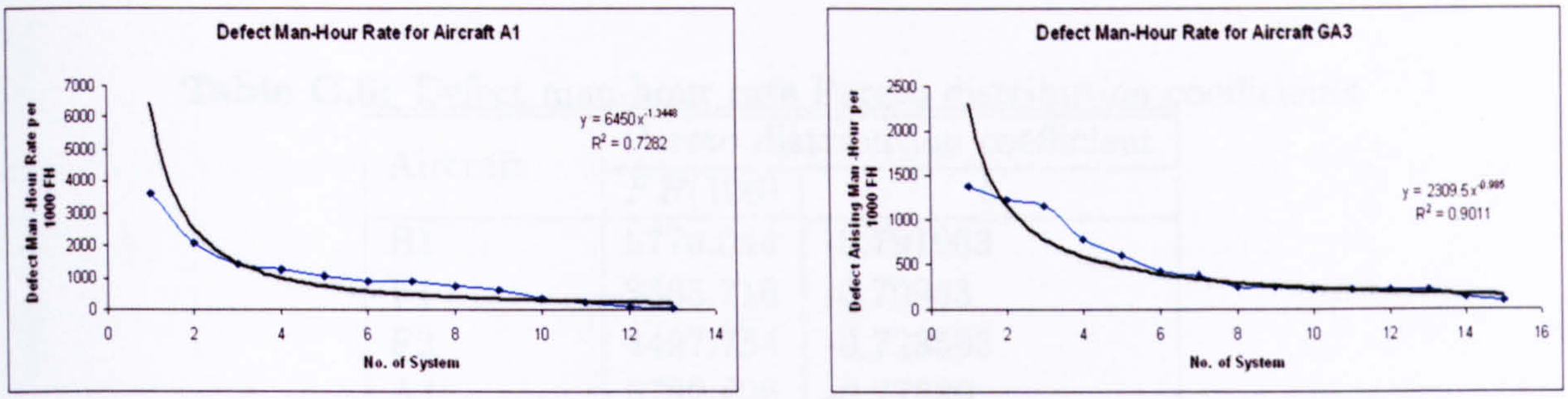

Figure C.8: Pareto distribution of real data in 1985 and 1993

As the same principle to predict aircraft failure rate, the highest defect man-hour rates of the real data have to be examined to confirm that the aircraft system $DMHR$ distribution follows the Pareto distribution (see Fig. C.8). From these two available data sets, the 40:70 portion has been discovered and be used as default in this methodology.

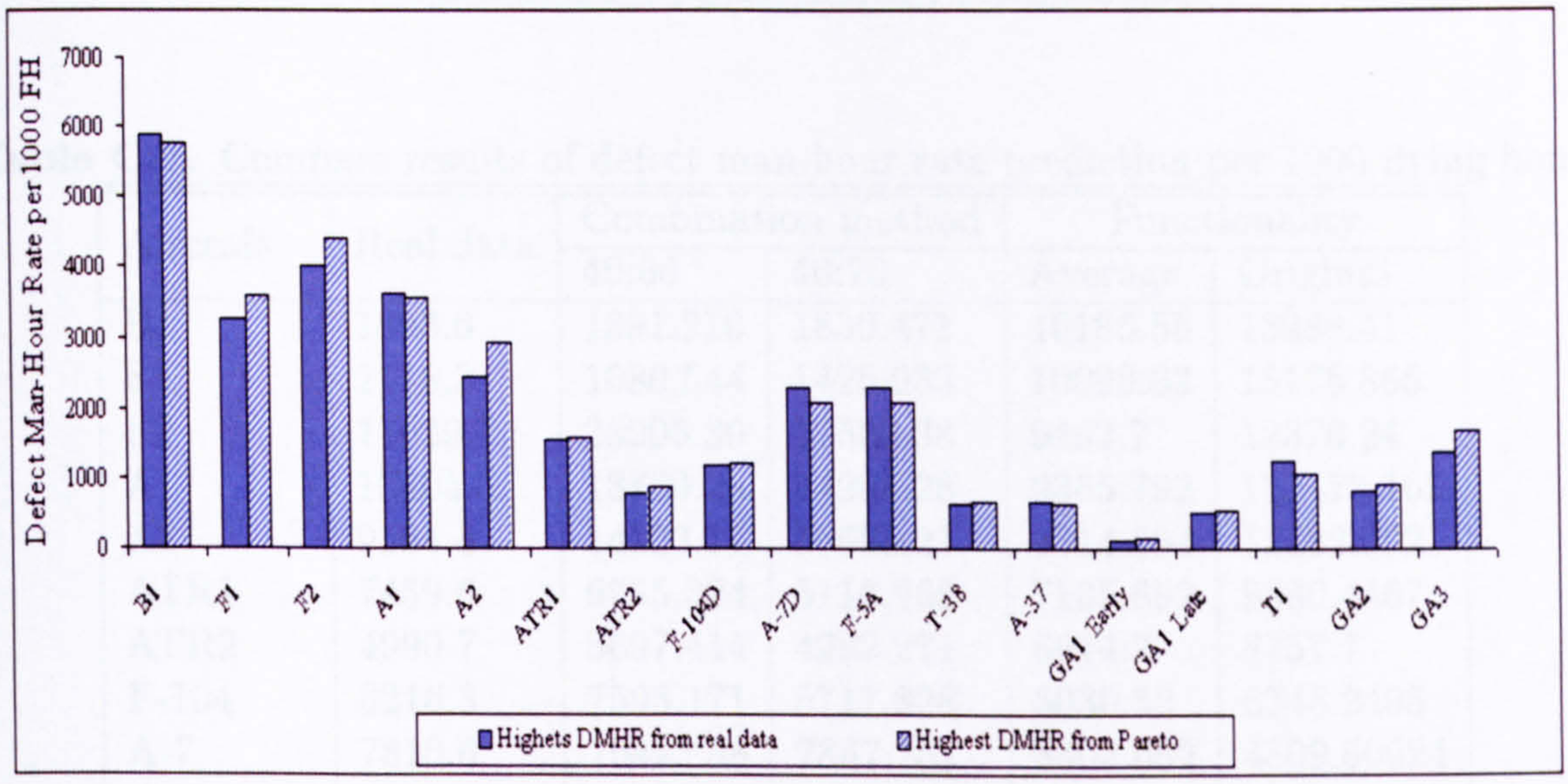

Figure C.9: Comparison between the highest defect man-hour rate from the real data and from the Pareto distribution representative

After the highest and the lowest aircraft system $DMHR$ have been determined, the Pareto distribution coefficients can be evaluated. Table C.6 shows the defect man-hour rate Pareto distribution coefficients of each aircraft. Finally, the total aircraft $DMHR$,

which is a summation of all assumed thirteen system $DMHR$ calculated from the Pareto distribution, can be calculated. Table C.7 shows the comparison between the total aircraft $DMHR$ calculated from the combination, functionality method and the two available real data.

Table C.6: Defect man-hour rate Pareto distribution coefficients

Aircraft	Pareto distribution coefficient	
	$FR(100)$	b
B1	5770.044	-0.791963
F1	3365.716	-0.70983
F2	4497.754	-0.723593
A1	3782.826	-0.77689
A2	2815.331	-0.76411
ATR1	1327.99	-7438
ATR2	1072.513	-0.69379
F-104	1396.812	-0.63395
A-7	2017.742	-0.7272
GA1 Early	2713.00	-0.7121
GA1 Late	2735.07	-0.7164
T1	1101.11	-0.6978
GA2	2207.76	-0.7648
GA3	702.41	-0.4843

Table C.7: Compare results of defect man-hour rate prediction per 1000 flying hour

Aircraft	Real data	Combination method		Functionality	
		40:60	40:70	Average	Original
B1	1893.6	1391.216	1830.471	10186.55	13288.41
F1	2118.3	1080.544	1426.933	10098.62	13176.865
F2	17029.7	23206.39	17580.38	9462.7	12370.24
A1	13405.5	18789.28	14289.28	9365.792	122473.165
A2	9584.4	14133.77	10695.21	9314.694	12182.502
ATR1	7459.6	6755.324	5118.266	7105.652	9380.4467
ATR2	4990.7	5697.414	4282.271	6614.7	8757.7
F-104	6216.3	7593.171	5711.828	5030.52	6748.2498
A-7	7810.6	10425.88	7867.151	3502.082	4809.50624
GA1 Late	3430	14183.74	10744.59	6574.655	3010.385
GA2	4500	11095.1	8384.3919	6614.7	3025.3
GA3	959	4435.54	3283.273	606.348	787.4534
T1	5040.0	5828.263	4383.341	9309.729	4029.0795

APPENDIX D

LIFE CYCLE COST ESTIMATION MODULE

This Appendix will show LCC estimation module and its model in details, which is based mostly on Woodford [53], Birkler [8] and Burns [11]. Some parts have been modified to make this model more simple and to avoid restricted and/or unavailable data. Fig. D.1 shows the overall outlook of the LCC estimation application dialog, which contains another five tap dialogs.

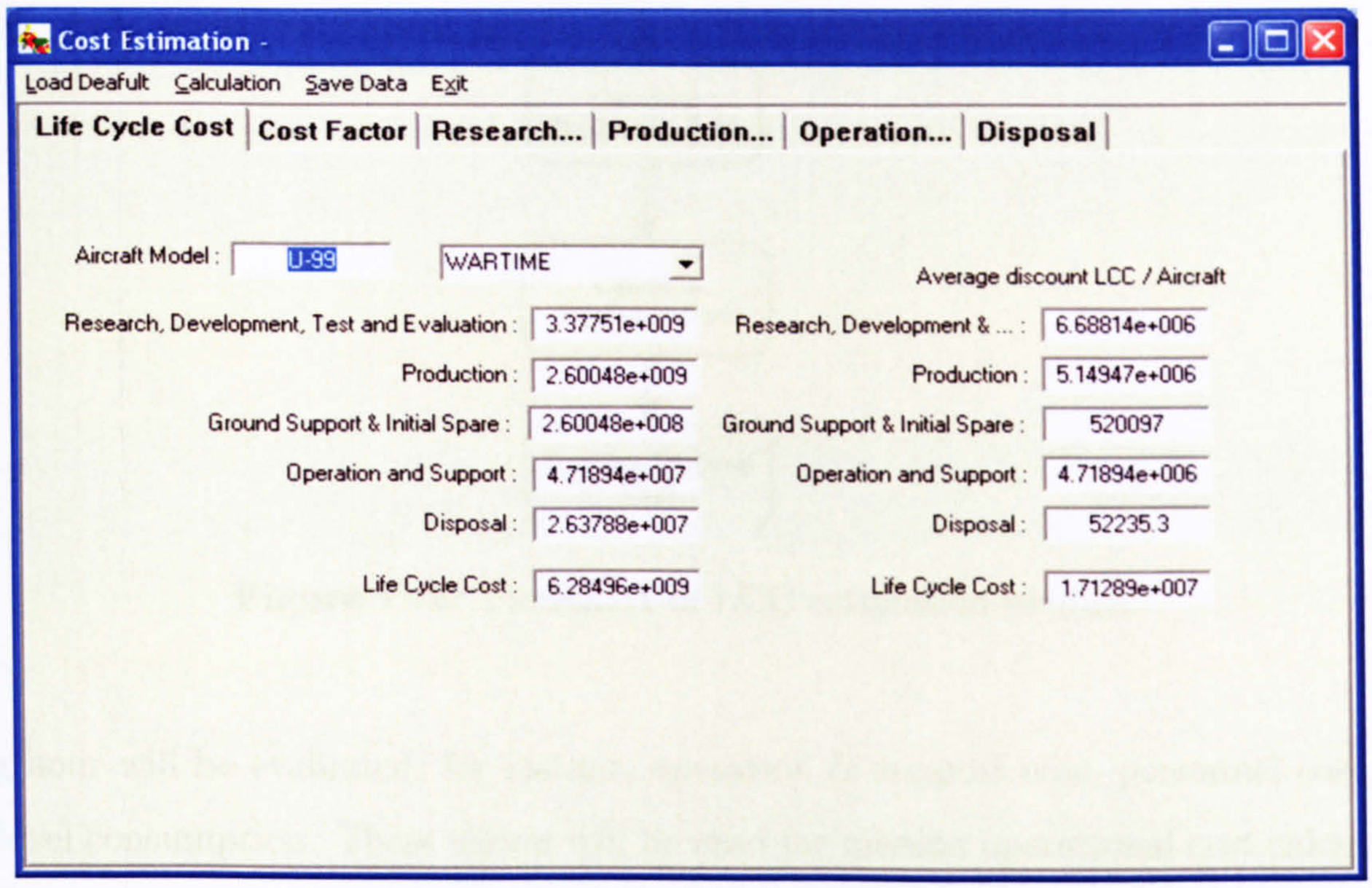

Figure D.1: Life Cycle Cost estimation application dialog

Similar to the other module, LCC estimation application dialog can load the default or pre-data directly from stored file or be given directly through the application dialog. Additionally, the pre-calculated unscheduled maintenance (DMHR) is automatically passed direct from the reliability & maintainability assessment module.

The next importance step is to choose mission scenario, in which an aircraft LCC will be evaluated. Then, the initial of the necessary parameter and variable can be done. Finally, after total aircraft LCC has been estimated, and the average costs per aircraft per

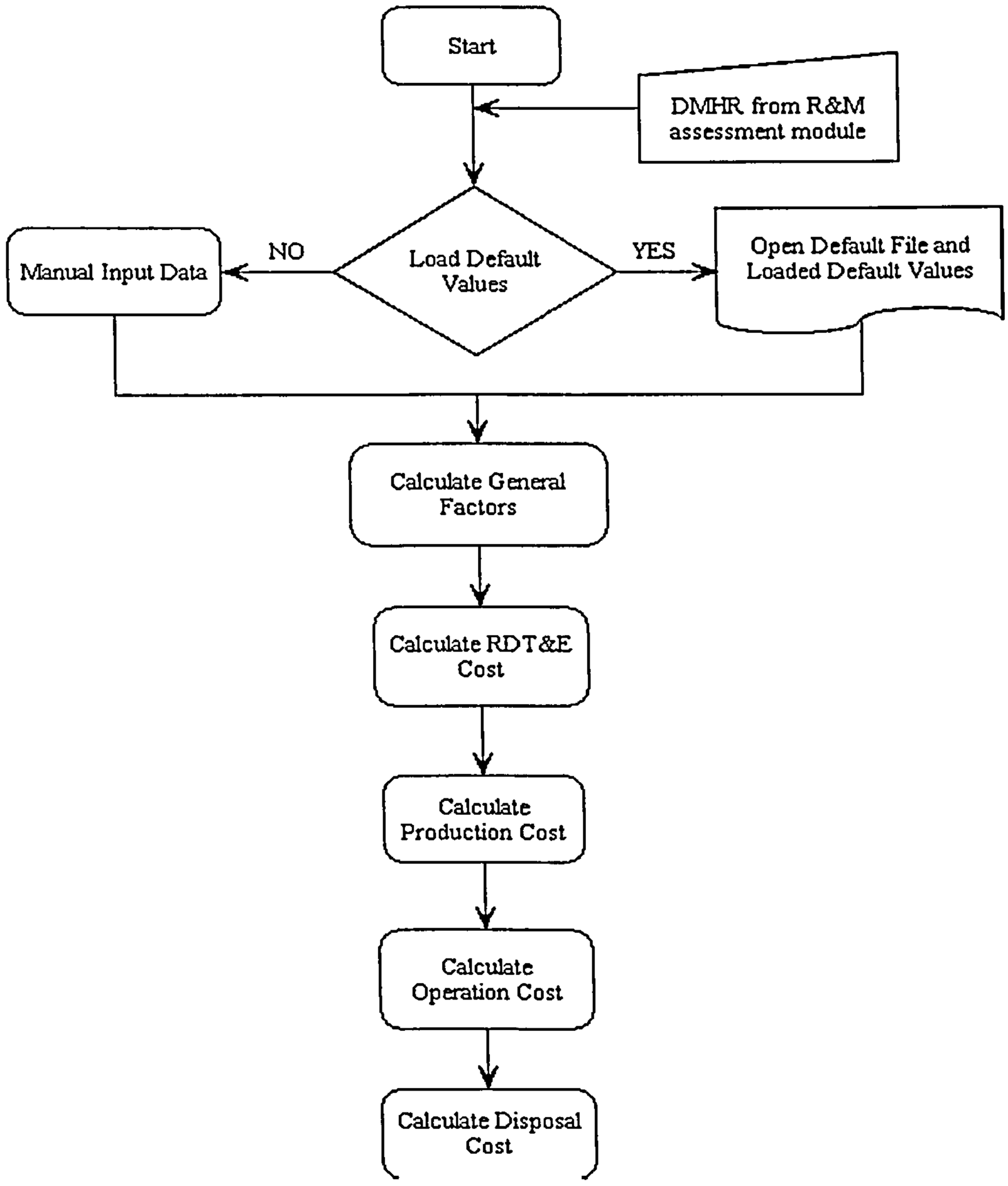

Figure D.2: Flowchart of LCC estimation module

flying hour will be evaluated; for instant, operation & support cost, personnel cost, and unit level consumption. These values will be used for mission operational cost calculation afterwards.

Fig. D.2 shows an overall flowchart of LCC estimation module. During the O&S cost estimation process, the O&S cost for wartime and peacetime operation will be separate calculated.

D.1 Parameter Initiate

Before the LCC can be evaluated, some global variables and assumed values have to be initiate. These values will be used in many different equations. These variables are:

1. Advanced technology factor: The advanced technology factor (FATF) value can be

estimated from a single equation presented by Woodford [53]. Unfortunately, his model is too details in design which excess this methodology; therefore, this value will be assumed as 1.275 throughout LCC estimation model.

2. Advanced design tool factor: This value is assumed as a constant value (FADT = 1.3) and is integrated mainly in RDT&E and production cost due to increasing usage of advanced composites and new technology.

3. Advanced technology testing factor: This factor is integrated aiming to cover flight test engineering planning, data reduction, manufacturing support, flight test instrumentation, spares, fuel and oil, pilot's salary, facility rental, and insurance during the flight test during the RDT&E process. This factor is assumed as constant variable (FATT = 1.2).

4. Number of partners: The number of partners is defined as the ratio of number of aircraft production to number of largest single buy from the program as:

$$NPART = \frac{N_{PROD}}{N_{LARGE}} \tag{D.1}$$

5. Airframe-only mass: This mass is equivalent to the airframe unit mass, and is defined by MIL-STD-1374. The airframe-only mass ($M_{Airframe}$) can be estimated as aircraft empty mass minus wheels, tires, tubes & brakes, engines, rubber or nylon fuel cells, starters and power unit, instruments, batteries & electrical power supply and conversion, avionics equipment, air conditioning, anti-icing & pressurisation units, cameras and other surveillance equipment, trapped fuel and oil.

6. Consumer Price index: This variable aims to include inflation within the cost of aircraft, which is a function of accounting year (YRACC) as shown in Eqn. (5.2).

7. Labour rates: The engineering (CLE), quality/tooling (CLT), and manufacturing labour rate (CLM) are based on 'then year' dollars, and can be given as following equations, which have an extra security factor (FS) built in [53].

$$CLE = (0.0191 \times YRACC^2 - 0.5432 \times YRACC - 37.964) \times FS \tag{D.2}$$

$$CLT = (0.0054 \times YRACC^2 + 1.0755 \times YRACC - 89.215) \times FS \tag{D.3}$$

$$CLM = (0.0132 \times YRACC^2 - 0.5627 \times YRACC - 13.679) \times FS \tag{D.4}$$

8. Advanced materials factor: This cost factor considers for using advanced materials (FAMA), which is a function of the percentage, by mass, of advanced materials used for structural application. This factor can be given as a function of aircraft empty mass.

$$FAMA = 4.4028 \times MAT^{4}_{Composite} - 5.7025 \times MAT^{3}_{Composite} + 2.8658 \times MAT^{2}_{Composite} + 0.3168 \times MAT_{Composite} + 1 \quad \text{(D.5)}$$

9. Collaborative factor: Woodford [53] developed a separate factor (FPART) to allow for the collaboration nature of modern aircraft programs with suggestion of Mr. P. Pugh, formerly of the Directorate of Project, Time, and Cost Analysis (DPTCAn), a division of the Ministry of Defence as:

$$FPART = NPART^{0.33} \quad \text{(D.6)}$$

10. Pay rates: Officer (OPR), Enlisted (EPR), and Civilian pay rate (CPR) are approximate average annual payment for U.S Air Force officer and engineer regarding to information from the open sources [33,34]. These rate have been set as default values as:

    - OPR = 50400 $
    - EPR = 22200 $
    - CPR = 42000 $

D.2 Research, Development, Test, & Evaluation Cost

This estimation model breaks the develop procedure into three major categories with several different activities. The total RDT&E cost is a summation of the multiples between the effort quantity in hours and its relevant labour rate.

D.2.1 Airframe Development Cost

Cost of airframe development can be broken down into following activities:

1. Engineering cost for the airframe development (CDAE)

$$CDAE = 0.066 \times M^{0.796}_{Airframe} \times V^{1.538}_{Max} \times N^{0.183}_{RDT\&E} \times FATF \times FAMA/FADT \times FPART \times CLE \quad \text{(D.7)}$$

2. Development support cost (CDDS)

$$CDDS = 0.0356 \times M_{Airframe}^{0.903} \times V_{Max}^{1.93} \times N_{RTD\&E}^{0.346} \times CPI \times FATF \times FS/FADT \times FPART \quad \text{(D.8)}$$

3. Flight test cost (CDFT)

$$CDFT = 0.00558 \times M_{Airframe}^{1.19} \times V_{Max}^{1.401} \times N_{RDT\&E}^{1.281} \times CPI \times FATT \times FS \quad \text{(D.9)}$$

4. Tooling cost (EDTP)

$$EDTP = 5.083 \times M_{Airframe}^{0.768} \times V_{Max}^{0.899} \times N_{RDT\&E}^{0.18} \times RATE^{0.066} \times FAMA/FADT^{0.5} \times FPART \times CLT \quad \text{(D.10)}$$

5. Development manufacturing cost (EDML)

$$EDML = 43.61 \times M_{Airframe}^{0.76} \times V_{Max}^{0.549} \times N_{RDT\&E}^{0.554} \times FAMA/FADT^{0.5} \times FPART \times CLM \quad \text{(D.11)}$$

6. Quality control cost (CDQL)

$$CDQL = 0.13 \times CDML \times CLT/CLM \quad \text{(D.12)}$$

7. Manufacturing material and equipment cost (CDMME)

$$CDMME = 96.77 \times M_{Airframe}^{0.692} \times V_{Max}^{0.639} \times N_{RTD\&E}^{0.803} \times CPI \times FAMA \times FLO \quad \text{(D.13)}$$

Total cost for development airframe ($CD_{Airframe}$) is a summation of above labour costs as:

$$CD_{Airframe} = CDAE + CDDS + CDFT + CDTP + CDML + CDQL + CDMME \quad \text{(D.14)}$$

D.2.2 Engine development cost

Woodford [53] explained that the constant 0.833 and 1.0E6 are added into model from Birkler [8] due to CPI value in 1980. Regarding to CPI value from The United States Bureau of Labour Statistics web site [49], the constant value 0.833 has been replaced by 0.842.

$$CDE = \left(\frac{-845.804 + 0.00002244 \times Thrust + 249.838 \times M + 0.313 \times TT4}{0.6 \times 0.8421 \times FADT} \times CPI \times FPART \times 1.0E6\right) \quad \text{(D.15)}$$

$$CDEF = 0.77 \times CPE \times (N_{RDT\&E} - N_{STAT}) \times (N_E + 1) \quad \text{(D.16)}$$

$$CD_{Engine} = CDE + CDEF \quad \text{(D.17)}$$

where M become 1 if an aircraft is not designed for supersonic vehicle.

D.2.3 Avionics development cost

This model to estimate avionics cost is based on the uninstalled avionics mass, which is approximated 90% of the total avionics mass, as follows:

$$CDV = 853820 \times WV \times FPART \times CPI \quad \text{(D.18)}$$

$$CDVF = 3950 \times WV \times (N_{RDT\&E} - N_{STAT}) \times CPI \quad \text{(D.19)}$$

$$CD_{Avionics} = CDV + CDVF \quad \text{(D.20)}$$

Total RDT&E cost is a summation of these three development costs as:

$$C_{RDT\&E} = CD_{Airframe} + CD_{Engine} + CD_{Avionics} \quad \text{(D.21)}$$

D.3 Production Cost

Similar to RDT&E cost, the production can be split into three main groups; airframe, engine, and avionics production. The summation of all three main component production costs brings to the total aircraft production cost.

D.3.1 Airframe Production Cost

During the production processes, the following activities and costs can be occurred. These can be estimated as:

1. Production engineering cost for the airframe development (CPAE)

$$CPAE = \Big[0.066 \times M_{Airframe}^{0.796} \times V_{Max}^{1.538} \times (N_{RDT\&E} + N_{PROD})^{0.183} \times FATF \times FAMA/FADT \times FPART \times CLE\Big] - CDAE \quad \text{(D.22)}$$

2. Production tooling cost (EPTP)

$$EPTP = \Big[5.083 \times M_{Airframe}^{0.768} \times V_{Max}^{0.899} \times (N_{RDT\&E} + N_{PROD})^{0.18} \times RATE^{0.066} \times FAMA/FADT^{0.5} \times FPART \times CLT\Big] - EDTP \quad \text{(D.23)}$$

3. Production manufacturing cost (EPML)

$$EPML = \Big[43.61 \times M_{Airframe}^{0.76} \times V_{Max}^{0.549} \times (N_{RDT\&E} + N_{PROD})^{0.554} \times FAMA/FADT^{0.5} \times FPART\Big] - EDML \quad \text{(D.24)}$$

4. Production quality control cost (CPQL)

$$CDQL = 0.13 \times CPML \times CLT/CLM \quad \text{(D.25)}$$

5. Production manufacturing material and equipment cost (CPMME)

$$CPMME = \Big[96.77 \times M_{Airframe}^{0.692} \times V_{Max}^{0.639} \times (N_{RTD\&E} + N_{PROD})^{0.803} \times CPI \times FAMA \times FLO\Big] - CDMME \quad \text{(D.26)}$$

D.3.2 Engine Production Cost

The engine production cost (CPE) is based on the aircraft turbine engine production cost developed by Birkler [8] and multiply by the effect of CPI value of year 1980, when this model has been developed, and CPI of aircraft design accounting year. Therefore, the total engine production costs (CP_{Engine}) can be given as:

$$CPE = \left(\frac{0.043 \times Thrust + 243.25 \times M + 0.969 \times TT4 - 2228}{0.8421}\right) \times CPI \times 1E6 \quad \text{(D.27)}$$

$$CP_{Engine} = CPE \times N_{PROD} \times N_E \quad \text{(D.28)}$$

D.3.3 Avionics Production Cost

The avionics production cost ($CP_{Avionics}$) is given as:

$$CP_{Avionics} = 3950 \times WV \times CPI \times N_{PROD} \tag{D.29}$$

Total production cost ($C_{Production}$) is then a summation of these three total production costs:

$$C_{Production} = CP_{Airframe} + CP_{Engine} + CP_{Avionics} \tag{D.30}$$

To estimate the trade value of the design aircraft, flyaway ($C_{Flyaway}$) and acquisition cost ($C_{Acquisition}$) will be evaluated as:

$$C_{Flyaway} = \frac{C_{Production}}{N_{PROD}} \tag{D.31}$$

$$C_{Acquisition} = \frac{C_{RDT\&E} + C_{Production}}{N_{RDT\&E} + N_{PROD}} \tag{D.32}$$

D.4 Ground Support Equipment and Initial Spares

The GSE&IS cost is about 10% of the aircraft flyaway cost, as described in chapter 5.

$$C_{GSE\&IS} = 0.1 \times C_{Flyaway} \tag{D.33}$$

D.5 Operation and Support

The operation and support cost ($C_{Operation}$) breakdown follows the methods and structure by the US Office of the Secretary of Defense [12] This O&S cost is estimated for one main operating base only; therefore, the cost for the individual aircraft contains the total deflated O&S cost divided by the number of aircraft on the base.

D.5.1 Personnel Cost

The personnel cost includes all expense for operation personnel, support personnel, and also service allowances, personnel support and training.

D.5.1.1 Operation Personnel Cost

Operation personnel cost (COM) is a summation of number of office, enlisted, and civilian in the first and second line operation multiply with their relevant annual payment rate as:

1. Number of active flight-crew member (NOMOF):

$$NOMOF = 0.923 \times FMOF \times N_{Operation} \tag{D.34}$$

where FMOF is the 'crew-ratio' (1.1 for fighter, 1.5 for bomber, 1.5 - 3.5 for transport).

2. Number of operation officer (NOMO):

$$NOMO = \left(0.40799 + 0.923 \times FMOF + FHY \times DMHR \times 6.708E-5\right) \times N_{Operation} + 3.0 \tag{D.35}$$

3. Number of operation enlisted (NOME):

$$NOME = \left(3.7246 + \frac{FHY \times SM}{301.5075} + \frac{FHY \times DMHR}{208.695622}\right) \times N_{Operation} \tag{D.36}$$

4. Number of operation civilian (NOMC):

$$NOMC = 0.0577 \times \left(1.67 + \frac{FHY \times DMHR}{208.695622}\right) \times N_{Operation} \tag{D.37}$$

5. Total number of operation personnel (NOM):

$$NOM = NOMO + NOME + NOMC \tag{D.38}$$

6. Total operation personnel cost (COM):

$$COM = NOMO \times OPR + NOME \times EPR + NOMC \times CPR \tag{D.39}$$

D.5.1.2 Support Personnel Cost

Support personnel cost (CSM) depends on number of operation aircraft and operation personnel on the base.

1. Number of support office (NSMO):

$$NSMO = 7.0 + 0.6155 \times N_{Operation} + 0.0555 \times NOMOF + 0.00837 \times NOM \tag{D.40}$$

2. Number of support enlisted (NSME):

$$NSME = 16.0 + 5.8974 \times N_{Operation} + 0.0921 \times NOM \tag{D.41}$$

3. Number of support civilian (NSMC):

$$NSMC = 0.02222 \times NOMOF + 0.0705 \times NOM \tag{D.42}$$

4. Total support personnel cost (CSM):

$$CSM = NSMO \times OPR + NSME \times EPR + NSMC \times CPR \tag{D.43}$$

D.5.1.3 Service Allowance, Personnel Support and Training Cost

This service allowance, personnel support and training cost (CSASTT) model aims to obtain all officer and enlisted training cost; training funds; and officer and enlisted permanent change of station.

1. Officer training cost (CSOT):

$$\begin{aligned} CSOT =& (0.0643 \times NOMO + 0.0028 \times NOM + 0.0001 \times NOME) \\ & \times OPR \end{aligned} \tag{D.44}$$

2. Enlisted training cost (CSET):

$$\begin{aligned} CSET =& (0.1294 \times NOME + 0.0232 \times NOM + 0.0077 \times NOMO) \\ & \times EPR \end{aligned} \tag{D.45}$$

3. Training funds (CSTF):

$$\begin{aligned} CSTF =& (0.0042 \times NOME + 0.052 \times NOMO + 0.1128 \times NOM) \times \\ & \frac{CPI}{0.739 \times 10^{-4}} \end{aligned} \tag{D.46}$$

4. Officer permanent change station cost (CSOPCS):

$$CSOPCS = 1795 \times \frac{CPI}{1.5884} \times (NOMO + NSMO) \tag{D.47}$$

5. Enlisted permanent change station cost (CSEPCS):

$$CSEPCS = 940 \times \frac{CPI}{1.5884} \times (NOME + NSME) \tag{D.48}$$

6. Total service allowance, personnel support and training cost (CSASTT):

$$CSASTT = CSOT + CSET + CSTF + CSOPCS + CSEPCS \tag{D.49}$$

D.5.2 Unit level consumption

Woodford [53] modified this model from the US Navy O&S cost estimating model FY-1979 with RAF Cost of support spreadsheet. This model can be split as follows:

1. Cost of Fuel, other petroleum, oil, and lubricants (COF):

$$COF = 1.213588 \times M_{Fuel} \times \frac{FHY}{T_{Sortie}} \times C_{Fuel} \times N_{Operation} \tag{D.50}$$

2. Maintenance material cost (COMMAT):

$$\begin{aligned} COMMAT =& (6.9313 + 0.1028 \times \frac{FHY}{12} \times (SM + DMHR) + 0.145 \times V_{Max}) \\ & \times 1.27199 \times FHY \times CPI \times N_{Operation} \end{aligned} \tag{D.51}$$

3. Miscellaneous support supply cost (COMSS): This cost is about 53.19 % of maintenance material cost (COMMAT).

$$COMSS = 0.5319 \times COMMAT \tag{D.52}$$

4. Depot level reparable cost (CODLR):

$$CODLR = 5.751 \times (SM + DMHR)^{1.2234} \times V_{Max}^{0.2486} \times FHY \times CPI \tag{D.53}$$

5. Temporary additional duty cost (COTAD):

$$COTAD = 6925.2077 \times N_{Operation} \times CPI \tag{D.54}$$

6. Transport cost (COUTRN): This cost is approximately 3.79 % of total above costs.

$$\begin{aligned} COUTRN =& (COF + COMMAT + COMSS + CODLR + COTAD) \\ & \times 0.0379 \end{aligned} \tag{D.55}$$

7. Other cost (COUOTH): This cost can be approximately estimated as 25 % of total unit level consumption cost until here.

$$\begin{aligned} COUTH =& 0.25 \times (COUTRN + COF + COMMAT + COMSS + \\ & CODLR + COTAD) \end{aligned} \tag{D.56}$$

8. Total unit level consumption cost (C_{Unit}): The C_{Unit} is simple a summation of all above described costs;

$$\begin{aligned} C_{Unit} =& COF + COMMAT + COMSS + CODLR + \\ & COTAD + COUTRN + COUOTH \end{aligned} \tag{D.57}$$

D.5.3 Contracts

Model from Woodford [53] defined this cost for the third and the forth line maintenance following structure of RAF and can be split into four main costs as:

1. Mechanical contract cost (COAC):

$$\begin{aligned} COAC =& \Big[(-9.7977 + 0.52085 \times (SM + DMHR) + 1.1902 \times M_{A/C} \times 2.2046E - 3) \\ & \times 1000 \times \frac{FHY}{160} \times N_{Operation} + (32.30965 + 7.688 \times (SM + DMHR)) \\ & \times FHY \times N_{Operation}\Big] \times \frac{CPI}{0.793} \end{aligned} \tag{D.58}$$

2. Engine contract cost (COEC):

$$\begin{aligned} COEC =& 1.9^{(N_E - 1)} \times \frac{(FRROR \times ERO) + ERM}{(1 + FPROR) \times DAR} \times 1000 \times \frac{CPI}{0.793} \\ & \times N_{Operation} \times FHY \end{aligned} \tag{D.59}$$

$$ERO = 5.574 + 4.527 \times Thrust + 70.71 \times FD \tag{D.60}$$

$$ERM = 8.9434 + 1.235 \times Thrust + 11.321 \times FD \tag{D.61}$$

where ERO is unit cost for an engine overhaul, ERM is unit cost for engine repair, FD = 1 if engine bypass ratio > 0, unless FD = 0, FPROR is the overhaul/repair ratio (here is assumed to be 0.4), and DAR is the depot arrival rate in operating hour (assumed to be 250 hours)

3. Avionics contract cost (COVC):

$$COVC = 0.5 \times N_{Operation} \times WV \times CPI \times FHY \tag{D.62}$$

4. Supply contract cost (COCT):

$$\begin{aligned} COCS =& (COF + COMMAT + COMSS + CODLR + COAC + COEC) \\ & \times 0.5 \end{aligned} \tag{D.63}$$

5. Total contract cost ($C_{Contract}$):

$$C_{Contract} = COAC + COEC + COVC + COSC \tag{D.64}$$

D.5.4 Sustaining Support Cost and Installation Support Funds

Woodford [53] showed that cost of replacement support equipment and modification kit procurement (CSEK) are approximate 0.55% of total flyaway cost of operating base. But the sustaining engineering support cost (CSSE) depends on labour, material and overhead costs. Therefore, the installation support funds (CSISF) are incurred by the personnel pay and allowances, material, and utilities needed for the maintenance of the base.

$$CSEK = 0.0055 \times C_{Flyaway} \times N_{Operation} \tag{D.65}$$

$$CSSE = 0.2396 \times CODLR + 0.098 \times (COAC + COEC) + 0.123 \times (COF + COMMAT + COMSS) - COSC - COUTRN \tag{D.66}$$

$$CSISF = 3565 \times \frac{CPI}{1.5884} \times NOSM \tag{D.67}$$

$$CSST = CSEK + CSSE + CSISF \tag{D.68}$$

Total O&S cost for one year is simply a sum of all of the precious calculated costs. As the aircraft will be operated for certain year; the 'discounted' value must be added for each year to reach the true total O&S cost.

$$C_{Operation\ 1\ year} = COSM + CSASTT + COULCT + COCT + CSST \tag{D.69}$$

$$C_{Operation} = C_{Operation\ 1\ year} \times \frac{1 - DEF}{RED} \tag{D.70}$$

where DEF can be calculated from Eqn. (5.8) and RED is economic discount rate (default value as 6% details see chapter 5).

D.6 Disposal

Woodford [53] developed a model to estimate disposal cost (CJT) based on material price in FY83 and validate with CPI factor; however, the final disposal cost is deflated following aircraft life time. Hence the deflated disposal cost ($C_{Disposal}$) can be given as:

$$CJM = 0.05 \times EPML \tag{D.71}$$

$$CJA = -5 \times (N_{PROD} + N_{RDT\&E}) \times (1 - MAT_{Composite}) \times W_e \times CPI \tag{D.72}$$

$$CJMAT = (N_{PORD} + N_{RDT\&E}) \times MAT_{Composite} \times W_e \times 27.86567 \times CPI \tag{D.73}$$

$$CJT = CJM + CJMAT + CJA \tag{D.74}$$

$$C_{Disposal} = CJT \times DEF \tag{D.75}$$

D.7 Life Cycle Cost

In this module, the total life cycle cost can be simply calculated as a summation of the different cost phases already calculated, apportioned to different number of aircraft, depending on the life cycle phase as:

$$LCC = \frac{C_{RDT\&E} + C_{Production}}{N_{RDT\&E} + N_{PROD}} + \frac{C_{GSE\&IS}}{N_{PROD}} + \frac{C_{Operation}}{N_{Operation}} + \frac{C_{Disposal}}{N_{RDT\&E} + N_{PROD}} \quad \text{(D.76)}$$

Figure D.7 - D.7 show the results of LCC estimation module for F-16 and Eurofighter during wartime and peacetime operation by using most values from Woodford [53] with some validated value from open sources; such as payment rates, CPI factor.

Aircraft Name : F-16 in PEACE TIME

Airframe Mass	5376.60	Kg	Uninst. Avionic Mass	512.42	Kg	Aircraft Mass	8645.65	Kg	Fuel Mass	1441.42	Kg
Max. Thrust	105.51	kN	Max. Velocity	2116.62	Km/h	Max. Mach	2.00		Max. Inlet-Temperature	1754.94	K
Adv. Materials	1.720	%	Disposal Labour	5.000	%	Economic Discount	6.00	%	Account Year	2000	
Year Entry Service	1977		Develop Aircraft	8		Static Aircraft	2		Test Aircraft	6	
Production Aircraft	3763		Operation Aircraft	150		Aircraft Crew	1		Annual Flying	320.00	Hrs
Life Time	20.00	Years									
Development			Production			Operation & Support			Disposal		
Airframe	2719.622	M$	Airframe	29680.906	M$	Personnel	190.137	M$	Advanced Materials	0.016	M$
Avionic	1671.384	M$	Avionic	28310.688	M$	Service Training	29.494	M$	Composite Materials	-370.335	M$
Engine	2345.629	M$	Engine	17624.297	M$	Contract	126.857	M$	Labour	787.897	M$
Software	1741.300	M$	Unit & Flyaway	20.095	M$	Install Support	16.052	M$			
						Unit Level	49.632	M$			
						Sustain Support	24.064	M$			
Total	8477.935	M$	Total	75615.887	M$	Total	436.236	M$	Total	417.578	M$
			Ground Support	7561.589	M$	Total 20.00 Yr	5003.591	M$	Deflated Disposal	130.203	M$
Total LCC			Discount LCC/AC			Cost/AC/FH					
RDT&E	8477.935	M$		2.248	M$	Personnel	2271.723	$			
Production	75615.887	M$		20.052	M$	Contract	575.466	$			
Ground Support	7561.589	M$		2.009	M$	Unit Level	592.991	$			
Operation	5003.591	M$		33.357	M$	Ground	313.978	$			
Disposal	130.203	M$		0.035	M$	Operation	5212.074	$			
Total	96789.205	M$		57.701	M$	Fly Away	20.095	M$			

Figure D.3: Result of F-16 LCC estimation in peacetime scenario

Aircraft Name : F-16 in WAR TIME

Airframe Mass	5376.60	Kg	Uninst. Avionic Mass	512.42	Kg	Aircraft Mass	8645.65	Kg	Fuel Mass	1441.42	Kg
Max. Thrust	105.51	kN	Max. Velocity	2116.62	Km/h	Max. Mach	2.00		Max. Inlet-Temperature	1754.94	K
Adv. Materials	1.720	%	Disposal Labour	5.000	%	Economic Discount	6.00	%	Account Year	2000	
Year Entry Service	1977		Develop Aircraft	8		Static Aircraft	2		Test Aircraft	6	
Production Aircraft	3763		Operation Aircraft	150		Aircraft Crew	1		Annual Flying	320.00	Hrs
Life Time	20.00	Years									
Development			Production			Operation & Support			Disposal		
Airframe	2719.622	M$	Airframe	29680.906	M$	Personnel	151.990	M$	Advanced Materials	0.016	M$
Avionic	1671.384	M$	Avionic	28310.688	M$	Service Training	24.050	M$	Composite Materials	-370.335	M$
Engine	2345.629	M$	Engine	17624.297	M$	Contract	0.000	M$	Labour	787.897	M$
Software	1741.300	M$	Unit & Flyaway	20.095	M$	Install Support	12.921	M$			
						Unit Level	42.556	M$			
						Sustain Support	20.576	M$			
Total	8477.935	M$	Total	75615.887	M$	Total	252.094	M$	Total	417.578	M$
			Ground Support	7561.589	M$	Total 20.00 Yr	2891.495	M$	Deflated Disposal	130.203	M$
Total LCC			Discount LCC/AC			Cost/AC/FH					
RDT&E	8477.935	M$		2.248	M$	Personnel	1815.956	$			
Production	75615.887	M$		20.052	M$	Contract	490.927	$			
Ground Support	7561.589	M$		2.009	M$	Unit Level	508.453	$			
Operation	2891.495	M$		19.277	M$	Ground	313.978 $				
Disposal	130.203	M$		0.035	M$	Operation	3011.974 $				
Total	94677.109	M$		43.621	M$	Fly Away	20.095	M$			

Figure D.4: Result of F-16 LCC estimation in wartime scenario

Aircraft Name : Eurofighter in PEACE TIME

Airframe Mass	5545.42	Kg	Uninst. Avionic Mass	724.47	Kg	Aircraft Mass	10073.35	Kg	Fuel Mass	2133.10	kg
Max. Thrust	179.85	kN	Max. Velocity	2116.62	Km/h	Max. Mach	2.00		Max. Inlet-Temperature	1829.93	K
Adv. Materials	33.680	%	Disposal Labour	5.000	%	Economic Discount	6.000	%	Account Year	2000	
Year Entry Service	1996		Develop Aircraft	9		Static Aircraft	2		Test Aircraft	7	
Production Aircraft	620		Operation Aircraft	39		Aircraft Crew	1		Annual Flying	300.00	Hrs
Life Time	25.00	Years									
Development			Production			Operation & Support			Disposal		
Airframe	5147.831	M$	Airframe	17616.028	M$	Personnel	45.918	M$	Advanced Materials	0.055	M$
Avionic	3254.535	M$	Avionic	6594.837	M$	Service Training	6.828	M$	Composite Materials	-42.993	M$
Engine	3265.192	M$	Engine	7916.164	M$	Contract	52.210	M$	Labour	490.467	M$
Software	2627.400	M$	Unit & Flyaway	51.818	M$	Install Support	3.856	M$			
						Unit Level	13.007	M$			
						Sustain Support	13.929	M$			
Total	14294.958	M$	Total	32127.029	M$	Total	135.748	M$	Total	447.530	M$
			Ground Support	3212.703	M$	Total 25.00 Yr	1753.317	M$	Deflated Disposal	104.274	M$
Total LCC			Discount LCC/AC			Cost/AC/FH					
RDT&E	14294.958	M$		22.726	M$	Personnel	2006.788	$			
Production	32127.029	M$		51.076	M$	Contract	551.495	$			
Ground Support	3212.703	M$		5.182	M$	Unit Level	568.442	$			
Operation	1735.317	M$		44.195	M$	Ground	690.904	$			
Disposal	104.274	M$		0.166	M$	Operation	5932.708	$			
Total	51474.281	M$		123.646	M$	Fly Away	51.818	M$			

Figure D.5: Result of Eurofighter LCC estimation in peacetime scenario

Aircraft Name : Eurofighter in WAR TIME

Airframe Mass	5545.42	Kg	Uninst. Avionic Mass	724.47	Kg	Aircraft Mass	10073.35	Kg	Fuel Mass	2133.10	kg
Max. Thrust	179.85	kN	Max. Velocity	2116.62	Km/h	Max. Mach	2.00		Max. Inlet-Temperature	1829.93	K
Adv. Materials	33.680	%	Disposal Labour	5.000	%	Economic Discount	6.000	%	Account Year	2000	
Year Entry Service	1996		Develop Aircraft	9		Static Aircraft	2		Test Aircraft	7	
Production Aircraft	620		Operation Aircraft	39		Aircraft Crew	1		Annual Flying	300.00	Hrs
Life Time	25.00	Years									
Development			Production			Operation & Support			Disposal		
Airframe	5147.831	M$	Airframe	17616.028	M$	Personnel	36.679	M$	Advanced Materials	0.055	M$
Avionic	3254.535	M$	Avionic	6594.837	M$	Service Training	5.448	M$	Composite Materials	-42.993	M$
Engine	3265.192	M$	Engine	7916.164	M$	Contract	0.000	M$	Labour	490.467	M$
Software	2627.400	M$	Unit & Flyaway	51.818	M$	Install Support	3.092	M$			
						Unit Level	10.420	M$			
						Sustain Support	12.105	M$			
Total	14294.958	M$	Total	32127.029	M$	Total	67.744	M$	Total	447.530	M$
			Ground Support	3212.703	M$	Total 25.00 Yr	865.989	M$	Deflated Disposal	104.274	M$
Total LCC			Discount LCC/AC			Cost/AC/FH					
RDT&E	14294.958	M$		22.726	M$	Personnel	1603.002	$			
Production	32127.029	M$		51.076	M$	Contract	438.448	$			
Ground Support	3212.703	M$		5.182	M$	Unit Level	455.395	$			
Operation	865.989	M$		22.205	M$	Ground	690.904	$			
Disposal	104.274	M$		0.166	M$	Operation	2960.647	$			
Total	50604.954	M$	101.355	M$	Fly Away	51.818	M$				

Figure D.6: Result of Eurofighter LCC estimation in wartime scenario

APPENDIX E

OPERATION MISSION SIMULATION MODULE

This module is the core of the entire program, because it links every submodule, which evaluate or measure aircraft performance and/or effectiveness, and apply these values to measure aircraft operational and cost-effectiveness, as shown in Fig E.1. Due to objective of this design methodology aiming to integrate a mission simulation within the early design stage, only general information and major conceptual design variables are available. Therefore, this mission simulation has been developed with some assumptions and simple models.

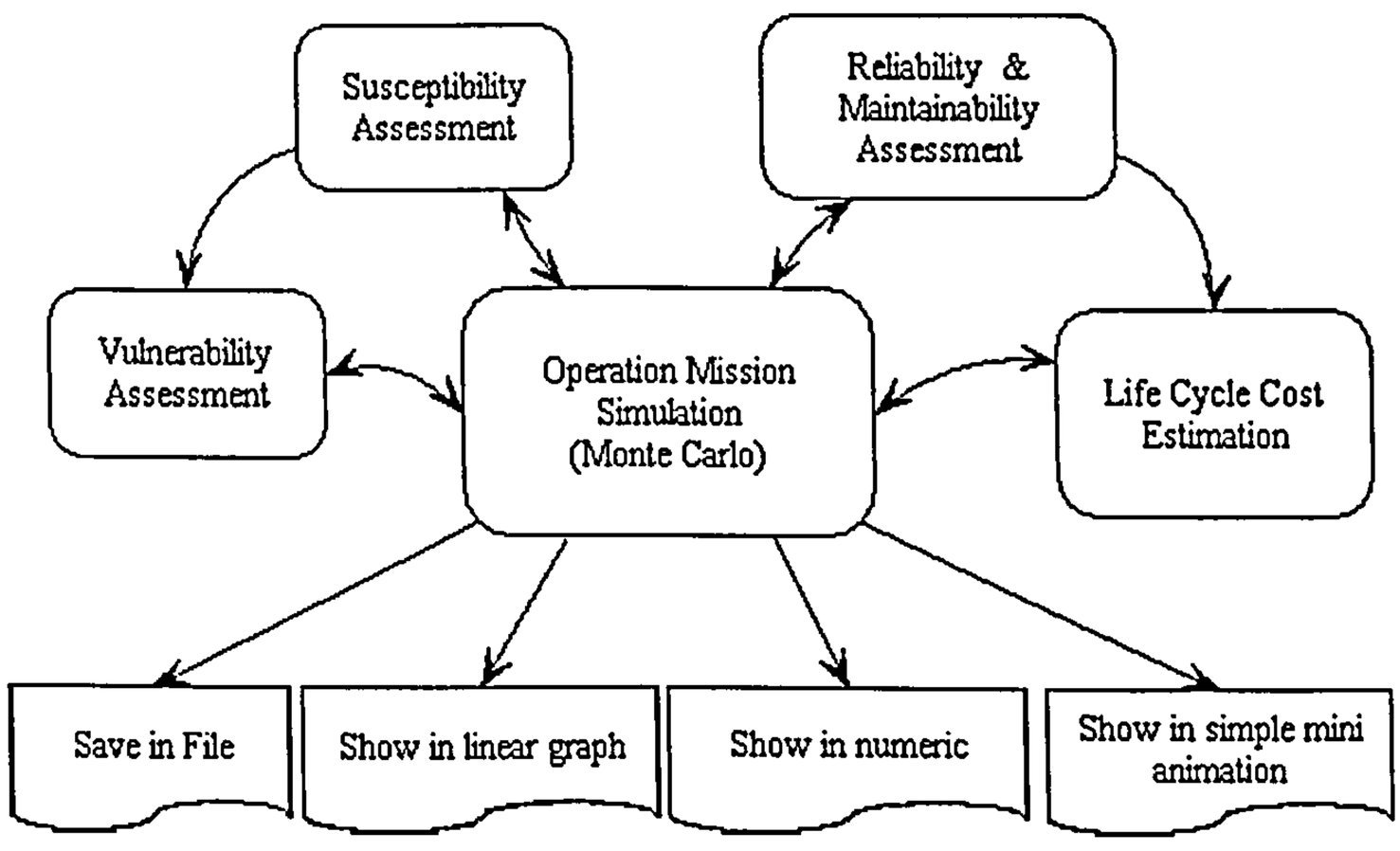

Figure E.1: Flowchart of entire application

E.1 Flowcharts of Alternative Studies Missions

The new generation of combat aircraft will be used as multi-roles air vehicle, but the performance and specification for each role is not the same. Therefore, primary mission for the designed aircraft has to be firstly established.

Finally, 'bombing' mission is chosen to be a model to develop this simulation due to specification of case study aircraft, U-99. Fig. E.2 - E.8 show all historical developed flowcharts for tactical and strategic combat missions.

CONTAINS PULLOUTS

Figure E.2: Flowchart of air superiority mission

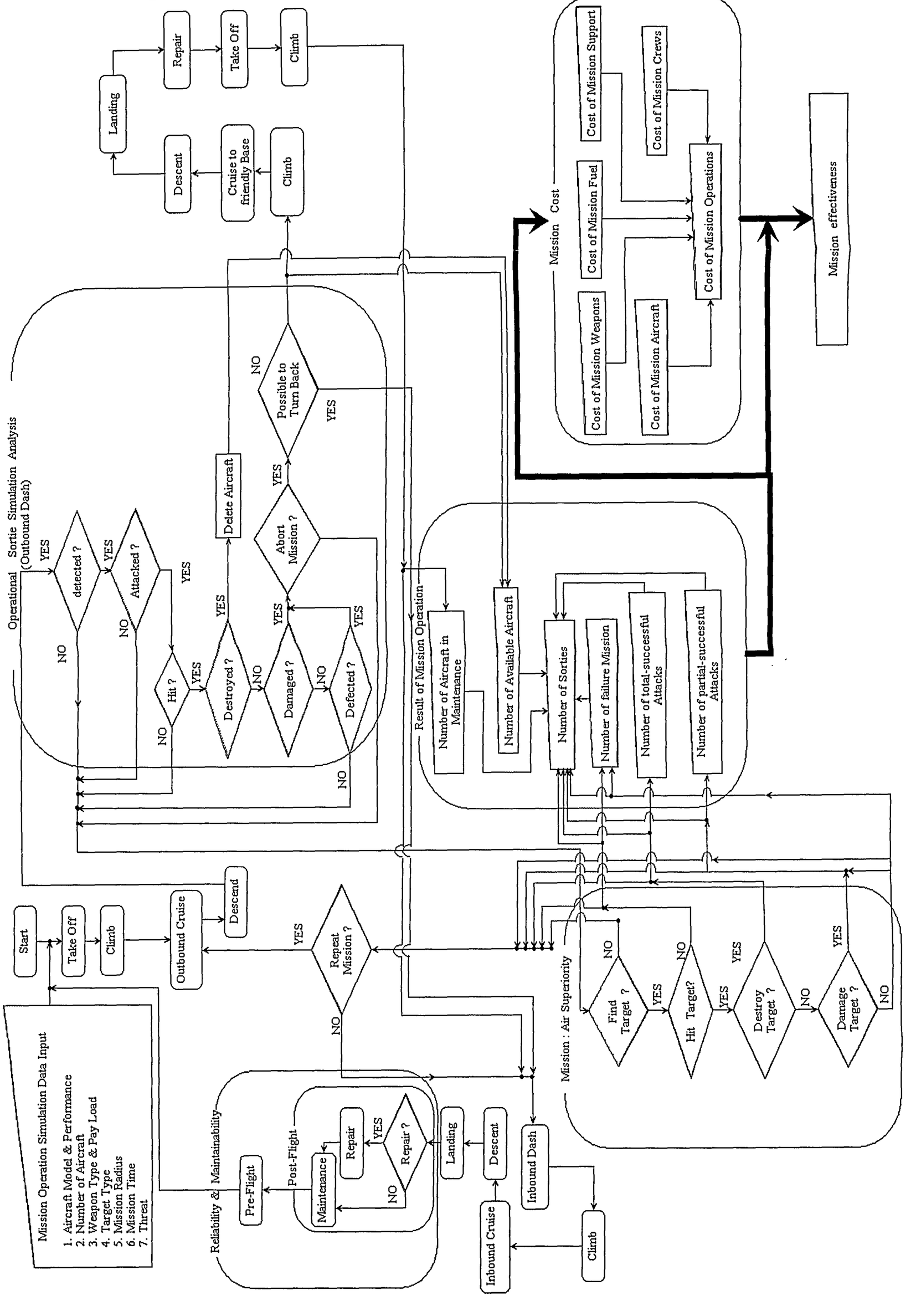

Figure E.3: Flowchart of patrol mission

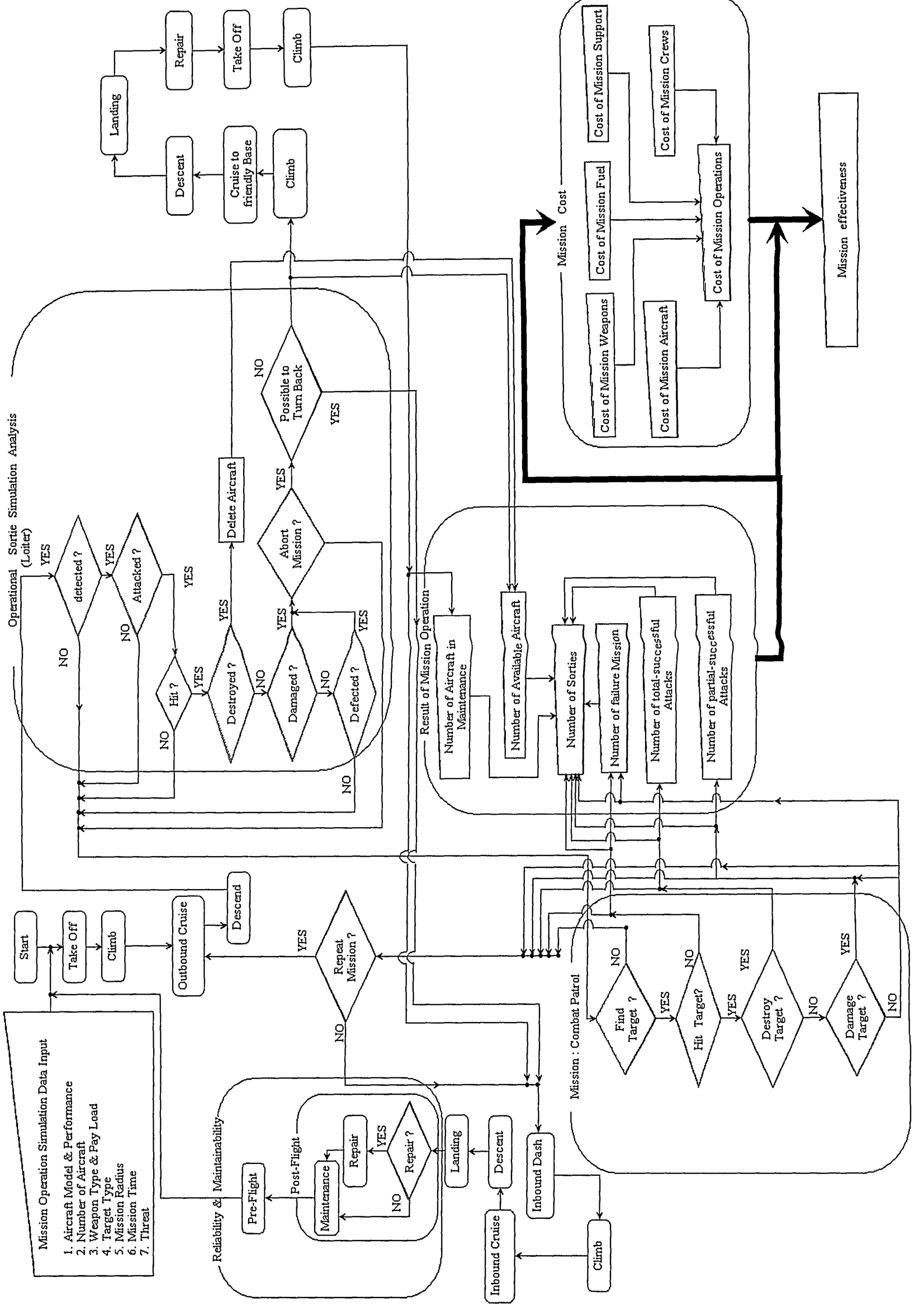

Figure E.4: Flowchart of long penetration mission (Hi-Lo-Lo-Hi)

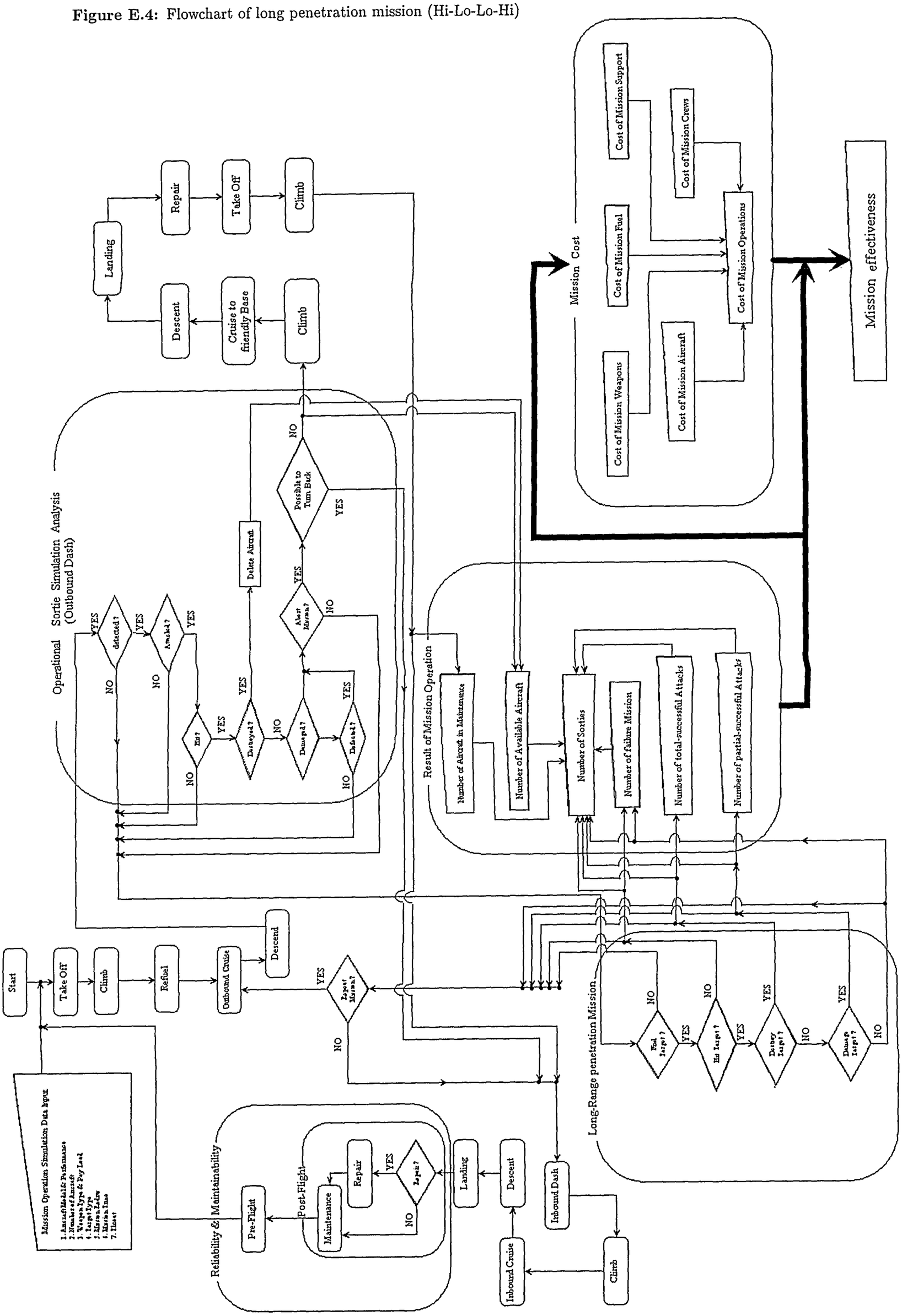

Figure E.5: Flowchart of escort mission

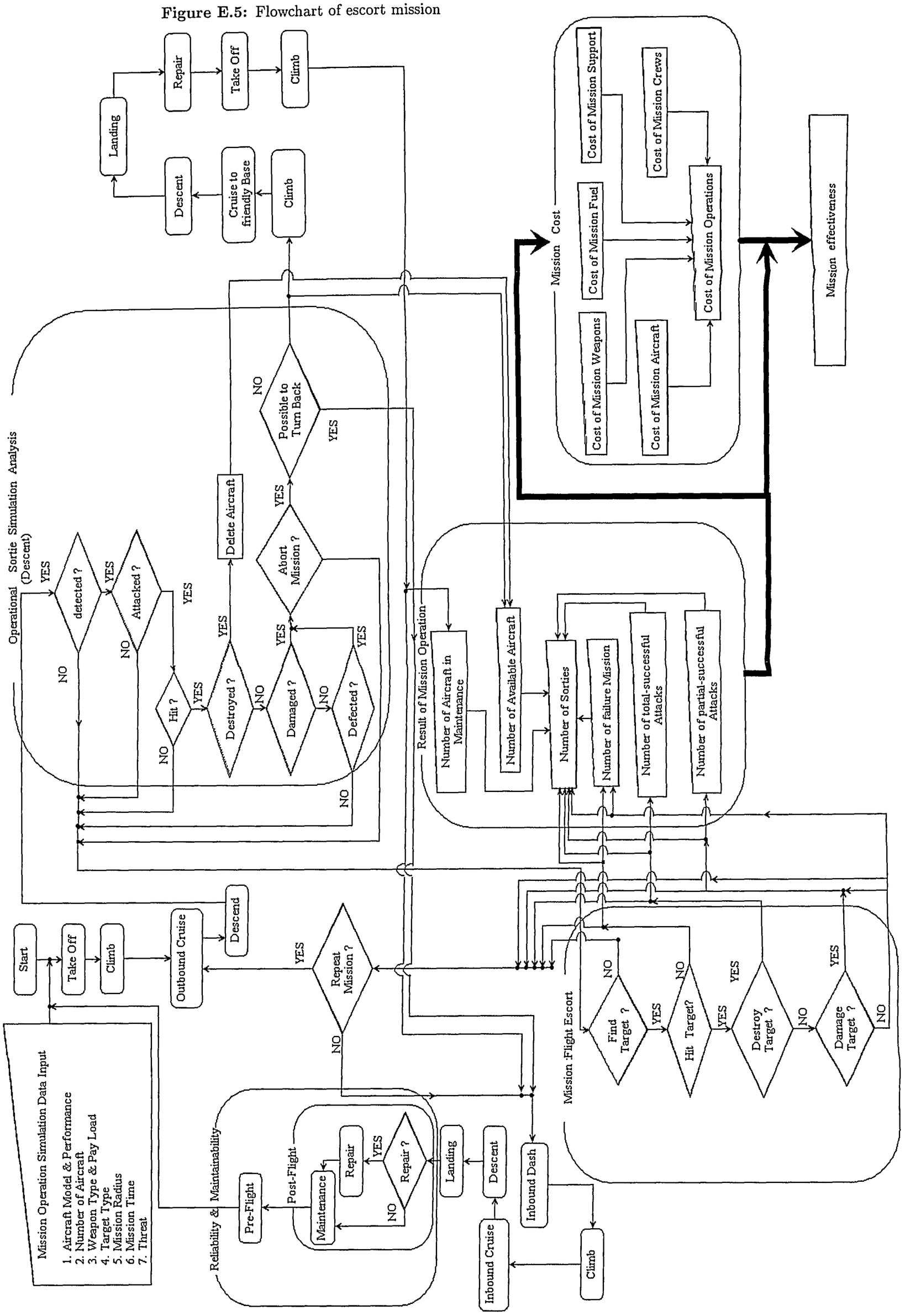

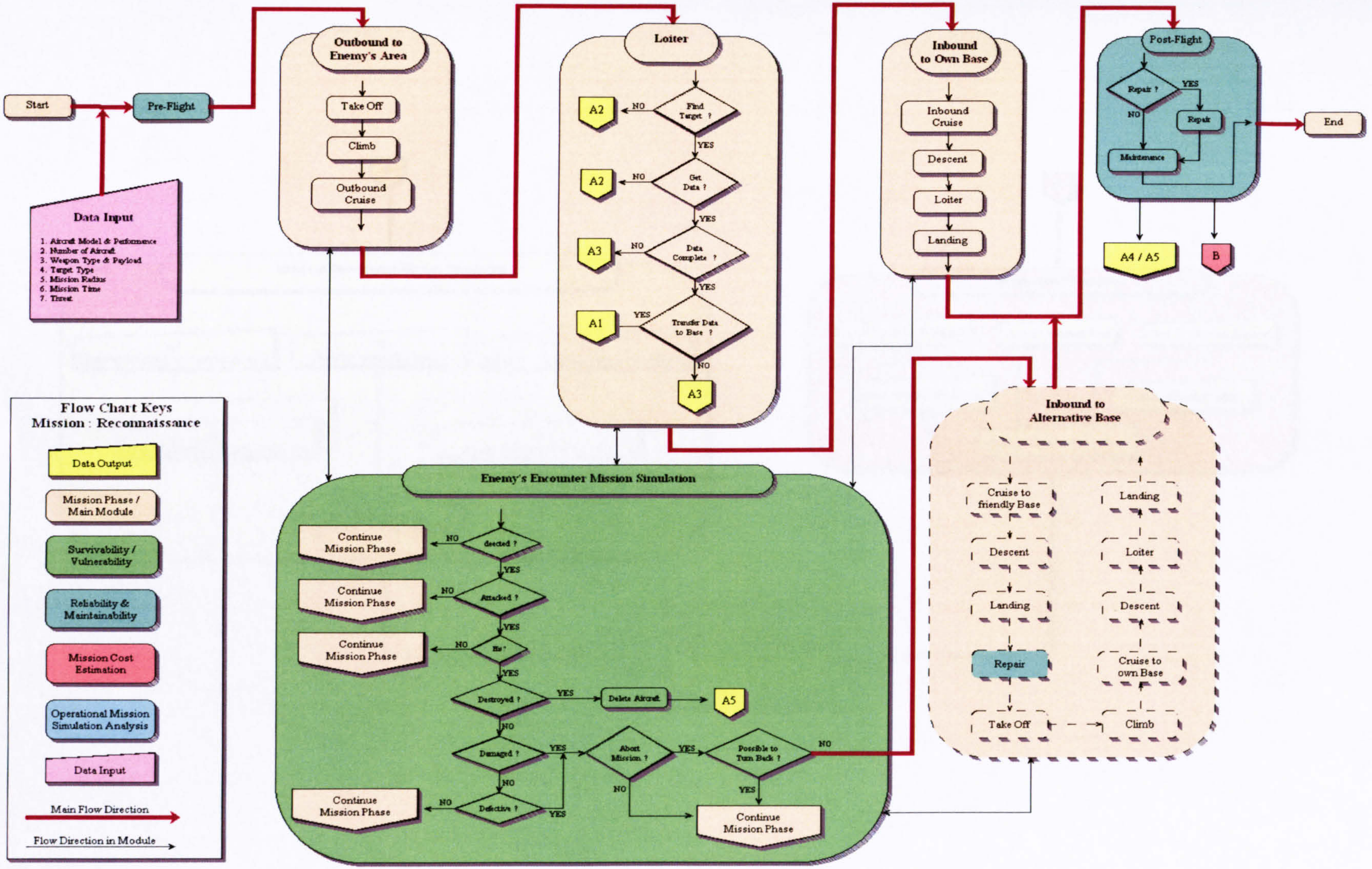
Start
Pre-Flight
Data Input
1. Aircraft Model & Performance
2. Number of Aircraft
3. Weapon Type & Payload
4. Target Type
5. Mission Radius
6. Mission Time
7. Threat
Outbound to Enemy's Area
Take Off
Climb
Outbound Cruise
Loiter
A2
NO
Find Target ?
YES
A2
NO
Get Data ?
YES
A3
NO
Data Complete ?
YES
A1
YES
Transfer Data to Base ?
NO
A3
Inbound to Own Base
Inbound Cruise
Descent
Loiter
Landing
Post-Flight
Repair ?
YES
NO
Repair
Maintenance
End
A4 / A5
B
Inbound to Alternative Base
Cruise to friendly Base
Descent
Landing
Repair
Take Off
Landing
Loiter
Descent
Cruise to own Base
Climb
Enemy's Encounter Mission Simulation
detected ?
NO
YES
Continue Mission Phase
Attacked ?
NO
YES
Continue Mission Phase
Hit ?
NO
YES
Continue Mission Phase
Destroyed ?
YES
Delete Aircraft
A5
NO
Damaged ?
YES
NO
Abort Mission ?
YES
Possible to Turn Back ?
NO
YES
NO
Defective ?
NO
YES
Continue Mission Phase
Continue Mission Phase
Flow Chart Keys
Mission : Reconnaissance
Data Output
Mission Phase / Main Module
Survivability / Vulnerability
Reliability & Maintainability
Mission Cost Estimation
Operational Mission Simulation Analysis
Data Input
Main Flow Direction
Flow Direction in Module

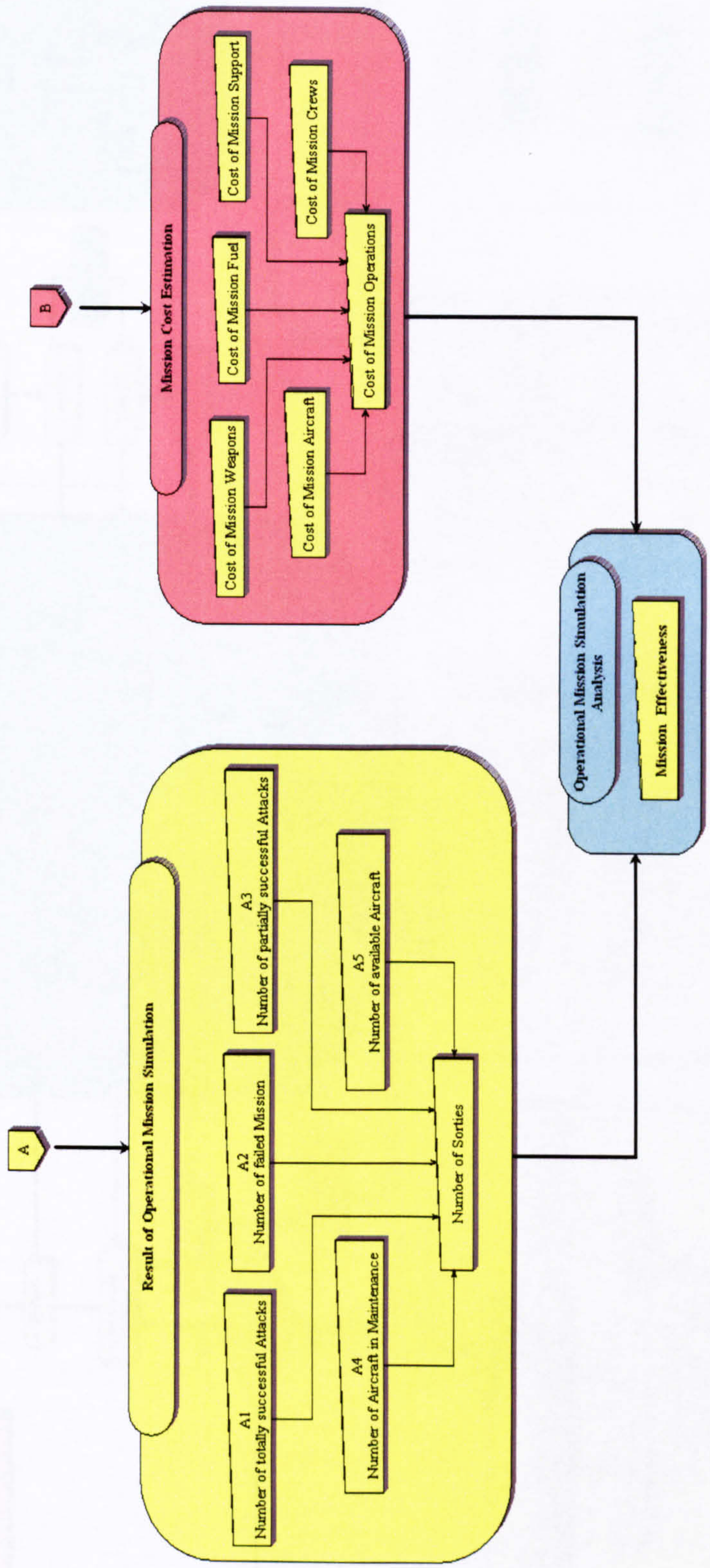
A
Result of Operational Mission Simulation
A1
Number of totally successful Attacks
A2
Number of failed Mission
A3
Number of partially successful Attacks
A4
Number of Aircraft in Maintenance
A5
Number of available Aircraft
Number of Sorties
B
Mission Cost Estimation
Cost of Mission Fuel
Cost of Mission Support
Cost of Mission Crews
Cost of Mission Weapons
Cost of Mission Aircraft
Cost of Mission Operations
Operational Mission Simulation Analysis
Mission Effectiveness

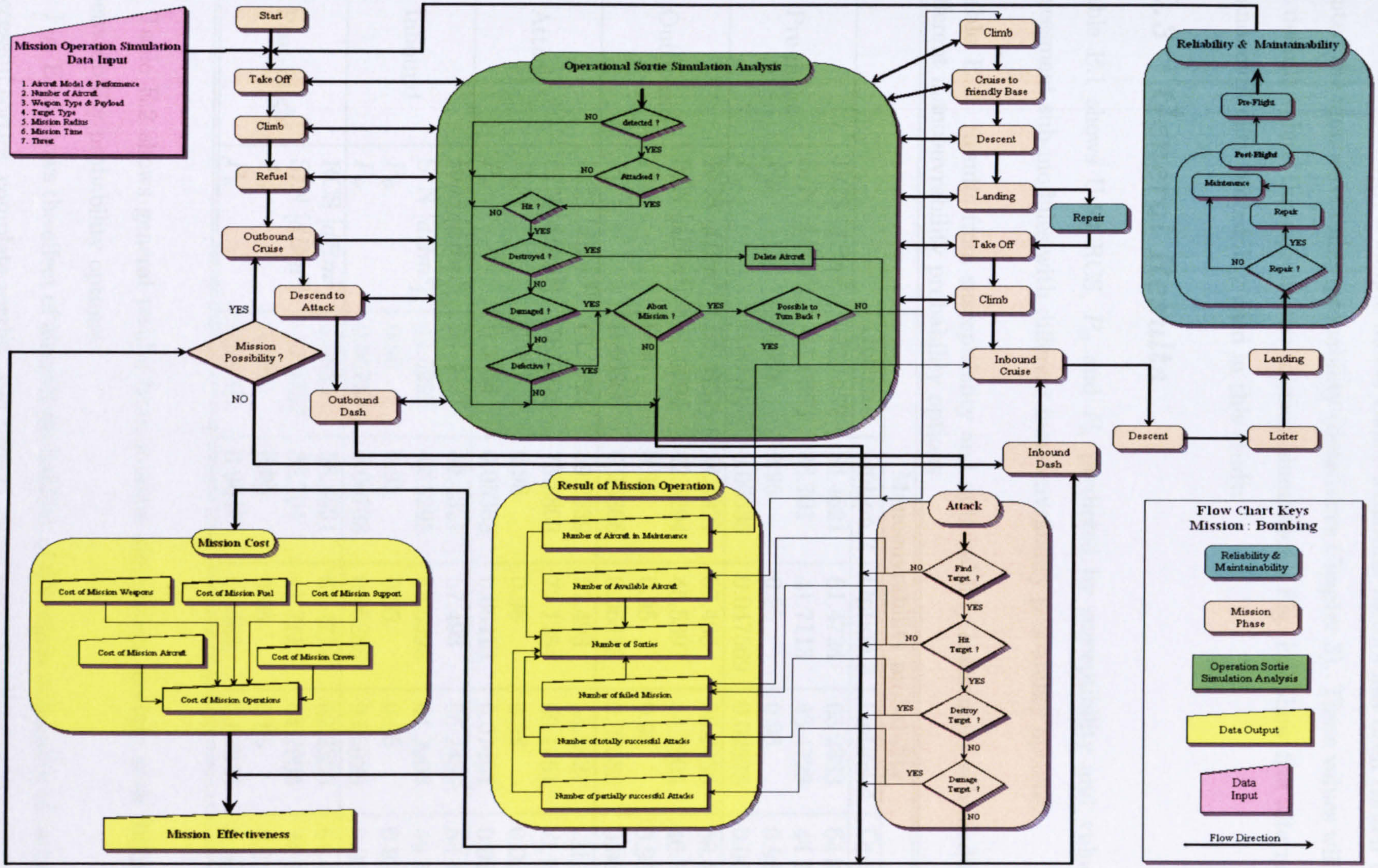
Mission Operation Simulation Data Input
1. Aircraft Model & Performance
2. Number of Aircraft
3. Weapon Type & Payload
4. Target Type
5. Mission Radius
6. Mission Time
7. Threat
Start
Take Off
Climb
Refuel
Outbound Cruise
Descend to Attack
Mission Possibility ?
YES
NO
Outbound Dash
Operational Sortie Simulation Analysis
detected ?
Attacked ?
Hit ?
Destroyed ?
Delete Aircraft
Damaged ?
Abort Mission ?
Possible to Turn Back ?
Defective ?
Climb
Cruise to friendly Base
Descent
Landing
Repair
Take Off
Climb
Inbound Cruise
Inbound Dash
Descent
Loiter
Landing
Reliability & Maintainability
Pre-Flight
Post-Flight
Maintenance
Repair
Repair ?
Result of Mission Operation
Number of Aircraft in Maintenance
Number of Available Aircraft
Number of Sorties
Number of failed Mission
Number of totally successful Attacks
Number of partially successful Attacks
Attack
Find Target ?
Hit Target ?
Destroy Target ?
Damage Target ?
Mission Cost
Cost of Mission Weapons
Cost of Mission Fuel
Cost of Mission Support
Cost of Mission Aircraft
Cost of Mission Crews
Cost of Mission Operations
Mission Effectiveness
Flow Chart Keys
Mission : Bombing
Reliability & Maintainability
Mission Phase
Operation Sortie Simulation Analysis
Data Output
Data Input
Flow Direction

E.2 Manoeuvrability Probability

In this methodology, a simple model called weighting factors has been chosen to represented the manoeuvrability probability (details see Chapter 3). These values will be used as default values throughout the mission simulation. Fig. E.9 show five alternatives of manoeuvrability probability used in this study.

E.3 General Results

Table E.1 shows U-99 RCS, P_D and P_K predicted by susceptibility and vulnerability assessment sub-modules with different manoeuvrability probability options.

Table E.1: Results from susceptibility and vulnerability assessment sub-modules with different manoeuvrability probability options

		Manoeuvrability probability				
		Option 1	Option 2	Option 3	Option 4	Option 5
Pre-flight	RCS $[dBm^2]$	-22.1452	54.4621	61.4724	63.2333	644827
	S/N $[dBm^2]$	-41.9063	38.701	41.7113	43.4723	44.7216
	P_D	0.001	0.95	0.95	0.95	0.95
	P_K	0.085146	0.06635	0.047569	0.02878	0.00999
Outbound	RCS $[dBm^2]$	54.4827	54.4827	57.493	56.2436	58.46
	S/N $[dBm^2]$	42.5294	42.5294	45.5397	44.2904	46.5089
	P_D	0.95	0.95	0.95	0.95	0.95
	P_K	0.06866	0.06866	0.06413	0.07088	0.06336
Attack	RCS $[dBm^2]$	61.4724	59.2539	57.493	54.4827	-21.7876
	S/N $[dBm^2]$	76.1048	73.8863	72.1254	69.1151	-7.1552
	P_D	0.98	0.98	0.98	0.98	0.003
	P_K	0.0386	0.05363	0.06413	0.07464	0.082157
Inbound	RCS $[dBm^2]$	54.4827	54.4827	57.493	56.2436	58.4621
	S/N $[dBm^2]$	42.5295	42.5295	45.5398	44.2904	46.5089
	P_D	0.95	0.95	0.95	0.95	0.95
	P_K	0.06738	0.06738	0.06285	0.06928	0.06198
Post-Flight	RCS $[dBm^2]$	0.6854	58.4621	61.4724	62.2333	64.4827
	S/N $[dBm^2]$	-19.0757	38.701	41.7113	44.2904	44.7216
	P_D	0.001	0.95	0.95	0.95	0.95
	P_K	0.08301	0.06475	0.0465	0.02824	0.00999

Table E.2 shows general results from mission simulation module with different manoeuvrability probability options.

Fig. E.10 shows the effect of aircraft probability of detection in number of sorties flown, successful sorties, complete sorties, and targets killed with the associated costs.

Manoeuvrability probability option 1

Flight phase	Aircraft views					
	Top	Right	Left	Front	Rear	Bottom
Preflight	0.00	0.00	0.00	1.00	0.00	0.00
Outbound	0.00	0.15	0.15	0.60	0.00	0.10
Attack	0.25	0.15	0.15	0.20	0.00	0.25
Inbound	0.00	0.15	0.15	0.00	0.60	0.10
Postflight	0.00	0.00	0.00	0.00	1.00	0.00

Manoeuvrability probability option 2

Flight phase	Aircraft views					
	Top	Right	Left	Front	Rear	Bottom
Preflight	0.25	0.00	0.00	0.75	0.00	0.00
Outbound	0.05	0.15	0.15	0.60	0.00	0.05
Attack	0.15	0.15	0.15	0.40	0.00	0.15
Inbound	0.05	0.15	0.15	0.00	0.60	0.05
Postflight	0.25	0.00	0.00	0.00	0.75	0.00

Manoeuvrability probability option 3

Flight phase	Aircraft views					
	Top	Right	Left	Front	Rear	Bottom
Preflight	0.50	0.00	0.00	0.50	0.00	0.00
Outbound	0.10	0.10	0.10	0.60	0.00	0.10
Attack	0.10	0.10	0.10	0.60	0.00	0.10
Inbound	0.10	0.10	0.10	0.00	0.60	0.10
Postflight	0.50	0.00	0.00	0.00	0.50	0.00

Manoeuvrability probability option 4

Flight phase	Aircraft views					
	Top	Right	Left	Front	Rear	Bottom
Preflight	0.75	0.00	0.00	0.25	0.00	0.00
Outbound	0.15	0.05	0.05	0.75	0.00	0.00
Attack	0.05	0.05	0.05	0.80	0.00	0.05
Inbound	0.15	0.05	0.05	0.00	0.75	0.00
Postflight	0.75	0.00	0.00	0.00	0.25	0.00

Manoeuvrability probability option 5

Flight phase	Aircraft views					
	Top	Right	Left	Front	Rear	Bottom
Preflight	1.00	0.00	0.00	0.00	0.00	0.00
Outbound	0.25	0.05	0.05	0.65	0.00	0.00
Attack	0.00	0.05	0.05	0.90	0.00	0.00
Inbound	0.25	0.05	0.05	0.00	0.65	0.00
Postflight	1.00	0.00	0.00	0.00	0.00	0.00

Figure E.9: Fives alternatives of manoeuvrability probability

Table E.2: Results from mission simulation module with different manoeuvrability probability options

	Manoeuvrability probability				
	Option 1	Option 2	Option 3	Option 4	Option 5
Sorties Flown	130	156	151	152	175
Complete Sorties	106	136	133	135	157
Targets Killed	78	107	110	96	115
Aircraft lost cost [M$]	26.0048	15.6029	15.6029	15.6029	0.00
Operational Cost [M$]	11.0655	13.7995	13.2599	13.5429	15.7375

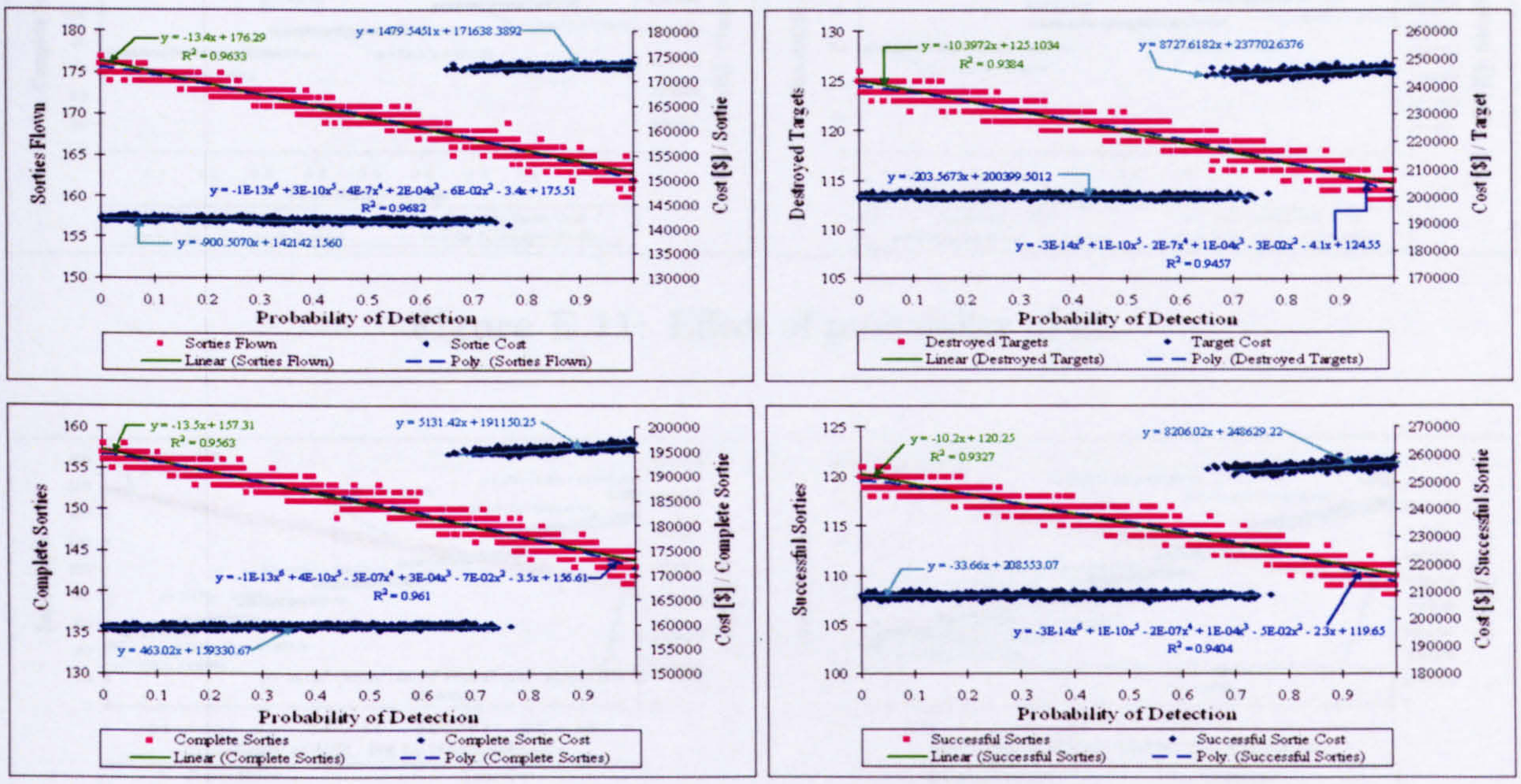

Figure E.10: Effect of probability of detection

Fig. E.11 shows the effect of aircraft probability of hit in number of sorties flown, successful sorties, complete sorties, and targets killed with the associated costs.

Fig. E.12 shows the effect of aircraft probability of kill on encounter with penetrators in number of sorties flown, successful sorties, complete sorties, and targets killed with the associated costs.

Fig. E.13 shows the effect of aircraft probability of kill on encounter with proximity warhead in number of sorties flown, successful sorties, complete sorties, and targets killed with the associated costs.

Fig. E.14 shows the effect of aircraft defect arising rate in number of sorties flown, successful sorties, complete sorties, and targets killed with the associated costs.

Fig. E.15 shows the effect of aircraft mean time to repair defect in number of sorties flown, successful sorties, complete sorties, and targets killed with the associated costs.

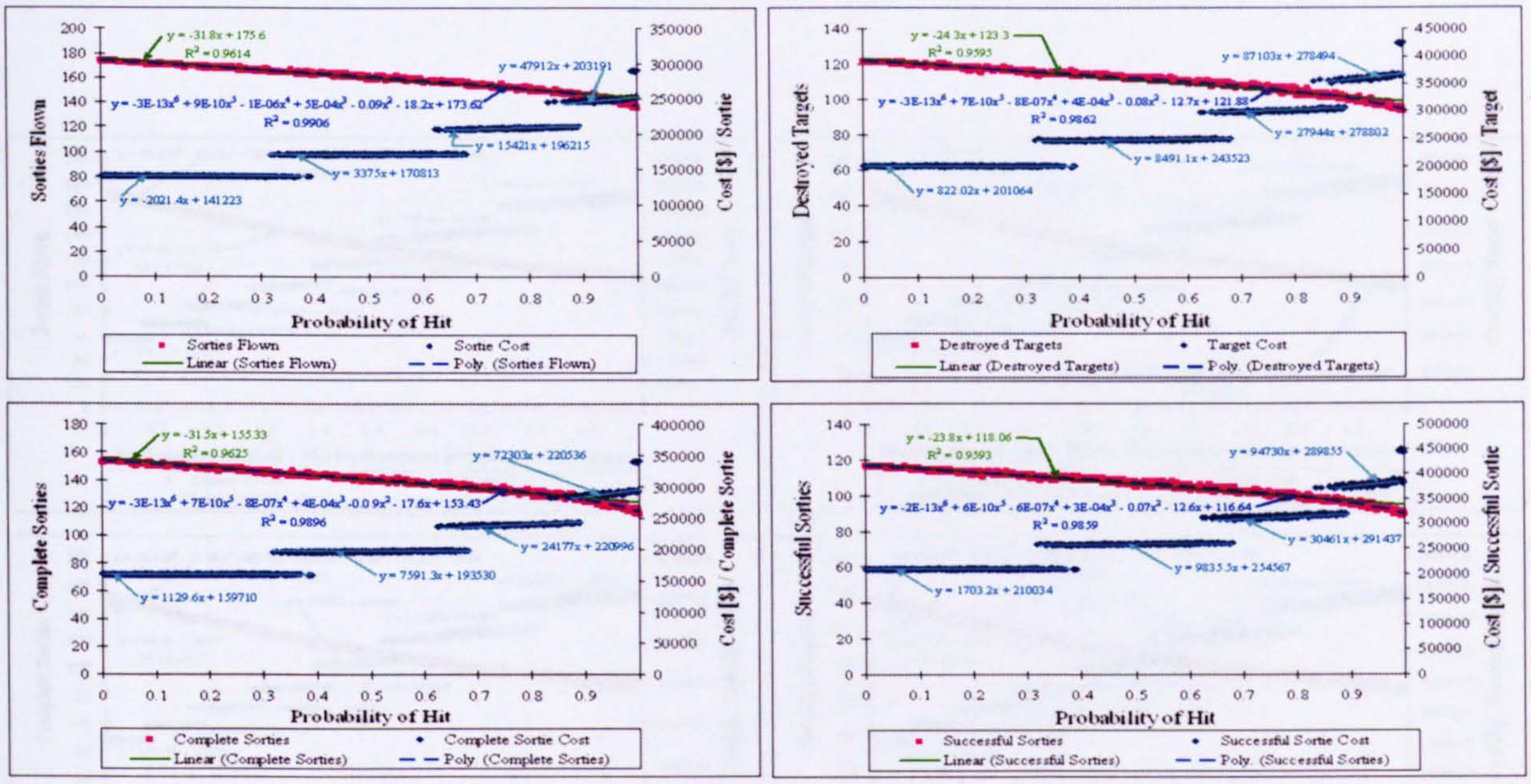

Figure E.11: Effect of probability of hit

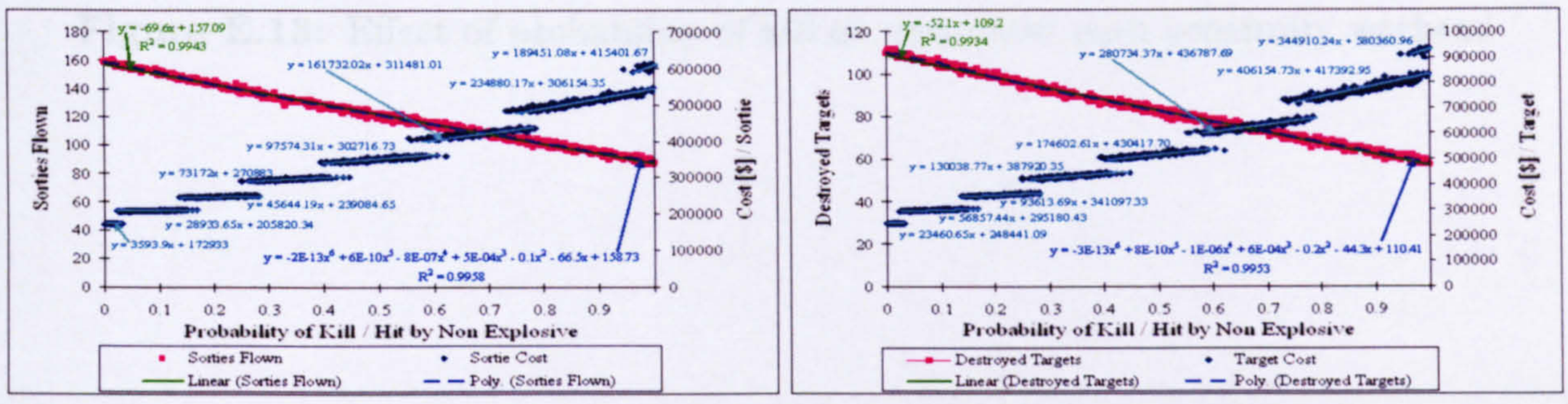

Figure E.12: Effect of probability of kill on encounter with penetrators

Fig. E.16 shows the effect of aircraft mean time to repair damage in number of sorties flown, successful sorties, complete sorties, and targets killed with the associated costs.

Fig. E.17 shows the effect of aircraft defect man-hour rate in number of sorties flown, successful sorties, complete sorties, and targets killed with the associated costs.

Fig. E.18 - E.30 show the effects of, and the relationships between susceptibility and vulnerability on the operational and operational cost MOEs.

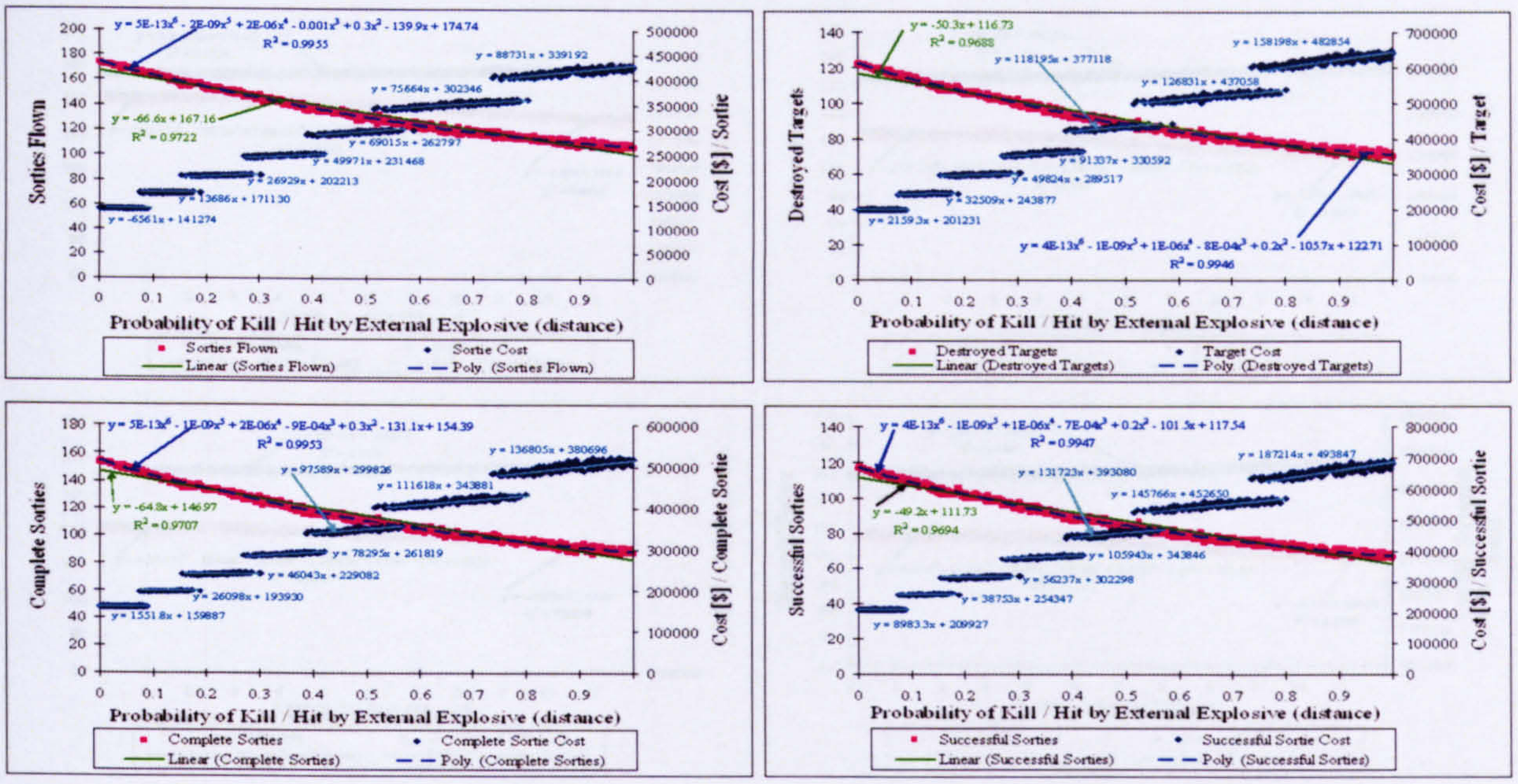

Figure E.13: Effect of probability of kill on encounter with proximity warhead

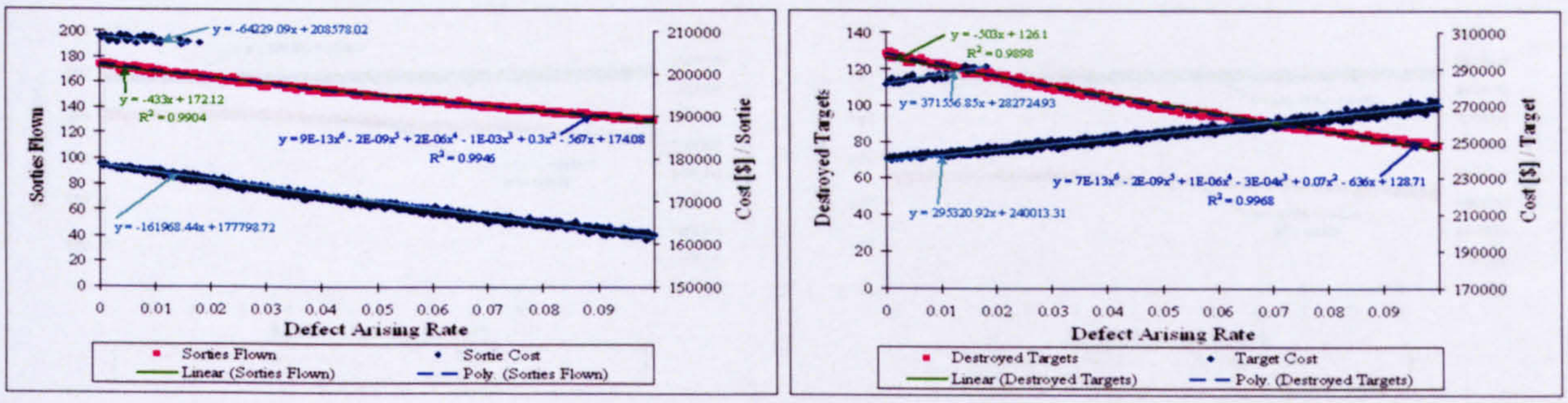

Figure E.14: Effect of defect arising rate

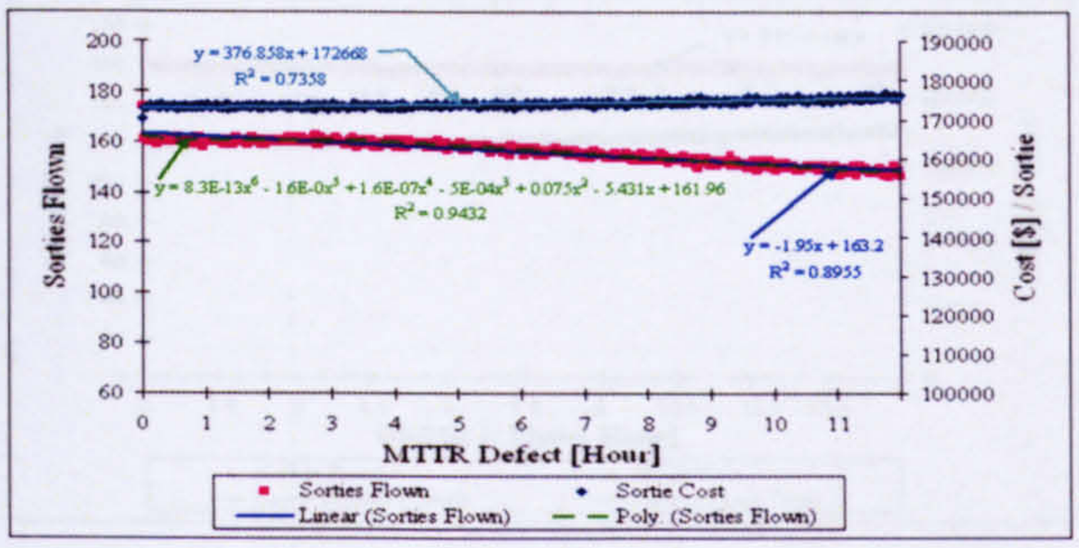

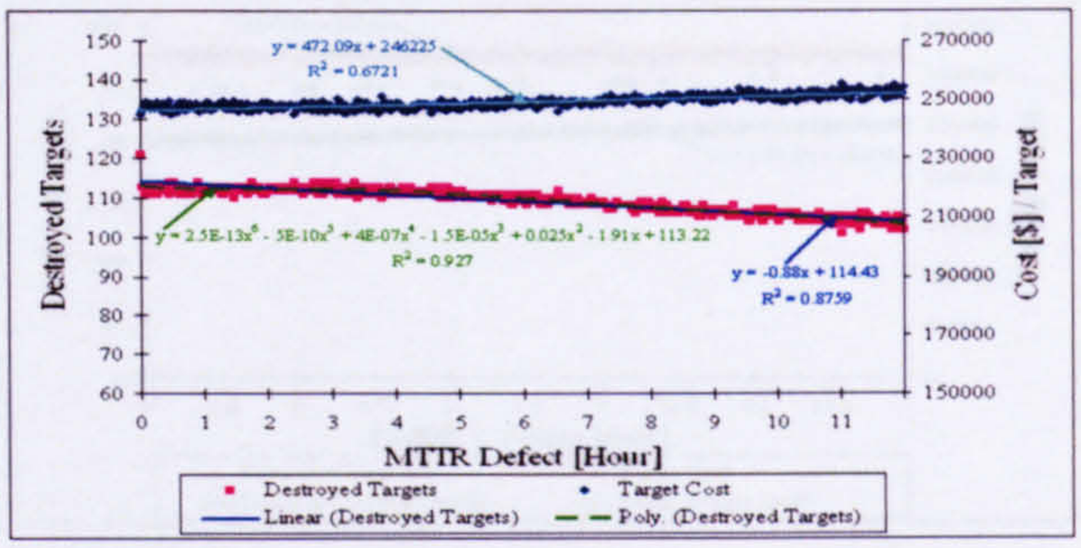

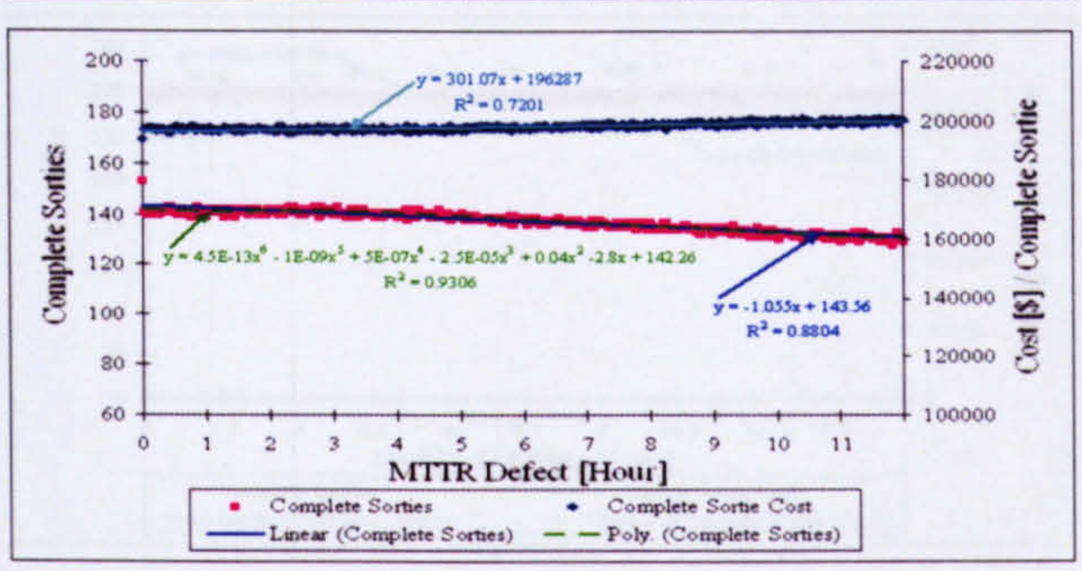

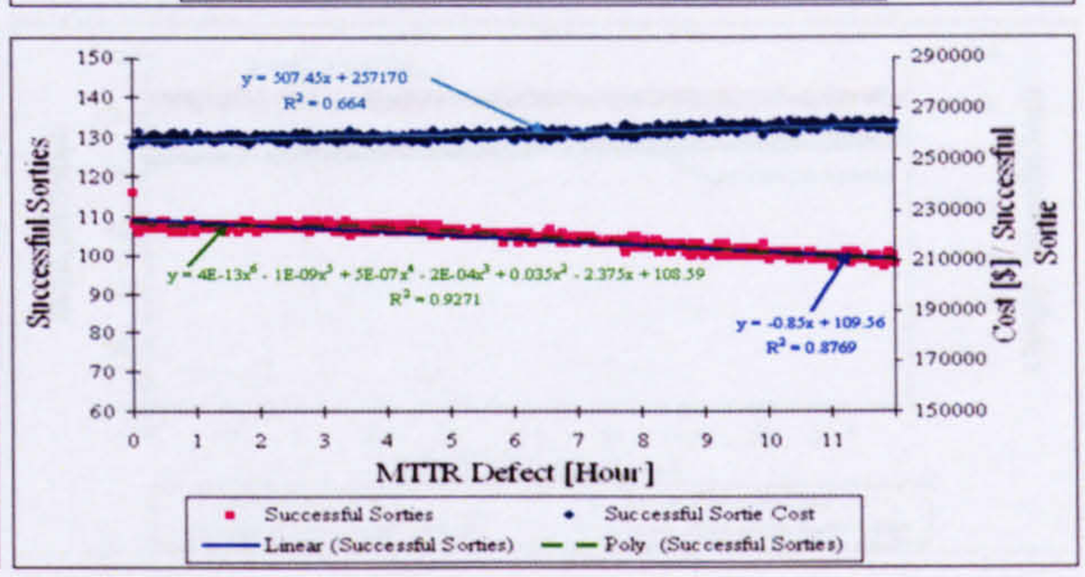

Figure E.15: Effect of mean time to repair defect

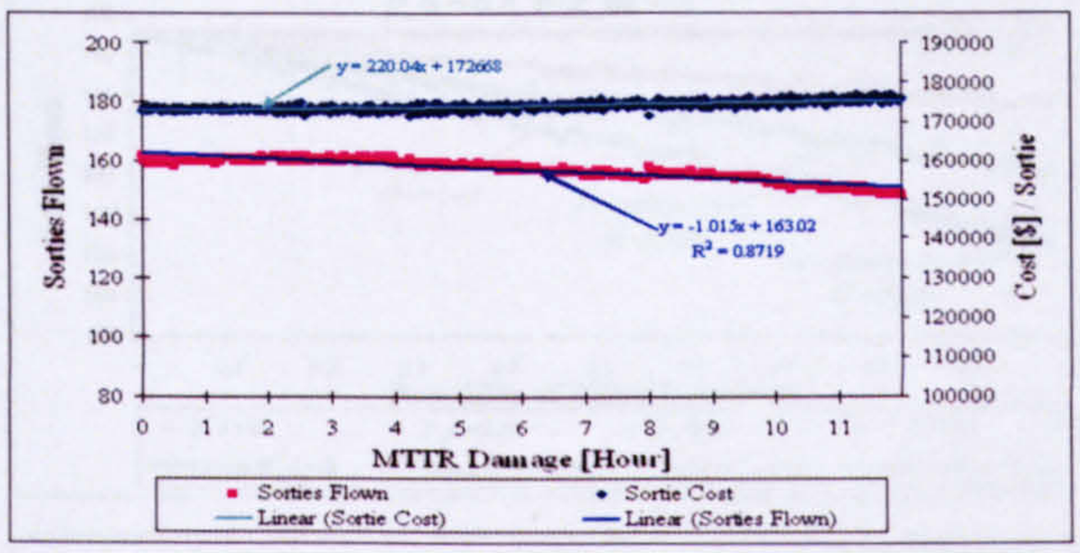

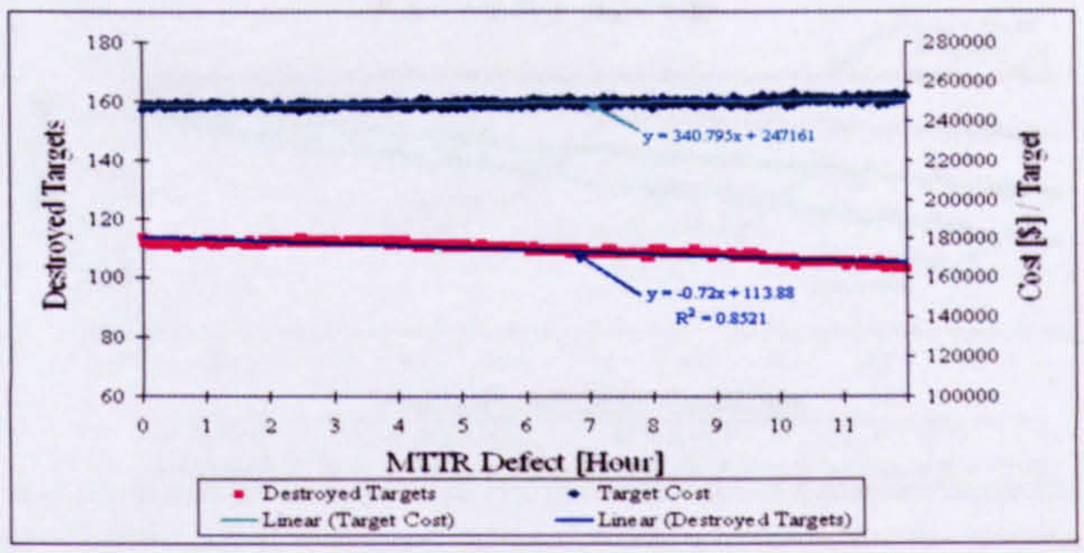

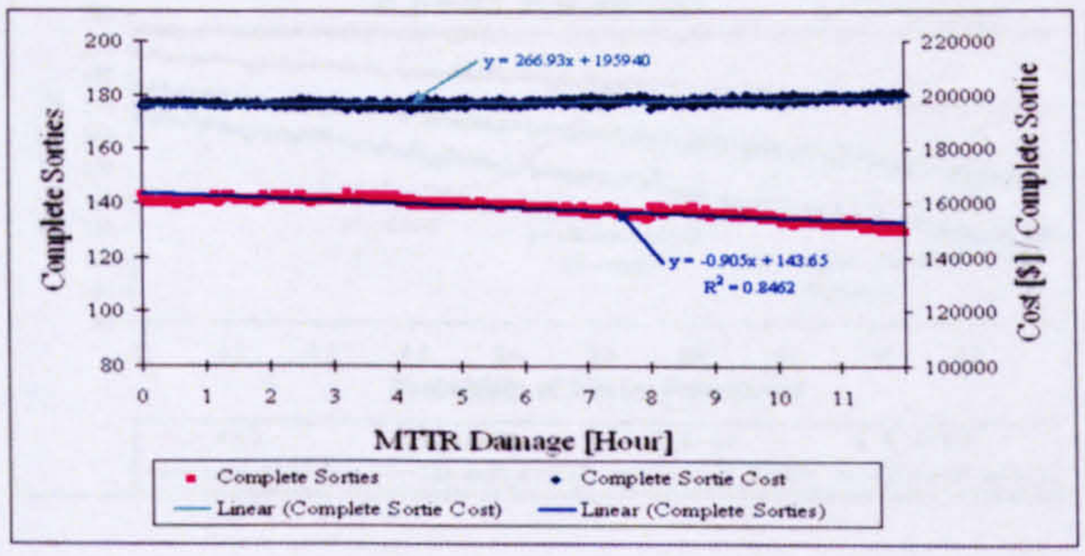

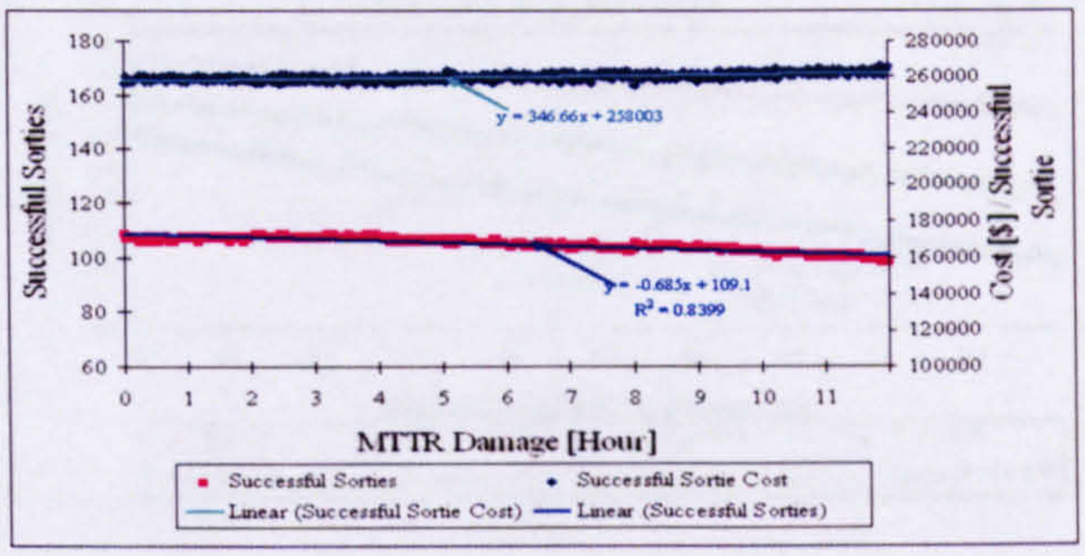

Figure E.16: Effect of probability of mean time to repair damage

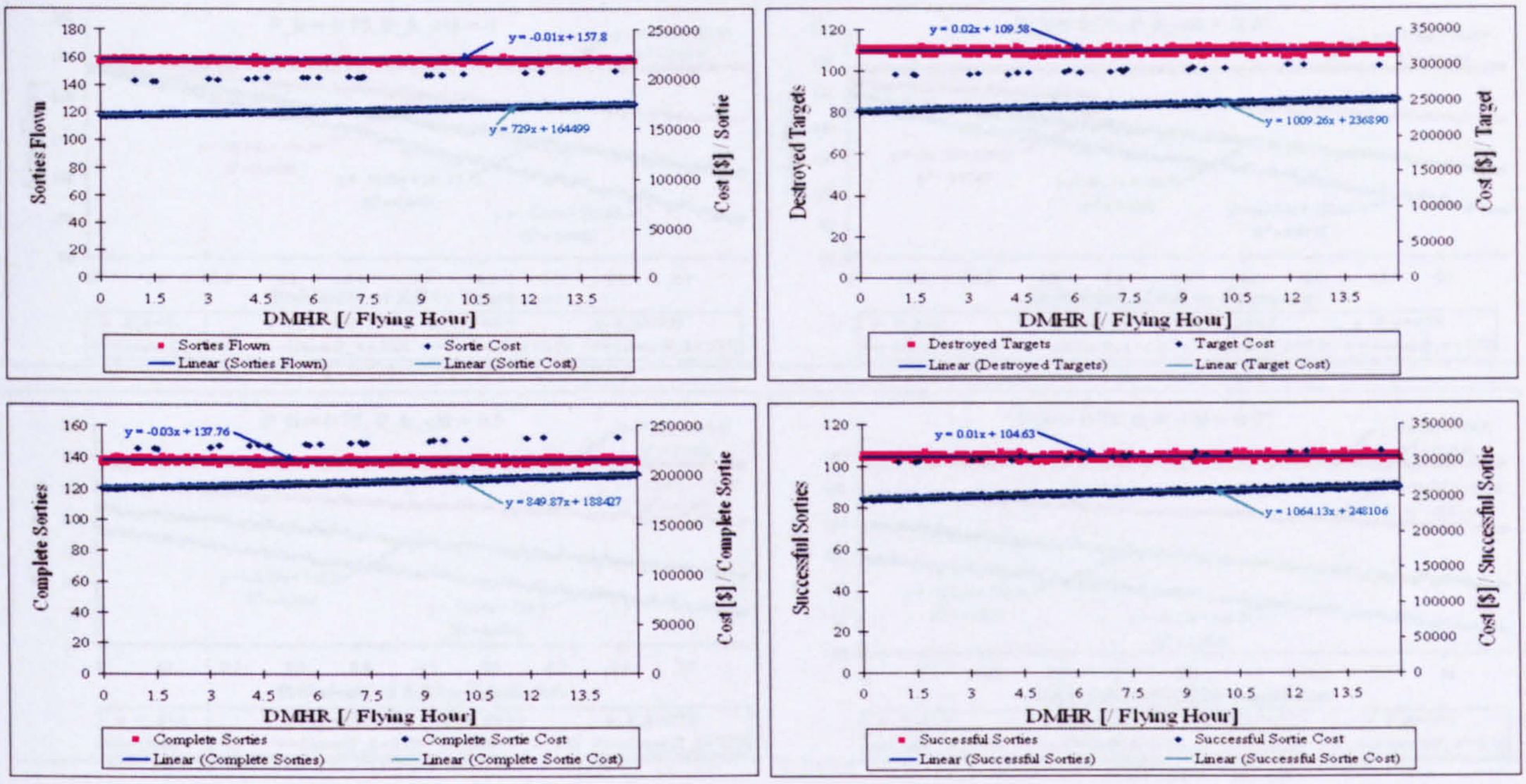

Figure E.17: Effect of probability of defect man-hour rate

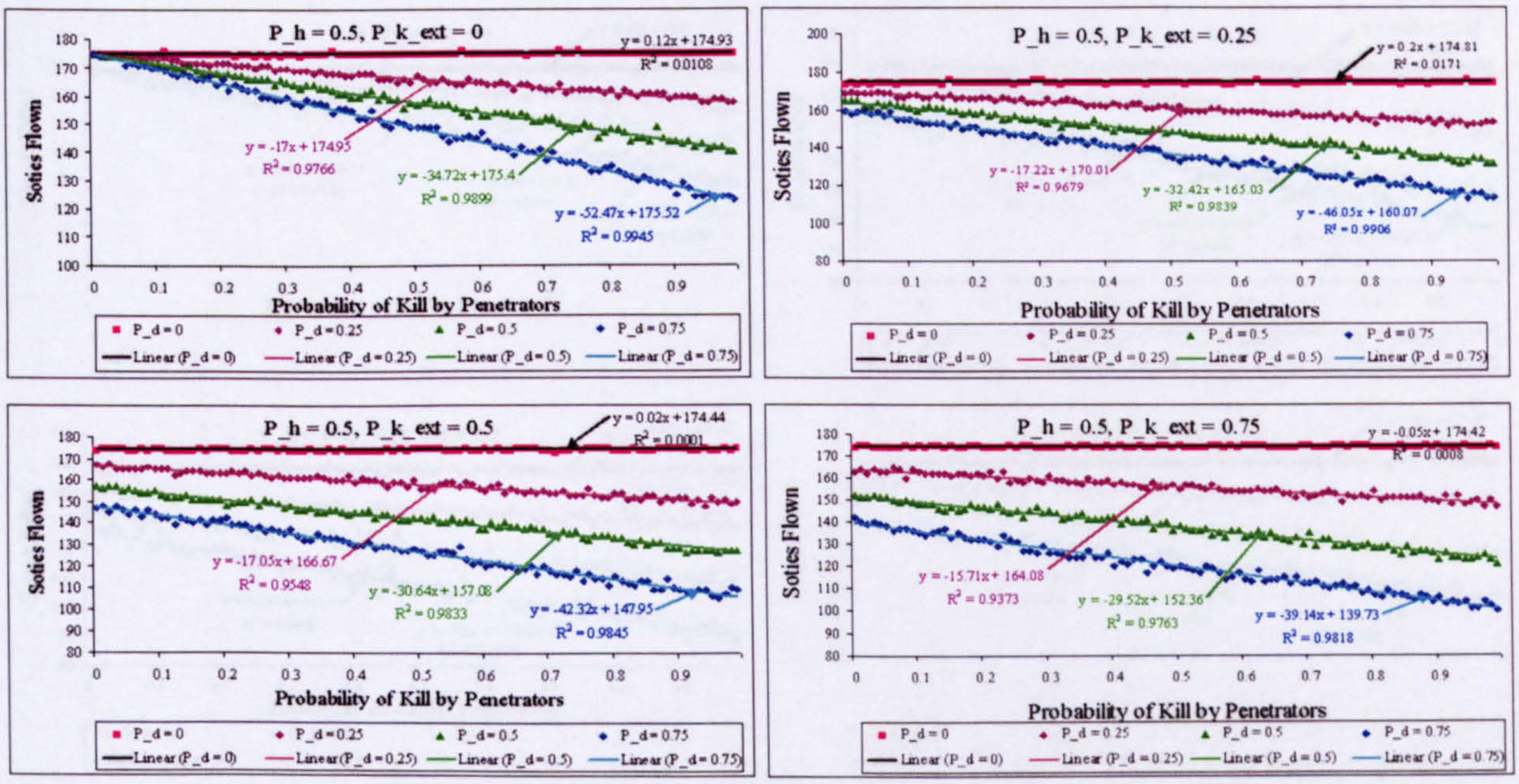

Figure E.18: Effect of P_D and $P_{K_{Non}}$ with increasing $P_{K_{Ext}}$ and $P_H = 0.5$ on the total number of sorties flown

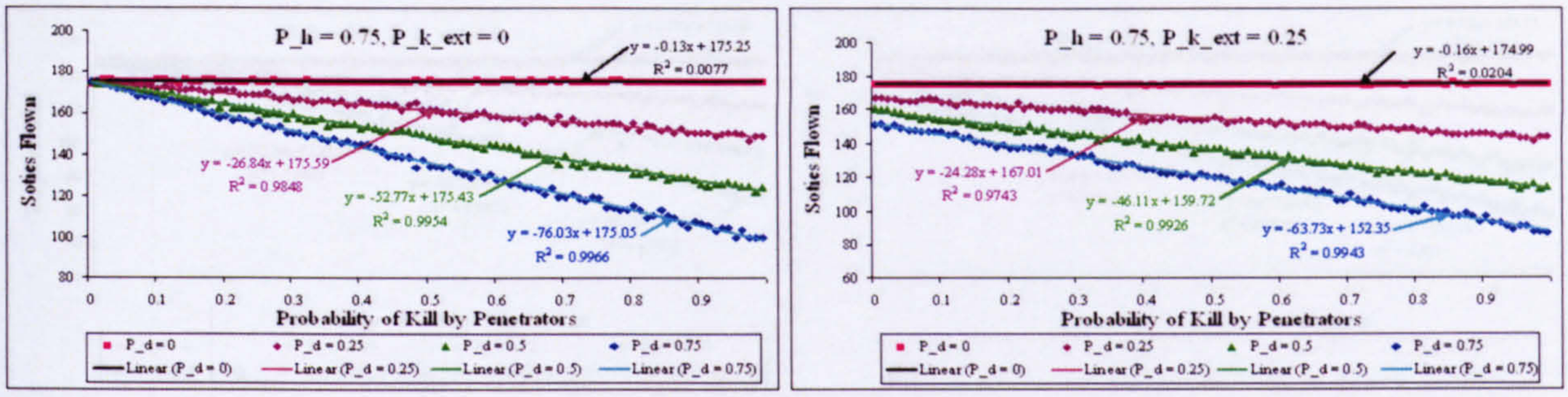

Figure E.19: Effect of P_D and $P_{K_{Non}}$ with increasing $P_{K_{Ext}}$ and $P_H = 0.75$ on the total number of sorties flown

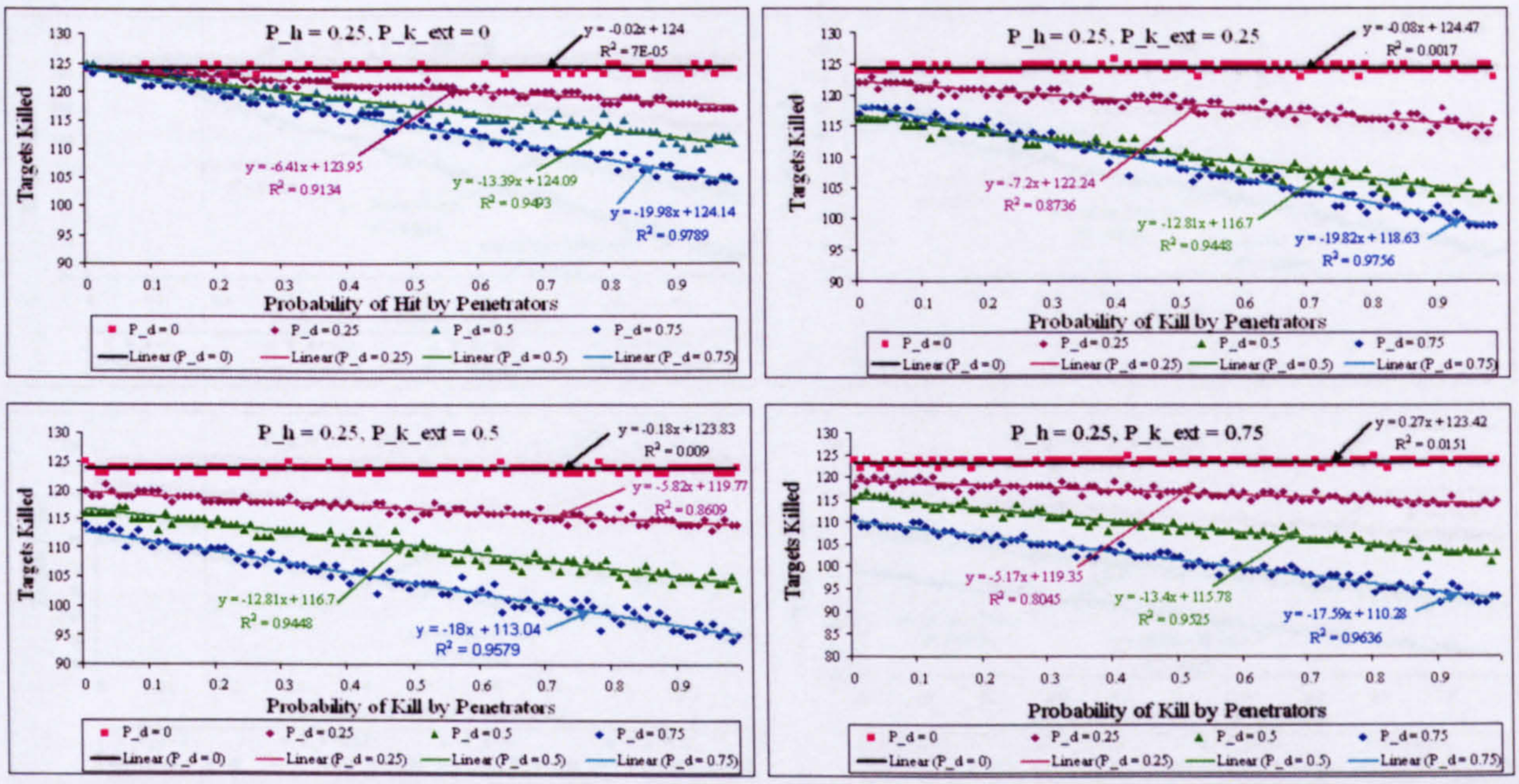

Figure E.20: Effect of P_D and $P_{K_{Non}}$ with increasing $P_{K_{Ext}}$ and $P_H = 0.25$ on the total number of targets killed

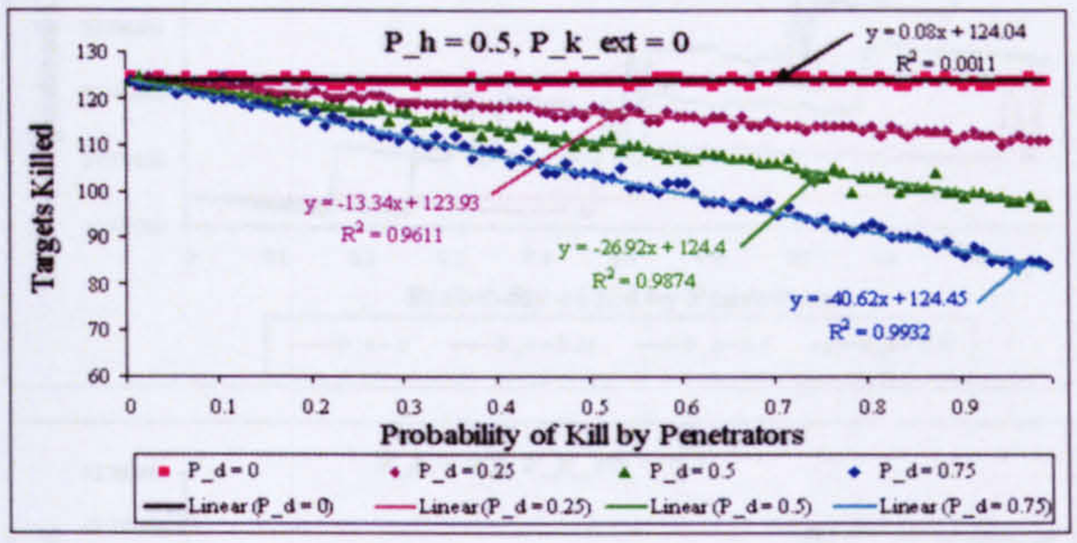

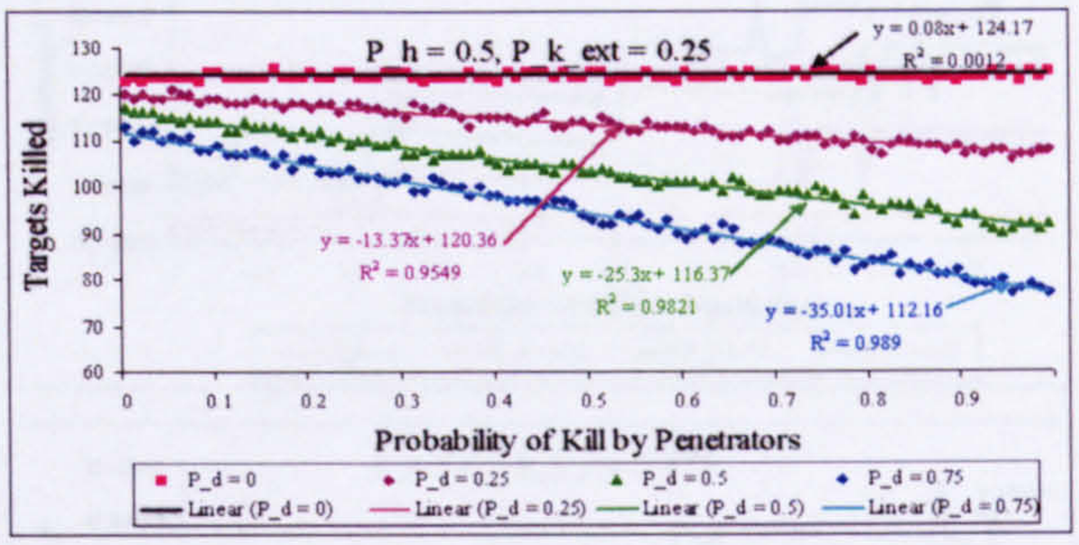

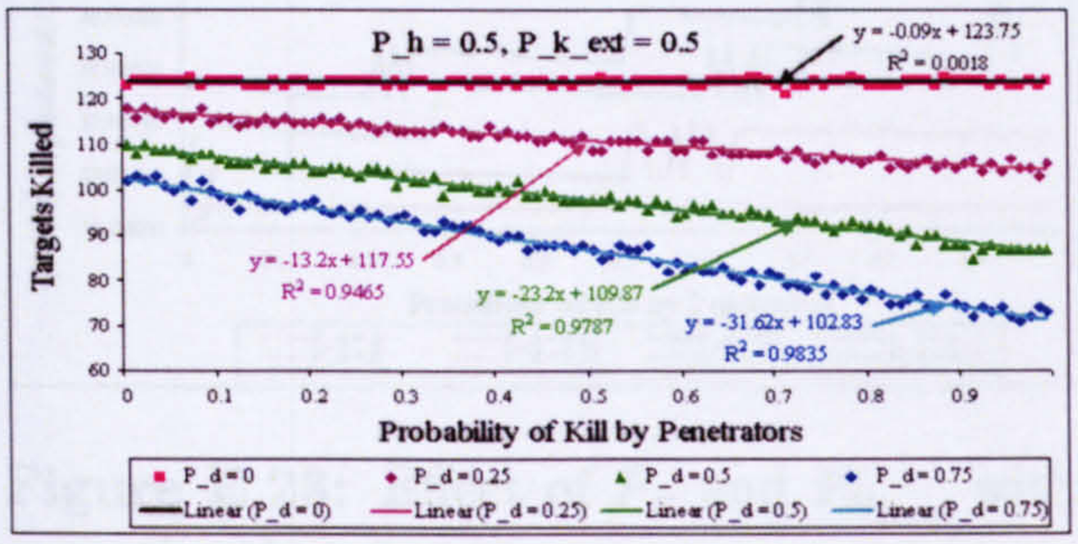

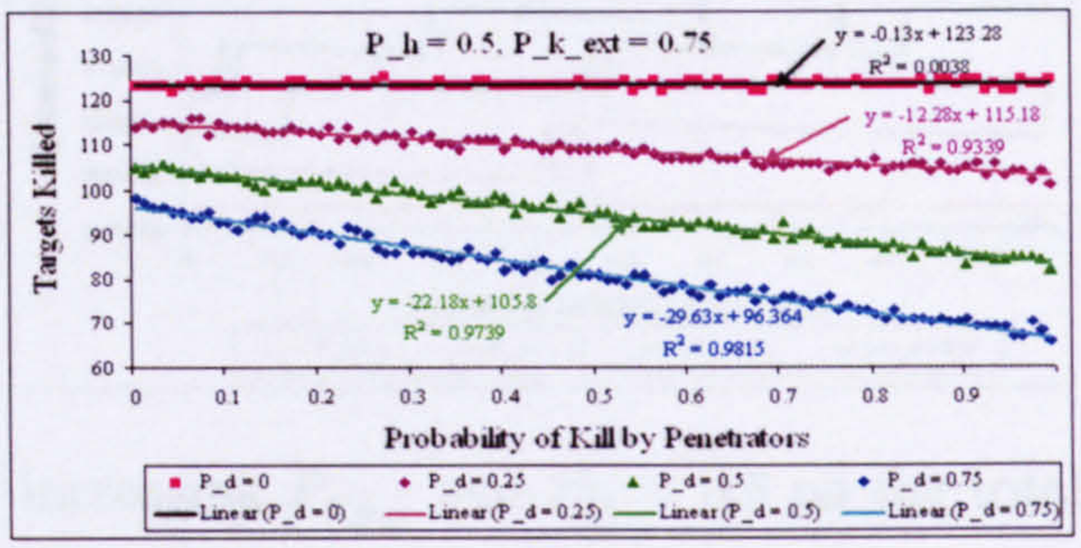

Figure E.21: Effect of P_D and $P_{K_{Non}}$ with increasing $P_{K_{Ext}}$ and $P_H = 0.5$ on the total number of targets killed

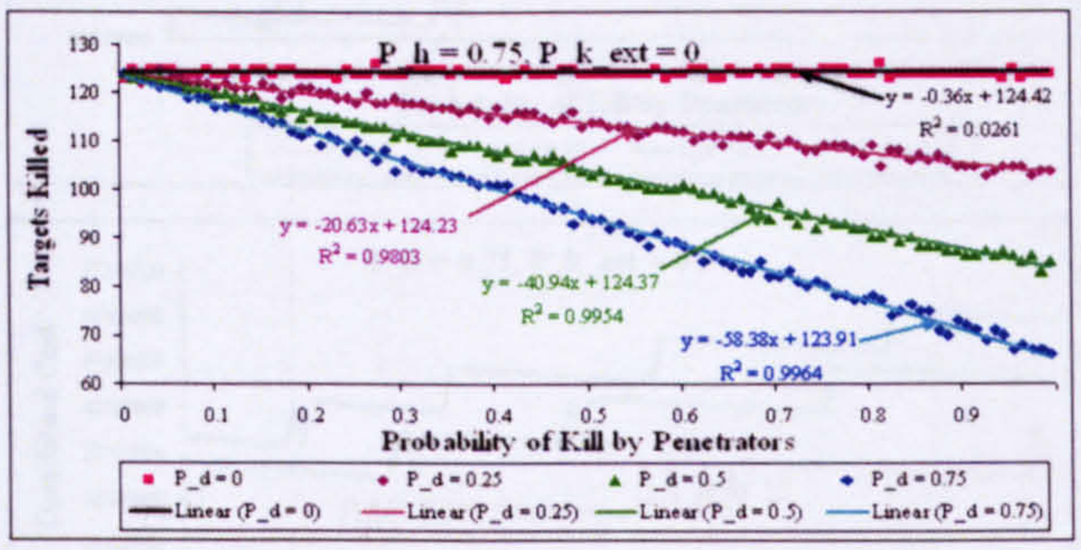

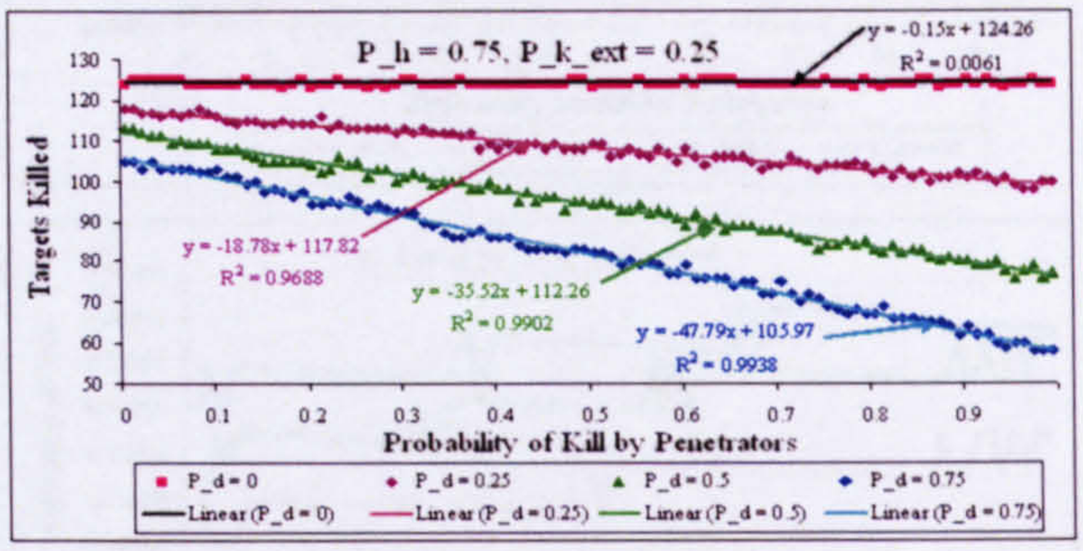

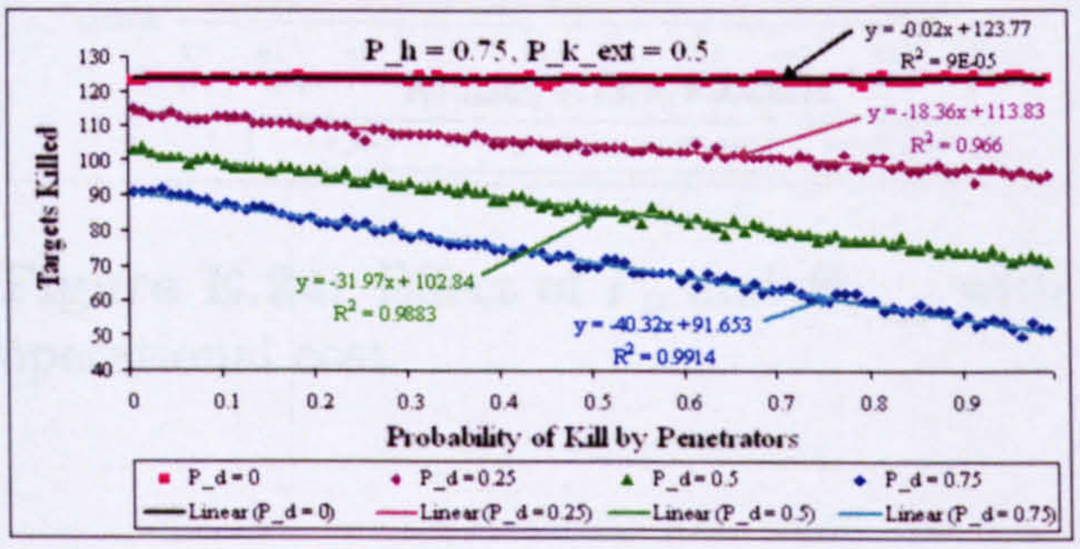

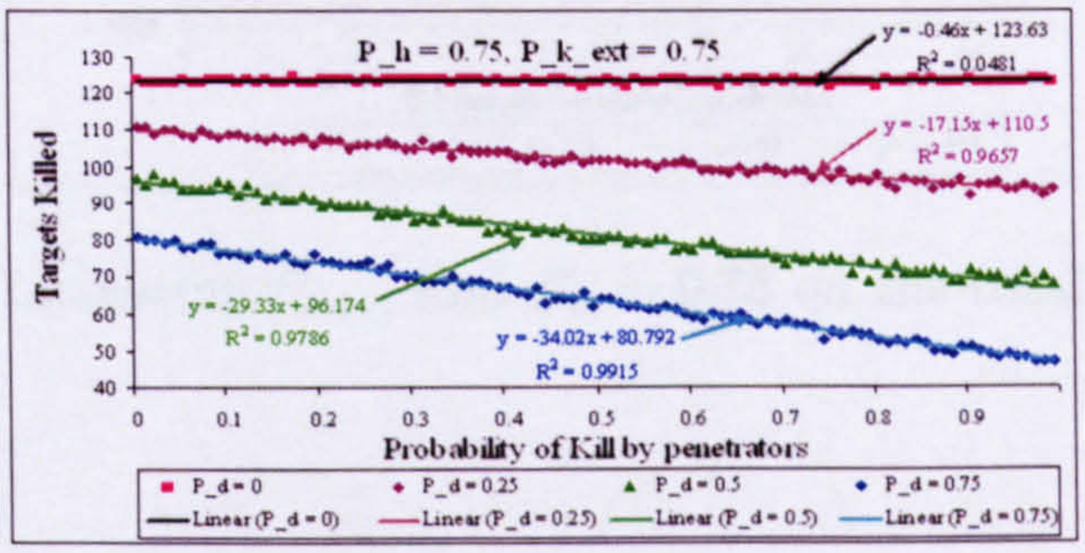

Figure E.22: Effect of P_D and $P_{K_{Non}}$ with increasing $P_{K_{Ext}}$ and $P_H = 0.75$ on the total number of targets killed

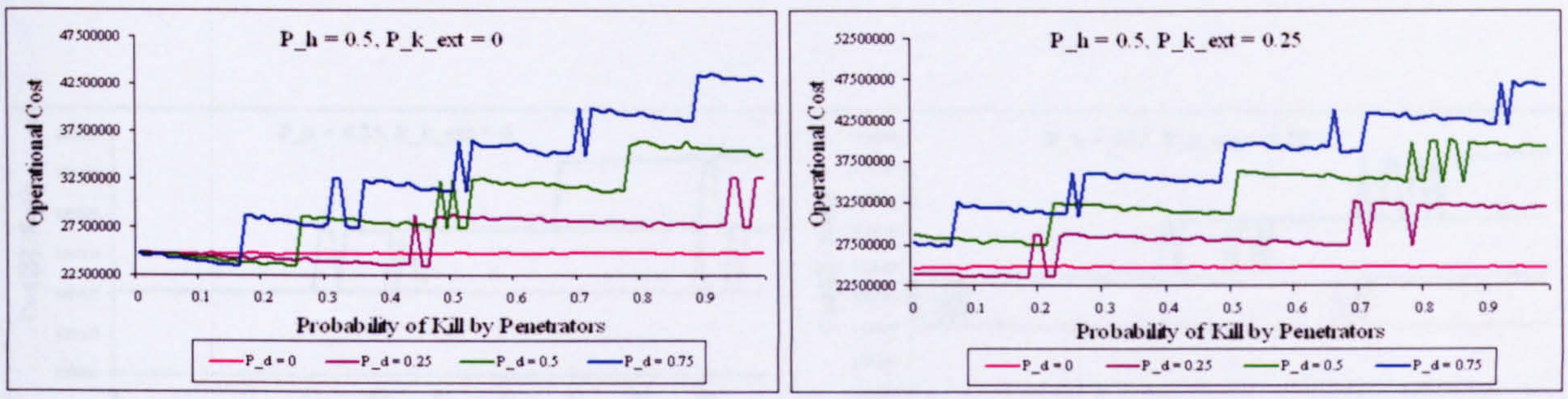

Figure E.23: Effect of P_D and $P_{K_{Non}}$ with increasing $P_{K_{Ext}}$ and $P_H = 0.5$ on the total operational cost

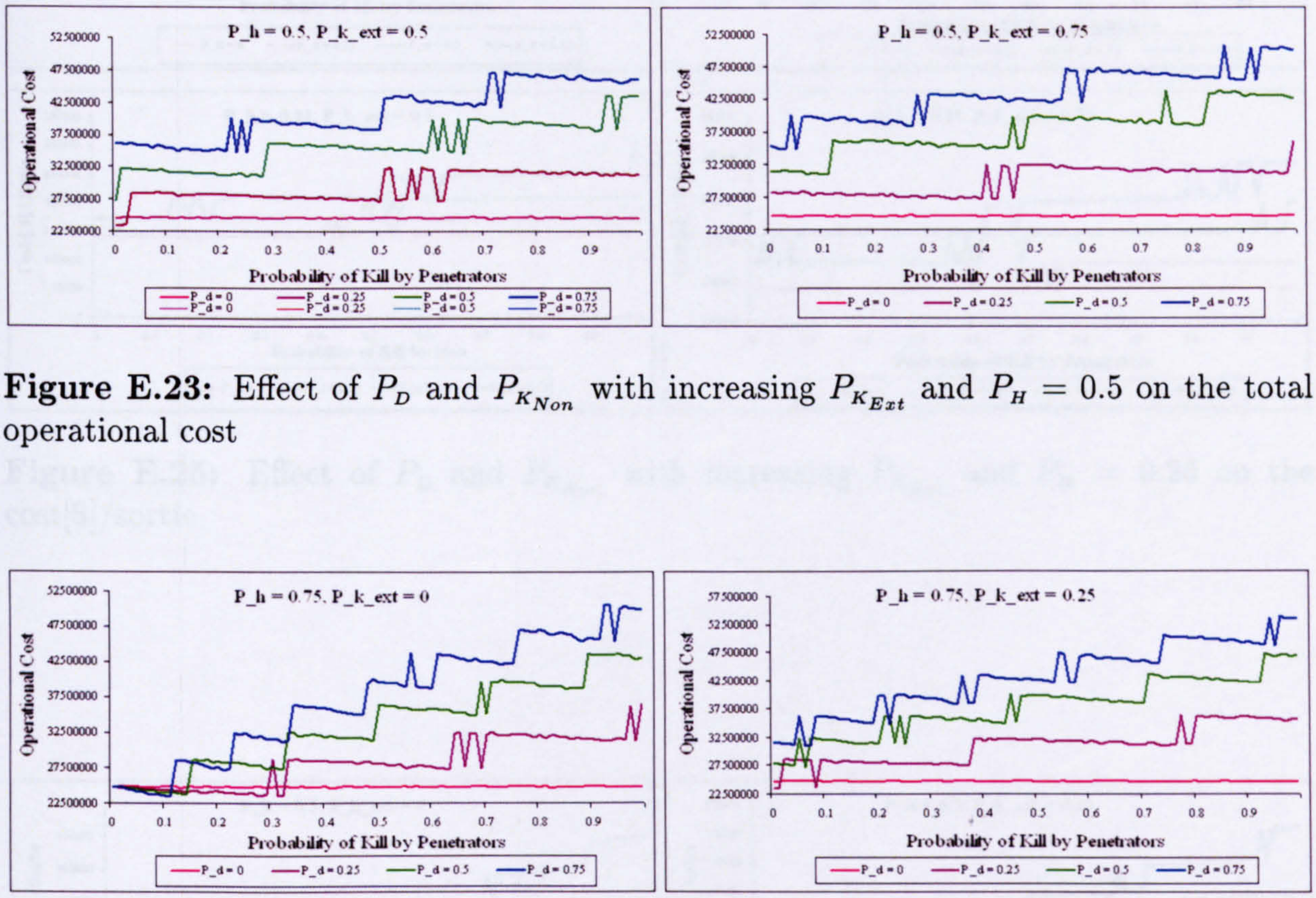

Figure E.24: Effect of P_D and $P_{K_{Non}}$ with increasing $P_{K_{Ext}}$ and $P_H = 0.75$ on the total operational cost

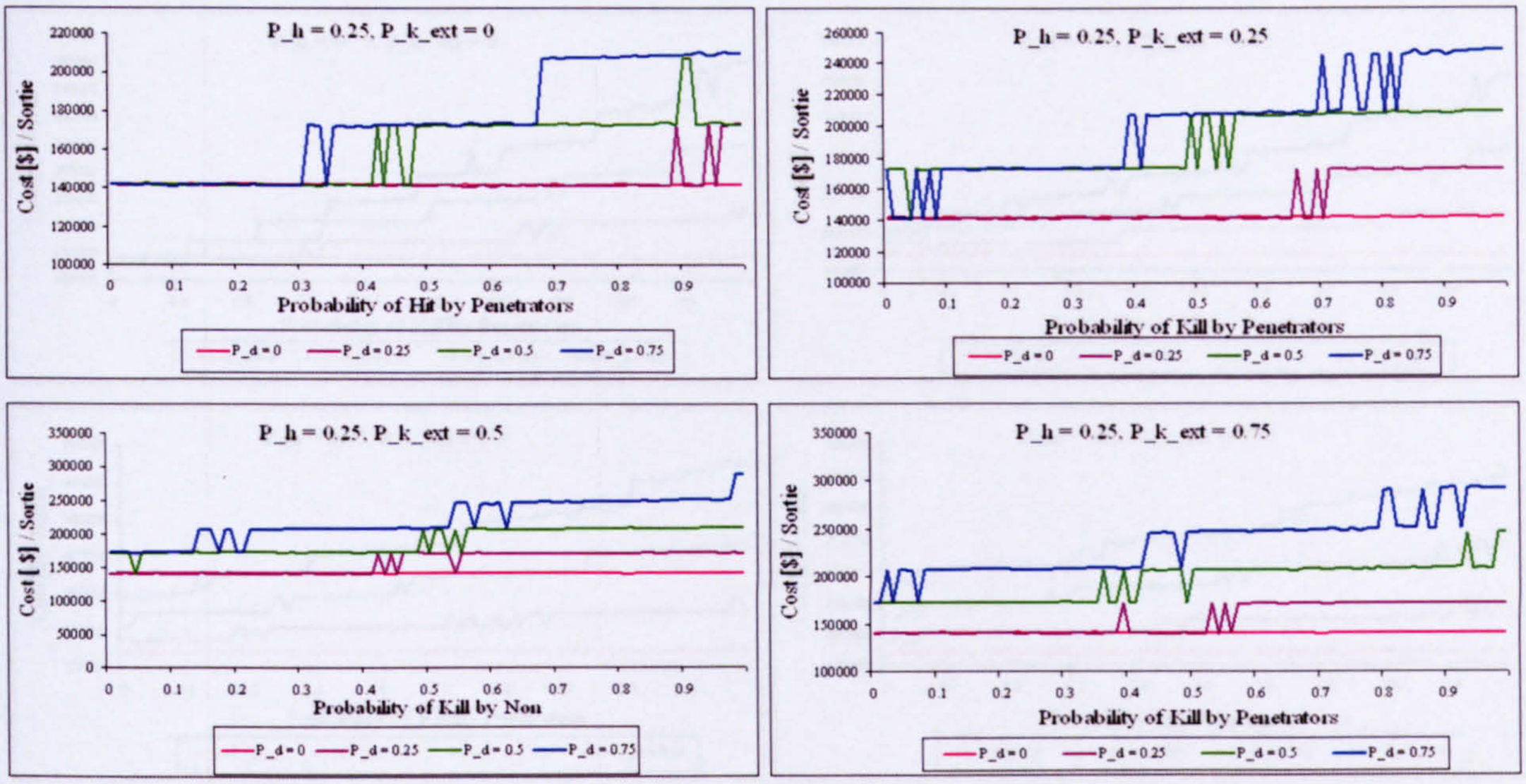

Figure E.25: Effect of P_D and $P_{K_{Non}}$ with increasing $P_{K_{Ext}}$ and $P_H = 0.25$ on the cost[$]/sortie

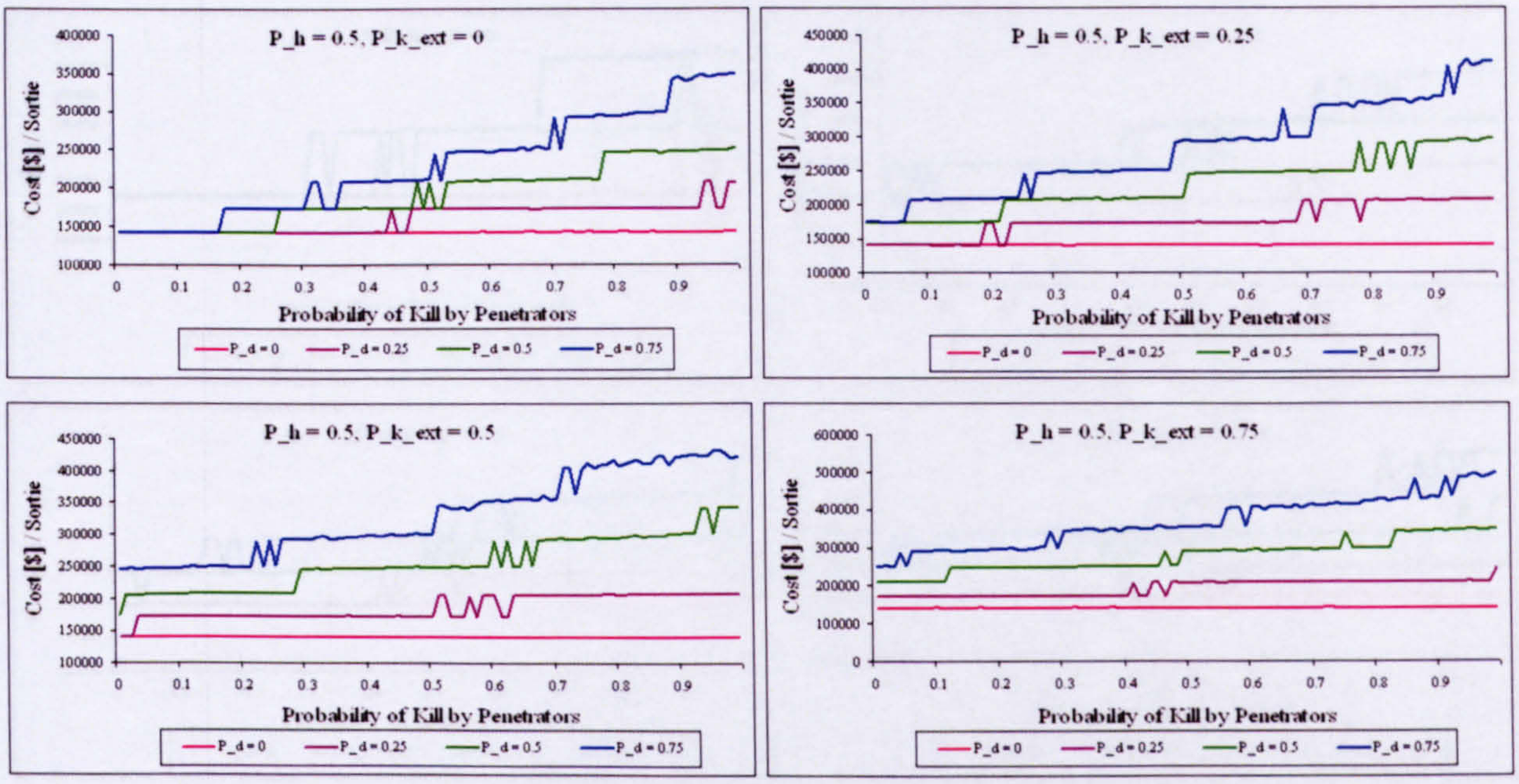

Figure E.26: Effect of P_D and $P_{K_{Non}}$ with increasing $P_{K_{Ext}}$ and $P_H = 0.5$ on the cost[$]/sortie

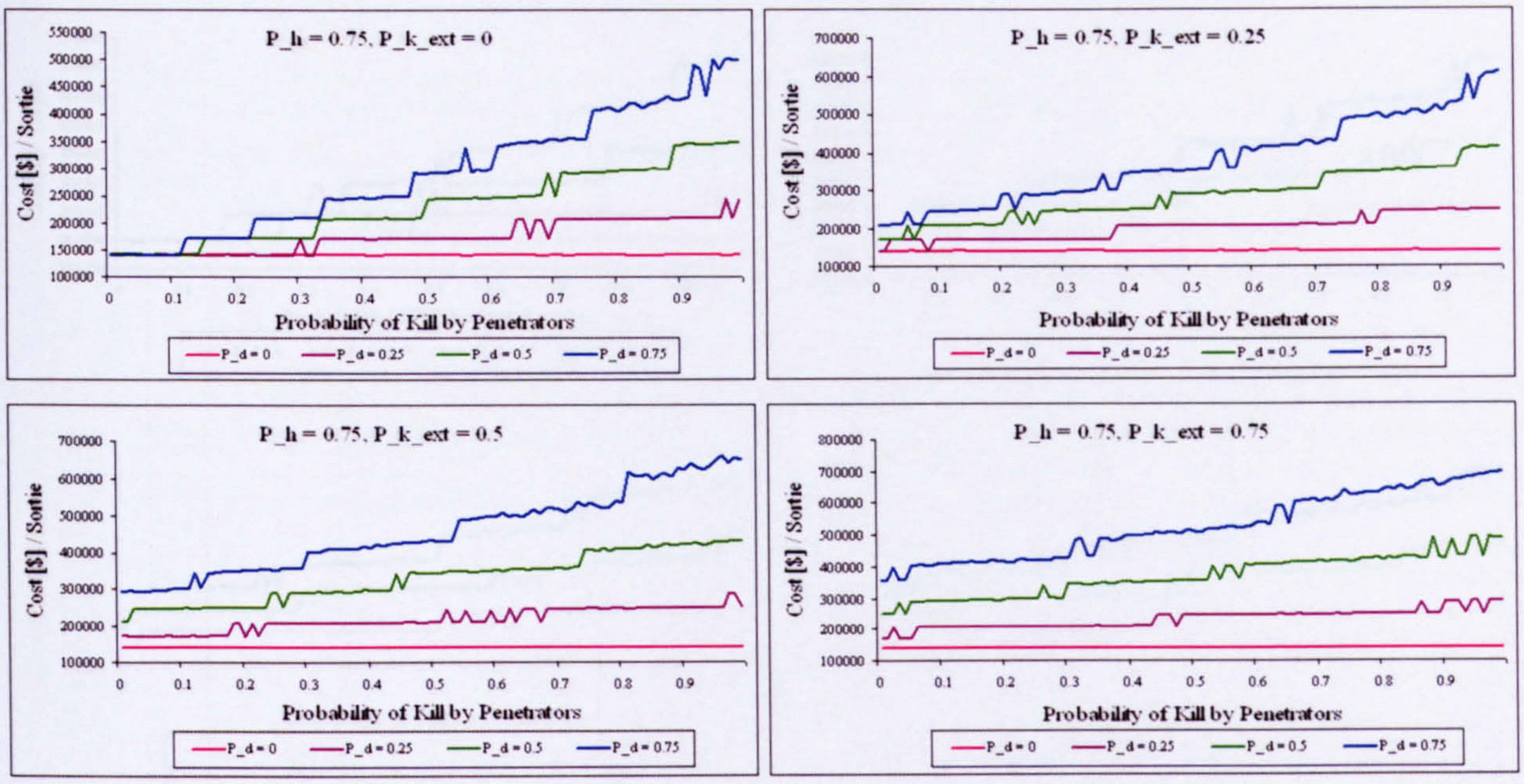

Figure E.27: Effect of P_D and $P_{K_{Non}}$ with increasing $P_{K_{Ext}}$ and $P_H = 0.75$ on the cost[$]/sortie

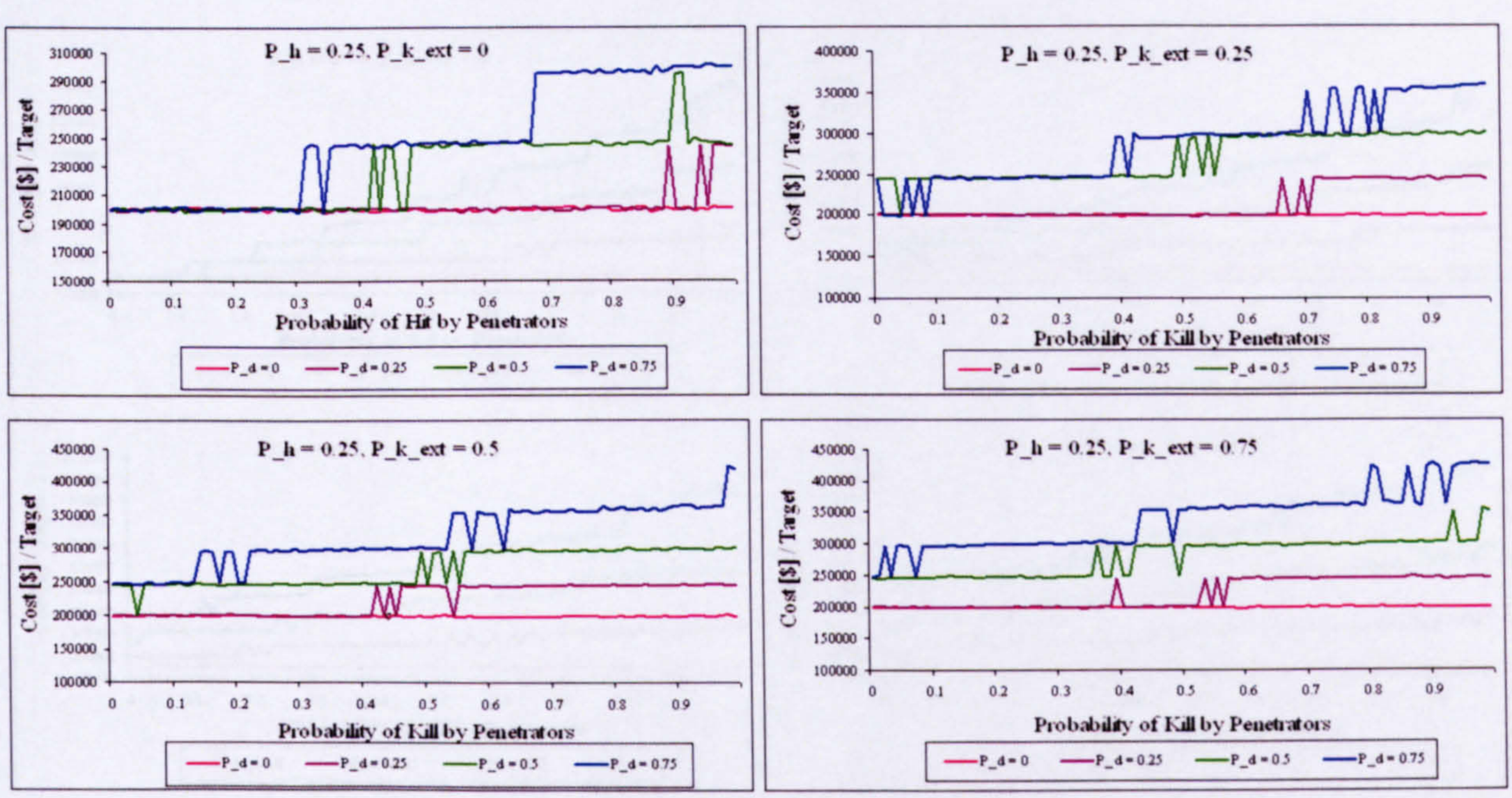

Figure E.28: Effect of P_D and $P_{K_{Non}}$ with increasing $P_{K_{Ext}}$ and $P_H = 0.25$ on the cost[$]/target

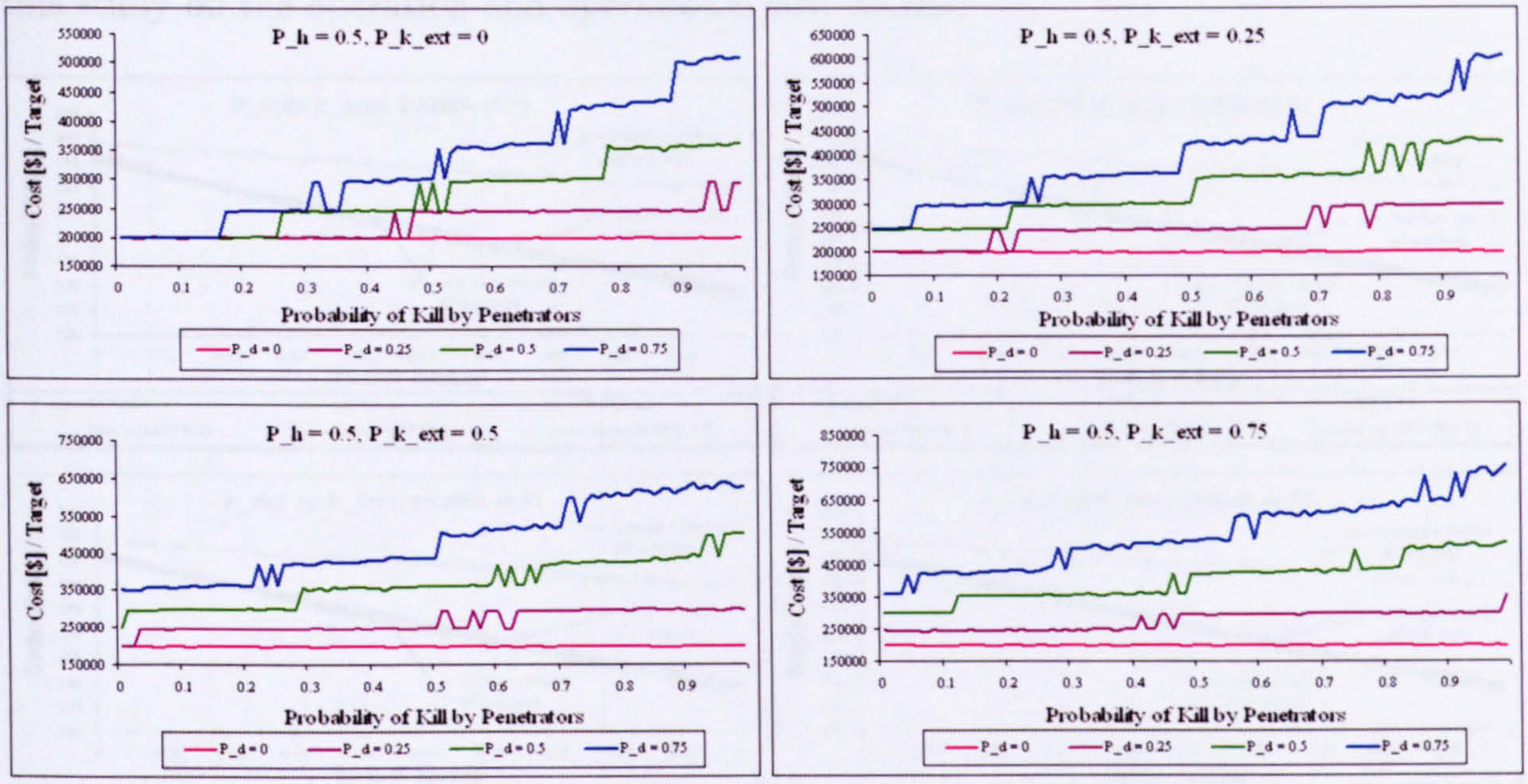

Figure E.29: Effect of P_D and $P_{K_{Non}}$ with increasing $P_{K_{Ext}}$ and $P_H = 0.5$ on the cost[$]/target

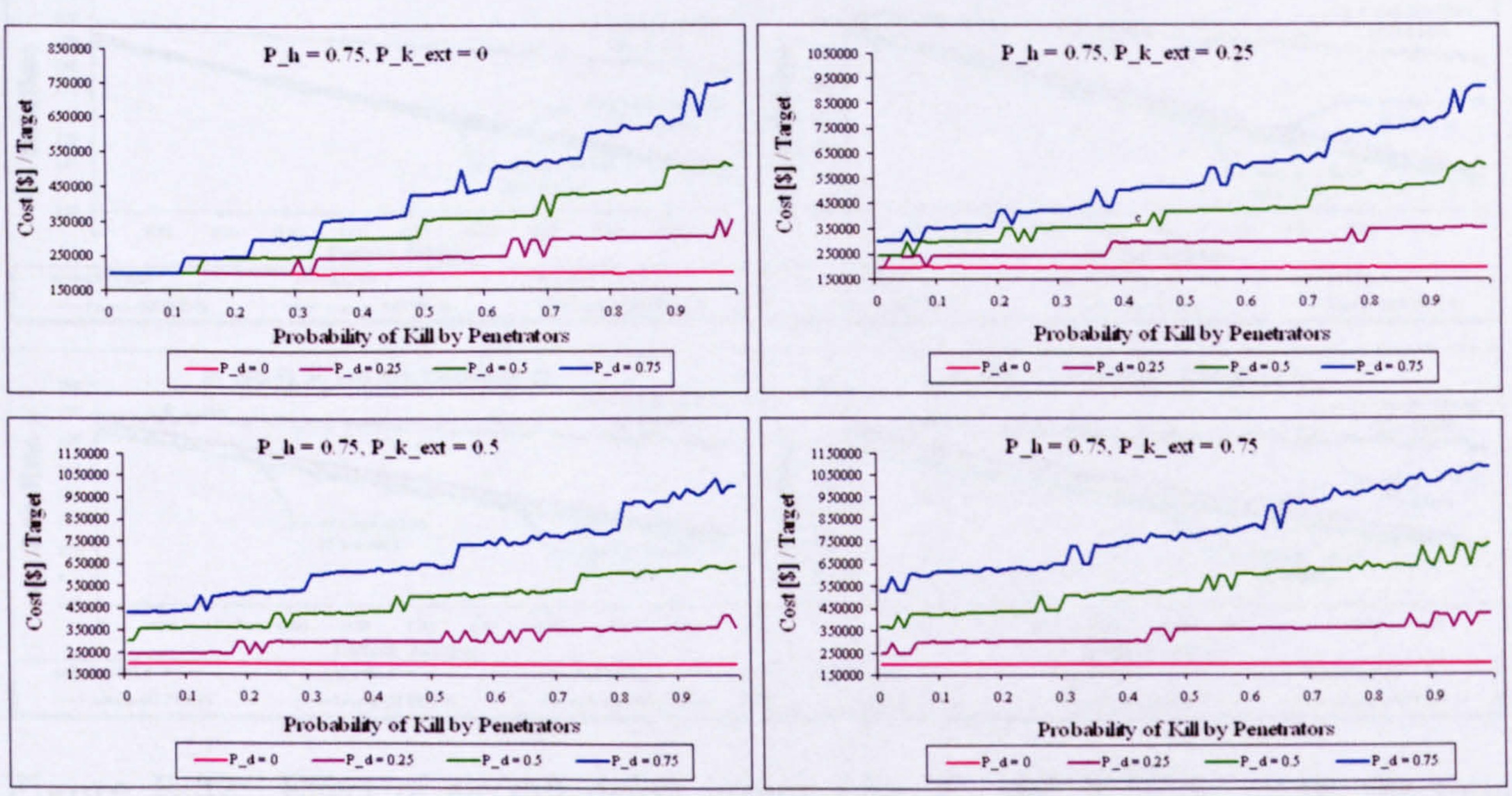

Figure E.30: Effect of P_D and $P_{K_{Non}}$ with increasing $P_{K_{Ext}}$ and $P_H = 0.75$ on the cost[$]/target

Fig. E.31 - E.49 show the results of the effect of all major aircraft MOPs predicted in this study on the operation and operational cost MOEs.

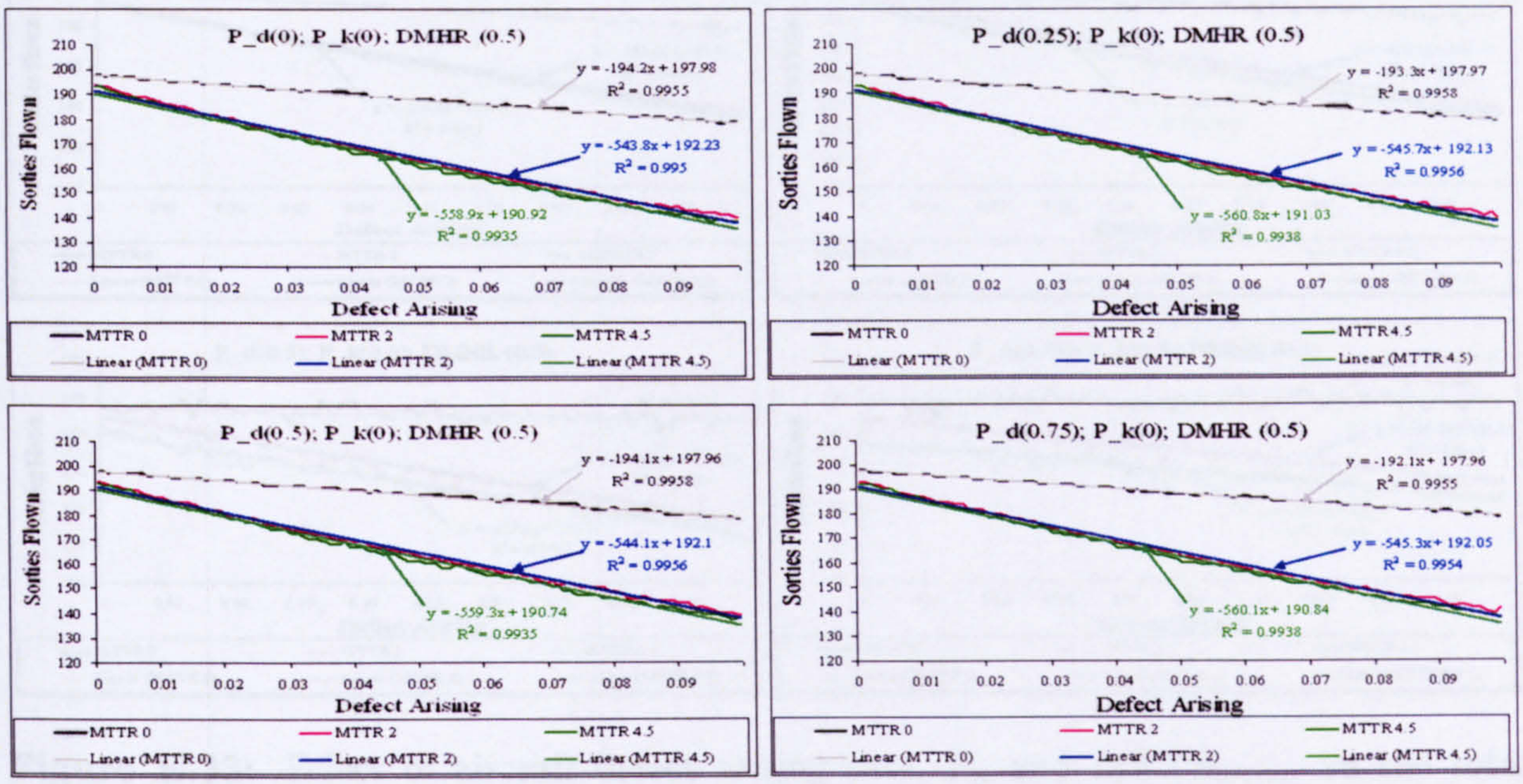

Figure E.31: Effect of aircraft defect arising rate, P_D and $MTTR_{Defect}$ on the total number of sorties flown with $P_{K_{Non}} = P_{K_{Ext}} = 0.00$

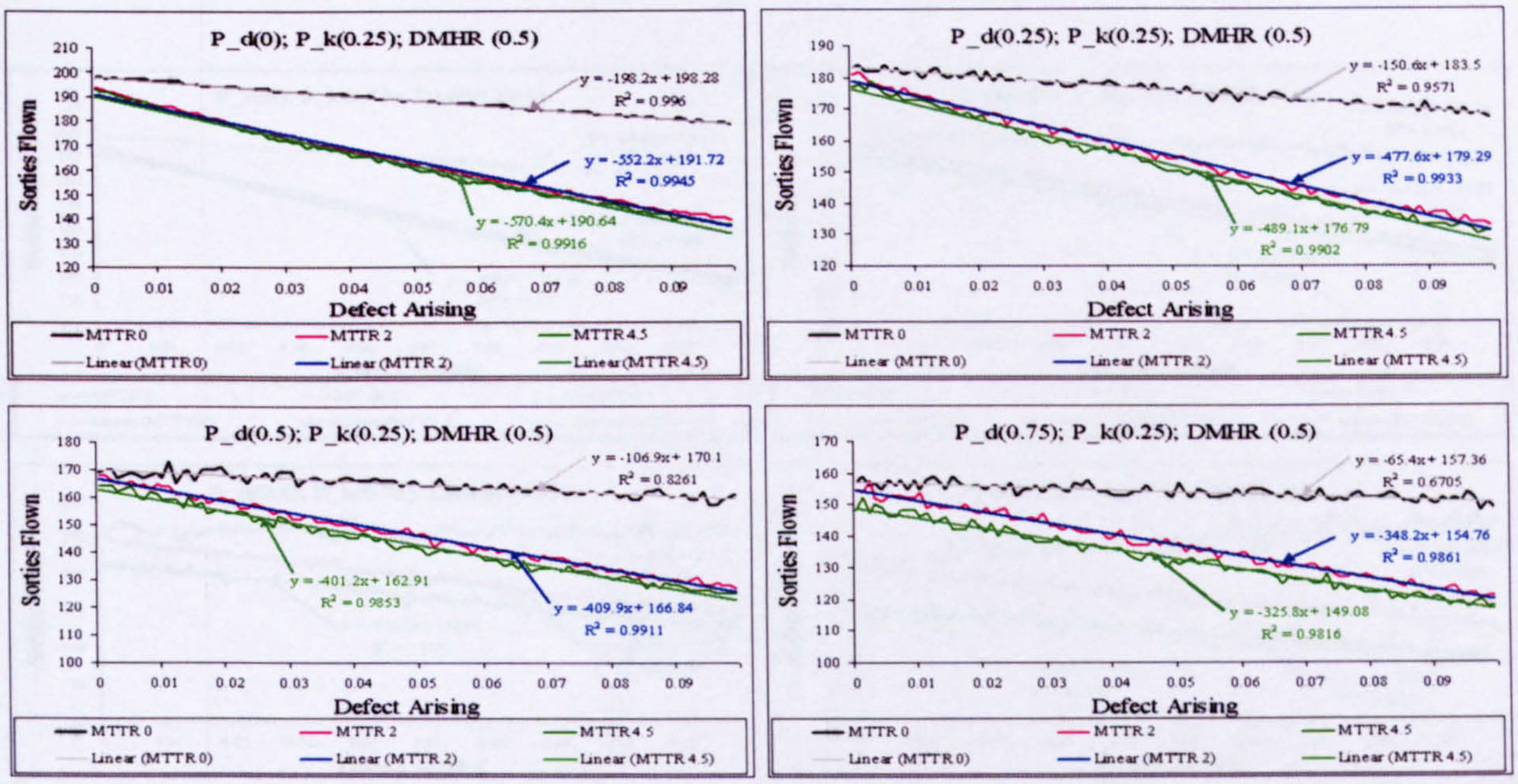

Figure E.32: Effect of aircraft defect arising rate, P_D and $MTTR_{Defect}$ on the total number of sorties flown with $P_{K_{Non}} = P_{K_{Ext}} = 0.25$

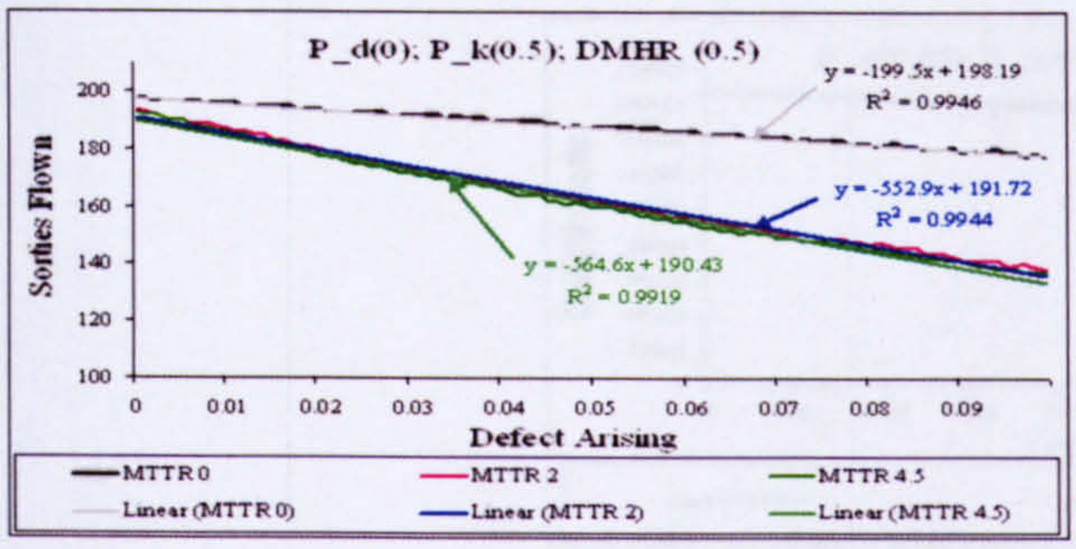

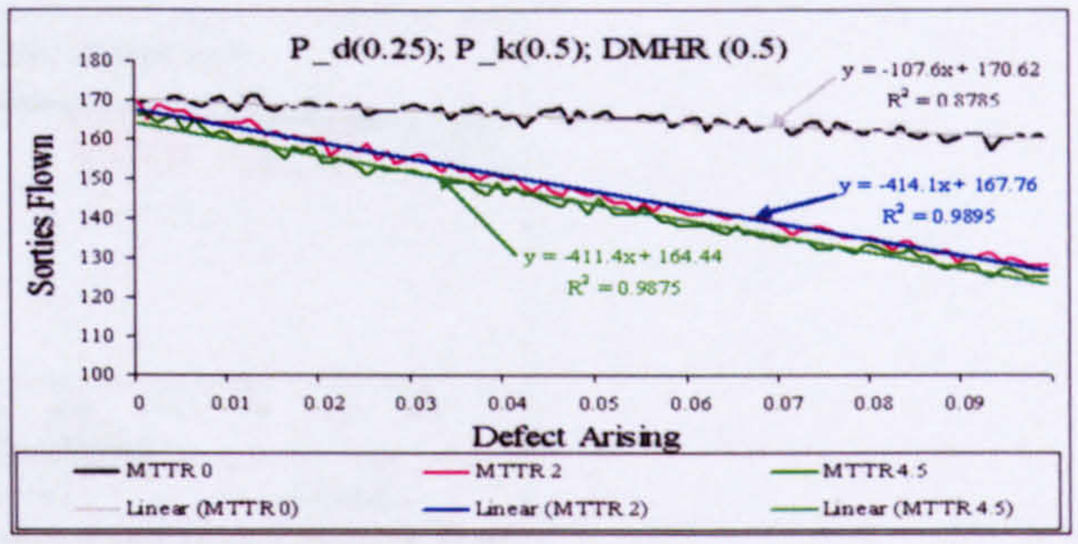

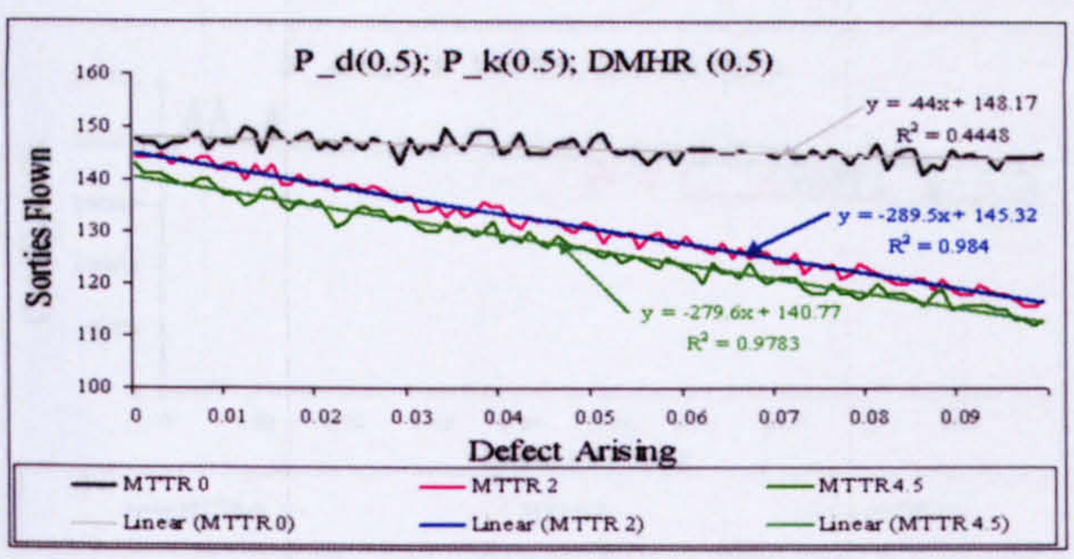

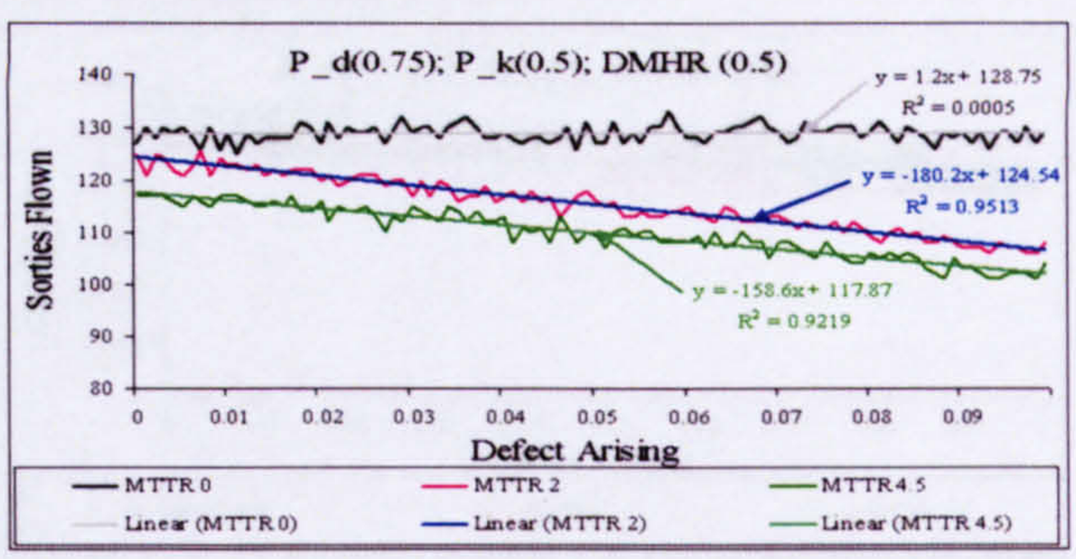

Figure E.33: Effect of aircraft defect arising rate, P_D and $MTTR_{Defect}$ on the total number of sorties flown with $P_{K_{Non}} = P_{K_{Ext}} = 0.50$

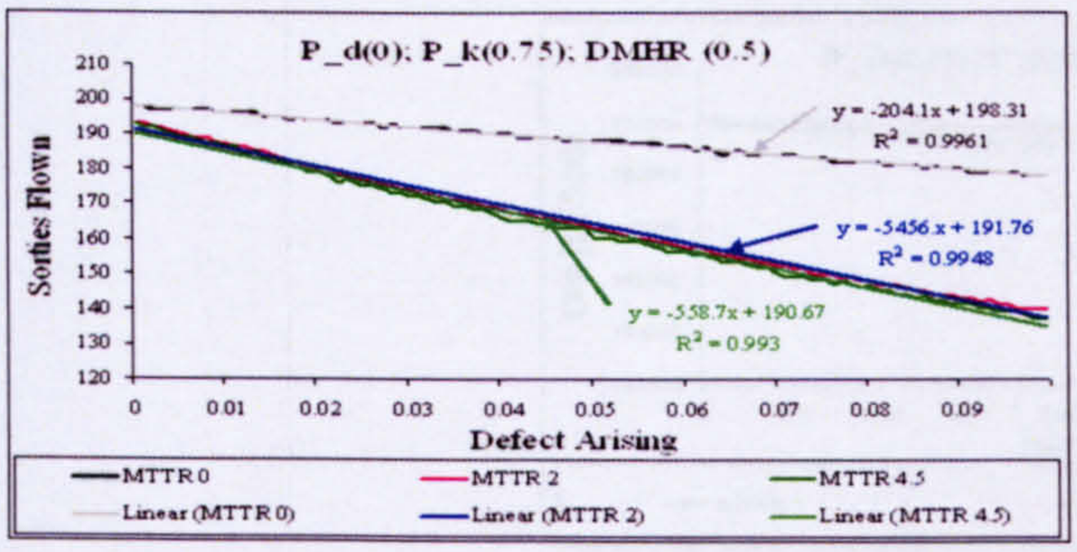

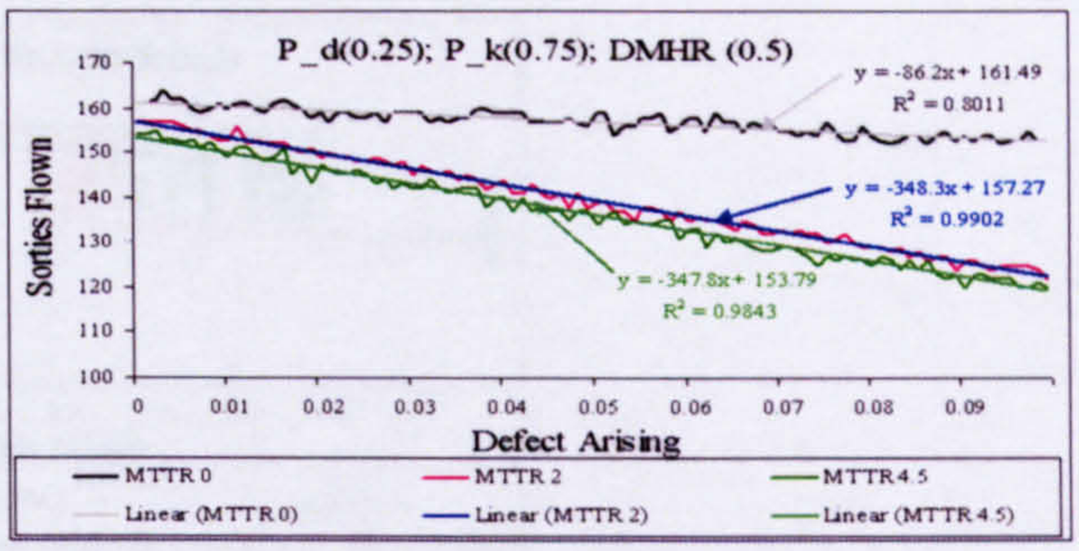

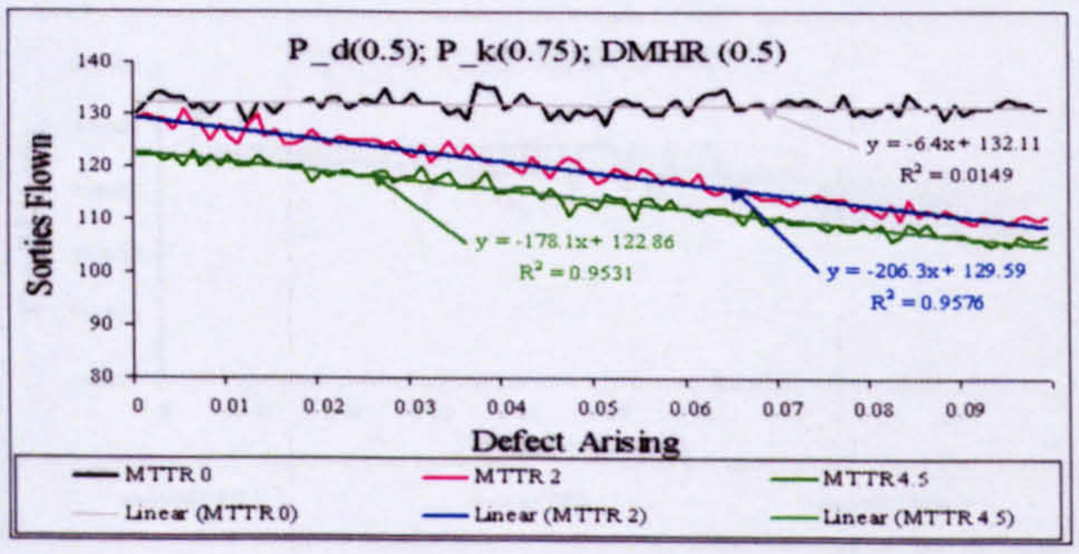

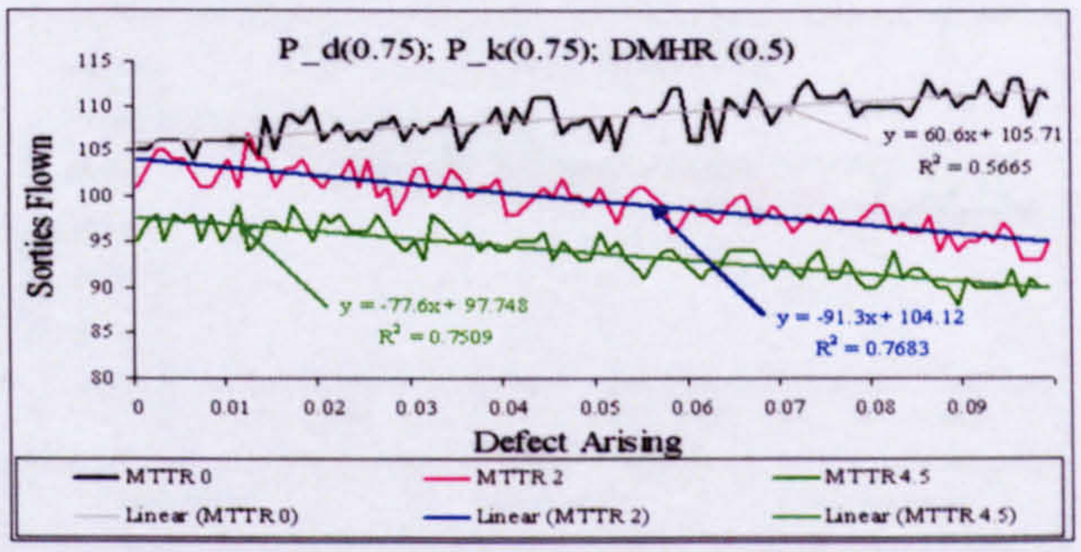

Figure E.34: Effect of aircraft defect arising rate, P_D and $MTTR_{Defect}$ on the total number of sorties flown with $P_{K_{Non}} = P_{K_{Ext}} = 0.75$

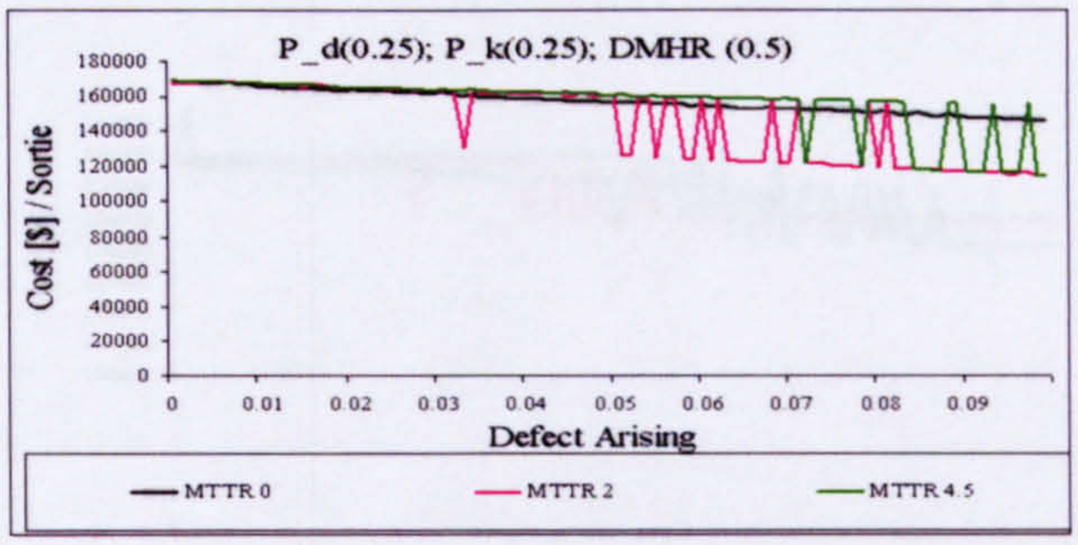

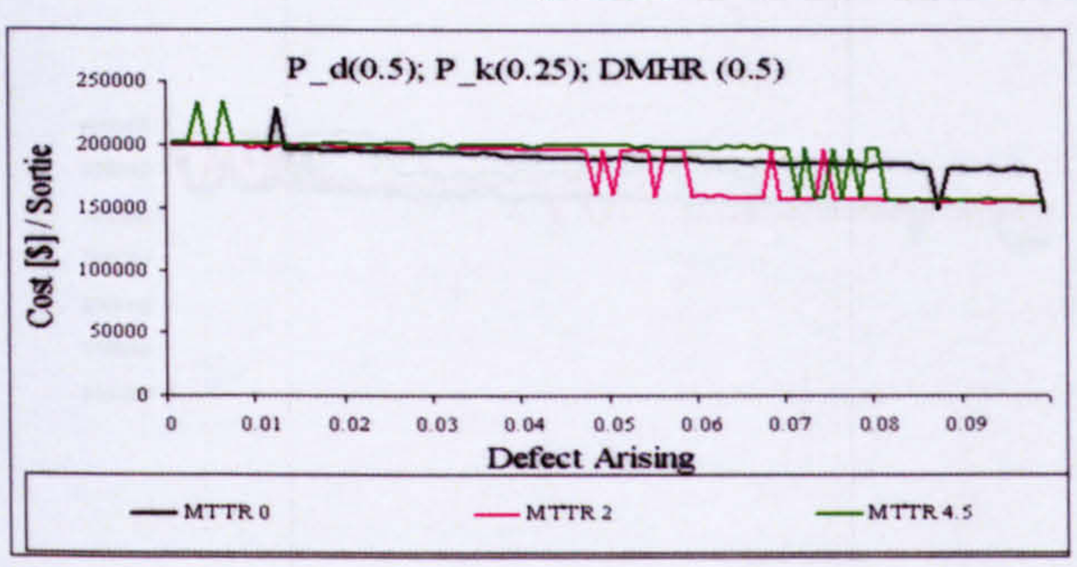

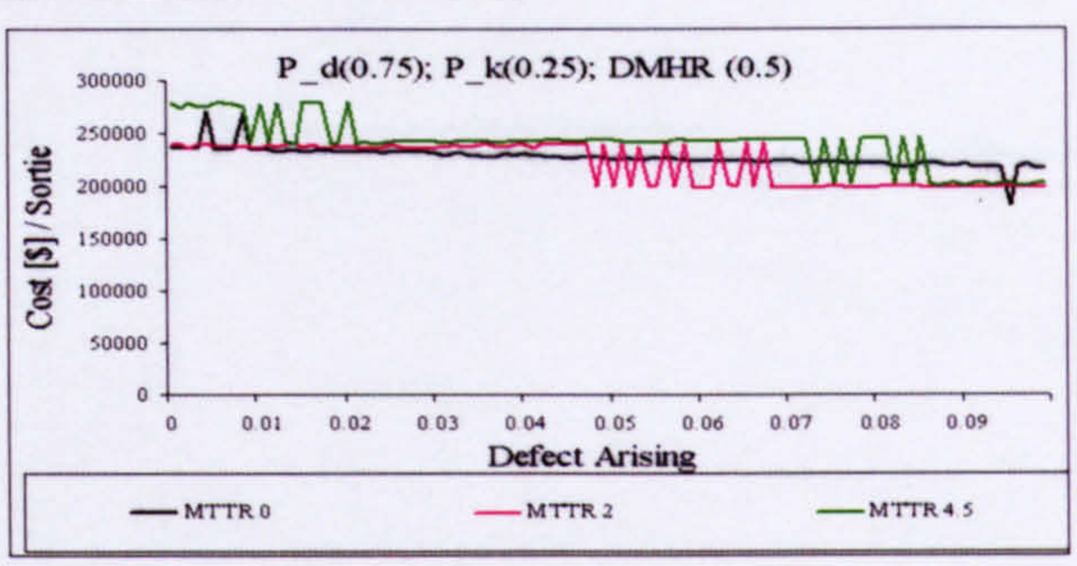

Figure E.35: Effect of aircraft defect arising rate, P_D and $MTTR_{Defect}$ on cost[$]/sortie with $P_{K_{Non}} = P_{K_{Ext}} = 0.25$

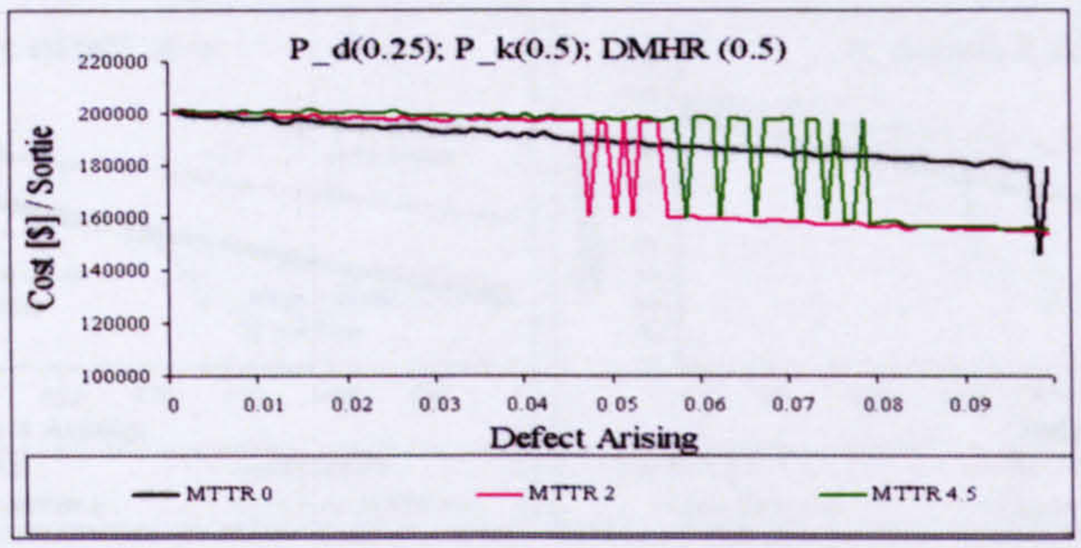

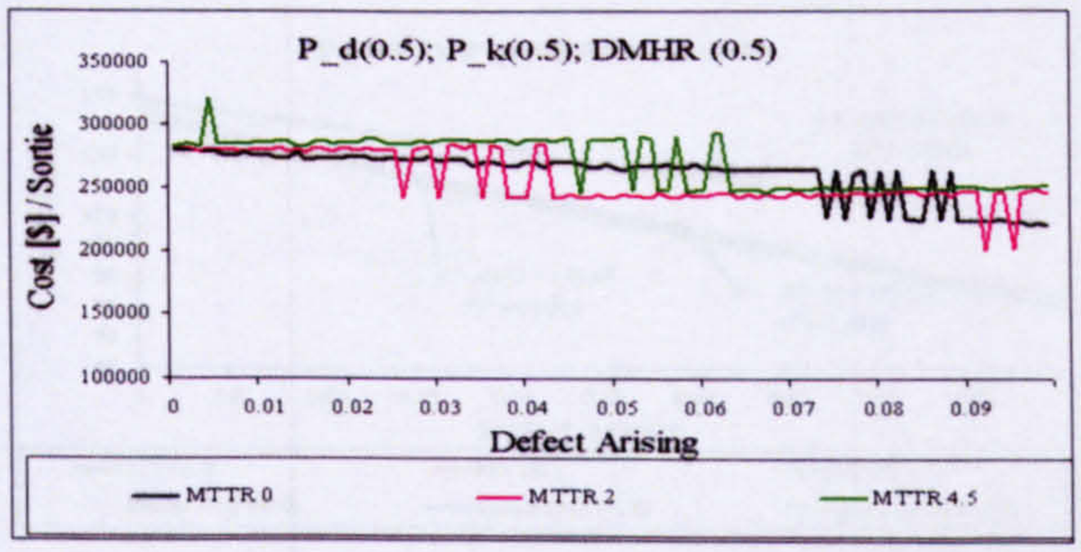

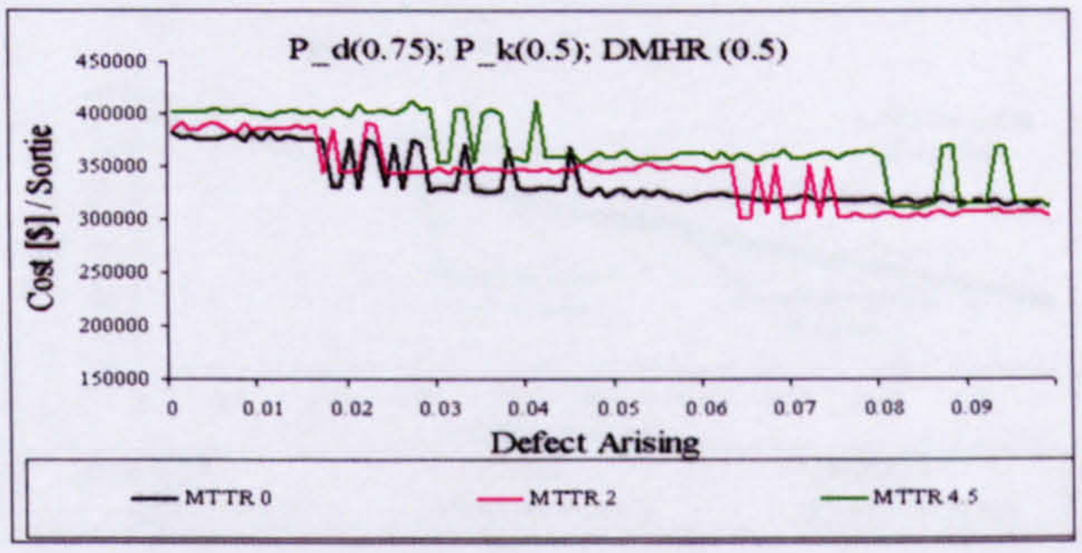

Figure E.36: Effect of aircraft defect arising rate, P_D and $MTTR_{Defect}$ on cost[$]/sortie with $P_{K_{Non}} = P_{K_{Ext}} = 0.50$

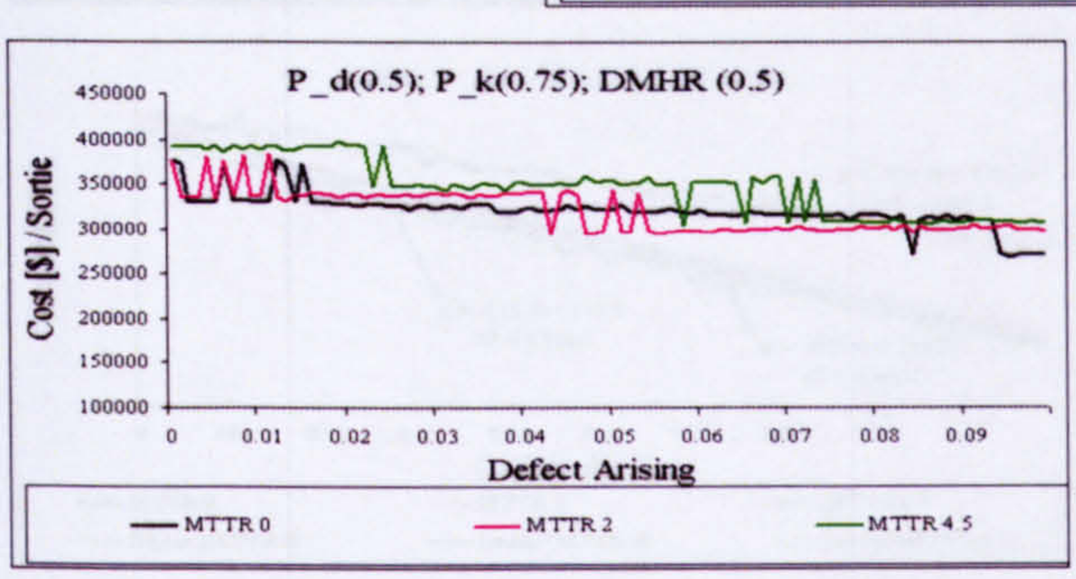

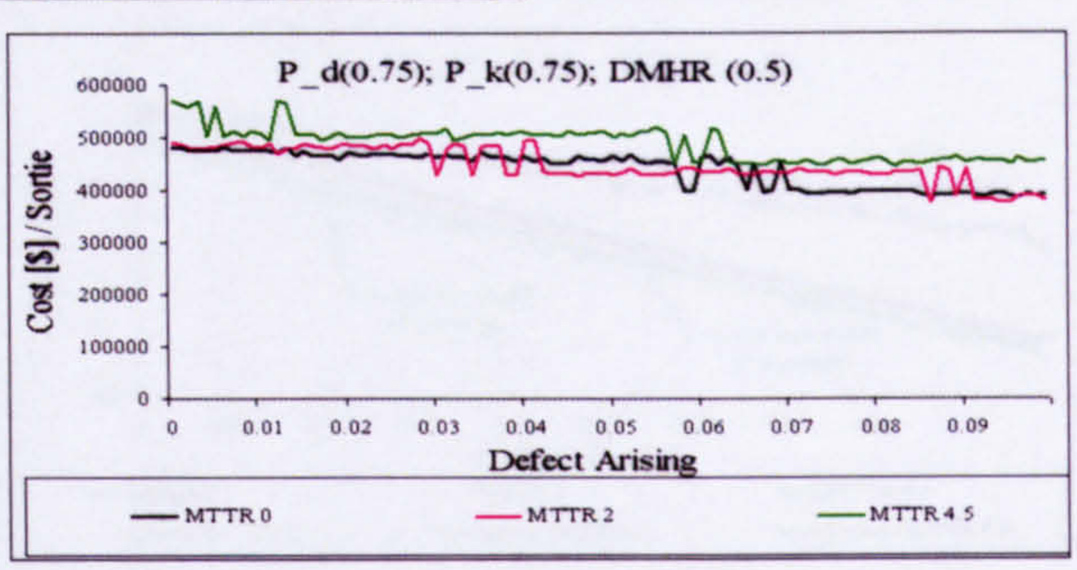

Figure E.37: Effect of aircraft defect arising rate, P_D and $MTTR_{Defect}$ on cost[$]/sortie with $P_{K_{Non}} = P_{K_{Ext}} = 0.75$

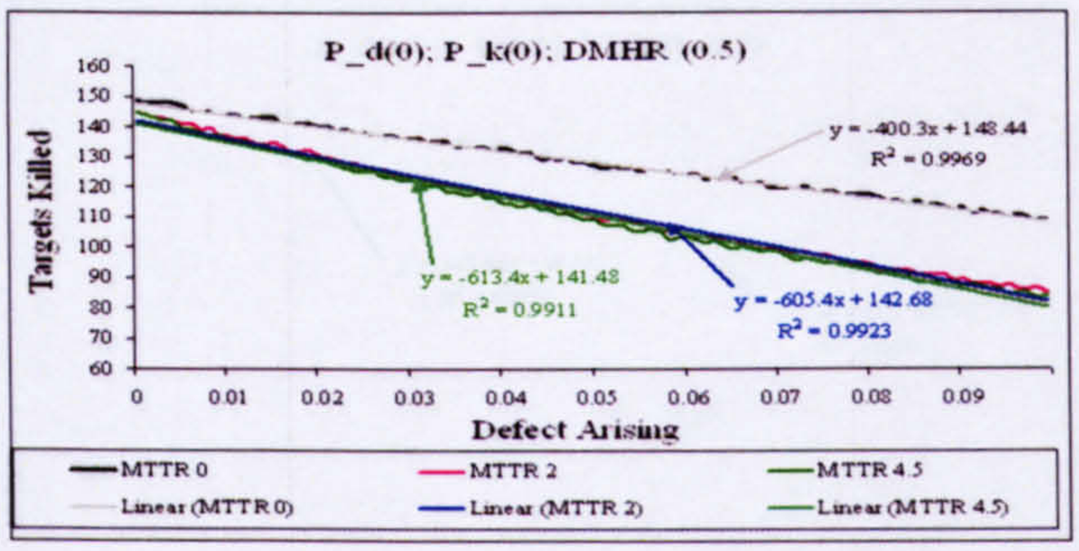

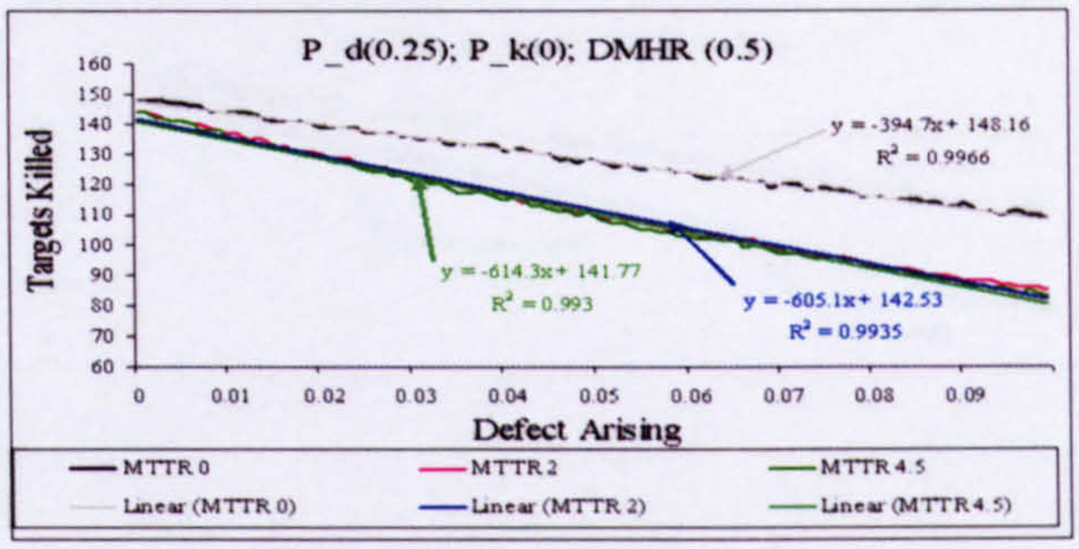

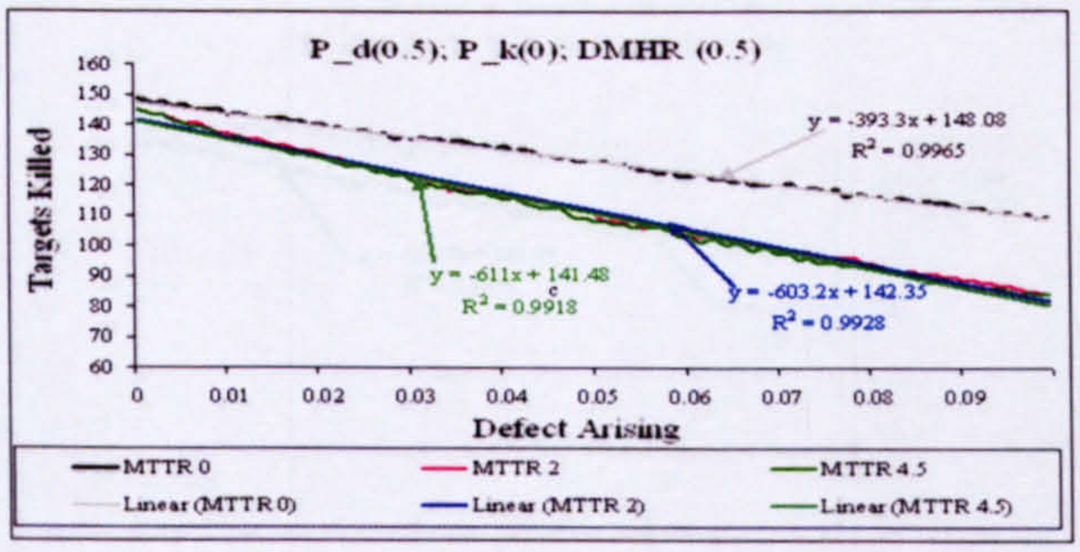

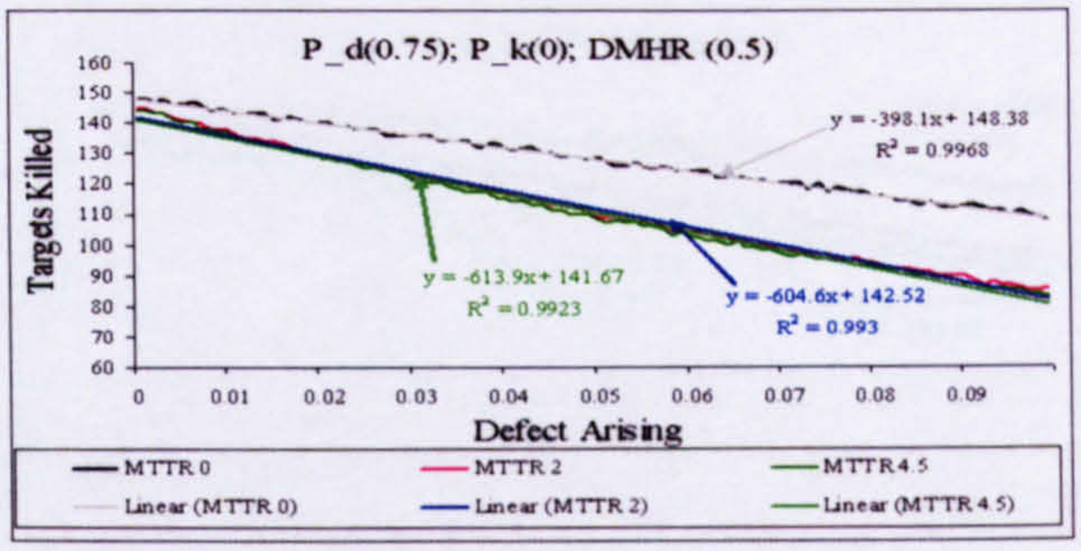

Figure E.38: Effect of aircraft defect arising rate, P_D and $MTTR_{Defect}$ on the total number of targets killed with $P_{K_{Non}} = P_{K_{Ext}} = 0.00$

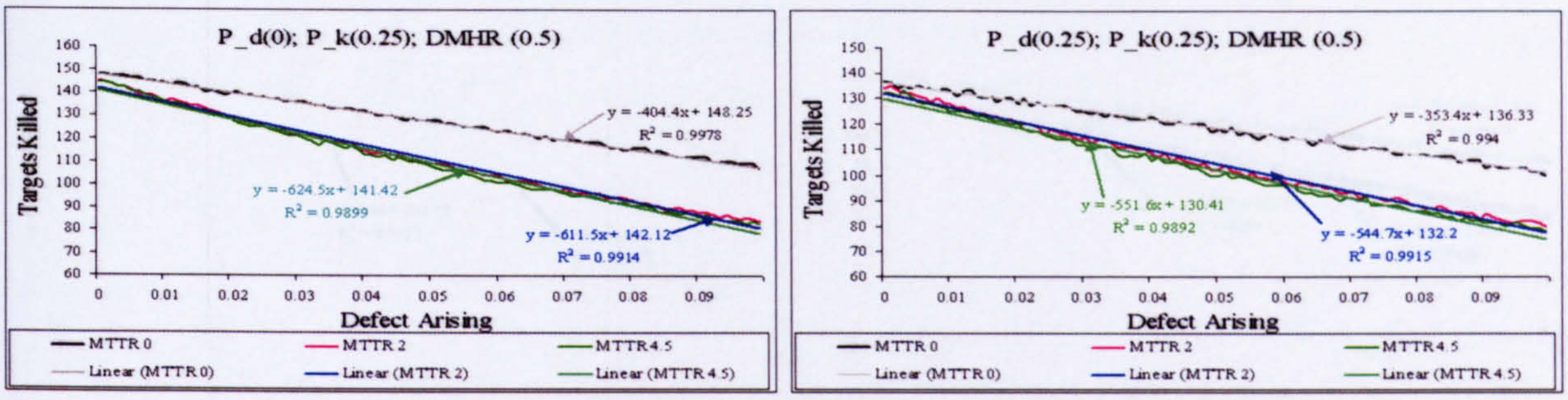

Figure E.39: Effect of aircraft defect arising rate, P_D and $MTTR_{Defect}$ on the total number of targets killed with $P_{K_{Non}} = P_{K_{Ext}} = 0.25$

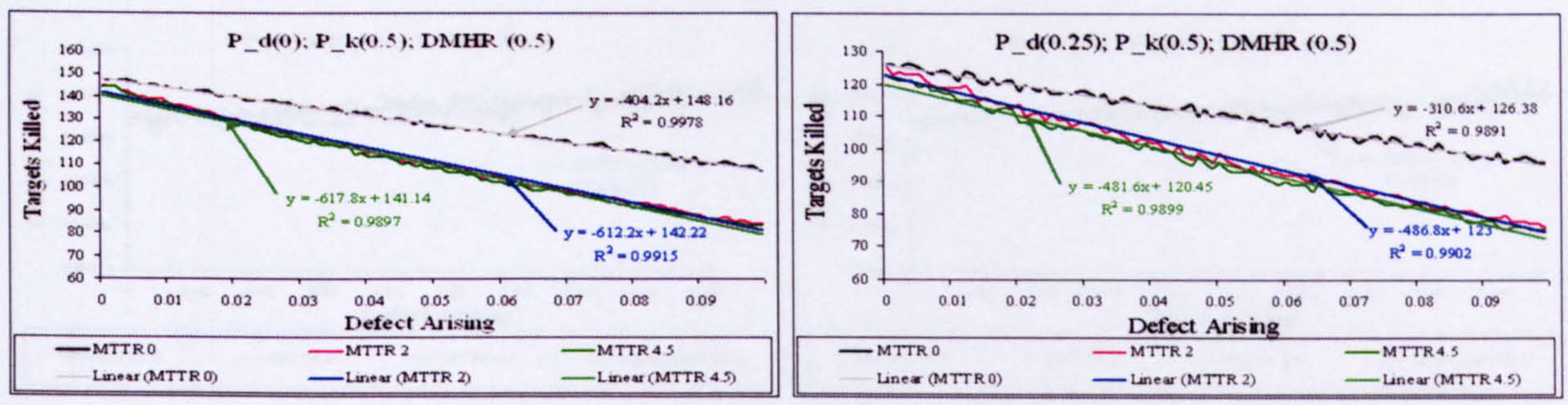

Figure E.40: Effect of aircraft defect arising rate, P_D and $MTTR_{Defect}$ on the total number of targets killed with $P_{K_{Non}} = P_{K_{Ext}} = 0.50$

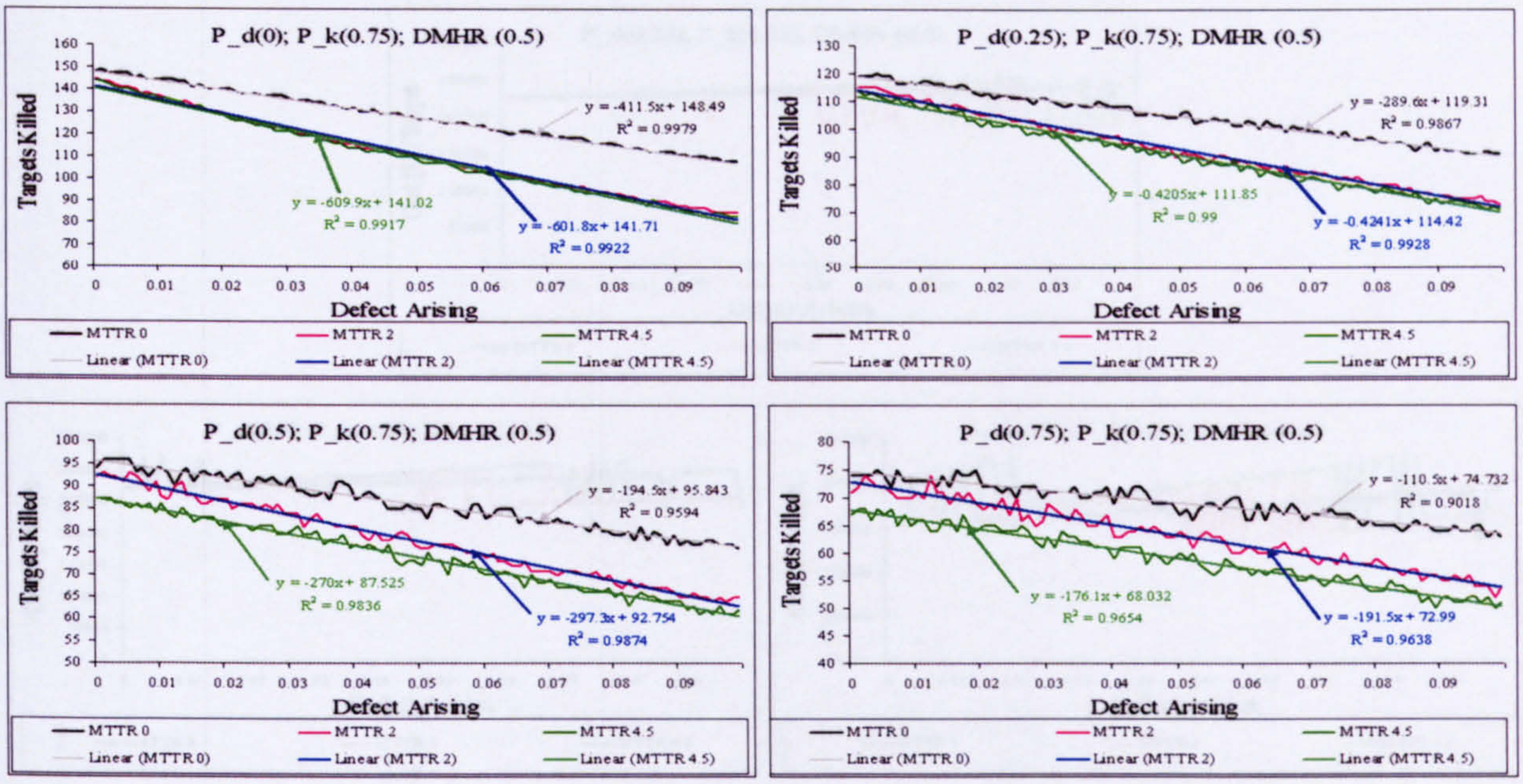

Figure E.41: Effect of aircraft defect arising rate, P_D and $MTTR_{Defect}$ on the total number of targets killed with $P_{K_{Non}} = P_{K_{Ext}} = 0.75$

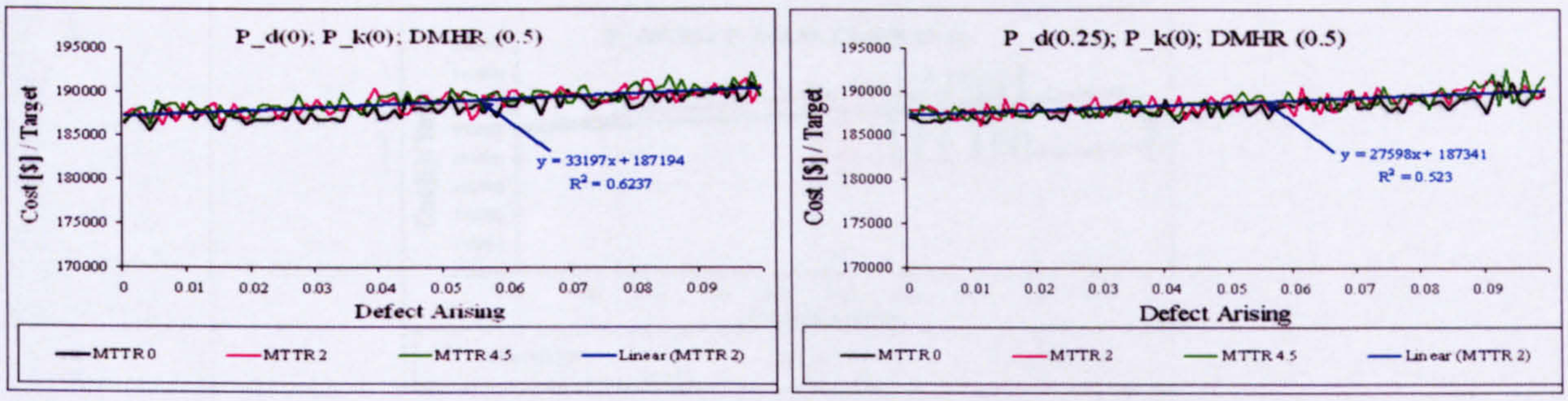

Figure E.42: Effect of aircraft defect arising rate, P_D and $MTTR_{Defect}$ on cost[$]/target with $P_{K_{Non}} = P_{K_{Ext}} = 0.00$

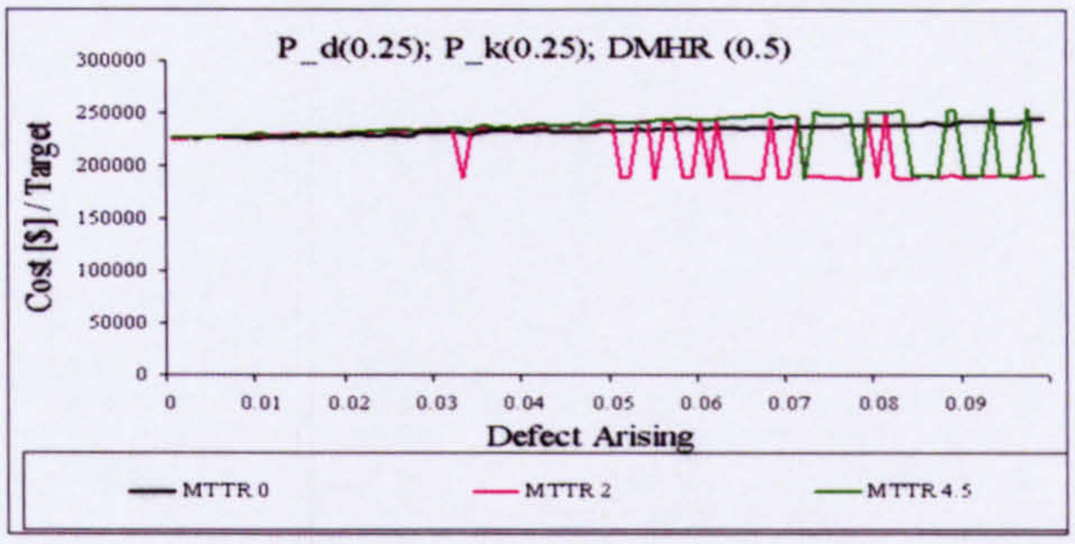

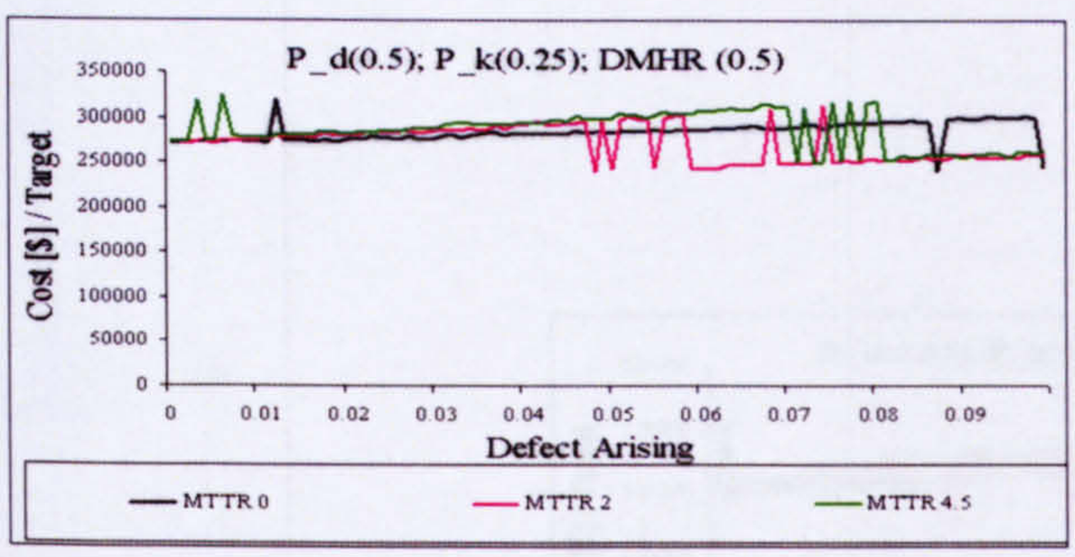

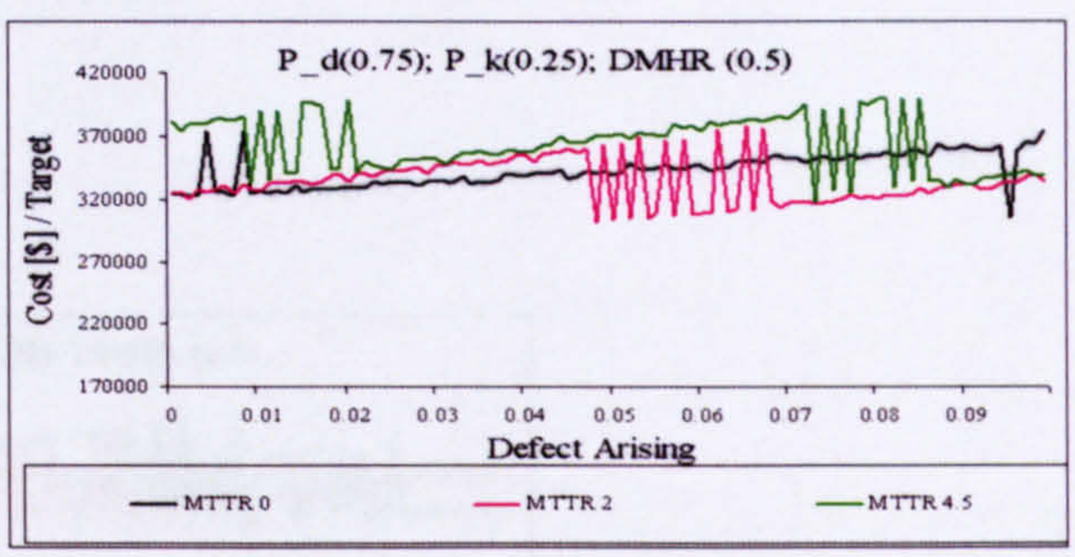

Figure E.43: Effect of aircraft defect arising rate, P_D and $MTTR_{Defect}$ on cost[$]/target with $P_{K_{Non}} = P_{K_{Ext}} = 0.25$

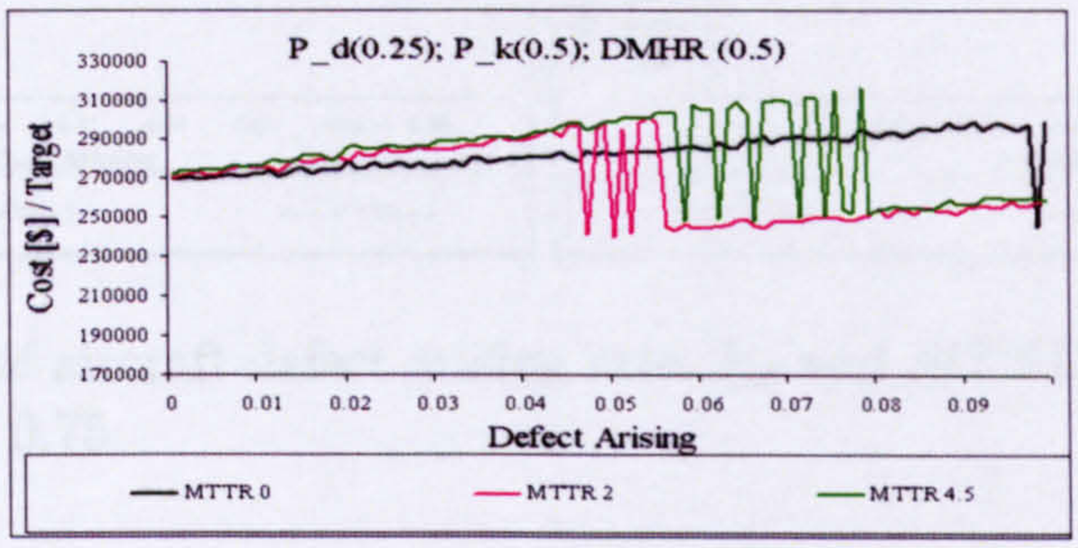

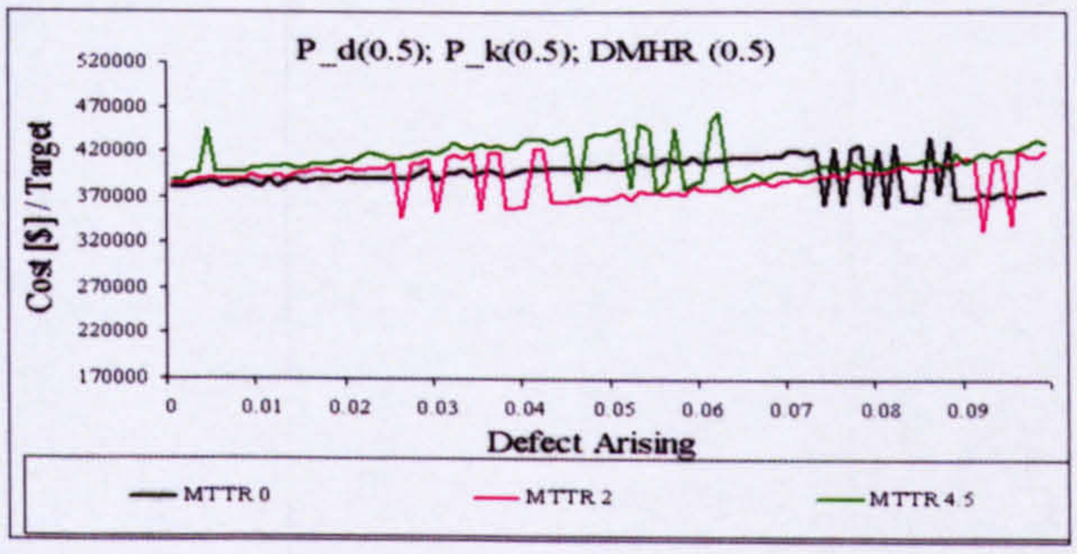

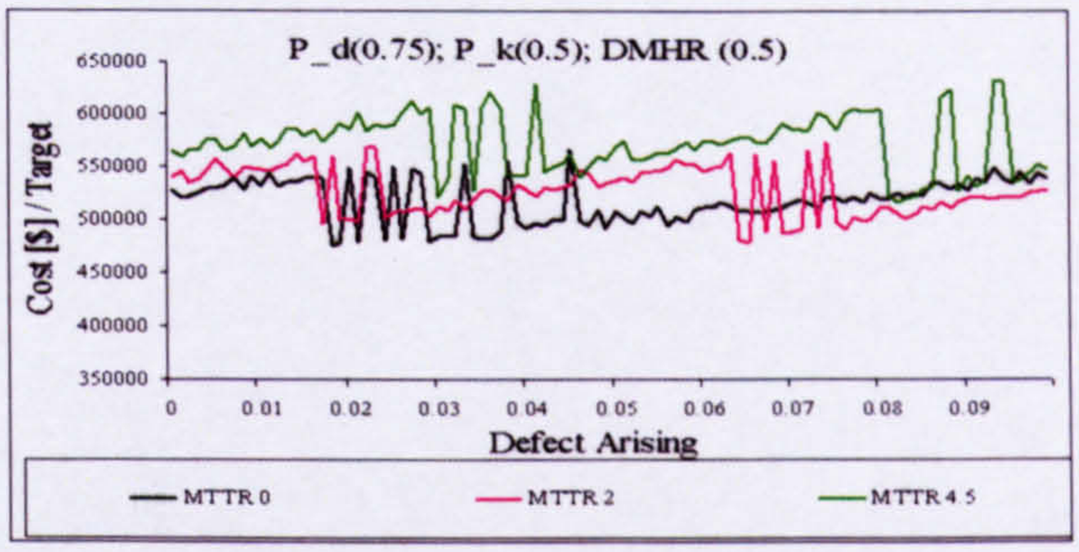

Figure E.44: Effect of aircraft defect arising rate, P_D and $MTTR_{Defect}$ on cost[$]/target with $P_{K_{Non}} = P_{K_{Ext}} = 0.50$

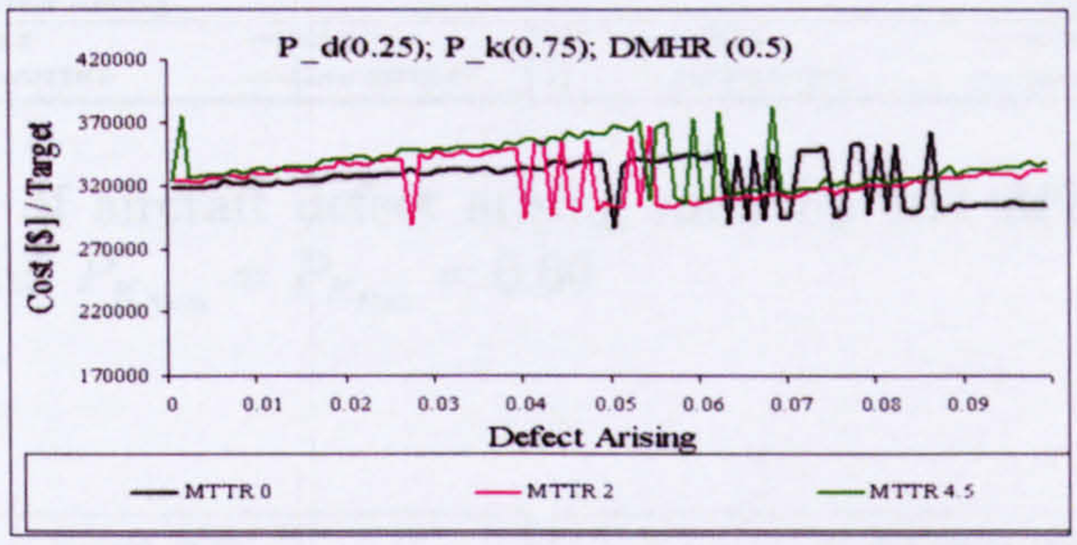

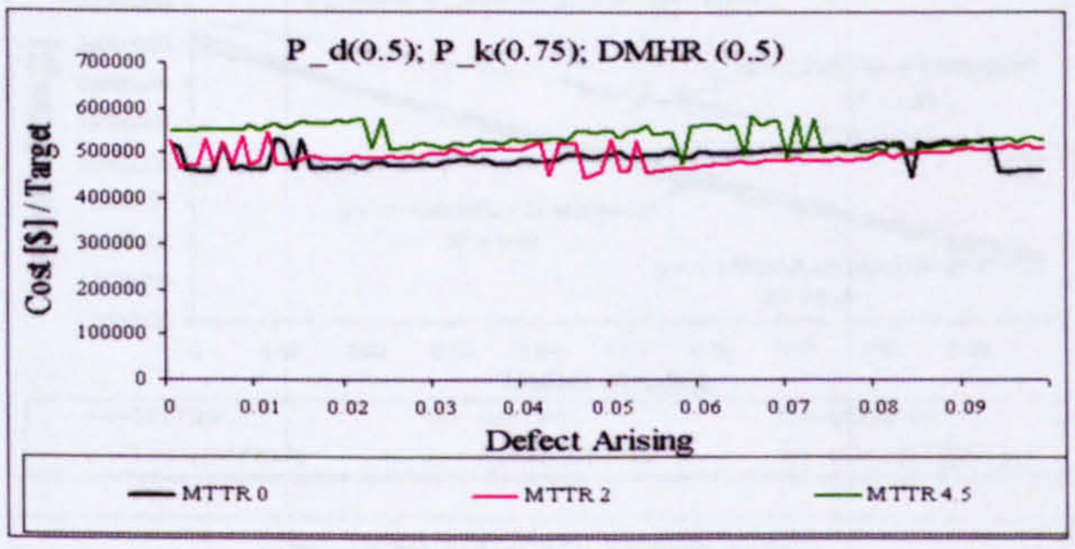

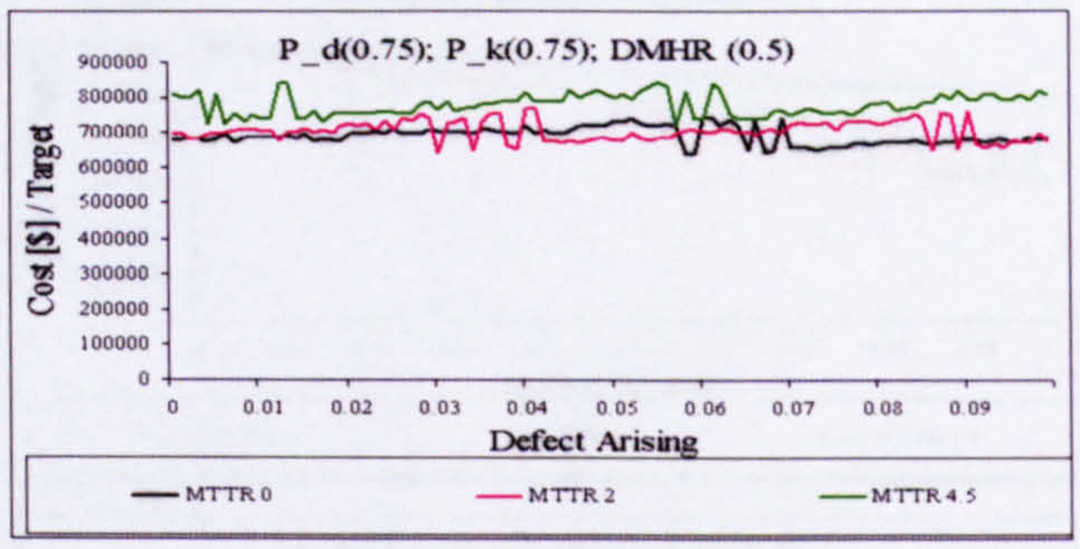

Figure E.45: Effect of aircraft defect arising rate, P_D and $MTTR_{Defect}$ on cost[$]/target with $P_{K_{Non}} = P_{K_{Ext}} = 0.75$

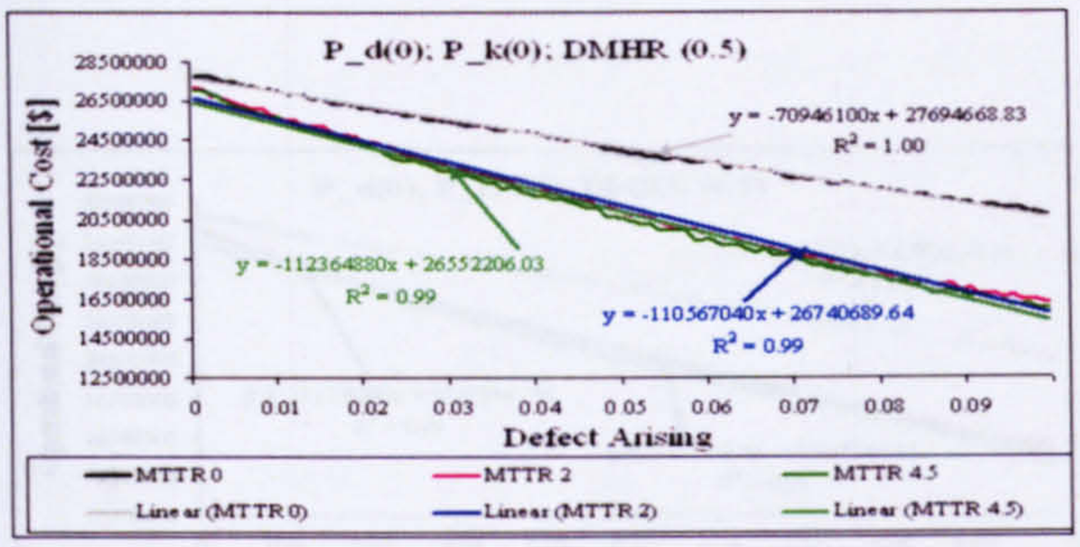

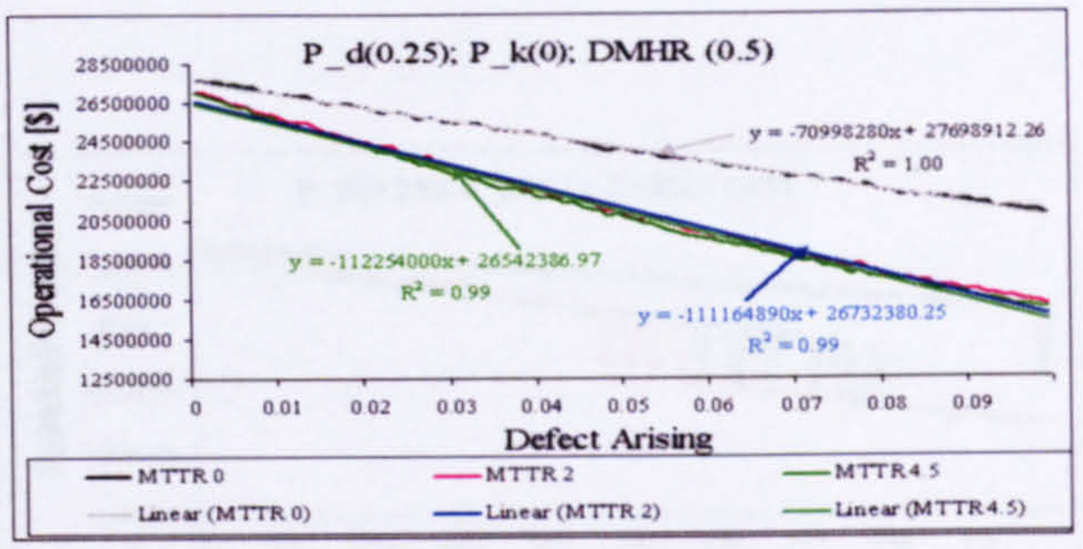

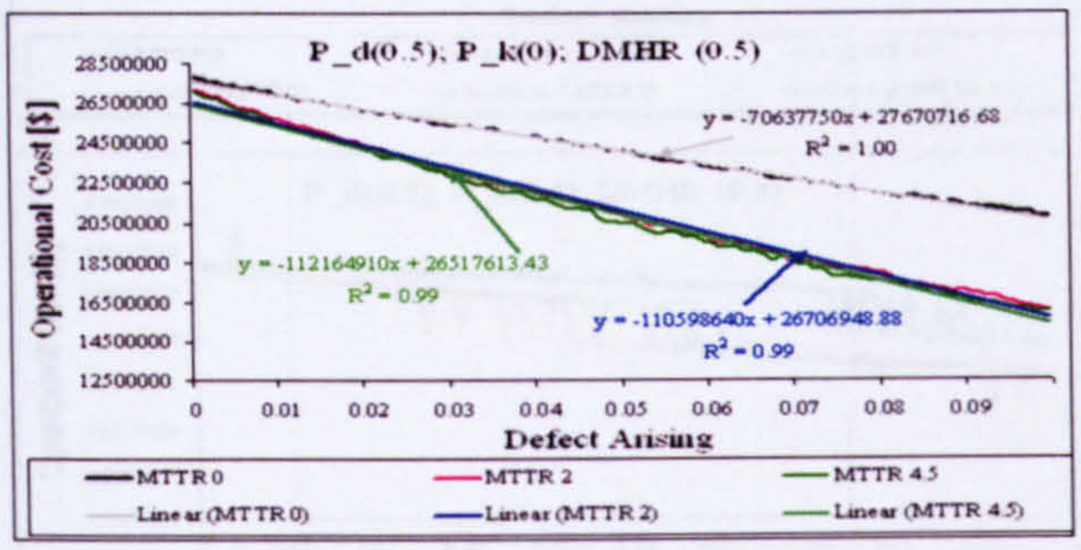

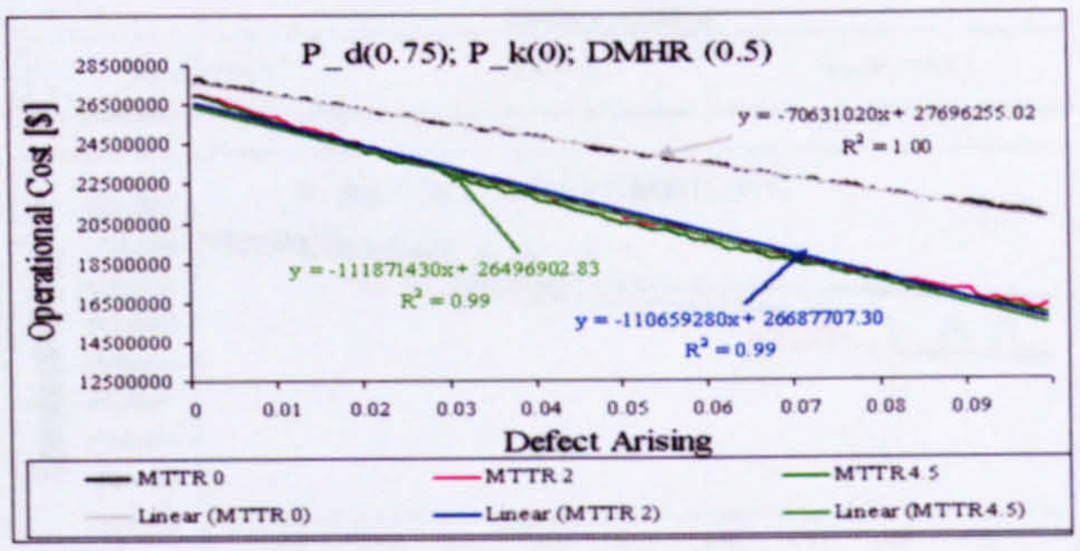

Figure E.46: Effect of aircraft defect arising rate, P_D and $MTTR_{Defect}$ on the total operational cost [$] with $P_{K_{Non}} = P_{K_{Ext}} = 0.00$

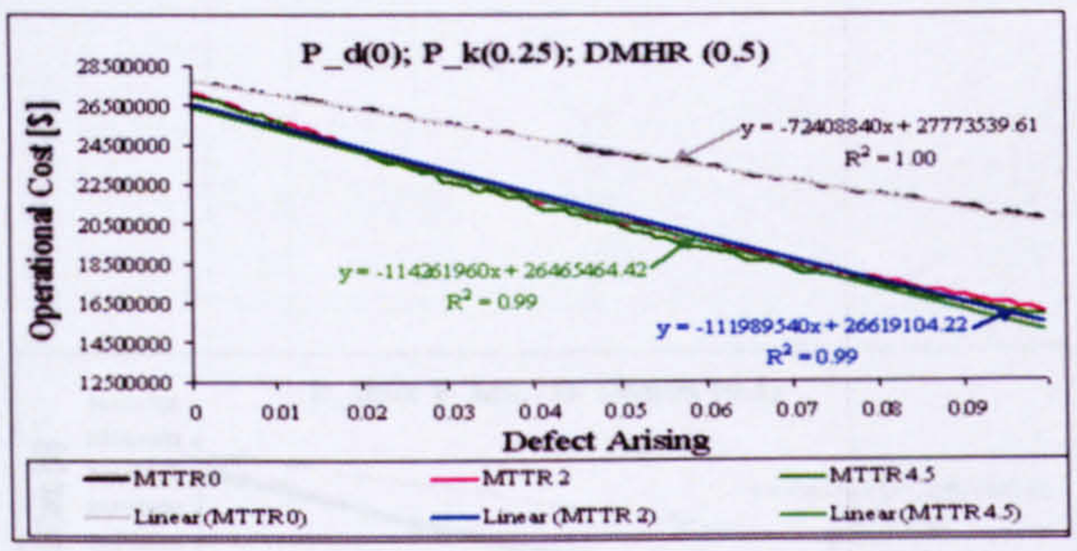

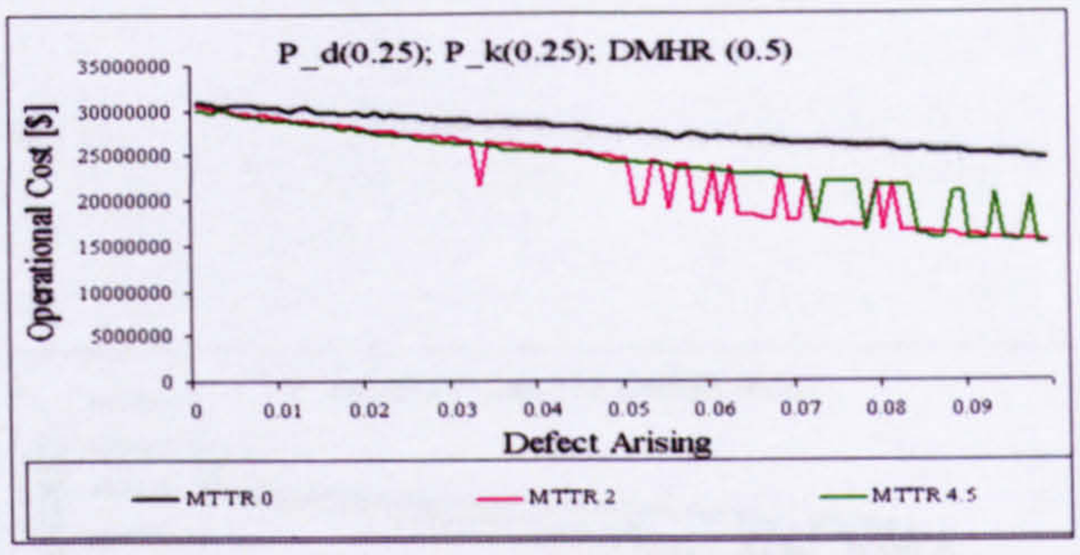

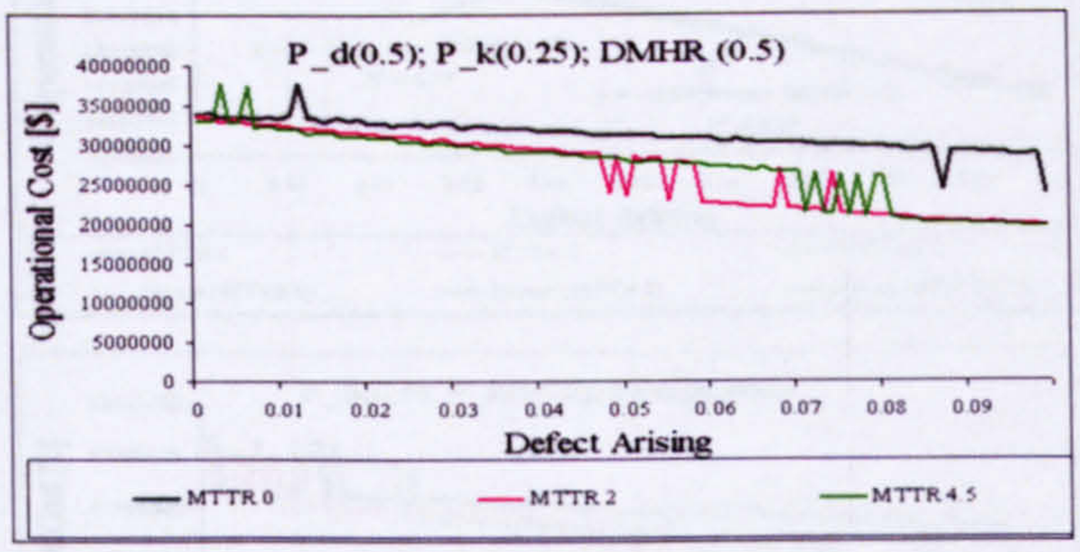

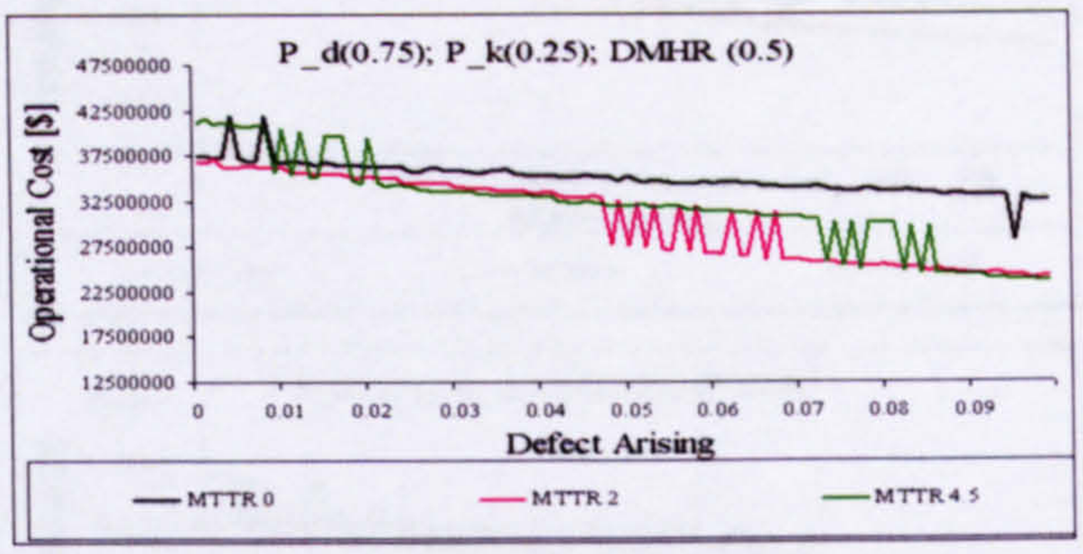

Figure E.47: Effect of aircraft defect arising rate, P_D and $MTTR_{Defect}$ on the total operational cost [$] with $P_{K_{Non}} = P_{K_{Ext}} = 0.25$

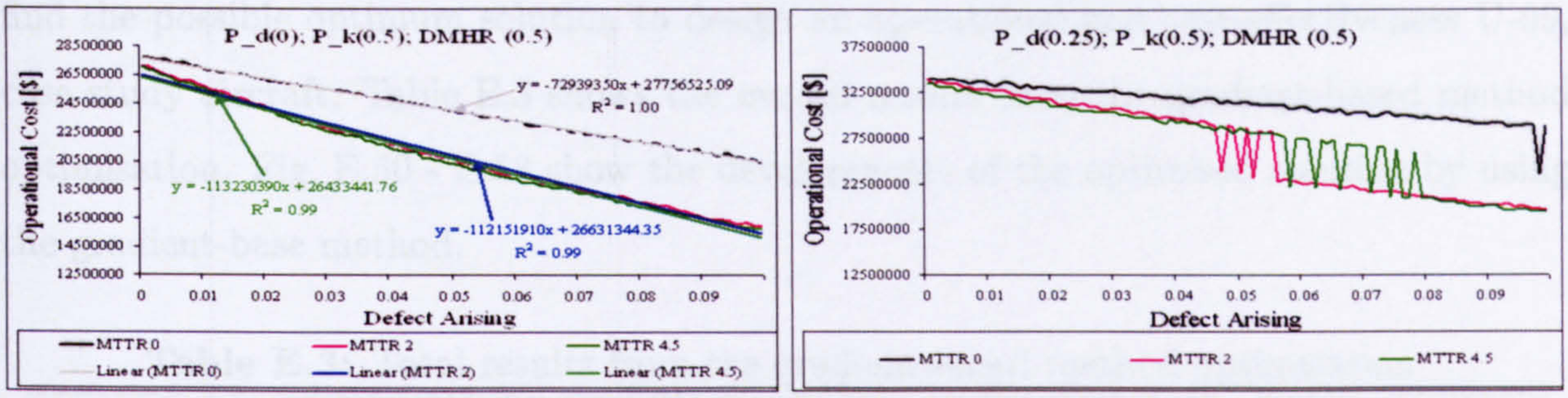

Figure E.48: Effect of aircraft defect arising rate, P_D and $MTTR_{Defect}$ on the total operational cost [$] with $P_{K_{Non}} = P_{K_{Ext}} = 0.50$

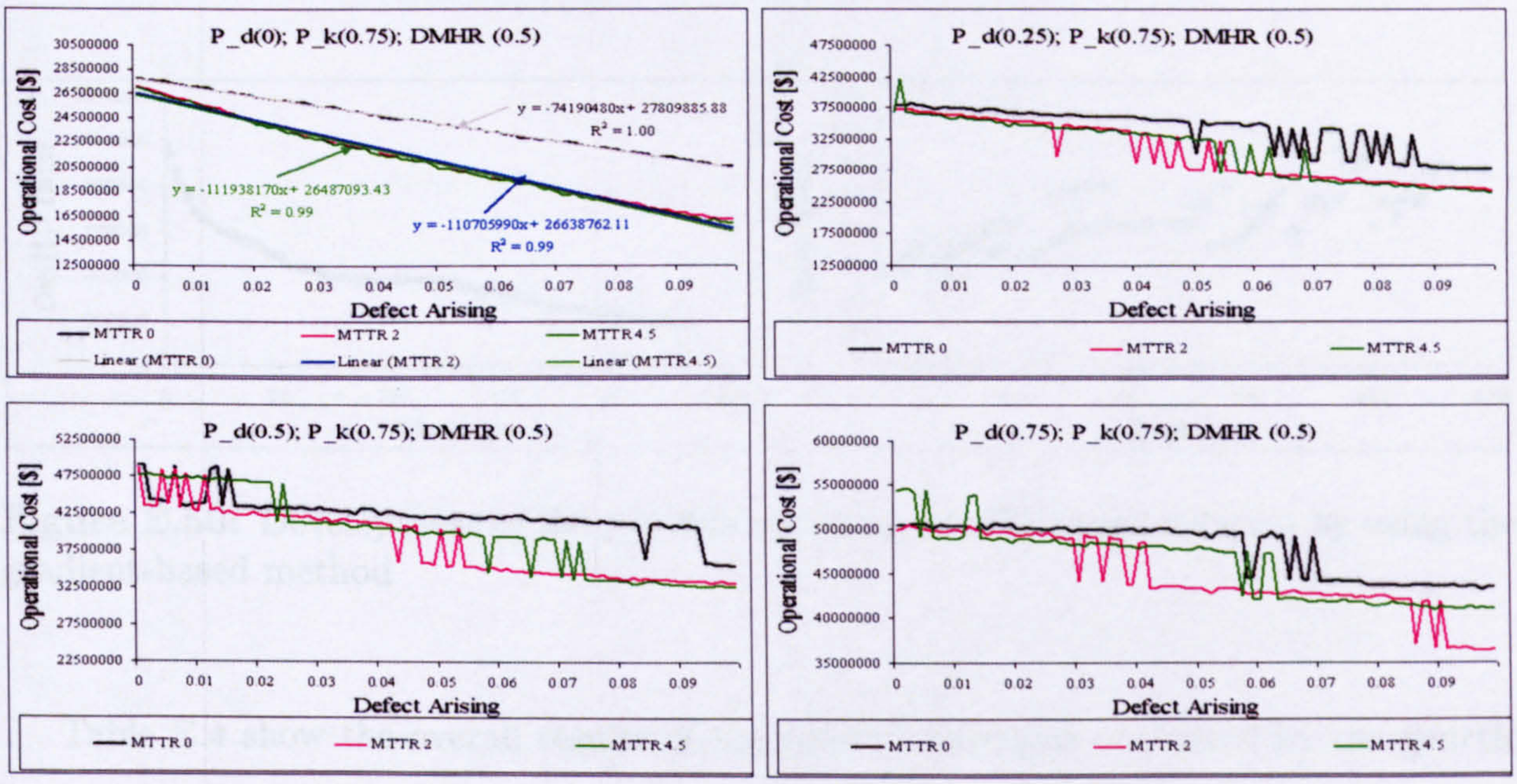

Figure E.49: Effect of aircraft defect arising rate, P_D and $MTTR_{Defect}$ on the total operational cost[$] with $P_{K_{Non}} = P_{K_{Ext}} = 0.75$

Following are results from two alternative optimisation by using six aircraft MOPS to find the possible optimum solution to design an operational and cost-effectiveness U-99, case study aircraft. Table E.3 shows the overall results from the gradient-based method optimisation. Fig. E.50 - E.53 show the developments of the optimised solution by using the gradient-base method.

Table E.3: Total results from the gradient-based method optimisation

	Minimise		Maximise	
	Cost[$]/Target	Cost[$]/Sortie	Targets Killed	Sorties Flown
Defect Arising	0.029519	0.099899	0.00494	0.00
P_D	0.062758	0.117555	0.29574	0.00
$P_{K_{Non}}$	0.371593	0.485130	0.007653	0.618059
$P_{K_{Ext}}$	0.515784	0.216124	0.148098	0.330151
$MTTR_{Defect}$	4.180827	6.534311	0.6544909	0.00
DMHR	0.00	5.374156	5.092504	4.074727
Sorties Flown	171	128	185	**198**
Complete Sorties	151	90	177	193
Successful Sorties	116	68	134	148
Targets Killed	120	78	**136**	150
Aircraft Killed	1	1	1	0
Cost [$] /Sortie	131547.125	**117821.8125**	142369.2188	143275.9844
Cost [$] /Target	**187454.6562**	193348.6094	193664.0000	189124.2969
Iterations	232	244	205	868

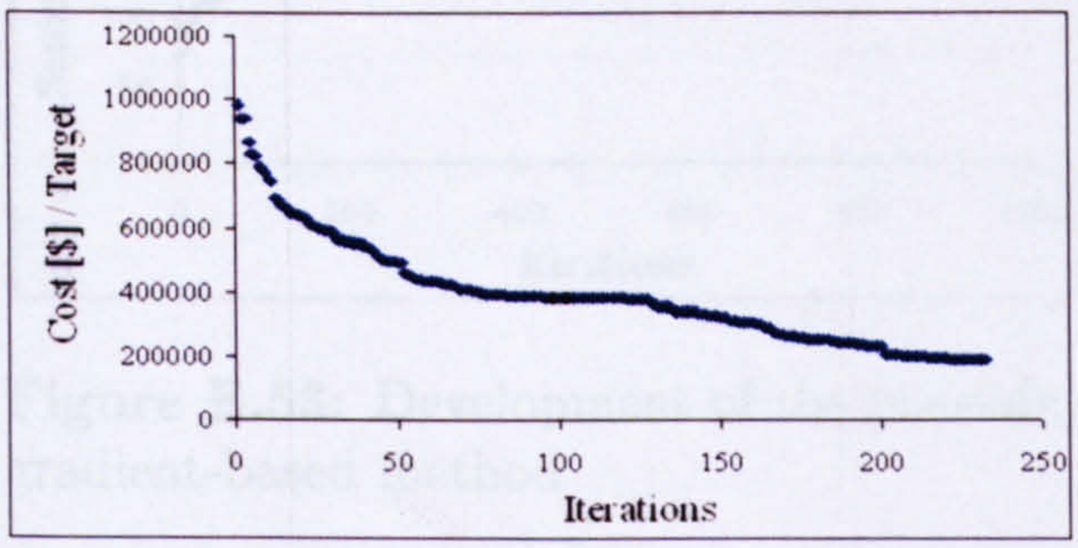

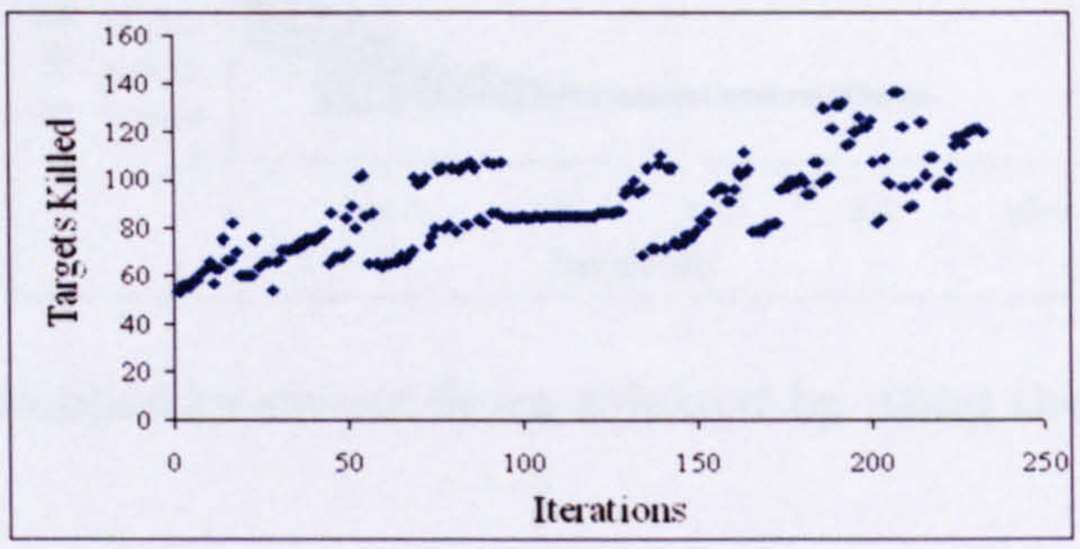

Figure E.50: Development of the possible minimum cost[$]/target solution by using the gradient-based method

Table E.4 show the overall results of the possible solutions optimised by the genetic algorithms, and Fig. E.54 - E.57 show the improvements of populations during the optimisation process.

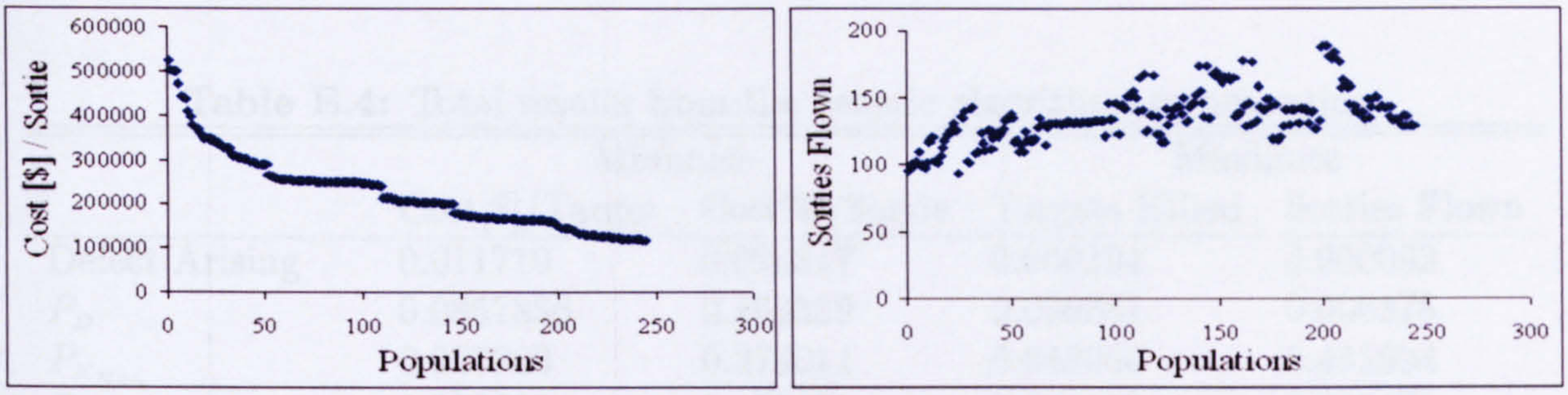

Figure E.51: Development of the possible minimum cost[$]/sortie solution by using the gradient-based method

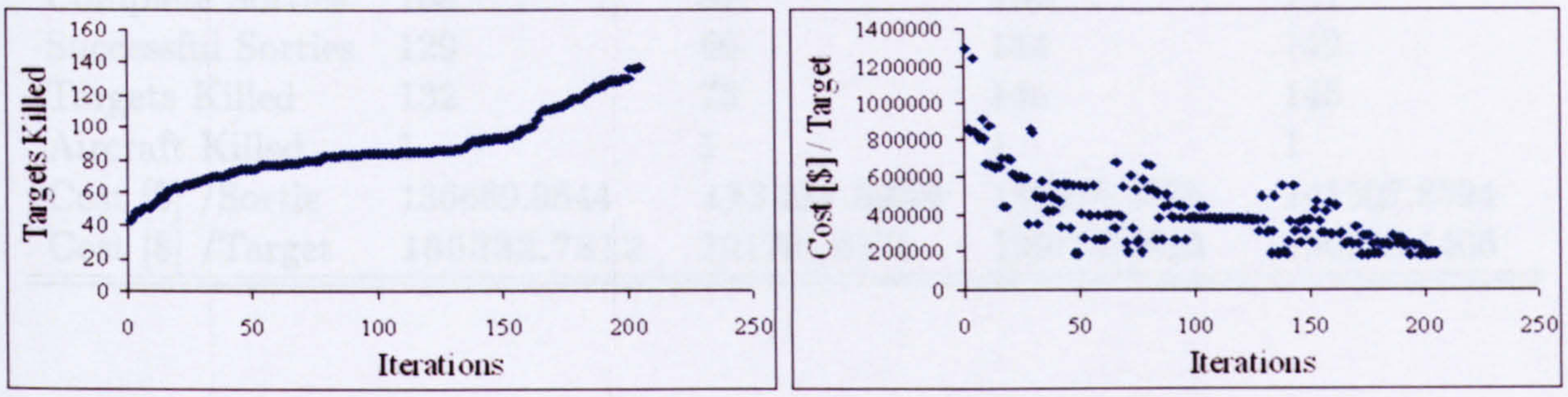

Figure E.52: Development of the possible maximum targets killed solution by using the gradient-based method

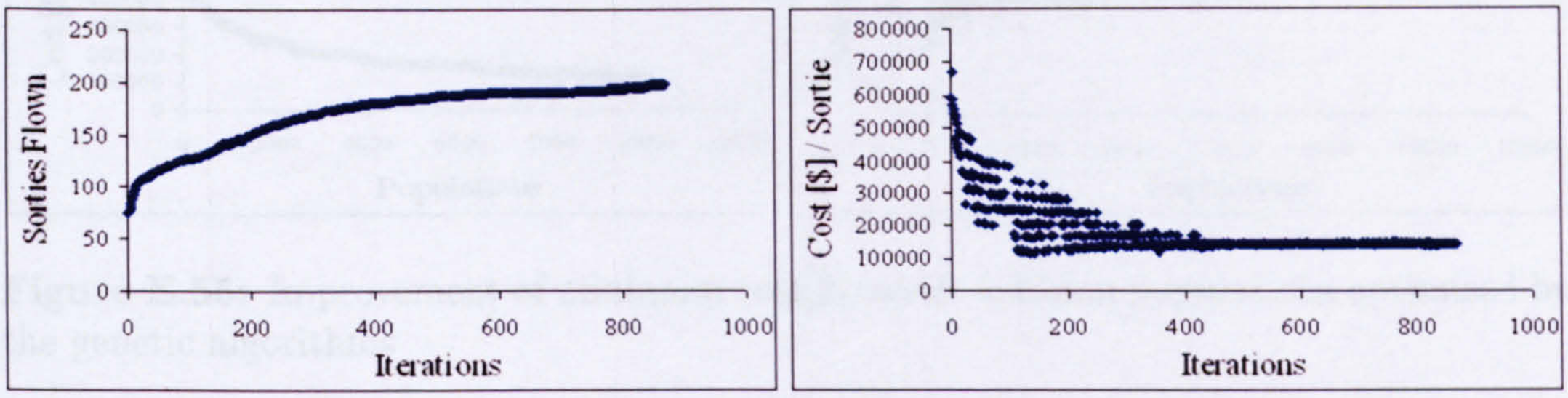

Figure E.53: Development of the possible maximum sorties flown solution by using the gradient-based method

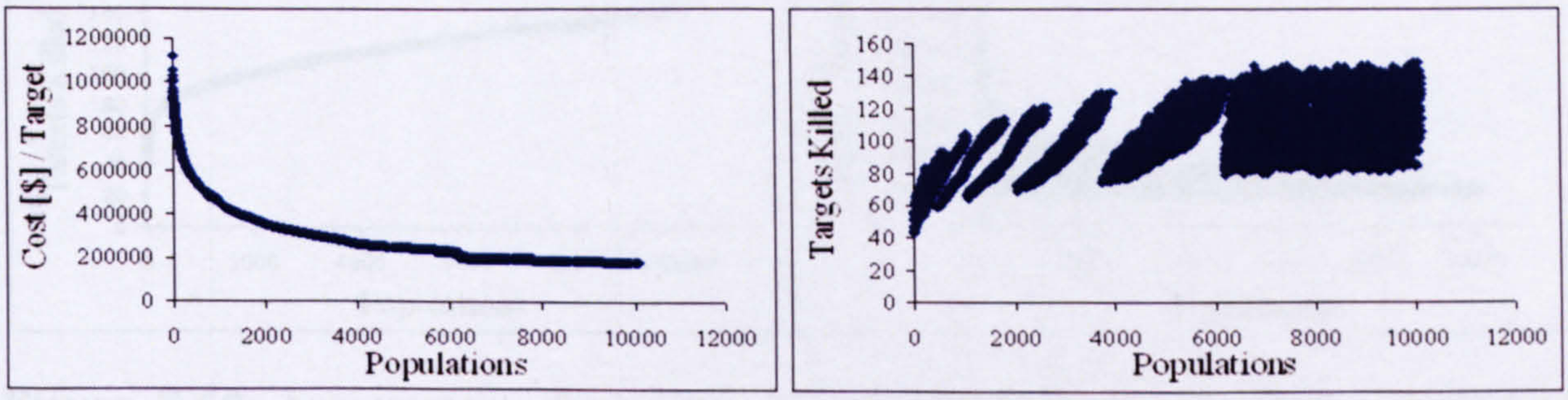

Figure E.54: Improvement of minimum cost[$]/target solution populations optimised by the genetic algorithms

Table E.4: Total results from the genetic algorithms optimisation

	Minimise		Maximise	
	Cost[$]/Target	Cost[$]/Sortie	Targets Killed	Sorties Flown
Defect Arising	0.011719	0.098817	0.000194	0.000092
P_D	0.0857886	0.169359	0.030381	0.006378
$P_{K_{Non}}$	0.927993	0.279011	0.048066	0.452994
$P_{K_{Ext}}$	0.138689	0.456199	0.000565	0.245471
$MTTR_{Defect}$	1.505455	7.514457	0.408179	1.979400
DMHR	0.075532	0.236438	2.873198	2.895339
Sorties Flown	179	125	194	**193**
Complete Sorties	168	87	**189**	187
Successful Sorties	129	66	144	142
Targets Killed	132	73	146	143
Aircraft Killed	1	1	1	1
Cost [$] /Sortie	136669.9844	**113487.3984**	142378.4375	141507.8594
Cost [$] /Target	**185332.7812**	191701.6875	189187.7813	190986.1406

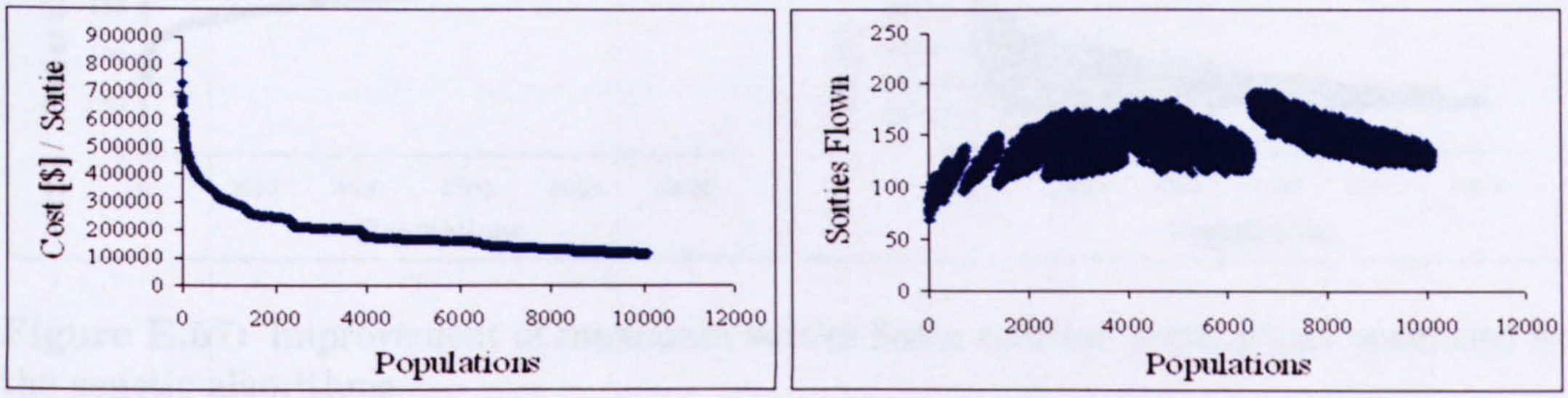

Figure E.55: Improvement of minimum cost[$]/sortie solution populations optimised by the genetic algorithms

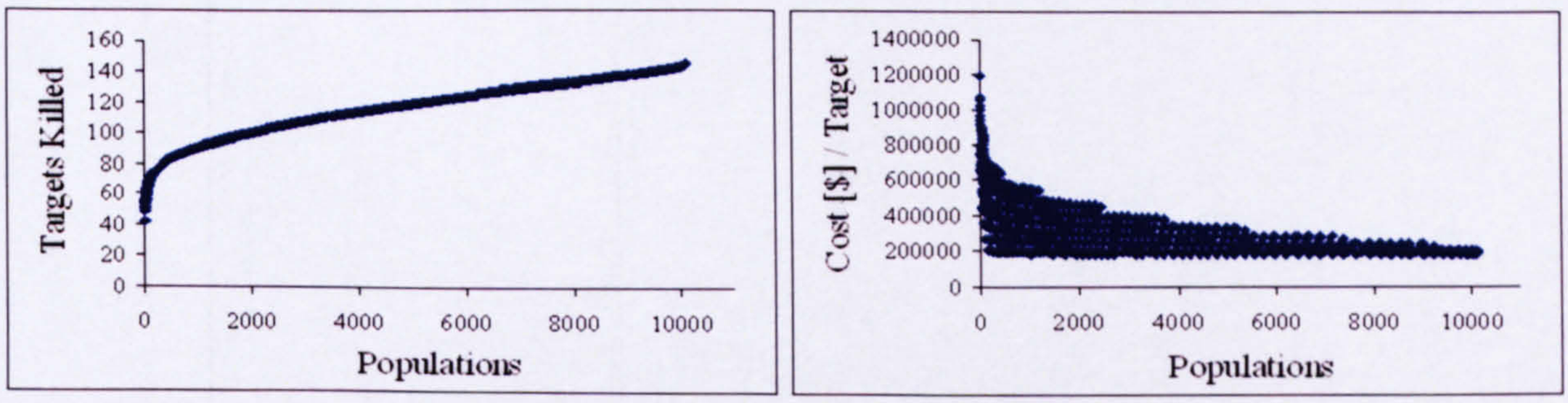

Figure E.56: Improvement of maximum targets killed solution populations optimised by the genetic algorithms

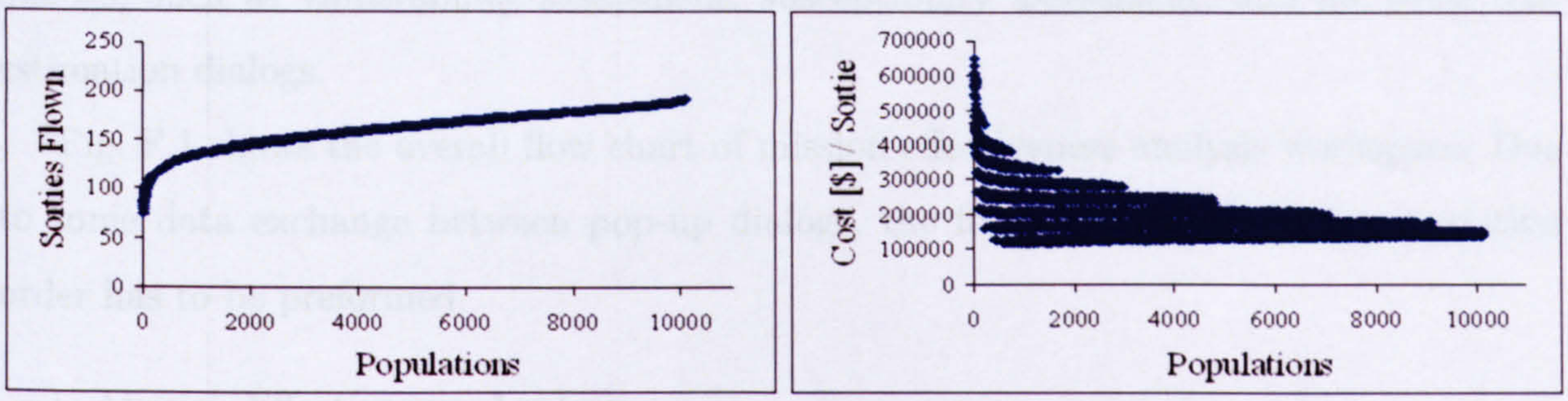

Figure E.57: Improvement of maximum sorties flown solution populations optimised by the genetic algorithms

APPENDIX F

MISSION EFFECTIVENESS ANALYSIS APPLICATION

This application has been developed by using Microsoft Visual Studio C++ version 6 as compiler. The program bases on Windows operating system, which offers easy usage, such as drag & drop, inter-active, and graphic display. The main application has been implemented in the form of one main workspace, which comprises 8 main individual projects. Each project can transfer data and be execute separately as pop-up windows dialogs, such as vulnerability assessment, susceptibility assessment, and life cycle cost estimation dialogs.

Fig. F.1 shows the overall flow chart of mission effectiveness analysis workspace. Due to some data exchange between pop-up dialogs, the following pop-up dialog execution order has to be preformed.

1. Mission Effectiveness Analysis
2. Vulnerability Assessment
3. Susceptibility Assessment
4. Reliability & Maintainability Assessment
5. Life Cycle Cost Estimation

CONTAINS PULLOUTS

Figure F.1: Complete flow chart of mission effectiveness analysis application

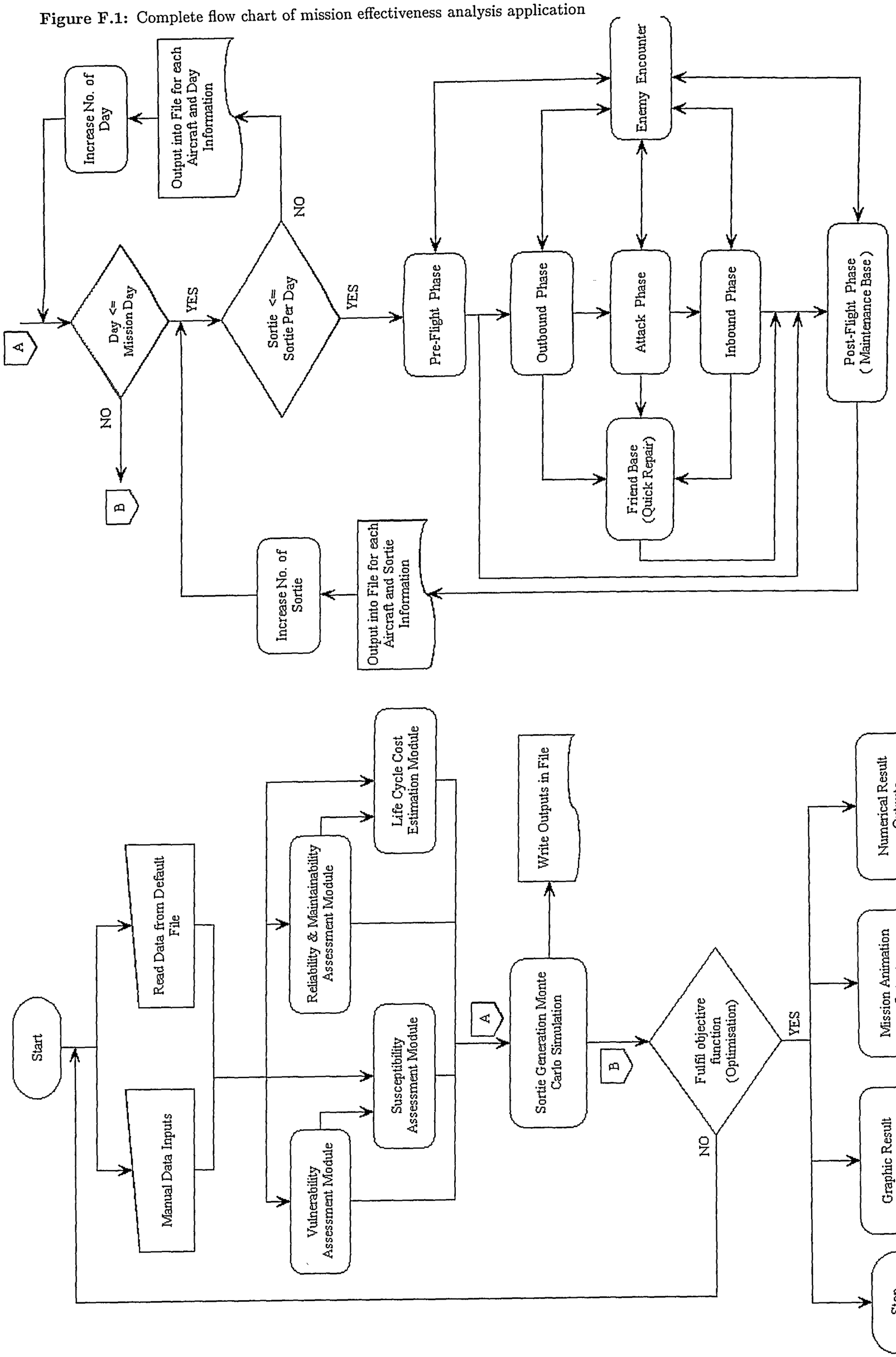

F.1 Mission Effectiveness Analysis

The first and main project is 'Mission Effectiveness Analysis', which will be firstly executed as the main application dialog, as shown in Fig. F.2. This application comprises 5 tab dialogs and several commands in the menu bar, which will load and run the remaining pop-up dialogs (projects).

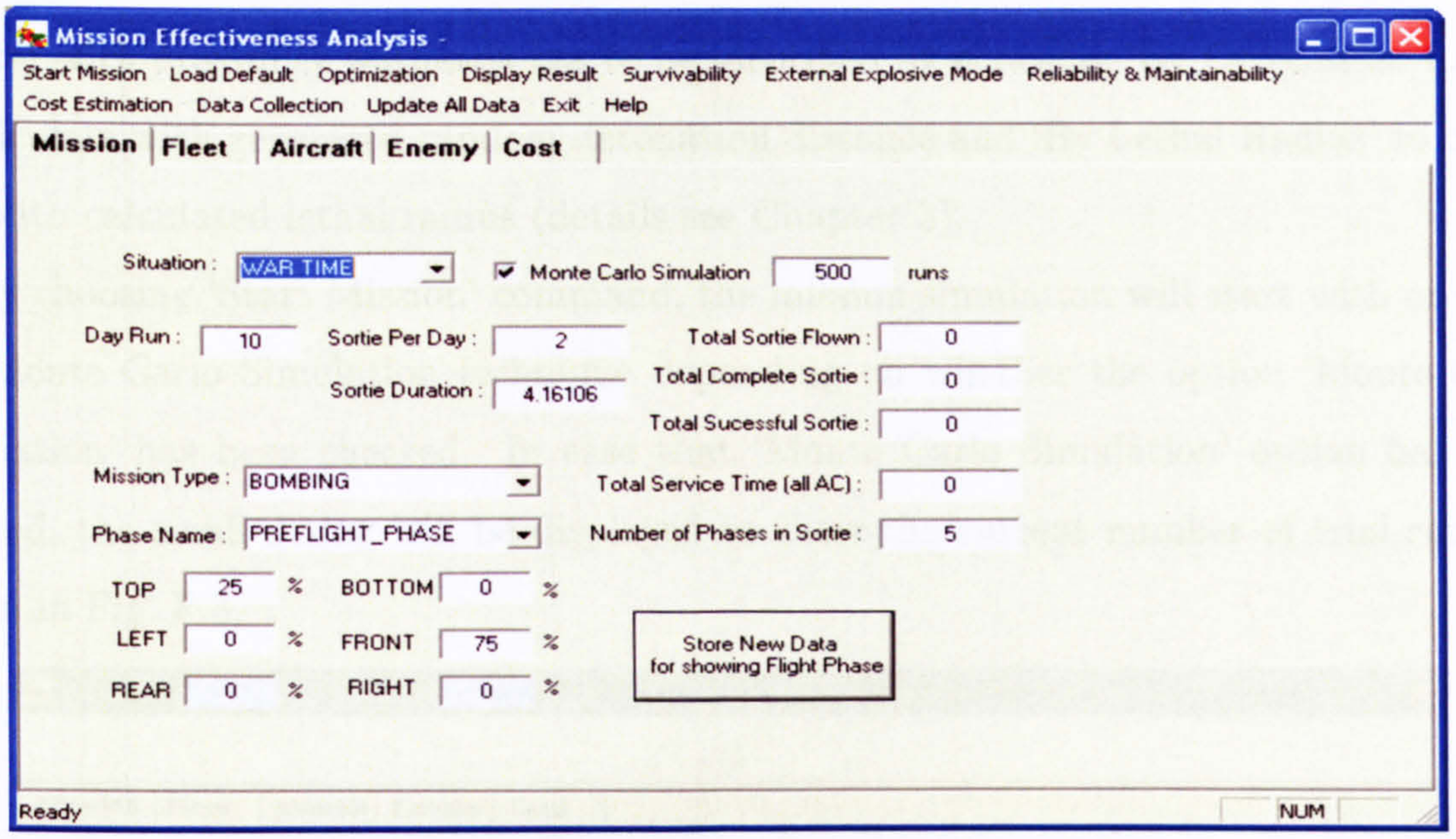

Figure F.2: Operation mission simulation application dialog

Firstly, the necessary variables have to be initialled by either loading directly from a file or directly giving in the application dialog. By using 'Load Default' command on the menu bar, the stored data in file namely 'input.dat' in the folder '...\input' will be loaded. In case that the file 'input.dat' does not exist or not locate in the folder '...\input', the windows browse dialog will be display. Therefore, the correct location or file can be indicated.

On the other hand, the threat and mission simulation information will be automatically loaded directly from the default file namely 'mission.dat', which is normally located in the same folder as 'input.dat'. On similar approach, if this file does not exist or locate in the folder, the browse dialog will be also display.

The next step is to execute the individual pop-up dialogs, as shown above. The vulnerability and susceptibility assessment pop-up dialogs will be shown by choosing the 'vulnerability' and 'susceptibility' sub-menus, which locate under the 'survivability' menu. The reliability & maintainability assessment pop-up dialog will be displayed, if

the command 'Reliability & Maintainability' has been chosen. By pressing command 'Cost Estimation', the life cycle cost estimation dialog will be popped up (details how to operate the vulnerability pop-up dialogs see section F.2, for susceptibility assessment see section F.3, for reliability & maintainability assessment see section F.4, and for life cycle cost estimation see section F.5).

Before the mission simulation starts, the calculation method for vulnerability on encounter with proximity warheads has to be identified by choosing 'By Detonation Range' to calculate with generated random detonation distance and 'By Lethal Radius' to calculate with calculated lethal radius (details see Chapter 3).

By choosing 'Start Mission' command, the mission simulation will start with or without Monte Carlo Simulation technique depending on whether the option 'Monte Carlo Simulation' has been checked. In case that 'Monte Carlo Simulation' option has been checked, the small dialog will be displayed to show the current number of trial runs, as shown in Fig. F.3.

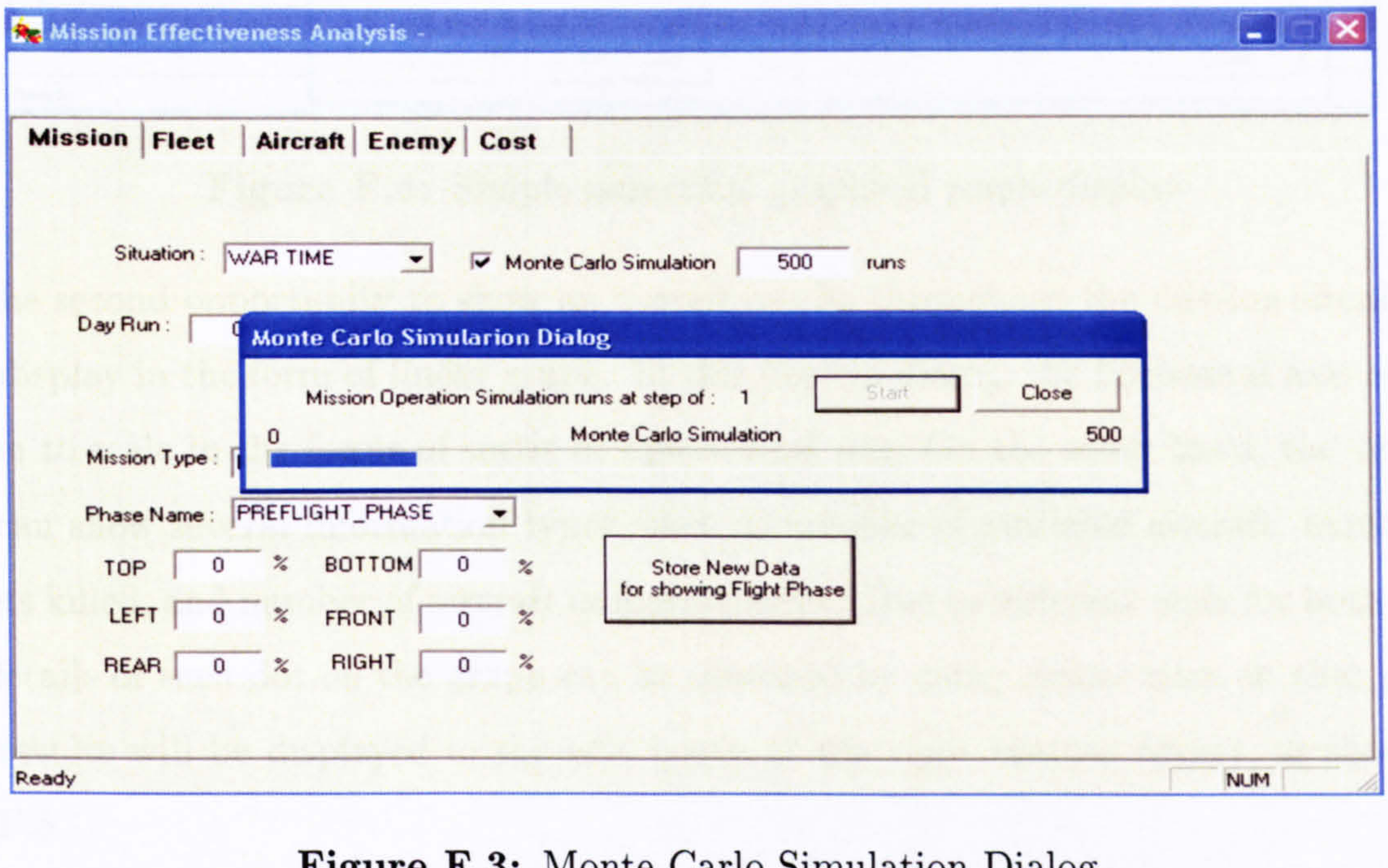

Figure F.3: Monte Carlo Simulation Dialog

There are three results display possibilities; i.e. Numerical, Linear Graph, and Simple Graphic Simulation display dialogs. Additionally, the general results in each sortie and operational day will be stored automatically into 'sortie.dat' located in the folder '...\output'. The details information of each aircraft will be also generated and stored into the file name 'aircraft**N**.dat', where **N** is a number of aircraft. The information during each flight phase will be stored into the file '**FlightPhase**.dat', where **FlightPhase**

is the flight phase name in the sortie.

The first results display option is numerical display dialog, which appears as Fig. F.4. The information of each sortie and operational day will be display in specific pop-up dialog, and by choosing 'Previous' and 'Next', the next and previous sortie or operational day information will be displayed.

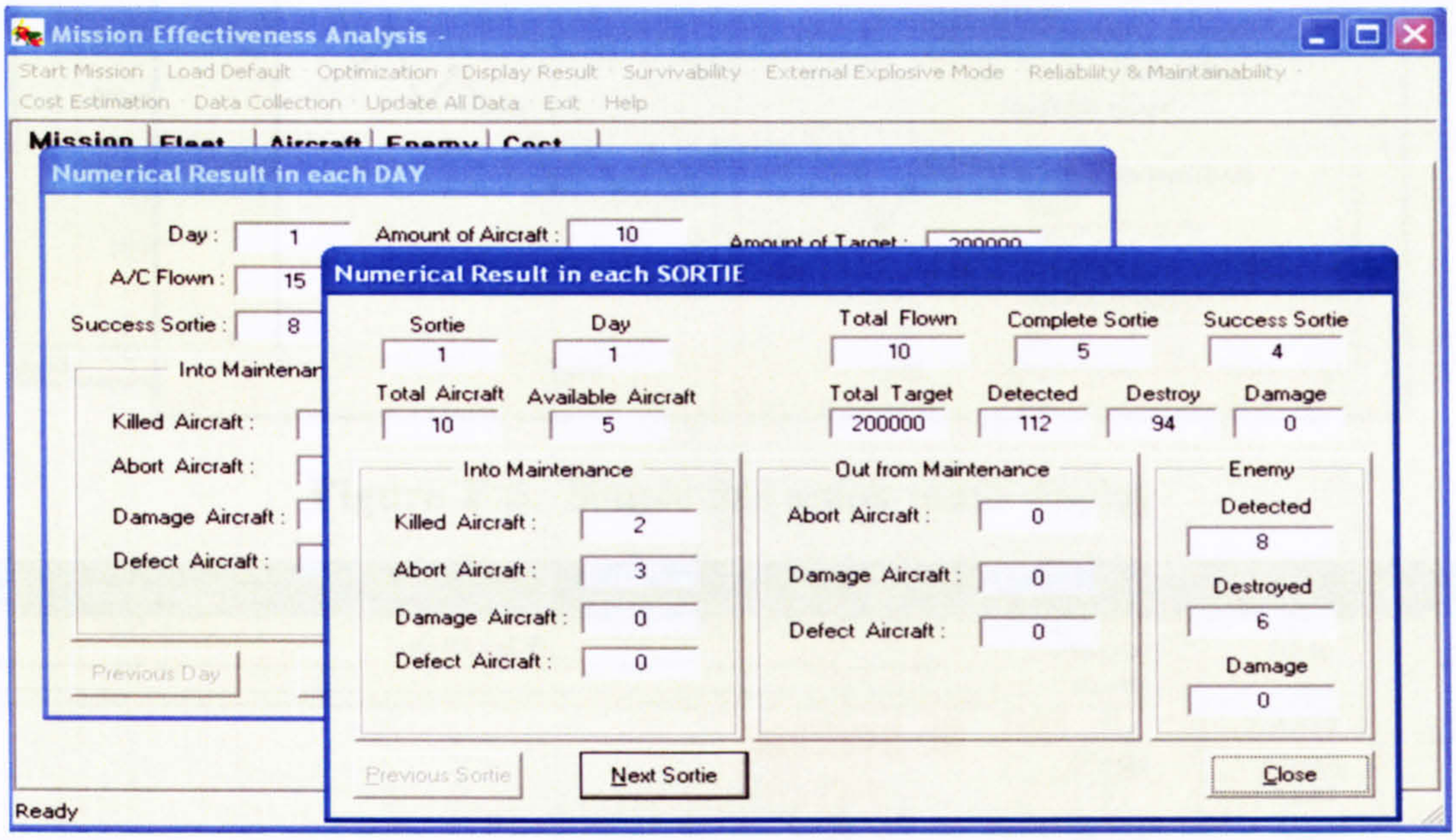

Figure F.4: Simple numerical graphical result display

The second opportunity to show an overall results throughout the mission simulation is to display in the form of linear graph. In this pop-up dialog, the horizontal axis can be chosen to scale in the forms of sortie or operational day. On the other hand, the vertical axis can show several information types, such as number of available aircraft, number of targets killed, and number of aircraft in maintenance. Due to different scale for both axes, the details of each dot on the graph can be obtained by using mouse click on that point. The results will be displayed in the edit boxes at the right bottom corner, as shown in Fig. F.5.

The last alternative to display the results is simple graphic simulation (semi-animate graphical) display. This option simulates and displays the entire results in every flight phases throughout the mission in motion. Aircraft status during the mission is represented by different colour (red = READY, purple = ABORT, grey = KILLED). During the simulation, if the encounters by threats or weapons release by the aircraft take place, dot lines with different colour will also be display (red = weapon released, green = threat encounter). Fig. F.6 shows one shot of entire simulation.

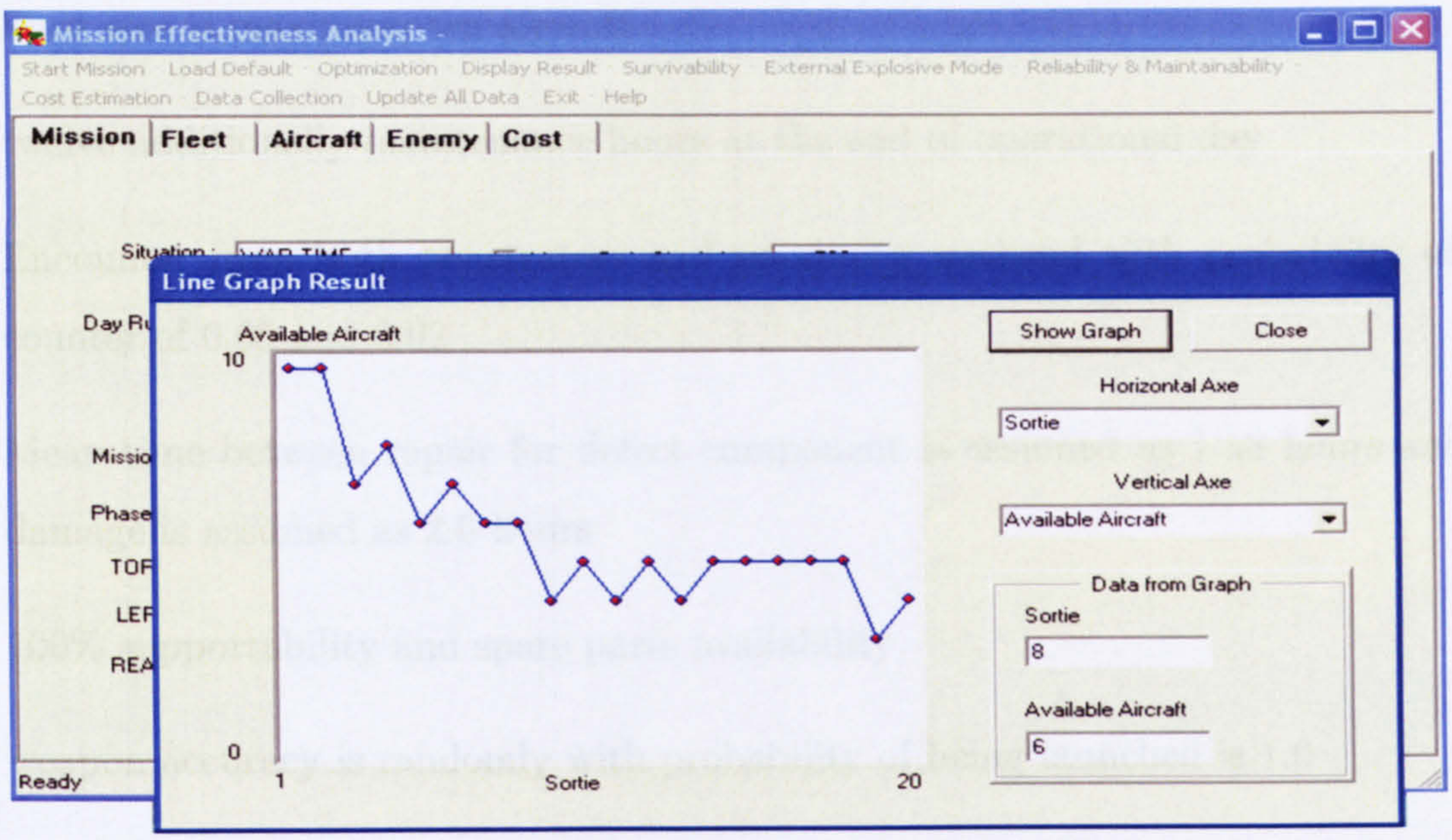

Figure F.5: Simple line graph result display

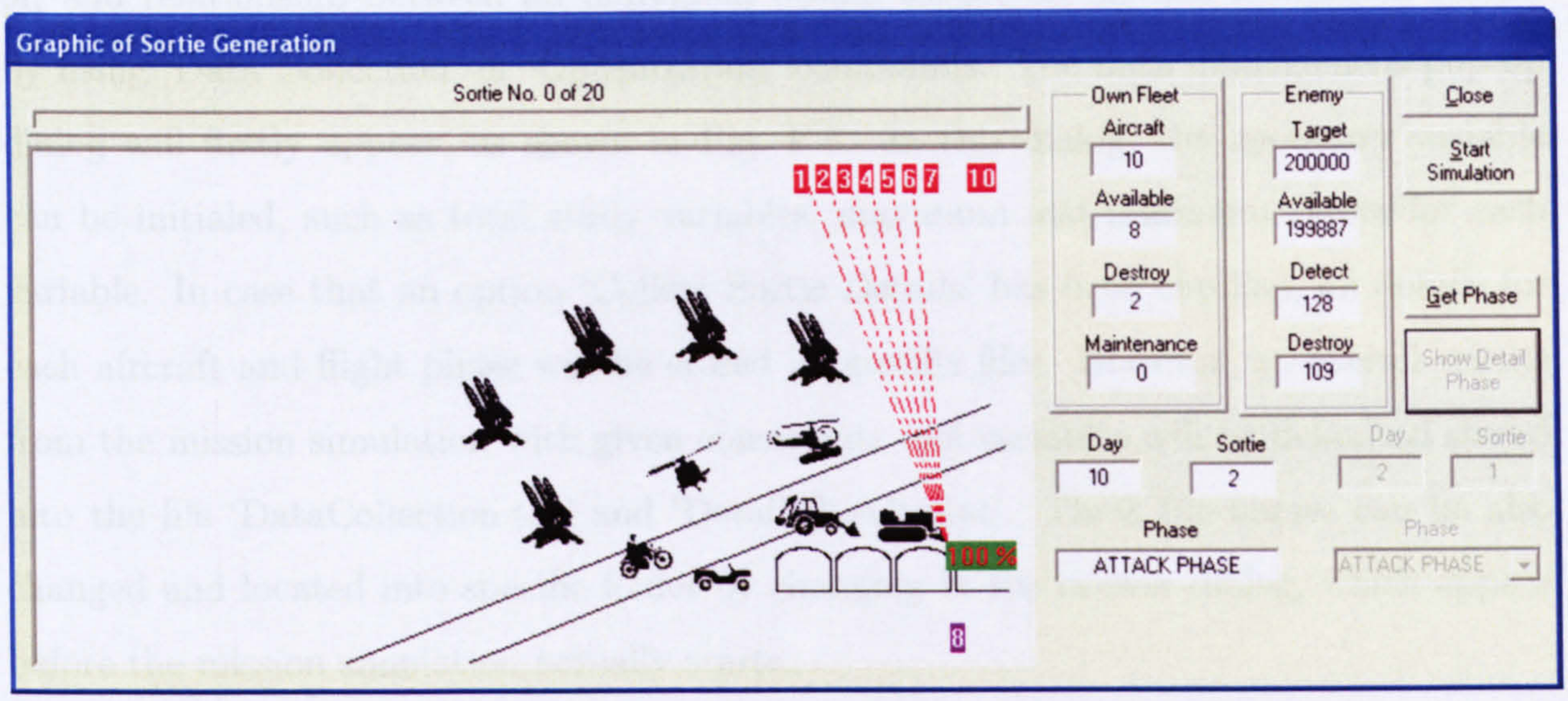

Figure F.6: Simple semi-animate graphical result display

Due to lots of information displayed in this pop-up dialog, an option to show only the occurrence in specific flight phase, sortie and operational day has been offered by pressing 'Get Phase' command and giving the specific sortie and operational day. To display the occurrence during the selected flight phase, sortie and operational day, the command 'Show Detail Phase' has to be chosen.

Fig. F.7 shows example of general results from an operation simulation with following constraints:

- Ten operational days with maximum two sorties per day

- Fleet size is maximum ten aircraft
- twelve additionally maintenance hours at the end of operational day
- Encounter from both penetrators and proximity warhead with probability of encounter of 0.05 and 0.02
- Mean time between repair for defect component is assumed as 1.53 hours and for damage is assumed as 2.6 hours
- 100% supportability and spare parts availability
- weapon accuracy is randomly with probability of being launched is 1.0

The mission effectiveness analysis application offers also alternative to investigate effect of, and relationship between an individual design aspect on mission simulation results by using 'Data Collection' or 'Optimization' commands. The data management pop-up dialog will firstly appear, as shown in Fig. F.8. In this dialog, the necessary variable can be initialed, such as total study variables, maximum and minimum values for each variable. In case that an option 'Collect Sortie Details' has been checked, all details for each aircraft and flight phase will be stored in specific files. However, an overall results from the mission simulation with given constraints and variables will be defaulted stored into the file 'DataCollection.txt' and 'DetailsResults.txt'. These file names can be also changed and located into specific folder by changing in the browse dialog, which appear before the mission simulation actually starts.

On similar approach, the optimisation constraints and variables can be also set throughout this pop-up dialog, such as minimise, maximise, and terminate with convergence. The default file name for 'GAlib' optimisation are 'GALibIter.txt' and 'GALibDetail.txt'. For 'Solver' optimisation, the 'SolverIter.txt' is the only results collection file.

F.2 Vulnerability Assessment

This application dialog can be executed by select command 'Vulnerability', which is a sub-menu in 'Survivability' menu. Fig. F.9 shows an application dialog.

By using the same principle as load default initial data from the specific file, the default file for this application dialog is 'vulner_input.dat'.

Fleet Size is 10 Aircraft; Simulation Period is 10 Days; Sortie per Day is 2

Prop. Abort: 0.0038 ; Prob. Encounter AAA: 0.0500 ; Prob. Encounter SAM: 0.0200 ; Prob. Damage: 0.0038 ; Prob. Defect: 0.0299

Time to Repair Defect: 1.5300 ; Time to Repair Damage: 2.6000 ; Time to Maintenance at End of Day: 12.0000 ; Cycle Time: 4.5819

Threat Defensive Level : HIGH

Day	*Sortie*	*Flown*	*EndSortieAvai*	*Abort*	*Kill*	*Damage*	*Defect*	*Re_Abort*	*Re_Dam*	*Re_Def*	*Main*	*QK_Re*	*Detect*	*Destroy*	*Damage*
1	1	10	9	1	0	0	0	0	0	0	1	0	9	6	1
1	2	7	10	3	0	0	0	0	4	0	3	0	6	6	0
2	1	9	8	2	0	0	0	0	0	0	2	0	8	6	0
2	2	8	9	0	1	0	0	0	2	0	0	0	6	4	0
3	1	8	8	1	0	0	0	0	0	0	1	0	7	6	0
3	2	8	9	1	0	0	0	0	2	0	1	0	5	3	0
4	1	9	9	0	0	0	0	0	0	0	0	0	8	8	1
4	2	9	9	3	0	0	0	0	3	0	3	0	7	5	0
5	1	8	7	2	0	0	0	0	0	0	2	0	7	7	1
5	2	7	9	2	0	0	0	0	4	0	2	0	5	5	0
6	1	8	7	2	0	0	0	0	0	0	2	0	8	8	0
6	2	6	8	1	1	0	0	0	3	0	1	0	4	3	1
7	1	8	8	0	0	0	0	0	0	0	0	0	4	3	0
7	2	8	8	3	0	0	0	0	3	0	3	0	7	7	0
8	1	7	7	1	0	0	0	0	0	0	1	0	7	2	0
8	2	7	8	0	0	0	0	0	1	0	0	0	6	4	0
9	1	8	7	1	0	0	0	0	0	0	1	0	7	4	0
9	2	7	6	1	1	0	0	0	1	0	1	0	7	6	0
10	1	6	6	1	0	0	0	0	1	0	1	0	4	3	0
10	2	6	7	1	0	0	0	0	2	0	1	0	5	4	0

Day	*Avai.*	*Abort*	*Kill*	*Damage*	*Return*	*Main.*	*Quick_Re*	*Flown*	*Sortie*	*Success*	*EnemyDect*	*EnemyDes*	*EnemyDam*
1	10	4	0	0	4	4	0	17	16	11	15	12	1
2	9	2	1	0	2	2	0	17	15	10	14	10	0
3	9	2	0	0	2	2	0	16	15	9	12	9	0
4	9	3	0	0	3	3	0	18	16	13	15	13	1
5	9	4	0	0	4	4	0	15	12	11	12	12	1
6	8	3	1	0	3	3	0	14	13	11	12	11	1
7	8	3	0	0	3	3	0	16	15	9	11	10	0
8	8	1	0	0	1	1	0	14	14	6	13	6	0
9	6	2	1	0	1	2	0	15	12	9	14	10	0
10	7	2	0	0	3	2	0	12	10	7	9	7	0

Total Takeoff : 154 ; Total Complete Sortie : 138 ; Total Successful Sortie : 96 ; End of Battle 7 Aircraft are serviceable
Total Enemy : 200000 ; Detected 127 times ; Destroyed 100 times ; Damaged 4 times ; Total Service Time : 661.11

Flying Hours Total Operation Cost : 6.0895 M$
Total Personnel Cost : 4.3953 M$
Total Unit Level Cost : 0.3459 M$
Total Maintenance Cost : 0.0000 M$
Total Ground Support Cost : 0.6198 M$
Total Weapon Cost : 7.9814 M$
Total Aircraft lost : 14.0624 M$

Figure F.7: Results from an operation simulation with manoeuvrability probability option 2

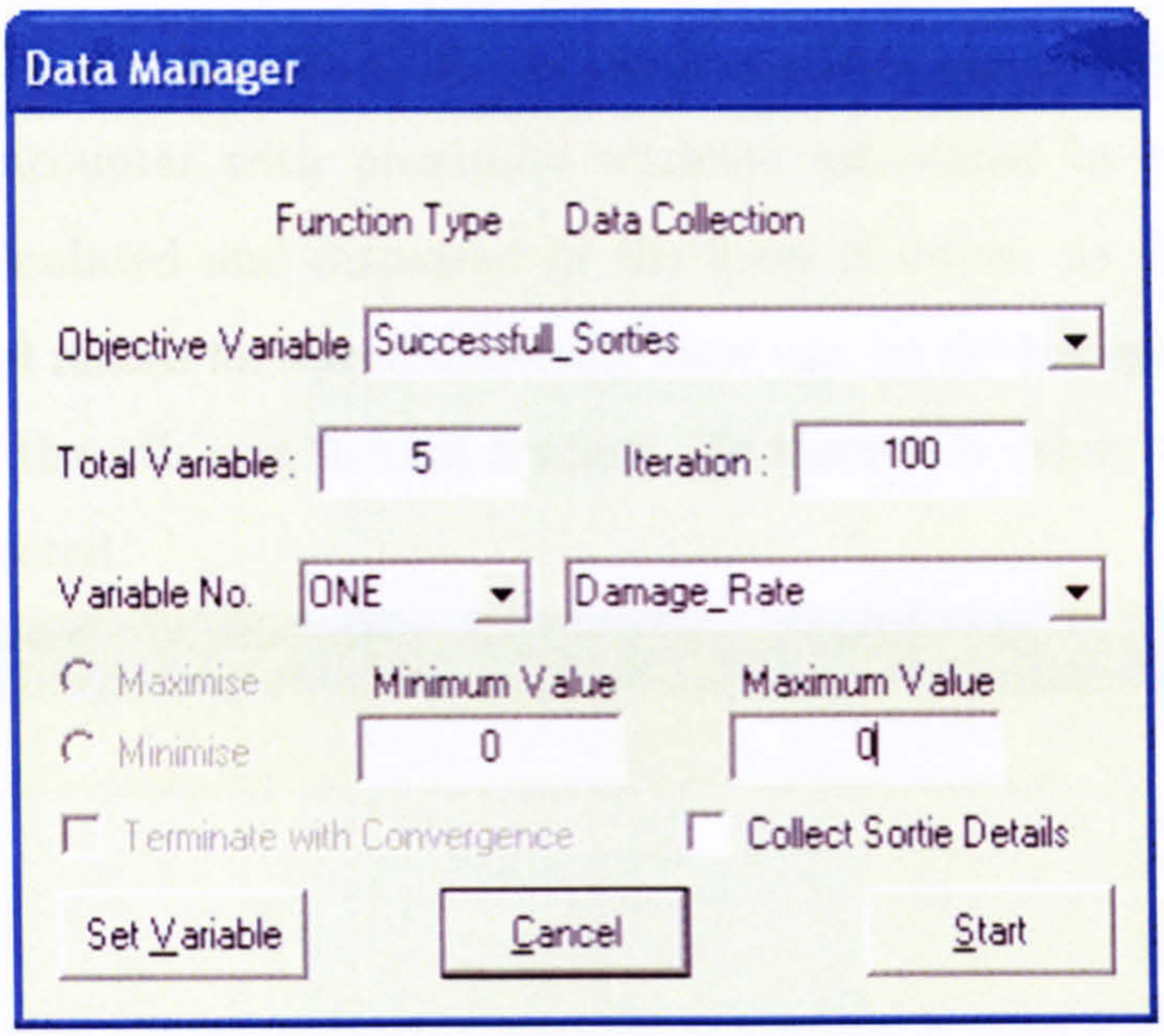

Figure F.8: Data Management Dialog

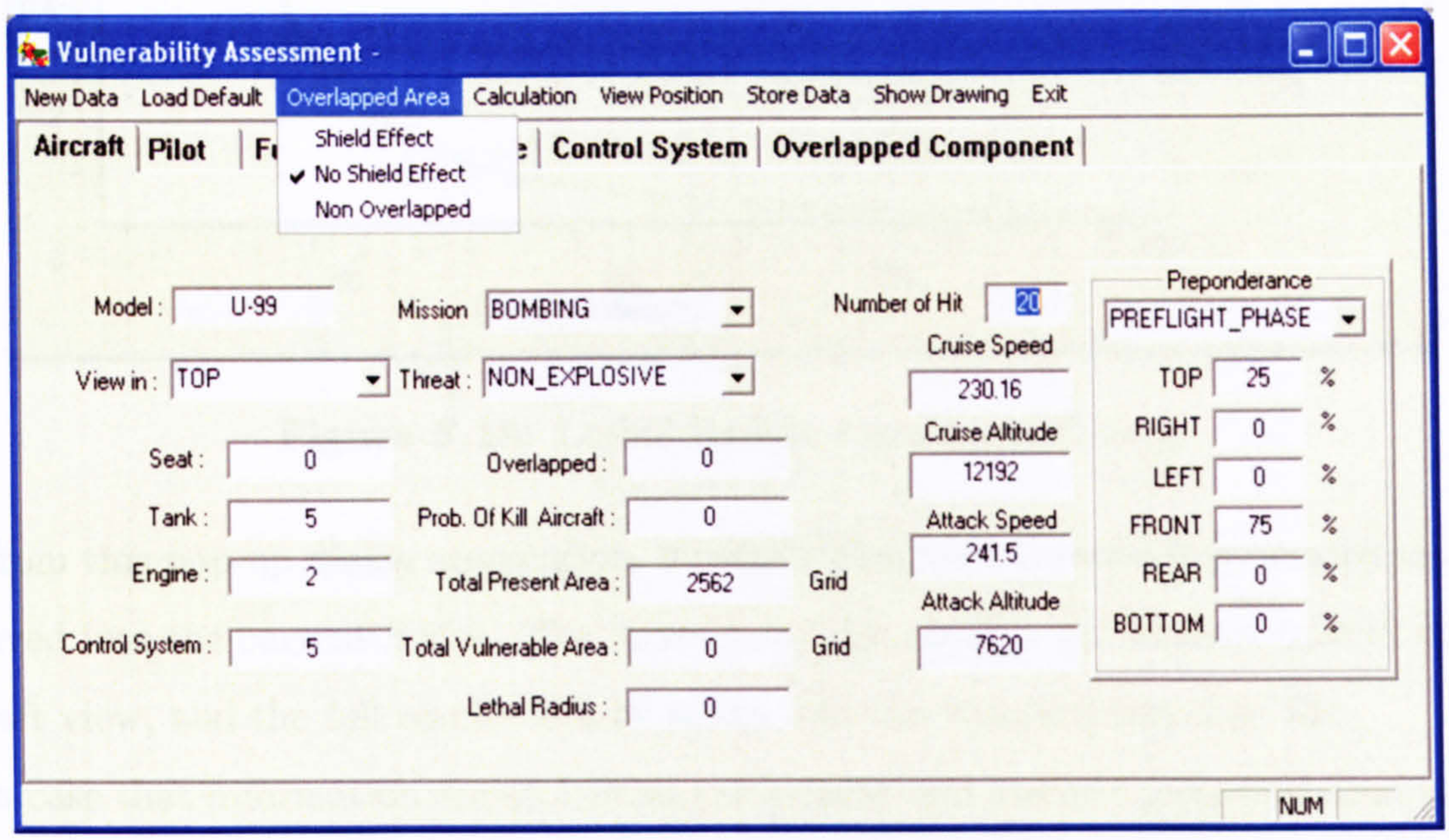

Figure F.9: Vulnerability Assessment Dialog

Next step is to choose overlapped area category from the menu 'Overlapped Area'. The probability of overlapped area and aircraft kill for every aircraft view will be calculated by pressing the command 'Calculation'. The average probability of kill (view in 'TOTAL') will be also calculated in conjunction with the weighting factor for each flight phase. However, by select specific aircraft view from the menu 'View Position', the information and probability of aircraft kill in selected aircraft view will be displayed.

In case that the threat type 'EXTERNAL_EXPLOSIVE' has been selected, both probability of kill on encounter with proximity warhead calculated by random detonation distance will be calculated and displayed in the form of curve, as shown in Fig. F.10. Therefore, the lethal radius for specific aircraft view can be determined and the user has to give the value in the edit box 'Lethal Radius'. To store this value, the command 'Save Data' has to be selected.

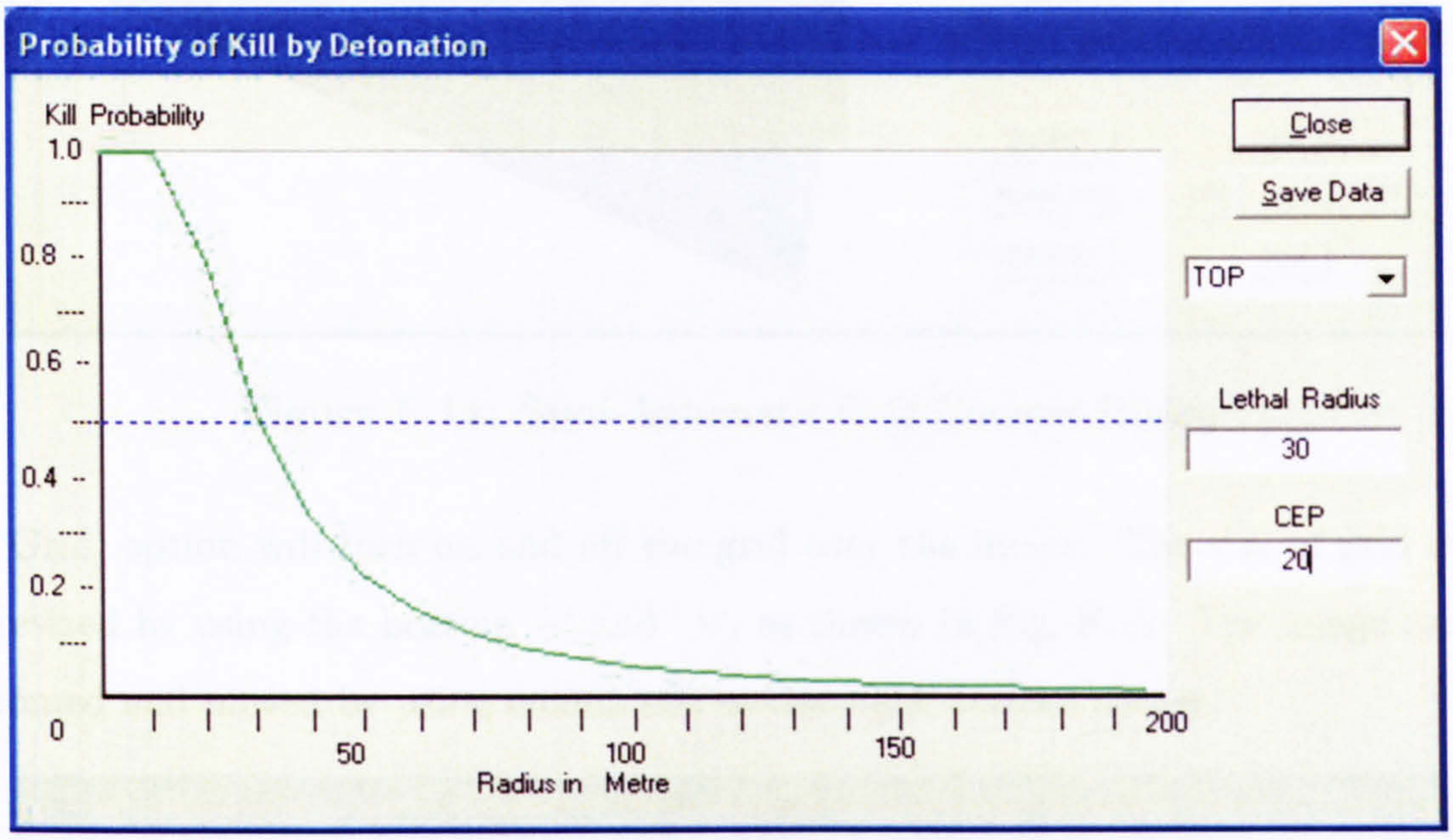

Figure F.10: Lethal Radius Assessment Dialog

From this pop-up dialog application, 2 default files are automatically created and will be saved into the current folder. The 'matrix.dat' file obtains the Makrov matrix of each aircraft view, and the full results will be saved into the 'vulnerability.day' file.

In case that information about critical component and aircraft presented area are not available, these information can be created from the semi-automatic grid counter option. However, the necessary information has to be initialed in the main application dialog, such as number of fuel tank, number of pilot, and number of overlapped area. After the command 'New Data' has been chosen, the aircraft drawing dialog will appear, as shown in Fig. F.11.

By choosing 'Load Drawing' command, the aircraft image in 'BMP' format can be loaded and displayed in the dialog. Regarding to the number of critical components, which have been given in the main dialog, their details have to be future given by using the scroll down menu and radio bottom, such as redundancy, position, and kill level. By pressing 'Save' for each critical component, its details will be stored into the memory.

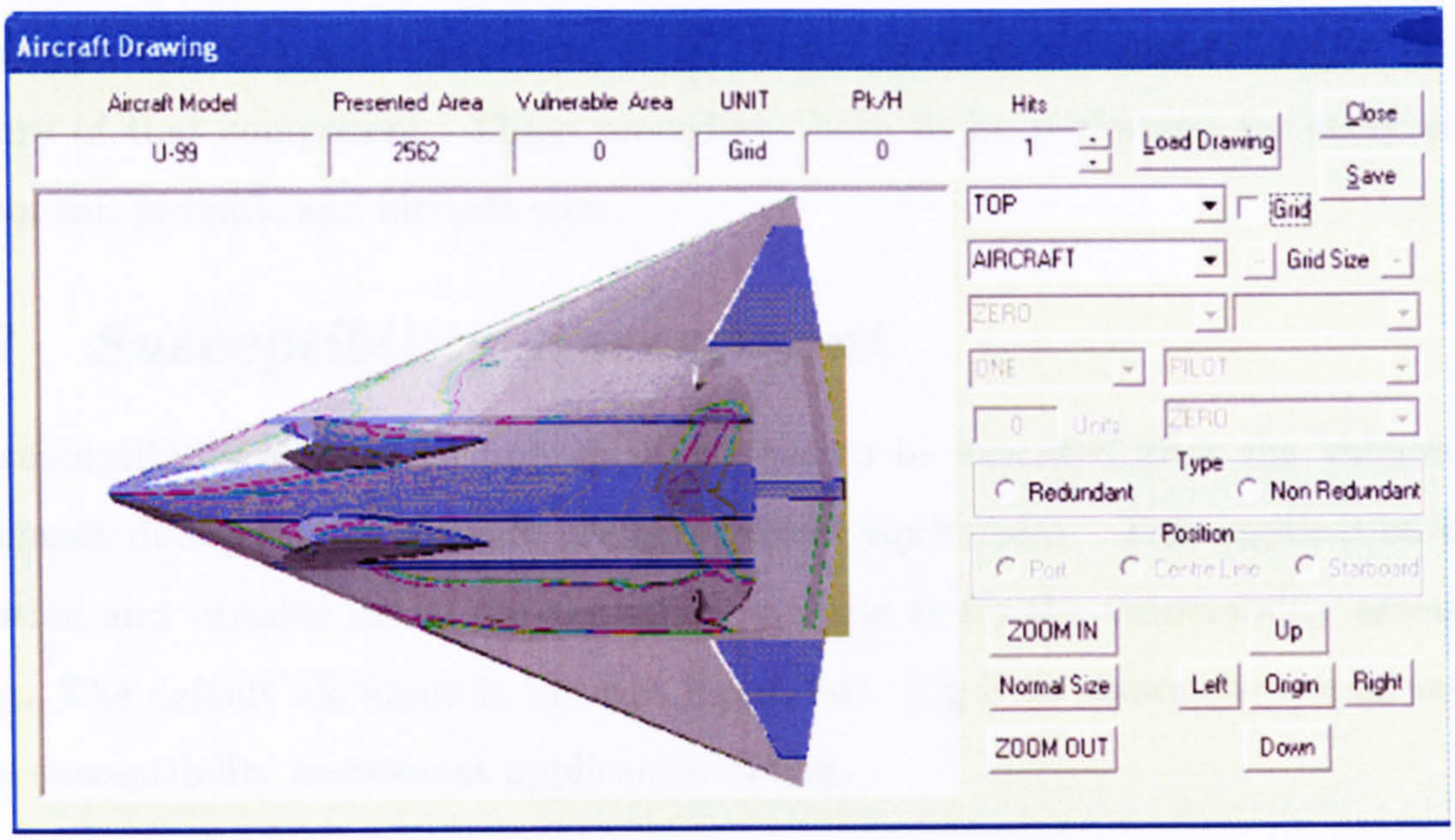

Figure F.11: Semi-Automatic Grid Counter Dialog

The 'Grid' option will turn on and off the grid over the image. The size of grid can be also resized by using the bottom '–' and '+', as shown in Fig. F.12. The image can also be zoomed and moved by using commands at the right bottom corner.

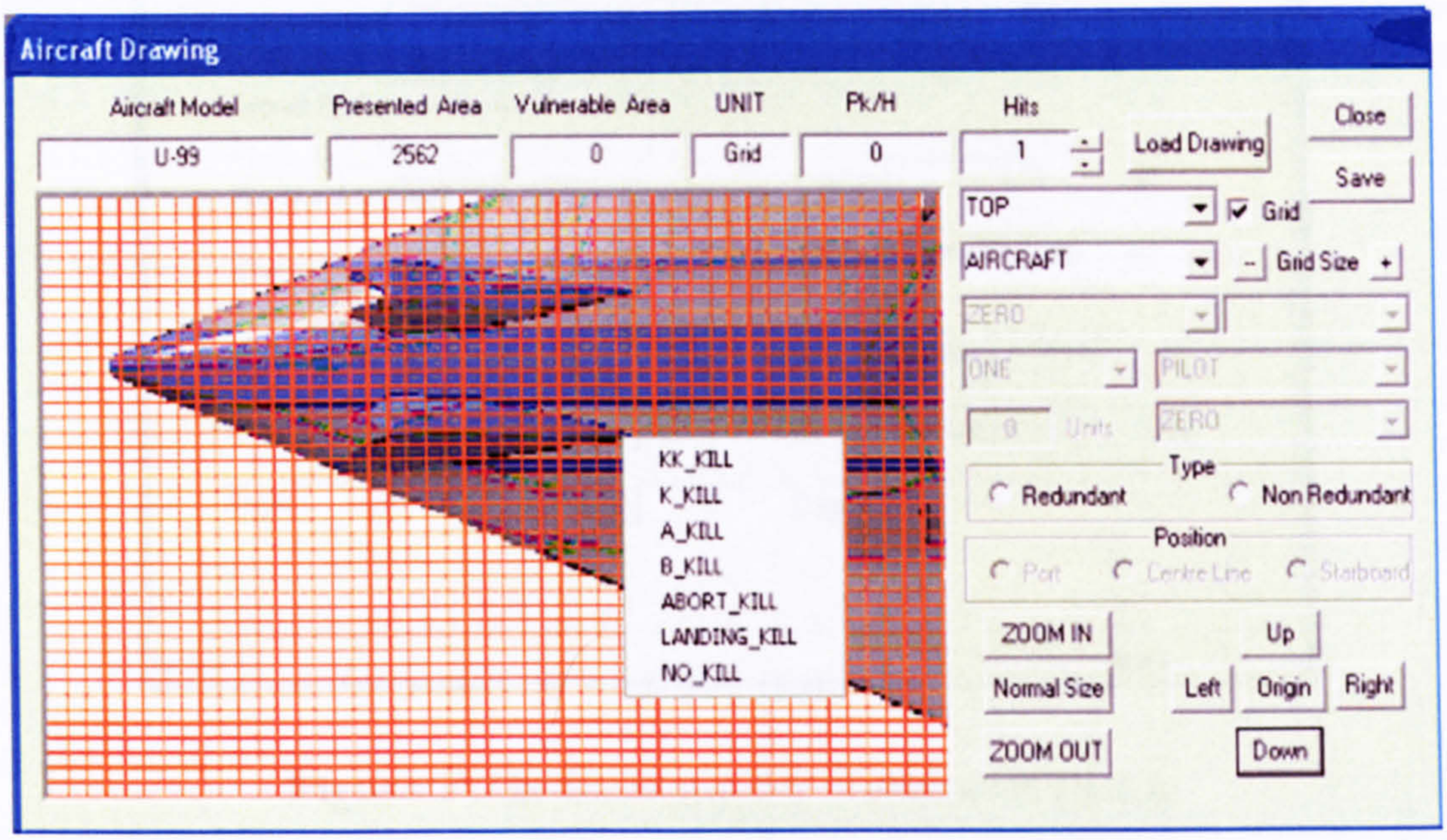

Figure F.12: Zooming and Moving Image Possibility

By pressing mouse right bottom, a small pop-up menu will be displayed. This menu offers the selection of kill level for each critical component. And by pressing left mouse bottom, the grid will be coloured mark depending on the kill level and automatically counted for the selected critical component. To stop counting grid for the selected critical

component, the command 'Save' has to be chosen to store to number of grid into the memory of that component. These procedures have to be performed for every critical component, aircraft, and aircraft view.

F.3 Susceptibility Assessment

The susceptibility assessment pop-up dialog has to be executed after the vulnerability assessment dialog due to aircraft presented area requirement. This application dialog execution and variable initial use the same principle as for the vulnerability assessment dialog. The default file name is 'suscept_input.dat'. Fig F.13 shows the overall outlook of the susceptibility assessment application dialog.

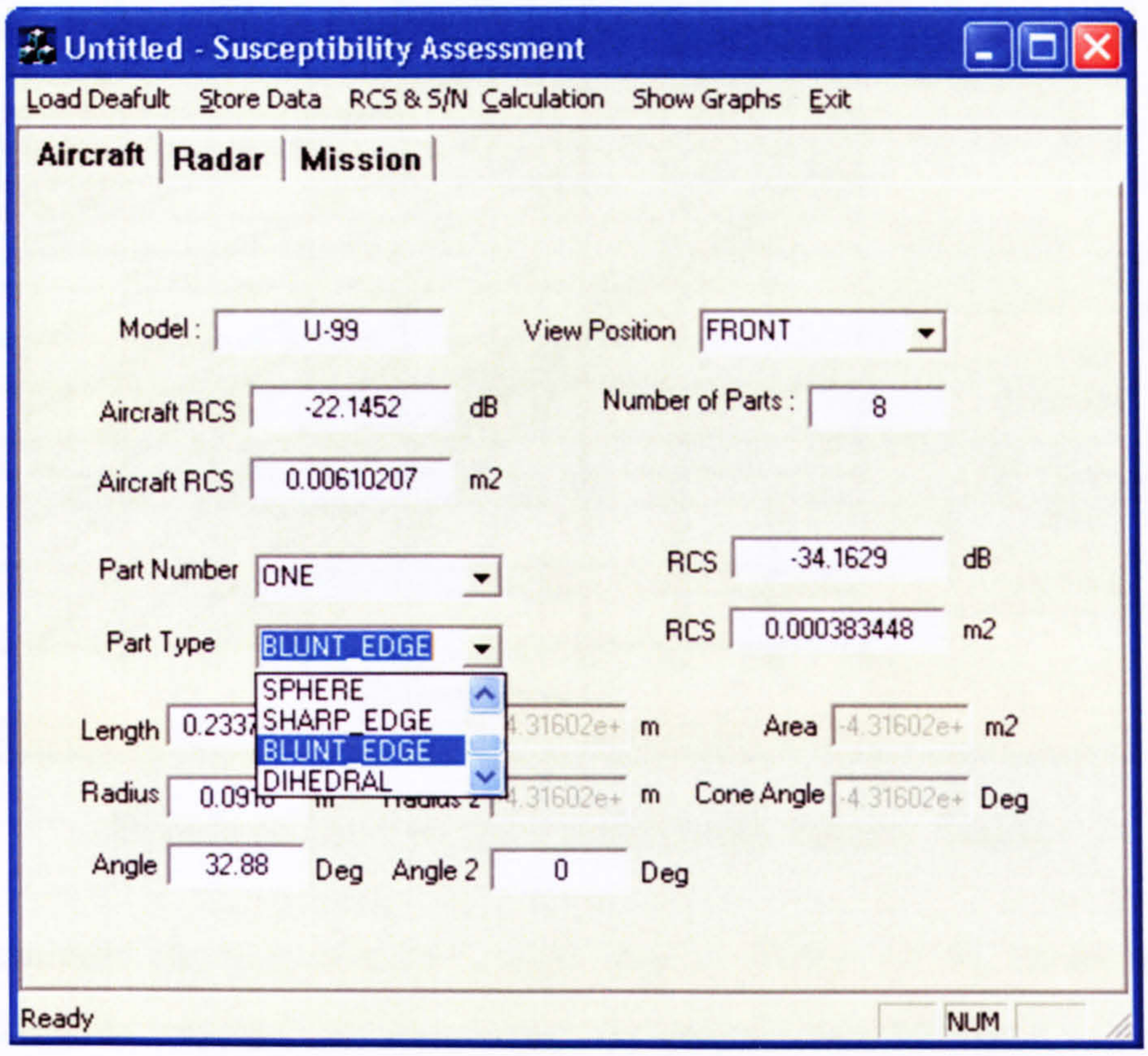

Figure F.13: Susceptibility Assessment Dialog

The next step is to calculate radar cross section and signal-to-noise ratio of the external aircraft shape by pressing command 'RCS & S/N Calculation'. Unfortunately, the aircraft probability of detection can not be calculated directly with this version; therefore, the pre-calculated graph has to be display by choosing command 'Show Graphs'. A new pop-up dialog will appear, as shown in Fig. F.14. There are 2 alternative of pre-calculated graph;

i.e. with and without scintillation effect. The selected graph will be displayed in the big square edit box in the left hand side of the dialog. The user has to give the probability of detection value in the 'P_D Value' edit box by using the S/N and P_n values displayed in the dialog. The P_D value will be stored in memory for the selected flight phase or aircraft view by pressing command 'Save Data'. The process has to be repeated to determine P_D for every aircraft view and flight phase.

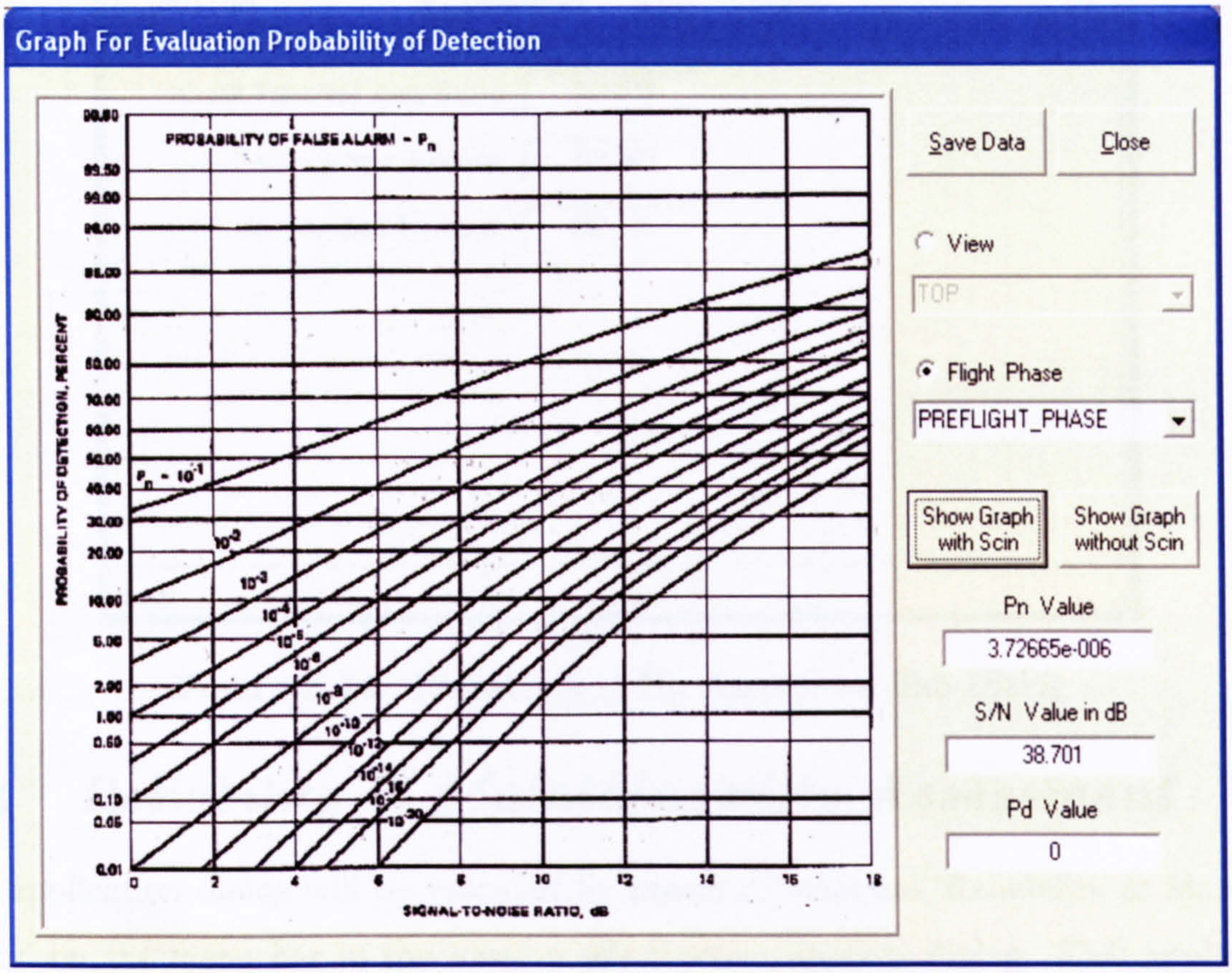

Figure F.14: Pre-Calculated Graph Display Dialog

After terminate the pre-calculated graph display dialog, all P_D values will be saved into the default file 'suscept.dat' by pressing command 'Save All Data'.

At the same time as calculation aircraft external radar cross section and signal-to-noise ratio, the probability of hit will be calculated by using 20 generated random miss distance. In case that the model to represent an aircraft presented area ('Carlton' or 'Shoe Box') has been change, the new probability of hit can also be new calculated by pressing command 'Recalculation', as shown in Fig. F.15.

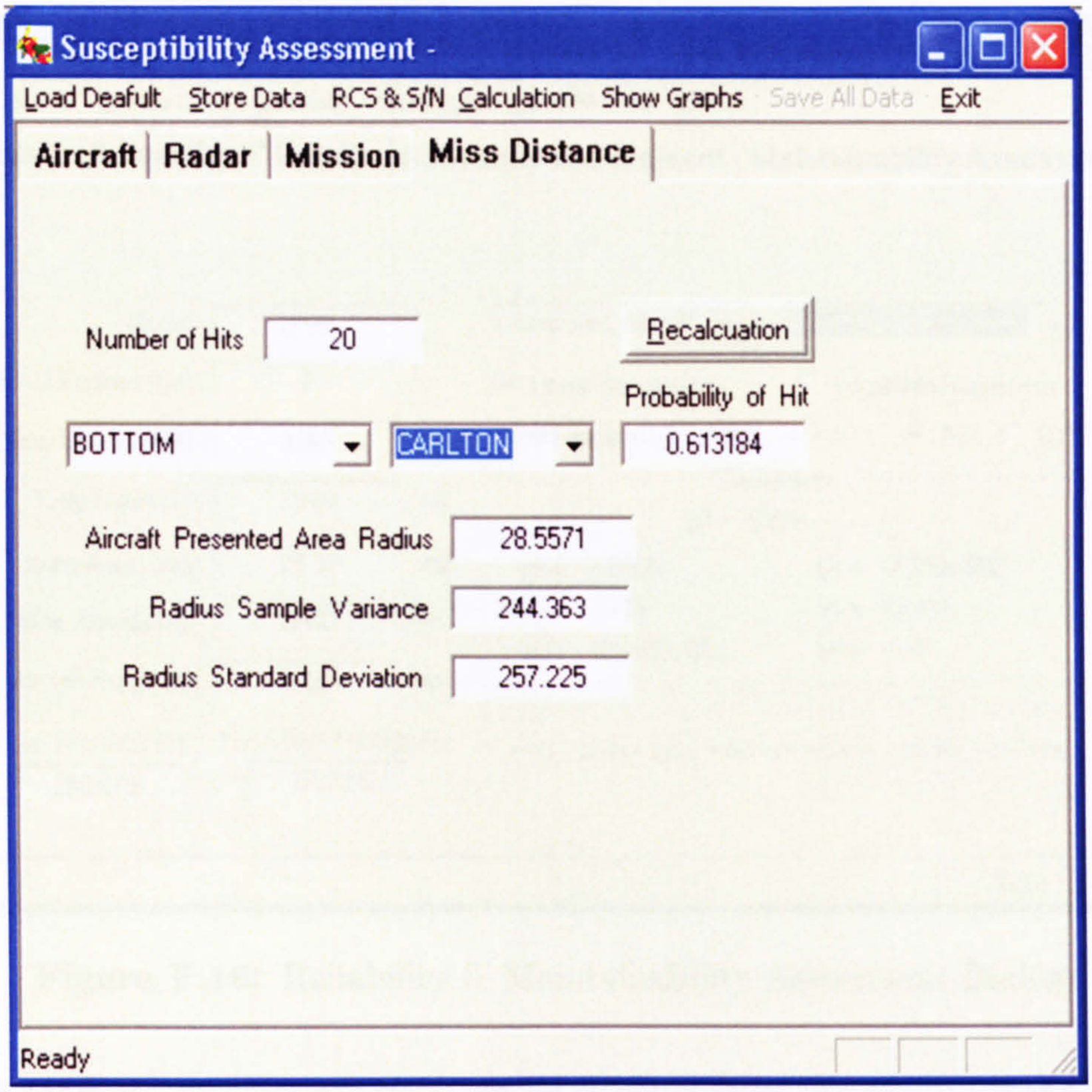

Figure F.15: Probability of Hit Assessment Tab Dialog

F.4 Reliability & Maintainability Assessment

This application dialog will be executed by pressing command 'Reliability & Maintainability' on the menu bar in the mission effectiveness analysis dialog. This application dialog comprises 3 tab dialog, as shown in Fig. F.16. By using the same approach to load default initial values for necessary variables, the information has to be stored into the file 'rel_main_input.dat'.

In case that the initial values are not correct or need to be changed, the new values can be given directly in the application dialog. These new values will replace in the memory by pressing command 'Update Data', and can be also save into file by pressing command 'Store Data'. The file containing new values will be created and named '**AircraftModel**_new_rel_main_data.dat', where **AircraftModel** is the same as shown in the dialog.

Before the aircraft failure rate and defect man-hour rate can be calculated, the necessary parameters have to be set by using pop-up menu and radio bottom in the application

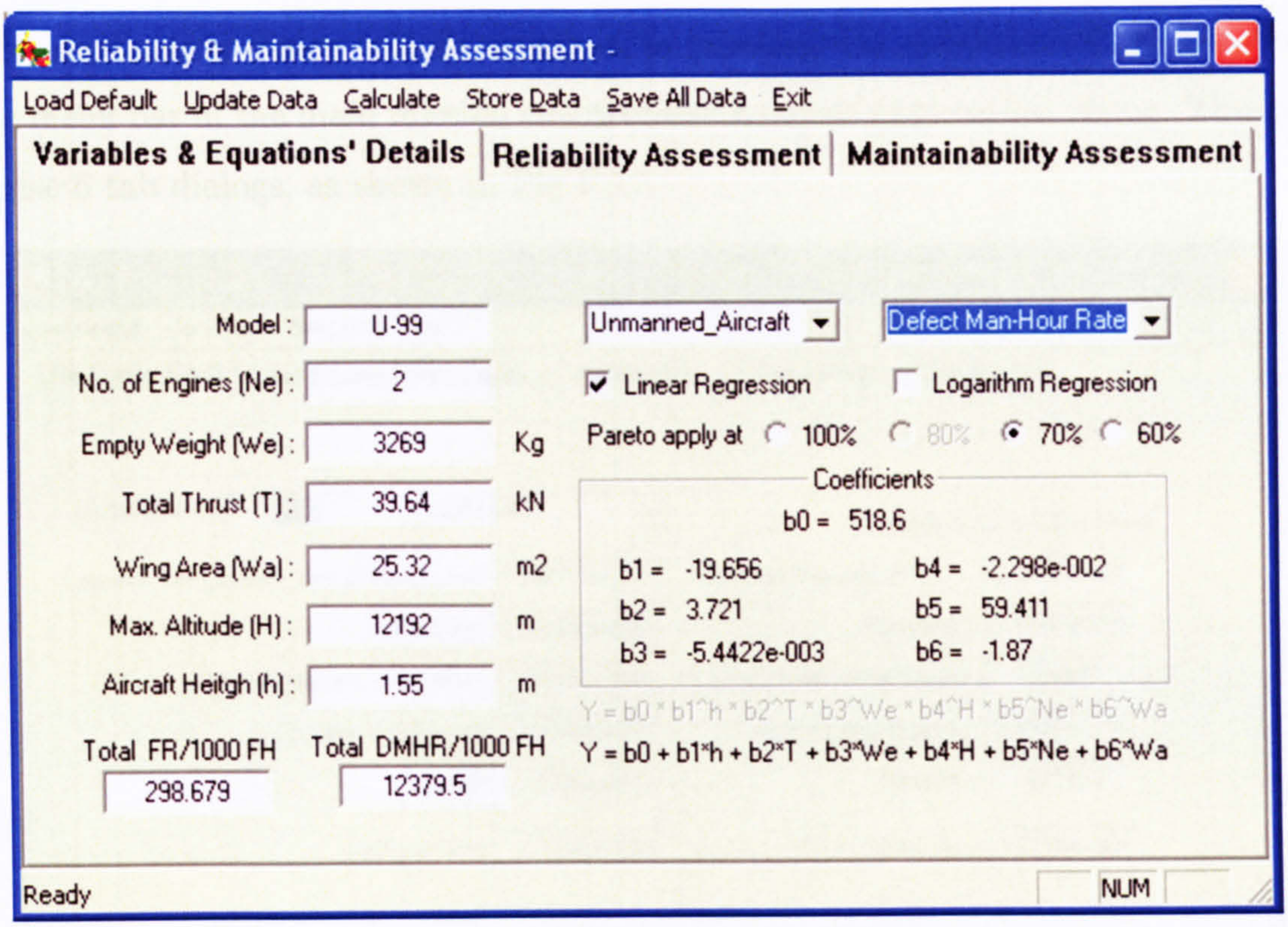

Figure F.16: Reliability & Maintainability Assessment Dialog

dialog. For example, the aircraft type can be selected from the pop-up menu positioning in the middle of the dialog or statistical analysis model to calculate the highest and the lowest failure rate or defect man-hour rate can be selected by using check box under the aircraft type pop-up menu.

By pressing command 'Calculation', the Pareto distribution coefficients, the remaining value either of failure rate or defect man-hour rate will be calculated, depending on the selected variable in the pop-up menu on right of aircraft type pop-up menu. Details of calculation will be also shown in the specific tab dialog.

To save all results into file 'reliability.dat', the command 'Save All Data' has to be chosen.

F.5 Life Cycle Cost Estimation

This application dialog has to be executed after the reliability & maintainability assessment dialog, and also cannot be terminated during the mission simulation runs. The reasons are that defect man-hour rate is one of the necessary variable to estimate aircraft life cycle cost, and the mission simulation need some values transferred directly from this application dialog.

The application dialog will be executed by pressing the command 'Cost Estimation' on the menu bar of the main mission effectiveness analysis application dialog. This dialog comprise 6 tab dialogs, as shown in Fig F.17.

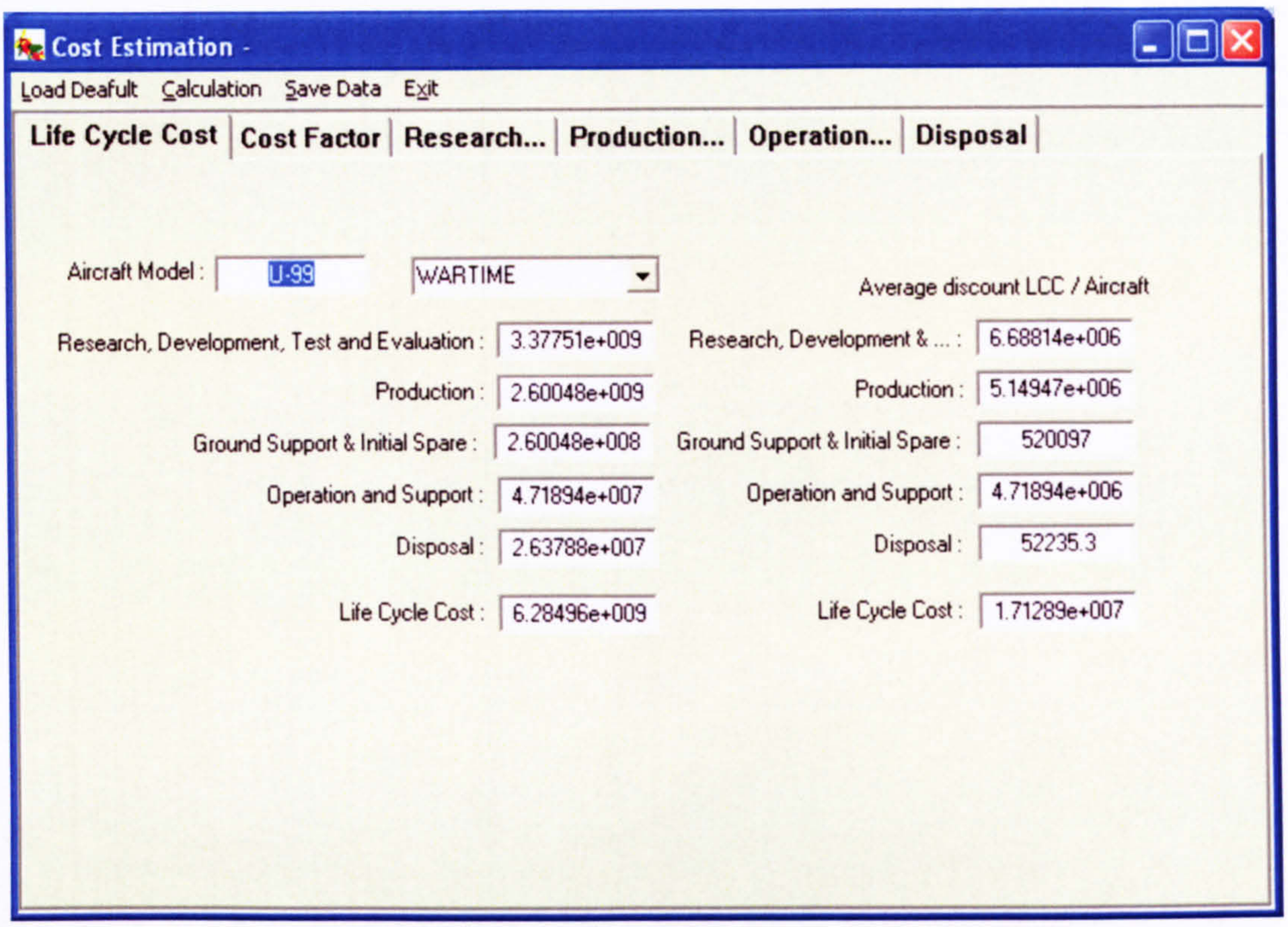

Figure F.17: Life Cycle Cost Estimation Dialog

The default initial values will be loaded from the file 'LCC_input.dat', when the command 'Load Default' has been chosen. Before actual calculation is performed, the user should also check the mission scenario in the pop-up manu because the application will calculate an aircraft life cycle cost based on the displayed scenario in that menu. Finally, the aircraft life cycle cost will be calculated by pressing command 'Calculation', and the results will be stored into the file 'lifecyclecost.dat' when the command 'Save Data' has been chosen.